620
C122r
no. 1-47

ENGINEERING LIBRARY
ALTBELD HALL STORAGE

DEPARTMENT OF ENGINEERING
UNIVERSITY OF CALIFORNIA
LOS ANGELES

June 1, 1951

ENGINEERING LIBRARY
ALTBELD HALL STORAGE

REPRINTS IN ENGINEERING

A limited number of copies are available for distribution. Please check the particular papers desired and return this list to: L. M. K. Boelter, Department of Engineering, University of California, Los Angeles 24, California.

1. "Air in Earth Fills Assures Stability", by E. R. Hallett, Jr., Engineering News-Record, June 1, 1950.

2. "Applications of a Mechanical Differential Analyzer to Electrical Engineering", by Earl Janssen and Don Lebell, Electrical Engineering, May, 1951.

3. "Applied Column Theory", by F. R. Shanley, Transactions of the American Society of Civil Engineers, Vol. 115, 1950, pp 698-750 (with discussions)

4. "Analysis and Design of Stiffened Shear Web", by Paul H. Denke, Journal of the Aeronautical Sciences, Vol. 17, No. 4, April, 1950, pp 217-231.

5. "Analysis of Magnetic Amplifier Equivalent Circuits", by Don Lebell, presented at the I.R.E. West Coast Convention, September 14, 1950.

6. "Analytical Studies in the Suppression of Wood Fires", by G. J. Tauxe and Ray L. Stoker, University of California, Department of Engineering, November, 1950.

7. "A Comparison of Several Heat and Mass Transfer Networks of Interest in Water Conservation", by H. F. Poppendiek and Myron Tribus, Transactions, American Geophysical Union, Vol. 32, No. 1, February, 1951, pp 49-56.

8. "Determination of Natural Frequencies of Piping Systems by an Electrical Analogy", by Eugene F. Murphy, Ph.D. Thesis, Graduate School of Illinois Institute of Technology, June, 1948.

9. "The Determination of Variables Included in a Composite Prediction of Matriculation in Engineering", by W. P. Wallace and H. W. Case, presented at the ASEE Annual Convention, June 22, 1950, Seattle, Washington.

10. "An Electronic Volume Counter", by D. L. Gerlough, Traffic Engineering, September, 1950.

11. "Erratum: On the Diffraction of an Electromagnetic Wave Through a Plane Screen", by J. W. Miles, Journal of Applied Physics, Vol. 21, No. 5, May, 1950, pp 468.

12. "Exercise Treatment of the Frozen Shoulder", by H. Jampol, Physical Therapy Review, Vol. 30, No. 6, June, 1950

DEPARTMENT OF ENGINEERING
UNIVERSITY OF CALIFORNIA
LOS ANGELES

June 1, 1951

REPRINTS IN ENGINEERING

A limited number of copies are available for distribution. Please check the particular papers desired and return this list to: L. K. Boelter, Department of Engineering, University of California, Los Angeles 24, California.

1. "Air in Pure Fluid Arrows Stability", by D. R. Dalton, Jr., Engineering News-Record, June 1, 1950.

2. "Applications of a Mechanical Differential Analyzer to Electrical Engineering", by Burt Jansen and Don Lobell, Electrical Engineering, May, 1951.

3. "Applied Column Theory", by W. H. Shanley, Transactions of the American Society of Civil Engineers, Vol. 115, 1950, pp 648-750 (with discussion)

4. "Analysis and Design of Shielded Sheet Coils", by Paul H. Dana, Journal of the Aeronautical Sciences, Vol. 17, No. 4, April, 1950, pp 217-231.

5. "Analysis of Magnetic Amplifier Saturable Circuits", by Don Lobell, originated at the I.A.S. West Coast Convention, September 11, 1950.

6. "Analytical Studies in the Expression of Wood Stress", by O. G. Ture and Ray L. Stoker, University of California, Department of Engineering, November 1950.

7. "A Comparison of Several Heat and Mass Transfer Patterns of Water Conservation", by R. F. Popperdick and Myron Tribus, Transactions, American Geophysical Union, Vol. 32, No. 1, February, 1951, pp 49-55.

8. "Determination of Natural Frequencies of Pulse Systems by an Electrical Analogy", by Eugene F. Murphy, Jr., Tunis, Graduate School of Aeronautics, Institute of Technology, June, 1950.

9. "The Determination of Vertical Inclined in a Composite Prediction of Natural Aviation in Engineering", by F. F. Wellins and H. W. Case, presented at the ASEE Annual Convention, June 22, 1950, Seattle, Washington.

10. "An Electric Volume Counter", by D. L. Ordway, Pacific Engineering, September, 1950.

11. "Pressure On the Diffraction of an Electromagnetic Wave Through a Plane Screen", by J. T. Wilson, Journal of Applied Physics, Vol. 21, No. 5, May, 1950, pp 509.

12. "Concrete Treatment of the Broken Shield", by H. Jumpel, Physical Review, Vol. 10, No. 61, June, 1950

620
C122r
no.1-47

13. "Experience Credit Toward the Professional Engineer's License for Technical Institute Study", by H. P. Rodes, Journal of Engineering Education, Vol. 41, No. 8, April, 1951, pp 472-473.

14. "Field Study of a Sheet Pile Bulkhead", by C. Martin Duke, presented at the Annual Spring Meeting of A.S.C.E., April, 1950, Los Angeles, California.

15. "How Can Standards of Achievement by Students in Lower Division Work be Made to Mean the Same to Junior and Senior Colleges?", by H. P. Rodes, Junior College Journal, January, 1951, pp 304-307.

16. "The Influence of Biaxiality on Notch Brittleness", by D. Rosenthal and W. D. Mitchell, Welding Journal Research Supplement, September, 1950.

17. "Influence of the Elastic Constants on the Partition of Load Between Rivets", by D. Rosenthal and W. D. Mitchell, Proceedings of Society on Stress Analysis Vol. 7, No. 2, pp 17-26.

18. "The Integration of Library Service with Teaching and Research, in Engineering School Libraries", by J. E. Allerding, Journal of Engineering Education, Vol. 41, No. 4, December, 1950, pp 145-148.

19. "The Interfacial Tension of Some Hydrocarbons Against Water", by W. F. Seyer and W. E. Rose, Journal of Physical and Colloid Chemistry, Vol. 55, No. 3, March 9, 1951, pp 439-447.

20. "Intermittent Heating for Aircraft Ice Protection with Application to Propellers and Jet Engines", by Myron Tribus, ASME Paper 50-A-55, presented at Annual Meeting, New York, November, 1950.

21. "Laboratory Demonstration Experiment - A Link Between Fundamentals and Applications", by D. Rosenthal and H. Baer, Journal of Engineering Education, Vol. 41, No. 3, November, 1950, pp 171-175.

22. "Microwave Spectrum of Methyl Mercaptan", by W. D. Hershberger and F. K. Hurd, The Physical Review, Vol. 82, April, 1951, pp 95.

23. "Multiple-Output Predetermined Counter", by D. L. Gerlough and H. R. Kaiser, Electronics, February, 1951. p. 122

24. "Mutual Solubilities of Hydrocarbons", by W. F. Seyer, Journal of the American Chemical Society, Vol. 72, pp 3162-3164, 1950

25. "A New Low Power Pulse Transformer for High Duty Cycle Operation", by W. L. Martin, University of California, Los Angeles, June, 1950 (M.S. Thesis)

26. "A Note on Subsonic Aerofoil Theory", by J. W. Miles, The Aeronautical Quarterly, Vol. 2, May, 1950, pp 23-33.

27. "On Downwash Corrections in Unsteady Flow", by J. W. Miles, Journal of the Aeronautical Sciences, Vol. 17, No. 4, April, 1950, pp 253.

28. "On the Equations of Longitudinal Stability", by J. W. Miles, Journal of the Aeronautical Sciences, Vol. 17, No. 12, December, 1950, p 815.

29. "On the Equations of Longitudinal Stability - II", by J. W. Miles, Journal of the Aeronautical Sciences, Vol. 18, No. 3, March, 1951, p 212.

30. "On Non-Steady Motion of Slender Bodies", by J. W. Miles, The Aeronautical Quarterly, Vol. 2, November, 1950, pp 183-194.

31. "On the Response of a Directive Antenna to Incoherent Radiation", by F. W. Schott, Proceedings of the Institute of Radio Engineers, June, 1951

32. "On Virtual Mass and Wave Drag at Subsonic Speeds", by J. W. Miles, Journal of the Aeronautical Sciences, Vol. 17, No. 10, October, 1950, p 667.

33. "The Oscillating Rectangular Airfoil at Supersonic Speeds", by J. W. Miles, Quarterly of Applied Mathematics, Vol. 9, No. 1, April, 1951, pp 47-65

34. "Promotional Systems of Variables for Engineering Faculties", by H. W. Case, Journal of Engineering Education, Vol. 41, No. 8, April, 1951, pp 464-470.

35. "Quasi-Stationary Airfoil Theory in Subsonic Compressible Flow", by J. W. Miles, Quarterly of Applied Mathematics, Vol. 8, No. 4, January, 1951, pp 351-358.

36. "Residual Stress and Fatigue Strength", by D. Rosenthal and George Sines, Metal Progress, p 76, July 1950, V. 58.

37. "A Segmented Electrical Element for Detecting Vehicular Traffic", by J. H. Mathewson, R. Brenner and R. J. Reiss, Proceedings of the Highway Research Board, 29th Annual Meeting, December, 1949, pp 374-383.

38. "Servo Theory Applied to Frequency Stabilization with Spectral Lines", by W. D. Hershberger and L. E. Norton, Journal of the Franklin Institute, Vol. 249, No. 5, May, 1950.

39. "Some Relations Between Harmonic and Transient Loading of Airfoils", by J. W. Miles, Journal of the Aeronautical Sciences, Vol. 17, No. 10, October, 1950, p 671.

40. "Some Statistical Considerations of the Jet Alignment of Rocket-Powered Vehicles", by A. L. Stanly, Journal of the American Rocket Society, December, 1950, pp 155-168.

41. "Special Abilities in Pre-Engineering Studies", by Harvey S. Moredock, Jr., University of California, April, 1950.

42. "Street and Highway Traffic", by T. W. Forbes, Handbook of Applied Psychology Chapter 50, Rinehart and Co., New York, 1950.

43. "A Study of the Response of an Airplane Landing Gear Using the Differential Analyzer", by W. C. Hurty, Journal of the Aeronautical Sciences, Vol. 17, No. 12, December, 1950, pp 756-764.

28. "On the Equations of Longitudinal Stability", by J. W. Miles, Journal of the Aeronautical Sciences, Vol. 17, No. 12, December, 1950, p 815.

29. "On the Equations of Longitudinal Stability - II", by J. W. Miles, Journal of the Aeronautical Sciences, Vol. 18, No. 3, March, 1951, p 212.

30. "On Non-Steady Motion of Slender Bodies", by J. W. Miles, The Aeronautical Quarterly, Vol. 2, November, 1950, pp 183-194.

31. "On the Response of a Directive Antenna to Incoherent Radiation", by F. V. Schott, Proceedings of the Institute of Radio Engineers, June, 1951

32. "On Virtual Mass and Wave Drag at Subsonic Speeds", by J. W. Miles, Journal of the Aeronautical Sciences, Vol. 17, No. 10, October, 1950, p 647.

33. "The Oscillating Rectangular Airfoil at Supersonic Speeds", by J. W. Miles, Quarterly of Applied Mathematics, Vol. 9, No. 1, April, 1951, pp 47-65

34. "Promotional Systems of Variables for Engineering Results", by H. W. Case, Journal of Engineering Education, Vol. 41, No. 8, April, 1951, pp 469-477.

35. "Quasi-Stationary Airfoil Theory in Subsonic Compressible Flow", by J. W. Miles, Quarterly of Applied Mathematics, Vol. 8, No. 1, January, 1951, pp 351-356.

36. "Residual Stress and Fatigue Strength", by D. Rosenthal and George Sines, Metal Progress, p 76.

37. "A Segmented Electrical Element for Detecting Vehicular Traffic", by J. H. Matheson, R. Brenner and R. J. Roles, Proceedings of the Highway Research Board, 29th annual Meeting, December, 1949, pp 374-383.

38. "Servo Theory Applied to Frequency Stabilization with Spectral Lines", by W. D. Hershberger and I. E. Morton, Journal of the Franklin Institute, Vol. 249, No. 5, May, 1950.

39. "Some Relations Between Harmonic and Transient Loading of Airfoils", by J. W. Miles, Journal of the Aeronautical Sciences, Vol. 17, No. 7, October, 1950, p 671.

40. "Some Statistical Considerations of the Jet Alignment of Rocket-Powered Vehicles", by A. L. Stanly, Journal of the American Rocket Society, December, 1950, pp 155-166.

41. "Special Abilities in Pre-Engineering Studies", by Harvey S. Moreock, Jr., University of California, April, 1950.

42. "Street and Highway Traffic", by T. W. Forbes, Handbook of Applied Psychology Chapter 50, Rinehart and Co., New York, 1950.

43. "A Study of the Response of an Airplane Landing Gear Using the Differential Analyzer", by W. C. Hurty, Journal of the Aeronautical Sciences, Vol. 17, No. 12, December, 1950, pp 756-761.

44. "The Summation of Fourier Series by Operational Methods", by L. A. Pipes, Journal of Applied Physics, Vol. 21, No. 4, April, 1950, pp 3162-3164. 298-301

45. "A Time-Method Study by Methods of High Speed Cimematography", by H. Baer, B. F. Cohlon, and A. R. Gold, Society of Motion Picture and Television Engineers Journal, May, 1951.

46. "Transient Loading of Supersonic Rectangular Airfoils", by J. W. Miles, Journal of the Aeronautical Sciences, Vol. 17, No. 10, October, 1950, pp 647-652.

47. "Wetting Properties of Some Enamel Glasses and Relations to Impact Resistance", by W.J . Knapp, Journal of American Ceramic Society, Vol. 33, No. 8, August, 1950, pp 258-262.

NAME _____

ADDRESS _____

_____

44. "The Summation of Fourier Series by Operational Methods", by L. A. Hipes, Journal of Applied Physics, Vol. 21, No. 4, April, 1950, pp 316-320.

45. "A Time-Method Study by Methods of High Speed Cinematography", by H. Baer, B. F. Cahlon, and A. R. Gold, Society of Motion Picture and Television Engineers Journal, May, 1951.

46. "Transient Loading of Supersonic Rectangular Airfoils", by J. W. Miles, Journal of the Aeronautical Sciences, Vol. 17, No. 10, October, 1950, pp 647-652.

47. "Melting Properties of Some Enamel Glasses and Relations to Impact Mortality", by W. W. Kemp, Journal of American Ceramic Society, Vol. 33, No. 8, August, 1950, pp 252-262.

NAME _____

ADDRESS _____

_____

Air in Earthfills Assures Stability

E. R. Hallett
Los Angeles, Calif.

SPECTACULAR earthfill failures have been caused by too much water in the fill. But when earthfill voids contain air as well as water, failure is not likely to result in a properly constructed fill.

Moisture and air content can be controlled when a fill is placed. But addition of fill material may increase the pressure so all the free air becomes absorbed in the water. This changes a well-made fill to a supersaturated condition and failure may result. Charts for field use that forecast this possibility have been developed by the author and are the subject of this article.

These charts were developed after a suggestion by R. R. Proctor and Loring E. Tabor of the Los Angeles Department of Water and Power. The author was employed as a field engineer on construction of the Baldwin Hills reservoir by the city. Construction of that earthfill was checked by this type of chart.

• **Moisture content important**—In constructing a rolled fill, one of the most important factors is the moisture content of the soil being compacted. The purpose of compaction is to make the fill so dense that failure by water saturation or other causes is not likely. For a given soil and a given method of compaction, a particular moisture content (optimum moisture content) of the soil will result in the most dense fill.

Compaction curves are drawn to determine the optimum moisture content. Unit weight (lb per cu ft) for several samples with different moisture content is determined to draw this curve. In all probability, no saturated samples will be used to prepare such a curve.

When a fill consolidates (by particles readjusting to decrease the voids as the fill rises), air and water in the voids are put under higher and higher pressures. With the pressure increased, air is absorbed by water until a saturated condition exists. (The possibility of the air escaping from the fill under pressure is neglected in this discussion. Such an omission will usually be on the safe side.) Then, if the particles further readjust so as to decrease the voids, the entire additional load will be carried by the incompressible water, and the pore pressure may become very high. The friction of the soil may thus decrease until a slide-out failure of a slope occurs. The charts developed by the writer are intended to predict without calculation just how great is the possibility of such a failure.

As rolled fills are constructed, a large number of field samples are taken to show conditions in the fill. Engineers can judge what future procedural changes seem wise. Simple laboratory tests on the field samples will give moisture content, unit weight as found in the fill and the specific gravity of the soil particles. These values together with an estimate of the temperature of the completed fill are used in the accompanying chart.

• **Using the chart**—For each combination of specific gravity and fill temperature, a separate chart is required. For example, if the specific gravity is 2.6 and the fill temperature is 50 deg F, the accompanying chart is used. The dry unit weight is plotted against moisture content. In most cases this point will fall within the group of curves plotted on the chart. For a 110-lb per cu ft sample with 17% moisture content, the plotted point falls on the third of the family of curves. This indicates that an additional pressure of 40 psi will be required fully to absorb existing air and result in a saturated condition.

For a field approximation, it may be assumed that increasing the height of a fill by 1 ft will increase the pressure by 1 psi. Thus, in the preceding example, an additional 40 ft depth of fill can safely be placed. But if more than 40 ft of fill is to be placed, a dangerous condition may develop. (Here the part of the weight of the additional fill supported by the soil skeleton is neglected—this being the side of safety.)

To correct this condition, the engineer may attempt to reduce the moisture content of the soil that is subsequently rolled. (Note that a reduction from 17 to 15% in our previous example will permit pressure to be increased to 140 psi.) If good compaction can be secured with a lower moisture content, the safety of the fill may be insured by this means. If good compaction cannot be obtained in the course of reducing the moisture content, then more accurate calculations

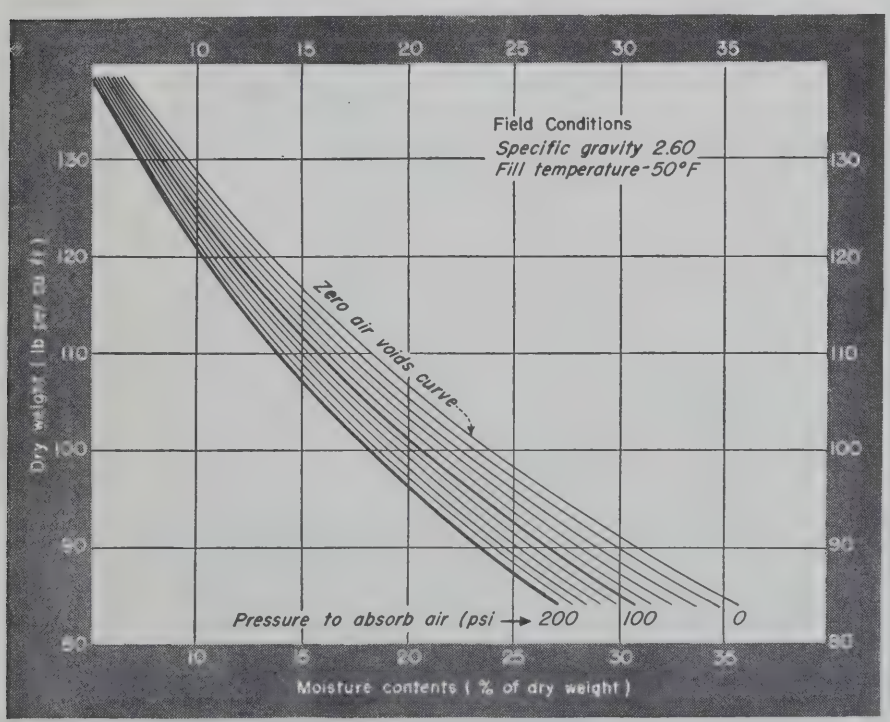

CHARTS such as this can be developed to predict pressure required to absorb air in a fill. This one is for a 2.6 specific gravity and a 50 F fill temperature.

of the pore pressures that may be expected to develop must be made. It may be desirable to install piezometers (if they are not already required) to determine actual pore pressure.

In some cases, pore pressures developed by consolidation will be dissipated through the fill if sufficient time is allowed. The field engineer in such case can reduce the rate of construction so that a dangerous condition does not develop.

It is conceivable that it might even be necessary to redesign the structure to secure safety if field experience and office calculations indicate a dangerous condition (one that cannot be relieved by reducing moisture content or slowing down rate of fill).

• **Consolidation computations**—Accurate calculations of consolidation where the soil is **not** saturated (i.e. where both a water and an air phase must be considered) are apt to prove difficult. The Terzaghi theory of consolidation uses the Darcy formula to calculate the additional amount of water that will be squeezed out from the soil. This is then made equal to the decrease in volume of the soil. Terzaghi's theory assumes (1) the complete saturation of the soil, (2) the validity of the Darcy law, (3) a constant coefficient of permeability and (4) one dimensional flow (upward). These may not always be true.

Modification of the Darcy formula by assuming polyphase flow involves the use of equations quite difficult for a field engineer to handle in time to be of any value to him in controlling the placing of a rolled earth fill. Thus, it appears that the alternative to the use of a chart such as presented herewith is to make no attempt at all to prevent future high pore pressures by controlling the rolled earth fill while it is being constructed. To attempt arbitrarily to place the fill in a relatively dry state may result in poor compaction, and use of the charts may indicate that it is not necessary to do this.

• **Basis of the chart**—Computation of the charts involves the degree of saturation, S, which is the ratio of the moisture content of a soil to its moisture content at full saturation. The curves on the charts correspond to various degrees of saturation where S is less than 1. The zero air voids curve corresponds to S = 1, or 100% saturation.

For each specific gravity, a plot of unit weight against moisture content can be made for a saturated condition. The other curves on each chart are computed by using Henry's Law that states that for a given temperature the amount of gas which a liquid will absorb is directly proportional to the pressure of the gas. Thus, for a given saturation (S), a curve can be drawn that is roughly parallel to the saturated condition curve. It then remains to select the saturations that will resist pressures of 20 psi, 40 psi, 60 psi, before a saturated condition exists.

Short-cut methods can be developed to simplify the plotting of these curves. For example, the entire series for a given temperature can be plotted against five horizontal scales, each scale representing a particular moisture condition.

AN ENGINEERING NEWS-RECORD REPRINT

June 1, 1950

Applications of a Mechanical Differential Analyzer to Electrical Engineering

EARL JANSSEN DON LEBELL

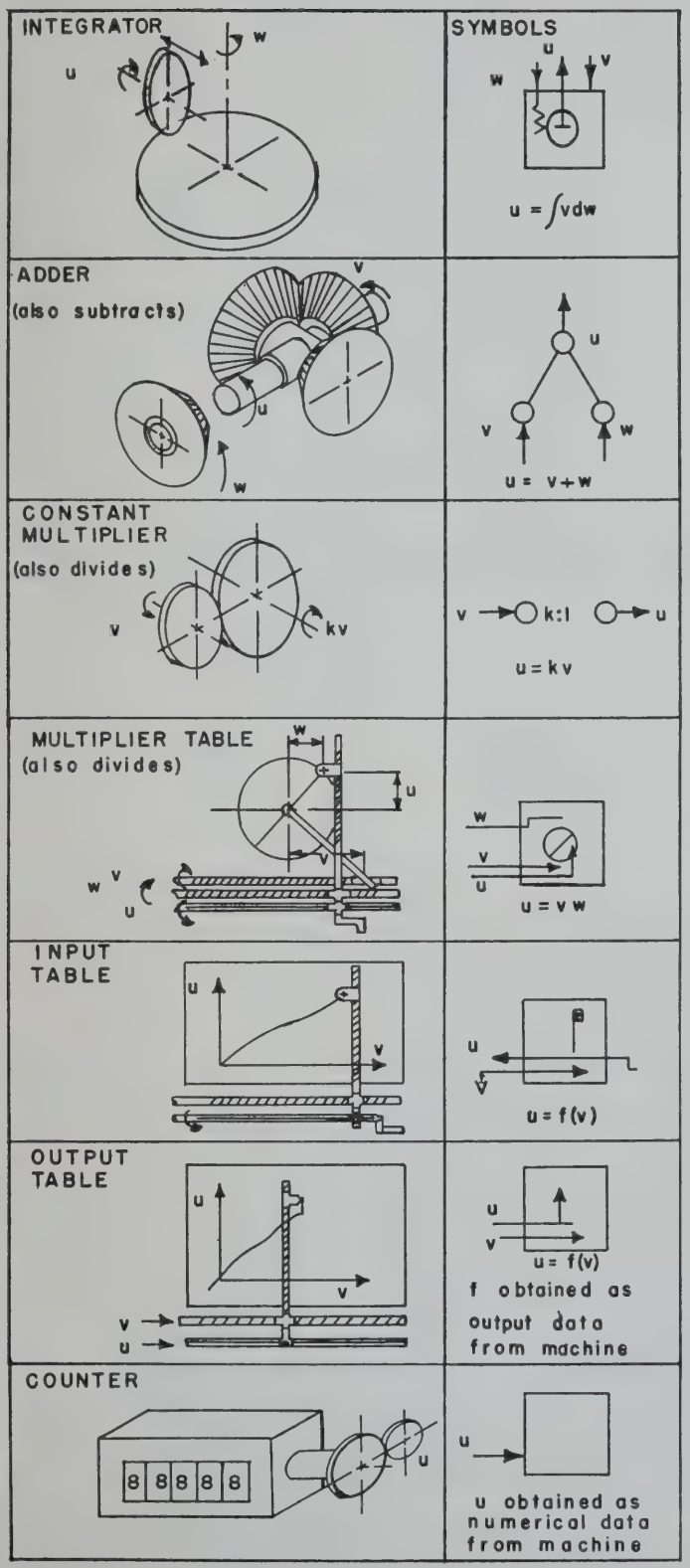

Figure 1(A). Basic components of a mechanical differential analyzer and their functions

The pertinence of the differential analyzer to the solution of certain types of electrical problems is explained by citing three examples. These examples have to do with magnetic amplifiers, pulse transformers, and particle (electron) accelerators.

THE PAST DECADE has produced an intensive and widespread series of developments in the computer field. Many dollars and man-hours have gone into computer projects with such extensive results that it has been difficult for the practicing engineer to obtain complete information on currently available computer facilities, their capabilities, and limitations. At the same time it is becoming increasingly important for the research and design engineer to have this information. He must be able to decide which computer, if any, should be employed to solve his particular problem. Too often, however, lack of information, or misinformation as to the characteristics of these devices, reduces the effectiveness of the engineer's efforts. It is the purpose of this article to point out the application to electrical engineering of one such computer, the mechanical differential analyzer. Accordingly, there follows a description of this computer and its application to the solution of representative problems in electrical engineering.

DESCRIPTION

THE OPERATING PRINCIPLES of the analyzer will be reviewed briefly since the detailed features have already been treated adequately in the literature.[1-3] The differential analyzer solves differential equations by construction within the machine of an analogue (model) of the equations to be studied. Quantities in the analogue correspond to variables in the equations to be solved; hence quantitative information about the equations can be obtained from an examination of the analogue quantities. Variables of the mechanical differential analyzer are represented by angular displacements of shafts which are interconnected to the various basic components of the machine. These basic components perform the mathematical operations indicated in Figure 1*A*. The particular selection and arrangement of components is determined by the form of the equations to be solved.

The real power of the analyzer lies in the special auxiliary operations and functions which can be produced as indicated in Figure 1*B* and the convenient means for supplying

Earl Janssen and **Don Lebell** are with the Department of Engineering, University of California, Los Angeles, Calif.

Acknowledgements for portions of this article are due the Engineering Pulse Transformer Research Project (Contract *W-28-099-ac-195*) of the University of California, sponsored by the Air Material Command.

Copyright, 1951, by the American Institute of Electrical Engineers and reprinted by permission of the copyright owner.

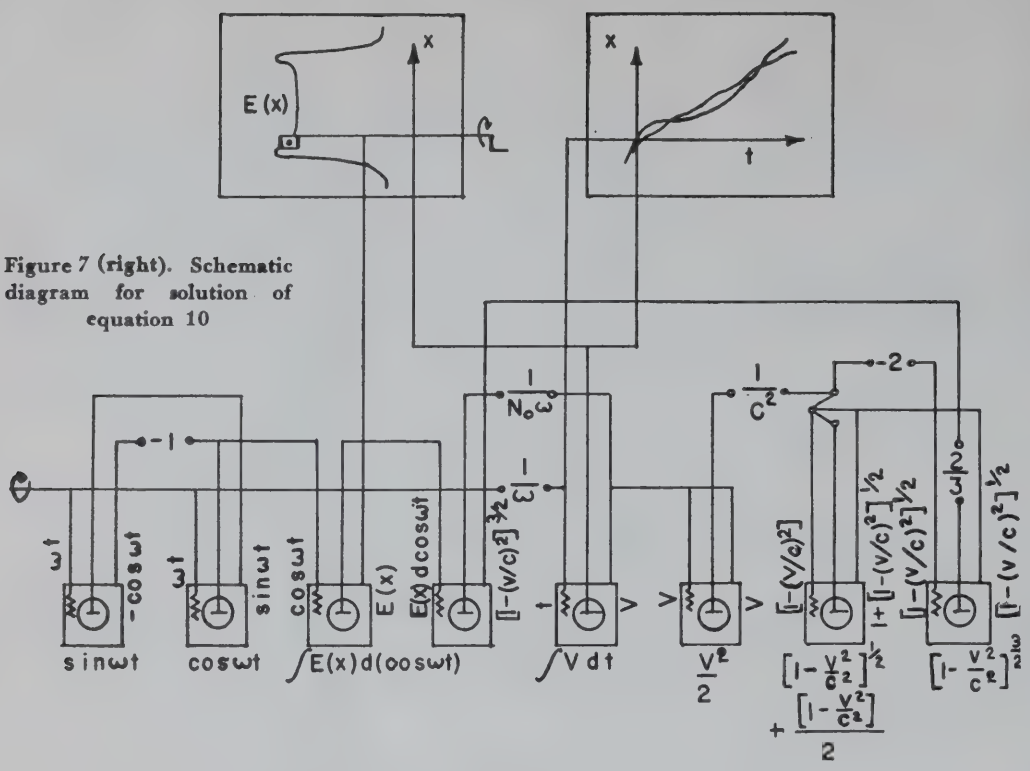

Figure 7 (right). Schematic diagram for solution of equation 10

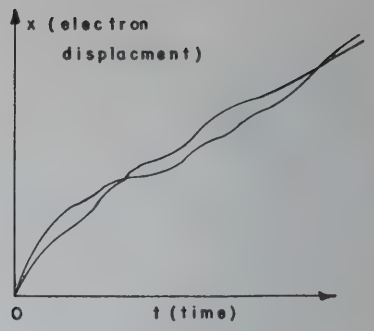

Figure 8 (above). Electron trajectories as obtained from the differential analyzer

be made to behave more nearly as the actual transformer by:

1. Considering the load resistance R_2 to vary as the actual load (perhaps a magnetron).
2. Employing the actual nonlinear characteristics of L_2 from core saturation data.
3. Increasing the number of loops, thereby simulating more nearly the distributed parameter characteristics of the actual transformer.

All these refinements could be made without adding appreciable complexity to the solution of the problem as obtained on the differential analyzer. However, these refinements would create considerable difficulty in achieving a satisfactory solution by other methods.

PARTICLE TRAJECTORIES

THE DESIGN of electron tubes, particle accelerators, and other devices utilizing the flow of particles under the influence of force fields often requires information about the trajectories of these particles. A typical example is the trajectory of a high-speed electron in a nonlinear electric field. The equation of motion in the particular direction X is

$$\mathcal{E}=\frac{d(mv)}{dt}$$

where $\mathcal{E}$ is the electric field intensity; m is the mass of the electron; v is the velocity of the electron; and t is time. The preceding equation becomes

$$\mathcal{E}=m\frac{dv}{dt}$$

except in applications where electron velocities approach the speed of light, in which case

$$\mathcal{E}=\frac{d}{dt}\left(\frac{m_0 v}{\sqrt{1-\left(\frac{v}{c}\right)^2}}\right)=m_0\left[1-\frac{v^2}{c^2}\right]^{-3/2}\frac{dv}{dt} \qquad (9)$$

where m_0 is the rest mass of the electron and c is the velocity of light. For an application of practical interest $\mathcal{E}$ varies in magnitude with distance x and sinusoidally with time; hence the relation

$$\mathcal{E}=E(x)\sin\omega t$$

where $E(x)$ is obtained from test data.

Combining this with equation 9 and integrating

$$v=\frac{1}{m_0}\int\left[1-\left(\frac{v}{c}\right)^2\right]^{3/2}E(x)\sin\omega t\,dt$$

$$=\frac{-1}{m_0\omega}\int\left[1-\left(\frac{v}{c}\right)^2\right]^{3/2}d\int E(x)d\cos\omega t \qquad (10)$$

Equation 10 is solved on the analyzer as shown in Figure 7. Solutions for various field conditions are shown in Figure 8.

The mechanical differential analyzer is capable of solving problems which can be formulated in terms of linear or nonlinear ordinary differential equations with constant or varying coefficients. Certain types of partial differential equations also can be solved on the differential analyzer by special techniques. There are now other computers which possess either greater speed, accuracy, or versatility in particular instances. However, because of its particular combination of these features it is the most suitable computer to employ for a large variety of problems and continues to be of great assistance to present-day technology.

REFERENCES

1. The Differential Analyzer of the University of California, **E. Janssen.** University of California Press, Berkeley, Calif., 1947.
2. Analogue Computer Facilities of the University of California, **L. L. Grandi, D Lebell.** University of California Press, Berkeley, Calif., 1950.
3. A New Type of Differential Analyzer, **V. Bush, S. H. Caldwell.** *Journal*, Franklin Institute (Philadelphia, Pa.), volume 240, 1945, pages 255–326.
4. Study of a Magnetic Amplifier with Self-Feedback, **D. Lebell.** Master of Science Thesis, University of California, Los Angeles, Calif., 1949.
5. *Reports I, II, III*, Pulse Transformer Contract *W-28-099-ac-195*, University of California, Los Angeles, Calif.
6. Some Studies of Pulse Transformer Equivalent Circuits, **C. K. Hadlock, D. Lebell.** *Proceedings*, Institute of Radio Engineers (New York, N. Y.), volume 39, number 1, January 1951, pages 81–3.

American Institute of Electrical Engineers
The Institute assumes no responsibility for statements made by contributors.

A Reprint From
ELECTRICAL ENGINEERING
Printed in the United States of America

5/14/'51 May 1951 issue

AMERICAN SOCIETY OF CIVIL ENGINEERS
33 WEST 39TH STREET, NEW YORK, N. Y.

Applied Column Theory

BY

F. R. SHANLEY

WITH DISCUSSION BY

MESSRS. WILLIAM R. OSGOOD, J. V. DU PLESSIS, JACOB KAROL, E. P. POPOV, JACK R. BENJAMIN, HERBERT A. SAWYER, E. C. HARTMANN, AND F. R. SHANLEY.

Paper No. 2410
Reprinted from TRANSACTIONS, Vol. 115, 1950, p. 698

AMERICAN SOCIETY OF CIVIL ENGINEERS

Founded November 5, 1852

TRANSACTIONS

Paper No. 2410

APPLIED COLUMN THEORY

By F. R. Shanley [1]

With Discussion by Messrs. William R. Osgood, J. V. du Plessis, Jacob Karol, E. P. Popov, Jack R. Benjamin, Herbert A. Sawyer, Jr., E. C. Hartmann, and F. R. Shanley.

Synopsis

The generalized Euler equation (involving the tangent modulus) is used as a basis for column strength analysis. The influence of the shape of the stress-strain diagram is shown by nondimensional column curves and an envelope formula is derived. The effects of initial eccentricity are investigated by interaction curves for combined bending and compression. Correction of test data, end fixity effects, and optimum design of columns are discussed briefly.

1. The Generalized Euler Theory

The failure of members under compressive loading has long been a subject of great interest to the structural engineer. In aircraft structures the phenomenon of instability is the basis for many strength calculations, because nearly all the structure is critical under some design condition that causes compressive loads. The demand for minimum structural weight has had two important effects—it has forced the aircraft designer to use special alloys and it has raised the level of design stresses well beyond the proportional limit, into the inelastic range. This combination of circumstances has made it necessary to abandon many of the formulas and methods that were satisfactory for heavier types of construction.

The search for more rational methods leads the investigator backward, chronologically, to the year 1757, when Leonhard Euler published his famous treatise on the strength of columns. The following quotation is taken from a translation [2] of the Euler paper by J. A. Van den Broek, M. ASCE:

> "To begin with I should indicate that this moment is not limited to elastic bodies, among which we have good reason to doubt that columns could be included. It concerns in essence a force by which any body resists a change in curvature, and it is totally immaterial whether such a body after

Note.—Published in June, 1949, *Proceedings*. Positions and titles given are those in effect when the paper or discussion was received for publication.

[1] Consultant, The Rand Corp., Santa Monica, Calif.; Lecturer, Univ. of California, Los Angeles, Calif.

[2] "On the Strength of Columns," by Leonhard Euler, translation by J. A. Van den Broek, *American Journal of Physics*, July–August, 1947, p. 315.

flexure is endowed with a force to re-establish its original shape or not. For this reason we might preferably designate this moment as stiffness moment (*moment de roideur*) because it occurs in all bodies that resist flexure, whether they are elastic or not."

The "moment" to which Euler referred was designated by him as $E\,k\,k$, the product of the modulus of elasticity and the square of the shape parameter. Today the product of E and the moment of inertia I replaces $E\,k\,k$ in the Euler formula.

The foregoing quotation shows that Euler did not intend to restrict his formula to the elastic range. Because Young's modulus and the tangent modulus were unknown in Euler's time, he could not have been more specific; but he left the door wide open for a general interpretation of the term E.

Since E is usually considered to be a constant (up to a certain stress), Euler's formula is restricted to the elastic range. In 1889, F. Engesser published a paper[3] in which he suggested that E be considered as the slope of the compressive stress-strain diagram, commonly called the "tangent modulus." (In a letter to the writer, Theodor von Kármán, M. ASCE, noted that he had independently made a similar suggestion in an early paper written in Hungarian). Several investigators later pointed out that this theory would not account for the fact that, when the strains are decreasing on one side of the column, during bending, the stresses will decrease at a rate given by the elastic modulus, E. In 1909, Mr. von Kármán[4] made a thorough analysis of column action and performed some very careful experiments, by which the double-modulus (or reduced modulus) theory was apparently substantiated.

The writer has shown[5,6] that the tangent-modulus theory is actually correct for predicting the load at which buckling of a perfect column will begin and that the double-modulus theory gives the upper limit for the load as the bending increases. Mr. von Kármán's own interpretation is clearly indicated by the following excerpts from his discussion of one of the writer's papers:[7]

"* * * the first equilibrium bifurcation from the straight equilibrium configuration occurs at a load given by the Euler formula when the Young's modulus is replaced by the tangent modulus. * * * The definition of the stability limit must be revised for nonreversible processes. * * * Although the Euler formula with the tangent modulus does not, in general, give the maximum axial load to which the column can be subjected without large deflection, it is conservative and therefore advisable to use this formula for practical computation of column loads. As I have shown in my paper of 1909, also the load deflection curve that starts from the upper limiting load in general soon assumes a negative slope. Consequently, it is difficult to determine the actual peak of the axial load. It will certainly be between the two values that correspond to the tangent and the reduced moduli. These two values can be respectively designated as the lower and upper limits of the critical load."

---

[3] *Zeitschrift fur Architektur und Ingenieurwesen*, 1889.

[4] "Untersuchungen über Knickfestigkeit," by Theodor von Kármán, *Forschungsarbeiten No. 81*, Berlin, 1910.

[5] "The Column Paradox," by F. R. Shanley, *Journal of the Aeronautical Sciences*, December, 1946, p. 678.

[6] "Inelastic Column Theory," by F. R. Shanley, *ibid.*, May, 1947, p. 261.

[7] *Ibid.*, p. 267.

The generalized Euler formula (which should perhaps be designated the Euler-Engesser formula) may now be written as

$$P = \frac{\pi^2 E_t I}{L^2} \quad \ldots\ldots\ldots\ldots\ldots\ldots\ldots\ldots (1)$$

in which P is an axial load on the column; E_t is the tangent modulus; and L is the length for a column with pinned ends. (The effects of end restraint are discussed in Section 8.)

To obtain the average axial stress f corresponding to the load P, Eq. 1 is divided by the cross-sectional area:

$$f = \frac{P}{A} = \frac{\pi^2 E_t I}{L^2 A} = \frac{\pi^2 E_t}{(L/\rho)^2} \quad \ldots\ldots\ldots\ldots\ldots\ldots\ldots\ldots (2)$$

in which $\rho^2 = I/A$ defines the least radius of gyration.

The following statement may be used as a basis for further discussion: The generalized Euler equation gives the load at which a perfect column will begin to bend.

The word "perfect" is used to describe a hypothetical centrally loaded straight column of uniform cross section and homogeneous material properties. It should be noted, too, that only primary bending failure is involved, not the bending that would result from a local instability failure. The statement takes care of another point that has sometimes caused confusion. It is well known that, in the elastic range, the buckling load is not a constant but increases with increasing deflection. In fact, for very large deflections the load required to maintain equilibrium may be considerably greater than the Euler load. In the inelastic range, too, it is possible for the column load to exceed the load given by the tangent-modulus formula, as previously noted. In both these cases, however, the generalized Euler formula is correct for predicting the load at which bending (or buckling) begins.

There are now two questions to answer:

(*a*) Shall the theoretical load at which bending of a perfect column begins be taken as the upper limit for structural design?

(*b*) How is this load further reduced by various imperfections that may exist in the actual structure?

It should not be difficult to agree on the answer to the first question. In the elastic range the column load will not exceed the Euler value by any appreciable amount until the bending deflection becomes quite large.[8] In the inelastic range the increase beyond the Euler value will depend on the variation of the tangent modulus with increasing stress. In the highly curved region of the stress-strain diagram (sometimes termed the knee) the tangent modulus drops very rapidly with increasing stress (shown subsequently in Fig. 5); consequently very little increase in load would be obtained. In the so-called plastic range, beyond the knee of the diagram, the tangent modulus usually has a relatively low value and does not change rapidly with increasing strain. The

[8] "An Introduction to the Theory of Elasticity," by R. V. Southwell, Oxford Univ. Press, Oxford, England, 2d. Ed., p. 434, Fig. 114.

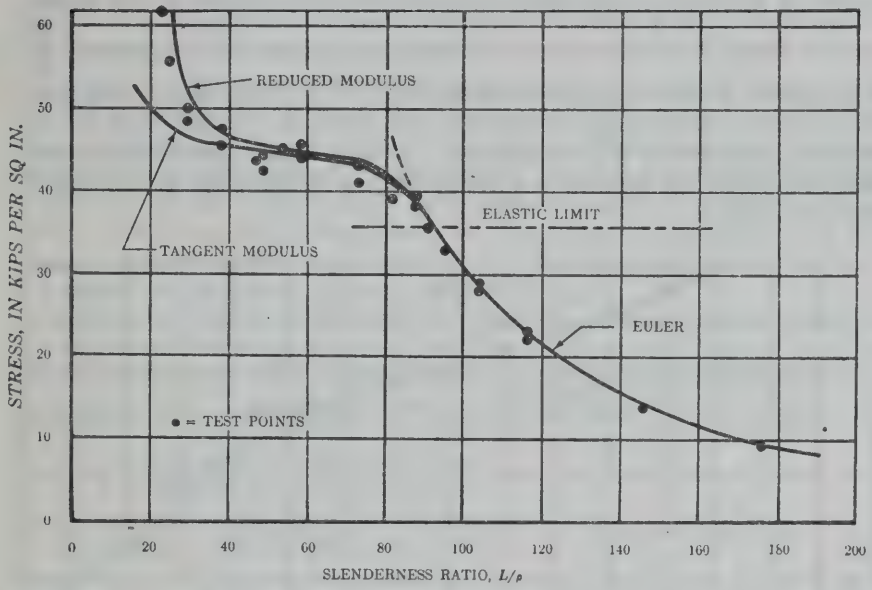

FIG. 1.—RECTANGULAR STEEL BAR WITH KNIFE-EDGE ENDS (THE ABBREVIATION "KSI" DENOTES KIPS PER SQUARE INCH—THAT IS, THOUSAND POUNDS PER SQUARE INCH)

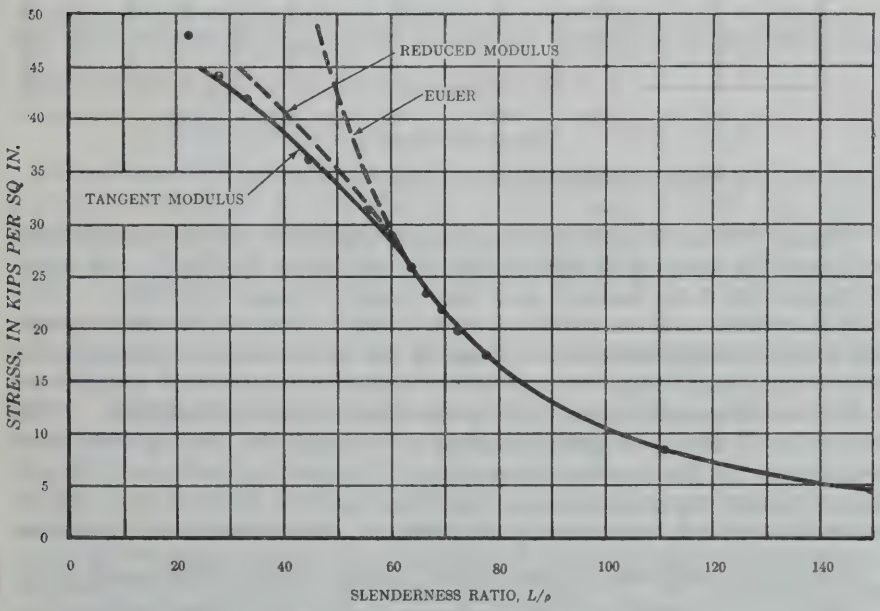

FIG. 2.—SQUARE ALUMINUM ALLOY COLUMN WITH SPHERICAL ENDS (24ST ¼ IN.)

maximum column load will therefore approach that predicted by the double-modulus theory,[9] which permits a relatively large increase for low values of $\frac{E_t}{E}$. It is doubtful whether any structural engineer would wish to take advantage of this factor in actual design, because in this region an increase in stress will involve a large amount of permanent set. It seems logical, therefore, to regard the beginning of the bending in a perfect column as the upper limit for structural purposes.

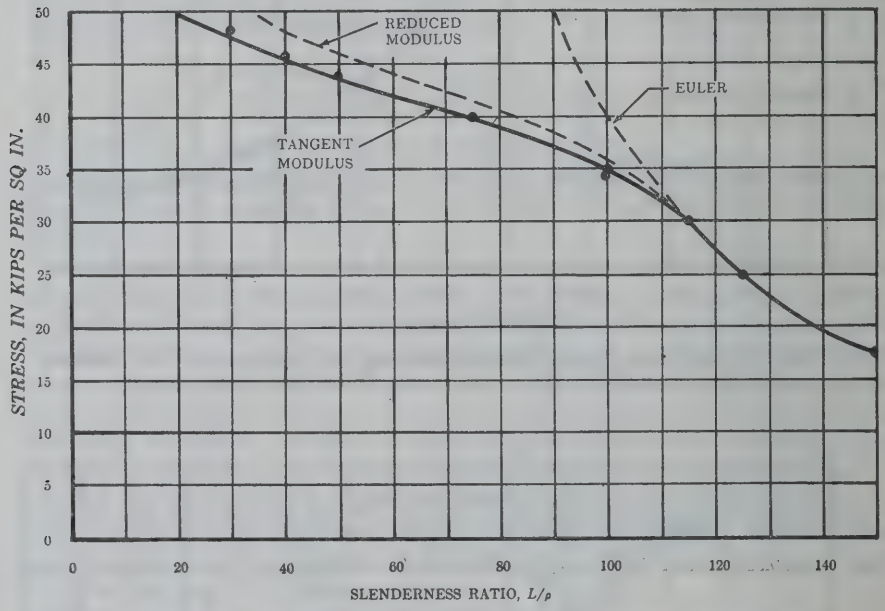

Fig. 3.—Solid Round Aluminum (17ST) Alloy Rod, with Flat Ends; Diameter 0.282 In.

Figs. 1,[4] 2,[10] and 3[11] show how test data compare with the generalized Euler equation. As denoted by the caption, the specimens for Fig. 1[4] were steel, of rectangular cross section, and were loaded through knife-edges. (The tangent-modulus column curve has been added.) The test points approach the double-modulus curves more closely in the region that lies well above the proportional limit. Mr. Van den Broek's tests[10] were made with square bars of 24ST aluminum alloy (see Fig. 2), using spherical steel loading blocks. (The symbol 24ST denotes a trade designation by which the alloy is commonly recognized. In the drawings, stresses are abbreviated ksi for kips—or thousands of pounds—per square inch, and psi for pounds per square inch.) Fig. 3[11] shows the results of tests made by the Research Laboratories of the Aluminum

[9] "The Double-Modulus Theory of Column Action," by William R. Osgood, *Civil Engineering*, March, 1935, p. 174, Fig. 2.

[10] "Column Formula for Materials of Variable Modulus," by J. A. Van den Broek, *The Engineering Journal*, December, 1945, p. 772.

[11] "Column Strength of Various Aluminum Alloys," by R. L. Templin, R. G. Sturm, E. C. Hartmann, and M. Holt, *Technical Paper No. 1*, Aluminum Research Laboratories, Pittsburgh, Pa., 1938.

Company of America, in Pittsburgh, Pa. The specimens were 17ST aluminum alloy of round cross section and were tested with flat ends (in these tests a fixity coefficient of 4 was developed).

It would be possible to devote the remainder of this paper to the reproduction of test data that show excellent agreement with the generalized Euler theory. Figs. 1, 2, and 3, however, should be sufficient evidence that the theory can be substantiated experimentally. In fact, it is doubtful whether any other structural theory could be verified so accurately by tests covering such a wide range of variables (materials, shape, method of loading, and end fixity). Even the departure of the test points from the tangent-modulus curve is predicted by the theory, as explained previously.

Although it may be agreed that the generalized Euler equation represents the upper limit for column strength, the engineer will very properly raise the second question, previously noted, regarding the reduction in strength caused by imperfections. The major imperfections may be classified as follows:

(*a*) Variations in material properties;
(*b*) Eccentricity of load application;
(*c*) Initial crookedness of the column; and
(*d*) Effects of end conditions:

Items (*b*) and (*c*) are usually classed together, since their effects are very similar. The effect of end conditions should probably be regarded as a separate problem, not as a type of imperfection. The difficulty in this case is the calculation of the degree of end restraint in actual structures.

Before these subjects are considered, it will be helpful to review some of the methods that are used in the engineering application of the generalized Euler theory.

2. Engineering Application of the Column Theory

To one who has not actually tried to use the tangent modulus in the Euler equation the lack of a formula that can be solved on a slide rule may appear to be a disadvantage. Actually, however, the entire column curve for a given material can be obtained in a few minutes, directly from the stress-strain diagram. The slope at various stress values is obtained by a straightedge.[12] These values of the tangent modulus may then be used, together with the corresponding stresses, to solve Eq. 3 (presented subsequently) for the slenderness ratio. It is interesting to plot the values of the tangent modulus against stress. This method will aid in obtaining a smooth curve and will also reveal how the stiffness of the material decreases as the stress is increased. Mr. von Kármán followed this procedure[4] in obtaining the column curve shown in Fig. 1. The curve presented by Mr. von Kármán is reproduced as Fig. 4. The reduced modulus is also shown in Fig. 4. It is important to note that the difference between the tangent modulus and the reduced modulus does not cause a very large reduction in stress on the column curve (Fig. 1). The reason for this

[12] "Compressive Stress-Strain Properties of Some Aircraft Materials," by P. E. Sandorff and R. K. Dillon, *Proceedings*, A.S.T.M., Vol. 46, 1946, pp. 1039–1052.

can be noted by writing Eq. 2 as follows:

$$\frac{L}{\rho} = \pi \sqrt{\frac{E_t}{f}} \quad \ldots\ldots\ldots\ldots\ldots\ldots\ldots\ldots\ldots\ldots (3)$$

At a given stress, a change in the value of the modulus will simply displace the column curve to the left or right, and then only by the square root of the ratio involved. For stress-strain diagrams with a relatively sharp knee, the difference between the two theories is almost negligible, over the range of slenderness ratios used in design.

Fig. 5 shows the tangent-modulus curves for several materials. The column curves derived from these curves are shown in Fig. 6. It is quite evident that the shape of the column curve may vary widely between different

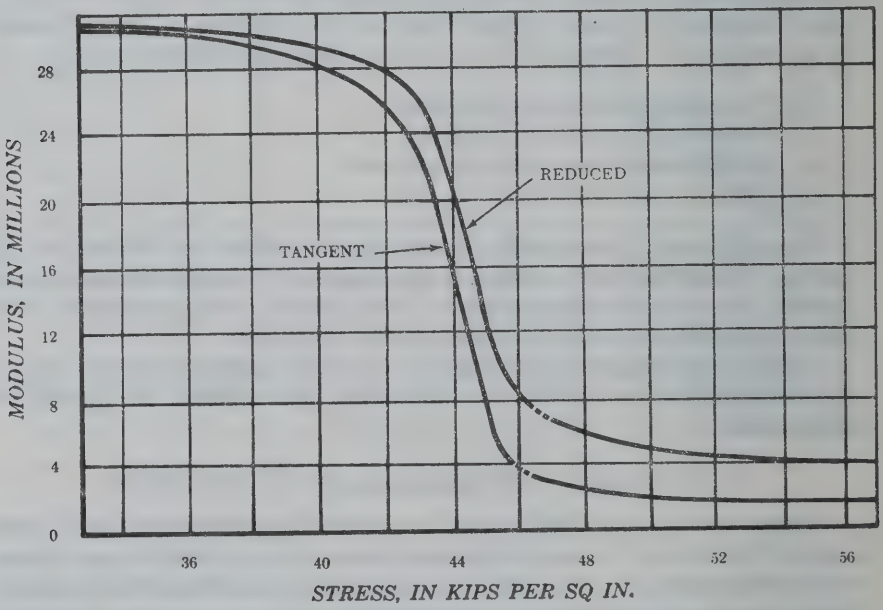

Fig. 4.—Relation Between Tangent Modulus and Stress

materials. With such an array of curves to be fitted, it is no wonder that engineers have used so many different types of empirical formulas for the "short-column" range.

One of the very practical advantages of the tangent-modulus method is that there is no need to define the "short column." One formula covers the entire range and it is impossible to make the mistake of using the wrong formula. It would be well to abandon the term "short column."

Some of the other engineering advantages of the generalized Euler equation will become apparent in the discussion of material variations and fixity effects. Before considering these questions, however, two very useful engineering tools will be discussed: The mathematical stress-strain diagram and the nondimensional column curve.

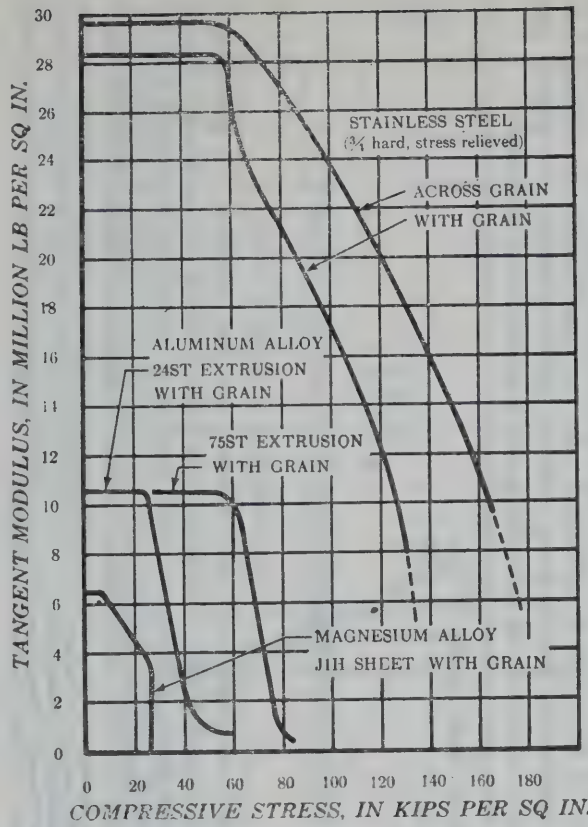

FIG. 5.—TANGENT-MODULUS CURVES FOR VARIOUS MATERIALS

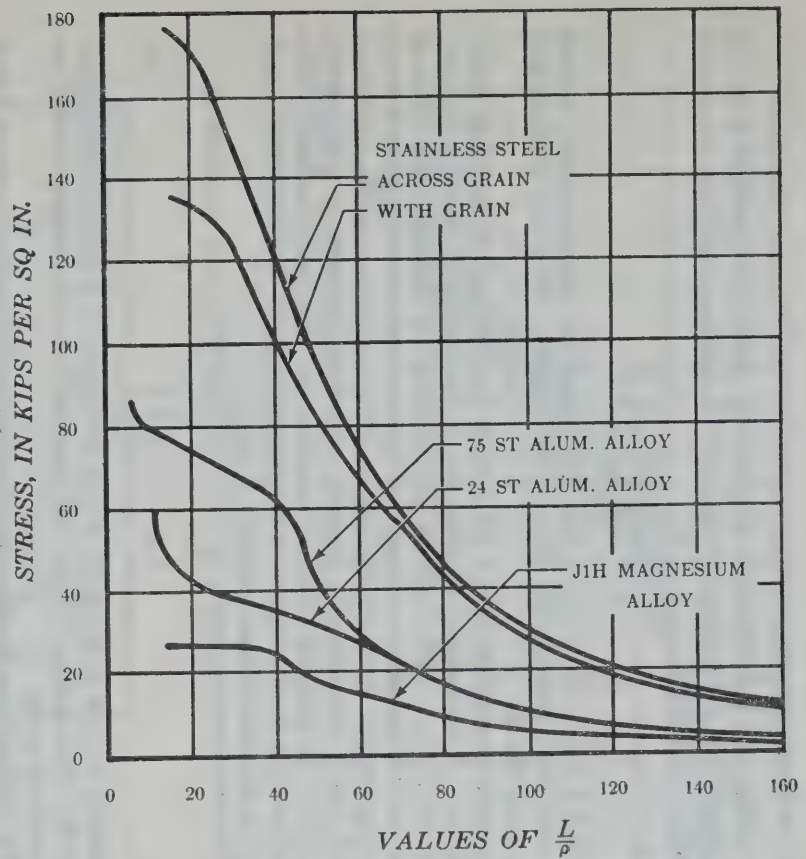

FIG. 6.—GENERALIZED EULER CURVES FOR VARIOUS MATERIALS

3. Mathematical Determination of the Tangent Modulus

W. Ramberg and William R. Osgood,[13] M. ASCE, have provided a method of expressing the stress-strain diagram by an equation which has the general form:

$$\epsilon = \frac{f}{E} + K\left(\frac{f}{E}\right)^n \quad \ldots\ldots\ldots\ldots\ldots\ldots\ldots\ldots (4)$$

in which ϵ is a strain; E is the modulus of elasticity (slope at origin); n is an exponent which controls the shape of the diagram; and K is a constant (see note under Eq. 5).

If the constants are known, the tangent modulus may be found by differentiation. A more general solution may be obtained by writing Eq. 4 in nondimensional form—which may be accomplished by dividing every value of stress, on the stress-strain diagram, by a base stress and every value of strain by a base strain. The base stress, f_o, is approximately equal to the yield stress (0.002) but is determined by drawing a line from the origin at a slope equal to 0.7 E. The resultant stress is designated the "secant yield stress." (The secant method is used because it is nondimensional.) The base strain, ϵ_o, is taken as the strain corresponding to E and f_o.

The stress-strain equation, in nondimensional form, may be written as

$$\frac{\epsilon}{\epsilon_o} = \frac{f}{f_o} + \frac{3}{7}\left(\frac{f}{f_o}\right)^n \quad \ldots\ldots\ldots\ldots\ldots\ldots\ldots\ldots (5)$$

in which $\epsilon_o = f_o/E$; and f_o is the secant yield stress for a secant modulus equal to 0.7 E. The constant 3/7 in Eq. 5 results from the selection of 0.7 E for the secant modulus.

Fig. 7 shows[13] the nondimensional stress-strain diagrams for various values of n. It is possible to determine n for an actual diagram by plotting it in nondimensional form on such a chart. Messrs. Ramberg and Osgood also present[13] a formula for determining n by a second secant yield stress.

The equation for the tangent modulus, in nondimensional form, may be obtained from Eq. 5:

$$\frac{E_t}{E} = \frac{1}{1 + \frac{3}{7}n\left(\frac{f}{f_o}\right)^{n-1}} \quad \ldots\ldots\ldots\ldots\ldots\ldots\ldots\ldots (6)$$

Curves representing this equation are reproduced in Fig. 8.[13]

4. Nondimensional Column Curves

The nondimensional column curve was first presented (to the writer's knowledge) in 1929.[14] Sometime later it was included in a handbook[15] printed by the federal government which establishes the allowable stresses used by

[13] "Description of Stress-Strain Curves by Three Parameters," by W. Ramberg and William R. Osgood, *Technical Note No. 902*, National Advisory Committee for Aeronautics, Washington, D. C., July, 1943.

[14] "Strength of Tubing Under Combined Axial and Transverse Loading," by L. B. Tuckerman, S. N. Petrenko, and C. D. Johnson, *Technical Note No. 307*, National Advisory Committee for Aeronautics, Washington, D. C., June, 1929.

[15] "Strength of Metal Aircraft Elements," *ANC-5*, Army-Navy-Civil Committee on Aircraft Design Criteria, U. S. Govt. Printing Office, Washington, D. C., 1942.

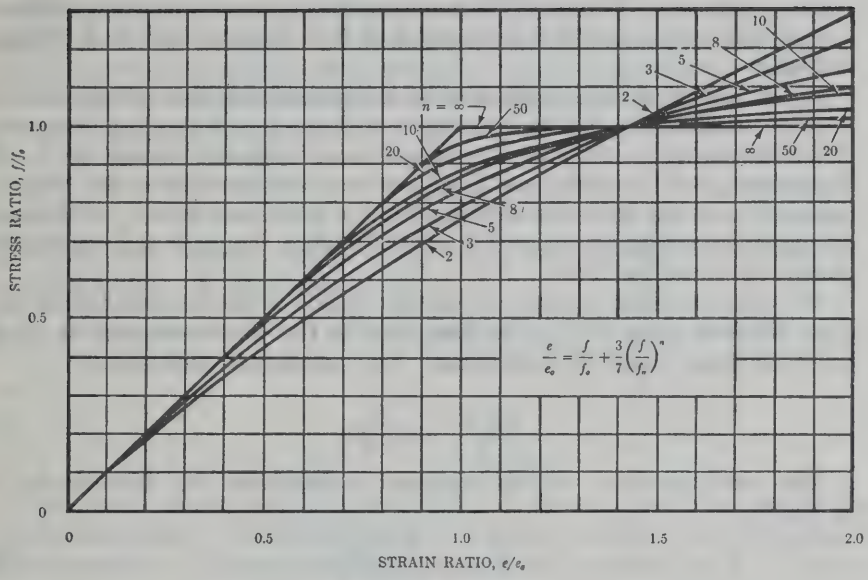

FIG. 7.—NONDIMENSIONAL STRESS-STRAIN DIAGRAMS

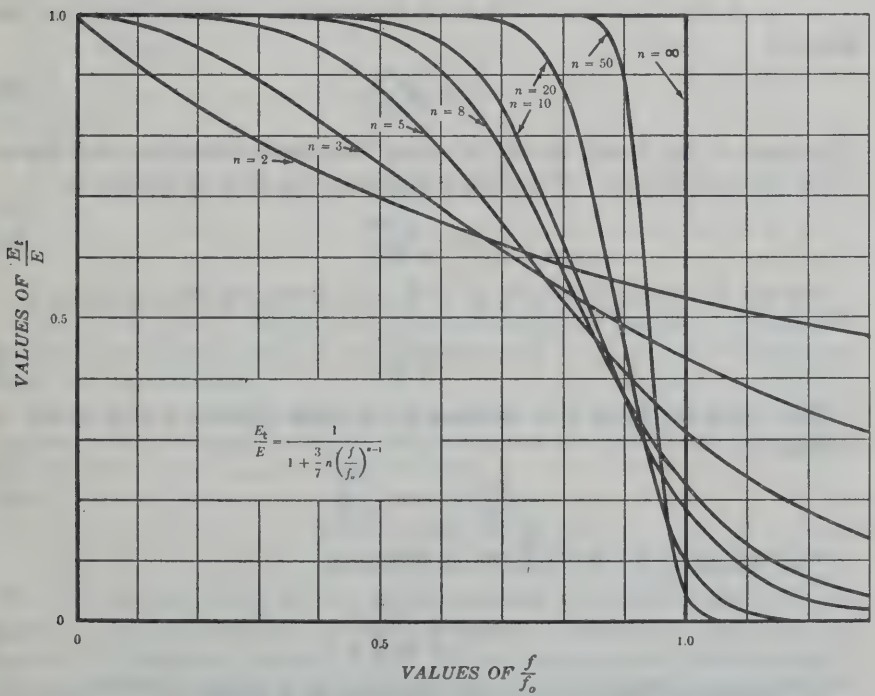

FIG. 8.—NONDIMENSIONAL TANGENT-MODULUS CURVES

airplane designers. The use of the nondimensional column curve in connection with aircraft stress analysis was described by F. P. Cozzone and M. A. Melcon in 1946.[16]

To reduce the column stress curve to nondimensional form, every point on the curve must be divided by a base value of stress, f_o, and also by a base value of slenderness ratio, $(L/\rho)_o$. The stress value originally chosen by L. B. Tuckerman, S. N. Petrenko, and C. D. Johnson[14] corresponded to the "column intercept" and was approximately equal to the 0.002 yield stress. If the nondimensional stress-strain diagram is used as a basis, the value of f_o will be the same as that used for Eq. 5.

To make the Euler (elastic) curves all coincide on the nondimensional diagram, the base value of $(L/\rho)_o$ is determined as the slenderness ratio at which the Euler stress equals the base stress. The equation for this point is

$$f_o = \pi^2 \frac{E}{(L/\rho)^2_o} \quad \ldots\ldots (7)$$

The nondimensional column equation is determined by dividing Eq. 2 by Eq. 7:

$$\frac{f}{f_o} = \frac{E_t/E}{\left[\dfrac{L/\rho}{(L/\rho)_o}\right]^2} \quad \ldots\ldots (8)$$

Let

$$R_f = f/f_o \quad \ldots\ldots (9)$$

and

$$B = \frac{L/\rho}{(L/\rho)_o} \quad \ldots\ldots (10)$$

The terms in Eqs. 9 and 10 may be called the column stress ratio and the reduced slenderness ratio. The column equation may now be written as

$$R_f = \frac{E_t/E}{B^2} \quad \ldots\ldots (11)$$

For the Euler (elastic) curve, $E_t = E$, from which the Euler equation is

$$R_f = \frac{1}{B^2} \quad \ldots\ldots (12)$$

The value of $(L/\rho)_o$ is a constant for a given material and is found by solving Eq. 7:

$$\left(\frac{L}{\rho}\right)_o = \pi \sqrt{\frac{E}{f_o}} \quad \ldots\ldots (13)$$

The expression for B is sometimes written as

$$B = \frac{1}{\pi} \sqrt{\frac{f_o}{E}} \frac{L}{\rho} \quad \ldots\ldots (14)$$

[16] "Nondimensional Buckling Curves—Their Development and Application," by F. P. Cozzone and M. A. Melcon, *Journal of the Aeronautical Sciences*, October, 1946, p. 511.

This form, however, conceals the physical significance of B. It is probably best to determine the constant $(L/\rho)_o$ for the material being investigated and then to use that value in Eq. 10 to determine B for any given slenderness ratio.

Messrs. Cozzone and Melcon[16] show that the curves of Fig. 8 may also be used for any type of buckling in which the equation has the form:

$$f = K \frac{E_t}{(a/b)^2} \quad \ldots\ldots (15)$$

in which K is a constant; and a and b are the two dimensions that affect the buckling stress. In this more general form,

$$B = \frac{a/b}{(a/b)_o} \quad \ldots\ldots (16)$$

and

$$\left(\frac{a}{b}\right)_o = \sqrt{K \frac{E}{f_o}} \quad \ldots\ldots (17)$$

The nondimensional column curve may be derived equally well from the load-length curves. Thus, test data can be plotted directly in nondimensional form, if desired. The column load, P, is divided by the base load, P_o, in which

$$P_o = f_o A \quad \ldots\ldots (18)$$

The effective column length, L, is divided by the base length, L_o:

$$L_o = \pi \sqrt{\frac{E I}{P_o}} \quad \ldots\ldots (19)$$

Then

$$R_f = \frac{P}{P_o} \quad \ldots\ldots (20)$$

and

$$B = \frac{L}{L_o} \quad \ldots\ldots (21)$$

Using Eqs. 18 to 21, any nondimensional column curve may be transformed directly into a design curve of load versus length, for a member of given material and cross section.

To express the nondimensional column curves in mathematical form it is necessary only to insert in Eq. 11 the expression for E_t/E from Eq. 6. The generalized column equation then becomes:

$$R_f + \frac{3}{7} n (R_f)^n = \frac{1}{B^2} \quad \ldots\ldots (22)$$

Eq. 22 is plotted in Fig. 9,[16] revealing a number of interesting points. The effects of varying the shape of the stress-strain diagram (by varying n) are greatest in the region where $B = 1.0$. Thus, it is apparent that the shape of the stress-strain diagram near the knee will have a relatively large influence on the column stress in this region.

5. The Envelope Equation

Fig. 9 shows that there is an envelope curve representing the minimum values of column stress. The equation for this envelope may be obtained from Eq. 22:

$$R_f = e^{-1/n} \quad \ldots\ldots (23)$$

from which

$$n = -\frac{1}{\log_e R_f} \quad \ldots\ldots (24)$$

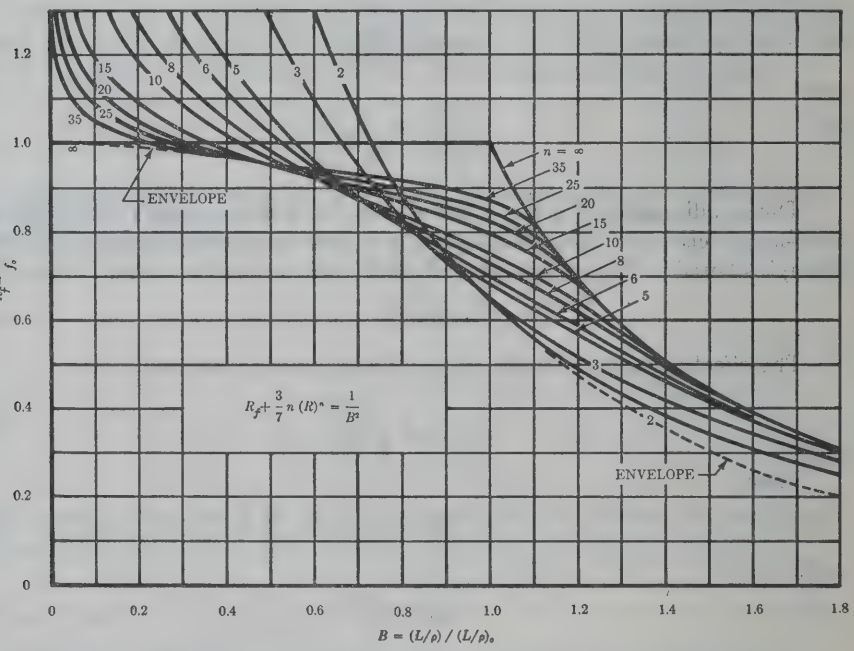

Fig. 9.—Nondimensional Tangent-Modulus Column Curves

Substituting the value of n in Eq. 24 into Eq. 22 gives the equation of the envelope curve:

$$R_f - \frac{3}{7} \frac{1}{e \log_e R_f} = \frac{1}{B^2} \quad \ldots\ldots (25)$$

Eq. 25 is based on the tangent-modulus theory, but it does not involve the tangent modulus; in fact, the only two material properties that enter into Eq. 25 are E (Young's modulus) and f_o (the secant yield stress). The physical significance of Eq. 25 is evident from Fig. 10. Together with the Euler curve, Eq. 25 bounds a region which encloses the column curves for all mathematical stress-strain diagrams (that is, all diagrams expressed by Eq. 22) that can be passed through the shaded area of Fig. 10(*a*); and it covers all positive values of n in Eq. 22.

Eq. 25 would be too conservative for most design purposes (at least for aircraft) since it does not permit the designer to take full advantage of available knowledge on the shape of the stress-strain diagram. Where weight saving is not too important, however, Eq. 25 could be used as a kind of over-all column curve for any material. It would then only be necessary to know the secant yield stress (the stress at which a line having a slope of 0.7 E cuts the stress-strain diagram) and the modulus of elasticity E.

The resemblance of the envelope curve to a parabola shows why parabolic curves have been found useful in representing the "short column" range. The relationship of various other column formulas is shown in Fig. 11. The equations of these formulas, in nondimensional form, are: Parabolic formula (exponent = 2):

$$R_f = 1 - \frac{B^2}{4} \quad \ldots\ldots (26)$$

straight line formula (intercept at $R_f = 1.0$):

$$R_f = 1 - 0.385\,B \quad \ldots\ldots (27)$$

Gordon-Rankine formula (with Ritter's constant):

$$R_f = \frac{1}{1 + B^2} \quad \ldots\ldots (28)$$

and Van den Broek formula:[17]

$$R_f = \sqrt{1 + \left(\frac{B^2}{2}\right)^2} - \frac{B^2}{2} \quad \ldots\ldots (29)$$

As a whole, the various empirical formulas form a "scatter band," as shown in Fig. 11.

6. Effects of Material Variations

From the discussion of nondimensional column formulas, it is obvious that the three primary material variables are the initial modulus of elasticity E, the secant yield stress f_o, and the shape of the knee of the stress-strain diagram (indicated by n).

It is unnecessary to consider E, as far as variations between lots of material are concerned. From an engineering point of view E can usually be regarded as constant for a given material or alloy and at a given temperature.

The secant yield stress based on 0.7 E is approximately equal to the conventional (0.002) yield stress.[13] For material-correction purposes either type of yield stress may be used. In general terms it can be stated that the compressive yield stress controls the height of the left end of the column curve. In the nondimensional form this stress controls the value by which all the ordinates of the diagram are multiplied. Therefore, it is the most important property, as far as material variations are concerned.

The specifications for structural materials to be used in compression should contain a minimum value for the compressive yield stress. The tensile yield

[17] "Theory of Limit Design," by J. A. Van den Broek, John Wiley & Sons, Inc., New York, N. Y., 1948, p. 103, formula IX.

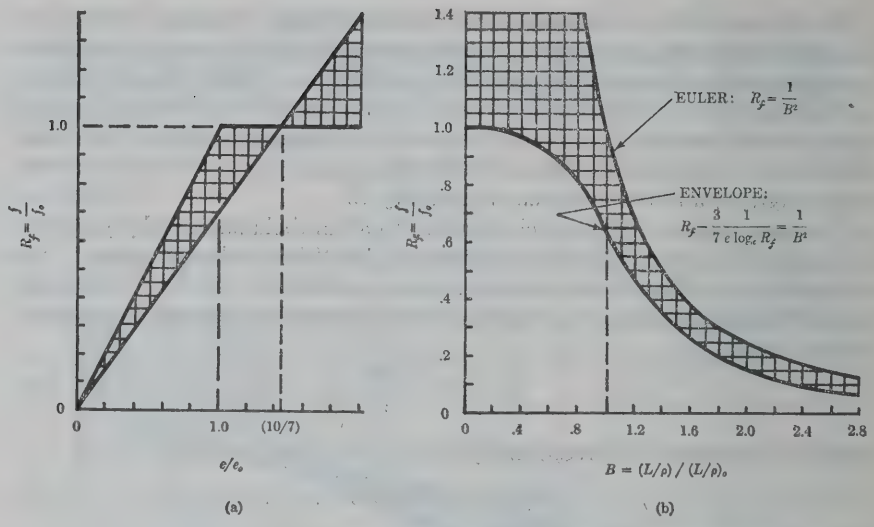

FIG. 10.—THE ENVELOPE COLUMN CURVE

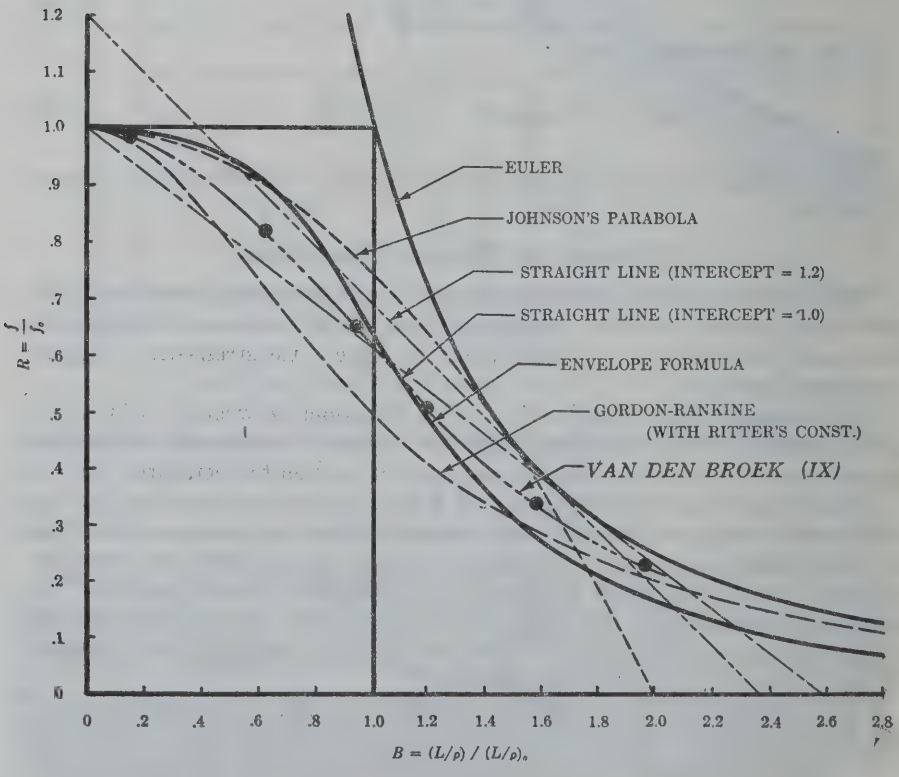

FIG. 11.—COMPARISON OF COLUMN FORMULAS IN NONDIMENSIONAL FORM

stress is sometimes a reasonably good substitute since the yield stresses in tension and compression are nearly the same, but this assumption can be misleading. Certain types of magnesium alloy show considerably lower yield stresses in compression than in tension. The "grain" (direction of rolling) may also have a pronounced influence (see Fig. 6). Most aluminum alloy sheet is straightened by stretching, which raises the tensile yield stress in one direction and raises the compressive yield stress in the other (cross grain).

To be entirely safe, it would be necessary to select, as a basis for the design column curve, the lowest probable value of compressive yield stress and the "flattest" type of diagram likely to be obtained (minimum values for f_o and n, when the stress-strain diagram is expressed mathematically). This procedure would take care of all material variations. (Theoretically the curve should be obtained from the two limiting values of n, with the envelope curve in between.)

In aircraft work many compression tests are performed to obtain allowable stresses for complicated types of construction. The results of such tests must be "reduced to standard," or to minimum specified values. Several methods are available, but the most logical is that using the nondimensional column curve. All test data may be divided by the constants corresponding to the test material, to obtain the nondimensional diagram. To convert back to "standard," the nondimensional values are multiplied by the constants for the standard material.

Fig. 12 shows a family of column curves for a high-strength aluminum alloy. The effects of varying the yield stress have been determined by the nondimensional system, assuming that the stress-strain diagrams remain affine (that is, that n does not vary).

Curves of this type may be used directly for "correcting" from one yield stress to another, as indicated in Fig. 12. Such curves may also be used directly for any type of buckling in which failure occurs by bending in one plane only, even though L/ρ is not the proper geometrical ratio. (This procedure is similar to the use of B for various types of buckling, as discussed in Section 4.)

7. The Effects of Eccentricity

The theories and formulas that have been discussed are all based on the conception of a perfectly straight, centrally loaded column. Since no actual column can fully meet this requirement, engineers have long been interested in the effects of eccentric loading. There is a definite need, also, for a sound method of design for columns that have design eccentricities of considerable magnitude. This problem therefore has two distinct phases: (*a*) The effects of small "incidental" eccentricities, and (*b*) the design of columns with known eccentricities.

For the design of columns that are nominally straight, it is customary and logical to consider small degrees of crookedness as equivalent to a certain initial eccentricity. There has been much discussion of the proper value to use for the equivalent eccentricity in actual design work, but obviously this problem comes under the heading of "tolerances" and must be controlled by the same processes that are used to control other tolerances in manufacture. It will be

assumed, therefore, that the designer either controls this variable by suitable specifications, shop practices, etc., or estimates a maximum value that is compatible with the kind of structures with which he is dealing. The question then becomes, is it necessary to make a further reduction in the column strength to account for the maximum probable equivalent eccentricity?

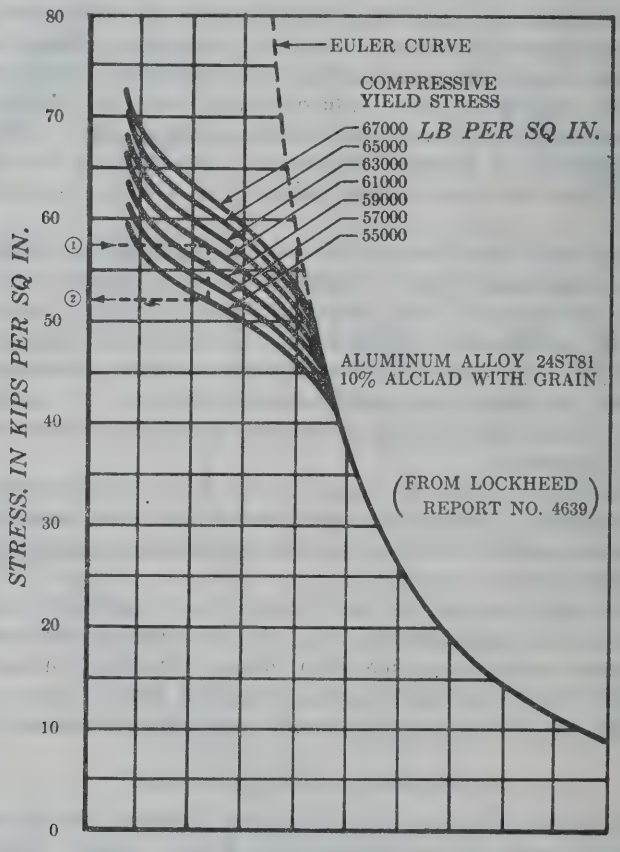

FIG. 12.—METHOD OF CORRECTING TEST DATA FOR YIELD STRESS

Before this question can be answered it is necessary to have a method of determining the effects of eccentricity. For the design of elastic members the answer is simple—use the secant formula. This well-known formula gives the maximum fiber stress that will be produced by a definite load (or average stress) in the column, provided that the stresses stay within the elastic range. If certain values are chosen for the eccentricity and the maximum permissible stress, the equation becomes a column formula.

For a material which has a very pronounced yield point, and a "flat-topped" stress-strain diagram, the secant formula can be used by substituting the yield stress for the maximum permissible stress. (It is still necessary to specify the

eccentricity, however.) For materials that do not exhibit this characteristic it is impossible to select a single value of maximum stress that will make the formula fit the test data. Furthermore, the shape of the secant column curve will have no relation to the shape determined by the tangent-modulus theory for zero eccentricity; yet it is obvious that the eccentric column curve must approach the basic column curve as the eccentricity approaches zero. Because of these shortcomings, the secant column formula cannot be considered as generally satisfactory.

The eccentric column was treated very thoroughly by Mr. von Kármán, in 1910.[4] He showed that, in the elastic range, initial eccentricity simply causes a constantly increasing lateral deflection as the axial load is increased. The curves are asymptotic to the Euler load, which therefore represents the maximum load for the eccentric elastic column. (This theory neglects the further increase in load at large deflections, previously discussed.)

For the inelastic case, Mr. von Kármán showed that increased eccentricity causes greater bending strains (for the same axial load), which force some of the material farther into the inelastic region of the stress-strain diagram. Thus, a lower value of effective modulus of elasticity is obtained. During loading, a point is finally reached where the internal resisting moment does not increase as rapidly as does the external moment. The external load must then decrease to maintain equilibrium. The maximum load reached in this process will depend on the slenderness ratio, the degree of initial eccentricity, the shape of the stress-strain curve, and the shape of the cross section.

This problem is extremely complex. Mr. von Kármán solved it for a particular material (steel) and cross section (rectangular) using the double-modulus theory to determine the internal resisting moment. Graphical integration methods were used. The resulting curves have been reproduced in many textbooks, but the exact solution has never been improved on, to the writer's knowledge. In fact, the recent discovery that the double-modulus theory (which Mr. von Kármán used) is not strictly accurate for small deflections further complicates the situation.

Mr. Van den Broek[10] has developed a formula for predicting the maximum load of the eccentric column. He assumes, in effect, that the stress-strain diagram becomes substantially flat at some known value of stress and that the column has bent to a point where opposite edges are working in these flat regions, one in tension and one in compression. By making some simplified assumptions as to the shape of the deflection curve, he obtains a formula for the maximum load, for a column of rectangular cross section. For materials having a curved stress-strain diagram, the Van den Broek method has the same limitation as the secant formula—there is no good definition for the "upper yield stress."

K. Ježek[18] has developed an algebraic method based on a simplified stress-strain diagram composed of two straight lines, one horizontal. He obtains factors by which the concentric column values are divided. Thus, the errors caused by the original assumptions are reduced, but for materials that have a

[18] "Approximate Theory of Eccentrically Loaded Steel Columns," by K. Ježek, *Der Stahlbau*, Vol. 8, 1935.

gradually curving stress-strain diagram the error may still be considerable. (The writer is indebted to Friedrich Bleich, M. ASCE, for the information on the Ježek method.)

These examples indicate that the eccentric column, in the inelastic range, cannot be treated adequately by any simple engineering formula or theory. The reason for this may be that there are in reality two problems—(1) stability under axial loading and (2) failure in bending. The stability problem is complicated even for zero eccentricity, but it can be handled by the tangent-modulus theory. Failure in bending is in itself a large subject, involving both the shape of the cross section and the shape of the stress-strain diagram.

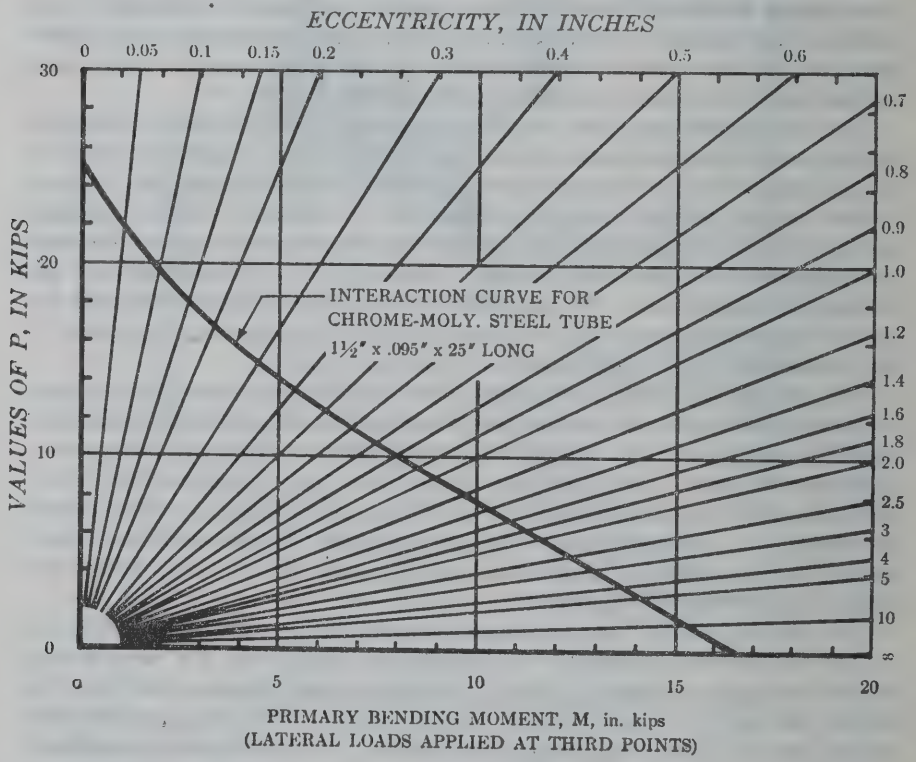

FIG. 13.—INTERACTION CURVE FOR COMBINED BENDING AND COMPRESSION

This situation is similar to one that existed about 1935, in aircraft structural analysis. There was no suitable formula for the strength of members subjected to combined bending and torsion. The solution was found in the interaction curve. This method has since become standard for handling many kinds of combined loading.[19]

Why not use the interaction curve to treat the eccentric column problem? The member can be regarded as being subjected to combined compression and bending, with the bending moment equal to $P\,e$ (e denoting eccentricity).

[19] "Basic Structures," by F. R. Shanley, John Wiley & Sons, Inc., New York, N. Y., 1944, Chapter 20 p. 340.

Interaction curves for combined bending and compression were obtained from tests of steel and aluminum alloy tubing by Messrs. Tuckerman, Petrenko, and Johnson.[14] In these tests the bending moment was applied by transverse loading at the third points, whereas in the eccentric column the bending moment must be considered as being applied at the ends of the member. Since the

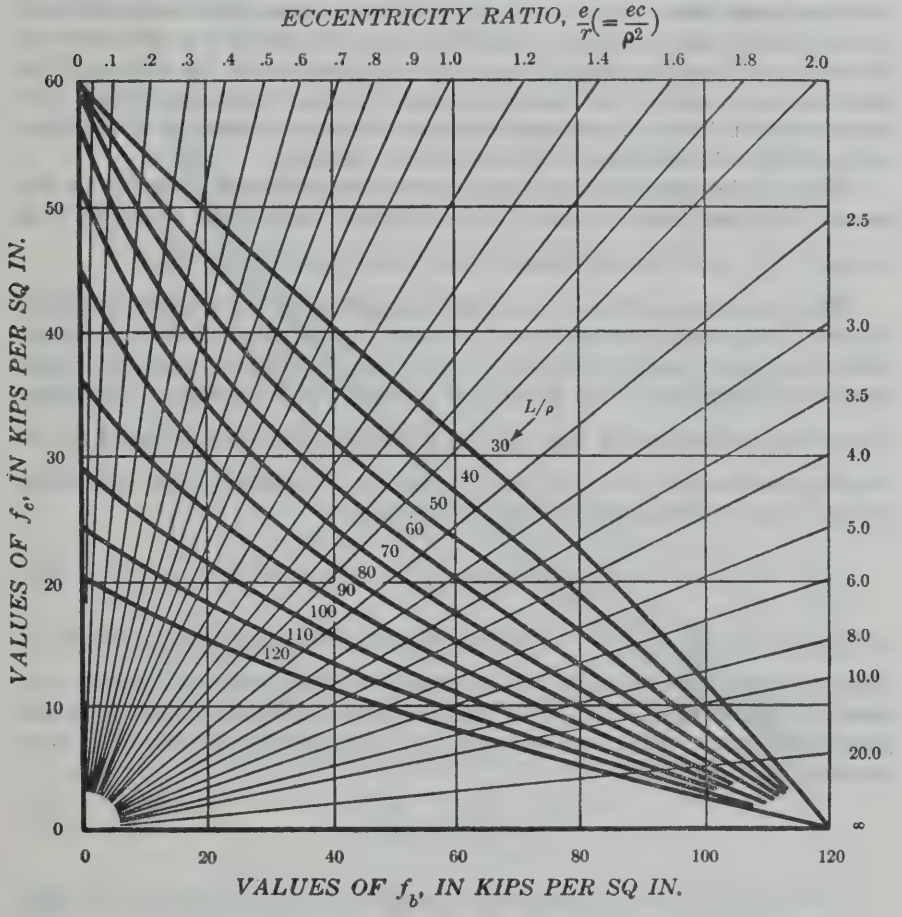

FIG. 14.—INTERACTION CURVES FOR CHROME-MOLYBDENUM STEEL TUBING

interaction curves for the two cases should be quite similar, the curves developed by Messrs. Tuckerman, Petrenko, and Johnson[14] will be used to illustrate the proposed method.

Fig. 13 shows a typical interaction curve for a single member under all possible combinations of axial compression and bending.[14] The two end points of the curve correspond to the column strength and to the ultimate bending moment, respectively. If it is assumed that the bending moment was applied at the ends of the member, as in an eccentric column test, the eccentricity (e)

is given by the ratio M/P. Straight lines of constant eccentricity therefore radiate from the origin, as shown in Fig. 13. The interaction curve may thus be used directly to determine the effects of eccentricity in axial loading.

Tests of different kinds and sizes of round tubing were made[14] and the results were plotted as interaction curves, both in terms of stress and in terms of stress ratios. Fig. 14 shows[14] that there is a family of curves for different values of the slenderness ratio. At low values of the slenderness ratio the curves tend to be straight, but at higher values there is a considerable sag (the result of the secondary bending moment caused by the deflection of the column). At zero bending stress the curves give a series of values that represent the concentric column curve; at zero axial stress the curves converge to a single value of f_b, which is the modulus of rupture for pure bending.

When the interaction curves are plotted in terms of stress, as in Fig. 14, the eccentricity lines denote values of the eccentricity ratio e/r, in which the core radius $r = \frac{\rho^2}{c}$; and c is the distance from neutral axis to outer fiber.

Fig. 14 may be converted to nondimensional form by either of two methods. Messrs. Tuckerman, Petrenko, and Johnson[14] divided the values of f_c by f_{co}, which was taken as the allowable stress for short columns (intercept value) and f_b was divided by f_{bo}, the modulus of rupture in pure bending. The resulting curves are like those of Fig. 14, with $\frac{L}{\rho}$-values replaced by values of B, the reduced slenderness ratio. For such a chart the eccentricity lines will define values of reduced eccentricity ratio, determined by

$$R_e = \frac{e}{e_o} \qquad (30)$$

in which $e_o = r\frac{f_{bo}}{f_{co}} = \frac{\rho^2}{c}\frac{f_{bo}}{f_{co}}$. To eliminate everything but the sag, divide all axial stresses by the concentric column stress for the member in question, instead of by the value of f_o. The following terms will then apply: f_{cr} is the allowable column stress for $e = 0$ and f_{bo} is the modulus of rupture in pure bending, and

$$R'_c = \frac{f_c}{f_{cr}}\left(= \frac{P}{P_{cr}}\right) \qquad (31)$$

$$R_b = \frac{f_b}{f_{bo}}\left(= \frac{M}{M_o}\right) \qquad (32)$$

$$R'_e = \frac{e}{e'_o} \qquad (33)$$

and

$$e'_o = \frac{\rho^2}{c}\frac{f_{bo}}{f_{cr}}\left(= \frac{M_o}{P_{cr}}\right) \qquad (34)$$

The terms in parentheses show that the ratios in Eqs. 31, 32, and 34 may all be expressed in terms of axial load and bending moment. Thus, test data may be converted directly into the nondimensional form. Conversely, the

nondimensional design charts may be used directly to find the allowable eccentric column load, if the load for the concentric column, and its ultimate bending moment, are known. The curves of Fig. 14 have been replotted in Fig. 15, in this reduced form. The actual slenderness ratio (L/ρ) has been retained, instead of the reduced slenderness ratio B. If B is used, the curves will be similar in shape; the eccentricity lines will remain unchanged.

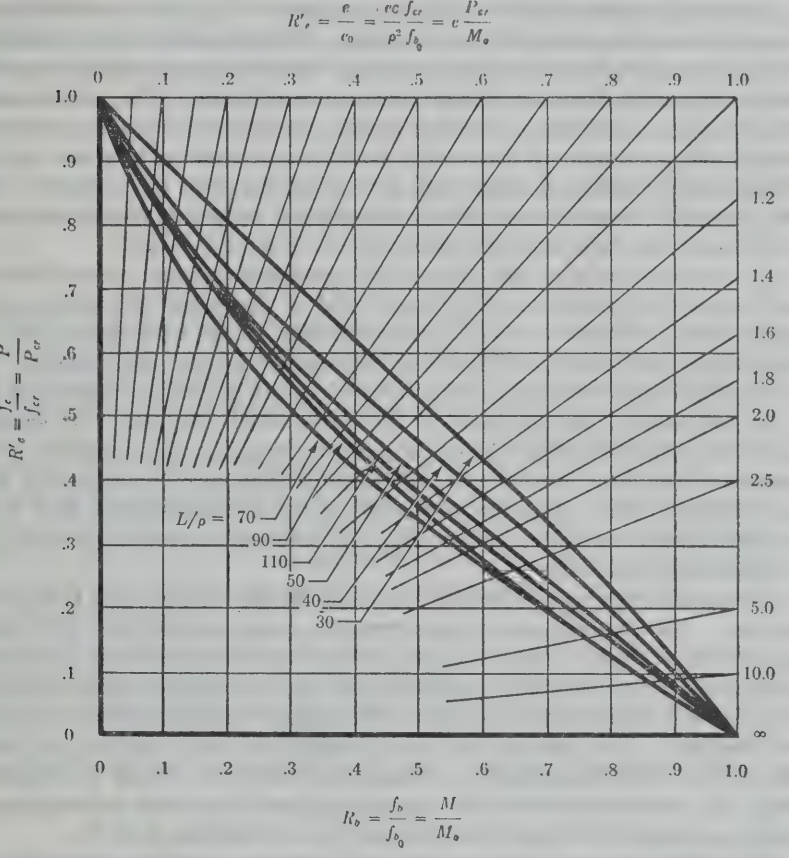

Fig. 15.—Reduced Interaction Curves for Combined Bending and Axial Loading

Fig. 15 indicates that the nondimensional interaction curves tend to lie within a definite band and that the amount of sag is a maximum for slenderness ratios in the region corresponding roughly to $L/\rho = 70$ (or to $B = 1.0$ to 1.2). At higher values of slenderness ratio, the interaction curves tend to become straighter again. If the bending moment had been applied at the ends of the member, the amount of sag would no doubt be greater.

Since the tests on which Figs. 14 and 15 are based did not truly represent the eccentric column, it would be unsafe to use them for design purposes, but they can be used to draw some interesting conclusions. One of the most valu-

able features of interaction curves is that their shape seems to be primarily a function of the kind of loading conditions involved and is little affected by other variables. Further research may indicate that a few sets of interaction curves, such as those shown in Fig. 15, could be used for a wide variety of columns. By using the reduced slenderness ratio B, it may be possible to show that the shape of the curves depends on the value of the exponent n for the nondimensional stress-strain diagram.

For small values of eccentricity the curves of Fig. 15 are converging and therefore must lie relatively close together. If the lowest curve is considered to apply for all values of slenderness ratio, the effect of eccentricity would be a reduction of all the column stresses by a constant factor. The nondimensional column curve would not be changed in this case; it would only be necessary to multiply R_e by a reduced value of f_o (or P_o) in converting to stress (or load). (The original value of f_o would still be used in the term B, however.) Thus, small eccentricities are more closely related to a reduction in the compressive yield stress than to a reduction in the effective column length.

It can be noted that the shape of the eccentric column curves derived by the interaction method must approach that of the concentric column, as the eccentricity approaches zero. This assumption agrees with theory and tests, as shown by the eccentric column curves presented by Mr. von Kármán.[4] One of the objectionable features of the secant formula is thereby eliminated (since it has no relation to the shape of the stress-strain diagram). It should be noted that the interaction curves need not be based on any particular column formula—they may be used with any formula that may be acceptable for the concentric column. Once the interaction curves are determined, they may be converted into eccentric column curves, or plotted as curves of reduction factors versus slenderness ratio.

Interaction curves are equally applicable to the case of large initial eccentricities. The convergence of the curves at a point representing pure bending permits the designer to take advantage of all that is known about the modulus of rupture. Even failure by local buckling may be included, although it is not yet possible to foresee what change in the shape of the interaction curves would be necessary. The case of combined bending and local buckling (no column effects) is a simple interaction problem and could very likely be handled by using the interaction curve for low slenderness ratios and substituting the crushing strength for the column strength in determining f_o or P_o.

The effect of small eccentricities may now be determined approximately. Assume, for example, that the equivalent eccentricity, e, for a thin-walled tube of mean radius R lies within the tolerance $\pm 0.025\,R$ (for a column 20 in. in diameter this would be $\pm$ 0.25 in.). The value of the core radius r $(= \rho^2/c)$ for such a tube is $R/2$. The eccentricity ratio e/r is therefore 0.05. The corresponding reduction in the column stress may be determined from Fig. 14 or Fig. 15. (If Fig. 15 is used, the eccentricity must be further reduced by using Eqs. 33 and 34.) The maximum reduction so determined is in the order of 6%, at $L/\rho = 70$. Since the curves are probably only slightly on the unsafe side at such low eccentricities, this result should be a fairly accurate indication of the reduction involved for the assumed case. The magnitude of the reduction

appears to be no greater than the usual variation in material properties and could be provided for (at least in part) in selecting a conservative value for the minimum compressive yield stress.

Mr. von Kármán[4] recommended that columns be designed on the basis of their concentric buckling strength and that the effects of initial eccentricities be taken care of in the safety factor. This recommendation is still sound and is followed in modern aircraft practice in the United States. (Although it is not specifically stated in the airworthiness requirements, the matter is provided for by a factor of safety to increase the applied loads, not to reduce the allowable stresses.) With the use of the tangent modulus in the column formula, together with proper control of manufacturing tolerances, the specification of a minimum compressive yield stress, and the reduction of all test data to minimum guaranteed properties, it would seem that the unknown factors in compressive loading are certainly no greater than those for any other type of loading and that no increase in the usual factor of safety is required.

8. Effects of End Restraint

In theory, end restraint has a very simple effect: It merely changes the effective column length. In practice, however, the accurate determination of the effects of end restraint for any column except a pin-ended column is a difficult problem. The situation that exists in aircraft structural analysis has been very well described by Paul E. Sandorff,[20] and there is little more that can be added at this time. Experience has shown that a fixity coefficient of 1.5 has been generally satisfactory for the design of the continuous compression panel forming the top of the wing structure. Mr. Sandorff shows that very little of this fixity is supplied by the supporting ribs. Edge restraint, chordwise curvature, and other effects usually provide the increase corresponding to the assumed fixity coefficient.

The long-standing conception of a fixity coefficient as a multiplying factor has perhaps given rise to an exaggerated idea of the effects of end restraint. Mr. von Kármán has shown[4] that the fixity coefficient can be used as a multiplying factor, but only for the elastic case (Euler formula). In the inelastic case the coefficient must be used indirectly, to obtain the effective length:

$$L_{\text{eff}} = L/\sqrt{C} \qquad (35)$$

It is easy to overlook this important fact in dealing with the generalized Euler equation. (The writer made this mistake in his own textbook!) It would have been much better if the effects of fixity had been introduced by a length coefficient in the first place, because length is really what is directly affected, not the buckling load nor the stress.

It is important to realize that efficiently designed structures cannot be made proportionately stronger by increasing the amount of end restraint. This fact, too, was pointed out by Mr. von Kármán[4] when he declared, in effect, that end restraint causes a marked increase in buckling strength only for long slender columns, not for shorter ones. In aircraft structures, for example, the com-

[20] "Notes on Columns," by Paul E. Sandorff, *Journal of the Aeronautical Sciences*, January, 1944, p. 1.

pression members are designed to develop ultimate stresses that approach the compressive yield stress.

Fig. 16 illustrates the effects of the fixity coefficient by column curves (24ST aluminum alloy) plotted for different degrees of end fixity C. Assume, for example, that a designer has used $C = 1$ to design a structure for the column stress f_1. If he now goes to considerable trouble to restrain the ends he may be able to develop a fixity coefficient C of 3.0, but the increase in stress thus obtained is almost negligible, as shown by case A, Fig. 16. On the other hand, assume that he has selected too high a value for the fixity coefficient (say, $C = 3.0$) and that in the actual structure it proves to be only $C = 1.0$. The

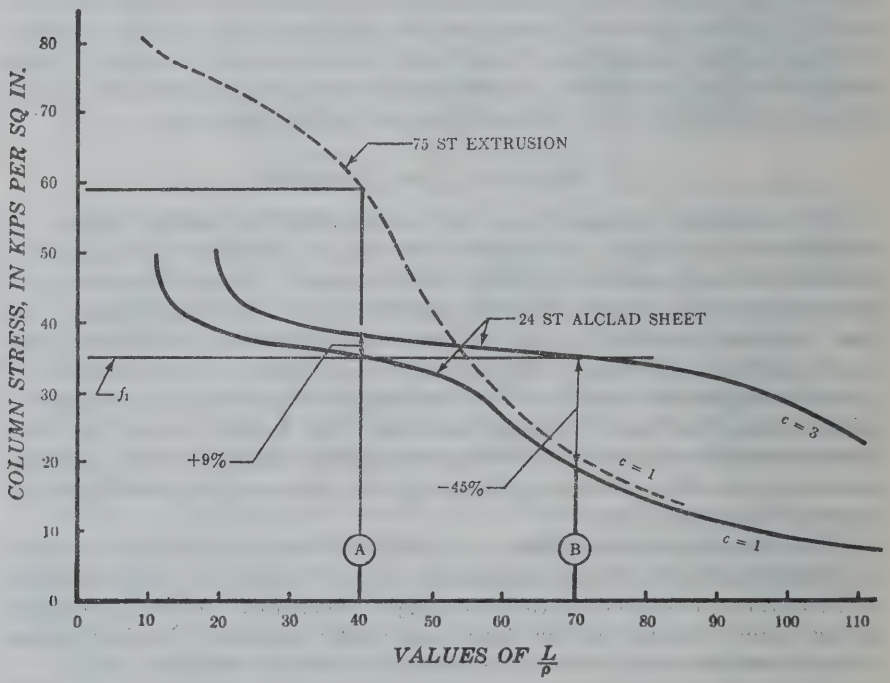

Fig. 16.—Effects of End Restraint (Curves Obtained from Tangent Modulus for Typical Material)

decrease in allowable stress is now quite large, as shown by case B. This situation is rather disturbing. An excess of actual fixity (over the assumed value) can do little good, but a lack of fixity (under the assumed value) can do much harm. Thus, conservatism should be used in selecting the fixity coefficient for use in design. Research on this subject cannot be expected to result in substantial weight savings for efficiently designed structures.

Fixity effects should be thought of as "length" effects. In aircraft wing structures, for example, changes in end restraint primarily affect the rib or bulkhead spacing. A few extra ribs represent the price that would be paid for being quite conservative in selecting the fixity coefficient for design. Fig. 16 also shows how the use of a material having a higher yield stress pays divi-

dends in the lower range of slenderness ratios, but such material would give little benefit at high slenderness ratios.

End restraint in an eccentric column reduces the effective eccentricity. An examination of the elastic case will show that the reduction increases as the column load is increased. In the inelastic case this effect should be even more pronounced. This condition is one more reason why, in actual structures, the effects of small eccentricities may prove to be relatively unimportant. The combined effect of large eccentricities and end restraint is an attractive subject for further research; the interaction curves previously described might be useful in this connection.

9. Design for Minimum Weight

The principles of structural design for minimum weight have been treated in some detail elsewhere.[21] In this paper the discussion will be confined to the procedure for determining the optimum design as applied to simple pin-ended columns of tubular cross section, using the generalized Euler theory. Since the weight of the column (for a given material) will be a minimum when the allowable stress is a maximum, the object is to find the maximum value of allowable stress in terms of the load P, the distance through which it must be transmitted L, and a "shape parameter" that controls the proportions of the cross section. If this is done for various materials, a direct comparison of weights may be made.

The generalized Euler stress formula, Eq. 2, contains one of the design variables, L, but it does not include the load P directly. The radius of gyration, being dimensional, cannot be used as a shape parameter. Since ρ^2 has the dimensions of an area, a ratio can be obtained by dividing it by A, giving the shape parameter:[22]

$$k = \frac{\rho^2}{A} \qquad (36)$$

Eq. 2 may now be written

$$f = \frac{\pi^2 E_t}{L^2}\left(\frac{\rho^2}{A}\right) A \qquad (37)$$

Substituting k for (ρ^2/A), (P/f) for A, and solving for f or P/L^2 gives the desired equations:

$$f = \pi \sqrt{E_t}\sqrt{k}\sqrt{\frac{P}{L^2}} \qquad (38)$$

or

$$\frac{P}{L^2} = \frac{f^2}{\pi^2 E_t k} \qquad (39)$$

The term P/L^2 is called the "structural index" or the "structural coefficient." (A nondimensional coefficient may be obtained by dividing by the elastic modulus, E.) Eq. 39 is more convenient to use than Eq. 38 since the value of

[21] "Principles of Structural Design for Minimum Weight," by F. R. Shanley, *Journal of the Aeronautical Sciences*, March, 1949, p. 133.

[22] "Structures of Minimum Weight," by H. Cox and H. Smith, *Reports and Memoranda No. 1923*, H. M. Stationery Office, London, 1943.

E_t depends on f. From a curve of tangent modulus versus stress the value of $\frac{f^2}{E_t}$ may be determined. Eq. 39 can then be plotted as allowable stress f against P/L^2, for different values of k.

For a thin-walled tube of average diameter D, the value of the shape parameter is

$$k = \frac{\rho^2}{A} = \frac{1}{8\pi}\left(\frac{D}{t}\right) \quad \ldots\ldots (40)$$

For the round tube, Eq. 39 then becomes

$$\frac{P}{L^2} = \frac{8f^2}{\pi E_t \frac{D}{t}} \quad \ldots\ldots (41)$$

From Eq. 41, it can be noted that high values of the stress (f) for a given material will be obtained at high values of the structural index (P/L^2) for large values of D/t. There is a limit to the value of D/t that may be used, however, because the local buckling or crushing stress decreases as D/t is increased.

The optimum stress and the corresponding $\frac{D}{t}$-ratio may be obtained graphically by plotting Eq. 41 as a family of curves for different values of D/t, after which another curve of local buckling stress against D/t is drawn, by which the curves are "cut off." If an equation for the crushing stress can be written in terms of D/t and E_t, the problem may be solved mathematically.

Mr. Timoshenko[23] has suggested an equation of the following type for local buckling:

$$f_{cr} = K\frac{\sqrt{E\,E_t}}{D/t} \quad \ldots\ldots (42)$$

(Recent developments in the theory of plasticity indicate that this may be considerably on the safe side.) If this value is substituted for f in Eq. 41, the following equation will be obtained:

$$\left(\frac{D}{t}\right)_{opt} = 2\left[\frac{K^2 E}{\pi (P/L^2)}\right]^{\frac{1}{3}} \quad \ldots\ldots (43)$$

It is interesting to note that the tangent modulus does not appear in Eq. 43 even though the equation applies to the inelastic range. Since E remains practically the same for any one class of alloys (steel, aluminum, etc.), the optimum value of D/t will be unaffected by changes in the shape or height of the stress-strain diagram: It depends only on the initial slope of the diagram.

By substituting the value from Eq. 43 in either Eq. 41 or Eq. 42, the optimum stress is obtained as a function of P/L^2:

$$\frac{P}{L^2} = \frac{8f^3}{\pi K E^{\frac{1}{2}} E_t^{\frac{1}{2}}} \quad \ldots\ldots (44)$$

Mr. Timoshenko[23] has shown that the theoretical value of K is about 1.2 but that much lower values are usually obtained in tests. For practical use

[23] "Theory of Elastic Stability," by S. Timoshenko, McGraw-Hill Book Co., Inc., New York, N. Y., 1st Ed., 1936, p. 442.

in design, Eq. 44 can be plotted for various materials[21] as shown in Fig. 17, where $K = 0.40$. The procedure for optimum design consists in determining the structural index for the case in question and selecting the optimum stress from such a chart. The load P is divided by the optimum stress to obtain the cross-sectional area. Eq. 43, or curves derived from it, may be used to deter-

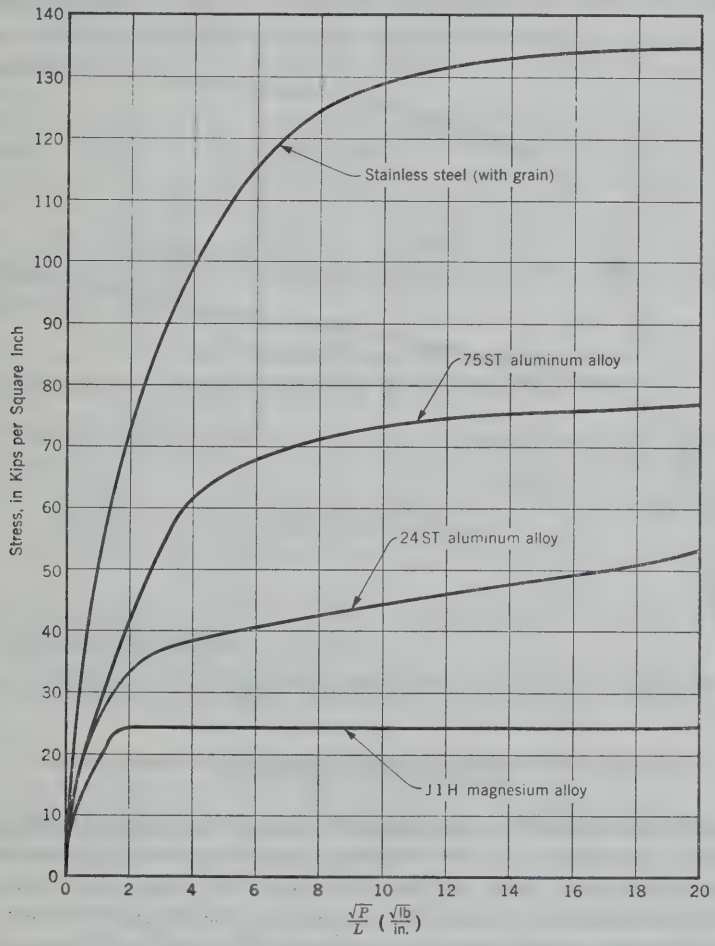

Fig. 17.—Optimum Column Stress for Round Tubes

mine the optimum ratio D/t, from which the mean diameter may be determined by the following equation for thin-walled tubes:

$$D = \sqrt{\frac{A}{\pi}\frac{D}{t}} \quad \ldots\ldots\ldots\ldots\ldots\ldots\ldots\ldots\ldots\ldots (45)$$

To show how the weight of a column is affected by the material and the loading conditions, the optimum stress may be divided by the relative density. If aluminum alloy is used as a base (density 0.10 lb per cu in.), the curves will

appear as in Fig. 18. (The square root of the structural index has been used in Figs. 17 and 18, to contract the scale.) It is important to note that curves of this type may be plotted directly from test data.[24] If all available data for a given type of loading were plotted on a single chart, the optimum conditions would be indicated by the envelope to the test points.[21] Application of the method, therefore, is not limited by the lack of a theory for optimum design.

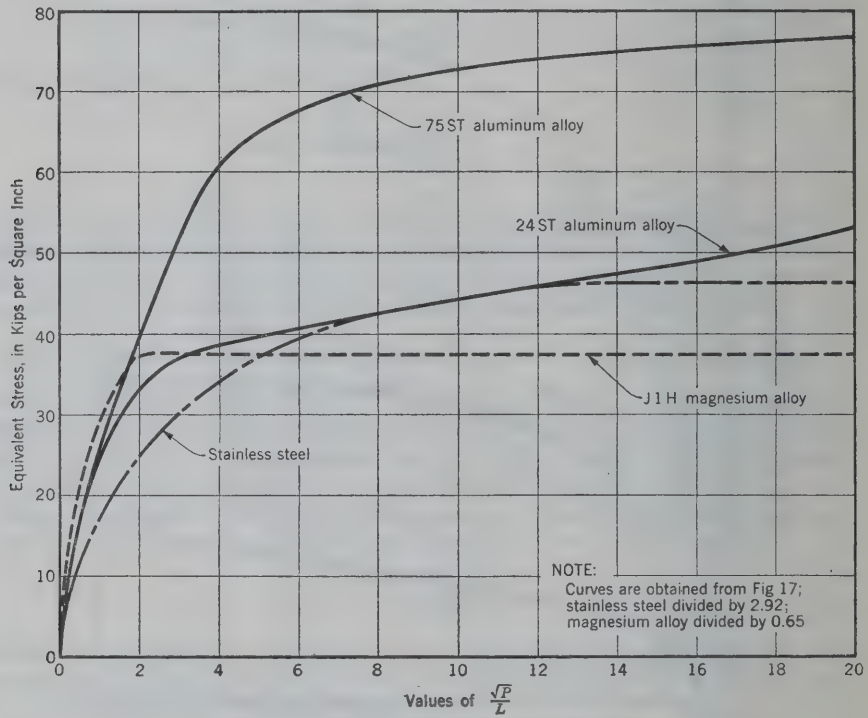

FIG. 18.—OPTIMUM COLUMN STRESS REDUCED TO SAME WEIGHT BASIS (ALUMINUM ALLOY USED AS BASE)

To apply the method to members such as those used in steel structures the same shape parameter (Eq. 36) could be used to determine the relationship between the structural index and the column buckling stress, as in Eq. 39. For the local buckling stress it would be necessary to use the ratio between one of the major cross-sectional dimensions (such as width) and the thickness of some part of the cross section. Since it is difficult to calculate the local buckling stress with accuracy, for such sections, a series of tests would be advisable in which the width/thickness ratio would be systematically varied. This procedure could be carried out for various basic shapes, such as I-beams, WF columns, and H columns. The results would be used in place of Eq. 42, to obtain curves similar to those in Fig. 17. A systematic program of this type would answer all questions regarding the efficiency of various cross-sections

[24] "Design Charts for Flat Compression Panels Having Longitudinal Extruded Y-Section Stiffeners and Comparison with Panels Having Formed Z-Section Stiffeners," by N. F. Dow and W. A. Hickman, *Technical Note No. 1889*, National Advisory Committee for Aeronautics, Washington, D. C., August, 1947.

shapes. It would show, for example, that beyond a certain value of the structural index any attempt to improve efficiency by revising the cross-sectional shape would be futile, at least for structural steel. More research of this type is needed, not only to supply valuable design information, but also to answer questions regarding the relative efficiency of various materials. For any structure that fails through buckling the term "strength/weight ratio" is misleading. The only way in which materials can be properly compared, in such cases, is through the use of optimum design procedures based on the structural index.

The round tube, loaded as a simple column, has been used as an example of the general method of optimum design. H. Cox and H. Smith extended the method to various other types of construction and loading conditions.[22] The National Advisory Committee for Aeronautics has determined the optimum design for flat panels with various types of stiffeners and for several different materials.[24] Some information is also available for shear webs and for shells loaded in bending.[21]

10. Recommendations and Conclusions

Eight general conclusions supported by this paper are:

(*a*) The generalized Euler formula, Eq. 2 (using the tangent modulus), is recommended for the design of columns that fail by primary instability;

(*b*) Specification of a minimum guaranteed compressive yield stress provides for most of the effects of material variations;

(*c*) The effects of small eccentricities may be provided for by the factor of safety;

(*d*) The interaction curves for combined bending and compression may be applied to eccentrically loaded columns;

(*e*) The effects of end restraint should be conservatively estimated in design;

(*f*) The coefficient of fixity should be replaced by an effective length coefficient;

(*g*) Tests are needed to determine interaction curves for various cross sections and materials; and

(*h*) Optimum design methods should be used to evaluate the efficiency of various types of construction and materials.

DISCUSSION

WILLIAM R. OSGOOD,[25] M. ASCE.—One aspect of the art of engineering consists in designing without adequate information. However much one may admire the artist, most engineers, nevertheless, would like the art reduced to a science. In what he calls "the generalized Euler formula," and modestly suggests calling the "Euler-Engesser formula," Mr. Shanley has made a signal contribution to column theory—that is, to science. The formula, in the writer's opinion, should be called the Euler-Shanley formula. It is true that Engesser first proposed it, but Engesser later gave it up in favor of the reduced modulus, or double-modulus, formula. It remained for Mr. Shanley to show that Engesser was right the first time.

Mr. Shanley has traced nondimensional column curves back to 1929. Actually they go back further than that, to May, 1918, when R. W. Hawken[26] introduced them.

In connection with the determination of the constants K and n in the stress-strain formula, Eq. 4, the preferable way (certainly for a new material) of determining these constants is the following: Write Eq. 4 as

$$e - \frac{f}{E} = K\left(\frac{f}{E}\right)^n \quad \ldots\ldots\ldots\ldots\ldots\ldots\ldots\ldots (46)$$

and take the logarithm of both sides:

$$\log\left(e - \frac{f}{E}\right) = n \log \frac{f}{E} + \log K \quad \ldots\ldots\ldots\ldots\ldots\ldots (47)$$

Now plot the observed values of $\log\left(e - \frac{f}{E}\right)$ against $\log \frac{f}{E}$ and draw a straight line through the plotted points that seem to lie along a straight line. The slope of this line will be n and the intercept on the axis of $\log\left(e - \frac{f}{E}\right)$ will be $\log K$. Alternatively, of course, $\left(e - \frac{f}{E}\right)$ may be plotted against f/E on log-log paper.

In connection with the interaction curves it may be well to emphasize that a bending moment M arising from transverse loads and an equal moment $P\,e$ arising from eccentrically applied longitudinal loads are not equivalent. If the interaction curve is obtained by transverse tests, as the curve in Fig. 13 was, then in using the curve for the design of an eccentrically loaded column, for

[25] Senior Structural Engr. (Acting), David Taylor Model Basin, Washington, D. C.

[26] "Column Analysis and Design," by R. W. Hawken, Univ. of Queensland and the Sydney Univ. Eng. Soc., Brisbane, Australia, 1918.

given e the load P read from the curve will be on the unsafe side—that is, the eccentrically loaded column will actually fail at a lower value of P. This becomes evident by considering Fig. 19. The moment diagrams on which Fig. 13 is based are like ABCD in Fig. 19, in which M is the maximum bending moment arising from the transverse loads. The corresponding diagram for terminal couples equal to M is AEBCGD. The maximum deflection produced by the terminal couples will be greater than that produced by the transverse loads. If an axial load is now added, it will take a smaller axial load to produce failure of the member loaded by the terminal couples than to produce failure of the transversely loaded member. (The terminal couples plus the axial load are the same as an eccentrically applied load.) On the other hand, if the interaction curve is obtained from tests on eccentrically loaded columns and the abscissas are $M = P\,e$, then in using the curve for the design of a beam-column for a given maximum moment from the transverse load the axial load P read from the curve will be conservative.

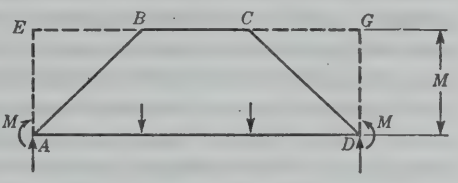

FIG. 19

In 1947 the writer suggested[27] a method of compromising between an unsafe design and an uneconomical one. The method assumes that the test data, in the form of an interaction curve, for example, are based on eccentrically loaded column tests. As intimated in the preceding paragraph, the eccentrically loaded column is a limiting case of a beam-column. The interaction curve for eccentric-load tests will be lower than the curve for any combination of axial and transverse loads, M being equal to $P\,e$ for the eccentric-load tests and equal to the maximum bending moment for transverse loads. As a practical matter it is easier to make accurate eccentrically loaded column tests than tests under combined axial and transverse load. The latter call for considerable art.

J. V. DU PLESSIS,[28] JUN. ASCE.—This comprehensive expression of the views of one who recently has shed further light on the fundamentals of column behavior is both refreshing and welcome.

It cannot be emphasized enough, however, that the "generalized Euler theory" is a "critical load" or "buckling load" theory and as such applies only to the "perfect" column or (the word used in this sense) "strut." Insisting, with the full rigor of Webster, that conditions existing are concentric loading, straightness, symmetricality, and homogeneity (even to postulating rigid monotonic rather than statistical location of atoms), it is possible to conceive a situation in which a column may be obtained in a straight loaded state, which, under some slight disturbance, will snap out of this position into the von Kármán nonstraight equilibrium bifurcation. In some cases, if the velocity of buckle is such as to induce large dynamic energy effects, the strut will surmount the barrier of increasing equilibrium loadings for larger deflections and

[27] "Beam-Columns," by William R. Osgood, *Journal of the Aeronautical Sciences*, March, 1947, p. 167.
[28] Research Student, Faculty of Eng., Bristol Univ., Bristol, England.

then, behaving according to the negative slope of the deflection-end-load curve, rush to catastrophic collapse. If this last condition were in danger of occurring, the use of the buckling criterion would deserve some support as a logical design basis in order to guard against the occurrence of the "perfect" column. Since the column in practice, perfect or otherwise, seldom occurs in splendid isolation, as in some types of water towers, but generally with some measure of restraint afforded in adjoining framing, it is not reasonable to fear the "runaway" of any incidentally occurring perfect column. Apart from the laboratory difficulty of securing the perfect straight equilibrium bifurcation, even in the "short column" compression test, practice adequately indicates that column failure is a matter of bending rather than buckling.

To cite a practical case, an old reinforced concrete frame building was subjected by new owners to warehouse type loading in the region of two to three times the design loading, and one of the columns under the loaded floor began to fail. Distortion was a gradual process (was not suddenly there) and proceeded so slowly as to allow adequate time for supporting timbers to be introduced. Whatever it was that happened, it certainly was not buckling. Apart from such records of column failures as may exist, the laboratory struggle to produce perfect pin-ended columns is sufficient testimony that column failure in civil engineering structures is a matter of bending rather than buckling, and that columns undergo bending deformation from the inception of loading.

On the basis of this observation it is impossible to agree with the author's statement (in Section 1) that:

> "It is doubtful whether any structural engineer would wish to take advantage of this factor [increasing equilibrium load with increasing deflections] in actual design, because in this region an increase in stress will involve a large amount of permanent set. It seems logical, therefore, to regard the beginning of the bending [that is, buckling] in a perfect column as the upper limit for structural purposes."

As a basis of discussion, accept the premise that a certain amount of permanent set is the maximum permitted for design purposes. If bending occurs from the beginning, due to some cause classified by buckling theorists under the term "imperfection" (as it undoubtedly will), the critical amount of permanent set will be induced at a lower load than in the case of the initially perfect but later buckling strut. The permissible load will therefore be different in practice from that derived from a buckling analysis. For other criterions of design, similar arguments will still apply. The greatest argument in support of buckling formulas is that there is no other theoretical analysis that does not presuppose knowledge either unobtainable or securable only by investigation or test, and, in any case, whose degree of variation has never been subject to control or even adequate determination. Until an adequate theoretical analysis not requiring unknown information exists, and until determined and specifiable systems of tolerances are used, it appears more practical to use empirical formulas and data, or practically proved formulas, rather than to rely on a formula based on a case unlikely to occur in practice. The interaction

curves described by the author are a valuable step in this direction; but they still involve undecided tolerances and, by so doing, only serve further to underline the need for investigation as to the range of tolerance that actually occurs in practice.

Although buckling formulas are more of academic interest, their value as one set of known boundary conditions to a complex region of structural actions should not be forgotten, and in this connection the author's clarification of the stress situation that may occur across a section is of the greatest value.

It is worthwhile to stress the fact, however, that this clarification (which, in effect, is a statement that the ratio of stress change to strain change applicable to analytical consideration of any fiber is, in some cases, for all the fibers, the ratio corresponding to the loading stress strain relationship) applies in some (and probably in most) instances to columns which for some reason (such as eccentric loading) bend right from the inception of the loading program. Any load analysis or distortion analysis of columns in the elasto-plastic range must therefore be subject to "co-analysis" as to whether all the fibers are being loaded or whether some are being unloaded. Analysis of the condition for loading to occur over the entire section has been made by D. C. Drucker,[29] Jun. ASCE, for the case of buckling of the perfect column, and extension can be made on similar lines to the more general "non-perfect" column problem. The case in which (given increasing end load) all fibers continue to load is obviously more tractable analytically since it is not necessary to have a stress-strain relation sensitive to "direction." In this category may also be placed those cases in which, if a fiber is subject to unloading, it is a fiber that has been subject to a past history of only elastic strain. Only the perfect, or near perfect, columns are likely to fall outside this category before reaching the maximum load they will carry; and, in general, this will be more likely to occur with materials having relatively steep-sloping strain-hardening curves. Therefore, the arguments that led the author to support the tangent modulus Euler formula are of much wider application.

Jacob Karol,[30] M. ASCE.—This comprehensive paper by Mr. Shanley is an admirable presentation of the theory underlying the present methods of stress analysis of compression members in aircraft design. The mathematical development of the nondimensional stress-strain diagrams and column curves may seem somewhat "impractical" to the civil engineer who uses allowable stresses in the design of columns of steel, concrete, or timber that are fixed by the design specifications at values well within the elastic range. In aircraft structures, however, the design stresses are in the inelastic range. Since airplanes are generally static tested for full design loads, it was necessary for the stress analyst to develop a design theory which, in the ideal case, would result in a structure that failed at slightly beyond the design load. Therefore, the detailed study, by the author, of the several phases of applied column theory is undeniably "practical."

The writer will confine his discussion to Sections 6 and 7.

[29] "The Plasticity of Metals—Mathematical Theory and Structural Applications," by D. C. Drucker, *Proceedings-Separate No. 27*, ASCE, August, 1950.

[30] Design Engr., Howard-Needles-Tammen & Bergendoff, Kansas City, Mo.

The method of correcting test data to "standard," as indicated in Fig. 12, is correct only for columns that fail by primary instability, since the affinely related column curves are derived from the tangent modulus. The horizontal scale marked "not used" is designated as "effective L/ρ" in the original Lockheed report (see Fig. 12). This value is actually the important variable in the general case, as will be evident subsequently.

It is supposed that a series of compression tests of sheet stiffener combinations have been made. Since the sheet and stiffener may each be subject to local buckling, the column curve plotted from the test data will not be affinely related to the tangent modulus column curve of the specimen material. It may be noted in passing that determination of f_c and L/ρ for a sheet stiffener combination is quite a problem in itself, but it is assumed that they have been determined somehow. It is desirable to plot the test data on a graph, which also has the Euler curve plotted thereon, to determine the point of intersection. The procedure for correcting the data for a test stress f_2 to standard is as follows:

Let: f_o be the yield strength for standard material; $K f_o$ be the yield strength for specimen material; f_1 be the stress for $(L/\rho)_1$, as reduced to standard; f_2 be the stress for $(L/\rho)_1$, read from the curve; and f_3 be the stress for $(L/\rho)_3 = (L/\rho)_1/\sqrt{K}$, read from the curve. Then, for the ratio $(L/\rho)_1$,

$$f_1 = \frac{f_3}{K} \quad \ldots\ldots\ldots\ldots\ldots\ldots\ldots\ldots (48)$$

The foregoing procedure is merely a verbal statement of the mathematics expressing the affine relationship between the test column curve and the derived column curve for the standard material. The interested reader can readily prove this for himself by assuming that the test column curve is mathematically expressible in terms of f_o and $K f_o$, as indicated elsewhere,[15] and by calculating the stresses f_1, f_2, and f_3. Hence, in the general case, correction to standard is a function of the shape of the test column curve, the yield strength ratio, and L/ρ.

The author's extended treatment of the effects of eccentricity in pin-ended columns is undoubtedly an indication of the importance of the subject. After rejecting the secant formula as inapplicable to materials not having a pronounced yield point, he suggests using interaction curves to solve the problem, and presents in Fig. 15 such a series of curves for axial loading and bending due to third-point loading. He assumes correctly that, for an initial moment due to constant eccentricity, the sag would be greater. He further states that the shape of these curves may be primarily a function of the kind of loading involved, which is also true. Hence, a number of sets of interaction curves would be necessary in design, unless there is some other approach to the problem.

After following the author's lead and verifying the statements referred to in the preceding paragraph, it occurred to the writer that the problem could be generalized so that one interaction curve would apply for various loadings, and perhaps for any shape of cross section and any type of stress-strain diagram. The reasoning was extremely simple. For any column subject to combined

bending and compression, the maximum stress on the section is the sum of the axial stress and the total bending stress. The total bending stress is itself the sum of the primary bending stress and the secondary bending stress due to lateral deflection. By using the total bending stress as a parameter, the type of loading is automatically cared for. If the total stress on the section is known, then, by deducting the axial stress, the total bending stress is obtained. The primary bending stress can then be determined by using the available theories of secondary bending.

The problem resolved itself into finding an expression which would equal the critical column stress for pure compression and the modulus of rupture for pure bending. The expression was originally determined to fit the test data in Fig. 14 for the entire range of R'_c and $L/\rho = 30$. It was later found that the same expression checked quite well any point taken at random from Fig. 14. This might be considered as an indication of its possible generality.

The total stress in combined compression and bending is given by the expression:

$$f_c + f_{bt} = f_{cr}\,[1 + (m - 1)\,(0.839 \tan \theta)] \quad \ldots\ldots\ldots\ldots (49)$$

in which

$$m = \frac{f_{bo}}{f_{cr}} \quad \ldots\ldots\ldots\ldots\ldots\ldots\ldots\ldots (50a)$$

and

$$\theta = \frac{5}{9} \text{ arc tan } \frac{f_{bt}}{f_c} \quad \ldots\ldots\ldots\ldots\ldots\ldots\ldots\ldots (50b)$$

Dividing through both sides of Eq. 49 by f_{cr},

$$\frac{f_c}{f_{cr}} + \frac{f_{bt}}{f_{cr}} = 1 + (m - 1)\,(0.839 \tan \theta) \quad \ldots\ldots\ldots\ldots\ldots (51)$$

The stress ratios are

$$R'_c + m\,R_{bt} = 1 + (m - 1)\,(0.839 \tan \theta) \quad \ldots\ldots\ldots\ldots\ldots (52)$$

in which

$$\theta = \frac{5}{9} \text{ arc tan } \frac{m\,R_{bt}}{R'_c} \quad \ldots\ldots\ldots\ldots\ldots\ldots\ldots\ldots (53)$$

Eq. 52 is plotted in Fig. 20(a) for various values of m. Since m is known for a particular problem—

$$R_{bt} = \frac{f_{bt}}{f_{bo}} = \frac{M_{bt}}{M_o} \quad \ldots\ldots\ldots\ldots\ldots\ldots\ldots\ldots (54)$$

—can be determined for any value of

$$R'_c = \frac{f_c}{f_{cr}} = \frac{P}{P_{cr}} \quad \ldots\ldots\ldots\ldots\ldots\ldots\ldots\ldots (55)$$

—and vice versa.

The remaining problem is to determine the primary bending stress f_b from the total bending stress f_{bt}. For any distributed loading (including the test third-point loading), as well as for initial curvature, the stress is given accurately enough by

$$f_b = (1 - \alpha)\,f_{bt} \quad \ldots\ldots\ldots\ldots\ldots\ldots\ldots\ldots (56a)$$

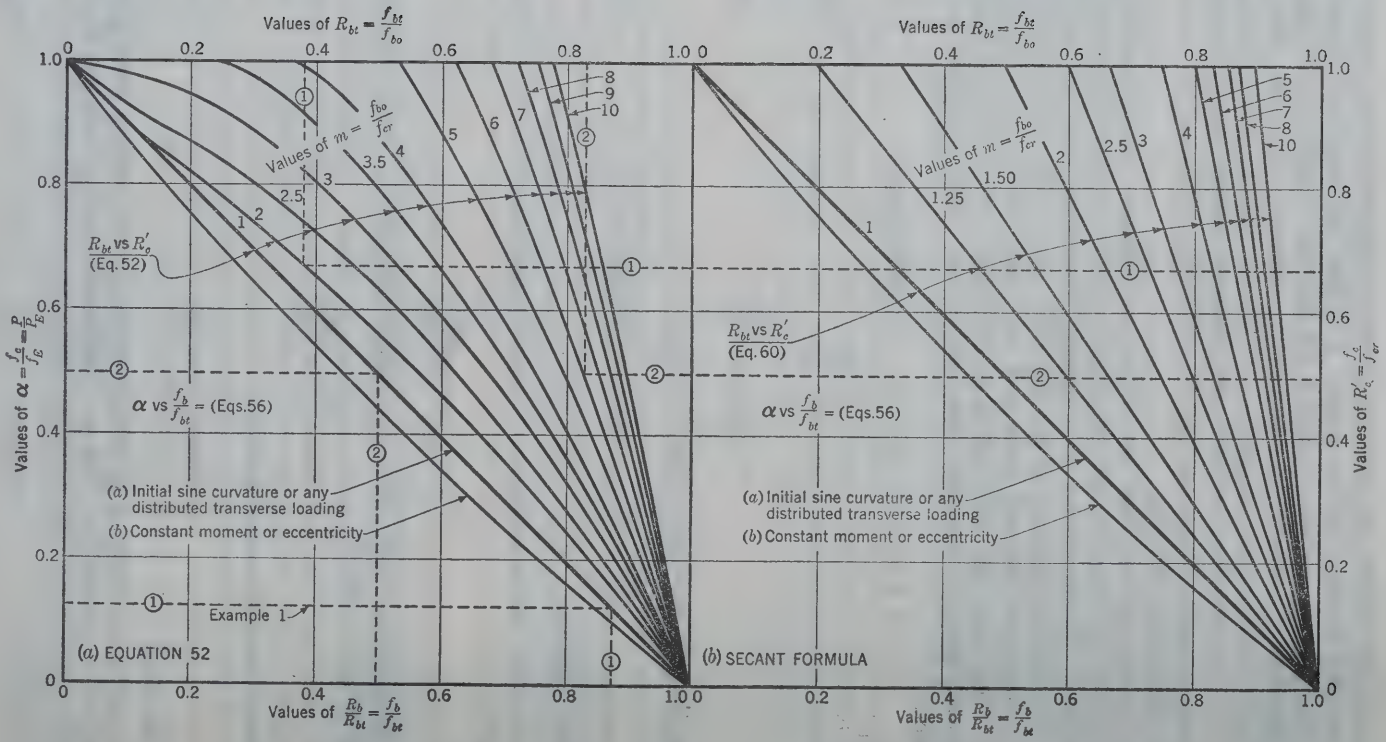
Values of $R_{bt} = \frac{f_{bt}}{f_{bo}}$
Values of $m = \frac{f_{bo}}{f_{cr}}$
R_{bt} vs R'_o (Eq. 52)
α vs $\frac{f_b}{f_{bt}}$ = (Eqs.56)
(a) Initial sine curvature or any distributed transverse loading
(b) Constant moment or eccentricity
Example 1
(a) EQUATION 52
Values of $\alpha = \frac{f_a}{f_c} = \frac{P}{F_o}$
Values of $\frac{R_b}{R_{bt}} = \frac{f_b}{f_{bt}}$
R_{bt} vs R'_o (Eq. 60)
(b) SECANT FORMULA
Values of $R'_o = \frac{f_o}{f_{cr}}$

FIG. 20.—INTERACTION CURVES FOR COMBINED BENDING AND AXIAL LOADING

and, for constant eccentricity of axial load,

$$f_b = \frac{1 - \alpha}{1 + 0.272\,\alpha} f_{bt} \ldots\ldots\ldots\ldots\ldots\ldots (56b)$$

in which

$$\alpha = \frac{f_c}{f_E} = \frac{P}{P_E} = \frac{f_c}{\frac{\pi^2 E}{(L/\rho)^2}} \ldots\ldots\ldots\ldots\ldots\ldots (57)$$

Hence the ratios

$$\frac{R_b}{R_{bt}} = \frac{f_b}{f_{bt}} = \frac{M}{M_{bt}} \ldots\ldots\ldots\ldots\ldots\ldots (58)$$

can be determined for any value of α, and vice versa.

Eqs. 56 are also plotted in Fig. 20(a). Thus, the problem of combined axial load and bending due to eccentricity or transverse loading is solved from one chart.

Two examples of the use of Fig. 20(a) applied to the data in Fig. 14 follow:

(1) Given: $L/\rho = 30$; and, in kips per square inch, $f_{bo} = 120$, $f_{cr} = 60$, $f_c = 40$, and $E = 29{,}200$. The problem is to compute f_b. From the assumed data, $m = 120/60 = 2$; $f_E = 320$ kips per sq in; $\alpha = 40/320 = 0.125$; and $R'_c = 40/60 = 0.667$. From Fig. 20(a), $R_{bt} = 0.38$; hence, $f_{bt} = 0.38 \times 120 = 45.6$ kips per sq in. From Fig. 20(a), $f_b/f_{bt} = 0.875$; hence, $f_b = 0.875 \times 45.6 = 39.9$ kips per sq in. From Fig. 14, test $f_b = 40$ kips per sq in.

(2) Given: $L/\rho = 120$; and, in kips per square inch—$f_{bo} = 120$, $f_{cr} = f_E = 20$, and $f_b = 50$. It is required to compute f_c. From the given data, $m = 120/20 = 6$; $f_b/f_{bo} = 50/120 = 0.417$. Guess $R'_c = 0.498 = \alpha$. From Fig. 20(a), $f_b/f_{bt} = 0.502$; hence, $R_{bt} = 0.83$. From Fig. 20(a), $R'_c = 0.498$, which checks the guess. Hence, $f_c = 20 \times 0.498 = 9.96$ kips per sq in. From Fig. 14, test $f_c = 10$ kips per sq in.

It is recognized that the addition of stresses in the inelastic range is a convenient fiction; but, in the foregoing treatment, Eq. 49 has the merit of being a close approximation to the experimental truth and of indicating the important variables in a problem not solved hitherto in the general case. Since Eq. 49 assumes a gradual change in the total stress as the loading changes from pure compression to pure bending, it seems logical enough to be generally valid. Furthermore, if f_{bo} is considered to represent not only the ultimate modulus of rupture, but also a limiting bending stress in general, the usefulness of Fig. 20(a) is extended. Thus, in aircraft design, it can be used for limit loads as well as for ultimate loads. The writer was able to check the test data by J. A. Van den Broek,[31] M. ASCE, on 1-in. mild steel round bars for both initial yielding and ultimate capacity by using the yield point as the limiting bending stress in the first case and 1.7 times the yield point as the modulus of rupture in the second case.

The column theory, from which the secant formula is derived, is also presented for comparison. The total stress is given by the expression:

$$f_c + f_{bt} = m\,f_{cr} \ldots\ldots\ldots\ldots\ldots\ldots (59)$$

[31] "Rational Column Analysis," by J. A. Van den Broek, *The Engineering Journal*, December, 1941.

Dividing through both sides of Eq. 59 by $m f_{cr}$,

$$\frac{f_c}{m f_{cr}} + \frac{f_{bt}}{m f_{cr}} = 1 \quad \ldots\ldots\ldots\ldots\ldots\ldots\ldots\ldots (60)$$

Expressed as stress ratios, Eq. 60 becomes

$$\frac{R'_c}{m} + R_{bt} = 1 \quad \ldots\ldots\ldots\ldots\ldots\ldots\ldots\ldots (61)$$

Eq. 61 is a family of straight lines, as represented in Fig. 20(*b*) for various values of m. It is obviously correct only for a value of $m = 1$. This is true in the short column range for structural steel, in which the limiting stress for both bending and compression is the yield point stress. For values of m greater than 1, it gives less conservative results than Eq. 52. The relation of primary to total bending stress is given by Eqs. 56, and use of the chart is similar to the method presented for Fig. 20(*a*).

E. P. Popov,[32] Assoc. M. ASCE.—An excellent comprehensive treatment of primary column failure has been presented in this paper. Emphasis on the tangent-modulus theory as a basis for column strength analysis is gratifying. In an earlier paper [6] Mr. Shanley capably justified the use of the tangent-modulus method for columns, theoretically. He showed that the bending of a column begins at the tangent-modulus load and that the consideration of a single critical section is sufficient to predict the capacity of a member. In this paper several graphs showing the agreement between this theory and tests are cited as supporting evidence for justification of the theory. However, these citations are limited to metals and it is noteworthy that even for reinforced concrete columns similar good agreement is found.[33]

Fig. 21 [33] shows the results of a series of tests on spirally reinforced concrete columns, in which ρ, the radius of gyration, is based on a transformed concrete section, and an average load-strain curve for a short column has been used to determine the tangent-modulus and reduced-modulus column curves. The agreement thus found is truly remarkable; and, although relatively few tests have been made on slender concrete columns, F. E. Richart and J. O. Draffin, Members, ASCE, T. A. Olson, and R. H. Heitman,[33] Assoc. M. ASCE, venture the following conclusion:[34]

> "It appears from the procedure followed that the strength of any long slender spiral column may be estimated from the properties of a short column of similar materials and arrangement of reinforcement."

However, in all these matters a word of caution must be given, as the tangent-modulus theory is adequate only if the material is stable with time.

---

[32] Associate Prof. of Civ. Eng., Univ. of California, Berkeley, Calif.

[33] "The Effect of Eccentric Loading, Protective Shells, Slenderness Ratios, and Other Variables in Reinforced Concrete Columns," by F. E. Richart, J. O. Draffin, T. A. Olson, and R. H. Heitman, *Bulletin No. 368*, Univ. of Illinois Eng. Experiment Station, Urbana, Ill., November, 1947, p. 103.

[34] *Ibid.*, p. 86.

Gradual plastic deformation of concrete, or creep of the material used, may substantially lower the carrying capacity of a column. The generalized Euler equation is a criterion of column strengths for loads of short duration and for materials that do not creep.

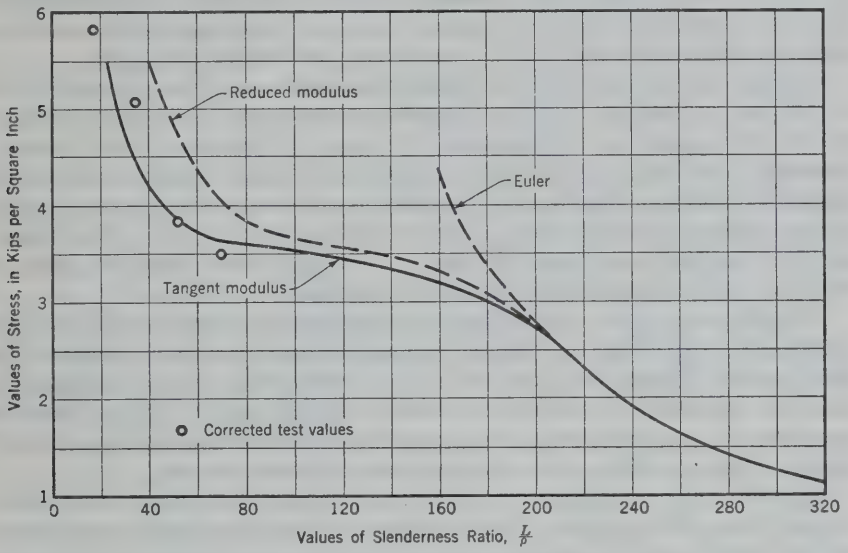

FIG. 21.—STRENGTH OF LONG REINFORCED CONCRETE COLUMNS
(Average Over-All Diameter of Columns, 12.40 In.; Average Core Diameter, 12.15 In.; and $\frac{\text{Maximum Length}}{\text{Diameter}} = 19.7$)

The writer is in agreement with the general conclusions reached by the author; but one of the basic assumptions made in the paper should be clearly kept in mind, as it is significant. After justifying the use of the tangent modulus in Euler's formula, an algebraic expression for a tangent modulus, stemming from the paper by W. Ramberg and William R. Osgood,[13] M. ASCE, is introduced by Mr. Shanley. This expression for the tangent modulus (Eq. 6) is obtained from Eq. 5 by differentiation. The latter expression with proper parameters is supposedly capable of representing, reasonably well, the stress-strain curve for any material in compression. Unfortunately, ordinary steel (which hardens after some yielding strain) cannot be represented accurately by Eq. 6, in that particular form. As may be noted from Fig. 7, none of the non-dimensional stress-strain curves resemble the entire range for an ordinary steel. Perhaps there are other cases in which a mathematical three-parameter expression for a stress-strain diagram is not adequate. Moreover, the author does not actually use these curves but goes even further and works with the tangents to such curves. Also, he calls attention to the shape of the knee (mathematically indicated by n) of the stress-strain diagram as having a relatively large influence on the column stress curves as this affects the tangent moduli considerably, in an important zone.

Messrs. Ramberg and Osgood [13] show that good agreement of computed-to-experimental tangent moduli is found for several materials whose curves may

be represented by a small value of parameter n. In such cases the value of n was always less than 20 and the knees of the corresponding stress-strain diagrams were not sharp. On the other hand, for the 1025 carbon steel which was also investigated, n is greater than 50 and a considerable discrepancy is indicated by the original data between computed and actual tangent moduli. To a large extent Mr. Shanley's argument rests on the adequacy of the empirical algebraic relation selected (Eq. 6), and it may not be fully adequate.

Finally, the writer wishes to comment on the term "short column" which is criticized in Section 2. What the author refers to as "short-column" range is usually termed the "intermediate" [35] range. The term "short column" generally is reserved for still shorter compression blocks. In the latter case the capacity is determined not by the instability phenomenon of an inelastic column but by an allowable deformation. Hence, retention of the term "short column" for this shortest range seems desirable to emphasize the transition point in column lengths from one kind of action to another.

The discussion given by Mr. Shanley regarding the end restraint is worthy of emphasis and repetition as it is not fully appreciated by some engineers. The development of interaction curves for combined bending and compression of members suggested by the author deserves further study. It is a practical expedient for accurate design of columns with any load eccentricity, although a large number of tests are necessary to establish such curves.

The foregoing remarks are not to be construed as detracting from the overall excellence of the paper. Even a single feature of the paper, such as the use of nondimensional forms for column formulas, is a valuable addition to civil engineering literature on columns. For completeness, in his concluding remarks, the author should comment on the limitation of the tangent-modulus column formula which occurs when $E_t = 0$; it even has a negative slope as in the case of an ordinary steel where it does not apply.

Jack R. Benjamin,[36] Assoc. M. ASCE.—The statement that the theoretical load at which bending of a perfect column begins is the upper limit for structural design leaves much to be desired. The design problem is not concerned basically with the upper limit for a theoretical column, but with the allowable design load on an actual column in a structure. The distance between the limit for such a column and this upper limit can be large and is difficult to analyze.

The "perfect" column does not exist. Every column is subject to variations in material and initial crookedness. These are items over which the designer has no control other than to set a limit for each. Eccentric load application always occurs and the eccentricity is normally variable about both principal axes. The end conditions in the usual structural column may be subject to analysis, but more often are not.

Taking the theoretical load at which bending of a perfect column begins as the upper limit for structural design and then modifying this limit in designing may be satisfactory for aircraft work, but it does not apply under

[35] "Mechanics of Materials," by P. G. Laurson and W. J. Cox, John Wiley & Sons, Inc., New York, N. Y., 1947, 2d Ed., p. 233.

[36] Asst. Prof. of Civ. Eng., Stanford Univ., Stanford University, Calif.

existing codes and specifications to civil engineering structures. Two possible general design criteria exist. The normal criterion for civil engineering structures is to consider the upper limit of column strength to be reached when the unit stress at any point in the primary column material reaches the yield point. In recent years, the other criterion of ultimate strength has been given much attention. However, no matter how the design is made, under normal working loads the stresses are within the elastic limit and the column acts elastically. If the column is a part of a complex structure, as most columns are, the load on the structure which will cause failure of any single column is very difficult to determine. If the yield point criterion is used, an approximation can be made, but if ultimate collapse is the basis, only a pure guess is possible. The structural designer must first consider the stresses in the column under working loads with some arbitrary limit set by code or specification which will determine the factor of safety. If superposition applies to the system, the factor of safety thus found is reasonable. However, when ultimate strength is the basis of design, a radical change in approach must be made by comparing the column in the structure with an isolated theoretical column in only a simplified mathematical structure at best. If the two can be compared at all, it can be only an arbitrary guess, pure and simple.

The tests of structural columns reported in the literature are open to the same kind of arbitrary decision as are designs by ultimate strengths. First, the experimental end conditions are unknown. Testing with flat ends certainly results in semielastic supports and the action of the column is not completely determined in either the elastic range or the plastic range. To accept test data with flat ends as a basis for design requires considerable imagination. The pin-ended testing is scarcely better since true pin ends are not obtained mechanically, and very small eccentricities can produce large stresses. Thus, tests of columns leave gaps in both experiment and application, the latter being virtually unbridged except by arbitrary opinion.

The design of columns in the elastic range by the secant formula is subject to question. First, only rarely are eccentricities constant throughout a column length. Eccentricities vary normally and exist about both principal axes. The further use of positive eccentricities combined with a reduced length coefficient based on a negative eccentricity places it in the same category with the parabolic and other empirical formulas.

The writer does not understand why eccentricity and end restraint are considered separately. End restraint is often the cause of eccentricity and then the two are inseparable. The same basic error contained in the secant formula is made in the paper. The idea of end restraint producing a reduced length is incompatible with positive eccentricities. Furthermore, eccentricities are not normally constant and occur about both principal axes.

The paper was found most challenging; it is a valuable contribution to the subject of columns.

HERBERT A. SAWYER, JR.,[37] JUN. ASCE.—This well organized and stimulating paper can be mainly criticized for its quick rejection of the secant

[37] Asst. Prof. of Civ. Eng., Univ. of Alabama, University, Ala.

formula. The secant formula is a special case of the general column formula:

$$f = \frac{P}{A} + \frac{M\,c}{I_e} \quad \ldots\ldots\ldots\ldots\ldots\ldots\ldots\ldots\ldots\ldots (62)$$

in which M is the actual maximum moment in the column from all possible causes. This expression is true even in the plastic range if the term c/I_e is properly modified. Contrary to what the author states in Section 7, the secant curve from this general formula has a very distinct relationship to the Euler column curve—in fact, the Euler Engesser curve is only a special case of the secant curve. The general column formula also appears to agree very well with the experimental results[14] cited by the author in his treatment of eccentricity. Thus these results (and evidently the entire problem of eccentricity) seem to have, in the general column formula, a theoretical basis which should be recognized, and which serves as a direct tie between the two main parts of the paper—one on perfect columns, and the other on eccentric columns.

To verify these statements, the value of M in the general equation must first be found. For this discussion, it is sufficient to do this only for the cases of the paper—for any initial eccentricity, e, and any initial moment from transverse loads, M_b, both of which are symmetrically distributed with respect to the transverse center line of the column. Examples of these cases are shown in Figs. 22(a) and 22(b). Many investigators have evaluated M for various conditions of eccentricity, curvature, or transverse loading.[38,39] Prominent among early investigators was J. M. Moncrieff,[40] M. ASCE, and the author[41] himself has suggested an approach to the problem.

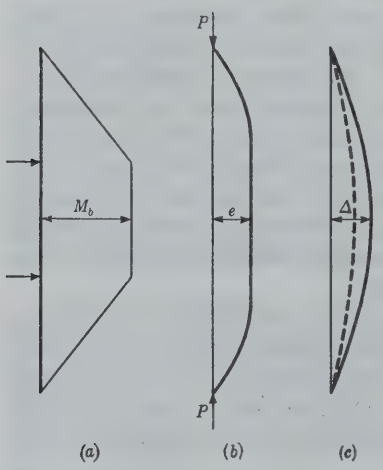

FIG. 22.—EXAMPLES OF INITIAL MOMENTS AND DEFLECTIONS

The writer's reason for adding another basically similar column formula to the existing superabundance is that a formula was needed for this discussion which, using the author's notation, would apply generally to the author's various examples of eccentrically and transversely loaded columns. Existing formulas have been developed, for the most part, for specific types of transverse loadings or eccentricities.

Successive approximations will be used, although the principle of superposition is true only in the plastic range as applied subsequently, and for infinitesimally small values of M_b and e. The moment M will be found at the midheight of the column, where it is a maximum.

[38] "Buckling of Elastic Structures," by H. M. Westergaard, *Transactions*, ASCE, Vol. LXXXV, 1922, p. 586.

[39] "Numerical Procedure for Computing Deflections, Moments, and Buckling Loads," by N. M. Newmark, *ibid.*, Vol. 108, 1943, pp. 1161–1234.

[40] "The Practical Column Under Central or Eccentric Loads," by J. M. Moncrieff, *ibid.*, Vol. XLV, June, 1901, p. 341.

[41] "Basic Structures," by F. R. Shanley, John Wiley & Sons, Inc., New York, N. Y., 1944, Chapter 19, p. 309.

The primary moments at the midheight will be $M_b + Pe$. These moments, distributed, for example, as shown in Figs. 22(*a*) and 22(*b*), each cause a transverse deflection, and, when added, would result in a deflection curve like Fig. 22(*c*). The total midheight deflection from these moments, Δ, calculated by any standard method, would be

$$\Delta = C_b \frac{M_b L^2}{\pi^2 E_t I} + C_e \frac{P e L^2}{\pi^2 E_t I} \quad \ldots\ldots\ldots\ldots\ldots\ldots (63)$$

in which C_b and C_e are constants depending on the shape of the curves corresponding to Figs. 22(*a*) and 22(*b*). Values of these constants, as defined by Eq. 63, are as follows:

Distribution of moment	C_b or C_e
Triangular (apex at midheight)	0.882
Third point trapezoidal (Fig. 22(*a*))	1.050
Quarter point trapezoidal	1.131
Rectangular (M_b or $P e$ constant)	1.26
Parabolic (vertex at midheight)	1.027
Sinusoidal (vertex at midheight)	1.000

The tangent modulus is accurate here only for infinitesimally small values of M_b and e, as shown by the author for perfect columns. For larger values, although not accurate, it is certainly more accurate than the elastic modulus.

The additional midheight moment, M_1, from the deflection Δ will be

$$P\Delta = M_1 = (C_b M_b + C_e P e) \frac{P L^2}{\pi^2 E_t I} \quad \ldots\ldots\ldots\ldots (64)$$

and the additional moment at any height will be P times the deflection at the height, producing a moment diagram geometrically similar to Fig. 22(*c*). This curve approximates a sine curve, with negligible error for the foregoing values of the constants, C_b and C_e, since its curvature usually approaches zero at either end and is maximum at the midheight. Assuming a sine curve, the additional midheight deflection from these moments will be $\frac{P \Delta L^2}{\pi^2 E_t I}$, and the additional midheight moment from this deflection will be

$$M_2 = P\left(\frac{P \Delta L^2}{\pi^2 E_t I}\right) = M_1 \frac{P L^2}{\pi^2 E_t I} \quad \ldots\ldots\ldots\ldots\ldots (65)$$

This increment of moment (with sine curve distribution again assumed), in turn, causes another increment of midheight deflection. This deflection, multiplied by P, gives the next increment of moment:

$$M_3 = M_1 \frac{P L^2}{\pi^2 E_t I} \frac{P L^2}{\pi^2 E_t I} \quad \ldots\ldots\ldots\ldots\ldots (66)$$

This process may be continued indefinitely, each successive increment of moment containing an additional term $\frac{P L^2}{\pi^2 E_t I}$. Totaling all these increments,

$$M = M_b + P e + (C_b M_b + C_e P e) \frac{P L^2}{\pi^2 E_t I} \times \left[1 + \frac{P L^2}{\pi^2 E_t I} + \left(\frac{P L^2}{\pi^2 E_t I}\right)^2 \cdots\right] \quad (67)$$

Summing up the geometric progression, and substituting this value of M in Eq. 62, the general column formula becomes

$$f = f_c + f_b + f_e + \frac{f_b C_b + f_e C_e}{\frac{\pi^2 E_t \rho^2}{f_c L^2} - 1} \quad (68)$$

in which $f_b = M_b c/I$; $f_e = P e c/I$; and $f_c = P/A$.

For the special case in which M_b and e are infinitesimal, when the term $\frac{\pi^2 E_t \rho^2}{f_c L^2}$ becomes unity, or $P = \frac{\pi^2 E_t I}{L^2}$, f will become infinite, indicating failure from instability. The curve of this failure will be the Euler-Engesser curve, the outermost curve of the infinite number of curves of f_c versus L/ρ, for the general formula, Eq. 68.

For the special case in which M_b and f_b are zero and e is constant throughout the length, C_e becomes 1.26. With this value the formula becomes practically identical to the secant formula, the series of Eq. 67 becoming practically identical to a secant series.

Many arguments can be advanced as to whether this approach and formula are useful in showing failure above the elastic limit for a material without a sharp knee on its stress-strain diagram. As indicated previously, it certainly becomes less accurate in these regions, except for very small values of M_b and e. In any case, the value of this approach will be similar to the value of the fictitious modulus of rupture in predicting pure bending failure.

The best answer to this question is to compare the general formula with the test results. This procedure has been used for the series of interaction curves in Fig. 14. In doing this, only the values for f_{bo} (the modulus of rupture), the value $f_{co} = 60$ kips per sq in. for average ultimate stress for a short perfect column, and a derived value of E_t for $f_c = 50$ kips per sq in., as given elsewhere,[14] were used; all other points were calculated, using a form of the general column formula, giving "stress" at ultimate loading:

$$f_c + \left(1 - \frac{f_c}{f_{co}}\right) f_{bo} = f = f_c + f_b + \frac{1.050 f_b}{\frac{\pi^2 E_t \rho^2}{f_c L^2} - 1} \quad (69)$$

The left-hand term of Eq. 69 (the "stress" at ultimate loading) is based on the reasoning that, if, for example, f_c is seven twelfths of f_{co}, failure will occur when the total bending stress exceeds five twelfths of f_{bo}. This result is prob-

ably not provable theoretically. Simplifying Eq. 69,

$$f_b = \frac{f_{bo}\left(1 - \frac{f_c}{60}\right)\left[1 - \frac{f_c}{\pi^2 E_t}\left(\frac{L}{\rho}\right)^2\right]}{1 + 0.05\frac{f_c}{\pi^2 E_t}\left(\frac{L}{\rho}\right)^2} \quad \ldots\ldots\ldots\ldots\ldots\ldots (70)$$

Curves plotted from Eq. 70 for $f_{bo} = 120$ kips per sq in., as indicated in Fig. 13 (and also the original[14] Fig. 10), did not check the experimental curves, especially at high eccentricity ratios. Further investigation showed that the experimental curves were plotted incorrectly. From the original source,[42] it can be deduced that the actual modulus of rupture varied from roughly 115 kips per sq in. to 135 kips per sq in., generally increasing with decreasing slenderness ratio and decreasing wall thickness. However, the original investigators[42] concluded that until some definite relationship was found it would be best to ignore this variation and use a constant value of 120 kips per sq in., thus making the experimental failure stresses relatively too high with respect to f_{bo}, and making the experimental curves plotted against this artificial limit err on the unsafe side for low slenderness ratios. Thus, through no fault of the author, the curves in Fig. 14 and Fig. 15 are inaccurate, on the unsafe side, in representing failure of compression tubing loaded transversely at the third points.

Curves were then plotted from Eq. 70 on the basis of a sliding value of f_{bo}, starting at 134 kips per sq in. for $L/\rho = 30$, and decreasing by 2 kips per sq in. for each increase of 10 in L/ρ, making $f_{bo} = 116$ kips per sq in. for $L/\rho = 120$. This very arbitrary variation seemed to fit the small amount of information[42] available concerning f_{bo}. It can be seen that the results, shown in Fig. 23, agree with the experimental curves very well. Discrepancies for $f_b > 96$ should be neglected because there were no tests in this region. The other discrepancies can probably be accounted for by the uncertainty as to f_{bo} and by experimental errors. These are especially large at small eccentricities and high axial loads, where any imperfection of the specimen tends to make experimental results very conservative relative to theoretical results.

Eq. 70 in general nondimensional form would be

$$R_b = \frac{(1 - R_c)(1 - R^2_L)}{1 + (C - 1)R^2_L} \quad \ldots\ldots\ldots\ldots\ldots\ldots (71)$$

in which C is either C_b or C_c as defined previously;

$$R^2_L = \frac{f_c}{f_{cr}} = \frac{\left(\frac{L}{\rho}\right)^2}{\left(\frac{L}{\rho}\right)^2_{cr}} = \frac{\left(\frac{L}{\rho}\right)^2}{\frac{\pi^2 E_t}{f_c}} \quad \ldots\ldots\ldots\ldots\ldots\ldots (72)$$

$$R_c = \frac{f_c}{f_{co}} \quad \ldots\ldots\ldots\ldots\ldots\ldots (73a)$$

[42] "Strength of Tubing Under Combined Axial and Transverse Loading," by L. B. Tuckerman, S. N. Petrenko, and C. D. Johnson, *Technical Note No. 307*, National Advisory Committee for Aeronautics, Washington, D. C., June, 1929, pp. 6–7.

and

$$R_b = \frac{f_b}{f_{bo}} \quad \text{or} \quad \frac{f_s}{f_{bo}} \ldots\ldots\ldots\ldots\ldots\ldots\ldots\ldots (73b)$$

Eq. 71 is plotted for constant e, a truly eccentric column, in Fig. 24. The author's radial lines showing eccentricity are very useful for this type of chart. For Eq. 71 and Fig. 24 they must be plotted for

$$R_e = \frac{R_b}{R_c} = \frac{f_{co}}{f_{bo}} \frac{c}{\rho^2} e \ldots\ldots\ldots\ldots\ldots\ldots\ldots\ldots (74)$$

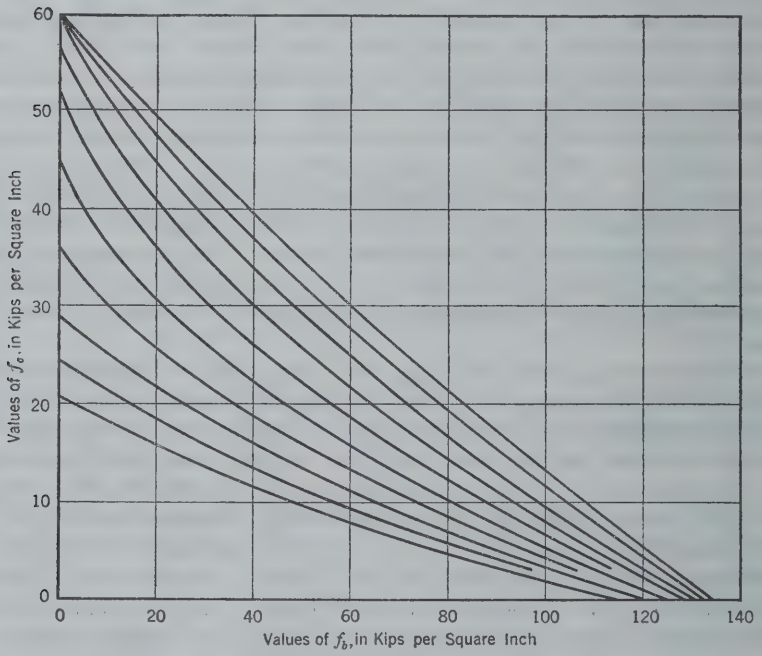

Fig. 23.—Theoretical Interaction Curves for Chrome-Molybdenum-Steel Tubing

Similar diagrams could be plotted very quickly for any one of the values of the constants, C_b or C_e, by computing the ten or more points at $R_e = 0$ required to determine the straight lines for R_L.

Eqs. 71 and 72 support the author's prediction that, since R_L depends upon L/ρ and E_t, the lines of the nondimensional curve (for example, Fig. 24) would change with the value of the exponent n if drawn for L/ρ instead of R_L. Drawn for R_L, the lines are independent of n; and one set of nondimensional lines (such as those in Fig. 24) are good for any column of constant $E\,I$ of any material with a certain type loading (such as the constant e of Fig. 24), within the limitations of the foregoing theory. These include, besides the limitations noted in the foregoing derivation, neglect of variation in tangent modulus (from size, shape, age, temperature, and direction and history of stress), failure in detail, and any imperfection not included in the terms M_b, C_b, e, and C_e.

To use Fig. 24 for a given material, f_{bo}, f_{co}, and the stress-strain curve must be known. Then, opposite each value of R_c should be placed the square of the corresponding maximum slenderness ratio for the material, $(L/\rho)^2_{cr}$, computed from the Euler-Engesser formula (using the stress-strain diagram to obtain E_t). Then, for a given member and load, the allowable e may be found directly. If the member and e are given, R_c must be found by trial and error,

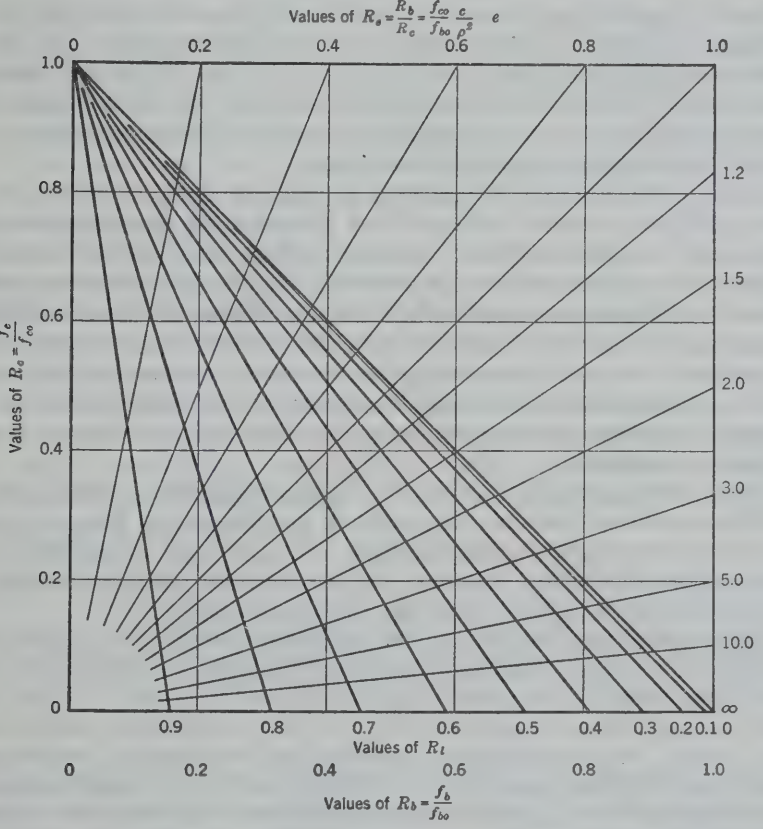

Fig. 24.—Reduced Interaction Lines for Eccentric Longitudinal Loading

two trials usually being sufficient. If the designer uses the concept of the factor of safety traditional to civil engineers, the design must be made on the basis of an ultimate load equal to the working load multiplied by the factor of safety, since f does not vary linearly with P.

Another check of Eq. 70 against experimental results was made, using the remaining data,[14] which was for duralumin tubing loaded in the same manner as the chrome-molybdenum-steel tubing. For these tests the value of the short perfect column strength had to be revised (for reasons similar to those for changing f_{bo} for the chrome-molybdenum-steel tests) to a value estimated at 38 kips per sq in. from the test data. The resulting theoretical and experi-

mental curves did not check as well as the steel curves, the discrepancy being from −4 kips per sq in. to +6 kips per sq in. for values of f_b up to 55 kips per sq in. Even though this difference is well within experimental error,[43] this check of Eq. 70 against experiment is not very strong evidence of its usefulness for materials less elastic than chrome-molybdenum-steel. More evidence, pro or con, is needed.

A second criticism of the paper concerns the envelope equation of Section 5, in which it is stated that this equation could be used as a kind of over-all column curve for any material where weight saving is not too important. In Fig. 11 the envelope equation is plotted along with various standard column formulas, which form a "scatter band," and it is stated that the resemblance of the envelope curve to a parabola shows why parabolic curves have been found useful in representing the short column range.

Actually, the parabolic, straight-line, and Gordon-Rankine-Ritter formulas have applications entirely different from the envelope equation, also their applications are more practical. Any one of these formulas has been set up empirically for columns of a single material and class with a certain probable degree of accidental eccentricity (from warpage, rolling tolerances, accidental damage, and eccentricity from the tolerances of theoretically concentric end connections). On the other hand, the envelope equation applies only to perfect columns made of an infinite variety of materials. Certainly any agreement between the various empirical formulas and the envelope formula is entirely coincidental.

The coefficients of B in Eqs. 26, 27, and 28 actually vary widely from material to material and class to class, even in nondimensional form, to provide for different expectancies of imperfection. Also, the actual coefficients used for carbon steel structural columns, for example, show better agreement between the empirical formulas than Fig. 11 would indicate.[44]

The empirical formulas, easy to use, and taking into account unpredictable eccentricities for a given material and class of columns, will always have great practical value for the purposes for which they were developed. On the other hand, it is hard to see a design situation in which the envelope equation would be of value. For extraordinary materials and eccentricities, experimental results along with the general column equation (using the tangent modulus so ably advocated by the author, and maximum tolerable values of accidental eccentricity) should be used, the generalized Euler equation being a special case of this application.

The fundamental importance of accidental eccentricity to routine column design is illustrated by an example. A "perfect" 14 WF 202 column, 30 ft long, would take an ultimate load of more than 2,100 kips according to the generalized Euler formula. Taking into account chance eccentricities, the American Institute of Steel Construction (AISC)[45] gives a 3/8-in. "out-of-lineness" rolling tolerance for this column, and it would probably not be too conservative

[43] "Strength of Tubing Under Combined Axial and Transverse Loading," by L. B. Tuckerman, S. N. Petrenko, and C. D. Johnson, *Technical Note No. 307*, National Advisory Committee for Aeronautics, Washington, D. C., June, 1929, p. 7.

[44] "Resistance of Materials," by Fred B. Seely, John Wiley & Sons, Inc., New York, N. Y., 3d Ed., 1947, p. 229.

[45] "Steel Construction," AISC, New York, N. Y., 5th Ed., 1947, p. 285.

to add a constant e of 1/8 in. from all other causes. Using the general column formula with $f_{bo} = f_{co} = 40{,}000$ lb per sq in., the ultimate load is about 1,420 kips. The allowable load on this column, using the parabolic formula in the 1946 AISC specifications,[46] equals about 784 kips, which when multiplied by the usual factor of safety[47] of about 1.8 agrees roughly with the foregoing result of 1,420 kips.

E. C. HARTMANN,[48] M. ASCE.—No structurally-minded engineer can read Mr. Shanley's excellent paper without finding much to stimulate his thinking, especially with regard to the significant part of the stress-strain curve for metals which lies above the range of purely elastic action. In his usual, clear, concise, and nonmathematical manner Mr. Shanley has covered some rather complicated concepts in a way which makes them more understandable, thus setting a good example to other engineering authors who do not always qualify for words of praise along these lines.

In the section of his paper dealing with the effects of eccentricity, Mr. Shanley has confined his attention to those members which fail in the plane of the applied bending moment. It might be well to point out that there is another classification of members, such as I-beams and H-beams, which may tend to fail at right angles to the plane of the applied moment, thus complicating the problem beyond that which is covered in Mr. Shanley's treatment. If an I-beam, for example, is loaded to failure as a column with the end load applied in the plane of the web, but eccentric with regard to the centroid, it is highly probable (assuming no local buckling) that the I-beam will fail by buckling in a direction at right angles to the plane of the web.

The problem of the lateral buckling of eccentrically loaded I-shaped and H-shaped columns is not an academic one in civil engineering practice and deserves more attention than it has received in the past. Among those who have contributed are S. Timoshenko[49] in 1936; Bruce Johnston,[50] M. ASCE, in 1941; and H. N. Hill, Assoc. M. ASCE, and J. W. Clark,[51, 52] Jun. ASCE, in 1948.

F. R. SHANLEY.[53]—The discussions of this paper by a number of experts have been most interesting and have contributed greatly to the knowledge of the subject. Most of the comments were of a constructive nature and were clearly presented. The writer wishes to thank the discussers collectively.

During the time that has elapsed since the preparation of the paper in the

---

[46] "Steel Construction," AISC, New York, N. Y., 5th Ed., 1947, p. 64.

[47] "Standard Specifications for Highway Bridges," A.A.S.H.O., Washington, D. C., 5th Ed., 1949, p. 242.

[48] Chf., Eng. Design Div., Aluminum Research Laboratories, Aluminum Co. of America, New Kensington, Pa.

[49] "Theory of Elastic Stability," by S. Timoshenko, McGraw-Hill Book Co., Inc., New York, N. Y., 1936, p. 243.

[50] "Lateral Buckling of I-Section Column with Eccentric End Loads in Plane of the Web," by Bruce Johnston, *Transactions*, A.S.M.E., Vol. 63, 1941, p. A-176.

[51] "Alcoa Structural Handbook," Aluminum Co. of America, Pittsburgh, Pa., 1948, p. 57.

[52] "Lateral Buckling of Eccentrically Loaded I-Section Columns," by H. N. Hill and J. W. Clark, *Proceedings-Separate No. 84*, ASCE, October, 1950.

[53] Prof., Univ. of California, Los Angeles, Calif.; Consultant, The Rand Corp., Santa Monica, Calif.

summer of 1947 a number of significant developments has occurred. Some of these have a bearing on the questions raised in the discussions and will therefore be mentioned briefly.

Mr. du Plessis mentions the case of a reinforced concrete column which bent gradually under heavy load and had to be supported laterally. This was evidently a case of instability as a result of compressive creep, a phenomenon which has been of some concern to the writer. Several years ago some experiments were made (at Lockheed Aircraft) in which a plastic (lucite) column, at room temperature, was subjected to a steady load equal to approximately two thirds of the buckling load determined under ordinary testing machine conditions. Careful measurements of lateral bowing showed a small but gradual increase over a period of several months; sudden buckling then occurred, with practically no warning.

Investigation of this phenomenon has since been under way by the writer and his associates at the Rand Corporation. Thomas Higgins has developed a method of predicting the deflection-time curve, using a procedure similar to that by which Theodor von Kármán,[4] Hon. M. ASCE, treated the eccentric column in the inelastic range. Creep curves were used as a basis, instead of the usual stress-strain diagram. Tests made at Battelle Institute, in Columbus, Ohio, show that column failure may occur under steady load at some time after initial application, the length of time depending on the average compressive stress, slenderness ratio, and temperature. It is of interest to note that complete collapse usually occurs before the bowing exceeds the core radius by any appreciable amount.

Mr. Karol's discussion of the interaction curves for combined bending illustrates how these curves can be derived by applying well known principles, and how they are related to the secant-modulus formula. This type of analysis may be useful in reducing the number of tests needed to establish the curves; however, the writer recommended the interaction curve method primarily because its simplicity permits the investigator to determine, with relatively few tests, the actual curves for various cross sections and materials. This seems to be important for members of complex cross section in which local buckling or other forms of instability may play a part.

It should be noted that an interaction formula is used for combined bending and compression in the manual[54] of the American Institute of Steel Construction. If secondary bending is not included in the computation of the bending stress, the formula would be represented by a straight line in Fig. 15, indicating unsafe values for slenderness ratios much greater than 40.

Mr. Popov states that the Ramberg-Osgood formula does not adequately represent the stress-strain diagram for some materials (such as ordinary steel), and that the writer's argument, to a large extent, "* * * rests on the adequacy of the empirical algebraic relation selected * * *." On the contrary, the

[54] "Steel Construction," AISC, New York, N. Y., 5th Ed., 1947, p. 284.

mathematical formulation of the stress-strain diagram should be regarded only as a convenience to be used when applicable. It was, perhaps, misleading to use the mathematical curves in presenting the nondimensional column curves. Any column curve or formula may be presented in this manner. In actual practice the tangent-modulus column curve is usually determined directly from the stress-strain diagram for the material.

Mr. Sawyer's remarks on the original data from which Figs. 14 and 15 were derived are important in connection with any attempt to apply a theoretical analysis to the interaction curves. As previously stated, however, these curves were presented only to illustrate the method and were labeled unsafe (see Section 7) for general use.

The writer certainly did not mean to add another column equation to the long list of empirical and semi-empirical equations. The remarks on the possible use of the envelope equation were intended to emphasize the point that all types of stress-strain curves would be safely covered by such an equation, if the value of f_o were defined as indicated.

Mr. Hartmann's remarks reveal another class of eccentric columns in which an additional interaction phenomenon must be considered—namely, the interaction between the eccentric bending moment in one principal plane and the induced or secondary bending moment in the other principal plane. Perhaps some of the analytical methods presented in the other discussions could be extended to include this unsymmetrical bending phenomenon, but one solution would be to find some interaction curves by actual tests. It might then be possible to convert the eccentric bending moment in one plane to an equivalent (reduced) bending moment in the other. From a practical point of view, however, the use of the straight-line interaction curve previously mentioned[54] might suffice, since the "sag" of the curves would probably be reduced. The lowest values of the allowable axial loads or bending moments thus obtained would of course be used.

In closing this discussion the writer would like to emphasize the importance of defining the level at which the analysis or investigation takes place. The most frequent criticism of the tangent-modulus theory is a statement to the effect that there is no such thing as a perfect column. Such a criticism can be applied to any scientific theory, since all such theories are based on idealizations or abstractions.[55] The only thing that can be discussed intelligently is the degree of abstraction involved and its relation to the actual phenomenon, which can never be completely described by words or equations.

In this paper the emphasis was on the application of the column theory in structural engineering. It was shown that an accurate estimate of the buckling load can easily be obtained from the compressive stress-strain diagram. A simple engineering method for reducing this load to account for eccentric loading was developed. Simple methods of reducing test data to standard

[55] "Science and Sanity," by Alfred Korzybski, Science Press, Lancaster, Pa., 3d Ed., 1948, p. 434.

values were presented. It is possible to move in either direction from this level. On the one hand, empirical equations may be fitted to the resulting curves, perhaps for handbook or specification purposes. On the other hand, one may attempt to analyze the action of the eccentric inelastic column in a detailed scientific manner.[56] Confusion of these levels of abstraction can lead only to arguments that have no end and delay real progress. The writer hopes that this paper will help to eliminate some of the confusion which seems to have surrounded the column problem for so many years.

[56] "Inelastic Column Buckling," by Tung-Hua Lin, *Journal of the Aeronautical Sciences*, March, 1950, p. 159.

Reprinted from JOURNAL OF THE AERONAUTICAL SCIENCES
Copyright, 1950, by the Institute of the Aeronautical Sciences and reprinted by permission of the copyright owner
April, 1950 Volume 17, No. 4

Analysis and Design of Stiffened Shear Webs

PAUL H. DENKE*

Douglas Aircraft Company, Inc.

Abstract

A simplified graphical solution of a previously published elastic energy analysis of shear panels is presented. Comparison is made between the results of the analysis and experimental data, and satisfactory agreement is found. A qualitative description of the failure of flat and curved shear panels is given, together with an example of the stress analysis of flat panels. It is concluded that a rational, easily applied, and satisfactorily accurate method has been developed for determining the stress distribution in stiffened shear webs. It is expected that future development, some of which has already taken place, will permit the prediction of ultimate loads not only for thin web beams but also for curved panels typical of wing and fuselage structure.

Introduction

The present paper provides a simplified graphical solution of a previously published shear panel analysis.[1] It also gives a comparison with test data and shows some of the applications in stress analysis and design. The previous paper presented a mathematical solution of the problem, but the results were not in a form suitable for practical calculation. This difficulty has been remedied through the discovery of a means of graphical presentation of the important variables.

The experimental comparison is with the N.A.C.A. data on diagonal tension beams.[2] Other experimental studies of the stress distribution in shear panels are available, but time did not permit a critical comparison with all. Agreement with test data is satisfactory in most cases, and such discrepancies as exist can probably be explained on the basis of difficulties involved in the testing technique.

The section on engineering applications is necessarily limited for lack of space, but it is hoped that the discussion given will serve as the basis for further development. It is deemed advisable, at present, to avoid particularizing too much with regard to the estimation of ultimate shear loads, because these depend on the detail design of the panel which varies a great deal among the various air-frame manufacturers. Greatest emphasis is therefore laid on the determination of the stresses existing in various portions of the panel for a given shear load. Whether or not these stresses will cause failure in any of the panel components requires additional correlation between analysis and test results.

Presented at the Structures Session, Annual Summer Meeting, I.A.S., Los Angeles, July 21–22, 1949.

* Structures Engineer.

Historical Survey

The following brief outline is not meant to be exhaustive but is intended only to trace the growth of the principal methods of shear panel analysis so far proposed.

Immediately after the publication of Wagner's classical treatise on the pure tension field,[3] it became clear that the assumption of zero diagonal compressive stress was entirely too conservative, even though it did provide a clear qualitative understanding of the behavior of thin-web beams in shear. In order to avoid this difficulty, three principal methods of analysis or design arose, of which the first was the purely experimental approach whereby components such as spar webs, wing panels, or fuselage panels were tested to destruction. This is the soundest means of determining the strength of a shear panel, provided suitable testing methods are employed. However, it is expensive and time-consuming and is not well adapted to certain purposes, such as the systematic search for optimum panel proportions, because of the large number of variables involved. Moreover, the experimental inaccuracies that inevitably creep in make it advisable to have on hand an analysis method that can serve as the basis for interpreting test results.

The second approach was through the modification of the Wagner equations. This was accomplished most simply by assuming that the principal diagonal compressive stress was not zero but constant and equal to its value at the critical buckling load. Analyses of this type have been developed by Langhaar,[4] Sechler and Dunn,[5] Niles and Newell,[6] Bruhn,[7] and others. These methods also tend to be conservative because many webs buckle at a negligible fraction of their ultimate strengths, and the computed diagonal compressive stresses, assumed constant after buckling, are therefore too small.

A more realistic modification of the Wagner equations was proposed by Kuhn.[8] In his analysis, the fraction of the shear load carried in diagonal tension is assumed to be given by an empirically determined function of the shear stress. The remainder of the load is carried as in a shear-resistant web. Since the various empirical constants have been evaluated to fit experimental results, the analysis can be expected to be reliable in the range covered by the test data, provided suitable testing techniques have been employed. The method is not well adapted to the analysis of heavy webs, since it provides

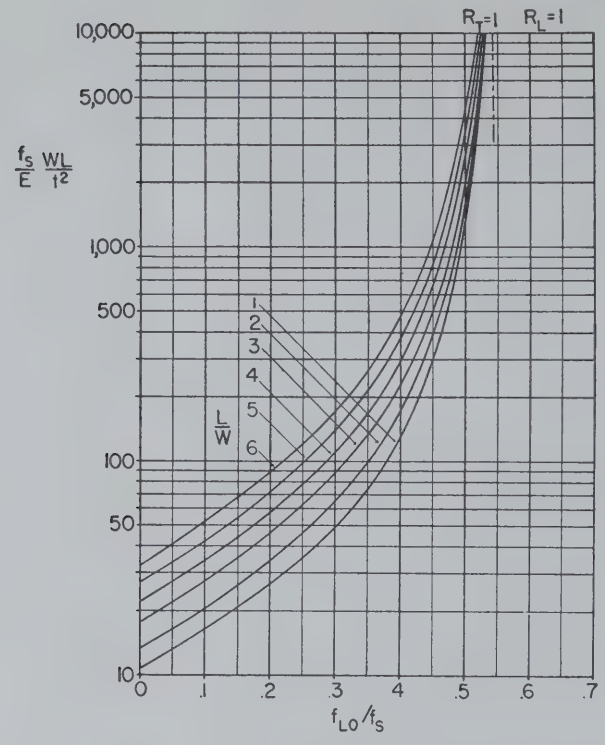

FIG. 1. Average web longitudinal tensile stress.

no means of computing the bending loads imposed on the stiffeners by the buckled sheet.

The third approach to the shear panel problem was simply to make use of established mathematical procedures to determine a reasonably close approximation to the true distribution of stress existing in the web and its stiffening elements. The mathematical instrument usually employed was the principle of virtual displacements, or minimum potential energy, various forms of which were developed by Rayleigh, Ritz, and Galerkin. These methods make use of the well-known expression for the strain energy stored in the buckled web.[10] The first analysis of this type appears to have been that of Kromm and Marguerre,[9] who applied the energy principle to the problem of the infinitely long shear panel subjected to stresses greater than critical, for the two cases of infinite and negligible transverse and longitudinal stiffening. The mathematical basis of the present paper, first presented in 1943, derives from the work of Kromm and Marguerre, although certain points of procedure are quite different. Recently, Levy and others have published analyses employing the energy method or the equivalent differential equations of von Kármán.

Besides the shear panel analysis, the writer has on hand certain unpublished investigations into the behavior of long, flat, and curved panels subjected to combined shear and compression.

Nomenclature

In the following discussion, "longitudinal" and "transverse" refer, respectively, to the long and short dimensions of the panel. Thus, web stiffeners on a thin-web beam are longitudinal stiffeners if they are closer together than the flanges; otherwise, they are transverse. On a fuselage panel the longerons are ordinarily closer together than the frames. The longerons are therefore longitudinal stiffeners, and the frames are transverse stiffeners.

NOTATION

The notation of reference 1 has been revised as follows:

W = panel width free to buckle, in.
L = panel length free to buckle, in.
t = web thickness, in.
f_s = average web shear stress, lbs. per sq.in.
E = effective web modulus of elasticity, lbs. per sq.in.
E_L = effective longitudinal stiffener modulus of elasticity, lbs. per sq.in.
E_T = effective transverse stiffener modulus of elasticity, lbs. per sq.in.
A_L = longitudinal stiffener cross-sectional area, sq.in.
A_T = transverse stiffener cross-sectional area, sq.in.
I_L = longitudinal stiffener moment of inertia, in.^{4}
I_T = transverse stiffener moment of inertia, in.^{4}
R_L = longitudinal stiffening ratio
R_T = transverse stiffening ratio
f_L = web average longitudinal tensile stress, lbs. per sq.in.
f_T = web average transverse tensile stress, lbs. per sq.in.
$\bar{\sigma}_1$ = web average diagonal tensile stress, lbs. per sq.in.
$\bar{\sigma}_2$ = web average diagonal compressive stress, lbs. per sq.in
W_L = longitudinal stiffener local bending load, lbs. per in.
W_T = transverse stiffener local bending load, lbs. per in.
M_L = longitudinal stiffener local bending moment, in.lbs.
M_T = transverse stiffener local bending moment, in.lbs.
G_s = panel secant shear modulus = f_s/γ_0, lbs. per sq.in.
γ_0 = average panel shear strain

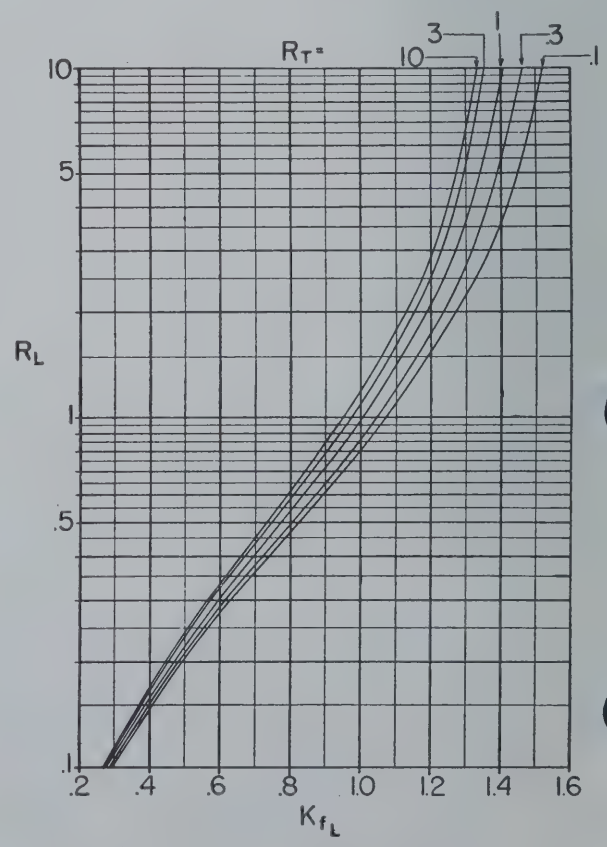

FIG. 2. Longitudinal tensile stress correction factor.

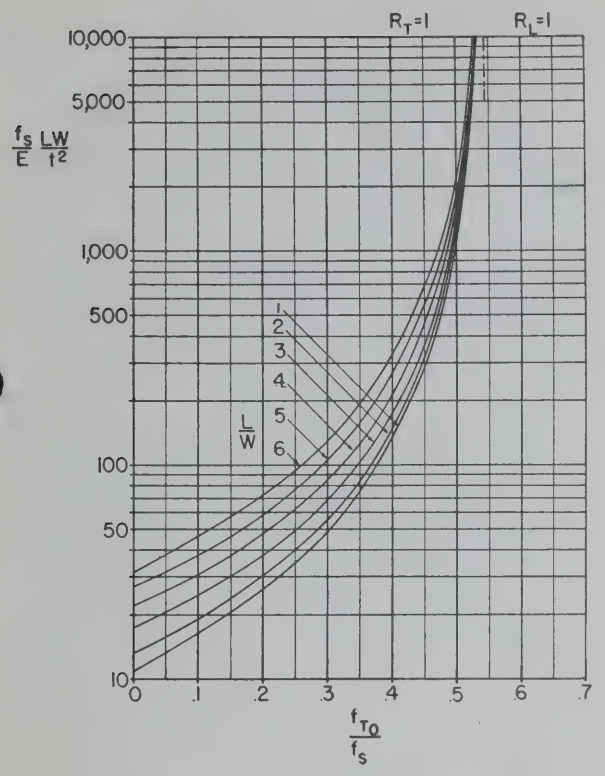

FIG. 3. Average web transverse tensile stress.

A_{L_s} = effective longitudinal stiffener area, sq.in.
ρ = stiffener radius of gyration, in.

GRAPHICAL PRESENTATION OF THE SHEAR PANEL ANALYSIS

The graphical method discussed in this section was developed in collaboration with D. M. Conner, of Douglas Aircraft. Mr. Connor also contributed to the section on the qualitative behavior of shear panels. Acknowledgment is likewise made to S. Noskoff from whose computations the design charts were constructed.

The four basic independent dimensionless groups involved in the analysis are the stress ratio $f_sWL/(Et^2)$, the panel aspect ratio L/W, and the transverse and longitudinal stiffening ratios R_T and R_L. The effect of the quantity R_Q of reference 1, which relates to the bending flexibility of beam flanges, is accounted for in a later paragraph by modifying R_T and R_L in order to avoid introducing a fifth or sixth independent variable. It is therefore necessary to plot the important panel stresses, such as the diagonal tensile stress $\bar{\sigma}_1$, as functions of four independent variables. In general, these are too many to plot, and the mathematics gives no clue as to how matters can be simplified.

However, it is found by calculation that the various panel stresses can be plotted as functions of the stress ratio and the panel aspect ratio for $R_T = 1$ and $R_L = 1$. The effect of the actual panel stiffening can then be accounted for by means of a multiplicative factor K, which is a function of R_T and R_L. In all cases, the ratio of the desired stress to some power of the shear stress is plotted rather than the stress itself, in order that the curves shall have asymptotes (see Figs. 1 to 17). As a result, it is possible to estimate values closely, even when they run off the curve sheet, and this happens only rarely because of the logarithmic scale for $f_sWL/(Et^2)$. The associated K factor is simply the ratio of the asymptotic value of the function for the given stiffening ratios R_T and R_L to its asymptotic value for $R_T = 1$ and $R_L = 1$. An example of the use of these charts is given in a later section.

The following quantities are presented graphically: f_L, f_T, $\bar{\sigma}_1$, W_L, W_T, M_L, M_T, and G_e. Most of the important panel loads and stresses are thus represented, and the remaining ones can be obtained by straightforward calculation. It was not found possible to plot the depth, length, and angle of the web buckles in simple fashion, but these are not ordinarily required in analysis. However, further investigation may disclose a means of plotting these quantities also.

The charts are based on a value of Poisson's ratio equal to 0.33.

It has been found that, by comparison with calculations made from the original analysis, the panel stresses obtained graphically are given to slide-rule accuracy. The charts therefore comprise a solution of the mathematical analysis complete and accurate enough for engineering purposes.

COMPARISON WITH TEST DATA

The stiffener stresses for the beams of series I, II, and III of reference 2 were computed and compared with

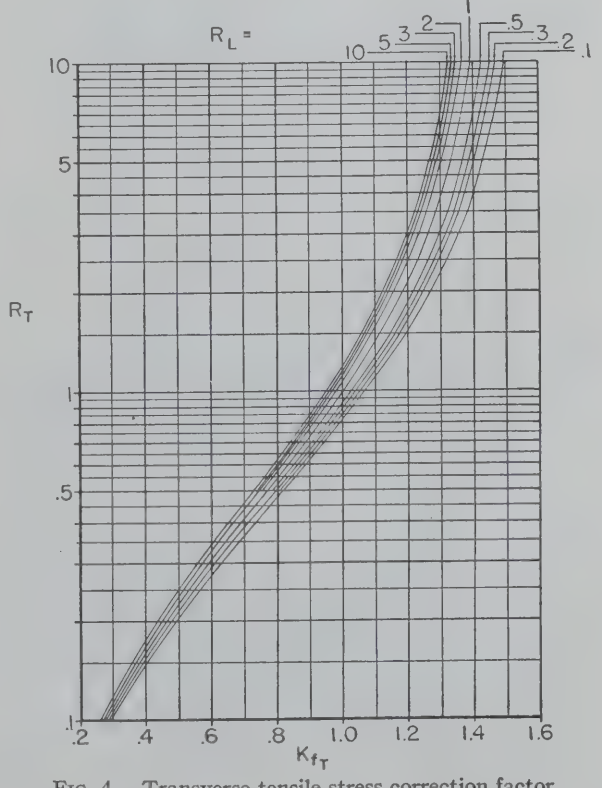

FIG. 4. Transverse tensile stress correction factor.

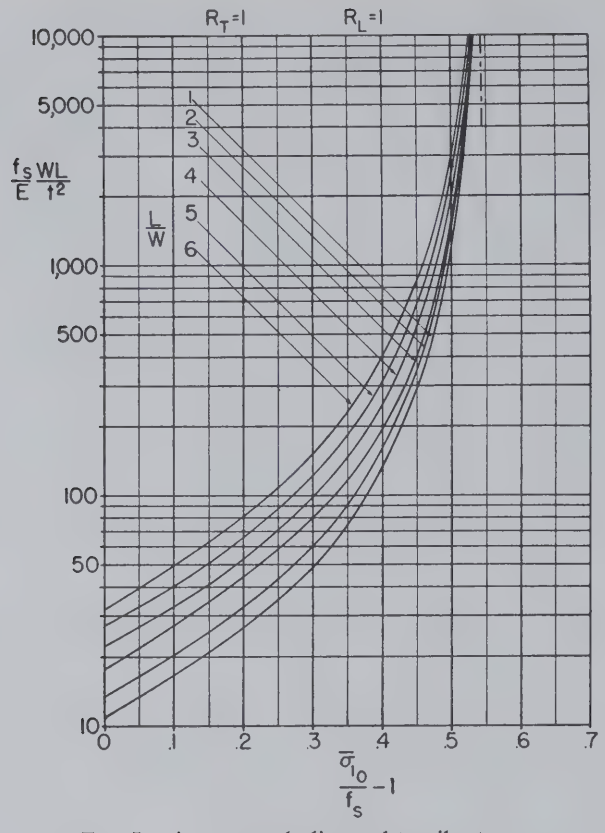

FIG. 5. Average web diagonal tensile stress.

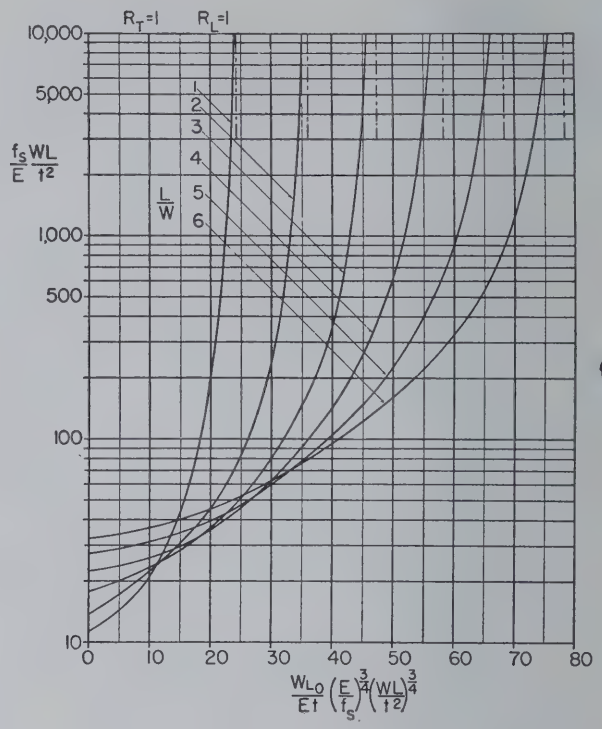

FIG. 7. Longitudinal stiffener local bending load.

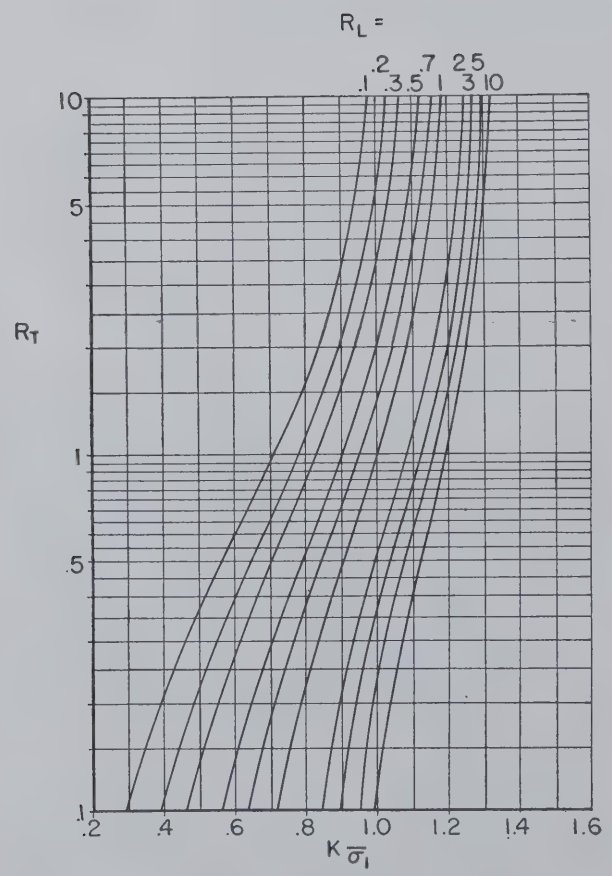

FIG. 6. Diagonal tensile stress correction factor.

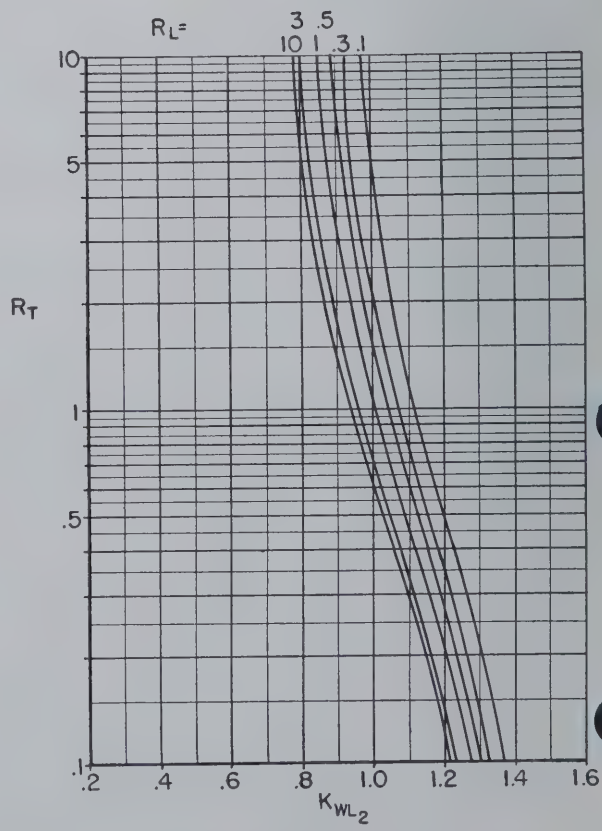

FIG. 8. Longitudinal stiffener local bending load correction factor.

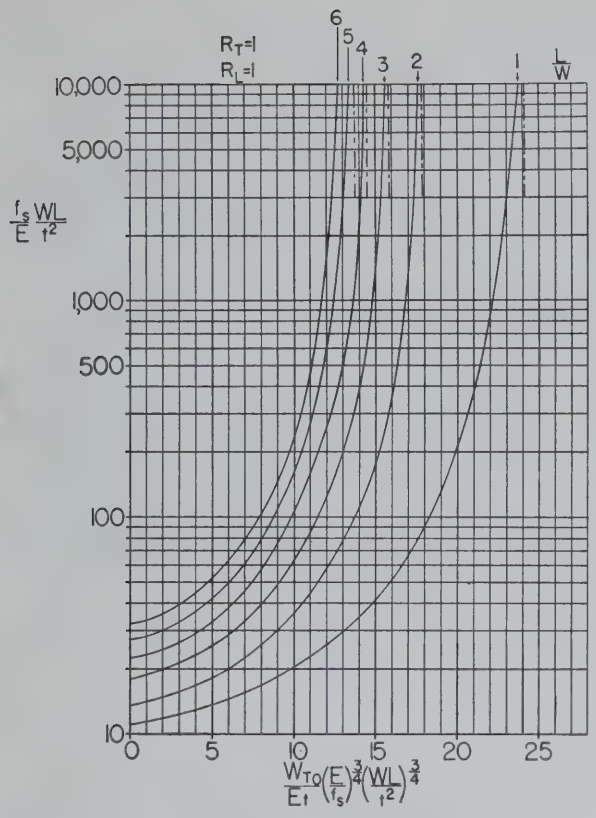

FIG. 9. Transverse stiffener local bending load.

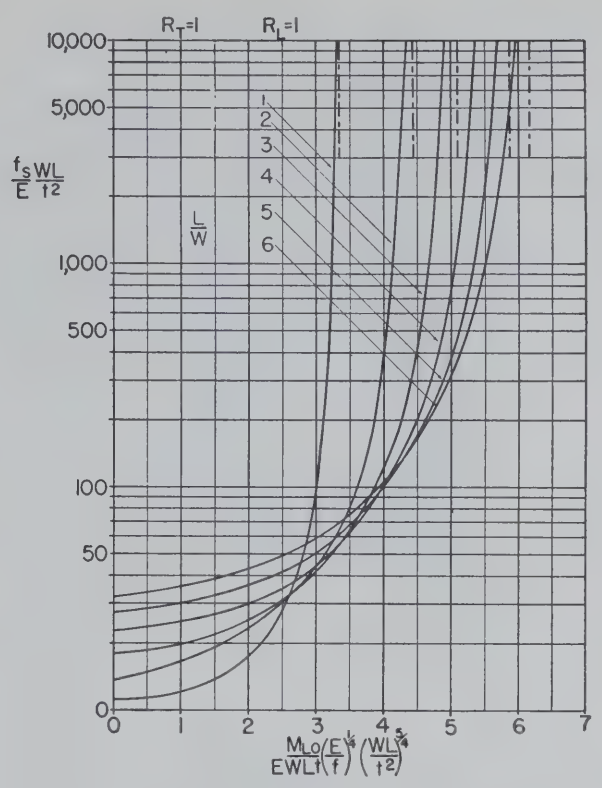

FIG. 11. Longitudinal stiffener local bending moment.

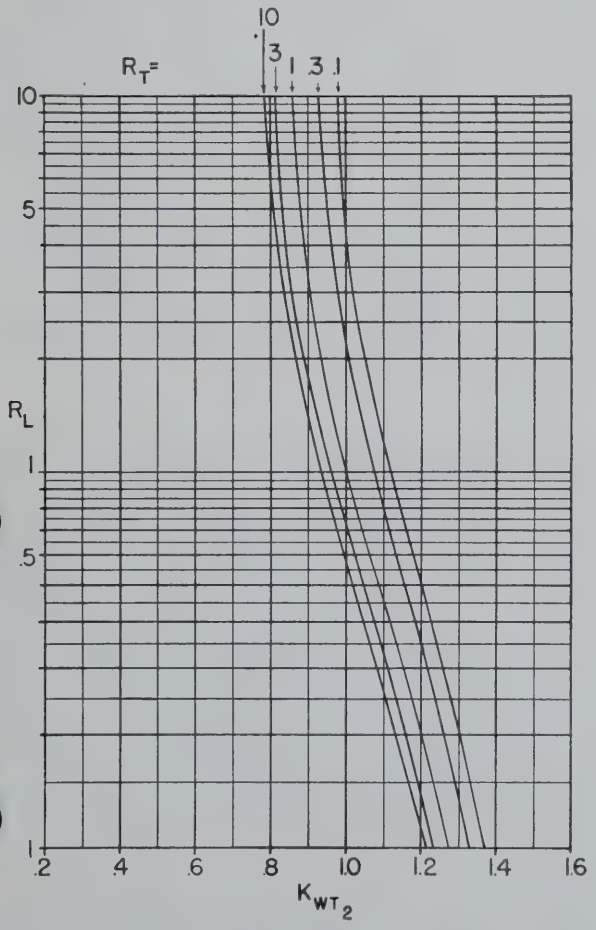

FIG. 10. Transverse stiffener local bending load correction factor.

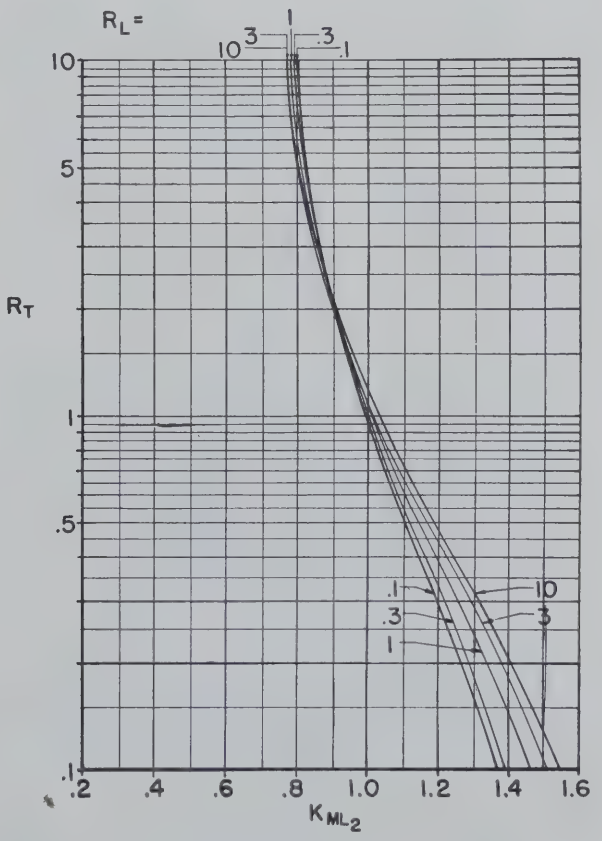

FIG. 12. Longitudinal stiffener local bending moment correction factor.

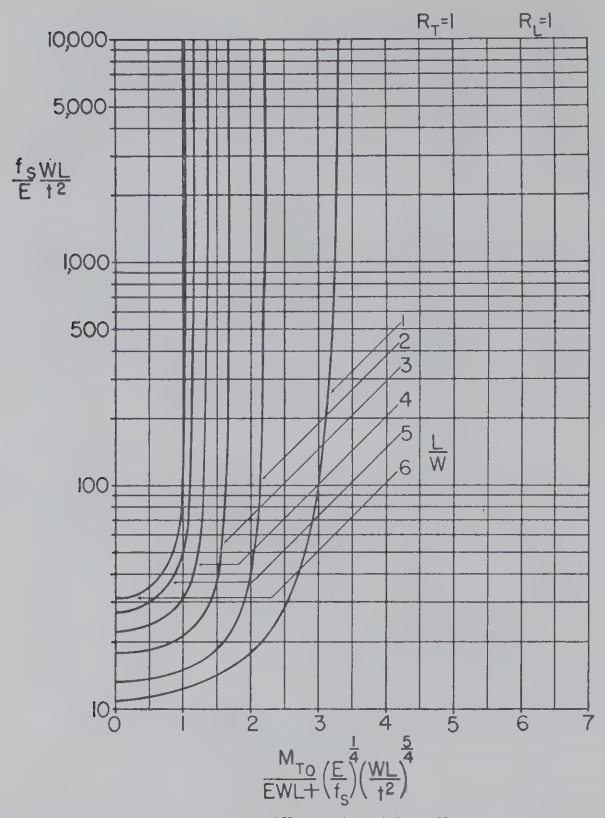

FIG. 13. Transverse stiffener local bending moment.

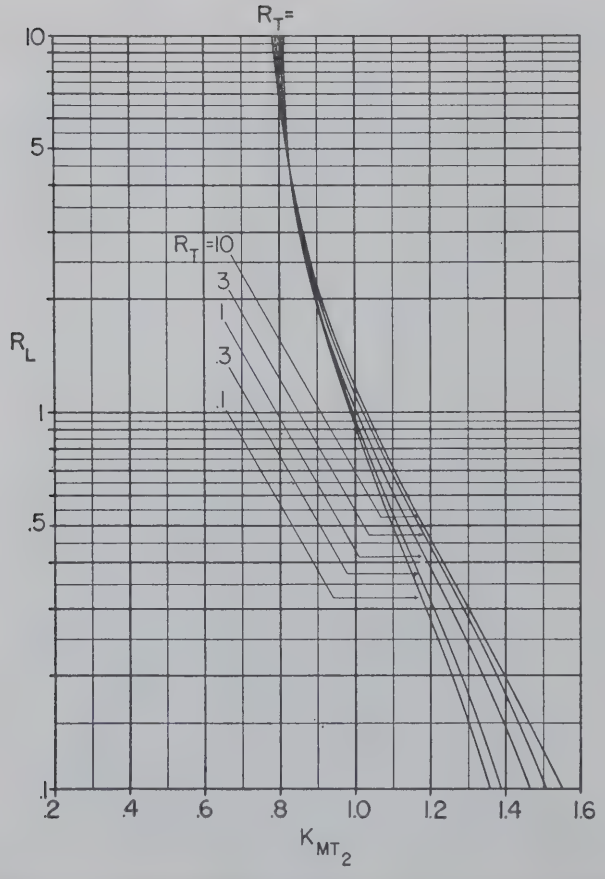

FIG. 14. Transverse stiffener local bending moment correction factor.

the test results, as shown in Figs. 18, 19, and 20. The method of computation is similar to the example given in a later paragraph. However, in the case of beams having stiffeners on one side of the sheet only (these are denoted by "S" in the beam code number), it was necessary to account for the fact that test stresses were measured only on the leg of the stiffener attached to the sheet, so that bending stresses were not eliminated. The correction was made according to the simple theory of flexure.

It should be noted that the computed stiffener stress is due only to the axial load introduced by the buckled web plus the bending due to the fact that the web is eccentric with respect to the stiffener. However, the range of test scatter indicates that extraneous stresses have affected the measurements. These additional stresses may be due to stiffener column action, stiffener torsional instability, or lateral loads imposed on the stiffener by the buckled web. However, the method of the present paper indicates that the web wrinkles produce small bending moments in the stiffener. If it be assumed that these moments are resisted only by the leg of the stiffener attached to the web, it is still only possible to account for a portion of the observed scatter.

In an effort to eliminate the extraneous stresses, the strain gage readings were averaged up and down the length of the stiffener.[2] But it does not follow that the resulting average would represent the sum of the compressive plus eccentric bending stress, as supposed. Thus, it is not surprising that the largest discrepancies between computed and test results occur for beams with single web stiffeners. (Beams having stiffeners on both sides of the sheet are denoted by "D" in the code number.)

It should be kept in mind in examining Figs. 18, 19, and 20 that no empirically determined functions have entered the analysis at this point, except the experimentally determined variation of effective web modulus with shear stress discussed later.

Analysis and Design

Failure of Flat and Curved Shear Panels

This section is a qualitative description of the behavior of both flat and curved shear panels at failure. It is believed that the present analysis may be applied, with suitable modifications, to curved panels in any case where the stiffening elements are sufficiently close together so that the sheet bounded by them is, for all practical purposes, flat. For example, a fuselage panel having a radius of curvature of 60 in., with longerons 6 in. on center, should come under this classification.

Web Failure

Shear panel webs normally fail through diagonal tension. Although basically simple, the mechanism of

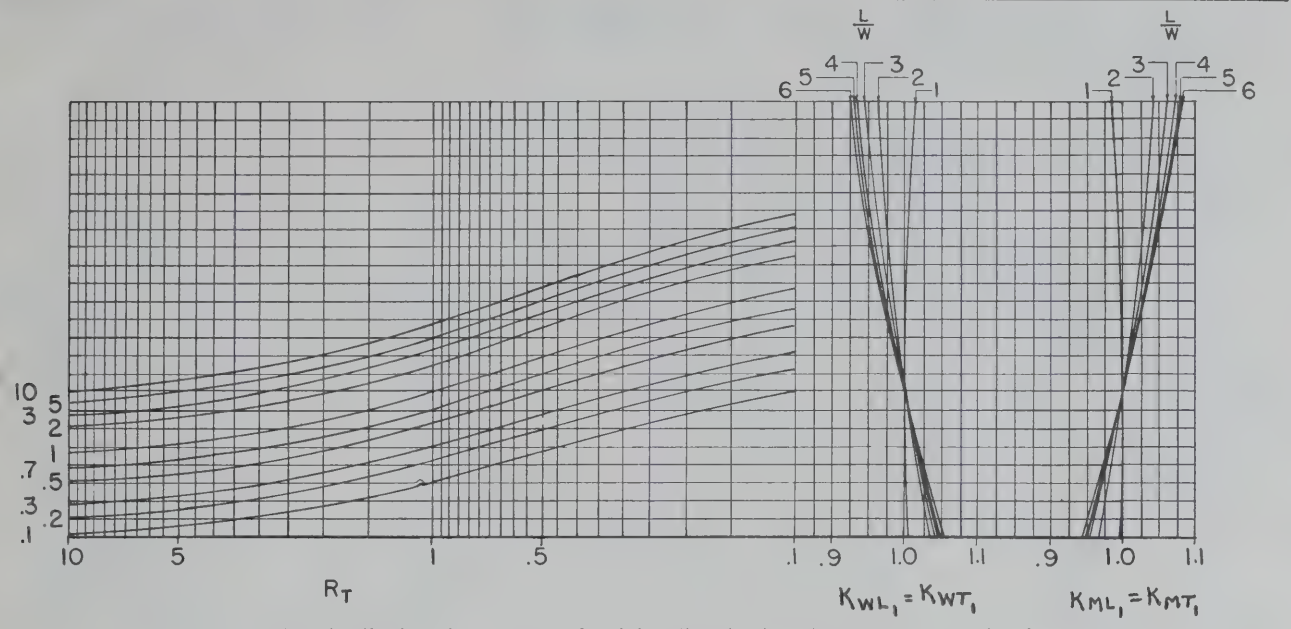

FIG. 15. Longitudinal and transverse local bending load and moment correction factors.

diagonal tension is complicated by the following factors: (1) The diagonal tensile stress is not uniform but, in the ideal web, tends to be maximum at the center and minimum at the edges. (2) The effect of wrinkling is to introduce bending stresses that add to the diagonal tension. These stresses likewise vary throughout the web and, in the ideal case, tend to a maximum at the center. (3) In the actual case, the riveted attachment of web to stiffeners produces stress concentrations that cause failure to start at the panel edges. Fig. 21 shows a diagonal tension failure.

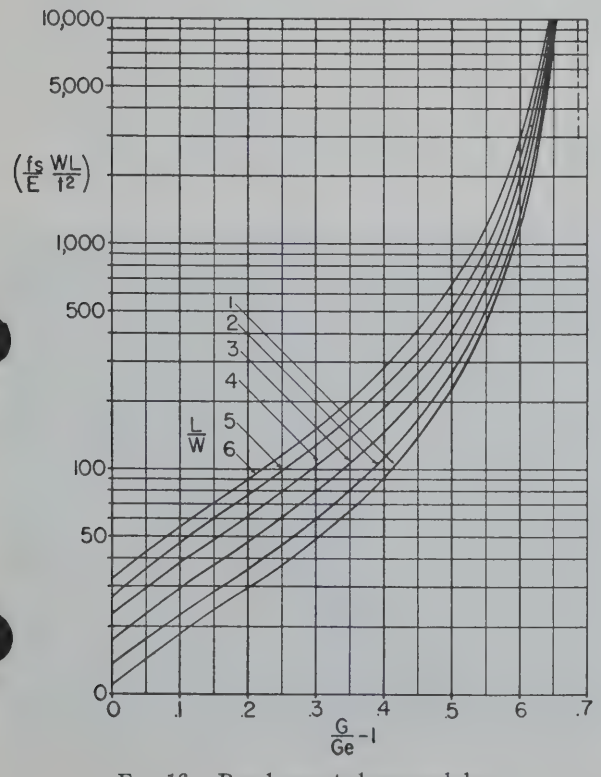

FIG. 16. Panel secant shear modulus.

Stiffener Failure

The term "stiffener" is here used in a general sense and may denote the stiffeners or flanges of a tension field beam, the stringers or ribs of a wing panel, or the longerons or frames of a fuselage panel. The following types of loads contribute to stiffener failure:

(*1*) *Axial Loads.*—In the case of a beam, the longitudinal tensile stress f_L is transmitted into the stiffener,

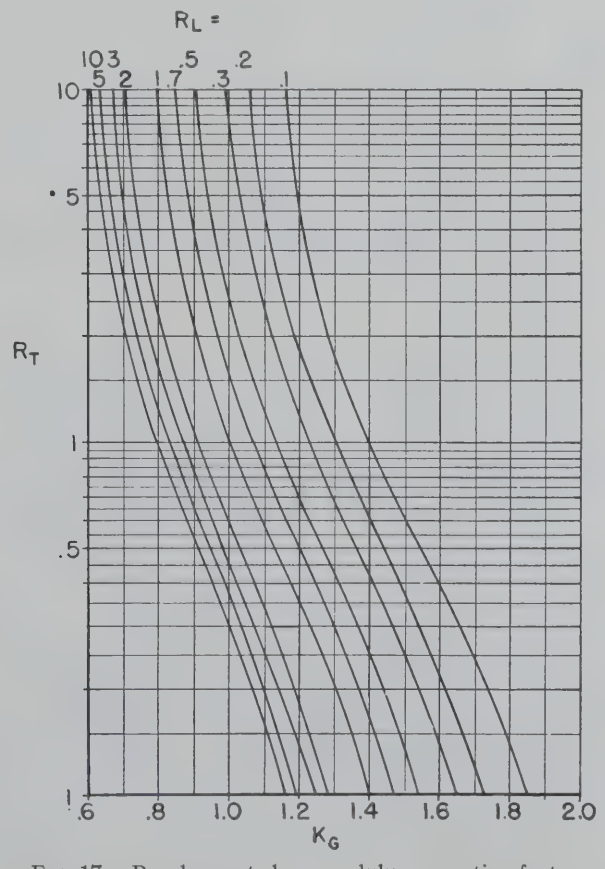

FIG. 17. Panel secant shear modulus correction factor.

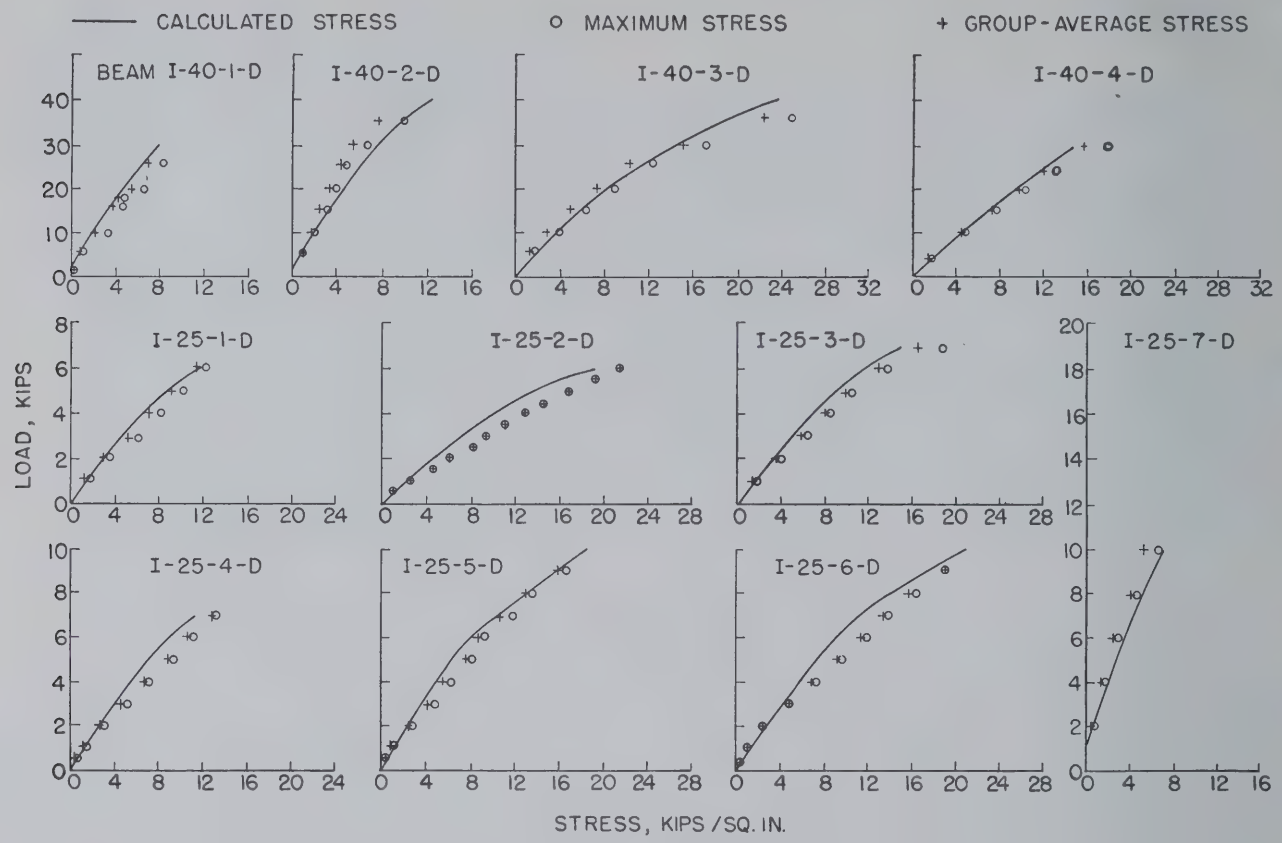

FIG. 18. Stiffener stress vs. shear load. N.A.C.A. beams series I.

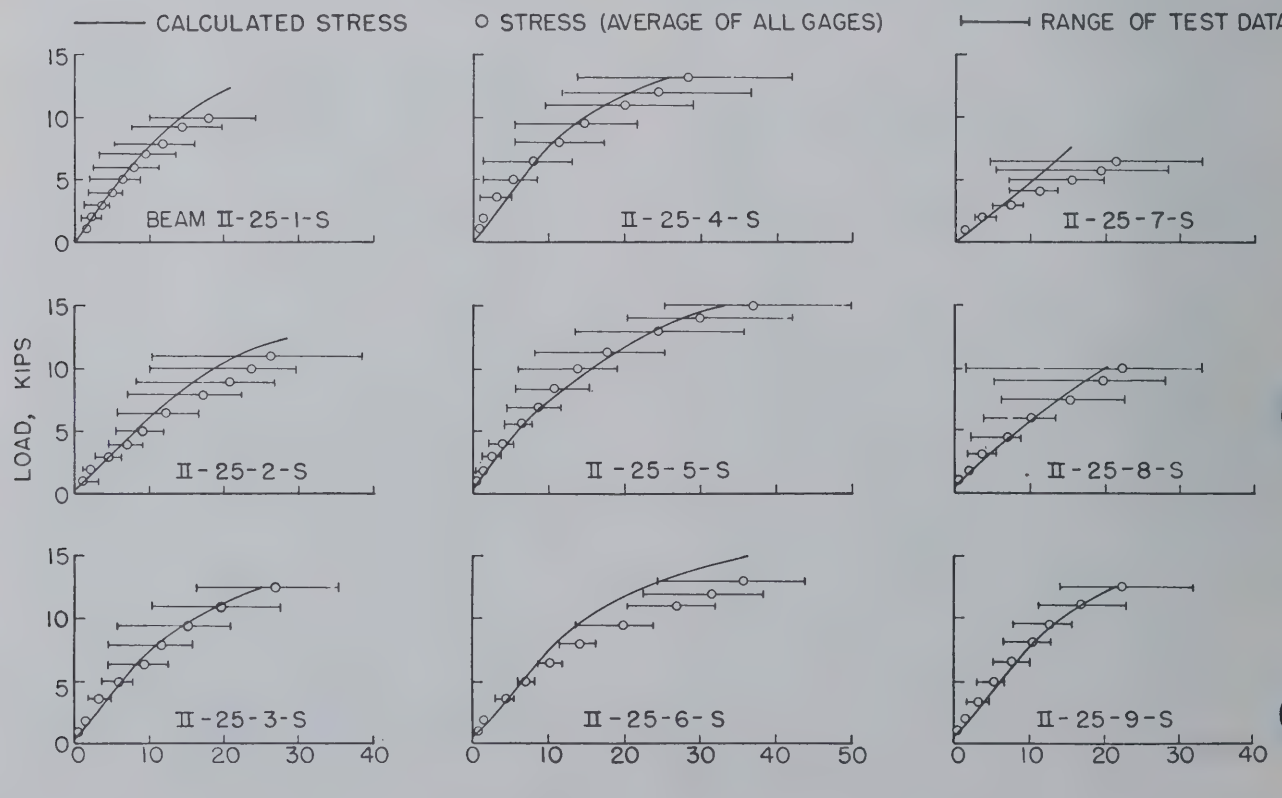

FIG. 19. Stiffener stress vs. shear load. N.A.C.A. beams series II.

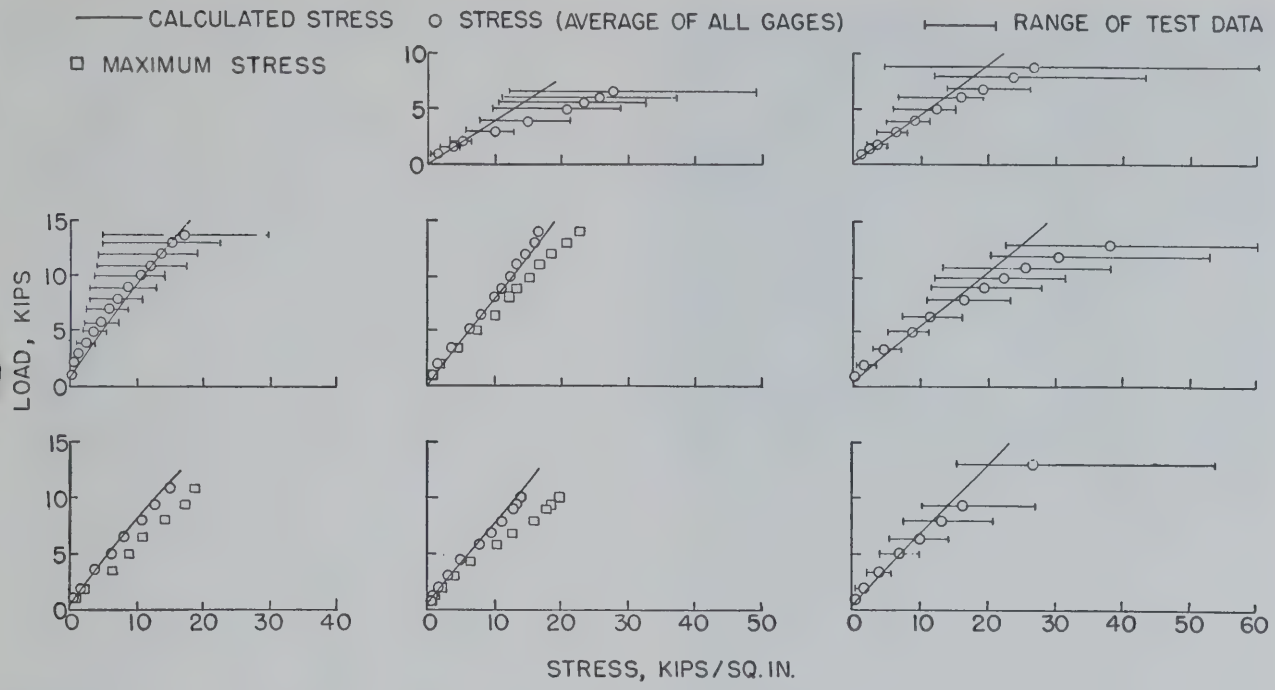

FIG. 20. Stiffener stress vs. shear load. N.A.C.A. beams series III.

producing the compression load P_L, as shown in Fig. 22. A stiffener that failed locally in axial compression is shown in Fig. 23. The transverse tensile stress f_T produces similar loads P_T in the flanges. In the case of a fuselage panel, the transverse tensile stress f_T has an inward component because of curvature, as a result of which radial loads per inch W_G are produced on the stringers (see Figs. 24 and 25), which in turn introduce compressive loads P_f in the frame.

(2) *Eccentric Bending Load.*—Besides producing compressive stress in the stiffener, the load P_L mentioned in reference 1 also introduces bending if the centroid of the stiffener does not lie on the skin line. Thus, in Fig. 26, the stiffener bending moment is $P_L z$.

(3) *Column Action and Torsional Instability.*—Beam stiffeners may have a tendency to fail as columns under the action of the stiffener axial loads. However, there are certain characteristics of shear panel behavior tending to minimize the likelihood of column failure, as is demonstrated by the following argument, which is thought to be valid in the case where the stiffeners are much closer together than the flanges.

Consider the curved stiffener shown in Fig. 27. The curvature may either be built in or be due to the bending effect of the various bending loads, discussed elsewhere, which are imposed upon the stiffener. The curve AB shown in the figure represents the mean deflection of the wrinkled skin, assumed to be the same as the deflection of the stiffener. Assuming that the length of the stiffener is sufficient so that the skin will act as a membrane over the distance AB, it follows that there must be certain distributed loads W_c, as shown, such

FIG. 21. Web diagonal tension failure.

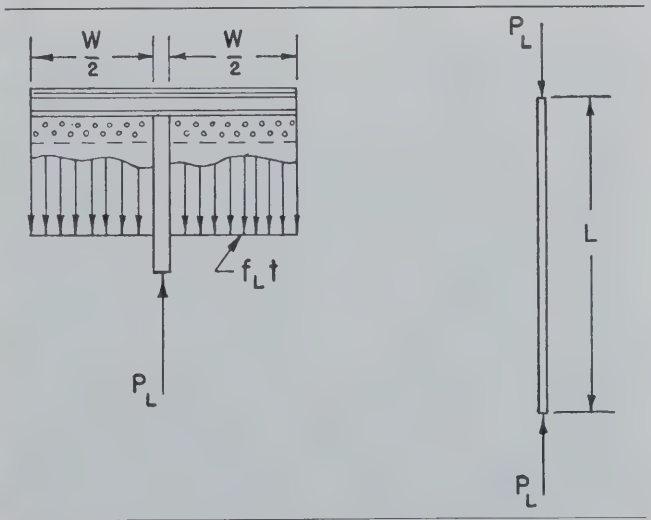

FIG. 22. Stiffener axial load.

FIG. 23. Stiffener axial load failure.

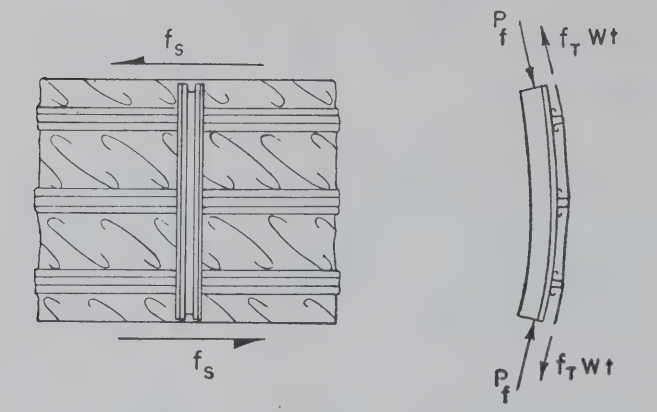

FIG. 24. Curved panel frame loads.

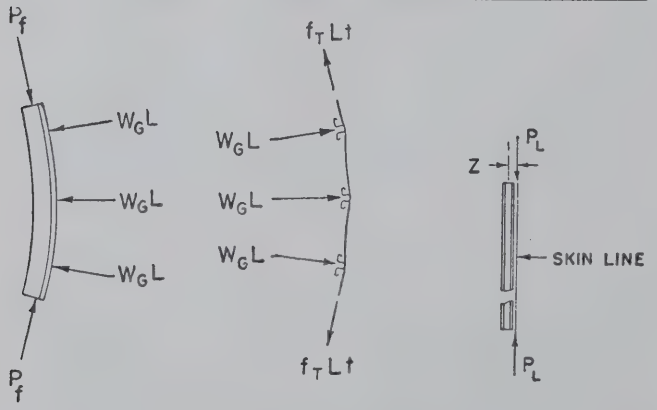

FIG. 25 (*left*). Curved panel frame loads. FIG. 26 (*right*). Stiffener eccentric bending moment.

that the combined bending moment of W_c and P_L about any point of AB is zero. Furthermore, the resultant at any point must be tangent to AB and equal to P_L. In the free-body diagram of the stiffener, CD is the centroidal axis. In this diagram also, the resultant load at any section of the stiffener is tangent to AB and equal to P_L. Consequently the moment about any point of CD due to the load P_L is equal to, but no greater than, $P_L z$. The column effect is therefore negligible.

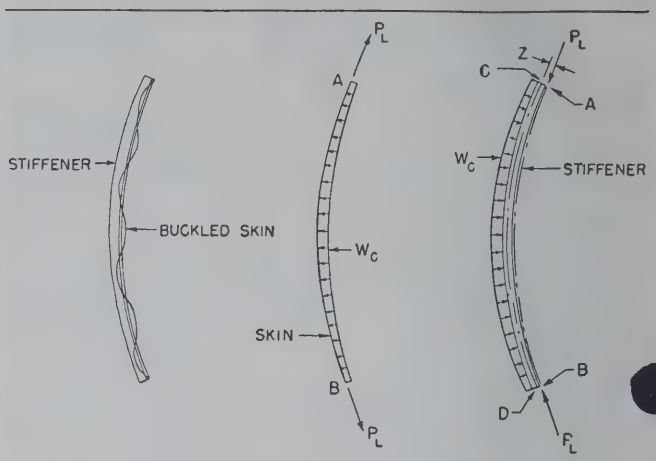

FIG. 27. Stiffener column action.

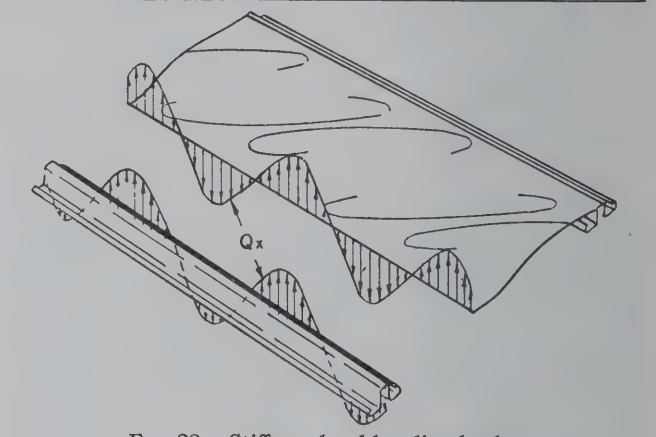

FIG. 28. Stiffener local bending loads.

In the case where the stiffeners are far enough apart to invalidate partially the above argument, because the web no longer bends with the stiffener near the panel center, the transverse tensile stress f_T begins to acquire a component tending to oppose lateral deflection so that the possibility of column failure is again inhibited.

The effect of the tension field in partially supporting the stiffener was first pointed out by Wagner,[3] who accounted for it by using a reduced column length in computing the strength of the upright.

Open section stiffeners on beam webs show a tendency to fail by torsional instability. Whether or not this type of failure is opposed by action of the web is not clear.

(*4*) *Stiffener Secondary Bending.*—The longitudinal and transverse tensile stresses f_L and f_T produce secondary bending stresses in the flanges and end stiffeners of beams. These stresses are of particular importance in the flanges of beams having widely spaced stiffeners.

(*5*) *Local Bending Loads.*—This is the term here used to denote the bending loads imposed on the stringer by the buckling of the web. The effect is illustrated in Fig. 28. The loads per inch Q_x produced on the stiffener are localized and sinusoidal in character. The maxima occur at points where the wrinkle crests intersect the

stiffener. The bending moments produced in the stiffener are in phase with the load. The loading shown in Fig. 28 is due to one panel only. If there are two adjacent panels, then the total stiffener load is the sum of the loads contributed by both panels. The resulting load on the stiffener is designated W_L. The stiffener moments are larger if the two loads are in phase than if they are out of phase. In particular, if the two adjacent panels are identical and equally stressed, then the stiffener moments are maximum if the loads are in phase and identically zero if they are 180° out of phase. Fig. 29 shows a stiffener failure apparently due largely to local bending moments induced by the buckled web.

(6) *General Bending Loads.*—These are the loads imposed on the longerons or curved fuselage panels as a result of the curvature of the tension field and are, in fact, identical with the loads W_G shown in Fig. 25. Reactions are provided by the frames as shown in Fig. 30. The stringer is thus a uniformly loaded continuous beam, with the maximum bending moments occurring at the frames. Fig. 31 shows a curved panel in which the longitudinal stiffeners failed under the action of the general bending load.

(7) *Torsional Loads.*—The local loads imposed on a stringer by two adjacent panels may combine to produce torsion instead of bending. This effect is particularly pronounced where the panels are identical and equally stressed, provided they buckle 180° out of phase as in Fig. 32. Fig. 32 also shows the resulting torsional loads on the stiffener.

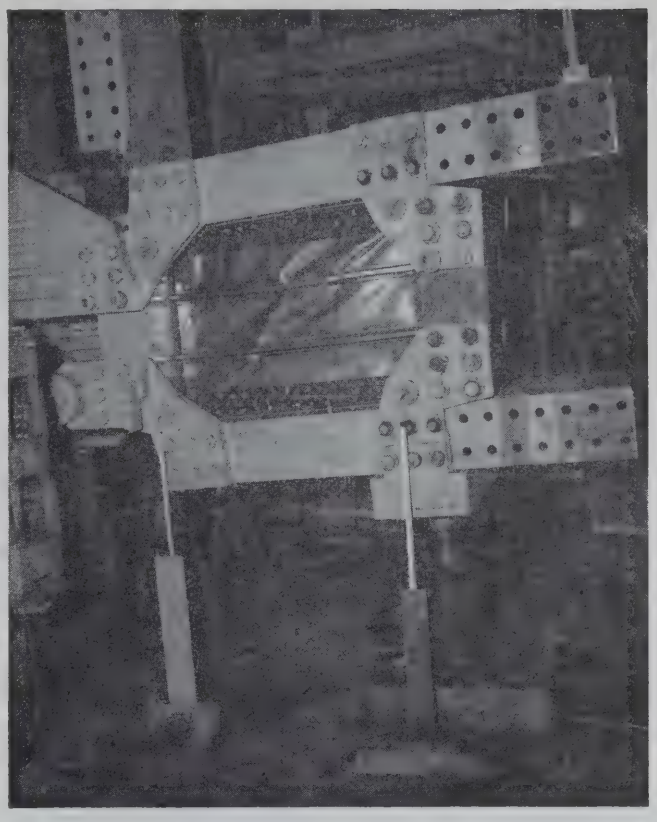

FIG. 29. Stiffener local bending failure.

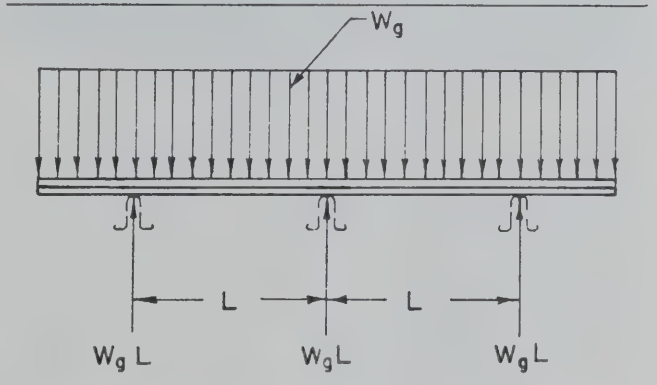

FIG. 30. Curved panel stiffener general bending loads.

Rivet Failure

The following loads contribute to rivet failure:

(1) *Shear Loads.*—The total shear on a transverse riveted seam or attachment is found by vectorially adding the stresses f_s and f_L. On a longitudinal seam or attachment, the total stress is the vector sum of f_s and f_T. In the panel shown in Fig. 33, the riveted attachment along the lower (transverse) edge failed in shear.

(2) *Tensile Loads.*—The same loads that produce stringer bending also tend to cause failure of skin-to-stringer rivets in tension (see Fig. 34). Actually, the general load W_G always acts radially inward; consequently, it always reduces the rivet tensile load. It is the local load W_L which is primarily responsible for panel failure by rivet tension. The total rivet load is equal to $(W_L - W_G)S_R$. However, it should be noted that, in curved panel tests, the panel frequently flattens out, thus reducing the load W_G and causing rivet tensile failure to occur under the action of W_L. Fig. 35 shows a rivet tension failure.

Stress Computation

It is believed that the various effects discussed above can be adequately evaluated on the basis of the present method. No example is given in what follows of the computation of loads in curved panels, but the flat panel

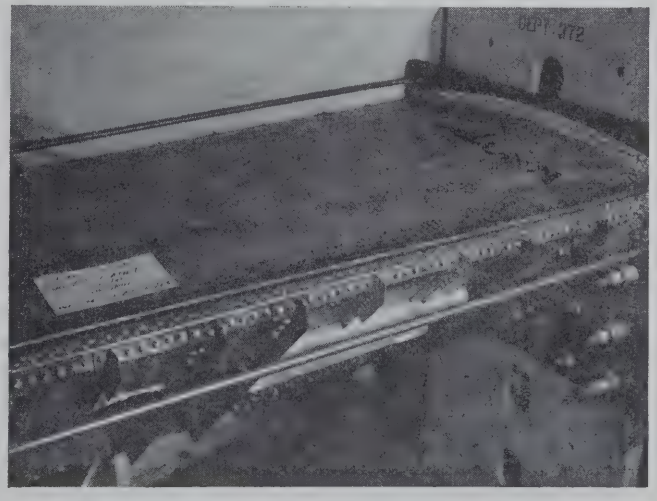

FIG. 31. Curved panel stiffener general bending failure.

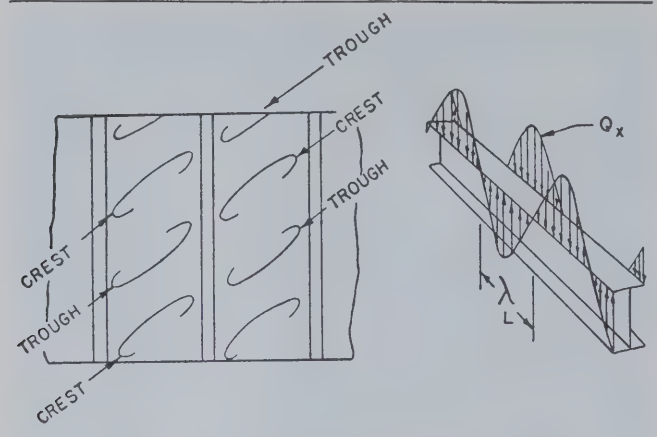

FIG. 32. Stiffener torsion loads.

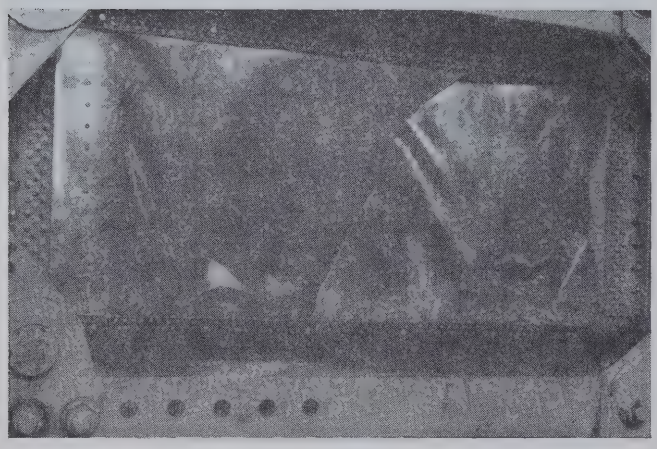

FIG. 33. Rivet shear failure.

example should serve to indicate the type of calculation required in curved panel analysis.

Analysis of Flat Panels

In flat panel analysis, the basic geometric data and loading are determined, values of the panel stresses are read from the charts for $R_L = 1$ and $R_T = 1$, these readings are multiplied by the correction factors corresponding to the true stiffening ratios, and the final stresses and loads are obtained by simple calculation.

Panel Dimensions

Fig. 36 shows the basic geometric data. The panel length L is the length of sheet free to buckle. Similarly, W is the buckled width. The longer dimension is always denoted L. In the case of single web stiffeners with a single row of rivets, the web buckles all the way to the rivet line, and W (or L) is measured from rivet row to rivet row. If the web stiffeners are double, the strip of skin between stiffeners should be considered unbuckled, and W is measured to the stiffener edges.

Shear Stress

In the case of a beam, the shear stress is taken as the total load divided by the distance between the centroids of the upper and lower riveted attachments times the sheet thickness.

Effective Modulus

Fig. 37 gives the effective web modulus of elasticity as a function of the shear stress for 24STAL and 75STAL materials. This empirical relation is based on load-deflection data derived from a large number of shear panel tests made at Douglas Aircraft. The use of these curves to account for panel behavior above the elastic limit of the web is justified by the agreement found in the previous section between test and analysis for the two kinds of material.

It is logical also to use some sort of effective modulus for the stiffening elements, but this would require a solution by successive approximations, since stiffener stresses are not known in advance. However, such a procedure can normally be avoided, since stiffeners, being in compression, are usually not so highly stressed as webs.

Stiffening Ratios

Basically, the stiffening ratios are given by

$$R_L = \frac{A_L}{Wt}\frac{E_L}{E}, \qquad R_T = \frac{A_T}{Lt}\frac{E_T}{E}$$

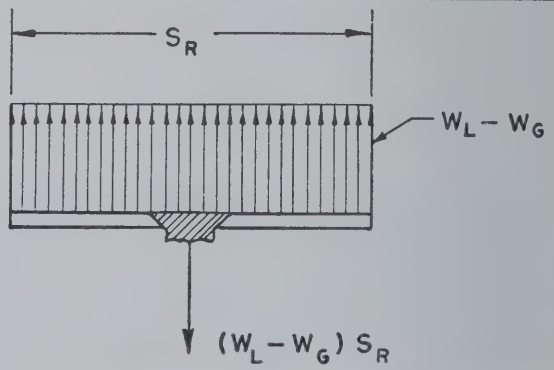

FIG. 34. Rivet tension loads.

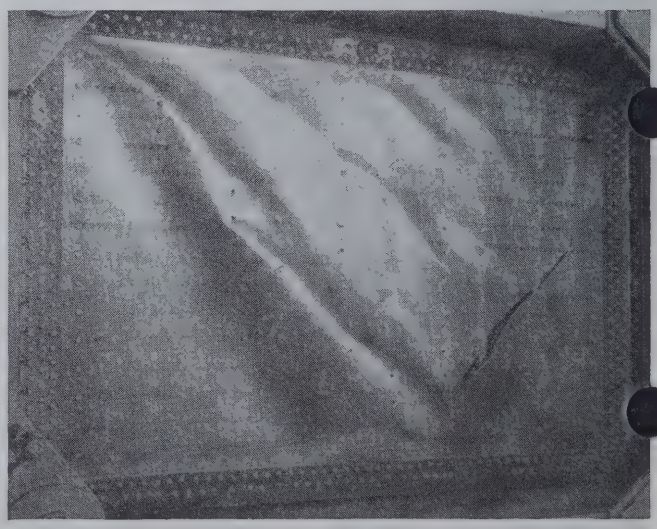

FIG. 35. Rivet tension failure.

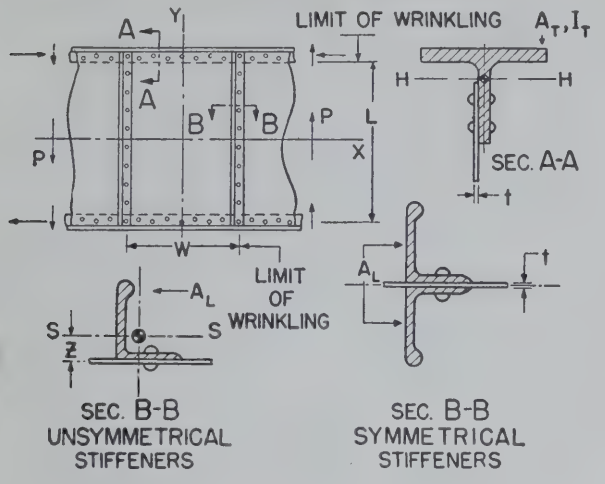

FIG. 36. Basic geometric data.

In these expressions, A_L is the amount of longitudinal stiffening associated with the area Wt of a transverse web section. Similarly, A_T is the transverse stiffener area associated with the area Lt of a longitudinal web section.

In the case of an interior panel of a beam (e.g., not the end panel), A_L is the area of one stiffener where there are single stiffeners or is the area of two stiffeners where there is double stiffening (see section BB, Fig. 36). A_T is the total area of both flanges.

In determining the longitudinal stiffening ratio for a beam, the bending flexibility of the flanges should be accounted for. This may be done by modifying the expression for R_L as follows:

$$R_L = \frac{(A_L/Wt)(E_L/E)}{\frac{W^3 A_L}{720L}\left(\frac{1}{I_{TU}} + \frac{1}{I_{TL}}\right)\frac{E_L}{E_T} + 1}$$

where I_{TU} and I_{TL} are the moments of inertia of the upper and lower flanges. This equation was derived by finding the area of an effective stiffener which, when combined with infinitely rigid flanges, gives the same average strain as the actual stiffener-flange combination under the same loading.

Where there are stiffeners on one side of the sheet only, the longitudinal stiffener area should be replaced by an effective value given by

$$A_{Le} = \frac{A_L}{[1 + (Z/\rho)^2]}$$

where Z is the distance from the stiffener centroid to the centerline of the web (see Fig. 36). This expression is due to Kuhn.[2] A similar correction may also be applied to transverse stiffeners. Where the stiffeners are double, no correction of this kind is required, but A_L should include the area of the strip of web between stiffeners.

Note that the value of E used in the stiffening ratios should be the effective value of the web modulus.

Example of Flat Panel Analysis

Determine the stress distribution in the beam shown schematically in Fig. 38. The design moment is 13,500 in.lbs. (compression on top), and the design shear is 1,225 lbs. per in.

$$f_s = 1{,}225/0.051 = 24{,}000 \text{ lbs. per sq.in.}$$

From Fig. 37,

$$E/E_0 = 0.487$$

$$E = 0.487 \times 10.6 \times 10^6 = 5.16 \times 10^6 \text{ lbs. per sq.in.}$$

$$\frac{f_s}{E}\frac{W_L}{t^2} = \frac{24{,}000 \times 8 \times 13.5}{5.16 \times 10^6 \times 0.051^2} = 193.0$$

$$L/W = 13.5/8 = 1.69$$

$$A_{Le} = \frac{0.127}{1 + (0.423/0.363)^2} = 0.0538 \text{ sq.in.}$$

$$\frac{A_{Le}E_L}{WtE} = \frac{0.538 \times 10.6 \times 10^6}{8 \times 0.051 \times 5.16 \times 10^6} = 0.271$$

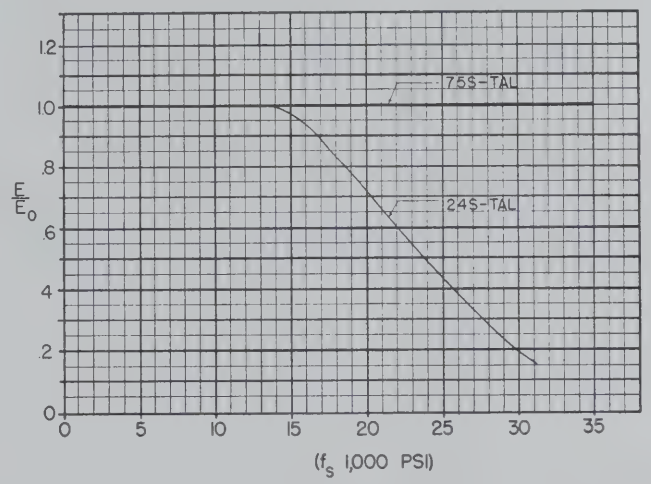

FIG. 37. Effective web modulus of elasticity.

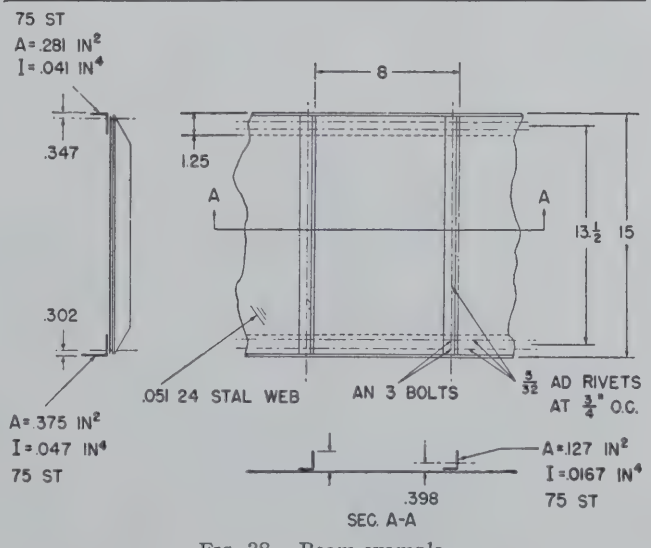

FIG. 38. Beam example.

$$\frac{W^3 A_{Le}}{720L}\left(\frac{1}{I_{T_U}}+\frac{1}{I_{T_L}}\right)\frac{E_L}{E_T}+1=\frac{8^3\times 0.0538}{720\times 13.5}\times\left(\frac{1}{0.041}+\frac{1}{0.047}\right)+1=1.130$$

$$R_L = 0.271/1.130 = 0.240$$

$$R_T = \frac{(0.281+0.375)\times 10.6\times 10^6}{13.5\times 0.051\times 5.16\times 16\times 10^6} = 1.960$$

(See Table 1.)

TABLE 1

Type of Stress	Uncorrected Value	K	Corrected Value
$(\bar{\sigma}_1/f_s)-1$	0.417	0.910	0.380
L/f_s	0.415	0.515	0.214
T/f_s	0.422	1.235	0.522
$\frac{W_L}{Et}\left(\frac{E}{f_s}\right)^{3/4}\left(\frac{WL}{t^2}\right)^{3/4}$	26.5	1.015×1.025	27.6
$\frac{M_L}{EWLt}\left(\frac{E}{f_s}\right)^{1/4}\left(\frac{WL}{t^2}\right)^{5/4}$	3.63	0.985×0.905	3.24

Web

$\bar{\sigma}_1 = (0.380+1)24{,}000 = 33{,}100$ lbs. per sq.in.

This figure should be multiplied by a factor to account for stress concentrations at the riveted attachment. A suggested correction is

$$\bar{\sigma}_{1_{design}} = \bar{\sigma}_1\left(\frac{S_R}{S_R-\sqrt{2}D}\right)K$$

where S_R = rivet spacing, D = rivet diameter, and K = concentration factor $\cong$ 1.1 for round-head rivets.

Stiffeners

$P_L = f_{L_1} t_w W = 2{,}100$ lbs.

$M_L = 3.24\,EWLt/(E/f_s)^{1/4}(WL/t^2)^{5/4} = 40.6$ in.lb.

$E/f_s = 5.16\times 10^6/24{,}000 = 215$

$WL/t^2 = 8\times 13.5/(0.051)^2 = 41{,}500$

$A_L = 127$ sq.in., $\quad I_L = 0.0167$ in.^{4}

$Z = 0.398 + (0.051/2) = 0.423$ in.

$C = 0.398$ or 0.602

Stress in leg attached to web:

$$f_b = -\frac{2{,}100}{0.127}\pm\frac{40.6\times 0.398}{0.0167}-\frac{2{,}100\times 0.423\times 0.398}{0.0167}$$
$$= -38{,}710 \text{ lbs. per sq.in. (compression)}$$

Caps

Compressive load due to transverse stress:

$P_T = f_t tL = 8{,}630$ lbs.
$P_T/cap = 8{,}630/2 = 4{,}315$ lbs.

Load due to design moment:

$P_M = 13{,}500/14.351 = 940$ lbs. (compression top cap)

The upper cap is critical.

Compressive stress:

$f_c = (4.315+940)/0.281 = 18{,}700$ lbs. per sq.in.

Bending stress at stiffener:

$f_b = F_L W^2 C/12I$

$F_L = 24{,}000\times 0.214\times 0.051 = 262$ lbs. per in.

$f_b = \frac{262\ (8)^2\ 0.903}{12\times 0.041} = 30{,}800$ lbs. per sq.in. (compression)

$f_{max.} = 18{,}700 + 30{,}800 = 49{,}500$ lbs. per sq.in. (compression)

Web-Stiffener Attachment

$W_L = 27.6Et/(E/f_s)^{3}/_{4}(WL/t^2)^{3}/_{4} = 44.2$ lbs. per in.

tension/rivet $= 44.2\times 0.75 = 33.2$ lbs. per rivet

Web-Cap Attachment

$f_L = 0.214\times 24{,}000 = 5{,}140$ lbs. per sq.in.
$f_{RT} = \sqrt{f_s^2+f_L^2} = 24{,}600$ lbs. per sq.in.
$F_{RT} = 24{,}600\times 0.051 = 1{,}252$ lbs. per in.
rivet load $= (1{,}252/2)\,0.75 = 470$ lbs. per rivet

Stiffener-Cap Attachment

$P_L = 2{,}100$ lbs.

If the load P_L is assumed to be transmitted entirely through the two bolts, then the load per bolt is 1,050 lbs. However, it appears to be good practice to consider that one of the stiffener rivets just below the cap helps to transmit the load, on the assumption that a small piece of web in the corner of the panel acts as a gusset.

Note in the above example that the depth of panel, L, was taken as the distance between the centroids of the upper and lower riveted attachments, assuming that these marked the limits of web buckling. In Table 1 the correction factor for W_L is given by $K_{W_L} = K_{W_{L_1}} K_{W_{L_2}}$.

CONCLUSION

A graphical method of applying the previously developed shear panel equations has been presented, and a comparison has been made between experimentally determined stiffener stresses and chart values. Reasonable agreement was found, and, where discrepancies appeared, it was possible that extraneous influences may have affected the test data. Since all of the aspects of panel behavior treated by the present method are part of a unified mathematical structure, it seems reasonable to suppose that verification of the predicted stiffener stress is at least a partial verification of the remainder of the analysis.

There is need for additional experimental investigation with regard to both the distribution of stress and the determination of allowable loads for the various panel components. In particular, the bending loads produced on the stiffener by the buckled sheet should be measured and compared with analysis values. In this connection, it should be mentioned that the charts for W_L and M_L give loads acting at the center of the stiffener, assuming conservatively that the crest of a web buckle intersects the stiffener at its midpoint. The same is true for the quantities W_T and M_T.

Besides the loads W_L and W_T, there are torsional stresses in the web itself, and these may have some effect on the stiffener. No explicit expression was given in reference 1 for web torsion, although one could be derived, and the energy of warping was accounted for in the analysis.

Although the loads W_L and M_L were small in the example analysis, their importance should not be discounted, because they increase rapidly with sheet thickness, for constant panel dimensions and shear stress.

It is concluded that a practical method of shear panel analysis has been developed. This method has a rational mathematical basis, is readily and easily applicable to engineering problems, and is capable of giving satisfactorily accurate results through the plastic range to failure of the panel. Although only the stress analysis of panels has actually been demonstrated, it is anticipated that additional investigation and refinement will establish the validity of the method as a means of predicting ultimate loads. It is further expected that the method will prove to be applicable not only to thin web beams but also to curved wing and fuselage panels. Some degree of success has, in fact, already been achieved in predicting ultimate loads for curved fuselage panels, although the results were not in a form suitable for publication at the time of preparation of the paper.

References

[1] Denke, P. H., *Strain Energy Analysis of Incomplete Tension Field Web-Stiffener Combinations*, Journal of the Aeronautical Sciences, Vol. 11 No. 1, pp. 25–40, January, 1944.

[2] Kuhn, P., and Peterson, J. P., *Strength Analysis of Beam Webs*, N.A.C.A. T.N. No. 1364, 1947.

[3] Wagner, H., *Flat Sheet Metal Girders with Very Thin Metal Webs*, N.A.C.A. T.M. Nos. 604, 605, and 606, 1931.

[4] Langhaar, H. L., *Theoretical and Experimental Investigations of Thin-Webbed, Plate Girder Beams*, Trans. A.S.M.E., Vol. 65, pp. 799–802, October, 1943.

[5] Sechler, E. E., and Dunn, L. G., *Airplane Structural Analysis and Design*, pp. 234–258; John Wiley & Sons, Inc., New York 1942.

[6] Niles, A. S., and Newell, J. S., *Airplane Structures*, 3rd Ed., Vol. II, pp. 156–178; John Wiley & Sons, Inc., New York, 1947.

[7] Bruhn, E. F., *Analysis and Design of Airplane Structures*, 1949 Ed., pp. C7.1–C7.12; Photo-Offset Company, Cincinnati, 1949.

[8] Kuhn, P., *Investigations on the Incompletely Developed Plane Diagonal-Tension Field*, N.A.C.A. Report No. 697, 1940.

[9] Kromm, A., and Marguerre, K., *Behavior of a Plate Strip under Shear and Compressive Stresses Beyond the Buckling Limit*, N.A.C.A. T.M. No. 870, 1938.

[10] Timoshenko, S., *Theory of Elastic Stability*, 1st Ed., pp. 307 and 391; McGraw-Hill Book Company, Inc., New York, 1936.

ANALYSIS OF MAGNETIC AMPLIFIER EQUIVALENT CIRCUITS*

By
Don Lebell
University of California
Los Angeles

From the viewpoint of circuit analysis, a magnetic amplifier consists of a combination of one or more a-c generators, load impedances, nonlinear reactors (transductors), and nonlinear resistances (rectifiers). The operation, physical features, and applications of magnetic amplifiers have been discussed considerably in the literature. It will suffice herein to point out that the [illegible] standard methods for treating these nonlinearities consist of (a) assuming linearity, or (b) approximating the nonlinearity by means of curve fitting polynomials or piece-wise-linear relations. The first [illegible] the latter [illegible] simplification of the problem but produces a closer approximation to the device under analysis.

The magnetic amplifier is a particularly difficult type of nonlinear problem in that for some common ranges of operation, its behavior is quite sensitive to the nonlinear characteristics. Hence the discrepancies introduced by the approximating procedures (a) and (b) may be prohibitively large (see Figure 1). Accordingly an investigation of certain methods for analyzing typical magnetic amplifier equivalent circuits has been conducted and is described as follows.

An equivalent circuit of a half-wave, single phase, magnetic amplifier with feedback was selected for study. This particular amplifier was chosen because it contains components which produce all the mathematical difficulties encountered in more complicated magnetic amplifiers. Further, although this circuit is relatively simple in form, it constitutes the "basic unit" of many more complex magnetic amplifiers.

The actual magnetic amplifier (Figure 2) consists of a series combination of an a-c source, a load, a selenium rectifier (to provide feedback as well as rectification) and a hypersil-core transductor (saturable reactor). The control, or saturating winding, is provided with a constant direct current generator of adjustable output.

An equivalent circuit of this amplifier (Figure 3) is a series combination of an a-c generator, a nonlinear resistance, and a

---

*Presented at the I. R. E. West Coast Convention September 14, 1950

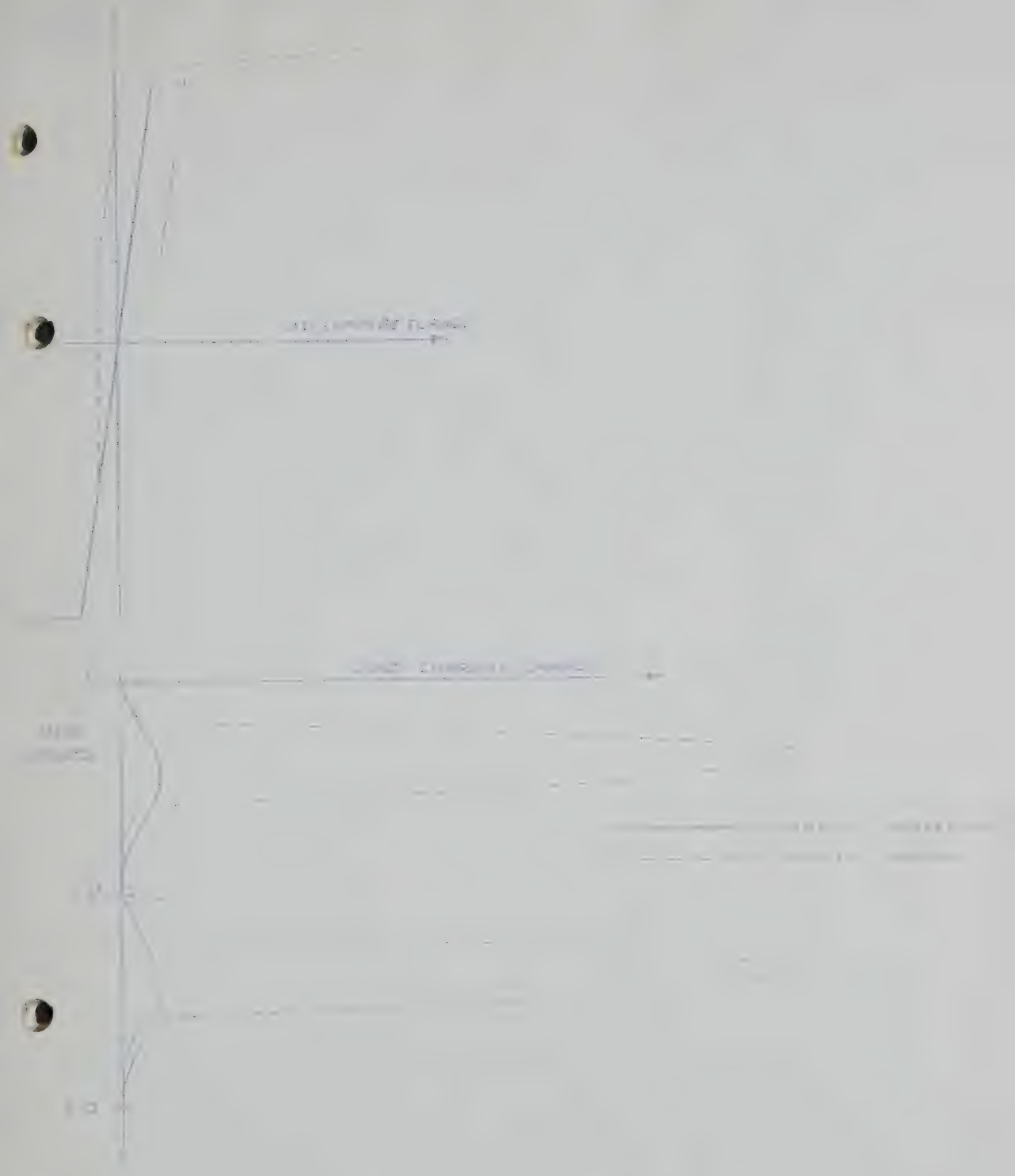

MAGNETIC AMPLIFIER
(WITH SELF-FEEDBACK)

Figure 2. Magnetic amplifier under study.

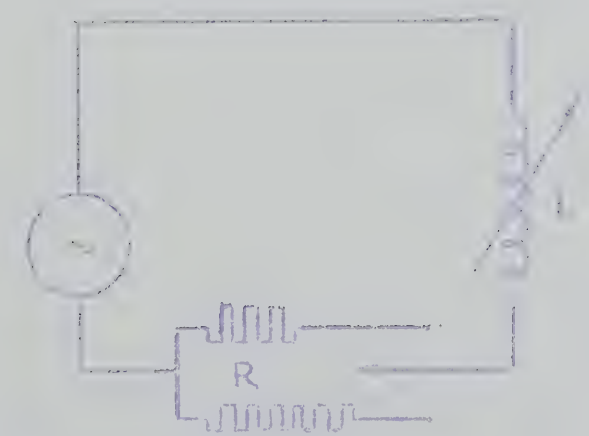

Figure 3. Equivalent circuit of magnetic amplifier.

nonlinear inductance. The differential equations for this circuit can be written:

$$L\frac{di}{dt} + Ri = E\sin\omega t \qquad (1)$$

where R is the sum of all resistance components contained in the load, generator, rectifier and reactor. It assumes two possible values depending on the direction of current flow.

L is the sum of the instantaneous values of inductance appearing in the load, generator, and reactor. It is dependent on saturation, hysteresis, instantaneous current, as well as the composition, heat treatment, and recent magnetic history of the core.

Solution of this equation is attempted by three distinct approaches described as follows.

I. Analytic Solution

Since R is a piece-wise constant function, a fairly obvious approach to the problem consists of replacing the nonlinear L by a piece-wise constant L thus reducing equation (1) to a linear equation containing piece-wise constant coefficients and can be solved analytically in the conventional step-wise manner.

II. Graphical Solution

A graphical solution is easily developed by replacing equation (1) by:

$$N\frac{d\Phi}{dt} + Ri = E\sin\omega t \qquad (2)$$

For sufficiently small Δt, $\frac{d\Phi}{dt}$ can be replaced by $\frac{\Delta\Phi}{\Delta t}$ and equation (2) becomes:

$$\Delta N\Phi + (R\Delta t)i = (E\Delta t)\sin\omega t \qquad (3)$$

If Δt is held constant throughout the solution, this equation can be solved graphically with accuracy limited only by the precision used and the Δt value selected (See Figure 4).

III. Differential Analyzer Solution

Equation (2) when integrated and written as

$$i = -\frac{1}{R}\int\frac{d\Phi}{dt}dt + \frac{E}{R}\int\sin\omega t\,dt \qquad (4)$$

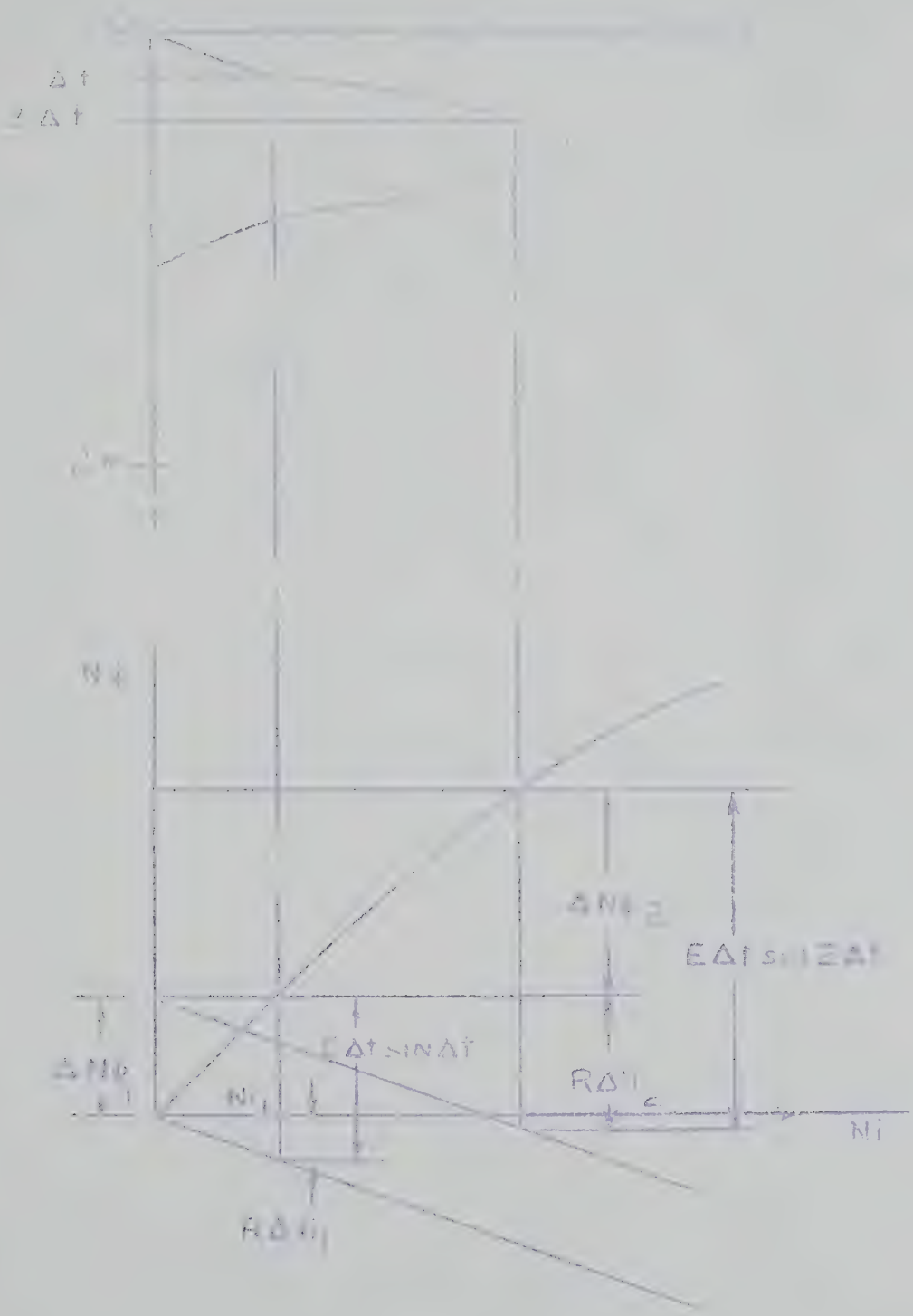

Figure 4. Graphical solution of equation (3).

can be solved on a differential analyzer. Current as a function of flux is supplied the machine by means of an input table directly from experimentally obtained magnetization curves. These curves may be [illegible] on a differential analyzer (See Figure 5 and Figure 6).

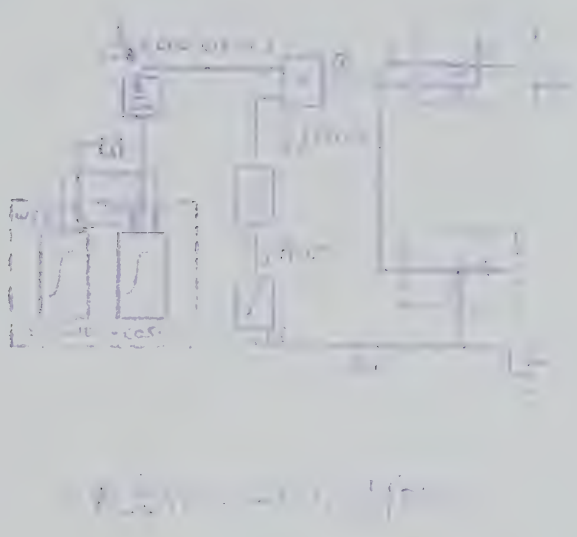

Figure 5. Schematic diagram showing solution of problem on the [illegible] differential analyzer.

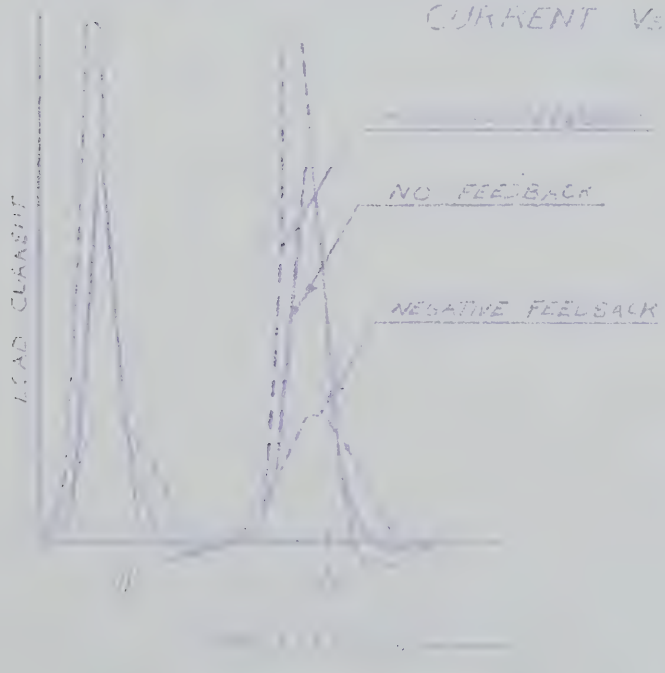

Figure 6. Solutions as obtained from the differential analyzer.

As a continuation of this study, the frequency response of a series connected, single phase magnetic amplifier was examined by means of the differential analyzer (Figure 7). For the assumed magnetization curve solutions were obtained for various a-c generator frequencies and transient starting times.

IV. Results and Conclusions

In any of the foregoing methods of analysis it is evident that the accuracy (and consequent value of the results obtained) is limited to the accuracy [illegible] or assumed. Over certain operating ranges large discrepancies are encountered if the magnetization curves are assumed linear and/or single-valued (no hysteresis). This extreme sensitivity to the magnetization characteristics is particularly evident where positive feedback and low impedance loads occur. Accordingly, the graphical, and differential analyzer solutions are most satisfactory since these methods incorporate actual B-H characteristics.

A single graphical solution is more rapid and less expensive than a single differential analyzer solution for this magnetic amplifier. On the other hand, if a number of solutions are to be obtained for different circuit values or initial conditions, or if the magnetic amplifier circuit increases in complexity, the reverse is true. That is, the graphical solution becomes laborious and time consuming, while the differential analyzer method is not seriously affected by the increased circuit or mathematical complexity. The analytical solution is the least desirable method from the standpoint of solution time and accuracy of results.

While the foregoing methods describe mathematical studies of an equivalent circuit of a magnetic amplifier, it should be kept in mind that other distinct approaches to this class of problem exist and should not be overlooked.

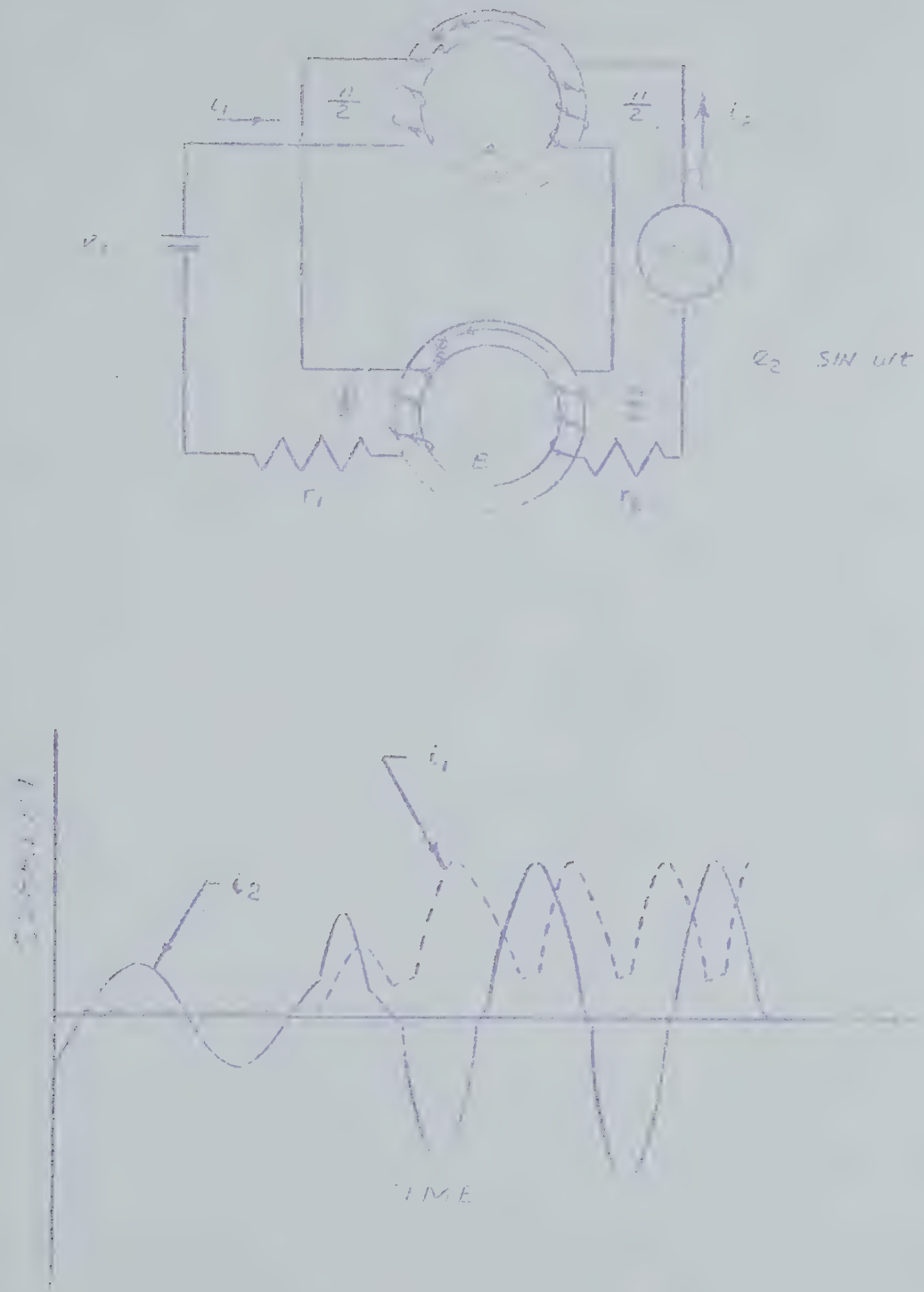

Figure 7. Series connected, single phase, magnetic amplifier and predicted current vs. time waveforms as obtained on the differential analyzer.

UNIVERSITY OF CALIFORNIA
DEPARTMENT OF ENGINEERING
LOS ANGELES

ANALYTICAL STUDIES
IN
THE SUPPRESSION OF WOOD FIRES

by

George J. Tauxe
Ray L. Stoker

NOVEMBER, 1950

UNIVERSITY OF CALIFORNIA
DEPARTMENT OF ENGINEERING
LOS ANGELES

ANALYTICAL STUDIES IN THE SUPPRESSION OF WOOD FIRES

BY

GEORGE J. TAUXE
RAY L. STOKER

NOVEMBER, 1950

CONTENTS

	Page
Abstract	ii
Nomenclature	iii
Introduction	1
Instantaneous Interfacial Temperature on Water Impingement	7
Analogous Studies in the Suppression of Wood Fires	11
Conclusions	44
Acknowledgment	45
Bibliography	45

ANALYTICAL STUDIES IN THE SUPPRESSION OF WOOD FIRES

By George J. Tauxe[1] and Ray L. Stoker[2]

ABSTRACT

This paper presents the results of two analytical studies associated with fire suppression of an idealized forest type fuel; certain aspects of the studies, however, are applicable to wood fires in general. A qualitative discussion of the burning and the suppression of wood fires is presented in the introduction. The first study concerns the instantaneous interfacial temperatures that occur when a drop of water impinges upon the hot surface of a burning piece of wood and shows for typical cases that the drop will not instantaneously vaporize or bounce off and that initially the relative wetting abilities of the suppressing agents may be of importance. The second study utilizes an electrical analogue computer to investigate the simulated thermal behavior of wood as it burns and is extinguished by surface cooling, by penetration cooling, and by oxygen dilution. One important result indicates that the minimum theoretical ratio of the quantity of water for suppressing a typical fire to the volume of the burning wood is in the order of 1/150. Laboratory and field test fires have given ratios in the order of 1/7, showing the large room for improvement in suppression techniques.

---

[1] *Lecturer in Engineering, University of California, Los Angeles 24, California.*

[2] *Formerly Research Engineer, University of California, Los Angeles 24, California (now Research Specialist, North American Aviation Inc., Downey, California). Member ASME.*

Paper for presentation at Annual Meeting of the American Society of Mechanical Engineers, Wood Industries Division, New York, N.Y., Nov. 27 - Dec. 1, 1950.

NOMENCLATURE

The following nomenclature is used in the paper:

A = cross sectional area, ft^2

a = a subscript to T to indicate ambient temperature or to E to indicate a voltage corresponding to T_a

b = a subscript to T to indicate burning temperature or to E to indicate a voltage corresponding to T_b

C = electrical or thermal capacitance, farads or Btu / °F

c = a subscript to T to indicate cooling temperature or to E to indicate a voltage corresponding to T_c

c_p = specific heat, Btu / lb °F

E = electrical potential, volts

e = a subscript to indicate that a particular term is an electrical quantity

H = latent heat of vaporization, Btu / lb

h = combined unit thermal conductance for convection and radiation, Btu / ft^2 °F hr

i = electrical current, amperes

k = thermal conductivity, Btu / hr ft^2 (°F / ft)

L = length, ft

m = conversion constant, ratio of thermal to electrical capacitance, Btu / °F farads

N = the number of meshes or elements in a system

n = conversion constant, ratio of electrical to thermal time; also a subscript to indicate a varying number

p = penetration distance, ft

Q = quantity of electricity or heat flux, coulombs or Btu

q = heat flow rate, Btu / hr

R = electrical or thermal resistance, ohms or °F / (Btu / hr)

r = radial distance, ft; also a subscript to T to indicate maximum reheating temperature or to E to indicate a voltage corresponding to T_r

s = a subscript to time, θ, to indicate water spreading time between sectors for the cylinder with two dimensional heat flow

T = temperature, °F

t = a subscript to indicate that a particular term is a thermal quantity

x = a lineal distance, ft

α = thermal diffusivity, ft^2 / hr

δ = equivalent thickness of water layer, in.

γ = weight density, lb / ft^3

θ = time, sec or hr

ϕ = conversion constant, ratio of electrical potential to temperature, volts / °F

INTRODUCTION

The spreading of fires in wood type fuels and their suppression involves many factors which enter in complicated and interrelated ways. A general analytical treatment of the entire problem is impossible, but insight in the phenomena involved is possible by separate considerations given to certain of the important phases. The results of two such analytical studies are presented herein, following a qualitative discussion of the burning and suppression of wood fires. The main emphasis in this work is toward typical forest type fuels and situations, certain aspects, however, are applicable to wood fires in general.

Qualitatively, the combustion of wood may be divided into two categories, which are (a) the burning of combustible gases and (b) the burning of carbon in the form of charcoal (1)[1]. The two combustion processes probably occur simultaneously during most of the combustion history of any given piece of wood, and it is probably only near the end of burning that charcoal burning alone exists.

If attention is given to a particular specimen of wood in a burning system of similar specimens, one may deduce its subsequent history to be somewhat as follows. Prior to the actual arrival of the active flame, the specimen's surface will be heated, usually first by radiation from the approaching flame, and later by convection while its interior becomes heated by conduction. Under certain circumstances the fuel system and its ambient conditions may be such that the temperature of the specimen under consideration reaches its kindling or ignition point as a result of radiation alone. Under other circumstances, however, the specimen may not ignite and possess its own flame until after being "licked" by the oncoming flame. The relative importance of radiation, convection, and conduction in burning as well as in suppression depends on many factors which in turn may vary among different fires.

Before the above mentioned specimen becomes ignited, several changes in it may have occurred because of heat absorption from its surroundings. Undoubtedly the first change is its reduction in moisture content, beginning at the surface and then gradually drying toward the interior. The completeness of and the rapidity of the drying operation depends largely upon the specimen's size, structure, and initial moisture content. Conceivably occurring simultaneously with the latter part of this drying phase, there begins the destructive distillation of the numerous hydrocarbons, alcohols, acetic acid, etc., present in wood. These substances which are normally liquids are ultimately

---

[1] *Numbers in parentheses refer to Bibliography at the end of the paper.*

volatilized — even cracked in some cases — and are driven out through the pores of the wood along with the secondary thermal reaction products such as carbon monoxide, carbon dioxide, and hydrogen Upon passing through the surface of the specimen into the immediate surrounding atmosphere, these gases may form a combustible mixture with the air, and their combustion will proceed directly if the surface temperature is high enough to ignite the mixture. Even if the surface temperature is below the ignition point of the combustible gases, they may be fired, nevertheless, by sparks or flames passing in the proximity of the specimen. In either case the specimen could be considered to be burning although it might temporarily be playing the role of a gas burner with its own contained gas generator.

From observations of laboratory and field test fires (2 & 3) it was not possible to detect a distinct transition from gaseous to charcoal burning. However, from the flames' motion and the lack of ash on observed specimens during the early stages of their combustion it was concluded that gaseous burning dominated. On the other hand near the completion of combustion, after the specimens had been reduced to glowing embers with little or no apparent flame, it seemed reasonable that this phase was largely one of charcoal burning. During the intermediate phases of combustion, it was observed that occasional flaming gas jets issued from the burning specimens while the amount of ash accumulated. This indicated the presence of both types of burning. The presence of gaseous combustion can assist the charcoal's burning by providing it with a hot ambient surrounding. Conversely, the burning charcoal provides a pilot light for the gases that issue out through the hot charcoal surface. Thus, the two combustions are not only compatible but may actually assist each other.

The foregoing qualitative description of the elements of wood combustion provides a basis on which to analyze the mechanisms of suppression. The most direct means of suppressing a fire involve (a) cooling the fuel to a point below its kindling or ignition temperature and (b) changing or modifying the atmosphere surrounding the fuel, or altering the fuel itself, in such a manner that a combustible mixture no longer exists. There are, of course, such indirect methods as isolating the burning fuel so that it will burn itself out. Also as each portion of a fire is extinguished, that portion will then no longer assist other regions to burn by aid of its transmitted heat, and this indirectly will have a beneficial effect in facilitating the suppression of the remainder

The first two means of direct suppression mentioned above are of principal interest here, and although they will be discussed individually, it is difficult to separate the two effects in any actual experiment. For example, cooling is undoubtedly an important factor in the blowing out of a match, but at the same time there is a good possibility that the fast moving stream of breath also dilutes the combustible mixture of air and the gases emitted from the match to such an extent that

combustion is no longer possible. Hence it is not obvious whether the match flame is extinguished because the fuel is cooled below its ignition point or if the gas mixture is made too lean by an excess of air. Both effects are undoubtedly responsible.

Extinguishment might conceivably be made with a very small amount of cooling provided the cooling could all be applied suddenly to a very thin layer on the surface of the burning wood. Assisting the extinguishment, there is the possibility that the cooled surface charcoal may act as an absorbing medium for the gases generated in the interior, thus momentarily reducing or even stopping the flow of gases which would otherwise diffuse out to support gaseous combustion. The surface could then presumably be below the ignition temperature of either the charcoal or the generated gases. Consequently, the temperature would be redistributed throughout the wood and a short time later the surface temperature might then again be well above ignition temperatures of either the charcoal or the gases. However, if only the surface were cooled, there is no reason to expect that the generation of gases within the hot interior would cease. Thus, consequently, one can readily imagine the resumption of conditions that existed before the extinguishment. With sufficient heat removal in the last instance, the new distribution of temperature following the extinguishment would have been below the ignition point of the fuels. Hence, if enough heat to make up this defecit is not provided by the surroundings, the fire would remain extinguished unless appreciable gas generation continued and sparks or other external ignitors were present.

Aside from immediate extinguishment another desirable effect that can result from cooling is a reduction of the destructive distillation process. To accomplish this second benefit effectively, the cooling should be such that the temperature of the wood itself, and not merely that of the flame, is reduced. Thus, it appears that the optimum cooling would require sufficient heat removal on the surface of the wood at least momentarily to stop the flame and enough interior cooling to suppress the destructive distillation and prevent rekindling after temperature readjustment.

It is practically impossible to apply an extinguishing agent on burning wood without in some way affecting the combustion mixture in the case of combustible gases or simply the oxygen availability in the case of charcoal burning. A low velocity stream of air entering the combustion zone would undoubtedly enhance the burning since the fuel to oxygen ratio in wood fires is usually on the rich side. Only with a somewhat stronger blast would an overly lean mixture result. In the suppression of forest type fires where explosives are used this principle has questionable value because of the danger of spreading the fire by blasting burning materials into unburned areas. Rendering the fuel-air mixture too rich for combustion is much more feasible in fire suppression than making the mixture too lean. Typical tactics are smothering with dirt to keep out air or dis-

placing the air by a gas which contains no available oxygen, such as carbon dioxide.

Undoubtedly the most effective agent for the suppression of wood fires is water. Owing to its high specific heat as a liquid and its very high latent heat of vaporization, it is potentially an excellent coolant. Upon evaporization its high specific volume also makes it capable of displacing a correspondingly large volume of air, hence giving it good smothering qualities. In fact, upon evaporation at 212° F at atmospheric pressure, one unit volume of water becomes approximately 1700 volume units of steam. Furthermore, steam is a fairly good absorber of radiation and thus provides a shielding effect that might serve to reduce the radiant heat transmitted by the fire being sprayed.

From our present knowledge it is difficult to evaluate the relative importance of each of the above mentioned functions of water in suppressing wood fires. All are useful and are present to some degree in water spray. In practice however, not all of the spray will reach the burning specimens and contribute directly to their cooling. Some of the spray will be carried away by wind and convection currents while some may be evaporated. Other drops may impinge on the hot surface but bounce or run off without providing any cooling. This latter loss of effectiveness may be remedied in part by increasing the affinity of water for wood as, for example, through the use of wetting agents.

A porous solid such as wood can under certain conditions be made to contain both adsorbed and absorbed water. Adsorbed water implies that a thin film of water exists over the surfaces of the porous walls (internal as well as external) whereas the absorbed water fills the interstices of the porous solid. To facilitate wetting wood in either manner, the water must have some affinity for the wood. This property can be enhanced by adding surface active agents such as wetting agents to the water.

Some wetting agents may have strong "spread wetting" characteristics. These agents must possess low surface tension and consequently probably aid adsorption. To have strong absorption characteristics, it would seem that strong capillarity and thus high surface tension would be needed. If this reasoning is correct, it would appear impossible to have both the best absorption and the best adsorption qualities simultaneously. Of course, from a practical standpoint the important thing may be to get sufficient water to the wood quickly and let the distribution between adsorption and absorption fall where it will.

One obvious difficulty to attaining well distributed wetting in forest fire control is that of approaching any burning specimen from more than one side. Consequently, only a portion of the surface area of any given specimen can be directly subjected to spray impingement. Even should the entire frontal area of the burning material experience spray impingement and become successfully

wetted, there is no good reason to expect that this wetting alone would effect an extinguishment since roughly one-half the original surface area involved in burning would remain unwetted. However, if the water would spread from the frontal surface around to the opposite side of each specimen, the situation would be greatly improved. Wetting agents should help accomplish this end.

The discussion to this point has centered around an individual specimen in a fire. It is felt that this approach should be the most logical one before attacking the overall complicated picture where for forest fires one would have to consider such effects as the fuel's size, shape, compactness, density, moisture content, initial temperature, and emissivity or absorbtivity of its surface, the air temperature and relative humidity, the barometric pressure, the wind velocity, the ground slope, the flame's emissive power, temperature, and shape, the physical and thermal properties of the suppressing agent, its affinity for the fuel, and its technique of use. In spite of man's long experience with wood fires, he has a very incomplete understanding of the real basic mechanisms of the burning and the suppression of these fires. Much basic analysis and investigation remains to be done in understanding and devising more effective ways of combating this drain on our natural resources.

In analytical studies it is recognized that it is not feasible to make an exact mathematical analysis of the complete action of suppression agents as they impinge upon a burning piece of wood and affect the temperature distribution with time within the piece. Due to difficulties in accounting for the changes in properties of the wood with temperature, the charring of wood at a varying depth so that its composition gradually approaches that of charcoal, and the flow of volatile gases through the wood pores toward the atmosphere, a complete mathematical description is practically unobtainable. However, by assuming that the material is either wood or charcoal depending upon the temperatures involved, it is possible by analyzing certain idealized systems to obtain results which are useful in indicating the order of magnitude of the desired quantities and their variations or in bracketing the results within certain limits.

The two analytical studies presented in this paper were conducted in order to gain an insight into the effect of the various heat transfer mechanisms as they influence temperature distributions with time on the surface and within a piece of wood as it burns and the fire is suppressed. The first study of the instantaneous interfacial temperature at the time of water impingement has been made in order to estimate how high the temperature of burning wood may be before the water which strikes it commences to boil upon contact. The second study has been made to investigate the thermal behavior in wood during burning and suppression by surface cooling, by penetration cooling, and by oxygen dilution. The first study was rather concise and was mathematical in nature. The second

study was quite comprehensive and was facilitated by the use of an electrical analogue computer, herein referred to as the thermal analyzer.

Certain assumptions and properties of the involved materials were common to both studies and are described below. The following assumptions were used:

1. Each material was taken to be homogeneous.
2. The effect of diffusion of volatile gases or liquids in the material was neglected.
3. It was assumed that there were no heat sources or sinks within the material.
4. The properties of the materials were assumed to be constant and not vary with temperature.

Properties to represent water, wood, and charcoal, the materials encountered in the analyses, were chosen by referring to several handbooks and by suggestions from W. L. Fons on the basis of his work in the measurement of ignition temperatures (4). The properties of water employed were those for standard conditions. To represent wood the average properties of ponderosa pine were used. Average values were likewise selected to represent charcoal. This information is presented in Table 1.

TABLE 1. PROPERTIES OF MATERIALS USED IN ANALYTICAL STUDIES

Quantity and Symbol	Units	Water	Wood	Charcoal
Thermal conductivity, k	Btu/(hr)(ft^2)(°F/ft)	0.36	0.1	0.05
Specific heat, c_p	Btu/lb	1.00	0.45	0.2
Weight density, γ	lb/ft^3	62.4	31	15
Thermal diffusivity, α ($\alpha = k/c_p \gamma$)	ft^2/hr	0.0058	0.0072	0.017

INSTANTANEOUS INTERFACIAL TEMPERATURE ON WATER IMPINGEMENT

The point might be raised that when burning wood is first attacked with water spray, the initial droplets impinging on the hot charred surface of the wood might immediately vaporize or bounce. This is because it seems impossible for a droplet to wet a surface that is well above the droplet's boiling point. As an example of this phenomenon, one can envision the action of a drop of water placed on the hot surface of an iron skillet where the drop immediately starts to boil and skitters about rapidly. If this activity occurs when water first strikes burning wood, wetting agents would probably have little, if any, initial advantage as boiling action would overshadow wetting action, and the bulk of the cooling would necessarily have to occur without the assumed advantage of wetting.

To investigate these phenomena use was made of a mathematical expression for the interfacial temperature of two semi-infinite solids following perfect contact with each other. This expression (derived in Ref. 5) is as follows:

$$T_o = \frac{k_1 T_1/\sqrt{\alpha_1} + k_2 T_2/\sqrt{\alpha_2}}{k_1/\sqrt{\alpha_1} + k_2/\sqrt{\alpha_2}} \quad \ldots\ldots\ldots\ldots\ldots\ldots\ldots\ldots\ldots\ldots\ldots\ldots [1]$$

where T_o is the interfacial temperature, T_1 and T_2 are the initial uniform temperatures of the two semi-infinite bodies indicated by the subscripts 1 and 2, and the remaining symbols are as defined in the nomenclature. This formula is valid at all times that these two semi-infinite solids of constant thermal properties are in perfect contact. Restricting attention to the instant of contact and and a limited time thereafter, considerable freedom of choice is permitted for the conditions of the two bodies. Since finite times are required for all finite thermal changes to occur in the interior of the bodies following the contact, only the properties and conditions existing on the two surfaces just prior to their contact are needed to substitute in Equation [1] for computing the interfacial temperature at the instant of contact and a limited time thereafter. Thus, for the computation of T_o the bodies may be finite and may even be liquid since a certain amount of time must elapse before convection within the liquid can affect the interfacial temperature. In particular, one of the bodies may be a piece of hot charcoal and the other a droplet of water providing the initial interfacial temperature determined according to this equation does not exceed 212° F, the boiling point of water.

Equation [1] has been used to compute the family of straight lines shown in Fig. 1. Here the initial surface temperature of charcoal, wood, and iron have been plotted against the initial water

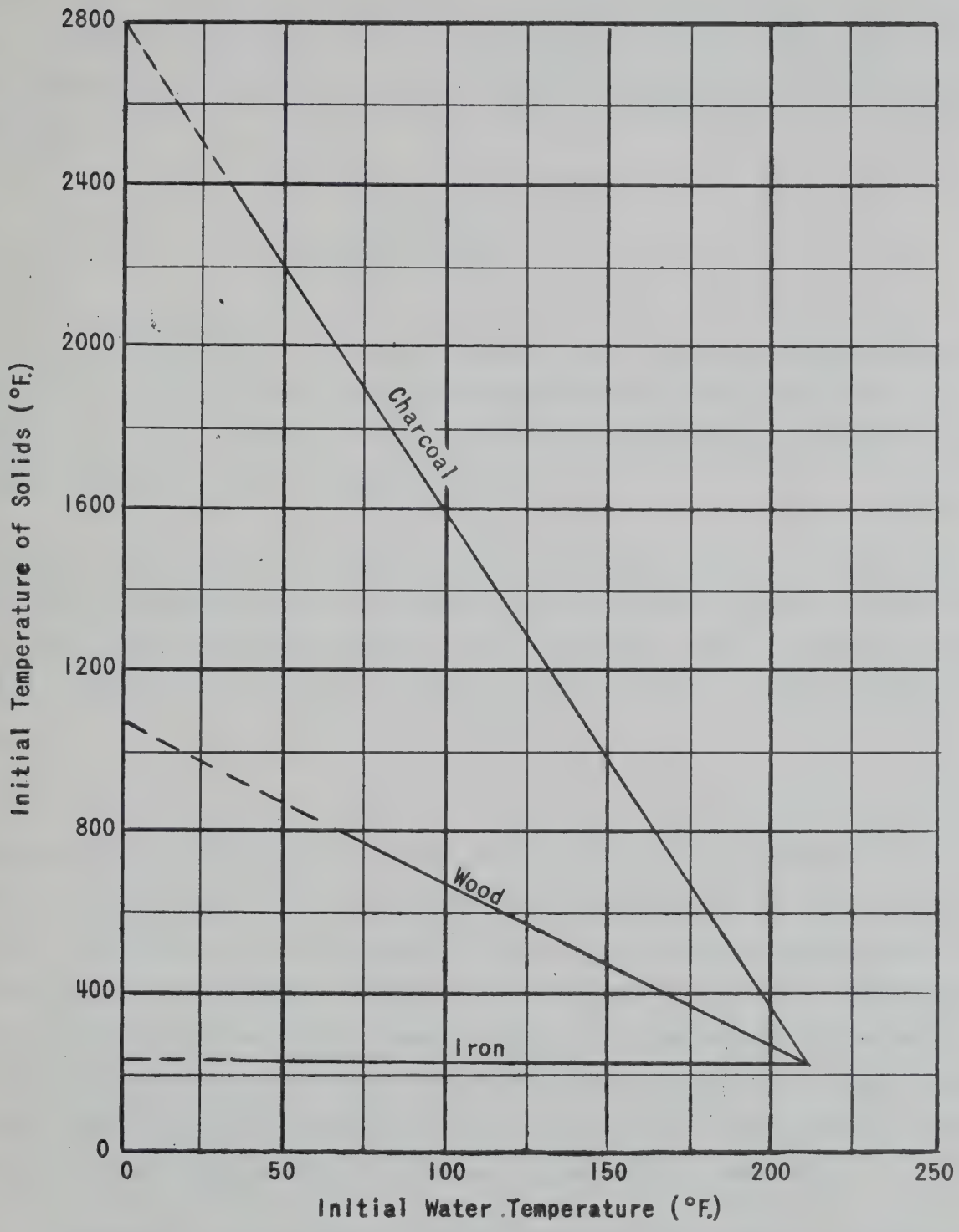

FIG. 1. TEMPERATURES OF WATER AND SOLIDS FOR AN INSTANTANEOUS INTERFACIAL TEMPERATURE OF 212°F.

temperature for the condition that the instantaneous interfacial temperature upon contact of the water on each of the solids would be 212° F. To make these computations it was necessary to determine only one additional point on each plot since each relation is a straight line going through the 212° F point for both axes. Letting subscript 1 in Equation [1] apply to water and subscript 2 apply to the solid materials, the solution was obtained by setting $T_1 = 0$ and by solving for T_2 to give a value of $T_o = 212°$ F. On substitution of $\alpha = k / c_p \gamma$ the following equation was obtained for these computations:

$$T_2 = 212 \left[1 + \sqrt{\frac{k_1 \, a_1 \, c_{p_1}}{k_2 \, a_2 \, c_{p_2}}} \right] \quad \cdots\cdots\cdots\cdots\cdots\cdots\cdots\cdots\cdots\cdots [2]$$

Values of the properties of the materials as given in Table 1 were substituted in Equation [2], and temperatures of 2810° and 1060° F were calculated for charcoal and wood, respectively. By using handbook values for its properties, a temperature of 233° F was similarly calculated for iron. Plotting these points yield the straight lines of Figure 1.

In Fig. 1 the lines are dashed below an initial water temperature of 32° F to indicate that these values do not have any physical significance due to the change in phase of water to ice. Similarly, the line for wood is dashed above an initial temperature of 800° F since at temperatures above this wood would be converted to a material whose properties more nearly resemble those of charcoal.

In analyzing the results shown in Fig. 1 it is interesting to note that for an initial water temperature of 75° F water would not commence to boil at the instant of impingement on hot charcoal unless the initial temperature of the charcoal were approximately 1900° F. Even for water at 100° F, the charcoal would have to be at approximately 1600° F for instantaneous boiling to occur. On laboratory scale fires (2) the highest temperatures measured on the surface of the burning wood were with one exception within one hundred degrees of 1570° F. If these results are representative (and they agree quite well with values reported by certain other investigators), it would indicate that the water drops will not instantaneously vaporize or bounce off upon impingement on burning wood and that initially the wetting ability of a suppressing agent may be of importance.

In attempting to verify these calculations a thermocouple was embedded just below the surface of a stick of charcoal, and heat was applied. The highest temperature obtainable in this experiment was 1300° F, and at this temperature water drops (initially at room temperature) wetted the surface instead of boiling instantaneously. Similar experiments were made using iron as the second material.

For this the initial iron temperature which caused water drops to boil instantly was 225° F. This very closely checked the calculated temperature as may be seen by reference to Fig. 1 for an initial water temperature of 70° F.

ANALOGOUS STUDIES IN THE SUPPRESSION OF WOOD FIRES

Some of the complex phenomena involved in the burning and suppression of wood fires has been discussed qualitatively in the Introduction. It has also been mentioned that in order to make a quantitative approach certain idealizations are necessary. Some of these idealizations were represented in the assumptions which were evolved in order that analytical solutions would be possible. Others entered in restricting the problem to typical cases representative of conditions actually encountered.

For these studies attention was focused on a single piece of wood and the analytical representation of the physical and thermal conditions encountered by it. The viewpoint was taken that this piece of wood was surrounded by like neighboring pieces, all of which were simultaneously undergoing the same sequence of treatment.

Certain values of temperature occuring during the sequence of burning, suppression, and reheating experienced by a piece of wood were selected for these studies. It was the aim to select temperatures as representative as possible of those occurring in the burning and the extinguishment of actual wood fires. Some of these were fixed by nature; however, most were selected as a result of experimental measurements compared with values observed and reported by other investigators. The initial temperature of the material to be burned was taken to be 100° F. Similarly, the ambient air temperature was selected as 100° F for the instances when no flame was present.

For the sequence of burning, the temperature at the surface of the piece of wood was taken to become 1500° F suddenly and to remain at that temperature until suppression started. The basis of this temperature selection is described briefly in the preceding section on interfacial temperatures. Assisted by radiation and convection from some source and by its own burning, the surface of the piece was assumed to be heated to this temperature while its interior was heated by conduction.

During burning, the transition of the wood to a substance whose properties resemble those of charcoal is somewhat gradual and depends upon the interior temperatures. On the basis of experimental measurements (3), a temperature of 800° F was selected for this transition of wood to charcoal. Consequently, wherever the interior of the piece was heated by conduction to between 800° and 1500° F, it was represented by a material having properties of charcoal; likewise, if heated below 800° F, the properties represented were those of wood.

Following the burning and attendant interior heating, suppression was represented by conditions made as typical as possible for surface cooling, penetration cooling, and oxygen dilution.

For the first two of these methods where water cooling was involved, the temperature of the wetted surface or interior was assumed to be at the boiling point of water, 212° F, as long as the water for suppression existed on or in the stick. This temperature of the wetted portion was maintained until the water was completely vaporized with the amount of heat abstracted from the wooden piece by each pound of water vaporized being taken as equal to the latent heat of vaporization (970 Btu / lb). That the temperature of the wetted portion woold be at or slightly less than 212° F was shown by the previously described studies of interfacial temperatures.

In these analytical studies the suppression of wood fires was idealized as consisting of two parts: (a) the flame and its associated heat generation was instantaneously stopped and (b) the surface temperature of the fuel was lowered and retained below its kindling temperature. The possibility of re-ignition due to combustible gases that might continue to be generated and be ignited by adjacent flame, sparks, etc., and produce a flash-back was not considered to exist in these analyses. Heat is necessarily removed from the fuel during part (b), but part (a) was assumed to be accomplished without the removal of heat.

Following the cooling period after which the heat of vaporization of the applied water is utilized, the surface temperature of the piece of wood will begin to rise as heat is conducted toward the surface from the hot interior. Heat is also lost to the ambient by convection and by radiation at the surface, and this will ultimately cause the surface temperature to decrease. Thus, at the surface a maximum temperature would be obtained at some time after the cooling period. If this maximum reheating temperature equaled or exceeded the assumed ignition temperature of the material, presumably re-ignition would occur with a resumption of burning about as it existed before the suppression. However, if the maximum reheating temperature were lower than the ignition temperature, presumably there would be complete extinguishment since conditions thereafter would improve with the surface temperature decreasing as time increased. Thus, the definition of complete extinguishment as used in these studies involved the application of a suppressing agent to cool the wood at or close to its surface to 212° F for such a time that following this cooling period the surface temperature would not exceed the ignition temperature.

The ignition temperature for wood is not a fixed quantity and varies with many factors. For dry cellulose the ignition point may fall between 400° and 600° F and averages 540° F. The ignition points for typical combustible gases volatilized out of wood ranges from about 950° to 1400° F. Using oven temperatures of 1000° to 1200° F, W. L. Fons (4) obtained an ignition temperature for ponderosa pine of 650° F. In later work using lower oven temperatures, Fons obtained values as high as 820° F. For these analytical studies a rekindling temperature of the wood was chosen to be 600° F. It might ap-

pear that this value is low in view of those reported above; however, the higher values were obtained for wood originally unburned and not for a wood material which had just been partially burned and suppressed. It seemed reasonable that re-ignition temperatures for this case would be lower than the original ignition temperature, and therefore a more conservative value was chosen.

For suppression by surface cooling, investigations were made which simulated the instantaneous application of water on the burning wood's surface for particular periods of time. Different runs were made with different cooling times in order to obtain a rather complete range of the subsequent maximum reheating temperatures. During the cooling period, the simulated rate of heat removal was measured. By integrating this cooling rate over the cooling period, it was then possible to determine the total heat removal. From this and the latent heat of vaporization, the total amount of water and the thickness of the water layer applied to the surface could be calculated.

The so called "penetration" type cooling was considered in an endeavor to evaluate the cooling effect that would result from the penetration of water into burning wood. Although the sort of cooling assumed involved a hypothetical penetration that would not occur in actual systems, it did lend itself readily to analysis and quite probably produced a comparable subsequent maximum reheating temperature to that which would result from more realistic penetration achieved with the same amount of cooling. Without attempting to elucidate the details of the mechanisms for accomplishing the end result, it was assumed that the "penetration" cooling runs represented the case where, after the initial burning, heat was removed suddenly so as to reduce the temperature to 212° F for a given depth into the material. The heat thus removed was taken to correspond to the latent heat of vaporization of a certain amount of water. This quantity of water might be assumed to be dispersed throughout the given depth instantaneously and to have no further effect beyond the cooling of the material to 212° F by its complete vaporization.

One aim of this investigation was to compare the effects of suppression by surface and by penetration cooling. To establish the equivalence of surface and "penetration" cooling, the various penetration distances, ϕ, were taken in such a way that the heat removed by the instantaneous "penetration" cooling corresponded to the heat removed in a given time of surface cooling. This is illustrated in the sketch of Fig. 2 where temperatures are plotted as ordinates against the distance within the slab from the surface as abscissae. Curve 1 illustrates, at the start of cooling, the distribution of temperature within the slab due to its burning. Curve 2 illustrates the temperature distribution at the end of a given time of surface cooling. The shaded area, A_1, then represents the amount of heat that is removed during this surface cooling period. For an equivalent "penetration" cooling run, the depth of "penetration", ϕ, was taken in such a way that the temperature was assumed to drop instan-

taneously to the cooling temperature, T_c = 212° F, for this depth, resulting in the removal of an equal amount of heat. The heat so removed by this "penetration" cooling is represented in the sketch by the shaded area, A_2, and as described, $A_1 = A_2$. After making surface and "penetration" cooling runs with this same amount of cooling, their effectiveness was compared by comparing their subsequent maximum reheating temperatures.

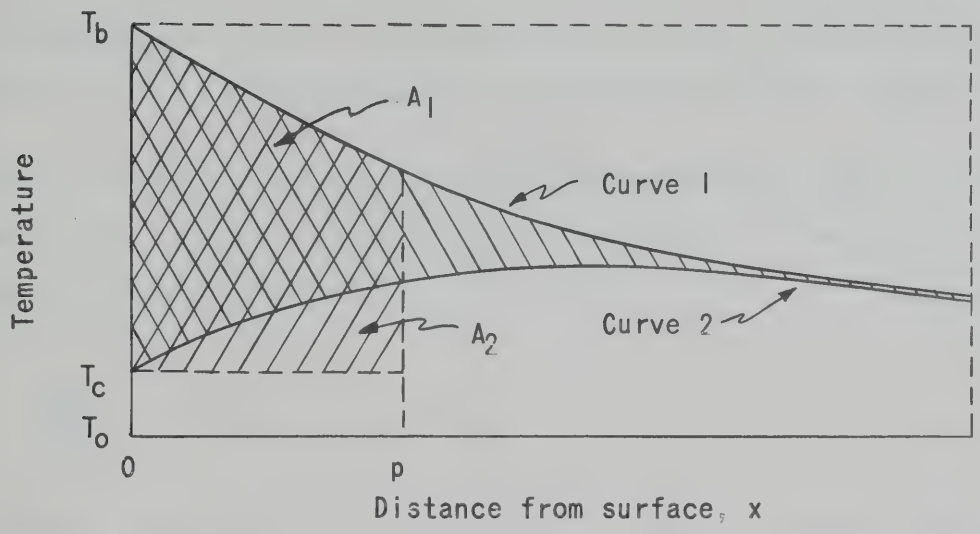

FIG. 2. TEMPERATURE DISTRIBUTIONS IN SURFACE AND "PENETRATION" COOLING.

The oxygen dilution runs represented the case where, after the initial burning, the flame of the burning wood was suddenly snuffed out (as though the extinguishment were being achieved with CO_2) and where with no applied cooling the surface temperature dropped gradually due to radiation and convection to the ambient. Complete extinguishment was represented for this method by finding the time required for the surface temperature to drop to 600° F.

Before going into details on the runs made on the various slabs or cylinders of wood with the three methods of suppression, information will be given on the general method of attack since that is believed to be of interest and as important as the immediate results.

Because of complications in the boundary conditions and in the involved phenomena, it would obviously be impractical, if not impossible, to solve these problems experimentally with the prototype of the thermal system or to make solutions mathematically even for the idealizations assumed. However, it is possible under certain circumstances to simulate systems involving heat conduction by means of

fairly simple electrical systems. The relative ease of measuring electrical quantities as compared to thermal quantities often makes an electrical analogy an attractive method for studying such problems in heat conduction. Because of these reasons, the suppression studies were attacked using an electrical analogue computer, called the thermal analyzer. The essential features of this analogy are developed for a one dimensional heat flow case. The development of the method for two and even three dimensional heat flow is in principle an extension of this one dimensional case and is not included.

The analogy is established by developing separately and then comparing the equations for temperature and for voltage in the thermal system and its electrical analogue respectively. Although the details establishing the thermal-electrical analogy are given in several articles and textbooks, they are offered here using a somewhat different approach from that usually presented.

Considering the homogeneous rod or slab of uniform cross sectional area, A, with the constant thermal properties depicted in Fig. 3 (a), the transient conduction of heat is defined by the Fourier-Poisson partial differential equation,

$$\frac{\partial T}{\partial \theta_t} = \alpha \frac{\partial^2 T}{\partial x^2} \quad \cdots\cdots\cdots\cdots\cdots\cdots\cdots\cdots\cdots\cdots\cdots\cdots\cdots\cdots\cdots\cdots [3]$$

and by the boundary conditions at the two ends of the slab. Here the thermal diffusivity,

$$\alpha = k / c_p \gamma \quad \cdots\cdots\cdots\cdots\cdots\cdots\cdots\cdots\cdots\cdots\cdots\cdots\cdots\cdots\cdots\cdots [4]$$

In these expressions the units of quantities are so chosen that distance, x, is measured in feet and time, θ, is measured in hours. The subscript, t, is used to indicate quantities in the thermal system.

Let the slab of Fig. 3 (a) be divided into N equal elements, each of length, Δx, as shown in Fig. 3 (b). The temperatures at the interfaces of each element will be designated as depicted in this figure. The subscript, n, is used to indicate the interface between the nth and the n-plus-first element and may be given the successive values:

$$1,\ 2,\ 3,\ - - - n,\ - - - (N - 1).$$

In applying Equation [3] to Fig. 3 (b), at any instant of time the second derivative term on the right hand side of the equation can be approximated by an expression involving finite differences as

$$\frac{\partial^2 T_n}{\partial x^2} \simeq \frac{(T_{n+1} - T_n)/\Delta x - (T_n - T_{n-1})/\Delta x}{\Delta x} = \frac{T_{n-1} - 2T_n + T_{n+1}}{(\Delta x)^2}$$

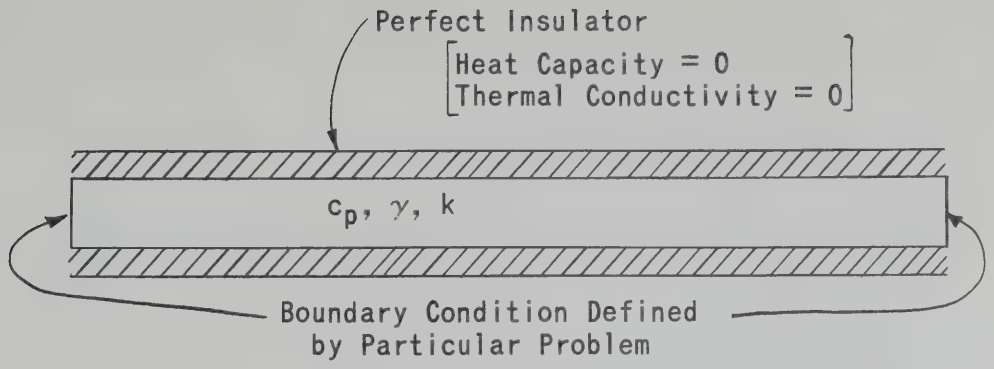

(a) THERMAL PROTOTYPE FOR SLAB

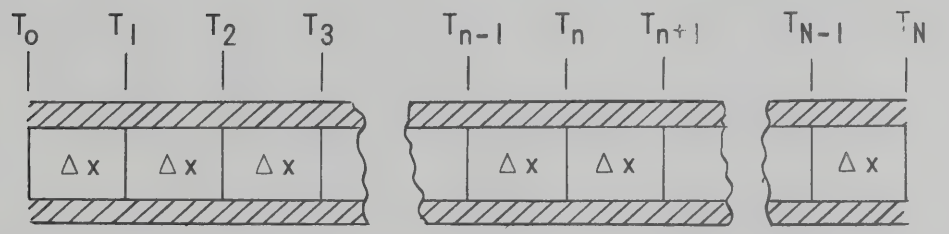

(b) DIVISION OF SLAB FOR APPLICATION OF DIFFERENCE EQUATIONS

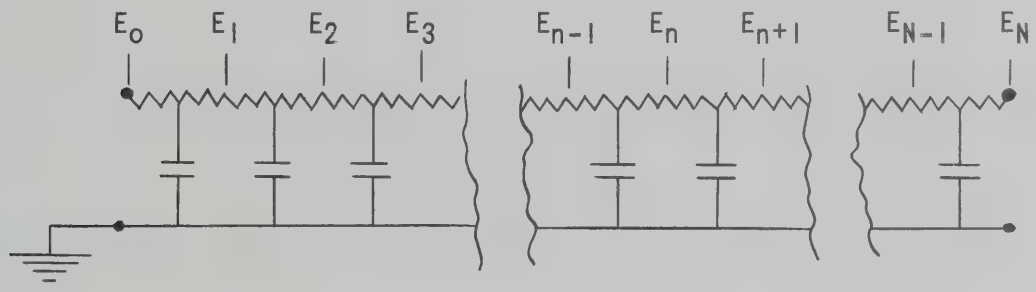

(c) ANALOGOUS ELECTRICAL NETWORK

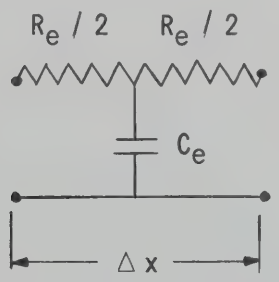

(d) SINGLE MESH FROM ELECTRICAL NETWORK

FIG. 3. ILLUSTRATION OF ANALOGOUS THERMAL AND ELECTRICAL CIRCUITS.

On substituting this in Equation [3] and by having n vary from 1 to $(N - 1)$, the temperature conditions in the slab may be represented by a system of $(N - 1)$ simultaneous approximate ordinary differential equations of the form:

$$\frac{dT_n}{d\theta_t} \simeq \frac{\alpha}{(\Delta x)^2} (T_{n-1} - 2T_n + T_{n+1}) \quad \cdots\cdots [5]$$

Expressions for the thermal resistance, R_t, and the thermal capacitance, C_t, of each element may be obtained by making use of the factor, $\alpha/(\Delta x)^2$, in Equation [5]. By substituting values of α from Equation [4] and by introducing the cross sectional area of the slab, A, this factor may be written as:

$$\frac{\alpha}{(\Delta x)^2} = \frac{k A}{\Delta x} \cdot \frac{1}{c_p \gamma A \Delta x} = \frac{1}{R_t} \cdot \frac{1}{C_t}$$

Thus, for each element

$$R_t = \frac{\Delta x}{k A} \quad \cdots\cdots [6]$$

$$C_t = c_p \gamma A \Delta x \quad \cdots\cdots [7]$$

On substituting these relationships in Equation [5] it becomes:

$$\frac{dT_n}{d\theta_t} = \frac{1}{R_t C_t} (T_{n-1} - 2T_n + T_{n+1}) \quad \cdots\cdots [8]$$

To develop the analogy it will next be shown that the electrical network of Fig. 3 (c) satisfies a system of ordinary differential equations similar in form to those in Equation [8]

The electrical system of Fig. 3 (c) consists of a series of N meshes, each of the type shown in Fig. 3 (d). The total electrical resistance in each mesh, which is the same as the resistance between condensers, is identical for each mesh and is equal to R_e ohms. (Quantities in the electrical system are distinguished by the use of the subscript e.) Likewise, all condensers are taken to have the same electrical capacitance, C_e, in farads. The voltages existing at the mesh junctions, which are midway between the condensers, are designated by the symbol, E, with subscripts like those for the temperature, T, to denote the various positions from points 0 to N. The electrical current flow in amperes in the corresponding resistors will be designated by the symbol, i, with the corresponding subscript. Thus, i_n represents the current flowing in the resistors joining at the point where E_n is obtained

In order to indicate the voltage at the condenser halfway between the points where E_n and E_{n+1} are obtained, the designation $E_{n+\frac{1}{2}}$ will be used. Similarly $E_{n-\frac{1}{2}}$ represents the voltage at the condenser halfway between the points where E_{n-1} and E_n are obtained.

The voltage, E_n, at the mesh junction may be expressed as:

$$E_n = \frac{1}{2}(E_{n-\frac{1}{2}} + E_{n+\frac{1}{2}}) \quad \cdots\cdots [9]$$

Taking the derivative of this expression with respect to time yields

$$\frac{dE_n}{d\theta_e} = \frac{1}{2}\left(\frac{dE_{n-\frac{1}{2}}}{d\theta_e} + \frac{dE_{n+\frac{1}{2}}}{d\theta_e}\right) \quad \cdots\cdots [10]$$

The general expression for the voltage developed across a condenser which is being charged with a current, i, is:

$$E = \frac{1}{C_e}\int i \, d\theta_e$$

By applying this,

$$E_{n-\frac{1}{2}} = \frac{1}{C_e}\int (i_{n-1} - i_n) \, d\theta_e$$

Taking the time derivative gives:

$$\frac{dE_{n-\frac{1}{2}}}{d\theta_e} = \frac{1}{C_e}(i_{n-1} - i_n) \quad \cdots\cdots [11]$$

By a similar process there can be obtained:

$$\frac{dE_{n+\frac{1}{2}}}{d\theta_e} = \frac{1}{C_e}(i_n - i_{n+1}) \quad \cdots\cdots [12]$$

Substituting Equations [11] and [12] into Equation [10] yields:

$$\frac{dE_n}{d\theta_e} = \frac{1}{2C_e}(i_{n-1} - i_{n+1})$$

By applying Ohm's law to the resistances, $R_e / 2$, between the midpoint and the edges of the mesh,

there can be obtained:

$$i_{n-1} = \frac{E_{n-1} - E_{n-\frac{1}{2}}}{R_e / 2}$$

$$i_{n+1} = \frac{E_{n+\frac{1}{2}} - E_{n+1}}{R_e / 2}$$

On substituting these two relations in the expression directly above, there results:

$$\frac{dE_n}{d\theta_e} = \frac{1}{R_e C_e} (E_{n-1} - E_{n-\frac{1}{2}} - E_{n+\frac{1}{2}} + E_{n+1})$$

Here the sum of the middle two terms in the bracket is equal to $-2E_n$ (from Equation [9]); therefore,

$$\frac{dE_n}{d\theta_e} = \frac{1}{R_e C_e} (E_{n-1} - 2E_n + E_{n+1}) \quad \cdots\cdots\cdots\cdots\cdots\cdots [13]$$

If in Equation [13] n is given the successive values from 1 to $(N-1)$, there will be obtained a system of $(N-1)$ ordinary differential equations which will represent the voltage conditions in the electrical network. These equations will be identical in form to the system of equations from Equation [8] except that these are exact equations whereas those for the thermal system are approximate equations. It should be noted that the degree of approximation depends upon the value of Δx; the smaller this is, the better the approximation becomes. Hence, except for this difference the voltage in the electrical network of Fig. 3 (c) can be made analogous to the temperature in the thermal system of Fig. 3 (a) if the corresponding boundary conditions are imposed.

In Equation [13] standard electrical units are used for the electrical quantities. When this is done, time for the electrical system, θ_e, is measured in units of seconds.

In order to interpret the quantities from the thermal system in terms of the analogous quantities from the electrical system, it is necessary to use certain conversion factors. These factors, designated as ϕ, m, and n, are as defined below.

$$\phi T = E \quad \cdots\cdots\cdots\cdots\cdots\cdots [14]$$

$$m C_e = C_t \quad \cdots\cdots\cdots\cdots\cdots\cdots [15]$$

$$n \theta_t = \theta_e \quad \cdots\cdots\cdots\cdots\cdots\cdots [16]$$

Here ϕ is a scale factor which may be arbitrarily selected in order to let a given number of volts potential difference represent a given value of temperature difference in degrees Fahrenheit. The factor, m, which converts thermal to electrical capacitance, may also be arbitrarily selected within the limits of availability of the condensers. Time for the two systems is related by the factor, n.

As indicated previously, units for the two systems are so chosen that time is measured in hours for the thermal system and in seconds for the electrical system. Thus, if n were to equal unity in Equation [16], one second of time on the thermal analyzer would represent the action during one hour in the thermal prototype. This would obviously be impractical particularly since manual switching was employed on the thermal analyzer. Therefore, it was necessary that the factor, n, be sufficiently large so that the timing would be accurate and so that significant amounts of time would not be lost in switching operations. On the other hand if too much time were allowed for measurements, accuracy would be lost due to the action of the leakage resistance of the condensers in the thermal analyzer. It had been estimated that the time constant of this condenser leakage was in the order of 10^4 seconds. Consequently, this indicated that a time factor should be selected so that runs could be made in less than 100 or 200 seconds. As a compromise, it was decided that a factor of $n = 3600$ would be used for the tests. A further advantage of this factor was that one second on the thermal analyzer runs would correspond to one second in the thermal system.

From a dimensional analysis of Equations [8] and [13], it can be seen that the $R\,C$ product terms in these equations must be of the dimensions of time — actually the so called "time constant" for the respective parts. Therefore, it follows that

$$n\,R_t\,C_t = R_e\,C_e \,.$$

By solving this expression for R_e and by substituting the capacitance ratio from Equation [15], the equation relating resistances in the two systems is obtained as

$$R_e = m\,n\,R_t \qquad \cdots\cdots\cdots\cdots\cdots\cdots\cdots\cdots\cdots\cdots\cdots\cdots\cdots\cdots\cdots\cdots [17]$$

Another pair of analogous quantities is of interest. For the electrical system the quantity of electricity, Q_e, in coulombs is given by:

$$Q_e = \int i\,d\theta_e = \int \frac{E}{R_e}\,d\theta_e = \int \frac{\phi\,T}{m\,n\,R_t}\,n\,d\theta_t = \frac{\phi}{m}\int \frac{T}{R_t}\,d\theta$$

with the equality being extended by using previously developed factors. By comparison of analogous quantities, it follows that the total heat flow, Q_t, in Btu is:

$$Q_t = \int \frac{T}{R_t} \, d\theta_t$$

Therefore,

$$Q_e = \frac{\phi}{m} Q_t \quad \ldots\ldots\ldots\

described immediately above for a slab. In either case the following expressions would be obtained:

$$R_t = \frac{1}{2\pi L k} ln \frac{r_{n+1}}{r_n} \quad \cdots\cdots [19]$$

$$C_t = c_p \gamma L \pi (r_{n+1}^2 - r_n^2) \quad \cdots\cdots [20]$$

Here L represents a length parallel to the axis of the cylinder, ln indicates the natural logarithm, and r_{n+1} and r_n are successive radial boundaries of the annular shaped elementary volume.

Calculating procedures for a cylinder are similar to those for a slab except that an axial length, L, is selected instead of the area, A, and that Equations [19] and [20] are used instead of Equations [6] and [7]. For the cylinder a certain amount of cut-and-try operation is frequently required in order to get the desired balance of values for Δr, R_e, and C_e. The arrangement of the resistors and the condensers in the electrical network is also similar to that for Fig. 3 (c) with the position of each condenser representing the mean radial position of the mass for each elementary volume.

For two dimensional heat flow in a cylinder the elementary volume is obtained by dividing the annulus shaped elements into equal sectors. Thus, the thermal capacitance representing the heat storage in the elementary volume is the same as that computed from Equation [20] divided by the number of radial sectors. The thermal resistance to heat flow in the radial direction is the same as that computed from Equation [19] multiplied by the number of radial sectors. By making use of Equation [6] the thermal resistance to heat flow in the tangential direction becomes.

$$R_t = \frac{2\pi r_m}{k L \Delta r} \div (\text{no. of sectors}) \quad \cdots\cdots [21]$$

where r_m is the mean radial position of the mass for the elementary volume. By using the previously defined conversion factors, values of electrical resistance and capacity may be computed for the thermal quantities. The arrangement of these circuit elements in the network is as depicted in the sketches of Fig. 9 and in the circuit diagram of Figure 10.

A necessary part of the analytical studies was to represent the heat lost by a burned piece of wood through convection and radiation to ambient temperatures Evaluations for this may be made using Newton's law of cooling, recast as indicated:

$$q = h A (T_1 - T_2) = \frac{T_1 - T_2}{1/h A}$$

where q = the heat flow rate, Btu / hr

h = the combined unit thermal conductance for convection and radiation, Btu / ft^2 °F hr

A = the surface area, ft^2

T_1 = the surface temperature of the wood, °F

$T_2 = T_a$ = the ambient air temperature, °F

Since temperature difference has been shown to be analogous to voltage difference, it will be seen upon comparison with Ohm's law, $i = E / R_e$, that the quantity, q, is analogous to the electrical current, i, and that the term, $1 / h A$, is analogous to the electrical resistance. The latter term must, therefore, be the thermal resistance due to the unit thermal conductance, h, and it may be written as

$$R_t = \frac{1}{h A}$$

Using Equation [17] to convert from thermal to electrical resistance and calling this electrical resistance R_h, there is obtained the expression,

$$R_h = m n \frac{1}{h A} \quad \cdots \quad [22]$$

Numerical values were assigned to the unit thermal conductance, h, by a consideration of the heat lost by convection and radiation to the surrounding air. The unit thermal convective conductance, h_c, was evaluated for free convection around a cylinder by using information in Reference 6. This was found to equal 2.5 Btu / ft^2 °F hr for T_2 = 100° F, T_1 = 600° F (taken as the average surface temperature of the wood during its reheating), and r_o = 0.025 ft (the outside radius used for cases representing cylinders). The unit thermal radiative conductance, h_r, was evaluated from plots in Reference 7, giving values of h_r for a Planckian (black body) radiator for various values of temperatures. For ambient and surface temperatures of 100° and 600° F, respectively, h_r is given as 4.0 Btu / ft^2 °F hr. The total or combined unit thermal conductance, h, is the sum of h_c and h_r or 6.5 for the indicated temperatures. Actually, the average surface temperature following suppression is probably less than 600° F since it varies between 212° F and the maximum reheating temperature, T_r. T_r might be anywhere between 212° F and 1000° F but was in the neighborhood of 600° F for the runs of greatest interest. Since the time-average would probably be less than 600° F, the value, h = 6.5, may be high for most runs. On the other hand, h_c is computed for free convection; actually the com-

posite effect of burning many sticks together would be to set up convection currents which would be greater than those that one stick alone could produce. The increased air velocity would cause a greater heat transfer, and h_c would be increased. After considering these effects, it was thought that a value of $h = 6$ would probably be most representative of actual conditions. However, to cover the possible deviations, various electrical resistors, R_h, were calculated and used in certain runs in the thermal analyzer to represent values of $h = 3.0$, 6.0, and 9.0 Btu / ft^2 °F hr. Physically, the resistor, R_h, is connected across the input terminals to the network as shown in Figures 4 and 10.

Investigations were conducted on different networks representing slabs or cylinders with temperature variations in one or two dimensions. In each network electrical capacitors and resistors were chosen to represent the thermal capacity and resistance of the prototype material, which was either wood or charcoal depending upon the initial heating. For the one dimensional case, the properties of the material in the slab or cylinder are represented by the resistors, R_1 to R_N, and the capacitors, C_1 to C_N, as shown in the schematic diagram of Fig. 4. To the left of the network is shown a D.C. power supply with a voltmeter, V_1, to measure the voltage, E_b, which was set at 200 volts to represent the burning temperature, 1500° F. The ground or zero voltage point, $E_a = 0$, was used to represent the initial and the ambient temperatures of 100° F. A small portion of the voltage appearing across the resistor, R_h, was amplified by a D.C. amplifier and applied to one channel of a two channel Brush recorder, where it was continuously recorded against time. This voltage represented the temperature of the surface of the slab or cylinder. By a similar arrangement the voltage drop across the first half of R_1 was simultaneously recorded on the second channel; from this voltage the current and then the heat flow rate could be determined. The voltmeter, V_2, was used to measure the voltage at the interface between the charcoal and the wood elements; here 100 volts was used to represent the demarcation temperature of 800° F. The timer and the switching and relay arrangement were used as part of the suppression sequence and will be described later.

Fig. 5 is a view of the thermal analyzer and its associated equipment. Aside from the switching panel in the top portion, the thermal analyzer is composed essentially of a series of electrical resistors and capacitances arranged with convenient receptacles in 45 units. Each unit consists of six fixed condensers and two variable resistors and may be used to form one mesh representing an elementary volume of a slab or a cylinder. The fixed condensers may be connected to have any nominal values in steps of 0.25 microfarads up to a maximum of 15.75 microfarads. Actual values as used were measured with a capacity bridge. The resistances could be varied up to 5.0 megohms. Connected externally to the thermal analyzer are the various meters, amplifiers, power supplies, timer, and two-channel automatic recorder.

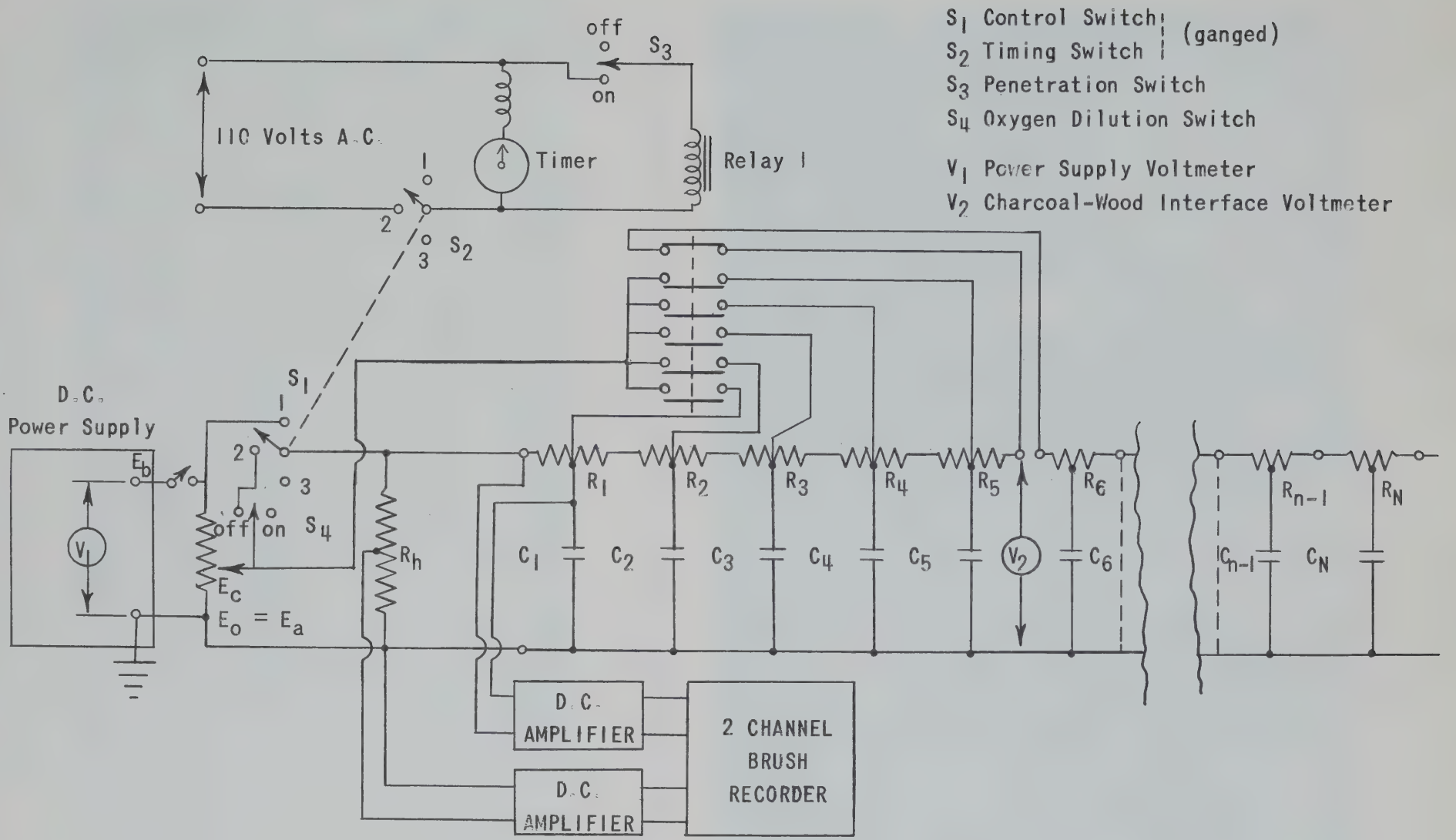

FIG. 4. SCHEMATIC DIAGRAM FOR THERMAL ANALYZER - ONE DIMENSIONAL RUNS.

FIGURE 5. THERMAL ANALYZER AND ASSOCIATED EQUIPMENT.

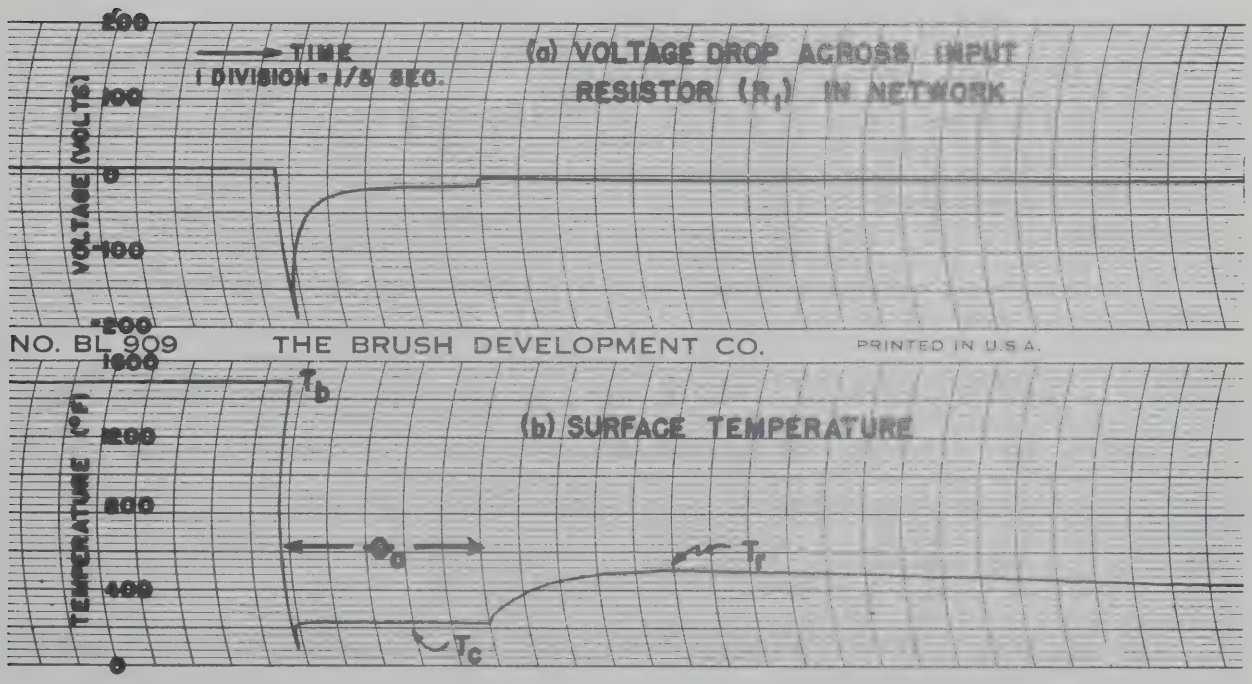

FIGURE 6. TAPE RECORD OF TYPICAL THERMAL ANALYZER SURFACE COOLING RUN.

The surface cooling runs were simulated on the thermal analyzer by the use of an arrangement whereby the network input terminals could be switched at certain times to voltages representing the prescribed temperatures. With the network initially uncharged and with all switches in their normally "off" position, the ganged $S_1 - S_2$ control switch shown in Fig. 4 would be set in position 1. Then when the power supply switch would be turned on, 200 volts, simulating the burning temperature would be applied to the input terminals of the network until V_2 indicated 100 volts at the charcoal-wood interface position. At this time the control switch would be placed in position 2 to simulate the start of surface cooling. Section S_2 would start the timer; section S_1 would switch the network input terminals to E_c = 16 volts, obtained by a voltage dividing arrangement from the 200 volt supply, to simulate the surface cooling temperature of 212° F. This would be applied for times ranging usually from 0.10 to 16 00 seconds. At the end of the surface cooling period as indicated by the timer, the control switch would be turned to position 3 where section 2 would stop the timer and where section 1 would cause the resistance, R_h, representing ambient, to be the only element connected accross the input terminals to the network. Thus, the voltage at the input terminals would rise and then fall, enabling the voltage representing the maximum reheating temperature, T_r, to be obtained from the recording tape. A typical tape record of a surface cooling run is shown in Fig. 6

The procedure used for the "penetration" cooling runs was similar to that for the surface cooling runs but with the following departures during the cooling period. It was necessary to short the condensers of the first few meshes to E_c = 16 volts in order to simulate the penetrating cooling which lowered the temperature to 212° F for the corresponding depths. The penetrating switch, S_3 of Fig. 4, would be turned to the "on" position for these runs causing the relay, R_1, to be actuated during the cooling period. This would cause six normally open contacts to close and short to the 16 volt point as many of the first six condensers of the network as were connected to the relay contacts. At the same time a pair of normally closed contacts would open the network just inside the point where the last condenser was shorted so that the remaining portion of the network would not be appreciably altered by these switching operations. Also the cooling time for these runs was kept as short as possible, a matter of a few hundredths of a second, in order to minimize any change in the voltage distribution of the interior. Separate runs were made in which from one to as many as six of the condensers would be so shorted in order to simulate various penetration depths and to determine the effect on the subsequent maximum reheating temperature.

The equivalence of the surface and the "penetration" cooling runs was determined by comparing the quantity of electricity removed during the cooling periods. As was depicted in Fig. 2 for the thermal prototype, this amounted to a comparison of the areas, A_1 and A_2, which represented the amount

of heat. For the surface cooling runs the quantity of electricity, Q_e, was determined by recording vs. time the voltage drop across the first half of R_1 (Fig. 4); this was converted to current, i, and integrated from the recording tape with a planimeter to get Q_e (in effect using $Q_e = \int i \, d\theta_e$) For the "penetration" runs the quantity of electricity was determined by making use of the relation, $Q_e = \int E \, dC_e$, and by taking into account the manner that both E and C_e varied with "depth" in the networks. The assumption was made that E varied linearly from $E_b = 200$ volts at the "surface" to $E = 100$ volts at the charcoal-wood interface. This assumption was valid to within three percent since the charcoal layer thickness was usually a small fraction of the total slab thickness or cylinder radius. The variation of C_e with "depth" was taken as it actually was computed and used in the networks. Thus, Q_e could be obtained for every "penetration" cooling run and compared by cross plots with the corresponding surface cooling runs in order to obtain an equivalent surface cooling run having a particular cooling time. Since the same heat removal would be involved, the two equivalent runs would require the same amount of water for suppression as viewed in this study and their effectiveness could be compared by observing their values of maximum reheating temperatures. The details in these comparisons required rather arduous calculations and are not included in this paper but are given in Reference 3.

Calculations for the water layer thickness, δ, for each run were made as follows. The quantity of electricity, Q_e, determined as indicated above, was converted to a quantity of heat, Q_t, by using Equation [18]. This quantity of heat was taken to be that given up by the vaporization of water of density, γ, spread over an area, A, to a thickness, δ. Thus, $Q_t = H \gamma A \delta$, where H is the latent heat of vaporization of water. On equating the two expressions for Q_t, there is obtained

$$\delta = \frac{m Q_e}{\phi H \delta A} \qquad \text{[23]}$$

Extinguishment by oxygen dilution was simulated in the runs by the aid of the oxygen dilution switch, S_4, which would be placed in the "on" position (Fig. 4). After the initial charging of the network, like that for the other types of runs, the control switch would be placed and left in position 2. Thus, there would be no simulated cooling and the network would discharge through R_h. From the tape recording the time for the surface temperature being represented to drop to 600° F would be obtained.

The slab for which one dimensional heat flow investigations were made was simulated by 10 electrical meshes representing charcoal, followed by 13 meshes representing wood. In addition to the properties listed in Table 1, the following numerical quantities were used in computing the electrical

parameters for this case:

A = 0.1 ft^2

ϕ = $\frac{1}{7}$ volts / °F

m = 300 Btu / °F farads

n = 3600 sec / hr

Each of the 10 charcoal meshes represented a Δx = 0.001 ft, for which a typical mesh contained:

R_e = 0.230 megohms

C_e = 1.065 microfarads

The wood meshes following had the first 5 meshes with Δx = 0.001 ft and the next 8 meshes with Δx = 0.002 ft. This gave a slab of a nominal 0.030 ft thickness that could be viewed as being a 0.060 ft thick slab which was suppressed simultaneously from both sides. For a value of h = 6.0 Btu / ft^2 °F hr, R_h was computed to equal 1.80 megohms.

To represent different degrees of establishment of the fire, various thicknesses of the charcoal layers were used in the runs. In addition to using 10 Δx's (0.010 ft) of charcoal elements, runs were made with only 2 Δx's (0.002 ft) and 5 Δx's (0.005 ft) of charcoal elements on the surface of the wood. Also in order to establish what was thought to represent the most severe condition of initial burning, a series of runs was made on a complete charcoal slab of 30 elements (0.20 ft) which was charged initially with a simulated uniform temperature of 1500° F throughout its thickness. For all practical purposes this was found to represent a semi-infinite slab since considerable reductions in the slab thickness did not appreciably affect conditions on the surface for the times employed.

The cylinder for the one dimensional heat flow investigations (radial symmetry) was simulated by 15 annular shaped elements of wood at the center (0.020 ft in radius) with 10 elements of charcoal for a surface layer (0.080 ft thick), giving a total radius of 0.030 ft. In addition to the materials' properties, the following numerical quantities were used in computing the electrical parameters for this case:

L = 1.00 ft

ϕ = $\frac{1}{7}$ volts / °F

m = 154 Btu / °F farads

n = 3600 sec/hr

In Table 2 the circuit parameters for this case are tabulated.

Similar to that for the slab case, two degrees of burning were represented for the cylinder by making runs using 5 and 10 Δr's of charcoal elements. Since the outside radius would change slightly with each of these charcoal layer thicknesses, the values of R_h would also change. For example, with h = 6.0 Btu/ft^2 °F hr, R_h was found to equal 0.588 and 0.490 megohms for the respective 5 and 10 Δr's of charcoal layer thicknesses.

For the slabs and cylinders thus far described, the cooling was considered to be applied instantaneously over the entire external surface, and in these cases the heat flow was unidimensional. Consideration was also given to a progressive cooling extending over the external surface of a cylinder giving rise to a two dimensional flow of heat, tangentially as well as radially. This treatment would approach conditions in practice where in fighting forest fires it is difficult to apply a suppressing agent on more than one side of the pieces of burning wood. Also from observations of model laboratory fires (3), it was quite apparent that the frontal area of burning cylindrically shaped wood specimens on the side of the water spray was readily wetted but that the water spread rather slowly over the rear surface. This resulted in a much greater water requirement for complete extinguishment than when both the front and rear surfaces were sprayed simultaneously, even though spreading over the rear surface could be facilitated somewhat by the use of wetting agents. Some features of this action are depicted in the sketch of Fig. 7. The line of symmetry appearing on the sketch is to some extent an idealization not actually realized unless the cylinder's axis is vertical because gravity influences the water film above the line somewhat differently from that below the line. Notwithstanding this discrepancy, it was felt that the more salient characteristics of the actual cooling were retained when this symmetry was employed.

In order to use the thermal analyzer to study the surface temperature and the heat loss by this sort of cooling, the spreading of the surface cooling over the rear of the cylinder was necessarily done in discrete steps rather than continuously. The wood and the charcoal represented in this burning cylinder were divided into elements as indicated in Fig. 9. The six sectors were numbered from 1 through 6, and the four radial divisions were designated by letters a, b, c, and d. Essentially, the dimensions were the same as for the cylinder with one dimensional heat flow with 5 Δr's and the same conversion factors were used in computing the electrical circuit parameters. The circuit parameters for one sector in this arrangement are given in Table 3. These are essentially the same for all sectors except for the small differences in values of C_e due to variations from their nominal

TABLE 2. CIRCUIT PARAMETERS

FOR CYLINDER WITH ONE DIMENSIONAL HEAT FLOW.

Mesh Number	Material Represented	Distance from Surface (feet)	R_e (megohms)	C_e (microfarads)
1	Charcoal	0.0010	0.0585	3 542
2	"	0.0021	0.0655	3.724
3	"	0.0030	0.0635	3.325
4	"	0.0040	0.0632	3 08
5	"	0.0050	0.0691	3 27
6	"	0.0060	0.0708	3 17
7	"	0.0072	0.0874	3 15
8	"	0.0082	0.0775	2 80
9	"	0.0092	0 0808	2 63
10	"	0.0101	0.0775	2.33
11	Wood	0.0111	0.0454	10.63
12	"	0.0121	0.0481	10.29
13	"	0.0131	0.0488	9.66
14	"	0.0140	0.0480	9 16
15	"	0.0150	0.0572.	8 87
16	"	0.0161	0.0662	8.86
17	"	0.0172	0.0727	8.39
18	"	0.0184	0.0864	8.31
19	"	0.0197	0.105	8.11
20	"	0.0213	0 147	8.45
21	"	0.0232	0.218	8.32
22	"	0.0258	0.429	8.18
23	"	0.0283	0.847	4.18
24	"	0.0290	0.447	0.507
25	"	0.0298	1.32	0.269

TABLE 3. TYPICAL CIRCUIT PARAMETERS

FOR ONE SECTOR OF CYLINDER WITH TWO DIMENSIONAL HEAT FLOW

Annulus	Material Represented	Distance from Surface (feet)	Radial Resistor (megohms)	Tangential Resistor (megohms)	C_e (microfarads)
a	Charcoal	0 - 0.0010	0.870	142.	0.249
b	Charcoal	0.0010 - 0.0056	4.48	27.5	1.03
c	Wood	0.0056 - 0.0101	2.79	11.1	3.61
d	Wood	0.0101 - 0.0145	3.70	2.05	5.17

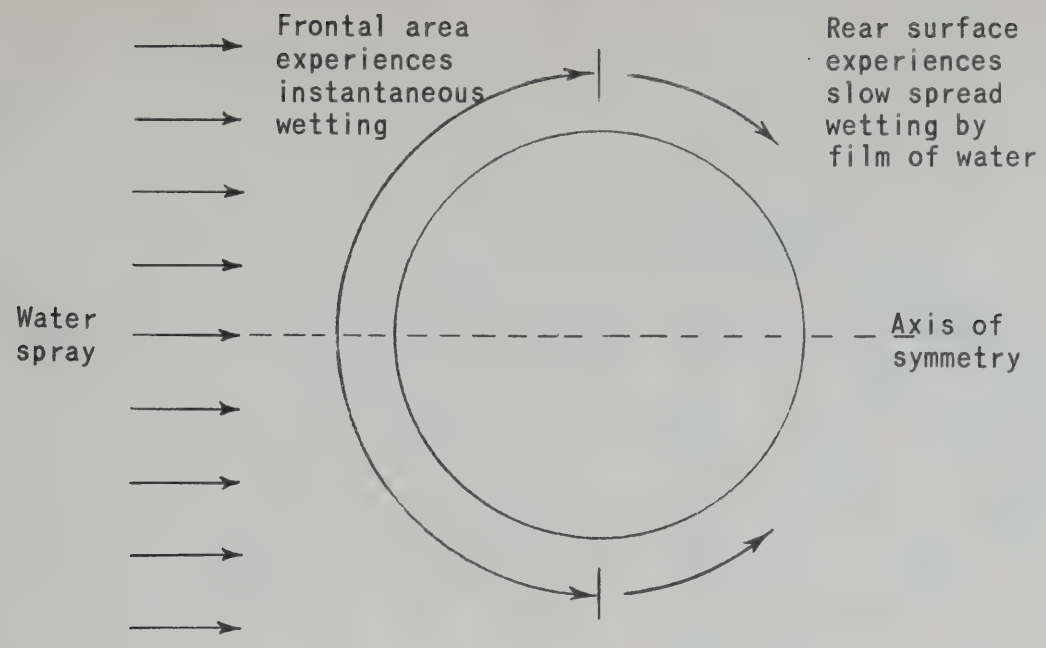

FIG. 7. WETTING OF A CYLINDER WITH WATER SPRAY FROM ONE SIDE.

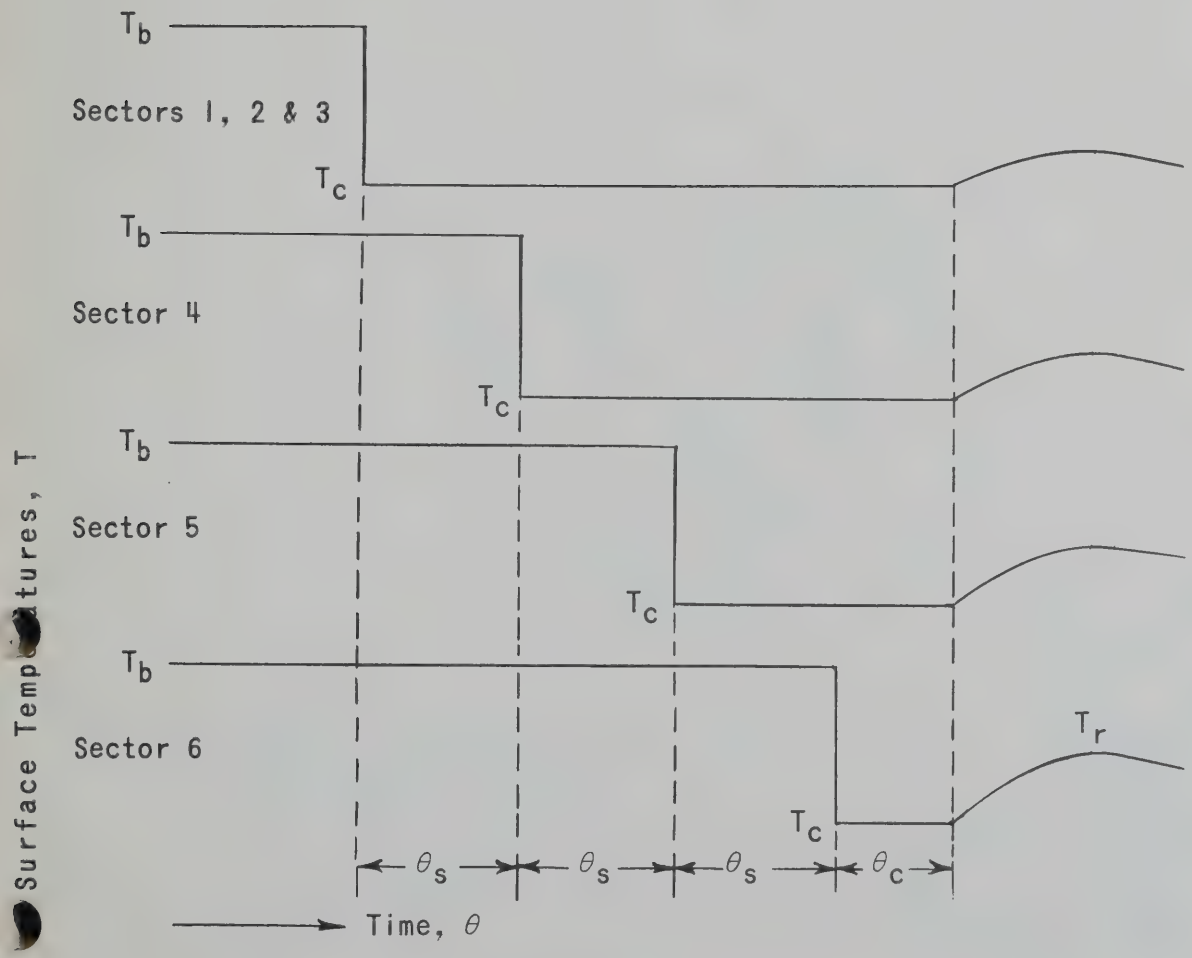

FIG. 8. SURFACE TEMPERATURE VARIATIONS OF SECTORS FOR CYLINDER IN TWO DIMENSIONAL RUNS.

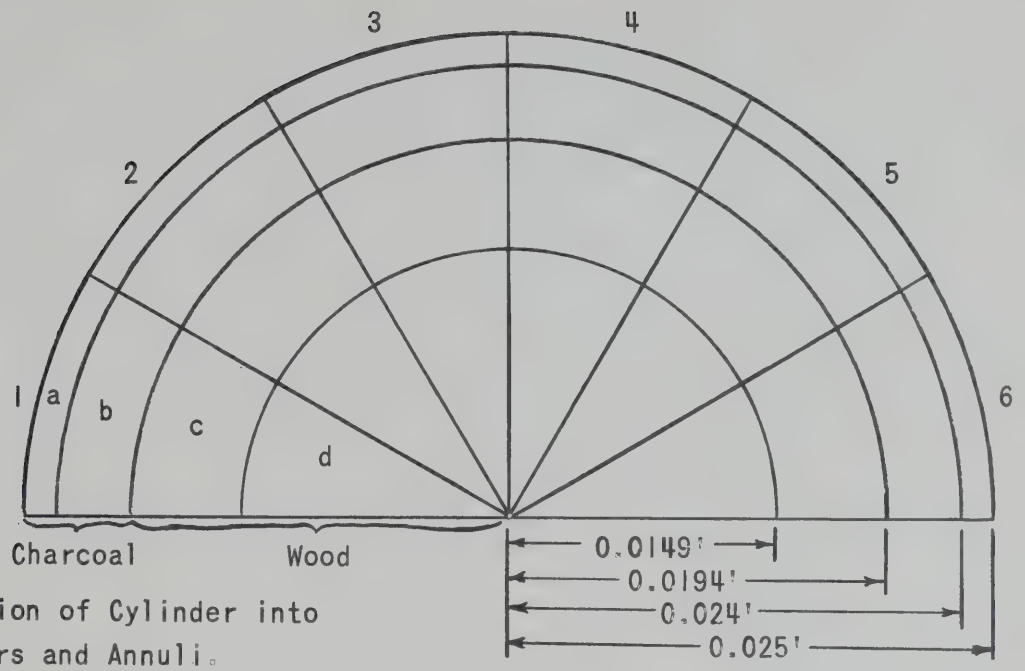

(a) Division of Cylinder into Sectors and Annuli.

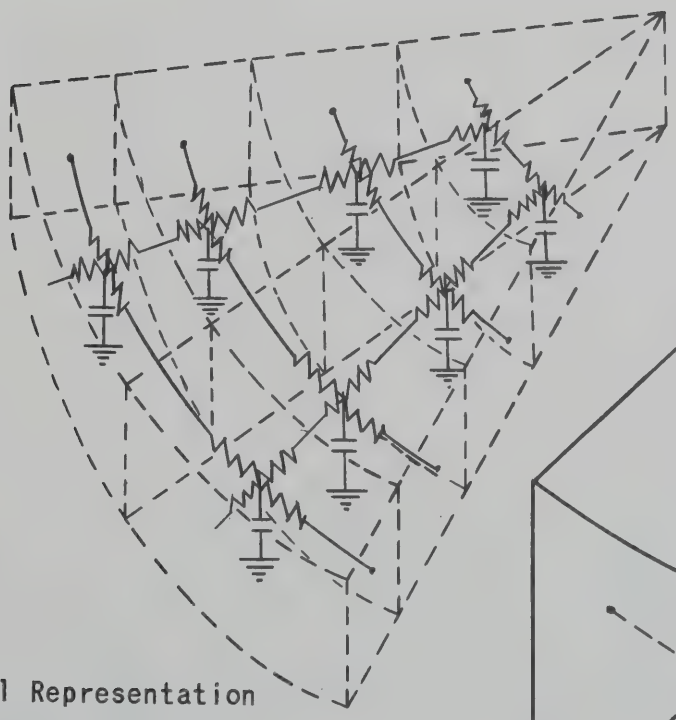

(b) Electrical Representation of Two Adjacent Sectors.

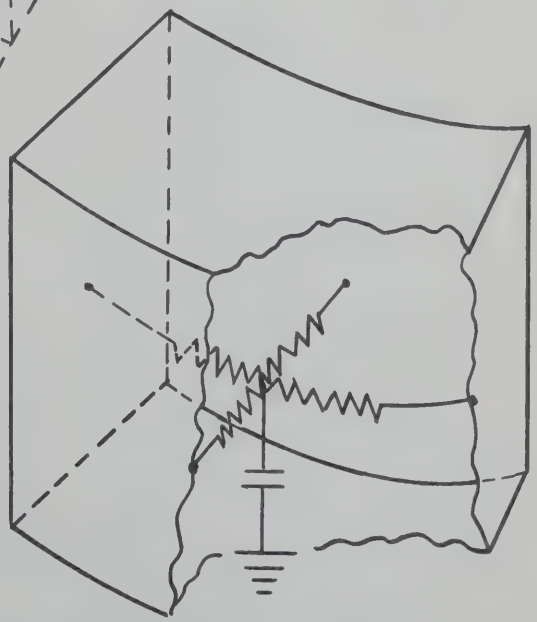

(c) Electrical Mesh Equivalent of One Element.

FIG. 9. SCHEMATIC REPRESENTATION OF CYLINDER FOR TWO DIMENSIONAL HEAT FLOW.

values.

Fig. 8 illustrates the variations in surface temperature for each of the various sectors during a typical run. At the instant when cooling commenced, the cylinder was assumed to possess a temperature distribution resulting from the burning temperature, 1500° F, being applied uniformly over the outside surface until the temperature at the charcoal-wood interface was 800° F. When this was achieved, a temperature of 212° F was instantaneously imposed on the front surface sectors 1, 2, and 3 with 1500° F still prevailing over the rear surface sectors 4, 5, and 6. After a prescribed time interval, designated as θ_s, the spreading time per sector, the surface of sector 4 was instantaneously reduced to 212° F. This same step-wise cooling was applied in turn to sectors 5 and 6 yielding a condition corresponding to the wetting being extended over the entire cylinder. After an additional time interval representing the cooling time for the last sector, θ_c, the 212° F temperature was removed from the entire surface, and the surface temperatures of the various sectors were allowed to take whatever values they would as determined by the ambient conditions and by the existing internal distribution of temperature. It is obvious from the longer heating and shorter cooling of sector 6 that it would achieve the highest T_r and be the most critical region in regards to rekindling.

The schematic diagram for investigations on the cylinder with two dimensional heat flow is given in Fig. 10. The network representing this case is shown in the lower part, and the details of switching are shown in the upper part. The voltages obtained from the D.C. power supply and the voltage divider were the same as those used for the other cases investigated. A ganged five section, seven position switch, S_1, was used as the control switch. Section 1 was connected to the first three sectors of the network while sections 2, 3, and 4 were connected to sectors 4, 5, and 6, respectively. Section 5 was used in the timer circuit in a manner similar to that for the one dimensional cases of Fig. 4 and is not shown in this schematic diagram. With S_1 in position 1, the network was made ready for charging. On turning to position 2, the switch applied the voltage, E_b, to all sectors causing the prescribed initial voltage distribution to be obtained in the network. When voltmeter, V_2, at the charcoal-wood interface reached 100 volts, the switch was turned to position 3 producing a voltage, E_c, across the first three sectors. After a time, θ_s, the switch was turned to position 4 producing a voltage, E_c, across sector 4. In a similar fashion positions 5 and 6 connected the input terminals of sectors 5 and 6 to E_c. After the cooling time, θ_c, for sector 6 had elapsed, the input terminals of all sectors were switched to their respective R_h resistors, and the value of T_r for the last sector was measured using a D.C. amplifier and a Brush recorder to record the voltage across the last sector's R_h. Another D.C. amplifier and Brush recorder were employed to record the voltage across a small resistance in series with the leads from each sector to the divider where E_c was obtained. This enabled the quantity

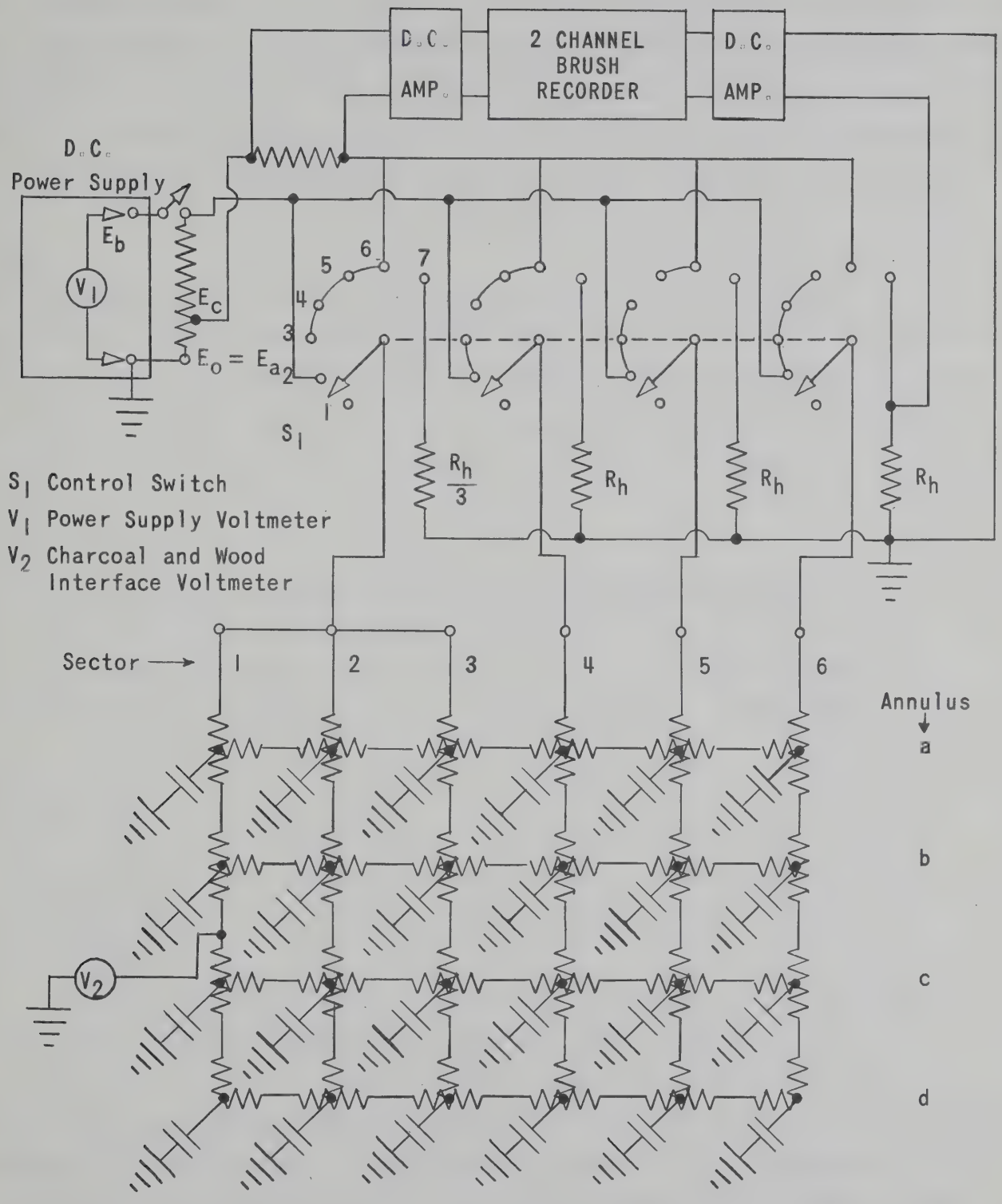

FIG. 10. SCHEMATIC DIAGRAM FOR THERMAL ANALYZER - TWO DIMENSIONAL CYLINDRICAL RUNS.

of electricity removed for the entire sequence of spread wetting and cooling to be measured so that the corresponding heat removal and average water film thickness might be calculated.

Only surface cooling runs with h = 6.0 Btu / ft^2 °F hr were employed in the investigations for the cylinder with two dimensional heat flow. Spreading times, θ_s, of 0.25, 1.0, and 8.0 seconds per sector were used with the cooling times, θ_c, for the last sector ranging from 0.25 to 8.0 seconds. The value of R_h for each sector was 7.05 megohms. Since the first three sectors were treated identically, each of their R_h resistances was effectively in parallel and was replaced by a single resistor of value $R_h / 3$.

Results from the previously described tests are presented in the graphs of Figures 11 to 15 and in Table 4. Though condensed considerably from a comprehensive research program, it is believed that the more representative and significant results are presented herein. In these figures, T_r, the maximum reheating temperature is plotted as ordinate. The cooling time, θ_c, is plotted as abscissae in Fig. 11, and on the rest, Figures 12 to 15, the equivalent water layer thickness, δ, is plotted as abscissae.

TABLE 4. SUMMARY OF OXYGEN DILUTION RESULTS

Case Investigated	No. of Charcoal Δx's or Δr's	h (Btu / ft^2 °F hr)	Extinguishment Time (seconds)*
Slab	2	6.0	1.8
Slab	5	6.0	1.7
Slab	10	6.0	7.2
Slab	all	6.0	25.3
Cylinder	5	3.0	4.4
Cylinder	10	3.0	12.7
Cylinder	5	6.0	2.2
Cylinder	10	6.0	7.8
Cylinder	5	9.0	1.5

* Time for surface temperature to decrease from 1500° to 600° F.

The effect of the degree of establishment of the fire for slabs can be seen from the curves for surface cooling of Fig. 11 and Fig. 12. This effect is also shown for the cylinder with one dimensional heat flow in Fig. 13 for both surface and "penetration" cooling. Comparisons of the above curves show a definite increase in the equivalent water layer thickness and the cooling time as the charcoal layer is made thicker, corresponding to the greater stored heat within the bodies in a more established fire.

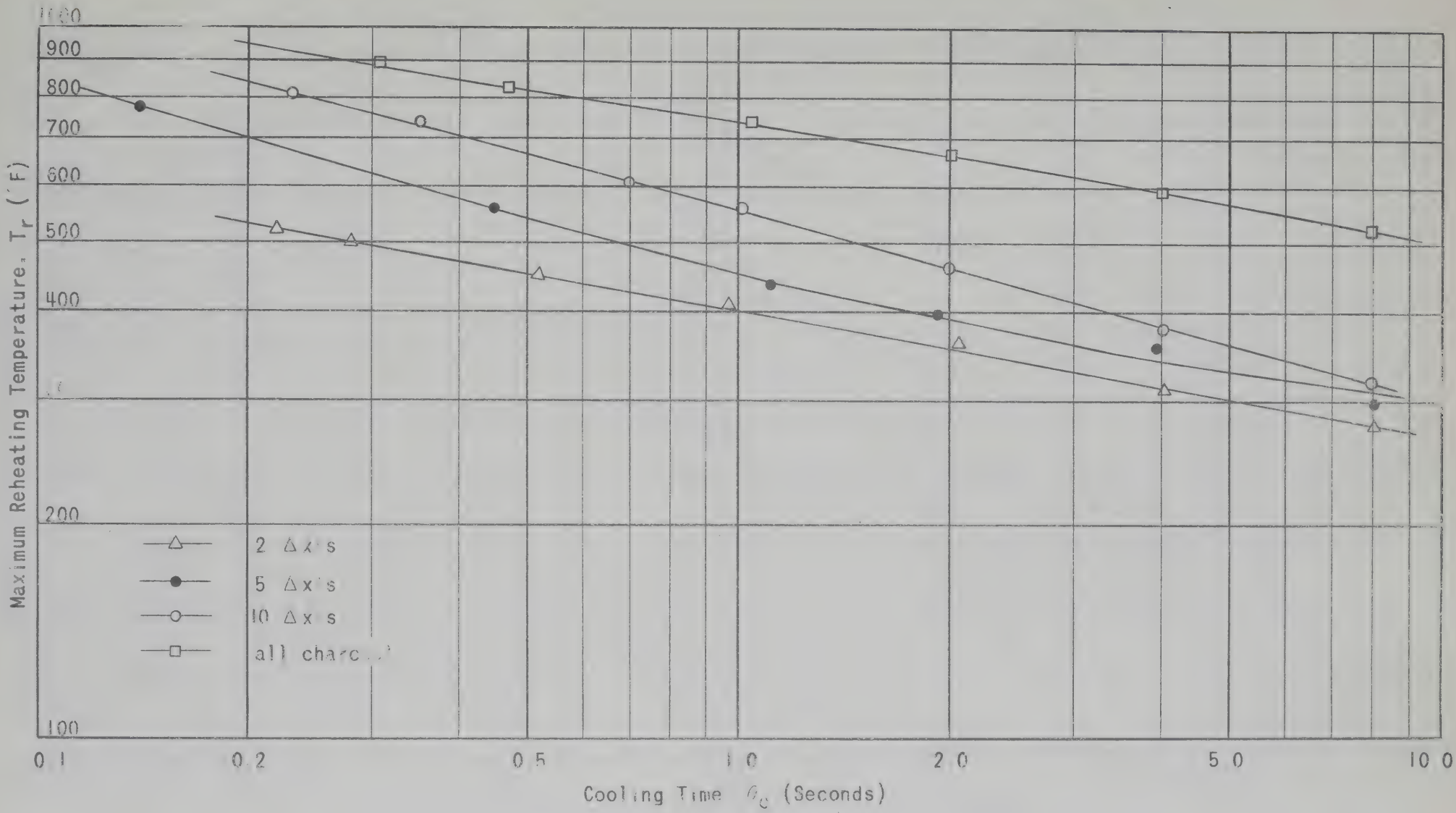

FIG. 11. THERMAL ANALYZER RESULTS FOR SLABS WITH ONE DIMENSIONAL HEAT FLOW

($h = 6.0$ Btu / ft^2 °F hr)

(Surface cooling)

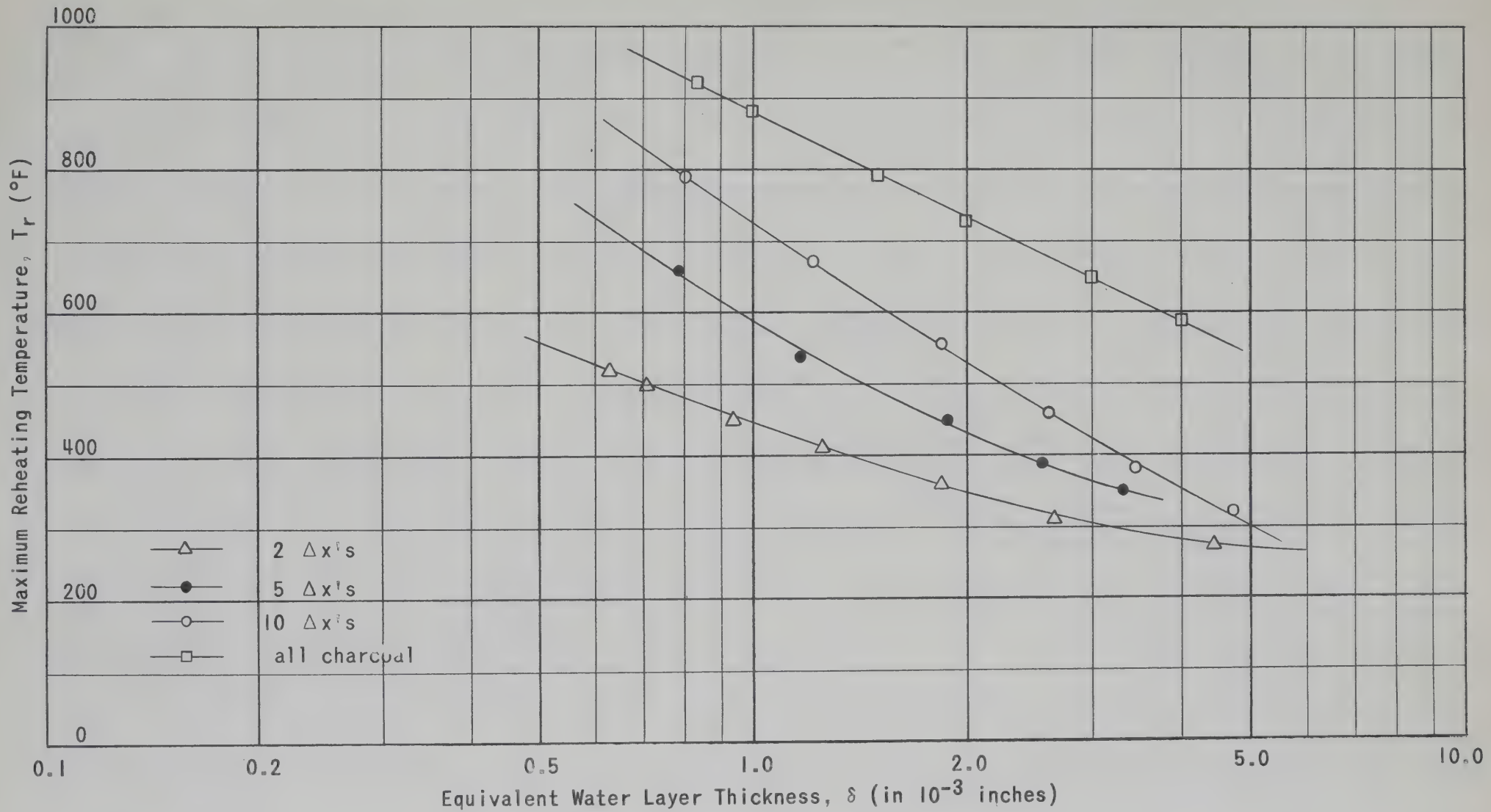

FIG. 12. THERMAL ANALYZER RESULTS FOR SLABS WITH ONE DIMENSIONAL HEAT FLOW.

($h = 6.0$ Btu / ft^2 °F hr)

(Surface cooling)

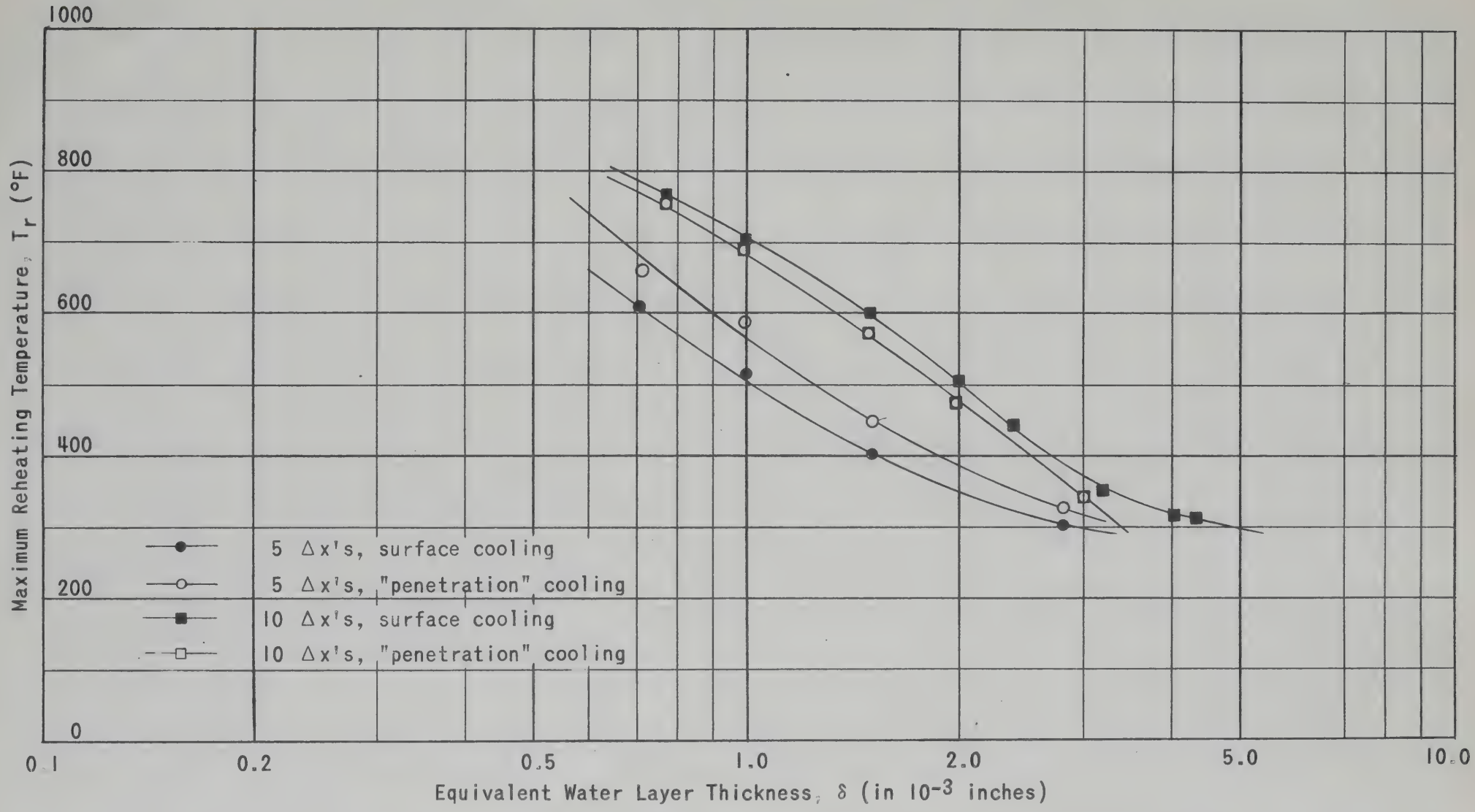

FIG. 13. THERMAL ANALYZER RESULTS FOR CYLINDER WITH ONE DIMENSIONAL HEAT FLOW.
($h = 6.0$ Btu / ft^2 °F hr)

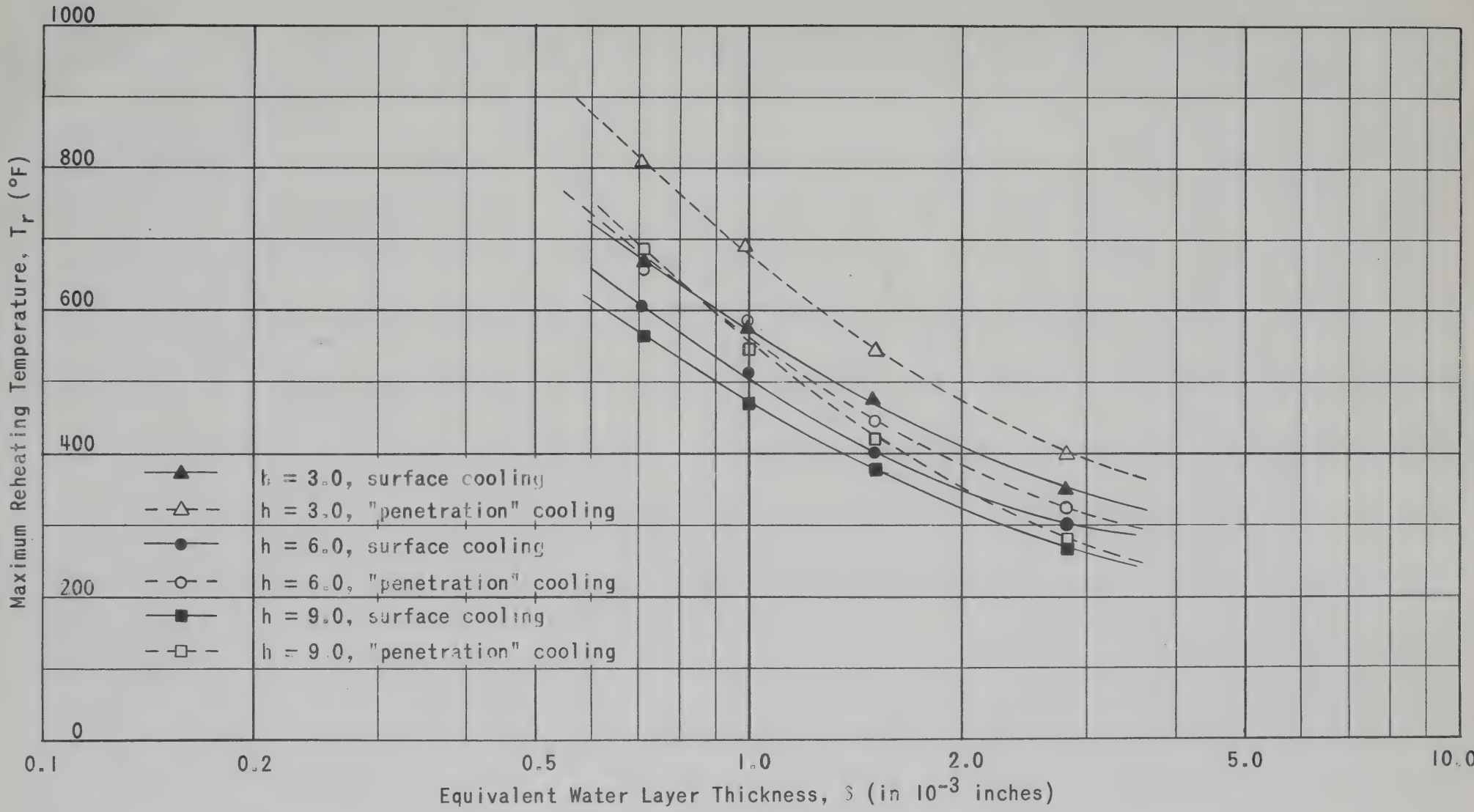

FIG. 14. THERMAL ANALYZER RESULTS FOR CYLINDER WITH ONE DIMENSIONAL HEAT FLOW.

(5 Δx's)

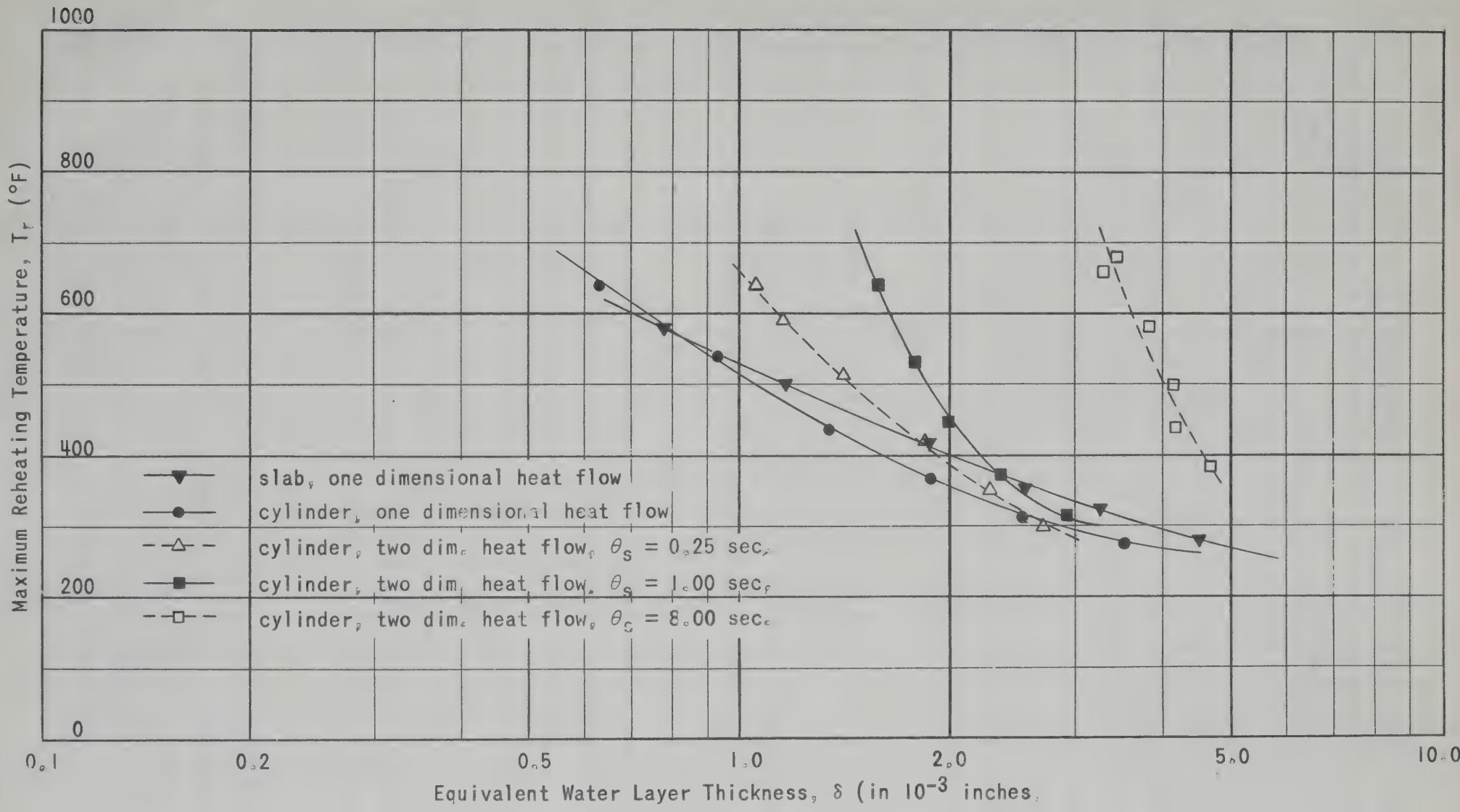

FIG. 15. COMPARATIVE THERMAL ANALYZER RESULTS.

(Surface cooling with 5 Δx's and h = 6.0 Btu / ft^2 °F hr)

A comparison of the effects of surface cooling and "penetration" cooling on extinguishment may be made from the curves plotted in Fig. 13 and Fig. 14 for the cylinder with one dimensional heat flow. It would appear from these curves that there is no clear cut advantage of "penetration" cooling over surface cooling. One might therefore conclude that as far as the effect of cooling is concerned in extinguishing a wood fire as viewed in these studies, the penetration ability of the suppressing agent is not of great importance. In the extinguishment of actual fires, however, there may be other factors or mechanisms present for which penetration of the suppressing agent may either directly or indirectly contribute to the overall effectiveness. On the other hand from observations made during laboratory and field test fires, it appeared that spread wetting was a desirable action in order that the fire might be extinguished on the side of a stick away from the spray. It is even conceivable that penetration action may be detrimental in slowing down spread wetting by causing the front part of the stick to become saturated with an excess amount of water that must first penetrate before it can build up to a sufficient thickness on the surface to spread wet.

The effect of h, the combined unit thermal conductance for radiation and convection, on the results may be seen in Table 4 and in the curves of Fig. 14 for the cylinder with one dimensional heat flow. For each type of extinguishment there was a noticeable spread in the results for h = 3.0, 6.0, and 9.0 Btu / ft^2 °F hr with greater amounts of the extinguishing agent needed for the smaller values of h.

The effect of the three spread wetting rates used in the surface cooling runs for the cylinder with two dimensional heat flow may be seen in the curves of Fig. 15. Comparable curves are also plotted for one dimensional heat flow in both the slab and the cylinder where instantaneous wetting on all sides was simulated. It was thought that the spread wetting rate of one second per sector most closely approximated the observed rates during suppression of laboratory model fires of similar sized specimens. Using this intermediate spreading rate, it can be seen that about two and one half times as much water was required for extinguishment as for the comparable instantaneous wetting case. Also it can be seen that the equivalent water layer thickness is decreased if the spreading rate is increased.

What was thought to be the most striking result of all these tests was the comparatively small amounts of water required for extinguishment. For example, a layer of water approximately one-thousandth of an inch thick suddenly applied over the surface of a 0.6 in. diameter burning wood cylinder should be sufficient to suppress the fire and prevent rekindling in the subsequent rise of surface temperature. This gives a ratio of the volume of wood to the volume of water required for extinguishment approximately equal to 150 / 1. In certain laboratory and field test fires (3), compa-

rable ratios were in the order of 7 / 1[1], thus showing the large room for improvement of techniques of extinguishing wood fires.

A comparison of curves for the one dimensional heat flow cases shows that results for a cylinder are fairly closely approximated by results for a slab with comparable number of elements of charcoal and values of h. This would tend to show that the geometry for these various cases does not influence the results as greatly as does the heat transfer in the portion of the material near the surface.

Times for extinguishment in the oxygen dilution runs are listed in Table 4. These decrease in about the manner expected with the higher values of h and with the smaller degree of fire establishment indicated by the lower number of charcoal elements. Except for the severe case of the uniformly heated complete charcoal slab, extinguishment times range from about two to eight seconds for the representative value of h = 6.0 Btu / ft^2 °F hr. These times are approximately five to ten times greater than the water cooling times from the comparable surface cooling runs where a T_r of 600° F was obtained.

---

[1] *In recent tests (8), W.L. Fons has obtained ratios as high as 117 / 1, for laboratory model fires and 56 / 1 for field test fires using burning stacks of logs.*

CONCLUSIONS

1. When water at ordinary temperatures strikes burning wood, it will not instantaneously boil, and consequently initial wetting should be possible.

2. The thicker water layers required for the greater depths of charcoal show that more suppressing action is needed for extinguishing the more established fires.

3. There appears to be no significant difference in the values of the maximum reheating temperature obtained for the "penetration" cooling runs and the equivalent surface cooling runs.

4. For all types of extinguishment the value of the unit surface conductance, h, which affects the ambient cooling, has a significant influence on the maximum reheating temperature.

5. A layer of water approximately one-thousandth of an inch thick suddenly applied over the surface of a 0.6 in. diameter burning wood cylinder should be sufficient to extinguish the fire and prevent rekindling. This gives a ratio of the volume of wood to the volume of water equal approximately to 150 / 1.

6. If the frontal area of a 0.6 in. diameter burning wood cylinder is instantaneously wetted and if four additional seconds are required for the wetting to cover the entire rear portion due to a finite rate of spread, the amount of water required for extinguishment will be about two and one-half times as great as would be required if the entire wetting were instantaneous.

7. The amount of water required to suppress a burning cylinder of wood is decreased if the rate of spread wetting is increased.

8. For one dimensional heat flow, results for a cylinder are fairly closely approximated by results for a slab.

9. Results for the oxygen dilution runs, representing CO_2 extinguishing, indicate that the times required for extinguishment range between about two and eight seconds for conditions that are believed to be most representative of actual situations.

ACKNOWLEDGMENT

The research represented in this paper was performed as a part of a more extensive program under a cooperative agreement between the University of California and the United States Forest Service. For their helpful cooperation and valued assistance, the authors are particularly indebted to Messrs. W.L. Fons and I.C. Funk of the Forest Service, and Messrs. L.M.K. Boelter, R. Bromberg, and B.R. Mead of the Department of Engineering, University of California, Los Angeles.

BIBLIOGRAPHY

1 "The Chemistry of Wood," by L.F. Hawley and L.E. Wise, American Chemical Society Monograph Series No. 28, The Chemical Catalogue Company, Incorporated, New York, New York, page 188.

2 "Technical Report Number 1 - Engineering Fire Control Research," by G.J. Tauxe, C.K. Hadlock, and R.L. Stoker, Cooperative Agreement Number A5Fs-103-72, University of California, Los Angeles, California, June 30, 1948.

3 "Technical Report Number 2 - Engineering Fire Control Research," by R.L. Stoker and G.J. Tauxe, Cooperative Agreement Number A5Fs-103-72, University of California, Los Angeles, California, January, 1949.

4 "The Heating and Ignition of Small Wood Cylinders," by W.L. Fons, California Forest and Range Experiment Station, Berkeley, California, April 16, 1948.

5 "The Conduction of Heat in Composite Infinite Bodies," by W.A. Mersman, W.P. Berggren, and L.M.K. Boelter, University of California Press, Berkeley, California, 1942, page 9.

6 "Heat Transfer Notes," by L.M.K. Boelter, V.H. Cherry, H.A. Johnson, and R.C. Martinelli, University of California Press, Berkeley, California, 1946.

7 "Heat Transmission," by W.H. McAdams, McGraw-Hill Book Company, Incorporated, New York, New York, 1942, page 63.

8 "Investigation of Use of Water and Chemicals for Forest Fire Syppression," by W.L. Fons, R.S. McBride, and E.E. Draves, California Forest and Range Experiment Station, Berkeley, California, May 9, 1950.

Transactions, American Geophysical Union Volume 32, Number 1 February 1951

A COMPARISON OF SEVERAL HEAT AND MASS TRANSFER NETWORKS OF INTEREST IN WATER CONSERVATION

Heinz F. Poppendiek and Myron Tribus

Abstract--Electrical networks descriptive of the heat and mass transfer processes occurring in the systems such as lakes, open fields, snow banks, and United States Weather Bureau evaporation pans, are presented and discussed. Suggestions for research and correlation of measurements are given on the basis of an examination and comparison of the networks.

Introduction--Exact solutions to most heat and mass transfer problems can only be obtained by the solution to the diffusion equation. There has been a growing appreciation, however, for the fact that many "field" problems may be solved with a satisfactory approximation by "network" methods, that is, treating in place of a system of spatially distributed quantities an approximately similar system comprised of "lumped" parameters. This method of analysis often results in a better overall view of the problem. It is the purpose of this paper to show how this network approach may be applied to the following systems involving large scale heat and mass transfer (evaporation): (a) an open field, (b) a melting snowbank, (c) a lake, and (d) an evaporation pan.

The treatment of problems in heat transfer [TRIBUS and MORRIN, 1948], mechanics [MILES, 1943], and electromagnetic radiation [McALLISTER, 1944], by the consideration of an equivalent network has permitted profitable analysis by analogic means, and what is equally important, has provided a terse graphic means of portraying the important variables in a complicated system. The thermal or mass flow network has the same significance in diffusion problems as has the free body diagram in mechanics. The important variables stand out unencumbered by non-essential details.

A brief search of the literature revealed that this mode of analysis has not been brought to bear upon the problems of large scale evaporation in such systems as open earth fields, lakes, or snowbanks. Many workers are active in this field, each, in general, attacking one portion of the network. If the presentation of the complete systems (via network representation) serves to show the common features in these many investigations, the purposes of this paper will have been met.

Symbols and subscripts--The following symbols are used:

A = area, sq ft
B = barometric pressure, inches Hg
f_c = unit thermal conductance, Btu/hr ft^2 °F
f_m = unit mass conductance, lb/ft^2 hr (lb/lb)
g = mass flux, lb/hr
H = specific humidity, lb water/lb air
k = thermal conductivity, BTU/hr sq ft (°F/ft)
L = latent heat of vaporization for water, BTU/lb
P = vapor pressure of water, in Hg
q = heat flux, BTU/hr
R = thermal resistance, °F/BTU/hr
t = temperature, °F
τ = temperature of receiver, °F
y = distance from surface, ft
$\triangleq$ means equal by definition

The following subscripts are used:

c = convection of heat
m = mass transfer
s = surface
∞ = "free stream"
dp = dew point
mr = mean radiant
f = mixed mean fluid

The network parameters--A simple example of the network technique may be found in the case of convective heat transfer to or from a fluid flowing in a pipe. (The heat conduction equation for a moving fluid is in many cases the same for the atmosphere as for the fluid in the pipe; only the boundary conditions and scale of turbulence are changed.) The thorough way of studying the details of the heat transfer mechanism is certainly to solve the fluid flow (hydrodynamic) and temperature (thermal) equations simultaneously. Even for such a simple system as flow in a pipe the problem is not easy, in fact, only for a few systems have the equations been solved. On the other hand, the compelling reason for solving these equations is the desire to predict the behavior of heat exchange equipment involving flow in tubes. Since this requires only the magnitude of the heat flow across the boundary, it is customary to define a "unit thermal conductance" (known also as a "heat transfer coefficient" and "film coefficient"; called "conductance" here to emphasize its role in the circuit) according to

$$q \triangleq f_c A(t_w - t_f) \quad \ldots\ldots\ldots\ldots\ldots\ldots\ldots\ldots (1)$$

where A is the area through which heat flows, and subscript w relates to the pipe wall.

The product $f_c A$ corresponds to the "conductance" of an electrical circuit; the reciprocal is referred to as a "thermal resistance" and is indicated in thermal circuits by the same symbol as is used for a resistor in electrical circuits.

How has the introduction of this symbol simplified the problem? Also, how does it relate to the solution we would obtain were we to solve the classical equations for the heat transfer in the fluid? The last question may be answered first. If the solution to the fluid flow and heat transfer equations were available we would have on hand some function which described the temperature distribution in the flowing fluid. This function would then be differentiated and the heat flow determined from the gradient of temperature at the wall of the tube, that is from

$$q \triangleq -kA(dt/dy)_{y=0} \quad \ldots\ldots\ldots\ldots\ldots\ldots\ldots\ldots (2)$$

From the definition of the conductance it is evident that the unit thermal conductance is related to the gradient of temperature in the fluid by the equation

$$f_c = -[k(dt/dy)_{y=0}]/(t_w - t_f) = -k\left\{\partial[(t - t_f)/(t_w - t_f)]/\partial y\right\}_{y=0}$$

The use of the unit thermal conductance for heat transfer then is a way of discussing the behavior of the all important gradient of dimensionless temperature at the boundary in the absence of information about the entire temperature field. This gradient (or the conductance) is a function of many parameters, which affect the hydrodynamic and thermal equation, the fluid properties, nature of boundary layer, flow velocity, and stability, all of which concern us. Lack of exact knowledge of the entire field does not prevent us from considering the conductance and also does not prevent us from measuring it.

If, in a thermal system, the temperature is a function of time, one must consider the effect of thermal capacity. It is evident that the analogous electrical quantity is the capacitance. In thermal circuits the accepted symbol for a capacitor is used. In an analogous fashion the defining equation for the unit conductance for mass transfer is given by

$$g \triangleq A f_m (H_S - H_\infty) \quad \ldots\ldots\ldots\ldots\ldots\ldots\ldots\ldots (3)$$

The definition for the conductance is seen to consider that the driving potential for mass transfer is the concentration (or specific humidity). Obviously other potentials could be chosen; the conductance would then take on a different numerical value and different units. The proper potential to take is probably the fugacity of the water, but the vapor pressure is easier to measure. If the vapor pressure is taken as the potential, but the conductance is retained in the manner defined above, the resulting equation for the mass transfer is

$$g = A f_m\, 0.62\, (P_S - P_\infty)/B \quad \ldots\ldots\ldots\ldots\ldots\ldots (4)$$

Associated with each pound of water evaporated, there is L, the heat of vaporization, approximately 1050 BTU/lb. The energy transfer associated with the evaporation process is therefore given by

$$q_e = A f_m\, 0.62\, L\, (P_S - P_\infty)/B \quad \ldots\ldots\ldots\ldots\ldots\ldots (5)$$

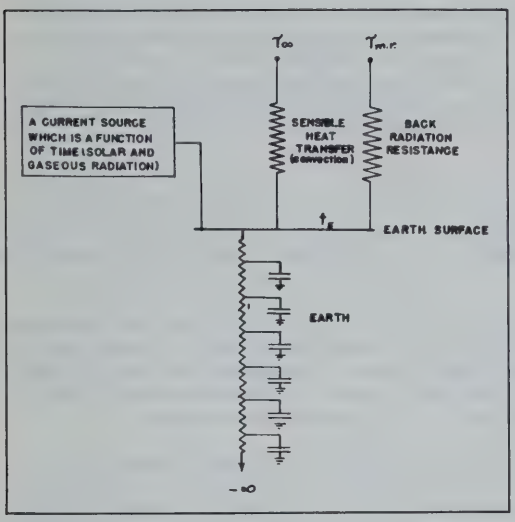
A CURRENT SOURCE WHICH IS A FUNCTION OF TIME (SOLAR AND GASEOUS RADIATION)
SENSIBLE HEAT TRANSFER (convection)
BACK RADIATION RESISTANCE
EARTH SURFACE
EARTH
-∞

Fig. 1--Thermal network for Earth system (in the absence of mass transfer)

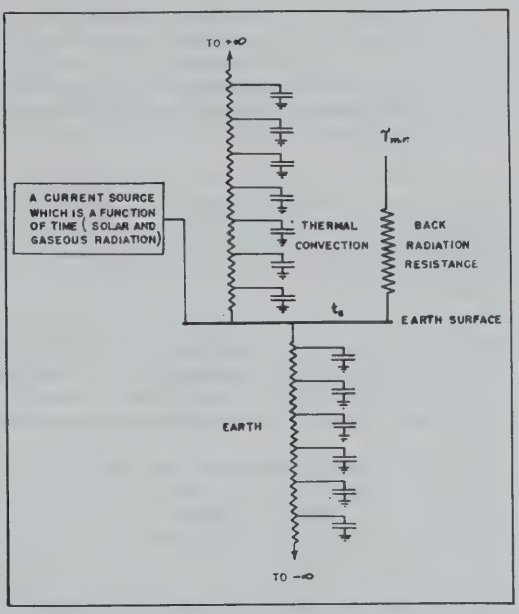

Fig. 2--Thermal network for Earth system with convective path in its more complete form (in the absence of mass transfer)

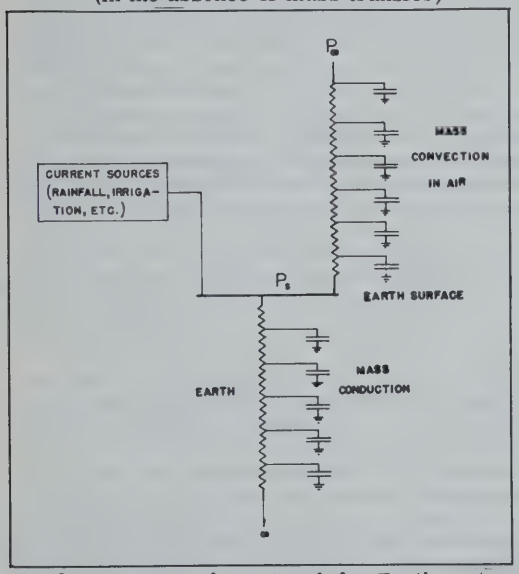

Fig. 3--Mass transfer network for Earth system

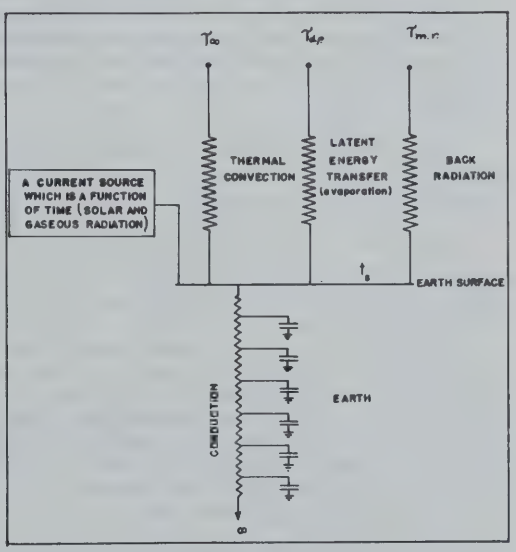

Fig. 4--Energy transfer network for Earth system with combined heat and mass transfer

The usual way of defining the thermal resistance is by means of the equation

$$q = \Delta t/R \quad \ldots\ldots\ldots\ldots\ldots (6)$$

The temperature difference to be used is somewhat arbitrary in most convection systems, the choice of temperature difference determining the magnitude of the resistance. For the mass transfer resistance one potential is taken as the temperature of the surface in question, the other, for reasons which will become apparent later is taken as the dew point of the air at the position where P_{∞} is measured.

The thermal resistance is therefore given by the following equation, obtained by eliminating q from the previous two equations

$$R_e = [(t_S - \tau_{dp})/(P_S - P_{\infty})](1.61/L)(B/f_m A) \quad \ldots\ldots\ldots\ldots\ldots (7)$$

If a temperature other than the dew point is used as the lower potential in the definition for the resistance for the evaporative process, negative values for R_e may occur. Since P_S corresponds to the saturation pressure at t_S and τ_{dp} corresponds to the dew point at vapor pressure P_∞, the equivalent resistance is always positive. Another method of treating the evaporative terms in the energy balance is to consider equivalent "sources" or "sinks" of current, as will be demonstrated when the effects of solar energy input are considered.

The fact that the thermal resistance turns out to be a function of the surface temperature as well as the free stream dew point should not be considered unusual. Thermal circuits in general are non-linear circuits and one must adopt the same techniques in treating them as are adopted by electrical engineers in studying networks containing vacuum tubes, relays or non-ohmic elements with thyrite.

The discussion which follows will be limited to systems in which there is no variation in network parameters with distance parallel to the surface from which the transfers occur. Such systems are the easiest to analyze, but if a complete solution is to be obtained, the effects of the upstream conditions on the downstream behavior should be included. In particular the effects of currents in lakes and of fronts in the atmosphere will not be included in the paper.

The thermal network for heat and mass flow in the open earth field system--Figure 1 shows the thermal circuit for an open Earth-field system. The Earth is considered to be made up of layers and to each layer there is assigned a resistance and a capacitance (that is, the distributed system is approximated by a resistance-capacitance (RC) network). The more finely the divisions are taken the more closely the behavior of the RC network will approximate the solutions to the diffusion equation. The solar input, being independent of the Earth temperature, is represented by a current source which follows a prescribed function of time. (A current source is a device which supplies a current to a network regardless of the potential as opposed to a potential source which maintains a constant potential regardless of the current drain. Practical electrical devices for this purpose function only in a limited range fixed by their design.) The convective heat flow resistance between the air and ground is represented by the resistor marked convection which is extremely variable in time. This resistance can be represented more completely by an RC network, similar to the one used for heat transfer in the Earth. The resistor marked "radiation" is representative of the "back radiation" resistance and is the predominant mode of heat transmission at night.

The lower potential for the radiant energy transfer from the Earth to outer space is the mean radiant temperature, that is, the effective temperature for radiation as measured by a radiometer integrating over a hemisphere.

Figure 2 reveals the heat-transfer network which contains the more complete convection circuit. The search for proper values of the eddy diffusivity in the Earth's atmosphere may be likened to the attempt to evaluate the indiviual resistors in the convection path of Figure 2.

In general, workers on the problem of heat transfer in the Earth have confined their attention to one part of the network or another. Thus, considerable data are available on heat flows in the Earth [PATTEN, 1909; SMITH, 1938, 1939], net radiation from the Earth to the sky [BOELTER, POPPENDIEK, YOUNG, and ANDERSEN, 1949], and solar irradiation [MOON, 1940]. Fewer data are available on the convective path [LETTAU, 1939]. Most workers use the Earth temperature as one reference, although if the problem is one of predicting heat flow it is seen that the surface temperature is the result of the currents in each part of the network and surface temperature should be treated as a dependent variable, not as the independent one.

In parallel with the thermal network there exists a mass-flow network. Figure 3 shows the network representation for the mass transfer. Moisture is exchanged between the Earth and air. The soil represents a resistance to the transfer of moisture which has been studied [SMITH, 1943] but seldom treated in conjunction with the resistance to convective transfer in the air.

Actually the heat- and mass-transfer networks are in action at the same time. The two modes of energy transfer affect one another in several ways. The moisture content of the soil influences the thermal conductivity and heat capacity of the Earth. The temperature at the Earth's surface influences the vapor pressure there. The moisture content of the air in turn affects the resistance to radiation and the magnitude of the nocturnal radiation.

Figure 4 shows the network which represents the combined transfers of energy to or from the Earth's surface. It would serve no useful purpose to add to the diagram the indications of how the

one resistance is affected by the current flows in other branches, but these mutual effects must be considered when "analyzing" the network.

The network for a snowbank system--Because the largest evaporation rate for snowbanks probably occurs when the snow is in the process of melting, this case will be considered. The case of the snowbank when the snow is not melting is simpler and can easily be treated when the more complicated case is understood.

Figure 5 shows the network drawn to represent the energy-transfer processes in the snowbank. As shown in Figure 5, the surface of the snowbank stays at 32° F while the snow is melting. A battery is indicated as maintaining the surface "potential" (temperature) constant in much the same fashion as the latent heat of fusion serves to hold the temperature fixed. (The current flow to or from the battery simulates the amount of heat transferred during melting or freezing.) The input energy from the Sun, indicated by the current source, is not all absorbed at the surface of the snowbank, but is rather absorbed in successive layers. The snowbank has a very low thermal conductivity and diffusivity. The heat transmission within the snowbank is represented by the RC network. The snowbank rests upon the Earth and the conduction of heat in the Earth is represented by the RC network shown. Radiation to the sky and convection to the air are shown as before.

The network for a lake--Figure 6 shows a network which has been drawn to illustrate energy flow paths for a lake system. In Figure 6, the various resistances which occur in the network within the lake are all functions of the turbulence occuring in the water. Thus the wind, the viscosity, the temperature distribution, and lake currents affect the magnitudes of the resistances. Like the case of the snowbank, the water does not absorb the solar energy at the surface of the lake, but rather there is a steady absorption from the top down. The absorptivity of the water depends upon its purity. Data on the absorptivity of pure water are given in MOON [1936] and HULBURT [1926]. These data indicate that at a level of one foot beneath the surface of the lake, 60 per cent of the energy has been absorbed. (The usual exponential law may be applied.)

The transfers of energy from the lake surface to the sky and air are accomplished by the same processes as exist in the Earth and snowbank systems. There will be a large difference between the evaporation rates from deep lakes as compared to shallow lakes. In a shallow lake (something just short of a marsh, say) a large fraction of the radiant energy will be absorbed at the bottom of the lake and considerable heat will be transferred by convection from the lake bottom to the water. This will lead to an instability and promote the convective transfer within the lake. Also, the capacity of the shallow lake will be less and the temperature of the surface will in general rise higher during the 24-hr cycle. Note that in a deep lake the solar radiation is absorbed in lesser and lesser quantities as one proceeds from the surface. This gives rise to a more stable daytime temperature distribution in the lake and does not promote convection.

The network for a pan--Because the evaporation pans are often used as a guide in the prediction of evaporation rates for lakes and other surfaces it is of interest to draw the equivalent network for the energy transfer processes occurring in a pan. Figure 7 shows a sketch of a standard Weather Bureau evaporation pan as installed in a typical location [U. S. WEATHER BUREAU, 1948]. Figure 8 indicates the equivalent network.

The relation between the resistances for convection and evaporation--WALKER, LEWIS, McADAMS, and GILLILAND [1937] and BOELTER, CHERRY, JOHNSON and MARTINELLI [1946] demonstrate that the conductances for heat and mass transfer should be proportional to one another. The latter reference shows that at temperatures near 50° F the ratio of f_c to f_m (conductance for heat transfer by convection to the conductance for mass transfer) is approximately 0.22 for an air-water system for either free or forced convection. These relations have been established for small scale convection systems, that is, wet bulbs, cooling towers, airplane wings in icing conditions, small spheres, flat plates, and other similar systems. There are good reasons to expect the relations to continue in large scale phenomena, but proof is at present lacking.

The two resistances will be proportional to one another provided, of course, the flow paths between them are the same. For this reason, the point at which the lower potential is selected must be the same for both heat and mass transfer. If the "air reference temperature" is taken at a five-foot level, then the "air dew point" should be taken at the same height. Eq. (8) gives the resistance for heat transfer

$$R_c = 1/f_c \; A \quad \ldots\ldots\ldots\ldots\ldots\ldots\ldots\ldots\ldots\ldots (8)$$

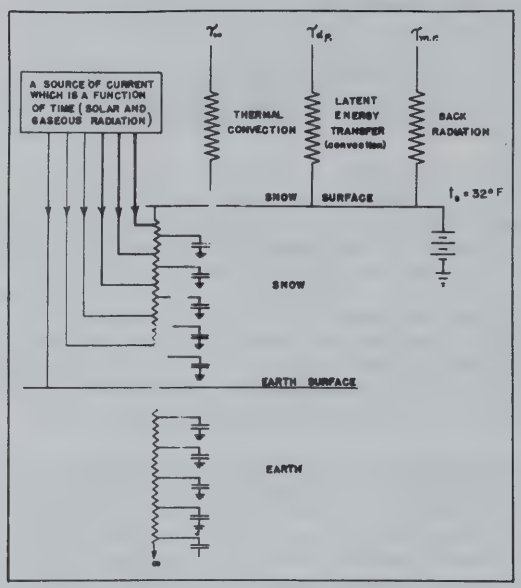

Fig. 5--Energy transfer network for a melting snowbank

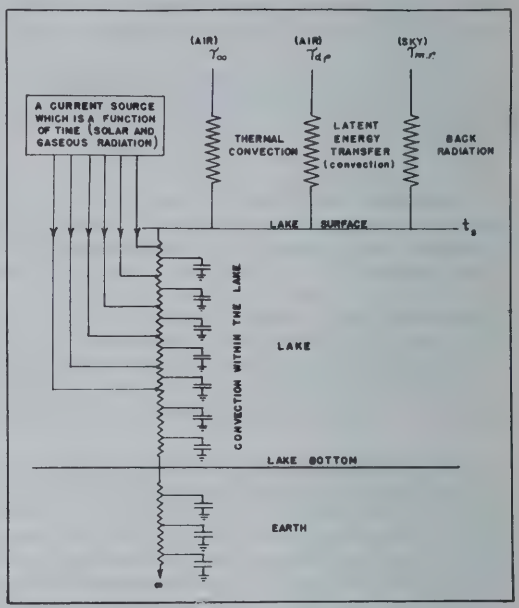

Fig. 6--Energy transfer network for a lake system

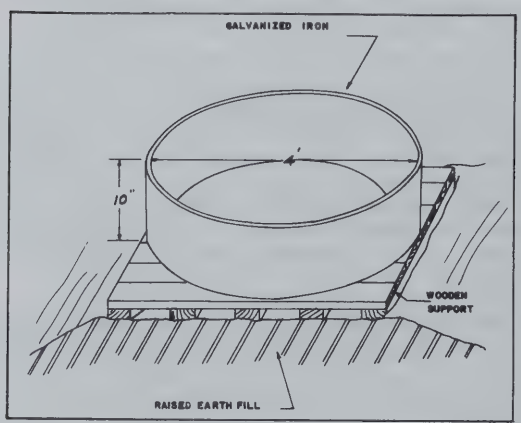

Fig. 7--Typical pan installation

Comparison with (7) indicates that the ratio of the two resistances, sensible to latent energy transfer, is given by

$$R_c/R_e = (f_m/f_c)[(P_s - P_\infty)/(t_s - \tau_{dp})]0.62\ L/B \quad \ldots\ldots (9)$$

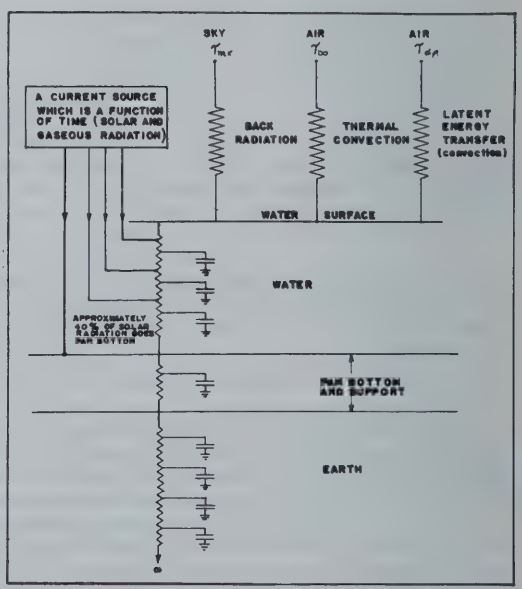

Fig. 8--Energy transfer network for pan system

Because of the previously mentioned ratio between the heat and mass-transfer conductances for a water-air system, the ratio between resistances noted in (9) is ultimately given by

$$R_c/R_e = 2.8(L/B)[(P_s - P_\infty)/(t_s - \tau_{dp})] \quad \ldots\ldots\ldots\ldots (10)$$

In the case of evaporation from a lake surface or from a melting snowbank the above ratio is a function of three parameters, the surface temperature, the free-stream dew point and the barometric pressure. The variation with barometric pressure is linear, hence a graph of this ratio as a function of two parameters will suffice. Figure 9 shows a graph of the ratio of the two resistances plotted against surface temperature with free stream dew point as a parameter for the

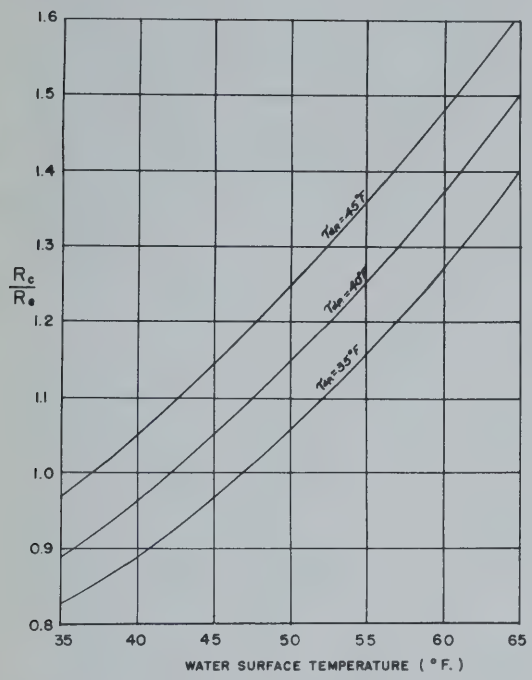

Fig. 9--Ratio of convective to evaporative resistances versus surface temperature for various free air dew points

lake and melting snowbank systems.

Some comments on the prediction of evaporation rates from lakes based upon consideration of the network characteristics--If wet- and dry-bulb air temperature, mean radiant temperature, back radiation resistance, latent heat resistance, sensible heat resistance, total hemispherical radiation, and water eddy diffusivity variations were known for the lake system, it would be possible to obtain a temperature solution by numerical or analog methods. If such a temperature solution were available, it would then be possible to calculate evaporation rates from the lake because the mass transfer potential would be known.

The most satisfactory and direct means of predicting the rate of evaporation from a surface is to know the magntiudes of the conductance, the surface vapor pressure and the vapor pressure in the free stream (wherever the "free stream" may be). This technique must be applied with care for the results are very sensitive to the accuracy of the measurements. For example, it is very difficult to determine the temperature of the surface of a lake. True, the water temperature may be measured, but it is the temperature at the interface which must be measured--a measurement taken two centimeters beneath the surface will be worthless, particularly at high evaporation rates where there will be steep gradients in the fluid. The vapor pressure of water changes very rapidly with temperature, and an error of five degrees F in temperature measurement may well mean an error of 65 per cent or more in predicted evaporation rate. The lake surface temperature may be measured by (1) making water temperature soundings in the uppermost water layers of the lake, or (2) dragging a light balsawood float, with an attached thermocouple under it, over the lake surface.

The determination of heat transfer convective conductances for the range of stability conditions encountered could be accomplished by measuring convective heat transfer rates and air temperature profiles over land. Such studies are at present being conducted by the Department of Engineering at the University of California.

Mass transfer convective conductances could be measured for a range of stability conditions over a smooth snowfield where ablation, radiation, and humidity measurements can be made; the classical work of SVERDRUP [1936] typifies the investigation that can be made.

Another technique for predicting evaporation is to set up an evaporation pan and multiply the ratio of areas of lake and pan by the pan evaporation rate and some empirically determined "coefficient." Until careful measurements have been made of the evaporation rates from a few lakes, such comparisons must necessarily be considered no more than enlightened guesses. A comparison of the networks for the pan and lake system indicated that few of the resistances are similar, the capacitances are unequal and the circuits are very different. Pan evaporation rates reveal little that could not be predicted from separate measurements of wind velocity, gustiness, humidity, solar irradiation and air temperature.

Energy methods, as consistently suggested by CUMMINGS [1940] are not satisfactory for lake systems, for these energy methods usually suggest that the energy is absorbed at the lake surface. It has been shown, however, that the absorption of the radiation occurs gradually with depth and that the surface temperature of the lake depends upon the magnitude of the convective resistances within the lake as well as the external ones. If the resistance to heat transfer within the lake were known, the energy method would have considerable value particularly when modified to take into account the actual processes occurring. Suppose that the conductance within the lake were known and the temperature beneath the surface were also known at a particular depth. If the surface temperature of the lake were known (but not necessarily with the precision required for

accurate knowledge of the vapor pressure), the rate of energy transfer to the lake surface (and thence to the air) might be computed. Now it is a curious circumstance, as Cummings has pointed out, that if the heat flow from the lake is given, the evaporation rate is not a very sensitive function of the unit mass conductance between the lake and the air. For example, if the unit mass conductance is large, the vapor pressure difference will be small and when the unit mass conductance is small the vapor pressure difference will be large. An accurate value of the conductances between the lake and air would not be necessary to the prediction of the evaporation rate. Unfortunately, there are available at present no methods for measuring the energy flux from beneath the surface of the lake. Until methods of measurement for either the water side resistance or the water side energy flux are available, the energy methods cannot be used for accurate prediction of evaporation rates from lakes.

References

BOELTER, L. M. K., V. H. CHERRY, H. A. JOHNSON, and R. C. MARTINELLI, Heat transfer notes, University of California Press, Berkeley and Los Angeles, pp. LVI-38 to XVI-43, 1946.

BOELTER, L. M. K., H. F. POPPENDIEK, G. YOUNG, and J. R. ANDERSEN, An investigation of aircraft heaters--XXX Nocturnal irradiation as a function of altitude and its uses in determination of heat requirements of aircraft, Nat. Adv. Com. Aeronautics, TN 1454, January, 1949.

CUMMINGS, N. W., The evaporation-energy equations and their practical application, Trans. Amer. Geophys. Union, pt. 2, pp. 512-522, 1940.

HULBURT, E. O., The transparancy of ocean water, J. Opt. Soc. Amer., v. 13, p. 553, 1926.

LETTAU, H., Atmosphärische Turbulenz, Ak. Verl. M. B. H., Leipzig, pp. 133-149, 1939.

McALLISTER, J. F., Equivalent circuit of an electromagnetic field, Gen. Elec. Rev., p. 9, March, 1944.

MILES, J. W., Applications and limitations of mechanical-electrical analogies, new and old, J. Acoust. Soc. Amer., v. 14, no. 3, pp. 183-192, January 1943.

MOON, P., The scientific basis of illuminating engineering, McGraw-Hill, 168 pp., 1936.

MOON, P., Proposed standard solar radiation curves for engineering use, J. Franklin Inst., v. 230, pp. 583-617, 1940.

PATTEN, H. W., Heat transference in soils, U. S. Dept. Agric. Bur., Soils Bull. 59, 1909.

SMITH, W. O., and H. G. BYERS, The thermal conductivity of dry soils of certain of the great soil groups, Soil Sci. Soc. Amer., Proc., v. 3, pp. 13-19, 1938.

SMITH, W. O., Thermal conductivities in moist soils, Soil Sci. Soc. Amer., Proc., v. 4, pp. 32-40, 1939.

SVERDRUP, H. U., The eddy conductivity of the air over a smooth snow field, Geofys. Pub., Norske Vidensk.-Akad. Oslo, v. 11, no. 7, 1936.

U. S. WEATHER BUREAU, Instructions for the installation and operation of weather bureau Class A evaporation stations, (instructions issued in conjunction with Weather Bureau Circular L), Washington D. C., August 1948.

WALKER, W. H., W. K. LEWIS, W. H. McADAMS, and E. R. GILLILAND, Principles of chemical engineering, McGraw-Hill, 591 pp., 1937.

TRIBUS, M., and E. H. MORRIN, Elementary heat transfer, University of California Press, Berkeley and Los Angeles, 130 pp., 1948.

Department of Engineering,
University of California,
Los Angeles 24, California

(Manuscript received March 20, 1950; presented at the Twenty-Fifth Regional Meeting, Davis, California, February 3, 1950; open for formal discussion until July 1, 1951.)

The Determination of Variables Included in a Composite Prediction of Matriculation in Engineering

by

W. P. Wallace, Lecturer, and

H. W. Case, Associate Professor

Engineering Department
University of California
Los Angeles

In 1949 at the A.S.E.E. Meetings held at Troy, the authors presented a paper entitled, "The Correlation of Industrial Criteria and Demand for Engineers." Following the presentation of this paper, correspondence with individuals who were interested in the possible applications of the technique seemed to indicate the desirability of investigating the relationship of national trends (as measured by various national economic indices) to the number of engineers graduating from the colleges in any given year. It was thought probable that by experimenting with a time lag for certain of the variables a technique of prediction might be developed that would prove to be experimentally interesting.

Utilizing the method developed by Gengerelli, the intercorrelations were determined on a yearly basis for several series of economic indices and engineering graduates for the same period of time. A time lag of one, two, three, and four years was introduced between the economic variables and the engineering graduates. Thus a whole series of possible intercorrelations were determined; such as the intercorrelations existing between economic variables of 1927, 1926, 1925, and 1924 and the number of engineers graduating in 1928.

Since it was recognized that economic variables show variations of large magnitude in periods of extreme national crises (such as war) and the causes of these sudden variations may not be related in the same manner

The Phenomenon of Individual Decisions in a Complex Institution of Mass-Production Be Explained Par

by

K. J. Wellman, Professor, and

Dr. V. Chase, Associate Professor

Department Psychology
University of California
Los Angeles

to the data being used as in a normal period, it was decided that the basic data used to obtain the intercorrelations would exclude the war period. Therefore, the period of 1920 to 1939 inclusive was used as the basis upon which the data was obtained for the regression equations shown in Figs. 1-8 inclusive. It is unfortunate that much of the data compiled before 1920 for these indices was not compiled on the same basis as for 1920 and the following period, and as a result would be misleading if included in the equation. The intercorrelations, which are shown in Table 2, were used to determine the weights to be assigned to each of the values used in the regression equation. The raw data from which these intercorrelations were obtained is shown in Table 1.

Figures 1 through 4 illustrate graphically the results of predictions when the graduation class of the previous year is retained in the correlation matrix (introducing essentially the concept of a one year lag in the graduating class). When taken over a twenty-year period, the extremely high relationship existing between succeeding graduating classes (0.97 in one equation) prevents the economic variables from exerting any significant contributing influence to the regression equation. It will be noted that the period 1940-1950 was predicted by using the regression equation based upon the data from 1920-39. It is apparent that if the relationship that is shown in these tables continues to be true, obviously one of the easiest methods of predicting the class of the next year would consist of using the class of the current year rather than calculating hypothetical attrition rates.

In order to determine if this hypothesis would hold if additional data were added into the correlation series, the data for the period of 1940 to 1947 inclusive was added to each of the series of variables (thus giving 28 cases as against 20 in the 1920 to 1939 series). A regression equation

was then computed for this period using the graduating class of the previous year (expressed as a 1 year lag), the wholesale price index (2 year lag), and the Dow-Jones Averages (2 year lag). On the basis of this regression equation the predicted number of engineering graduates for the year 1948 was 29,700, while the actual number was 27,500. For the year 1949 the predicted number was 41,000, while the actual was 41,800, and for 1950 the predicted is 45,200--the actual at the writing remains to be determined. This relationship is shown graphically in Fig. 9 and in its accompanying tables. It is to be noted that a slight drop in the correlation (0.91) with the preceding graduating class is evident (probably brought about by the inclusion of the war years) which in turn allows the economic indices to exert a slightly greater effect on the regression equation.

Because of the high intercorrelations obtained between the current and the graduating class of the preceding year, it was decided to exclude this factor from the correlation matrix (the matrix would then only include economic variables) and to apply Gengerelli's technique to determine whether a regression equation could be worked out from these variables that would not suffer from the excessive loading resulting when the preceding graduating class was included in the matrix. Using the economic data from 1920 to 1939 and introducing the time lags as indicated previously, a series of regression equations were solved. The results obtained are shown graphically in Figures 5, 6, 7, and 8. As in the first study, it will be noted that the regression equation obtained for this period was then used to predict the trend for 1939 to 1950. An examination of these curves seems to indicate that with the economic variables used the four year time lag gives a closer approximation to the actual number of engineering graduates

than any of the other curves. The results might seem to indicate that at least the possibility exists that eventually a series of economic indices may be determined which when used with the correct time lag may bear a close relationship to actual conditions.

In conclusion, it should be pointed out that, while the method seems to show promise, the entire procedure is undoubtedly open to some question due to the possibility of having spurious correlations occur in the variables comprising the time series, either because of unmeasurable intangibles in the variables or because of lack of data accumulated for a sufficient length of time to afford to produce a significant correlation. It is the hope of the authors that other investigators may apply the method to time series to aid in determining its usefulness as a prediction device.

References

1. J. A. Gengerelli, Psychometrica, September, 1948.

2. N. Wiener, "Extrapolation, Interpretation and Smoothing of Stationary Time Series." John Wiley and Sons.

Table 1 - Raw Data

Year	Grad. 4 yr. lead Y	Grad. 3 yr. lead X1	Energy X2	Wholesale Price Index X3	National Income X4	Production Index X5	Consumer's Price Index X6	Dow-Jones Assoc. X7	Gov't. Non-war Exp. X8	Grad. 2 yr. lead X9	Grad. 1 yr. lead X10	Enroll-ment X11	Grad. Current X12
1920	69	66	110	193	64	86	146	69	33	64	52	77	43
1921	67	69	91	122	75	67	131	66	44	66	64	81	52
1922	65	67	90	120	87	84	123	81	32	69	66	85	64
1923	67	65	119	126	96	101	124	89	32	67	69	88	66
1924	68	67	107	123	99	94	124	91	33	65	67	92	69
1925	67	68	110	130	101	103	128	119	29	67	65	93	67
1926	66	67	121	125	108	110	129	140	31	68	67	94	65
1927	79	66	118	119	112	109	125	157	30	67	68	95	67
1928	92	79	117	121	115	113	124	197	31	66	67	96	68
1929	97	92	126	119	129	126	124	204	33	79	66	96	67
1930	103	97	112	108	121	104	122	162	38	92	79	97	66
1931	100	103	97	91	113	86	111	80	49	97	92	97	79
1932	97	100	83	81	91	67	99	42	74	103	97	98	92
1933	98	97	90	83	85	79	94	52	61	100	103	98	97
1934	100	98	95	94	91	86	98	89	91	97	100	99	103
1935	114	100	100	100	100	100	100	100	100	98	97	100	100
1936	130	114	113	101	113	118	101	148	122	100	98	100	97
1937	131	130	121	108	120	130	105	118	107	114	100	130	98
1938	138	131	105	98	120	102	103	104	100	130	114	130	100
1939	132	138	114	97	132	125	101	125	121	131	130	163	114

All data reduced to 100% for the year 1935, and are expressed as a percentage.
The economic data, enrollment, and current graduates are for the years shown; the other data for graduates include a lead of 4, 3, 2 or 1 year.

(1) Journal of Engineering Education
(2) Minerals Year Book, Bureau of Mines
(3) Handbook of Basic Economic Statistics, 1949

Table 2 - Correlation Coefficients - Data: 1920-1939

		Grads. 3 yr. lead X1	Energy X2	Wholesale Price Index X3	Nat'l. Inc. X4	Production Index X5	Consumer's Price Index X6	Dow-Jones avg.(lows) X7	Gov't. Non War Exp. X8	Grads. 2 yr. lead X9	Grad. 1 yr. lead X10	Enroll-ment X11	Grads. Current X12
Graduates (4 yr. lead)	Y	0.97	0.08	-0.58	0.60	0.44	-0.76	0.18	0.87	0.92	0.86	0.78	0.83
Graduates (3 yr. lead)	X1		-0.01	-0.61	0.57	0.37	-0.77	0.05	0.87	0.97	0.91	0.84	0.85
Energy	X2			0.38	0.59	0.88	0.36	0.79	-0.12	-0.15	-0.22	0.21	-0.18
Wholesale Price Index	X3				-0.41	0.04	0.88	0.09	-0.54	-0.66	-0.75	-0.45	-0.77
National Income	X4					0.80	-0.29	0.73	0.30	0.47	0.41	0.66	0.41
Production Index	X5						-0.03	0.80	0.25	0.22	0.16	0.53	0.23
Consumer's Price Index	X6							0.21	0.81	-0.82	-0.91	-0.57	-0.95
Dow-Jones Avgs. (Lows)	X7								-0.11	-0.11	-0.17	0.38	-0.10
Gov't. Non-War Exp.	X8									0.87	0.88	0.72	0.89
Graduates (2 yr. lead)	X9										0.96	0.83	0.81
Graduates (1 yr. lead)	X10											0.82	0.95
Enrollment	X11												0.75

Table 3 - Correlation Coefficients - Data: 1920-1947

		Grad. 1 yr. lead X2	Grad. Current X3	Enroll-ment X4	National Income X5	Production Index X6	Wholesale Price Index X7	Dow-Jones Avgs. X8	Govt. Non-War Exp. X9
Grads. 2 yr. lead	X1	.912	.67	.90	.51	.46	.40	.30	.88
Grads. 1 yr. lead	X2		.85	.92	.51	.49	.23	.19	.88
Grads. Current	X3			.64	.57	.61	.04	.10	.72
Enrollment	X4				.39	.37	.39	.30	.81
Nat'l. Income	X5					.97	.26	.46	.58
Prod. Index	X6						.38	.42	.53
Wholesale Price Index	X7							.29	.21
Dow-Jones Avgs.	X8								.24

$$r = \frac{(n.\Sigma xy) - (\Sigma x.\Sigma y)}{\sqrt{[n.\Sigma x^2 - (\Sigma x)^2]\,[n.\Sigma y^2 - (\Sigma y)^2]}}$$

Calculations and Results

The correlation coefficients for various economic data and graduates are shown in Table 2.

From this table, it will be observed that for a one year lead on economic variables, the highest correlation coefficient is 0.95, relating engineering graduates of one year with those of the preceding year. In other words, the best correlation of engineering graduates is with those for the preceding year. (The column marked "Graduates-Current" refers to graduates for the same year as the data on economic variables.)

Using these correlation coefficients, the coefficients for the regression equation are found as follows:[3]

$$oB = r_{12} = 0.95 \quad \text{(Current graduates)}$$
$$r_{o12}$$

$$o\,B_2 = -.22 - .95(-.18) = .00$$

$$o\,B_3 = -.75 - .95(-.77) = -.04$$

$$o\,B_4 = .41 - .95(.41) = +.02$$

$$o\,B_5 = .16 - .95(.23) = -.06$$

$$o\,B_6 = -.91 - .95(-.95) = -.01$$

$$o\,B_7 = -.17 - .95(-.10) = +.07$$

$$o\,B_8 = .88 - .95(.89) = +.03$$

$$o\,B_{11} = .82 - .95(.75) = +.11$$

$$oB_{11} = r_{o11} = 0.11 \text{ (Enrollment)}$$

Regression equation is:

E.G. = (0.95) (Grads. of prec. year) + (0.11) (Enrollment)

The results from this equation are illustrated in Fig. 1.

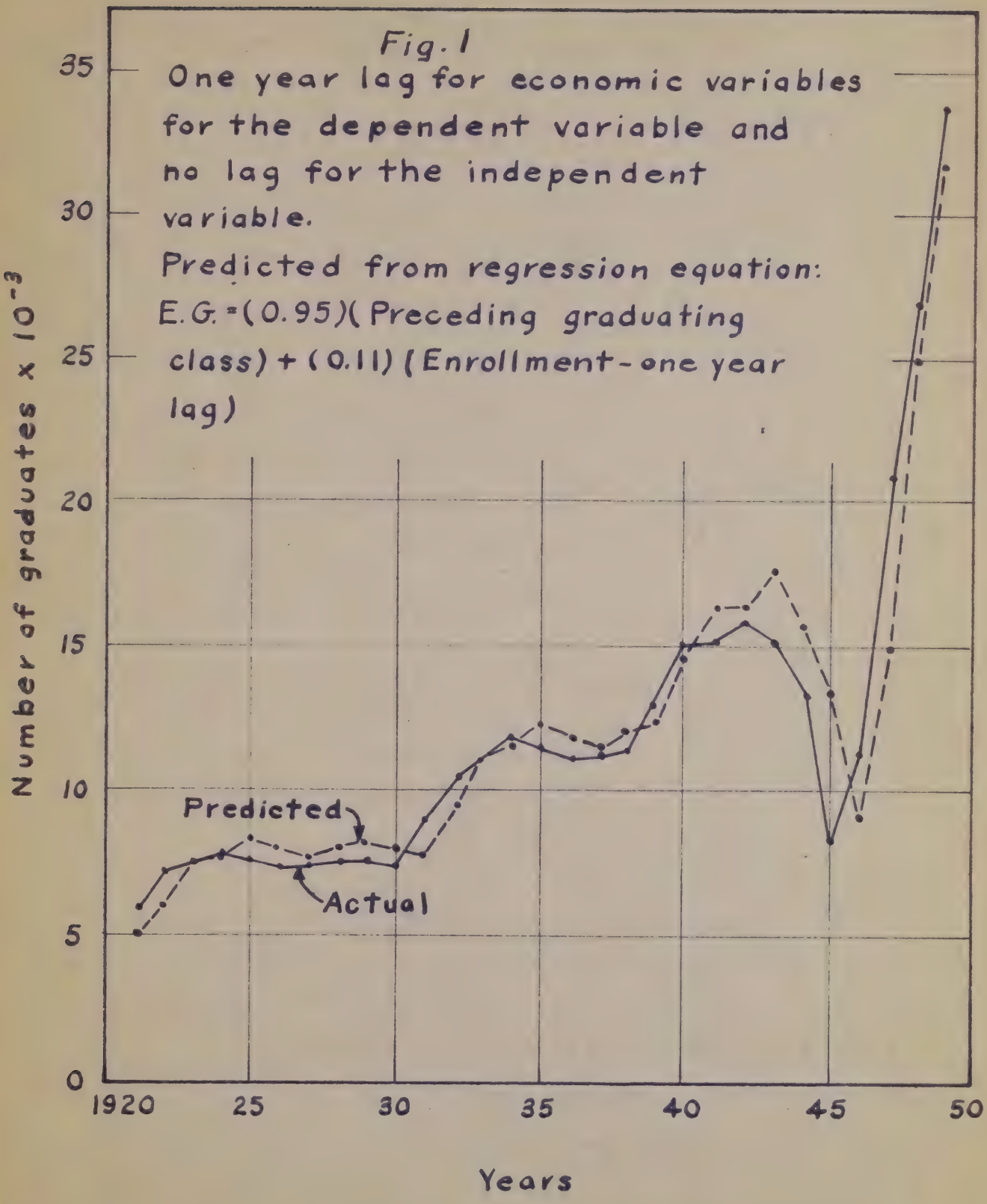
Fig. 1
One year lag for economic variables for the dependent variable and no lag for the independent variable.
Predicted from regression equation:
E.G. = (0.95)(Preceding graduating class) + (0.11)(Enrollment - one year lag)
Number of graduates x 10^{-3}
35
30
25
20
15
10
5
0
Predicted
Actual
1920
25
30
35
40
45
50
Years

The correlation coefficients for 2, 3, and 4 year lags and the corresponding calculations of regression coefficients follow:

Calculations for 2 y ar lead

$o\ B_{10} = r_{o10} = 0.96$ (Prev. year graduates)

$o\ B_2 = -.15 \quad -.96(-.22) = \ .06$

$o\ B_3 = -.66 \quad -.96(-.75) = +.06$

$o\ B_4 = \ .47 \quad -.96(\ .41) = +.07$

$o\ B_5 = \ .22 \quad -.96(\ .16) = +.07$

$o\ B_6 = -.82 \quad -.96(+.91) = +.05$

$o\ B_7 = -.11 \quad -.96(-.17) = +.05$

$o\ B_8 = +.87 \quad -.96(\ .88) = +.02$

$o\ B_{11} = +.83 \quad -.96(\ .82) = +.04$

$o\ B_{10} = +.81 \quad -.96(\ .95) = -.10$

$o\ B_4 = 0.07$ (National Income)

$o\ B_2 = \ .06 \quad -.07(+.59) = +.02$

$o\ B_3 = \ .06 \quad -.07(-.41) = +.09$

$o\ B_5 = \ .07 \quad -.07(\ .80) = +.01$

$o\ B_3 = 0.09$ (Wholesale Price Index)

Regression equation is:

Graduates = (Grad. of preceding year) (0.96) + (National Income) (0.07) + (Wholesale Price Index) (0.09)

The results from the preceding regression equation are illustrated in Fig. 2.

Fig.2

Two year lag for economic variables for the dependent variable and one year lag for the independent variable.

Predicted from regression equation:

E.G. = (0.96)(Preceding graduating class) +(0.07)(National Income) +(0.09) (Wholesale Price Index)

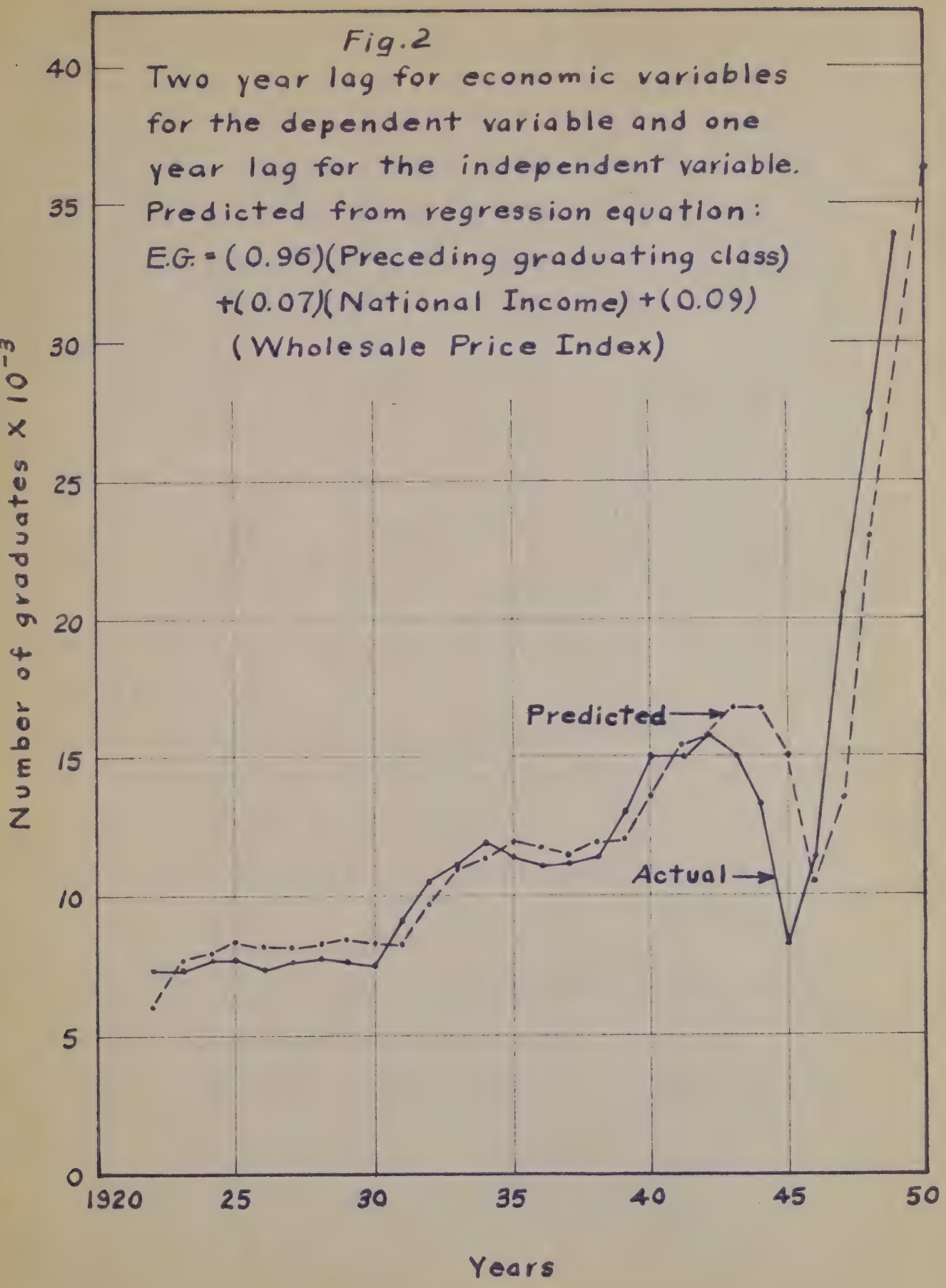

Calculations for 3 year lead

$o\ B_9 = r_{o9} = 0.97$ (Prev. year graduates)

$o\ B_2 = -.01 - .97(-.15) = +.14$

$o\ B_3 = -.61 - .97(-.66) = +.03$

$o\ B_4 = .57 - .97(.47) = +.11$

$o\ B_5 = .37 - .97(.22) = +.16$

$o\ B_6 = -.77 - .97(-.82) = +.03$

$o\ B_7 = .05 - .97(-.11) = +.16$

$o\ B_8 = .87 - .97(.87) = +.03$

$o\ B_{10} = .91 - .97(.96) = -.02$

$o\ B_{11} = .84 - .97(.83) = +.03$

$o\ B_{12} = .85 - .97(.81) = +.06$

$o\ B_5 = 0.16$ (Production Index)

$o\ B_2 = .14 - .16(..88) = .14 - .14 = 0$

$o\ B_4 = .11 - .16(.80) = .11 - .13 = -.02$

$o\ B_7 = .16 - .16(.80) = .16 - .13 = +.03$

$o\ B_{12} = .06 - .16(.23) = .06 - .04 = +.02$

Regression equation is:

Graduates = (0.97) (Graduates of prec. year) +

(0.16) (Production Index)

The results from this equation are illustrated in Fig. 3.

Fig. 3

Three year lag for economic variables for the dependent variable and two year lag for the independent variable.

Predicted from regression equation:

E.G. = (0.97)(Preceding graduating class) + (0.16)(Production Index)

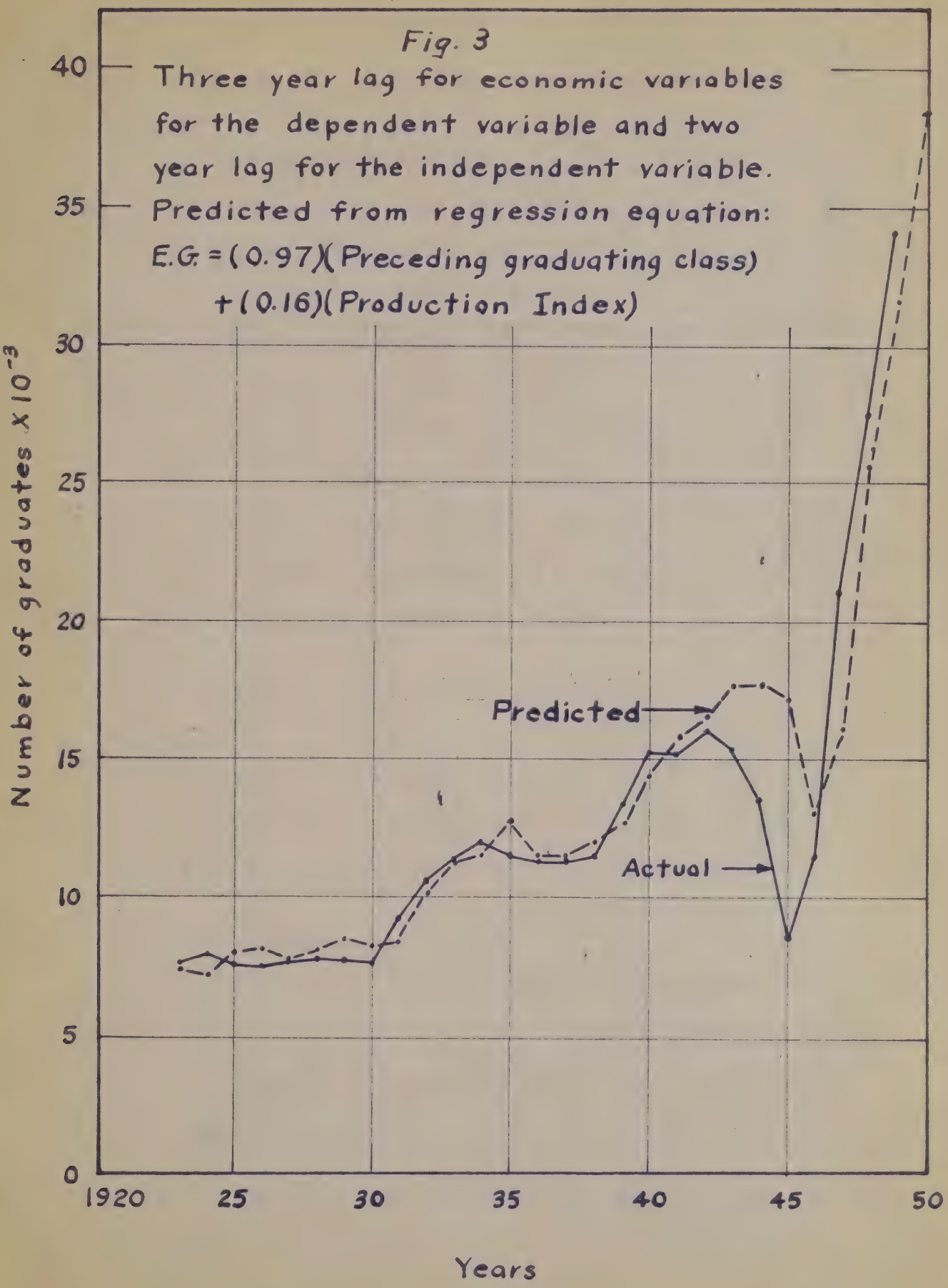

Calculations for Graduates - 4 year lag

- $B_1 = r_{o1} = 0.97$ (Previous Graduating Class)

- $B_2 = .08 - (.97)(-.01) = .09$
- $B_3 = -.58 - (.97)(-.61) = .01$
- $B_4 = .60 - (.97)(.57) = .05$
- $B_5 = .44 - (.97)(.37) = .08$
- $B_6 = -.76 - (.97)(-.77) = -.01$
- $B_7 = .18 - (.97)(.05) = .13$
- $B_8 = .87 - (.97)(.87) = .02$
- $B_9 = .92 - (.97)(.97) = -.02$
- $B_{10} = .86 - (.97)(.91) = -.02$
- $B_{11} = .78 - .97(.84) = -.04$
- $B_{12} = .83 - .97(.85) = +.01$

- $B_7 = 0.13$ (Dow-Jones averages)

- $B_2 = .09 - .13(.79) = .09 - .10 = -.01$
- $B_4 = .05 - .13(.73) = .05 - .10 = -.05$
- $B_5 = .08 - .13(.80) = .08 - .10 = -.02$

Regression equation is:

Graduates = (0.97)(Graduates of prec. year)
+ (0.13)(Dow-Jones Averages)

Results from this regression equation are illustrated in Fig. 4.

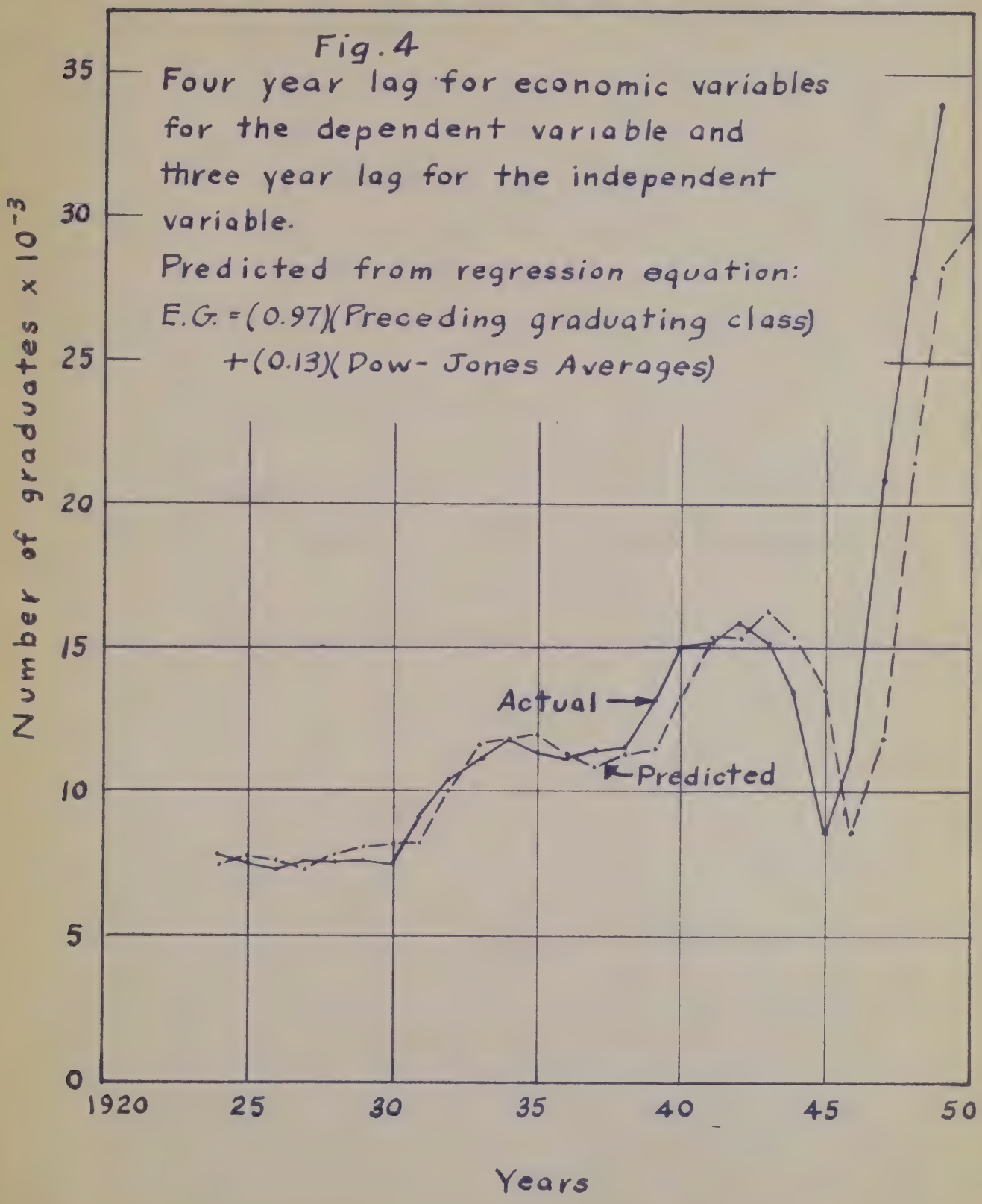
Fig. 4
Four year lag for economic variables for the dependent variable and three year lag for the independent variable.
Predicted from regression equation:
E.G. = (0.97)(Preceding graduating class)
+ (0.13)(Dow-Jones Averages)
Number of graduates x 10^{-3}
35
30
25
20
15
10
5
0
Actual
Predicted
1920
25
30
35
40
45
50
Years

Calculations for 1 year lag for Economic Variables

o $B_8 = r_{o8} = 0.88$ (Govt. N-W Exp.)

o $B_2 = -.22 -(.88)(-.12) = -.11$

o $B_3 = -.75 -(.88)(-.54) = -.27$

o $B_4 = .41 -(.88)(.30) = .15$

o $B_5 = .16 -(.88)(.25) = -.06$

o $B_6 = -.91 -(.88)(.81) = -1.62$

o $B_7 = -.17 -(.88)(-.11) = -.07$

o $B_3 = 0.15$ (National Income)

Regression equation is:

Graduates = (0.88)(Govt. Non-War Expenditures) + (0.15)
(National Income)

Results from this regression equation are illustrated in Fig. 5.

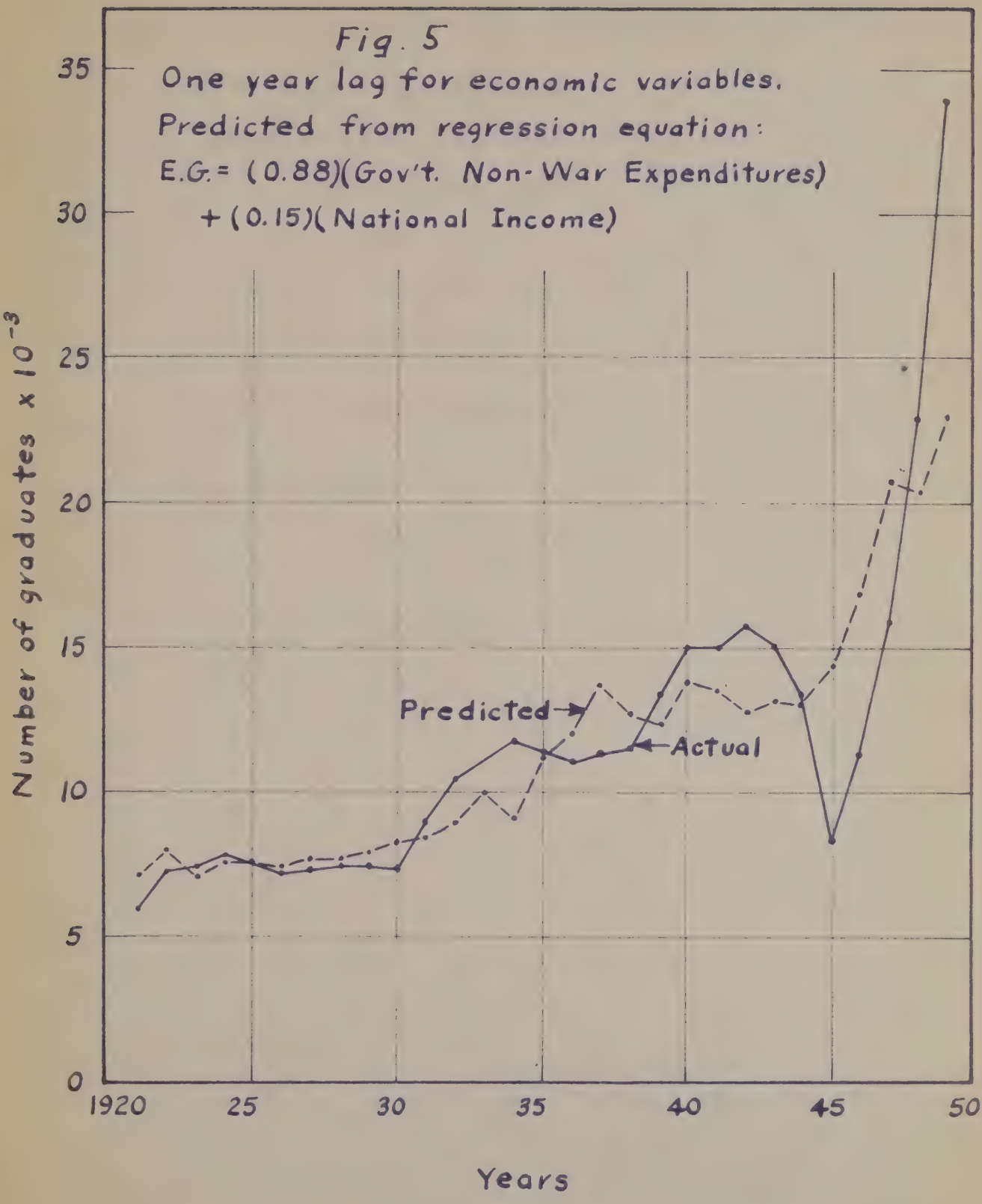
Fig. 5
One year lag for economic variables.
Predicted from regression equation:
E.G. = (0.88)(Gov't. Non-War Expenditures)
+ (0.15)(National Income)
Number of graduates x 10^{-3}
35
30
25
20
15
10
5
0
1920
25
30
35
40
45
50
Years
Predicted
Actual

Two-year lag for economic variables

$o\ B_8 = r_{o8} = 0.87$ (Govt. N-W Exp.)

$o\ B_2 = -.15 - .87(-.12) = -.04$

$o\ B_3 = -.66 - .87(-.54) = -.19$

$o\ B_4 = .47 - .87(.30) = +.21$

$o\ B_5 = .22 - .87(.25) = 0$

$o\ B_6 = -.82 - .87(.81) = -1.53$

$o\ B_7 = -.11 - .87(-.11) = -.01$

$o\ B_4 = 0.21$ (National Income)

Regression equation is:

E.G. = (0.87) (Govt. Non-War Exp.) + (0.21)

(National Income)

Results from this regression equation are illustrated in Fig. 6.

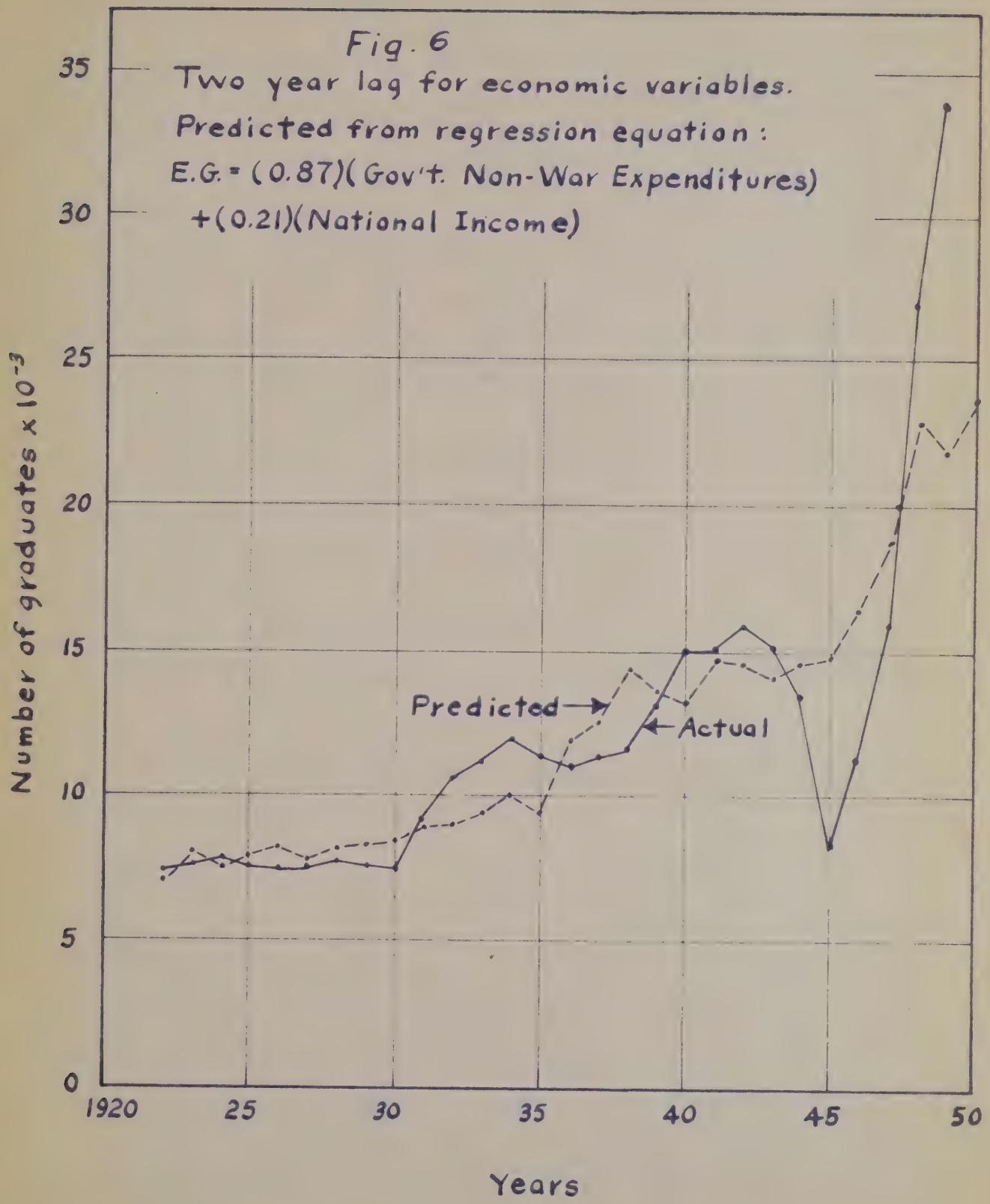
Fig. 6
Two year lag for economic variables.
Predicted from regression equation:
E.G. = (0.87)(Gov't. Non-War Expenditures)
+(0.21)(National Income)
Number of graduates x 10⁻³
35
30
25
20
15
10
5
0
1920
25
30
35
40
45
50
Years
Predicted
Actual

Three-year lag for economic variables

o $B_8 = r_{o8} = 0.87$ (Govt. Non-War Exp.)

o $B_2 = -.01 - .87(-.12) = +.10$

o $B_3 = -.61 - .87(-.54) = +.14$

o $B_4 = .57 - .87(.30) = +.31$

o $B_5 = .37 - .87(.25) = +.15$

o $B_6 = -.77 - .87(.81) = +.49$

o $B_7 = .05 - .87(-.11) = +.15$

o $B_4 = 0.31$ (National Income)

o $B_2 = .10 - .31(.59) = -.08$

o $B_5 = .15 - .31(.80) = -.10$

o $B_7 = .15 - .31(.73) = +.08$

Regression equation is:

E.G. = (0.87) (Govt. N-W Exp.) + (0.31) (National Income)

Results from this equation are illustrated in Fig. 7.

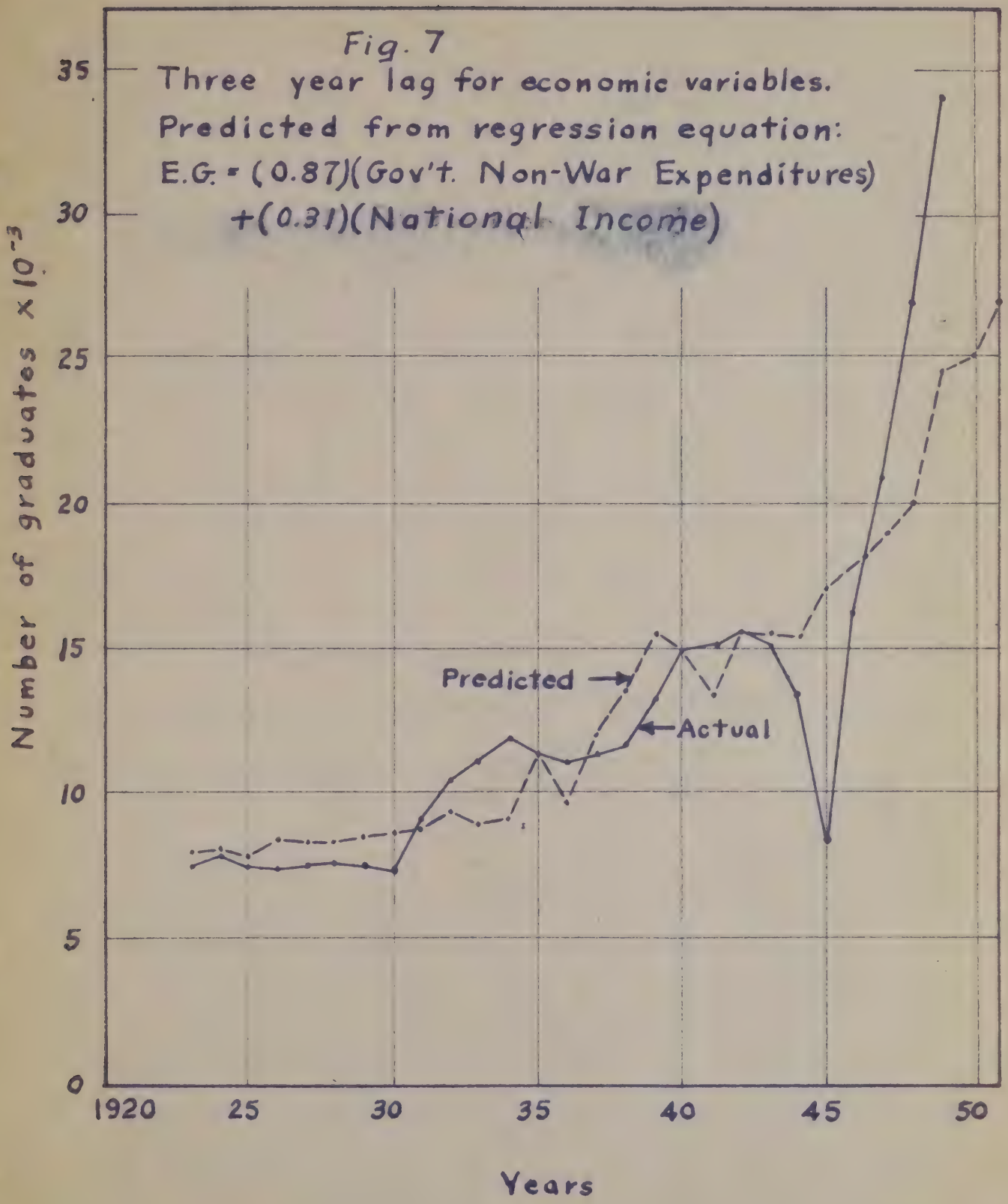
Fig. 7
Three year lag for economic variables.
Predicted from regression equation:
E.G. = (0.87)(Gov't. Non-War Expenditures)
+(0.31)(National Income)
Number of graduates x 10⁻³
35
30
25
20
15
10
5
0
1920
25
30
35
40
45
50
Years
Predicted
Actual

Four-year lag for economic variables

o $B_8 = r_{o8} = 0.87$ (Govt. Non-War Exp.)

o $B_2 = .08 - .87(-.12) = .18$

o $B_3 = -.58 - .87(-.54) = -.11$

o $B_4 = .60 - .87(.30) = .34$

o $B_5 = .44 - .87(.25) = .22$

o $B_6 = -.76 - .87(.81) = -1.47$

o $B_7 = .18 - .87(-.11) = .28$

o $B_4 = 0.34$ (National Income)

o $B_2 = .18 - .34(.59) = -.02$

o $B_5 = .22 - .34(.80) = -.05$

o $B_7 = .28 - .34(.73) = +.03$

Regression equation is:

Graduates = 0.87 (Govt. Non-War Exp.) + 0.34 (National Income)

Results from this equation are illustrated in Fig. 8.

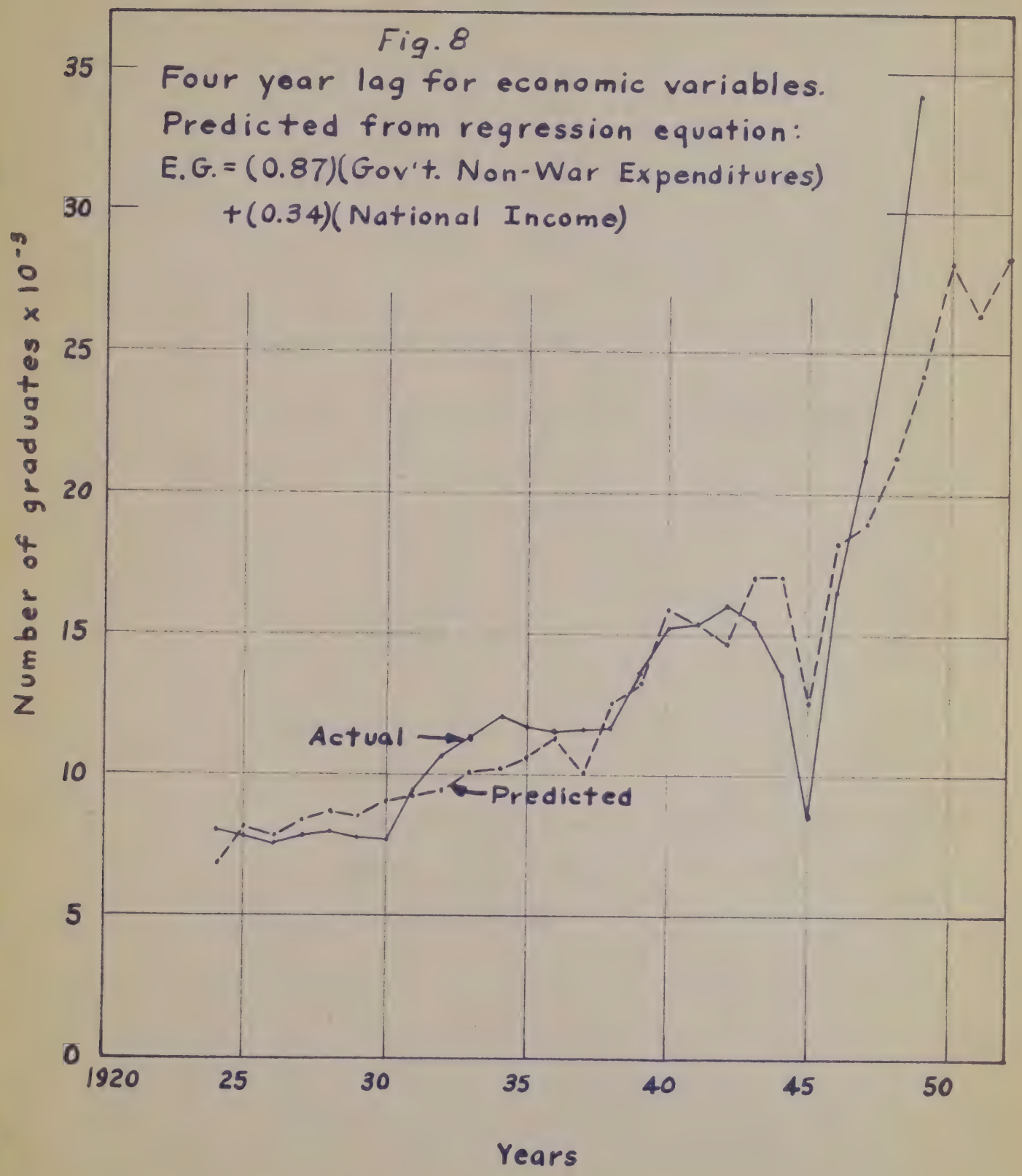
Fig. 8
Four year lag for economic variables.
Predicted from regression equation:
E.G. = (0.87)(Gov't. Non-War Expenditures)
+(0.34)(National Income)
Number of graduates x 10⁻³
35
30
25
20
15
10
5
0
1920
25
30
35
40
45
50
Years
Actual
Predicted

Calculations - X_1 - Graduates - 2 yr. lead

$\phi B_2 = \underline{\quad 2 \quad} = 0.91$ (Graduates 1 year lead)

$\phi B_3 = .67 - .91(.85) = -0.10$

$\phi B_4 = .90 - .91(.92) = +0.08$

$\phi B_5 = .51 - .91(.51) = +0.04$

$\phi B_6 = .46 - .91(.49) = +0.01$

$\phi B_7 = .40 - .91(.23) = +0.21$

$\phi B_8 = .30 - .91(.19) = +0.18$

$\phi B_9 = .88 - .91(.88) = +0.08$

Significant B's are ϕB_4, ϕB_7, ϕB_8, and ϕB_9. The highest is $\phi B_7 = 0.21$. Hence:

$\phi B_7 = 0.21$ (wholesale price index)

$\phi B_4 = .08 - .21(.39) = 0.0$

$\phi B_8 = .18 - .21(.29) = +0.12$

$\phi B_9 = .08 - .21(.21) = +0.04$

Significant B is $\phi B_8 = 0.12$ (Dow-Jones Averages)

Regression equations is:

Graduates (2 year lead) = (0.91) (Graduates 1 year lead) + (0.21) (Wholesale Price Index) + (0.12) (Dow-Jones Averages)

Two year lead

					Predicted	Actual
$z^{22}=(.91)(-1.18)+(.21)(+2.84)+(.12)(-1.19)=$	-1.08	+0.60	-.14	= -0.62	9300	7500
$z^{23}=(.91)(-0.88)+(.21)(+0.13)+(.12)(-1.26)=$	-0.80	+0.03	-.15	= -0.92	7300	7200
$z^{24}=(.91)(-0.83)+(.21)(+0.05)+(.12)(-0.90)=$	-0.76	+0.01	-.11	= -0.86	7600	8000
$z^{25}=(.91)(-0.75)+(.21)(+0.28)+(.12)(-0.70)=$	-0.68	+0.06	-.08	= -0.70	8800	7800
$z^{26}=(.91)(-0.80)+(.21)(+0.17)+(.12)(-0.66)=$	-0.73	+0.04	-.08	= -0.77	8200	7600
$z^{27}=(.91)(-0.85)+(.21)(+0.43)+(.12)(+0.02)=$	-0.78	+0.08	- 0	= -0.70	8800	7800
$z^{28}=(.91)(-0.80)+(.21)(+0.24)+(.12)(+0.53)=$	-0.73	+0.05	+.06	= -0.62	9300	7900
$z^{29}=(.91)(-0.78)+(.21)(+0.01)+(.12)(+0.94)=$	-0.71	+0	+.10	= -0.61	9400	7800
$z^{30}=(.91)(-0.80)+(.21)(+0.09)+(.12)(+1.91)=$	-0.73	+0.02	+.23	= -0.48	10300	7700
$z^{31}=(.91)(-0.83)+(.21)(+0.01)+(.12)(+2.08)=$	-0.76	+0	+.25	= -0.51	9600	9200
$z^{32}=(.91)(-0.50)+(.21)(-0.41)+(.12)(+1.06)=$	-0.46	-0.08	+.23	= -0.41	10800	10700
$z^{33}=(.91)(-0.17)+(.21)(-1.06)+(.12)(-0.92)=$	-0.16	-0.22	-.11	= -0.49	10400	11300
$z^{34}=(.91)(-0.05)+(.21)(-1.44)+(.12)(-1.84)=$	-0.05	-0.30	-.22	= -0.57	9700	12000
$z^{35}=(.91)(+0.11)+(.21)(-1.36)+(.12)(-1.60)=$	+0.10	-0.28	-.19	= -0.37	11200	11600
$z^{36}=(.91)(+0.03)+(.21)(-0.94)+(.12)(-0.70)=$	+0.02	-0.20	-.08	= -0.26	11800	11200
$z^{37}=(.91)(-0.05)+(.21)(-0.71)+(.12)(-0.44)=$	-0.04	-0.15	-.05	= -0.24	12000	11400
$z^{38}=(.91)(-0.02)+(.21)(-0.68)+(.12)(+0.70)=$	-0.01	-0.14	+.08	= -0.07	13100	11600
$z^{39}=(.91)(+0.03)+(.21)(-0.41)+(.12)(-0.01)=$	+0.02	-0.08	+ 0	= -0.06	13200	13300
$z^{40}=(.91)(+0.38)+(.21)(-0.79)+(.12)(-0.34)=$	+0.35	-0.17	-.04	= +0.24	15400	15100
$z^{41}=(.91)(+0.78)+(.21)(-0.83)+(.12)(+0.17)=$	+0.71	-0.17	+.02	= +0.56	17500	15200
$z^{42}=(.91)(+0.81)+(.21)(-0.79)+(.12)(-0.05)=$	+0.74	-0.17	+ 0	= +0.57	17600	16000
$z^{43}=(.91)(+0.99)+(.21)(-0.37)+(.12)(-0.22)=$	+0.90	-0.08	-.04	= +0.78	19200	15300
$z^{44}=(.91)(+0.83)+(.21)(+0.20)+(.12)(-0.53)=$	+0.76	+0.04	-.06	= +0.74	18700	13500
$z^{45}=(.91)(+0.43)+(.21)(+0.39)+(.12)(+0.12)=$	+0.39	+0.08	+.01	= +0.48	17100	8500
$z^{46}=(.91)(-0.65)+(.21)(+0.43)+(.12)(+0.48)=$	-0.59	+0.09	+.06	= +0.74	18700	11500
$z^{47}=(.91)(+0.01)+(.21)(+0.51)+(.12)(+0.89)=$	+0.01	+0.10	+.10	= +0.21	15200	18500
$z^{48}=(.91)(+2.07)+(.21)(+1.23)+(.12)(+1.21)=$	+1.89	+0.26	+.15	= +2.30	29700	27500
$z^{49}=(.91)(+3.50)+(.21)(+2.76)+(.12)(+1.21)=$	+3.20	+0.58	+.15	= +3.93	41000	41800
$z^{50}=(.91)(+4.02)+(.21)(+3.33)+(.12)(+1.21)=$	+3.67	+0.70	+.15	= +4.52	45200	----

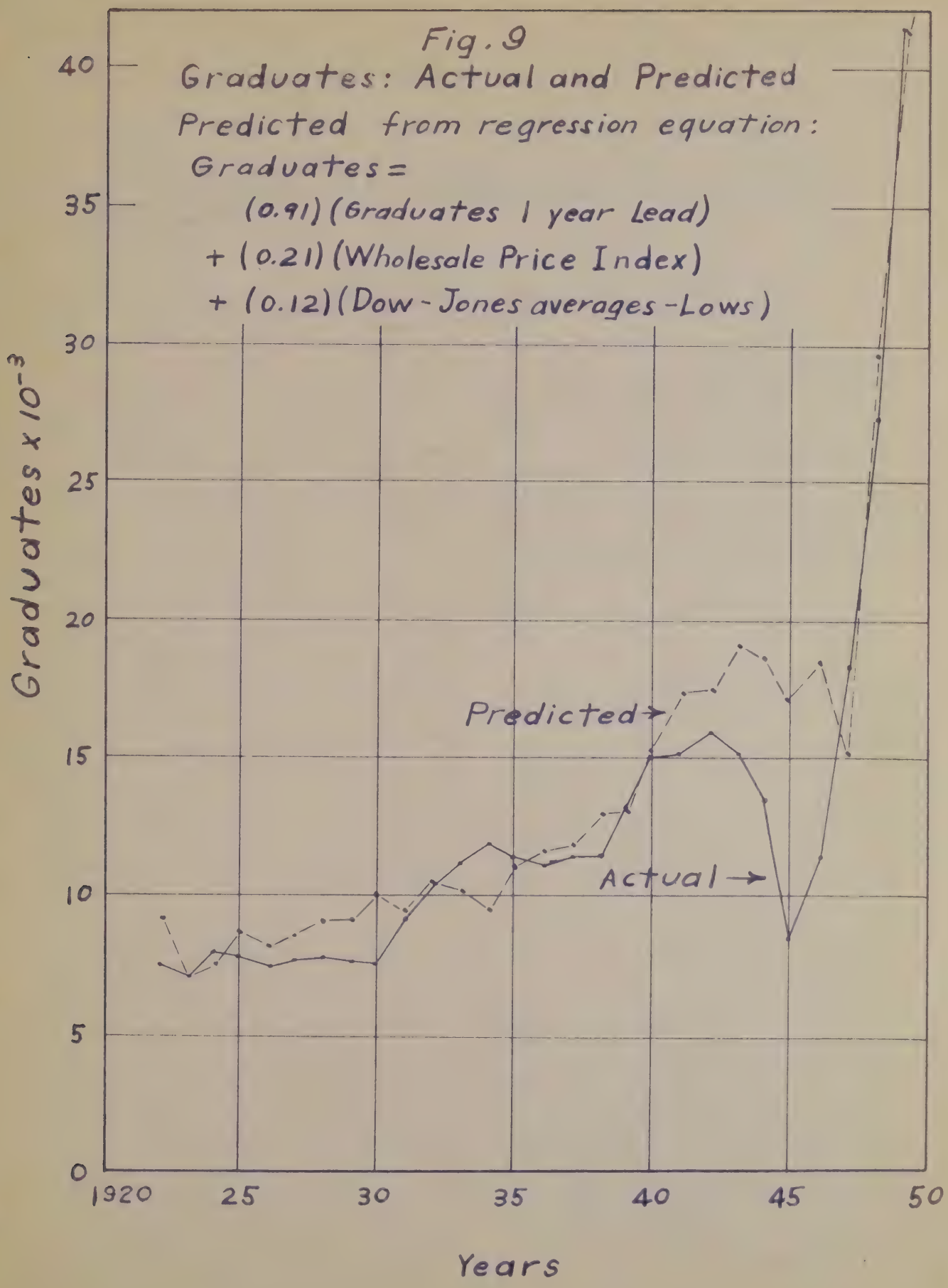
Fig. 9
Graduates: Actual and Predicted
Predicted from regression equation:
Graduates =
(0.91) (Graduates 1 year Lead)
+ (0.21) (Wholesale Price Index)
+ (0.12) (Dow - Jones averages - Lows)
Graduates x 10⁻³
40
35
30
25
20
15
10
5
0
Predicted →
Actual →
1920
25
30
35
40
45
50
Years

An Electronic Volume Counter

By D. L. Gerlough (Jun. Mem., ITE)
Assistant Engineer, Institute of Transport and Traffic Engineering,
University of California

A FOUR-LANE electronic volume counter has been developed recently by the Los Angeles office of the Institute of Transportation and Traffic Engineering for use in its research studies. This counter is quite advantageous in that the equipment need not be located at the side of the road, but may be located some distance away, using wires to connect it with the roadway detectors. During a recent series of tests in Los Angeles, telephone lines more than eight miles long were used for transmission.

The unit is composed of four separate electronic circuits which operate four electromagnetic counters; each circuit contains provision for dividing the number of axles by two. Provision has been made so that the four-lane counter can be operated in conjunction with the Vehicle Speed Distribution Recorder previously described.[1] With this arrangement, the counter registers the volume in each lane continuously, while speed is being measured in one lane by means of the Speed Distribution Recorder. Such information is useful to traffic engineers and to enforcement authorities in studying lane utilization, enforcement needs, congestion, etc. Figure 1 shows how a tap switch is provided in order to select the lane in which speed is to be measured.

The detector used to actuate this counter is the Institute's detector recently described before the Highway Research Board.[2] By connecting together appropriate segments of this detector it is possible to provide pickups for individual lanes and at the same time to minimize double recording of vehicles straddling the lane markers. When speeds are to be measured, two detector strips must be provided, while with volume alone only one detector is required. Figure 2 shows the arrangement of pickups recently used on one-half of Wilshire Boulevard in Los Angeles, at a point where Wilshire is essentially a freeway.

Figure 3 is a photograph of the counter and its separate power supply. The present power supply is operated from the 110-volt alternating current supply. The Institute expects within the near future to construct a modified version of this counter which will have facilities for periodically recording the count on a paper tape and which may be operated either from a 6-volt d-c source or from a 110-volt a-c source.

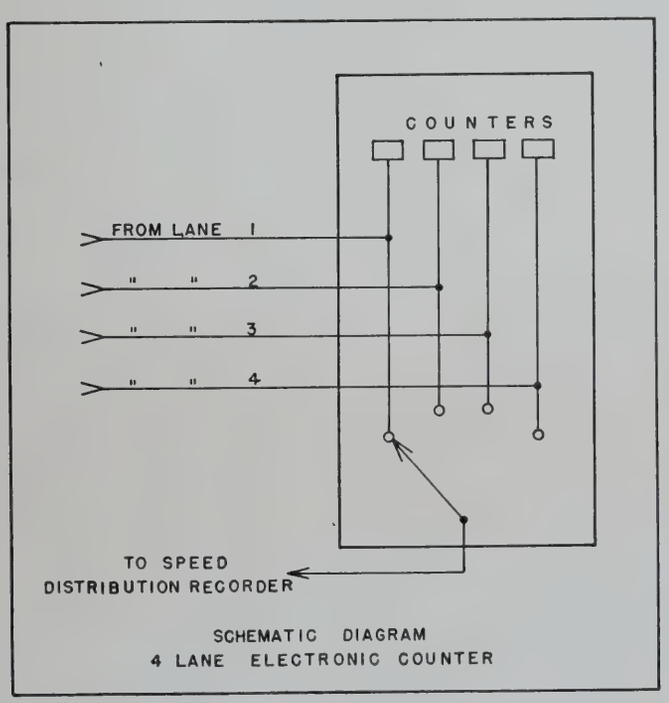

Fig. 1
Interconnection of Four-Lane Counter and Speed Distribution Recorder. The input from each lane is connected directly to the electronic counter for that lane. By means of a tap switch, the speed distribution recorder can be connected to any lane.

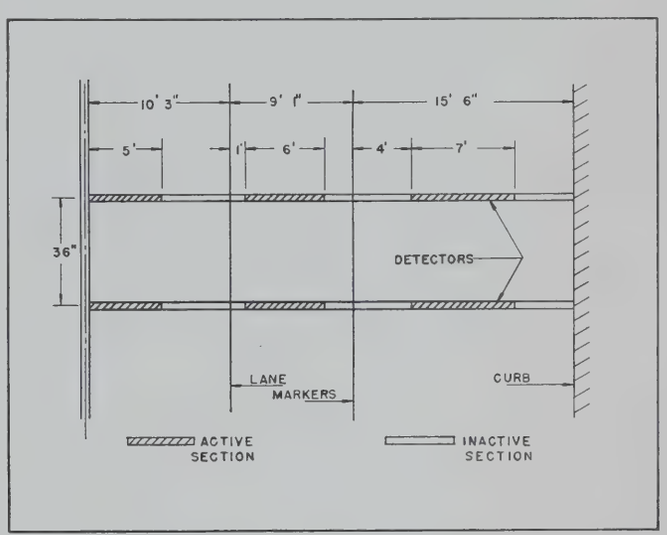

Fig. 2
Arrangement of Detectors on south side of Wilshire Boulevard. By a combination of active and inactive sections it is possible to minimize the misses and for double counts of cars straddling the lane markers.

Fig. 3
The Four-Lane Counter and Its Separate Power Supply

[1] "Applications of Electronic Techniques to Traffic Instrumentation," by Robert Bromberg and D. L. Gerlough. Proceedings of the Highway Research Board, Vol 28, pp. 348-353.
[2] "A Segmented Electrical Element for Determining Vehicular Traffic" by J. H. Mathewson, R. Brenner, R. J. Reiss. Presented at the 29th Annual Meeting of the Highway Research Board, Washington, D. C., December 16, 1949.

Reprinted from JOURNAL OF APPLIED PHYSICS, Vol. 21, No. 5, 468, May, 1950
Copyright 1950 by the American Institute of Physics
Printed in U. S. A.

Errata: On the Diffraction of an Electromagnetic Wave through a Plane Screen

[J. App. Phys. **20**, 760 (1949)]

J. W. MILES
Department of Engineering, University of California, Los Angeles, California

THE scattering cross section for plane, electromagnetic waves normally incident upon a circular aperture in an infinite, plane, perfectly conducting screen given by us in a recent paper[1] was calculated erroneously. This error, in turn, was due to an error in the computation of the aperture susceptance (B). The results have been recalculated, and Figs. 9 and 10 in the original paper should be replaced by those given here.

The error in our calculations was brought to our attention by Professor Harold Levine (Harvard University), who has carried out similar (variational) calculations,[2] using as first and second approximations to the aperture field $[1-(r/a)^2]^{\frac{1}{2}}$ and $A_1[1-(r/a)^2]^{\frac{1}{2}}+A_2[1-(r/a)^2]^{\frac{3}{2}}$, respectively. Our calculation, which uses the static approximation $[1-(r/a)^2]^{\frac{1}{2}}$ for the leading term for small βa and the incident field for the remaining terms, does not predict the first maximum of the scattering cross section as accurately as that of Levine. (We obtain $(T/T_0)_{\max}=1.63$ at $\beta a=1.5$; Levine obtains $(T/T_0)_{\max}=1.78$ at $\beta a=1.4$.) But it is somewhat more accurate

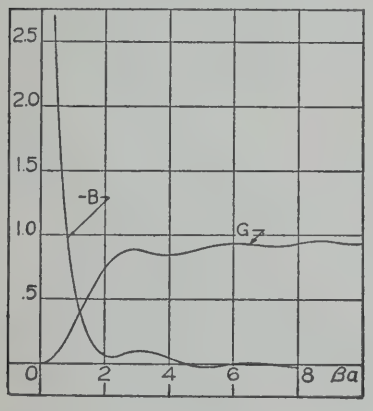

FIG. 9. The conductance and susceptance of a circular aperture for normal incidence of a plane, electromagnetic wave.

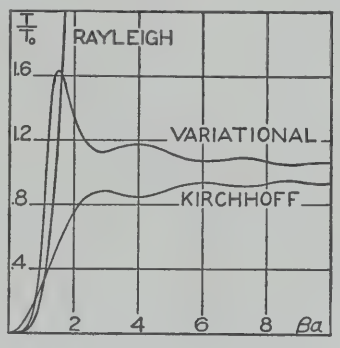

FIG. 10. Scattering cross section (relative to geometric) of a circular aperture for normal incidence of a plane, electromagnetic wave.

(relative to Levine's first approximation) for large βa, all of which is as should be expected from the nature of the field approximations.

Two other errors in the paper should be pointed out. Equation (86b) should have read

$$B_\sigma(\beta a)=\sum_{m=0}^{\infty}\frac{(-)^m(\beta a)^{2m+1}}{(2m+2)[\Gamma(m+\frac{3}{2})]^2}-(3\pi/8\beta a). \qquad (86b)$$

(This error was typographical and not connected with the calculations.) Moreover, contrary to our statement, Magnus[3] *did* solve the integral equation which he formulated for the Sommerfeld problem,[3] and we should have stated merely that his solution was not as direct as the Wiener-Hopf approach.

[1] J. App. Phys. **20**, 760–771 (1949).
[2] Progress Report 6, Cruft Laboratory, Harvard University, Contract N5-ORI-76 (January 1, 1948).
[3] W. Magnus, Zeits. f. Physik **117**, 168 (1941). See also W. Magnus and F. Oberhettinger, *Formulas and Theorems for the Special Functions of Mathematical Physics* (Chelsea Publishing Company, New York, 1949), pp. 142, 143.

Exercise Treatment for the Frozen Shoulder

Hyman Jampol

The term "frozen" to describe a shoulder joint with limited motion has had wide usage. Dorland's medical dictionary defines a frozen shoulder as "a disability of the shoulder joint due to fibrositis and characterized by limited abduction and rotation of the arm." Codman described it as "a condition in which the axis of the shaft of the humerus is nearly at right angles to the axis of the spine of the scapula, and remains so, no matter in what direction the arm is moved." The frozen shoulder, according to Mosely, is one in which all movements at the gleno- and acromiohumeral joints are abolished, although motion of the upper limb on the trunk is still present, occurring through movements in other joint areas.

Storms emphasizes the limitation of motion present in this condition, and also points out that there is an abnormality of the cuff muscles and painful spasm in the spinati, pectoral, latissimus dorsi, and rhomboid muscles. The clinical picture of the chronically frozen shoulder, as described by Behrend, is evidenced by limitation of motion and symptoms of an abduction or adduction contracture. "The movements of internal and external rotation, of abduction and adduction, and of circumduction are impaired. In extreme cases no glenohumeral movement exists. Pain may exist on a slight touch of the joint, on certain or all motions of the joint, or on attempts to move the joint passively. The pain may vary from mild to excruciating, which deprives the patient of his sleep and generally causes a debilitated condition. There is usually pain in the muscles surrounding the joint."

Although there is agreement among most observers as to the clinical symptoms of the frozen shoulder, the exact causes of the limitation of motion are controversial. There are those who believe that adhesions are the sole cause, while others attribute it to various other mechanisms.

In 1872 Duplay described periarthritis and recorded the presence of adhesions within the subacromial bursa. (Lippman is of the opinion that Duplay referred to what today is called the frozen shoulder.) Codman listed adhesions as the primary cause of limitation of joint motion. Among these were adhesions between the bicipital groove and the tendon of the long head of the biceps, and adhesions in the extension of the joint underlying the infraspinatus and subscapular muscles. Mumford and Martin explained the marked loss of function of severe painful shoulders as being due to adhesions but did not specify their location. According to Watson-Jones, limitation of movement by muscle guard rapidly progresses to limitation by adhesion formation, and in severe cases, generalized adhesions of the whole pericapsular tissue lead to a frozen shoulder. Engelman believes that there are adhesions of the folds of the inferior aspect of the relaxed capsule, in addition to adhesions of various other surfaces about the head of the humerus. Inman is of the same opinion, and adds that the other adhesions are probably in the region of the superior aspect of the head, perhaps underneath the insertion of the rotator cuff.

According to Baer, the cause of the limitation of motion is purely a mechanical one; the swelling of the subdeltoid bursa results in its inability to pass under the coracoacromial ligament during abduction.

Buchholz believed that the stiffness is caused not so much by adhesions as by retraction of the muscles and periarticular structures. Sir Colin MacKenzie was of the opinion that a stiff shoulder did not necessarily mean that adhesions in the joint were binding the head of the humerus to the glenoid cavity. He maintained that the two factors to be borne in mind are the adduction contracture, which is especially favored by gravity, and the weakness or paresis of the muscles which elevate the limb.

Abstracted from a Master's thesis completed at Stanford University, Division of Physical Therapy, in March, 1950, entitled "The Exercise Program for the Shoulder with Limited Motion." The entire work may be borrowed through any university or public library by addressing Interlibrary Loan, Stanford University.

Magnuson analyzed the mechanical disadvantages of an adherent deltoid muscle. He showed how that muscle, which normally inserts down on the shaft of the humerus, becomes adherent to the greater tubercle of the humerus, thus reducing its leverage and its power. As a result, the great bulk of the muscle is being wasted, exerting a pull between two points on the humerus—namely, the head and the deltoid tubercle.

Further causes are listed by other investigators. Lippman and Hitchcock and Bechtol are of the opinon that tenosynovitis of the long biceps tendon is a possible cause of the frozen shoulder. Inman also mentions myostatic contracture as a cause of the limitation of motion. King and Holmes believe that a relaxed capsule is a frequent cause of a stiff and painful shoulder. This is brought about by the pain produced when motions are attempted; hence muscle guard and disuse are the contributing factors.

Dr. Bechtol explains that once the frozen shoulder is established, the pathology is about the same in any case, involving an adherence and contracture of the capsule in the inferior portion of the shoulder joint, probably associated with a mild static contracture of the various muscles of the rotator cuff. Further, adhesions which may arise in the subacromial bursa are probably producers of pain, but they are not important as causative factors of stiffness.

How do these adhesion formations and muscular contractures occur? What is the predisposing factor (or factors) which makes for their appearance? Again there are various opinions on these points.

Any tissues making up the shoulder joint, if injured, can contribute to a frozen shoulder. Trauma to the joint can cause injury which, in turn, causes a frozen shoulder. Injury to joint cartilage may produce chondromalacia which, in turn, produces pain and immobilization leading to a frozen shoulder. Muscle tears may produce a frozen shoulder.

According to Wagner, the physiological process by which a shoulder becomes frozen by adhesions can best be summarized as follows: First, a degenerative lesion of some sort must be present in order that adhesions form in the joint. This lesion makes for the production of fibrocytes which may form in the inferior capsular folds about the head of the humerus and about the bursae and the tissue surrounding it. These adult cells are non-elastic and the frozen shoulder results. If the shoulder complex has been injured severely enough so that edema occurs, the presence of the fluid, which is rich in protein, is an aid to adhesion formation.

Many times the injury to the shoulder may go unnoticed, as in the case of a Colles' fracture, where the patient has attempted to break his fall on his outstretched hand and extended arm. The patient's arm is placed in a sling and cast and the shoulder is untreated. Perhaps six weeks later when the arm cast is removed, the patient is surprised to find that he has a stiff, painful shoulder. The rupture of some of the tissues within the shoulder joint has started the process and this, together with immobilization, has produced the frozen shoulder.

Watson-Jones, in an excellent discussion of adhesions, states that joint stiffness after injury is due to the adhesions of the capsular plications, and this may result from the organization of any exudate in the periarticular tissues.

Codman depicted the inflammatory reaction after calcified material has been forced into the bursa, adding that adhesions form as a result of the reaction. MacKenzie wrote that the possibility of a stiff shoulder following any injury or inflammation of the shoulder joint should always be borne in mind. He has seen it occur after rheumatic inflammation of the shoulder, fractures of the upper end of the humerus, falls on the shoulder, and after bullet wounds of the neck region and of the shoulder joint, without much obvious injury to the muscles.

Any trauma about the shoulder region that produces pain and causes the patient to hold the arm at the side for a considerable length of time may lead to a frozen shoulder. That a stiff and painful shoulder is seen, following trivial as well as severe injuries of the joint, is noted by Hammond. His findings show that a simple strain or contusion, resulting from blows or falls, may produce tears of the ligamentous attachments and effusion from the synovial membrane, or even injury to the joint cartilage, all of which would prevent a speedy return of function. In his opinion the dislocated shoulder is a common cause of the frozen joint, due to fixation and improper after-care.

Steindler mentions the fact that contusion of the shoulder occurs with any gross injuries of the upper extremity. When the patient recovers from a major injury, he gradually notices increasing symptoms in the shoulder joint, which in time may become the outstanding feature of the whole complex.

Gordon's opinion is that a painful intra-, peri-, or extra-articular lesion of the shoulder will produce a protective spasm of the muscles, thus controlling its movements; furthermore, if this spasm is maintained, contracture results. As an example of an extra-articular lesion which can produce a stiff shoulder he cites Colles' fracture, a lesion

where there has been no injury directly to the shoulder. The patient attempts to immobilize the shoulder by holding the arm at the side. An example of a periarticular lesion is the simple, acute, subacromial bursitis. Here, if muscular spasm has prevented pain from movement in the shoulder, an impaired shoulder remains. This is due to muscle contracture, and pain is referred to the insertion of the deltoid muscle.

A swollen bursa is listed as one of the causes of a shoulder with limited motion. Baer maintained that the swollen bursa prevented all except the first ten degrees of abduction, due to its impingement against the coracoacromial ligament. It can be seen that the persistence of this condition would result in muscular contractures and still further limit motion in the joint. In addition, Baer describes the atrophy of the supraspinatus and infraspinatus muscles as "appreciable," which in itself contributes to limitation of motion in the shoulder joint.

Instances have occurred in which there was definitely no history of the injury to the shoulder itself and yet a stiff shoulder resulted. For instance, the forearm or hand may be injured, with the shoulder protected from all strain. Here the contributory factor is simply immobilization. This type of etiology results in a frozen shoulder for which there is a better prognosis than that accompanied by specific joint trauma. The stiffness results from the contracture of the periarticular structures which have not been used and tend to contract. For example, frozen shoulders are seen after heart attacks in which the patient has lain in bed for a period.

In summary, various factors which may contribute to the condition commonly called frozen shoulder are: bursitis, cuff injuries, periarthritis, contusions, tenosynovitis, muscle tears, and long immobilization from any cause. As is readily discernible, these processes are interrelated. Any one or a combination of these conditions can cause a frozen shoulder.

Exercise Program

The object of treatment of the frozen shoulder is to regain the full range of pain-free motion in each direction. In 1932 Martin demonstrated that lateral or external rotation of the humerus was necessary for full elevation of the arm. It is now general knowledge that this external rotation of the humerus moves the greater tubercle posteriorly and thereby allows the head of the humerus to glide under the acromion during elevation of the humerus. The statement "the essential object of the treatment of the frozen shoulder is to regain the range of external rotation" emphasizes the principle that, unless external rotation is restored, there will be limitation in the degree of abduction or forward flexion possible.

Watson-Jones has said that successful treatment of the stiff shoulder may be summed up in two words, active exercise. This of course is the opinion of one authority, but it has now become a primary method of treatment prescribed by many orthopedic surgeons for the alleviation of the frozen shoulder. Another physician has said "the most important treatment method of all (for the frozen shoulder) is active, voluntary motion, purposely made by the patient." Often no description of specific exercises desired is included in the prescription. However, it is possible with a knowledge of the functional anatomy of the shoulder complex to analyze the motions desired and to plan specific exercises carefully in order to achieve specific results.

Three types of exercise procedures in the armamentarium of the physical therapist are: passive movement, active exercises, and forced motion. It is understandable that forced motion might be construed by some to be identical with manipulation, and as such is outside the realm of the physical therapist. One point to the contrary is the fact that manipulation is usually carried out by the physician under anesthesia, while forced motion, as performed by the physical therapist, uses no such measures. In using forced motion, the physical therapist attempts primarily to obtain normal muscle elongation and breaking up of minor adhesions. By comparison, the physician's objective in manipulation is the breaking up of major joint adhesions.

Before embarking on a description of various exercises, it is necessary to list a few principles which govern the administration of voluntary exercises:

1. Complete arm elevation through 180 degrees can only be carried out with external rotation of the humerus; therefore, a primary object of active exercise is to regain the range of external rotation.

2. In the early stages of treatment, elevation should be attempted in the sagittal plane rather than in the coronal. Elevation in the coronal plane, or abduction, may be attempted only after external rotation is free to some extent.

3. The exercise should not be done at too *slow* a speed in the beginning. Progression should be toward slower exercises.

4. The exercises should be done smoothly and without halting or jerking movements.

5. A sharp watch should be kept for substitution or trick movements on the part of the patient.

6. The patient should not attempt any exercise which would reinforce faulty habit patterns, such as elevation of his shoulder during abduction of the arm.

7. The use of resistance exercises is efficacious in obtaining the relaxing of the antagonists. This is based on Sherrington's law of reciprocal innnervation, and, inasmuch as part of the problem is a contracture of one group of muscles and a weakness of the opposing group, it can be seen that the encouragement of movements of abduction against resistance would help to relax the aforementioned contracted muscles.

8. Wherever possible, apparatus may be used for resistance or holding in preference to manual resistance. The patient knows just to what extent the apparatus will go but may be unsure and wary of the hands of the physical therapist.

9. The patient must be urged to practice active exercises for a few minutes hourly through the day.

10. The patient's tolerance to pain, his reaction to previous treatments, and his daily condition should be considered.

11. The problem must be carefully explained to the patient and his cooperation obtained. The patient's mental attitude and cooperation is extremely important in the re-education of disordered skeletal function. (In fact, Mosely is of the opinion that often the mental development of the patient determines the end result obtained.)

12. It must be remembered that one will encounter uncooperative patients, ignorant patients, and patients subject to weather changes and occupational strains, and the physical therapist must adjust and arrange the administration of the treatment according to the reactions that develop from these factors.

13. The adjacent areas should be considered as well as the shoulder joint.

Mobilizing the Head of the Humerus

The first group of exercises are those aimed toward mobilizing the head of the humerus. Because of the fact that in the frozen shoulder the head of the humerus is held high in the glenoid fossa, either by adhesions, muscle spasm, or muscle contraction, this first step is necessary. The proof of this fact can easily be seen on a patient with a frozen shoulder. Normal arm elevation produces a declevity on the superior aspect of the shoulder during abduction, and, during flexion of the humerus, this hollow is evident on the superior-posterior aspect of the shoulder. The patient with the stiff shoulder exhibits no such deformation as a result of the tight position of the head of the humerus. The declevities produced are a result of the downward motion of the humeral head during abduction and the backward and downward motion of the head during flexion. This motion of the humeral head has been called by Mennell the "involuntary" motion of the joint, and he maintains that voluntary joint motion, namely, flexion, extension, and so forth, cannot be performed until the involuntary motion is restored. This concept is the basis for the first group of exercises.

These are performed in a position which relaxes the musculature of the area. They are called "pendulum" exercises. With the body erect, the upper limb hangs at the side, and if the body is bent forward with relaxed shoulder muscles, the limb hangs as a pendulum. It can and will swing as would a weight supported by a string if the body is swayed. This entails no muscular action of the shoulder muscles except suspension support.

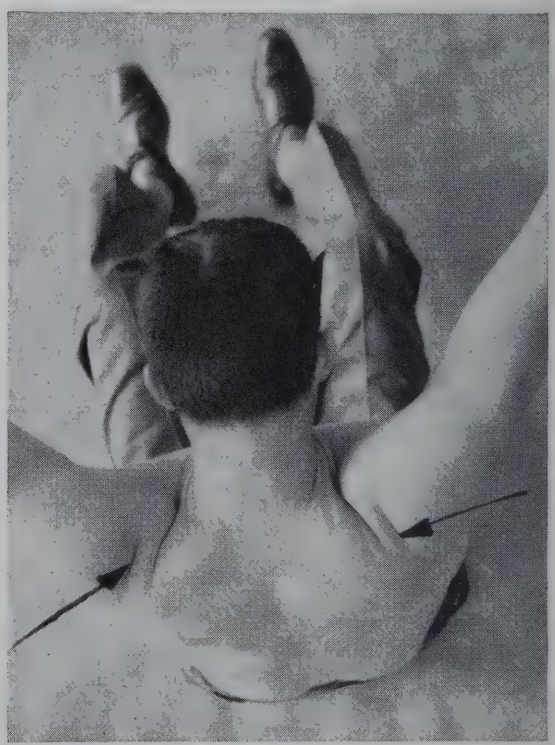

Figure 1. Illustrating the declevities produced on the superior aspect of the shoulder during arm elevation. These declevities are due to the downward motion of the head of the humerus during elevation of the arm. In frozen shoulder patients these cannot be produced.

1. Patient bends forward from the hips allowing the arm to hang down freely. He is then given a weight, varying from three to twenty pounds, which he grasps and allows to swing slowly forward and backward in the anterior-posterior plane. This motion is not to be accomplished by the shoulder musculature; rather, a slight movement of the body starts the motion which continues almost by itself. It should be noted that the angle to which the trunk can bend may depend on tight hamstrings, and scapular limitation may prevent forward bending by causing pain as the humerus flexes.

2. Patient assumes the same position as in the preceding exercise. Now the trunk is rotated slightly so that the arm swings from side to side.

3. Patient, in the same relaxed position, moves the trunk so that the hand describes a small circle, gradually enlarging the circle to about eighteen inches in diameter. This is to be done in both clockwise and counter-clockwise directions. If the patient is able, he should supinate his hand at the lateral edge of the circle. For the home program the patient should perform the above exercises with a flatiron or some such object in his hand.

4. Patient stands, arms at sides, a weight in each hand. He swings one arm across his body in front of him, at the same time swinging the other across his body behind him, taking care to see that the trunk does not rotate.

It can be understood that the above exercises, combined with the tension exerted by the weights added, can serve a dual purpose. First, they serve as a passive stretch on the joint capsule, due to the weight plus the motion; and, second, they serve to mobilize the head of the humerus by purely mechanical means. These exercises cause no pain and should be used whenever possible. Care should be taken not to keep the patient bent over for too long a period and to give him relief by removing the weight from his hand and having him stand erect periodically. Usually he can perform the exercise ten times without undue strain. Progression in these exercises can be accomplished by increasing the size of the arc or circle which the hand describes, and by more repetitions with shorter or no rest periods.

Increasing the Range of External Rotation

These exercises may be done at the same time as the exercises for the mobilization of the head of the humerus, or they can be done after a period of time during which only mobilization exercises have been carried out.

After some freedom (however slight) of the head of the humerus is evidenced, the next step is to increase the range of external rotation. That this is necessary has been shown previously, for complete elevation cannot be accomplished until rotation of the humerus is possible.

The objectives of these exercises are:

1. To increase the range of external rotation and stretch the tight musculature (adductors and internal rotators of the humerus)
2. To increase the strength of the external rotator muscles
3. To re-establish neuromuscular patterns of use and thereby re-establish the smooth, integrated "scapulo-humeral rhythm"

1. Patient lies supine on plinth with elbows at his sides, flexed so that the hands point to the ceiling. Patient attempts to externally rotate the arm by pulling hands out to the sides toward the plinth.

2. Patient stands with his back to the wall, elbows at sides flexed ninety degrees. Palms facing ceiling. Patient attempts to pull hands toward wall, thus externally rotating the humerus.

3. Patient lies supine on plinth with hands clasped behind his head and elbows forward. He then pulls his elbows toward the plinth. When this motion is extremely painful, it should be done against resistance given manually by the physical therapist. This makes use of the reciprocal innervation principle, and the patient often finds the exercise is no longer painful, or pain is decreased.

4. Patient stands with his back to the wall with hands clasped behind his head and elbows forward. Patient pulls his elbows back toward the wall.

5. Patient stands with one hand on top of his head. He attempts to touch the opposite ear by reaching laterally over his head. The elbow should be kept well back if possible.

6. Patient lies supine on plinth, holding one edge with hand of affected arm. Patient then rolls away from holding hand and returns.

7. Patient stands with wand behind back, locked in both elbows, and elbows flexed to ninety degrees. Externally rotate the arms and return.

8. Patient stands facing stall bars. With elbow flexed to ninety degrees, the patient grasps rung with hand of affected arm, using underhand grip, and slowly turns *away* from the affected arm, taking short steps, and returns.

(Exercises with pulley weights can be attempted, after the patient has recovered some motion in the

joint and strength in the joint muscles, when more mobility of the joint is desired.)

9. Patient stands with his unaffected side facing the pulleys. His affected arm is by his side with elbow flexed to ninety degrees. Holding the handle of the pulley with an underhand grasp, he externally rotates his arm and returns.

10. Patient stands facing the pulleys, arms abducted to ninety degrees, elbows flexed to ninety degrees, palms facing the floor. Patient grasps pulley handle with overhand grip and rotates humerus backward. Care should be taken to see that the rope of the pulley is not parallel to the floor but that the patient stands above the pulley so that the distance of the rope from the floor increases as it approaches the patient. This insures a steady pull through the full range of motion.

Increasing the Range of Internal Rotation

In the last analysis, the function of the arm is to place the hand in a position of use. Therefore, even if full abduction is achieved, if the patient still cannot place his hand behind him, the total functional range has not been re-established. It is for this reason that the range of internal rotation must be increased to include these areas.

The objectives of these exercises are:

1. To regain the full range of internal rotation and stretch the tight structures in the area of the shoulder joint which may serve to limit rotation
2. To increase the strength of the internal rotator muscles

One word of caution is necessary here. Due to the tightness of the internal rotators, these exercises should not be used until a fair range of external rotation is present. Otherwise a reinforcement of faulty mechanics may occur.

1. Affected arm is behind back, forearm supinated; hand grasps one end of wand which is held by other hand overhead.
   a) By use of wand, the lower hand is pulled up as far as possible.
   b) Now the lower hand pushes up, with the upper hand offering resistance.

2. Wand behind buttocks is grasped in overhand grip by both hands. Bring wand *up* along the back by bending the elbows and then return.

3. Patient faces stall bars, grasping rung with affected arm about head height. With overhand grip, patient proceeds to walk under arm and return. Elbow should be kept straight.

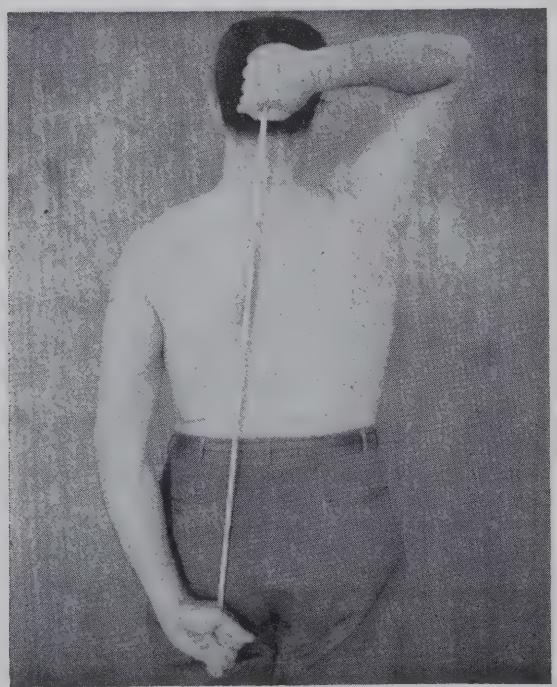

Figure 2. Use of the wand to increase the range of internal rotation and hyperextension. Top hand pulls the bottom hand up.

Figure 3. Here the wand is pushed up against the resistance of the upper hand. Again, internal rotation and hyperextension motions are improved.

Figure 4. The "London Bridge" exercise. View at left shows starting position, and the right-hand view shows the final position. This exercise is excellent for stretching the scapulo-humeral musculature.

4. Patient stands with one foot away from stall bars and back to bars. He grasps rung at hip height with both hands, using overhand grip. Patient does knee bends. These may be slight at first, progressing to deeper bends.

5. Patient stands with his back to the pulleys, arms abducted to ninety degrees, elbows flexed ninety degrees, palms facing forward. Patient grasps pulley handles with overhand grip and rotates humerus internally. It may be necessary to stand behind the subject and support his elbows in order to insure internal rotation in good alignment.

Increasing the Mobility of the Shoulder Girdle

Due to the inactivity of the affected arm, frequently the whole shoulder complex is limited in motion. As a result, exercises should be given to mobilize the girdle. These exercises, like the preceding ones, are not specific. (Due to the close interaction of all the muscles and joints of the shoulder complex, it is impossible to isolate one single motion or muscle and work on it.) Therefore, exercises for mobilizing the shoulder girdle will, of necessity, include exercises for abduction and adduction.

The objectives of these exercises are:

1. To mobilize the shoulder girdle
2. To strengthen the shoulder girdle musculature

1. Patient stands with elbows flexed and hands on shoulders. He then flexes the humerus and returns it to position. Progression is to abduction in the coronal plane. The scapula must not be allowed to elevate abnormally.

2. Patient stands, hands clasped behind neck, elbows forward. The elbows are pushed forward, abducting scapulae. The same exercise can be done with the patient supine. This aids in freeing the scapula and stretches the posterior shoulder muscles.

3. Patient either stands or lies supine. He shrugs his shoulders. Progression can be accomplished by having patient stand with weights in either hand and shrug. This exercise aids in mobilizing the shoulder girdle and, if done with weights, offers a passive stretch to the structures holding the humeral head high in the glenoid fossa.

4. Patient, on hands and knees, places his hands further and further away from his knees.

5. Wand is grasped with overhand grip, arms flexed to ninety degrees. With elbows *straight,* the wand is pushed away from the body, abducting the scapulae. Wand is then pulled to the body, adducting the scapulae.

6. a) With one end of the wand in the palm of the hand of the affected arm and the other end held in the other hand, patient pushes down, giving traction to the affected side.

b) With traction now established, he proceeds to push the affected arm through the first ninety degrees of elevation (abduction and flexion), taking care to keep the pressure constant and the hand supinated as much as possible.

c) Exercise is repeated, continuing on through full range of abduction.

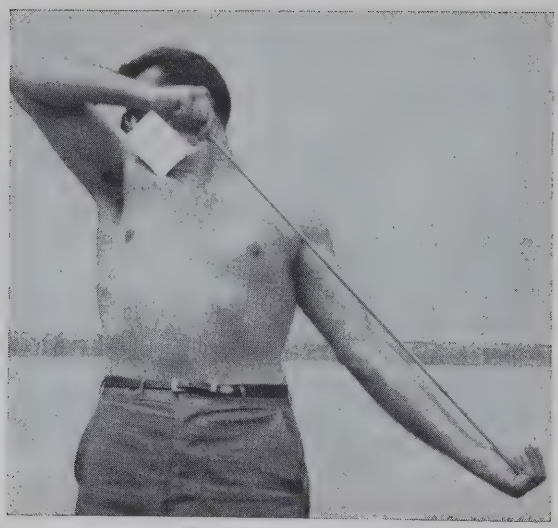

Figure 5. The use of the wand for self-applied traction. The right hand is giving traction to the left during attempted abduction of the left arm. This exercise is valuable as a mobilizing agent and as an aid to reducing pain during arm motions. The affected arm should be externally rotated during this exercise.

7. Patient stands, hands at sides, grasping wand with an overhand grip (dorsum of hand anterior). He flexes the arms to the overhead position and then drops the wand behind the neck. From here, he returns to the overhead position and down to starting position.

8. With patient's affected side facing stall bars, bar is grasped at shoulder level with underhand grip, forearm along the other rungs. (Forearm perpendicular to floor.) Patient does knee bends, doing all the work with his legs and not pulling with his arms. Grip is raised at end of series.

9. Facing stall bars, hands grasp rung with overhand grip at shoulder height. Patient does knee bends, progressively raising hands to next rung at conclusion of series. Care should be exercised here to see that the patient does the motion with the legs while the arms are just supported. No force is to be exerted at the shoulder joint.

10. With patient's affected side facing stall bars, rung at shoulder height is grasped with hand of affected shoulder, using overhand grasp. With elbow straight, body turns toward elbow.

11. With back to stall bars, patient grasps rung closest to his head with both hands, using underhand grip, flexes knees, and returns to position.

12. Patient stands facing pulley weights.

a) With the arms flexed to ninety degrees and using the overhand grip, he pulls the handles of the pulleys down to his sides, keeping the elbows straight.

b) With his arms at ninety degrees of flexion and grasping the handles with an overhand grip, patient flexes his elbows and abducts his scapulae. His arms must be kept parallel to the floor.

13. Patient stands with his back to the pulleys, hands at his sides, grasping the handles with an underhand grasp.

a) He then flexes his arms to the horizontal.

b) Same exercise as 2a, but with overhand grip

c) Patient stands with his back to the pulleys, arms abducted to ninety degrees, elbows extended, palms facing forward. He then pulls the handles forward until they meet at the midline of the body at eye level. Care is taken to keep the elbows straight.

A few "tricks" are sometimes valuable to have in one's armamentarium. They may perhaps be of value in some instance where all else fails, and may mean the difference between success and failure with a patient:

If the patient is disturbed because he is unable to move his arm, have him bend forward, allowing his arm to hang down; then have him swing the arm pendulum-fashion in an anterior-posterior plane. At the peak of his anterior swing, catch his hand, hold him in that position, and have him stand erect; lo, his arm is now elevated to about ninety or a hundred degrees.

If it is possible to get the patient to concentrate on some other part of the body during exercises it will be of great assistance. For example, have him do knee bends with his hands resting on the stall bars. He invariably complains of the strain on his quadriceps, forgetting at the time that his arm has been elevated past its usual range.

In order to assist the depressors of the head of the humerus, the therapist can hold the head down manually while the patient voluntarily elevates his arm.

In addition to self-traction with the wand, self-traction can be applied by the patient merely by having him pull his affected arm with his good hand.

Much has been said in this work concerning the necessity of securing external rotation of the humerus *before* attempting abduction. This is an extremely important concept in the planning of an exercise program for a patient.

First, external rotation is necessary in order that the greater tubercle of the humerus slide easily under the acromion. If this is not possible, the

range of abduction is limited and pain is produced when the patient attempts abduction.

Second, with the weakness of the external rotators (which is present in a stiff shoulder), the placing of the arm in external rotation places the tendon of the long head of the biceps in a most advantageous position to assist the weak functional group in keeping the head of the humerus down in the glenoid.

Last, the constant placing of the arm in external rotation will serve to develop the weak external rotators and, in so doing, strengthen them much sooner, so that they may reach the point at which they can once again take over their function as depressors of the head of the humerus.

Of much value and practicality is the large strap whose use is advocated by Furscott. This is a webbing strap about two inches in width and about ten feet long, with a buckle on one end. With the patient standing, the strap is placed around the humerus just above the insertion of the deltoid muscle. It is then run under the contralateral foot of the patient and cinched up tight. As the patient voluntarily abducts his arm, the strap acts as an assistant to the depressors of the humerus by mechanically holding the head of the humerus down. The fact that the patient is in complete control of the tension at all times makes for relaxation, and the device functions very well. In addition, it can be used in exactly the same way with the patient lying supine on a plinth. Here gravity is "eliminated" and pain is minimized.

Another device, which is of recent origin and is being used extensively by its originator, is the swinging beam, capable of being loaded on either end with graduated weights. This is Dr. Storms' design. Since the function of the rotators of the humerus is to hold the head of the humerus in the glenoid fossa and thereby allow the deltoid muscle to lever the arm up, it is essential that these rotators be strong before abduction exercises are started. If they are not sufficiently strong, the deltoid muscle will only force the head of the humerus up against the acromion and produce further trauma. Storms found in a number of his cases that the rotators were not sufficiently strong to swing the beam, unloaded. After an exercise regimen, during which the external rotators are strengthened to where they can swing the beam with fifteen pounds or more loaded on it, the ability to abduct the arm returns. The deltoid is now able to lift the arm into full abduction.

In summary, an exercise program for the treatment of the stiff shoulder should have specific objectives. Exercises given have been divided into categories which parallel the sequence of treatment. Of first importance are the exercises in the first group, exercises for the mobilization of the head of the humerus. Following those come, in order, exercises to increase the range of external rotation, exercises to increase the range of internal rotation, and exercises to increase the mobility of the shoulder girdle. From these groups, exercises which are applicable to the particular case can be chosen and varied as desired by the physical therapist.

Bibliography

1. Dorland, E., The Illustrated American Medical Dictionary, W. B. Saunders Co., Philadelphia, 1927.
2. Codman, E. A., The Shoulder, The Author, Boston, 1934.
3. Mosely, H. F., Shoulder Lesions, Charles Thomas Co., Springfield, Ill., 1945.
4. Behrend, H. J., Physical Treatment of the Frozen Shoulder, New York State Journal of Medicine, Vol. 48, No. 9, May, 1948.
5. Duplay, S., On Scapulo-humeral Periarthritis, Paris Clinical Lectures, Medical Press, 1900, Vol. 69.
6. Lippman, R. K., Frozen Shoulder; Periarthritis: Bicipital Tendonitis, Archives of Surgery, Vol. 47, No. 3, Sept., 1943.
7. Mumford, E. B., & Martin, F. J., Calcified Deposits in Subdeltoid Bursitis, Jour. of the Amer. Med. Assoc., Vol. 97, Sept. 1931.
8. Watson-Jones, R., Fractures and Joint Injuries, Vol. II, Williams and Wilkins Co., Baltimore, 1943.
9. Baer, S. S., Operative Treatment of Subdeltoid Bursitis, Bulletin, Johns Hopkins Hospital, No. 3, June-July, 1907.
10. Buchholz, C. H., The Stiff and Lame Shoulder, Jour. of the Amer. Med. Assoc., Vol. 97, Sept. 1931.
11. MacKenzie, Sir C., The Action of Muscles, Paul B. Hoeber, Inc., New York, 1918.
12. Magnuson, P. B., Fractures, J. B. Lippincott Co., Philadelphia, 1942.
13. Lippman, R. K., Bicipital Tenosynovitis, New York State Jour. of Med., Vol. 44, Oct. 15, 1944.
14. Hitchcock, H. H. & Bechtol, C. C., Painful Shoulder, Jour. of Bone and Joint Surgery, Vol. 30-A, No. 2, Apr. 1948.
15. King, J. M., & Holmes, G. W., The Diagnosis & Treatment of 450 Painful Shoulders, Jour. of the Amer. Med. Assoc., 89:23, Dec. 3, 1947.
16. Watson-Jones, R., Adhesions of Joints and Injury, British Medical Journal, Vol. 1, May, 1936.
17. Hammond, R. H., The Stiff and Painful Shoulder, Rhode Island Medical Journal, Vol. 1, No. 11, November, 1917.
18. Steindler, A., & Marxer, J. L., Traumatic Deformities & Disabilities of the Upper Extremity, Charles C Thomas, Springfield, Ill., 1946.
19. Gordon, D., Observations on Impaired Shoulder Function and Methods of Treatment, Annals of Surgery, Vol. 90, Sept., 1929.
20. Martin, C. P., A Note on the Movements of the Shoulder Joint, British Journal of Surgery, July, 1932.
21. Fulton, John F., editor, Howell's Textbook of Physiology, W. B. Saunders Co., Philadelphia, 1946.

Reprinted from The Physical Therapy Review, Vol. 30, No. 6, June 1950.

Reprinted from the JOURNAL OF ENGINEERING EDUCATION, Vol. 41, No. 8, April, 1951
Printed in U. S. A.

Experience Credit Toward the Professional Engineer's License for Technical Institute Study*

By HAROLD P. RODES

Assistant Director of Relations with Schools and Assistant Professor of Engineering, University of California, Los Angeles

Stimulated in 1929 by the Wickenden report on engineering education, which included a major section on technical institute training, the tie between professional engineering and the technical institute type of engineering education has been becoming gradually closer and more friendly. Some of the tangible evidences of this relationship are the establishment of the Technical Institute Division of the American Society for Engineering Education and the Subcommittee on Technical Institutes of the Engineers' Council for Professional Development. Just as the medical profession, for example, recognizes that its effectiveness is due partially to the quality of its nurses and medical assistants, so does the engineering profession now recognize in the main that its effectiveness is due partially to the quality of its technicians and engineering aides.

We know, of course, that this improved relationship is not free from areas of irritation to the engineer and the technician, both in industry and in education. Some of the basic problems which remain to be solved include the lack of agreement on terminology, the difficulties encountered in the transfer of technical institute graduates into a professional engineering curriculum, and the establishment of a general policy concerning the granting of experience credit for technical institute training toward the professional engineer's license. For the purposes of this discussion we shall limit ourselves to the last of these problem areas.

Results of Survey of State Policies

Several months ago Dean L. M. K. Boelter requested the Executive Secretary of the National Council of State Boards of Engineering Examiners to undertake a survey of the practices employed in the various states with respect to the granting of experience credit for training of technical institute type. Accordingly, each member state was asked to indicate whether or not it gives experience credit for training received in ECPD accredited technical institute curricula.

The replies were extremely interesting for several reasons. They indicated not only a wide variation in practice from one state to another, but in several cases a complete lack of understanding of the question.

A tabulation of the replies received to date shows that six of the thirty-two states replying grant full experience credit toward a professional engineer's license for ECPD accredited technical institute training; seven states grant no credit; six states grant partial credit; the boards of five states have not yet decided upon a policy for granting credit; five states answered the question as relating to ECPD accredited "engineering" curricula; and three states frankly admitted that they did not understand the question.

* Presented before the Annual Meeting of the Pacific Southwest Section of the American Society for Engineering Education at the University of Southern California, December 28, 1950.

If the states replying with an unequivocal answer can be taken as an adequate sampling, it would appear that the boards in approximately one-fourth of the states are granting full experience credit for ECPD accredited technical institute training toward the professional engineer's license; that about one-fourth are granting no credit whatsoever; that another fourth are granting partial credit; and that in the final fourth the state boards have not yet considered the problem. However, in addition to this last fourth it is apparent that many other states have made their decisions in this matter tentative and subject to change on the basis of additional evidence and argument.

Although it is not the purpose of this paper to launch a crusade for complete standardization in the acceptance of experience credit for technical institute training, I do believe that it is somewhat embarrassing and difficult for the engineering profession to explain why the licensing boards in some states grant full credit while the boards in other states grant no credit for ECPD accredited technical institute training.

Before describing the policy which, in my opinion, represents the most rational and realistic approach to this problem, it might be well to review briefly some of the arguments which have been advanced by the two extremes mentioned previously. The state boards which grant full credit have proceeded on the assumption that two years of technical institute training is the equivalent of two years of engineering training insofar as professional preparation is concerned, an assumption that is questionable in the minds of many. The opposite point of view can perhaps be best presented by quoting the reply received from a member of one of the state boards:

"This matter has not as yet come before the Kentucky Board, but I think I can safely say that we will not give experience credit for work in technical institutes. Having sat in on a number of meetings of ECPD when this situation was discussed I can further say that ECPD certainly does not consider attendance at technical institutes, even though accredited, as having anything to do with registration as a Professional Engineer. I think the reason that ECPD has undertaken this work at all was because they have felt that something of the sort should be done in order to insure a supply of competent technicians but they do not expect the technical institutes to be considered as training Professional Engineers. The two things are entirely separate and distinct."

Like many other issues, this one also has two sides. Each of us probably has an opinion on this particular issue which may be quite close to one side or the other. I suspect, however, that the majority of us, as well as of the state licensing boards, will eventually agree that the ultimate solution lies somewhere between the two extremes.

California Plan

Of the several plans for granting partial credit, I believe that the "California Plan" has the greatest promise. In Section 409 of the California Administrative Code, the State Board of Registration for Civil and Professional Engineers was granted the authority to (1) "give partial credit for the completion of an approved curriculum of technical institute type," and (2) "accept the technical institute type curricula which have been approved by the Engineers' Council for Professional Development."

In order to implement the above legal authorization, the California Board adopted the following resolution: "Moved by Mr. Sullivan, seconded by Mr. Sorensen, that graduates from a technical institute curriculum accredited by the Engineers' Council for Professional Development be given one year's credit toward experience. . . . Motion carried." *

Stated differently, this resolution means that accredited technical institute train-

* Minutes of the California Board of Registration for Civil and Professional Engineers, May 17, 1949.

ing, which is normally of about two years in duration, is considered to be the equivalent of about one year of professional engineering training. An examination of ECPD accredited technical institute curricula indicates that such an evaluation is not far from the actual fact. For example, one accredited technical institute curriculum in the State of California includes courses in Applied Mathematics through Calculus, Aircraft Drafting and Detail Design, Applied Mechanics, Engineering Shop, Technical Report Writing, Elementary Physics, Aerodynamics, and Stress Analysis. Although the objective, and therefore the content of these courses differs considerably from that of the four and five year ECPD accredited engineering curricula, experience has shown that the graduate of such a curriculum who indicates aptitude for professional engineering training can probably complete a four year professional curriculum in about three years. Thus, the decision by the California State Board to grant one year of experience credit for the completion of approximately two years of ECPD accredited technical institute training appears to be a realistic and practical one.

There are undoubtedly those, even in this state, who feel that the Board should not grant any credit, or that it should grant full credit for ECPD accredited technical institute training. There are others who feel that the Board should not restrict the granting of partial credit to those curricula which have been accredited by ECPD. I believe we would all agree, however, that unless certain standards are maintained the licensing of professional engineers is meaningless. Possibly ECPD accreditation is not the only or even the best method of maintaining sufficiently high standards for purposes of registration. Nevertheless, until some of the closely related problems such as terminology and transfer are solved, ECPD accreditation appears to be the only sound educational basis for the granting of experience credit toward the professional engineer's license.

At the present time there are only two institutions in the State of California which are offering technical institute curricula that would qualify for partial experience credit. Even if this number should be greatly increased by the accreditation of technical institute curricula in other private and public institutions, the total number of technical institute graduates applying for professional registration will never be very large. Nevertheless, if the engineering profession is to maintain its current development in a true professional sense, and at the same time avoid some of the errors and inconsistencies which have been plaguing certain other professions, it appears desirable and even essential that the "California Plan" for the granting of experience credit for technical institute training should be continued in this state and considered in some appropriate form in other states.

FIELD STUDY OF A SHEET PILE BULKHEAD

by

C. Martin Duke

Assistant Professor of Engineering
University of California
Los Angeles

Paper presented at Annual Spring
Meeting of American Society of
Civil Engineers, April 27, 1950,
Los Angeles, California

NOT FOR PUBLICATION

SYNOPSIS

Results of a field study of structural performance of a flexible anchored bulkhead are presented in this paper. The bulkhead retains a 55-foot height of fine sand hydraulic fill in Long Beach Harbor, California. A coarse granular dike extends for half the height on both inside and outside. Instrumentation was provided for measurement of soil pressure, tie rod tension, and deflection during and after the filling operation.

It was found that during filling the lateral soil pressure distribution was approximately in proportion to weight of overlying fill, with a lateral pressure coefficient of about 0.7. After completion of filling the lateral pressures above wale increased sharply while those below decreased; this is attributed to settlement of fill and accompanying partial support of fill on the tie rods and wale.

Design implications of the test results are indicated.

INTRODUCTION

The Need for Full-Scale Tests.

The flexible bulkhead is an outstanding example of the great group of problems in foundations and earth structures which are not amenable to accurate analysis on account of insufficient understanding of the performance of the real system. In the case of bulkheads the problem can be expressed in three parts: (1) the bulkhead, the backfill, and the supports at anchor and toe all deform in accordance with some as yet unformulated functions of soil and bulkhead load-deformation characteristics; (2) the factors determining relations between lateral and vertical soil pressures under idealized conditions are still incompletely understood; and (3) the quantitative influence on lateral pressures of such prototype phenomena as tide fluctuation, pore pressure, settlement of fill, and construction irregularities is not understood.

Efforts toward determination of the fundamental parameters of bulkhead performance have led, as with many other soil problems, to the conclusion that further advance must lean heavily on scientific studies of prototype structures. An opportunity for an investigation of this type arose when the Port of Long Beach, California, as part of its development program, planned the construction of two large hydraulically filled piers bordered by anchored steel sheet pile quay walls. This led to the cooperative program of investigations of the bulkhead at Pier C in Long Beach Harbor which is the subject of this paper.

Scope and Objective of Investigation.

The structural performance of the east bulkhead of Pier C, Long Beach Harbor (Figure 2), during and after hydraulic filling of the pier, was investigated by means of instruments installed at two test stations. The pier was filled to Elev. +17 and has an outboard bottom elevation of -38 at the test locations. A coarse granular dike placed on both sides of the bulkhead to Elev. -10 prior to filling provided a degree of reinforcement. The essentially non-plastic fill material consisted of a fine sand containing varying amounts of silt.

Conclusions

The Pier C failure is an outstanding example of the great group of problems in foundations and earth structures which are not amenable to accurate analysis by means of the traditional theoretical or the purely empirical approach. In the case of Pier C the problem can be pictured as that of (1) the settlement, or overfill, on the property of Union Oil Company of California and (2) the resulting lateral displacement of soft and relatively impervious clay deposits. (3) the factors dominating relations between lateral and vertical displacements were practically not known; and (4) the quantitative influence on lateral pressures of such complex phenomena as thixotropy, pore pressure, rebound of fill, and consolidation irregularities is not understood.

Efforts toward determination of the fundamental parameters of soil-steel pressure have led, as with many other soil problems, to the conclusion that theoretical methods must lean heavily on scientific studies of prototype structures. In particular for an investigation of this type arose when the Port of Long Beach, California, as part of its development program, planned the construction of two large additionally filled piers bordered by sunbonded steel sheet pile bulkheads. This led to the cooperative program of investigations of the bulkhead on Pier C in Long Beach Harbor which is the subject of this paper.

Structural Performance

The structural performance of the east bulkhead of Pier C, Long Beach Harbor (Figure 2), during and after hydraulic filling of the pier, was investigated by means of instruments installed at two test stations. The pier was filled to +10, and has an outboard bottom elevation of -38 at the test locations. A row of tubular tiles placed on both sides of the bulkhead to Elev. -10 prior to filling provided a degree of reinforcement. The resulting composite bulkhead consists of tiles and sheet piles varying amounts of silt.

Provision was made at the principal test station for measurement of total deflection of bulkhead and anchor, relative deflection at various elevations on the bulkhead, bending strain in bulkhead, tension in tie rods, soil pressures at various elevations, and water pressures at significant locations in the fill. These measurements, except for soil and water pressure, were duplicated at another test station. Observations were made over a period of eight months, from February to October, 1949, with principal activity during the filling operation from February to June.

The investigation probed the distribution and magnitude of soil pressure against the bulkhead and its variation with height and age of fill. The effectiveness of the dike in carrying a part of the lateral pressure was also studied.

Organization.

The Long Beach Harbor Department purchased and installed the instruments. Active participants for the Harbor Department were R. R. Shoemaker, Chief Harbor Engineer, and B. N. Hoffmaster and T. J. Thorley, Engineers.

The University of California, Department of Engineering, Los Angeles, planned the instrumentation and conducted the tests and analyses. L. M. K. Boelter is Chairman of the Department. D. P. Krynine, Visiting Professor, advised in the planning. The author was in immediate charge. Students in Engineering who participated were D. L. Wheeler, E. R. Hallett, V. S. Peterson, R. J. Reich, and E. Carlson.

The Soil Mechanics Committee, Los Angeles Section, American Society of Civil Engineers, gave considerable study to the test program and made numerous valuable suggestions. Committee members were T. R. Dames (Chairman), F. J. Converse, C. M. Duke, L. T. Evans, S. S. Green, T. M. Leps, and D. F. Warren.

Preliminary Qualitative Analysis.

As a basis for discussion of the planning and interpretation of the tests there is first presented a qualitative analysis of the performance of a typical hydraulically filled bulkhead. The cross-section of Figure 1 is considered, which

is similar to Pier C bulkhead except for omission of the rock dike. It is assumed that water level remains constant at Elev. +4 inside and outside of bulkhead, that bulkhead is fixed at Elev. -38 and simply supported at Elev. +4, and that friction between soil and bulkhead is negligible. Discussion is subdivided according to phenomena before and after completion of filling.

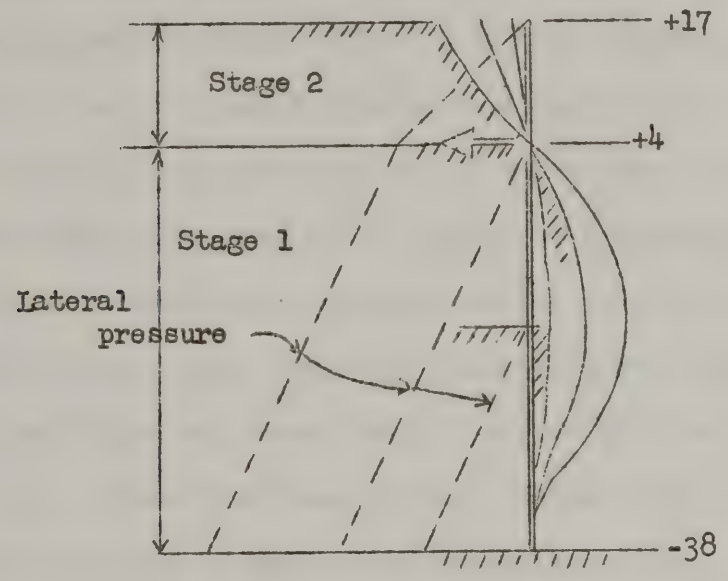

Fig. 1. Deflection of a Hydraulically Filled Bulkhead

Active pressure, pressure-at-rest, and passive pressure of soil against bulkhead are the limits to be considered in evaluating the behavior of this ideal system during the filling operation. In Stage 1 of Figure 1, with fill level below the wale, deflection of bulkhead is qualitatively suitable for development of lateral pressure between the limits of active pressure and pressure-at-rest. In Stage 2 the influence of the cantilever portion above the wale is felt, and in addition the unbuoyed fill density causes a sharper rate of increase in vertical pressure. The deflection of the cantilever portion continues to be inward, as in Stage 1, so that lateral pressures against the cantilever will be between the limits of pressure-at-rest and passive pressure. If Stage 2 were carried to a great height the trend of deflections below and above the wale would tend to reverse; this would represent an unusual bulkhead. Then it should be anticipated

that pressures against the bulkhead during filling will be somewhat less than pressure-at-rest below the wale, somewhat greater above. If the fill is highly fluid the range between active and passive pressures will be small, so that this difference will not be easily detectable.

During and after the filling operation the fill settles. This fact in itself might cause minor changes in the above distribution of lateral pressure because of the influences of wall friction, diminishing fluidity, and horizontal consolidation. But a factor of greater importance exists: the tie rods (and at Pier C also the wale) are contained in the fill. Fill settlement results in the tieback system supporting part of the weight of overlying fill. This causes lateral pressure redistribution because the tie rods act as cables to support vertical load and thus their reaction on the bulkhead increases lateral soil pressures at and above wale level; also, because vertical pressure below the tie rods is reduced, lateral pressure against bulkhead below wale level is decreased. This is a consideration of major significance in design.

The rock dike (Fig. 2) will influence pressures over its lower portion. The inner dike (references 3, 5, and 6) transmits some of the fill pressure to the ground beneath the bulkhead. The outer dike provides a minor passive resistance and confines the ground on the outside, giving plausibility to the above assumption of fixity at Elev. -38.

Passive resistance at the base has not been specifically dealt with above because the Pier C tests did not adequately cover this important item. It should also be pointed out that bulkheads constructed on land, followed by dredging on the outboard side, should be considered in a separate class.

STRUCTURE AND MATERIALS

Construction of Pier C.

The Pier C quay wall (Fig. 2) consists of a bulkhead of 78-foot MZ-38 steel sheet piles anchored by means of 3-inch tie rods at 6-foot intervals to a concrete-capped batter-pile anchor set 62 feet back of the bulkhead centerline. A

continuous wale consisting of two 15-inch channnels is bolted to the inside of the wall. Tie rods are on a slope of one in 27, which may be considered as horizontal for structural analysis. The timber anchor piles are 3 feet center to center in two rows battered each way from the anchor centerline. The quay wall was designed by the Long Beach Harbor Department; contractor was the United Construction Company.

After completion of pile driving, installing of wale and tie rods, and concreting of anchor cap, the 3-inch maximum size rock dike was placed by clam-shell (Fig. 4) on both sides of the wall, sloping at its natural angle of repose. Actual dike profiles are given in Fig. 7. Pumping of fill into the pier from dredges working in the harbor began in mid-December, 1948. In mid-February, 1949, deposition began at Station 27 + 30, and by mid-June, 1949, filling had been substantially completed at both test stations. Figs. 3 through 6 show the fill at various stages.

Dike Material.

The rock used in the dike was obtained from a quarry in the hills west of San Pedro. According to B. M. Page, Geologist, it is classified as: "Diabase. A dark-colored igneous rock composed of augite, feldspar, and iron greenstone." Particles are angular and fairly hard. Specific gravity is 2.42. Study of the screen analyses made at the quarry gave the following grading:

Square Screen Size	Average Per cent Passing
3 inch	90
1-1/2 inch	55
3/4 inch	30
1/4 inch	15

Angle of repose, measured from dike cross-sections after placing, was 32° (Fig. 7). Fig. 15 shows a typical sample of dike material where it collected on the wale during placing.

Fill Material.

Both fill and natural ground consist of recent alluvium brought to the

[illegible]	[illegible]
[illegible]	[illegible]
[illegible]	[illegible]

harbor by the Los Angeles River. The fill was dredged hydraulically from the vicinity of the river delta.

Exploration and testing of soils was carried out by L. T. Evans, Foundation Engineer, who studied samples from 69 borings in the harbor area. Four of the borings were made in Pier C prior to filling and extended to about Elev. -100. After completion of filling a boring was made through the fill opposite each test station. "Undisturbed" samples of 3-inch diameter were taken at 3-foot intervals in 23 of the borings, including those in Pier C, and classification samples were taken in the remainder. Laboratory density, mechanical analysis, triaxial compression, permeability, and consolidation tests were made on a large number of samples representing all soil types encountered; approximate tests were made to estimate maximum and minimum void ratios, and Atterberg limits were established for the few plastic soil types encountered. These data, as they pertain to Pier C, are summarized in Table 1, where data on dike properties are also included.

Consolidation tests of the fill itself have not been made, but data on similar soils from other parts of the harbor gave the following representative figures:

Soil	Compressive Index
Fine Sand	0.05
Silty Clay	0.15

Compressive index is defined as the decrease in void ratio per 100% increase in pressure on a preconsolidated specimen. For the fine sands of the fill, possible range of maximum and minimum void ratios was about 0.6; permeability coefficients ranged between about 10 and 35×10^{-4} cm./sec.; per cent passing sieve No. 200 ranged between 5 and 15, approximately. Lenses of coarse and medium sand and occasional lumps of organic clay were present.

Table 1. Generalized Soil Properties

Location	Gradation	Angle of Internal Friction	Cohesion lb./sq.ft.	Specific Gravity	Coefficient of Permeability cm./sec.	Unit Weight lb./cu.ft.
Dike	Graded 3" to $\frac{1}{4}$"	32°[a]	0	2.42	--	60[b]
Below Elev.-38	Fine Sand[e]	38°	0	2.67	25×10^{-4}	55[c]
Elev.-38 to -32	Silty Clay[e]	13°	1000	2.72	--	48[c]
Elev.-32 to +4	Fine Sand[e]	37°	0	2.67	25×10^{-4}	55[c]
Elev.+4 to +17	Medium Sand[e]	38°	0	2.67	100×10^{-4}	105[d]

a. Measured as angle of repose from dike profiles.

b. Assumed submerged unit weight.

c. Submerged unit weight.

d. Field unit weight.

e. Grain size limits (mm): Clay below .005 Silt .005 to .05, Very Fine Sand .05 to 0.1, Fine Sand 0.1 to 0.22, Medium Sand 0.22 to 0.5, Coarse Sand 0.5 to 1.0. Gradations given in table were assigned on basis of predominant proportions.

INSTRUMENTATION

Scheme of Instrumentation.

Much study was given to the problem of how best to observe the behavior of the soil and bulkhead. General features are shown in Figs. 7, 8, and 9. Sta. 27 + 30 on the east bulkhead line of Pier C (Fig. 2) was instrumented for measurement of soil and water pressures against the bulkhead and for measurement of tie rod tension on, bending moment in, and deflection of the bulkhead. Sta. 30 + 30, 300 feet to the south, was used as a check station with duplicate instrumentation except for soil and water pressure. Measurements consisted of the following:

At Both Test Stations

Deflection of points on upper half of bulkhead by reference to a plumbed vertical beam.

Tension in tie rods by means of pairs of Carlson strain-meters attached to three tie rods at each test station.

At Sta. 27 + 30 Only

Pressure of soil against bulkhead by means of nine Carlson stress-meters. Four of these instruments were installed in the fill above the dike. Five were installed in the dike, three inside and two outside the bulkhead.

Water pressure on stressmeters and on inside of bulkhead, and pore pressure in the fill, by means of six standpipe piezometers.

In addition there were undertaken at both test stations measurements of bulkhead strain by Whittemore mechanical strain gage and of total deflection of bulkhead and anchor by transit. Precision and consistence of these measurements was so poor that they have been disregarded.

Tides and fill elevations were referred directly to points on the bulkhead in order to eliminate errors due to regional subsidence. Nominal datum is Mean Lower Low water. Real elevations can be estimated by reference to subsidence contours of the area.

Leads from the Carlson instruments, which are electric recording, were brought to a plug-in panel specially fabricated for this use (Fig. 9).

Observations were made three or four days apart during the placing of the fill, which occupied a period of about three months. On selected days, observations were made at two hour intervals during a maximum tidal range. Readings at decreasing frequency were made up to October 5, 1949, when the tests were discontinued because insufficient instruments to justify further observations remained active after this date. See reference 4 for full explanation of the instrumentation. Most significant features are given below.

Tie Rod Tension.

Six tie rods, three at Sta. 27 + 30 and three at Sta. 30 + 30, were instrumented with two Carlson strainmeters each for measurement of tie rod tension. The strainmeters are described in references 1 and 7. Fig. 16 shows the elements of the standard instrument; that used in the tests was of slightly smaller diameter and lacked the end flanges shown. The strain-sensitive element consists of two coils of wire, one of which stretches while the other shortens when the ends of the meter are displaced relative to one another. Use of Carlson strainmeters in preference to a bonded type strain gage such as the SR-4 gage was adopted in order to assure longer life to the installation and to avoid uncertainties as to waterproofing and as to possible shifts in zero reading.

A portable Wheatstone bridge set is used to observe the ratio of the resistances of the two coils and their total resistance in series; change in resistance ratio is a linear function of strain, and change in total resistance is a linear function of change in temperature. A temperature correction to strains computed from resistance ratios is required on account of the difference in coefficients of thermal expansion of meter and of tie rod.

Figs. 17 and 18 show the method of attachment of the strainmeters to the tie rods -- an arrangement designed to cancel out the effects of bending in the rods. This was worked out in consultation with Mr. Carlson and with Mr. David Pirtz. The strainmeter was slipped through the holes in the lugs (Fig. 18) and

[illegible] recording, which was electric recording, was [illegible] specially constructed for this use (Fig. 9).

[illegible] were made three or four days apart during the flowing of the [illegible] period of about three months. On selected days, observa- [illegible] at two hour intervals during a maximum total range. Reading at [illegible] were made up to October 7, 1910, when the cocks were discon- [illegible] Laurer Manometer [illegible] Instrument [illegible] [illegible] value 0.14 bars. [illegible] [illegible] [illegible]

[illegible]

[illegible] were at 6th. 27 + 30 and three at 6th. 30 + 7th, were [illegible] with two Gardner sphygmometers each for measurement of the rod tension. [illegible] are described in reference 1 and 7. Fig. 16 shows the elements [illegible] instrument; both used in the tests was of slightly smaller [illegible] the rod changes shown. The strain-sensitive element consists [illegible] wire, one of which remembers while the other unscreen when the [illegible] are displaced relative to one another. One of [illegible] [illegible] to a bonded type strain gage such as the SR-4 gage was [illegible] easier to measure Langer 1414 to the installation and be avoid uncer- [illegible]

[illegible] [illegible] [illegible] [

securely clamped with the Allen set screws in such a manner that about three fourths of the range of resistance ratio was available for tensile strain measurement. Precision of individual observations corresponded to about 150 psi. stress.

Before taking initial readings all tie rods in the vicinity of the test stations were adjusted as nearly as possible to the same length by means of the turnbuckles.

Difficulty was encountered with the strainmeters due to lack of protection of lead wires against tensile forces due to the drag of the settling fill. When the fill level reached Elev. +8, the strainmeters began to become inoperative one by one until when the fill had reached its full height there were only three strainmeters left, one at Sta. 27 + 30 and two at Sta. 30 + 30. Fortunately the loss of strainmeters was a gradual process and it was possible to continue computations of tie rod tensions by using data from only one strainmeter on a rod. For these computations it was assumed that bending strains had been largely accounted for under the lower tensions.

Soil Pressure.

Nine Carlson stressmeters with ranges of 20 and 40 psi., were used for the measurement of soil pressure against the bulkhead. See Fig. 11 and references 2 and 7. These instruments, which have a fine record of stress measurement in concrete and have been previously used for soil on several occasions, were adapted to this soil pressure problem through conferences with the manufacturer and with the inventor. Fig. 7 shows the stressmeter locations, at Station 27 + 30 on the bulkhead line. Pressure on the outer face causes pressure in the film of mercury which in turn deflects the diaphragm proper: this deflection is measured with a Carlson strainmeter unit. The least reading corresponds to less than 50 lb./sq. ft.

The stressmeters were calibrated for soil pressure in the laboratory by the manufacturer, using a stiff rubber pad as the bed and applying load in a testing machine over the flat area of the top plate by means of an annular block.

Calibration for water pressure was carried out at the site of the tests by suspending the stressmeters at known distances below the water surface. Fig. 13 gives soil and water calibration curves for P-4, a typical stressmeter. The two curves are different because of the differences in manner of loading.

The stressmeters were mounted in 22-inch steel plates as shown in Fig. 12. Reaction for the pressure was provided by two steel bars which also served to stiffen the plate; on account of the sufficient thickness of the inner plate of the stressmeter these bars provided essentially the same support as the annular block used in the soil pressure calibration. The steel plates were held in the bulkhead troughs by means of spring friction clips. Figs. 10 and 12 illustrate these details. After the stressmeters had been firmly screwed in place, the two steel plates on the inboard side and the one on the outboard side were lowered into position, pressed into the bulkhead troughs by a diver (Fig. 14), and securely welded to the bulkhead at their tops only.

A number of difficulties, most of which were overcome, were encountered in the installation and use of the stressmeter. Some of these were: early unsteadiness of zero readings; inadequacy of friction clips; damage to stressmeters during installation; and broken lead wires. Probable validity of measurements in the dike was questioned from the first on account of large size of dike fragments.

Water Pressure.

Pressure of water against stressmeters and against bulkhead was determined during the early stages of filling by direct observation of tide elevation; after closure of the last corner of the pier the water rose inside, and both inside and outside water elevations were observed. After the fill rose above inside water level the tide data were supplemented at Sta. 27 + 30 with piezometer readings at three elevations (Fig. 7) on the back face of the bulkhead; three additional piezometers were installed to give information about ground water in the fill. The piezometers consisted of 1/2- or 3/4-inch pipes running to simple filter-type

pore pressure points. Readings of water level were made to the nearest 0.1 foot by sounding.

Bulkhead Deflection.

Deflection of bulkhead points was determined by means of the vertical reference beam shown in Figs. 7, 9, and 19. Plumbing of the beam was achieved by means of a precise level tube mounted at the top. Relative deflection measurements were made to the nearest 0.01 inch with a portable dial gage stand placed perpendicular to bulkhead and at minimum distance to reference beam at the various points observed. Provision was also made for observing anchor deflection by means of a special fin (Figs. 6 and 7) bolted to the cap and projecting up through the fill, but transit observations of deflection of both anchor and bulkhead were insufficiently precise. Thus it was decided to postulate zero deflection of the wale and to utilize the reference beam exclusively for deflection determinations.

PRESENTATION OF RESULTS

Results of the Pier C bulkhead tests are presented in Tables 2 through 5 and in Fig. 20.

Tie rod tension measurements at both test stations are given in Table 2 and are summarized in Tables 3 and 4. Due to successive breaking of strainmeter leads the composite values in Table 2 become more approximate with the passage of time after about April 6, but enough strainmeters remained in action to the end of the tests to provide measurements.

Tables 3, 4, and 5 summarize all measurements at the two stations. Free body diagrams of the bulkhead at Sta. 27 + 30 on 19 dates up to August 17, are drawn in Fig. 20; tie rod tension values have been divided by six for these diagrams to give anchor pull per linear foot of bulkhead. Measurements of water pressure by piezometer have been used in computing soil pressures from stressmeter readings; hydrostatic excess, which is small and has not been shown in this figure, can be computed from data in Table 5.

Table 2. Tie Rod Tensions

Values in kips.

Date (1949)	Station 27 + 30				Station 30 + 30				
	Tide Elev. (ft.) (a)	Sta. 27+18 (b)	Sta. 27+42 (b)	Composite (c)	Tide Elev. (ft.) (a)	Sta. 30+18 (b)	Sta. 30+30 (b)	Sta. 30+42 (b)	Composite (c)
4-15		6	10	8		5	5	1	0
19		6	11	8		-7	2	2	0
19		4	11	8		-5	3	2	0
23	4.2 in. 1.7 out.	22	24	23	5.1 in. 1.9 out.	8	22	7	12
26	5.0 in. 2.0 out.	28	24	26	5.0 in. 2.0 out.	3	17	11	10
26	5.3 in. 4.0 out.	18	25	22	5.0 in. 3.0 out.	9	21	13	14
26	5.5 in. 6.0 out.	24	27	26	5.6 in. 5.6 out.	3	7	0	3
29	5.6 in. 3.9 out.	30	23	26	5.2 in. 3.1 out.	4	26	21	17
5-3	5.5 in. 4.4 out.	32	30	31	5.5 in. 4.5 out.	19	33	26	25
6	6.6 in. 4.4 out.	46	42	44	6.6 in. 3.7 out.	11	40	34	28
10	8.2 in. 2.5 out.	30	53	42	8.2 in. 3.7 out.	33	48	41	41
14	10.5 in. 3.7 out.		62	58	10.5 in. 3.7 out.	49	122	62	78
17	4.8	72	76	74	4.7	48	109		73
20	4.0	138	97	118	4.0	63	162	67	97
24	4.4		155	155	5.0	73	183	63	106
6-3	5.7		182	182	6.0	71	194	55	107
11	0.5		205	205	1.0		266	76	153
7-12	3.6		209	209	3.8		255	49	135
8-5	8.0		198	198	8.0		257	55	139
5	5.5		197	197	5.5		265	57	143
5	4.0		214	214	3.7		267	62	147
6	2.0		212	212	1.6		269	64	149
6	0.7		219	219	0.7		269	66	150
17	6.0		229	229	5.6		291	83	169
24	2.8				3.7		297	92	176
10-5	3.0				3.2		293		172

(a) Both inside and outside free water levels given where appropriate.

(b) Horizontal line in column indicates where one of the two strainmeters went out of action. Increases from this point based on one strainmeter only. S-3 and S-4 at Sta. 27 + 30 gave erratic values which have been discarded.

(c) While strainmeters still in action on all tie rods, computed as average. Increases thereafter obtained by averaging individual increases.

Table 3. Summary of Measurements: Station 27 + 30

Date (1949)	Fill Elev. (ft.)	Tide Elev. (ft.) (a)	P_v at El.-10 (kips/sq.ft.) (b)	Tie Rod Tension (kips)	Horiz. Defl. at El. -9.5 (in.)	Soil Pressure (kips/sq.ft.)						
						Inside Face					Outside Face	
						Elev. +12.3	+7.3	+0.7	-7.3	-14.9	-22.8	-32.8
2-17	-32		0							.00	.00	.00
25	-30		0							.00	.56	.38
3-1	-29		0							.22	.70	.26
4	-27.5		0							.40	.69	.27
8	-27		0							.50		
13	-26		0							.73	.86	.36
17	-22		0		.02					.77	.84	.38
22	-22		0		.05					1.40	.94	.50
26	-21		0		.00					1.00	.99	.33
29	-21		0		.00					.96	1.15	.30
4-2	-18		0		.11					.80	.98	.31
6	-17.5		0		.02					.80	1.03	.28
9	-14		0		.04					.90	1.02	.40
12	-11	1.2	0		.09					1.20	1.32	.53
15	- 8.5	2.7	.08	8	.42					1.10	1.22	.42
19	- 7	3.5	.17	8	.52				.00	1.06	1.20	.45
23	- 1	4.2in. 1.7out.	.50	23	.82				.17	1.33	1.47	.60
26	3.2	5.3in. 4.0out.	.73	25	1.89			.00	.55	1.19	1.61	1.05
29	5.8	5.6in. 3.9out.	.88	26	2.15			.11	.50	1.06	1.38	1.27
5-3	7.5	5.5in. 4.4out.	1.00	31	2.48		.00	.00	.76	1.06	2.40	1.12
6	7.8	6.6in. 4.4out.	1.07	44	2.57		.08	.00	.55	1.00	1.47	.87
10	9.4	8.2in. 2.5out.	1.17	42	2.78		.08	.26	.86	.98	1.90	1.04
14	12.0	10.5 in. 3.7out.	1.42	58		.00	.38	.56	1.04	1.62	2.30	1.12
17	12.1	4.8	1.52	74	3.39		.73	.68	1.25	1.84	1.98	.98
20	13.1	4.0	1.59	118	3.33		.26	.85	1.48	1.59	1.60	.96
24	16.0	4.4	1.94	155	3.42		.55	.23	1.14	1.70	1.58	.95
6-3	16.3	5.7	2.01	182	3.36		.67	1.30	1.04	1.74	1.35	.60
11	16.5	0.5	2.14	205	3.40		.70	1.18	.71	2.52	1.88	.85
7-12	16.5	3.6	2.07	209	3.46		1.28	.00	.58	2.53	1.58	
8-5	16.5	8.0	1.96	198	3.37		1.79	.00	.68	2.79	.80	.6
6	16.5	0.7	2.09	219	3.37		1.85	.00	.24	2.33	.95	
17	20.5	6.0	2.43	229	3.37	2.70	2.36	.00	.55	1.62	.69	1.07
24	20.5	2.8	2.49		2.41	2.85	2.60	.00	.48	1.30	.87	
10-5	20.5	3.0	2.48		3.63			.00	.57	1.85	.74	

(a) Both inside and outside free water levels given where appropriate.

(b) Vertical soil pressure (computed).

Table 4. Summary of Measurements: Station 30 + 30

Date (1949)	Fill Elev. (ft.)	Tide Elev. (ft.) (a)	P_v at El.-10 (kips/sq.ft.) (b)	Tie Rod Tension (kips)	Horiz. Defl. at El. -9.5 (in.)
3-1	-35		0		
17	-30.5		0		.00
22			0		.02
26			0		.13
29			0		.08
4-2			0		.17
6	-28.5		0		.13
9	-26		0		.14
12	-25		0		.10
15	-23		0	0	.14
19	-22		0	0	.16
23	-20	5.1 in. 1.9 out.	0	12	.86(c)
26	-14.5	5.0 in. 3.0 out.	0	10	1.16
29	- 6	5.2 in. 3.1 out.	.22	17	1.60
5-3	- 3	5.5 in. 4.5 out.	.38	26	2.02
6	0.5	6.6 in. 3.7 out.	.58	28	2.28(d)
10	4.5	8.2 in. 3.7 out.	.80	41	2.58
14	9.0	10.5 in. 3.7 out.	1.05	78	
17	10.2	4.7	1.38	73	3.57
20	12.0	4.0	1.62	97	3.66
24	12.7	5.0	1.63	106	3.69
6-3	12.5	6.0	1.56	107	3.86
11	15.5	1.0	2.13	153	
7-12	15.5	3.8	1.99	135	
8-5	16.0	8.0	1.83	139	3.69
8-6	16.0	0.7	2.20	150	3.69
8-17	21.5	5.6	2.53	169	3.67
8-24	21.5	3.7	2.62	176	3.67
10-5	21.5	3.2	2.65	172	3.92

(a) Both inside and outside free water levels given where appropriate.

(b) Vertical soil pressure (computed).

(c) Level tube reset after this measurement. Following values have been increased 0.20 in., to allow for deflection between 4-23 and 4-26, value having been estimated from measurements at Sta. 27 + 30.

(d) Same as (c) except added 0.30 to account for estimated 5-6 to 5-10 deflection.

Table 5. Piezometer Readings: Station 27 + 30

Values in ft. above M.L.L.W.

Date (1949)	Time	Tide	Piezometer						Inside Water Level	Fill Elev.
			H-1	H-2	H-3	H-4	H-5	H-6		
4-19	3:00 P	4.2	4.0	4.0	4.4	4.1	4.0	4.0	Tide	-7
4-23	12:00 M	1.5	3.2	3.3	2.8	2.2	4.8	3.8	3.4	-1
5- 3	3:00 P	4.4	6.5	4.3	4.2	4.5	4.5	4.5	5.5	7.5
5- 6	3:30 P	4.6	5.8	4.5	4.9	5.1	5.1	4.9	6.6	7.8
5-10	2:30 P	2.7	7.1	4.4	2.3	4.4	5.7	5.5	8.2	9.4
5-14	3:15 P	3.7	7.5	5.4	3.0	5.2	5.6	5.4	10.5	12.0
5-17	3:20 P	4.8	5.8	5.8	4.5	5.7	6.3	5.7	-	12.1
5-20	2:10 P	3.8	7.1	5.2	3.7	5.0	5.9	5.8	-	13.1
5-24	3:15 P	4.2	5.6	4.6	3.7	4.9	5.9	5.6	-	16.0
6- 3	3:30 P	5.9	Bel.5.4	5.0	5.6	6.3	6.3	5.1	-	16.3
6-11	5:30 A	0.9	"	2.6	1.0	2.3	2.6	4.6	-	16.5
7-12	4:30 P	3.7	"	4.1	3.5	3.5	3.8	3.8	-	16.5
8- 5	7:10 P	8.0	"	6.2	7.0	6.4	5.9	5.5	-	16.5
	10:00 P	4.8	5.5	6.0	5.1	5.3	5.6	5.6	-	16.5
	10:40 P	4.0	5.5	5.5	3.9	4.4	5.4	5.4	-	16.5
8- 6	12:05 A	2.0	Bel.5.4	4.6	2.3	3.3	4.0	4.2	-	16.5
	2:00 A	0.7	"	3.5	1.2	2.5	3.0	3.1	-	16.5
8-17	4:40 P	6.0	"	5.3	5.3	5.3	5.5	5.0	-	20.5
	5:45 P	5.2	"	5.3	5.2	-	-	-	-	20.5
8-24	4:00 P	3.4	"	4.1	3.3	3.4	3.8	4.1	-	20.5
10- 5	3:00 P	3.0	"	4.3	4.6	4.5	4.7	4.2	-	20.5

| | | |

BULKHEAD PERFORMANCE DURING FILLING

The result of greatest importance which it was hoped to obtain from the tests is the distribution of lateral pressure of fill against the bulkhead and its variation with significant parameters. Thus the program was laid out with lateral pressure as center of attraction. A large quantity of direct and indirect data on this subject has been obtained, all of which is interrelated. To organize these data, analysis has been subdivided according to phenomena before and after completion of the hydraulic fill.

In utilizing the deflection and tie rod tension measurements to supplement lateral pressure measurements during filling, the following procedure was adopted: (1) Determine best lateral pressure coefficients based on stressmeter observations only; (2) Tentatively adopt a hypothesis concerning nature of support of the bulkhead; (3) Compute deflections and tie rod tensions from steps (1) and (2) and compare with measured quantities.

Outward Soil Pressure.

Analysis of soil pressures from stressmeter observations during filling operation has been made in terms of a single coefficient of lateral pressure; distinction between coefficients above and below the wale has not seemed justified on account of imperfect homogeniety of fill and anticipated small magnitude of actual differences. This analysis required first an estimation of vertical pressures (Tables 3 and 4) which has been made on the basis of soil densities in Table 1. It is assumed here that friction between bulkhead and fill is negligible during the filling operation.

Fig. 21 shows the measured lateral soil pressures at Sta. 27 + 30 plotted against vertical pressure at Elev. -10, which increases in accordance with the increase in weight of fill above that elevation. Vertical pressure at the level of a particular stressmeter is obtained by moving the origin to the right by the amount of fill weight between Elev. -10 and the stressmeter. Thus the slopes of the stressmeter "curves" in Fig. 21 are the lateral pressure coefficients, values

of which are indicated on the figure. Stressmeters P-5, P-8, and P-11 have not been included here as P-5 and P-11 are on the outside of the bulkhead and all are in the dike where a different coefficient should be expected.

Soil pressures against the bulkhead are also shown in Fig. 20. During the filling operation (up to about May 24), these pressure distributions can be used to estimate the value of the lateral pressure coefficient. By use of a template ruled with theoretical lateral pressure lines (broken at ground water level) corresponding to various assumed lateral pressures coefficients, and assuming the soil submerged below Elev. +4, the values indicated on the figure were obtained.

As a result of the above determinations the lateral pressure coefficient of the fill material during the filling operation has been taken at 0.7.

Lateral Pressures in Dike.

Stressmeter measurements within the dike, as had been anticipated, were inadequate for reliable lateral pressure determinations on account of the large size of fragments. Initial observations were inconsistent with reasonable theoretical values, but it is thought that subsequent small increases superposed on the initial values may be rough approximations to the actual increases.

Deflection of the inner dike is qualitatively suitable for development of a lateral pressure between the limits of pressure-at-rest and active pressure. Active pressure coefficient for the Dike is about 0.3, based on approximation that angle of internal friction equals angle of repose equals 32°. Pressure-at-rest for this coarse granular material may be approximated at 0.5 (reference 6). Because the relative deflection of the bulkhead was appreciable (nearly 4 inches in a 42-foot span, Tables 3 and 4) the lateral pressure coefficient of the inner dike has been taken at 0.3 for purposes of analysis. Because top of dike deflects it is believed that it does not reduce lateral pressures to the 0.3 value over its full height; see pressure diagram, Fig. 22, and compare reference 3.

Study of performance of the stressmeters on the outside face, as given in

Table 3 and Fig. 20, reveals a definite passive resistance provided by the outer dike. Both stressmeters indicated increases of approximately 0.5 kip/sq. ft., at about the time the fill reached Elev. +4. Prior to this increase it may be considered that active pressure existed, for earth sloping at its angle of repose is everywhere just short of incipient failure. Then for purposes of analysis the following generalization is made:

Fill Level	Passive Resistance of Outer Dike
Elev. +4	Lateral pressure coeff. = 0.3
Elev. +17	Additional 0.5 kips/sq. ft. for full height of dike.

Theoretical versus Observed Performance.

Pressure distribution for fill elevations +4 and +17, based on the foregoing interpretations of stressmeter measurements, are presented in Fig. 22. Tide and ground water levels have been taken at Elev. +4 for this purpose. Pressure due to the dike inside the bulkhead has been estimated by drawing straight lines between values computed for fill at Elev. -10 and for dike at Elev. -38: this makes allowance for gradually increasing effectiveness of the dike, with depth, in transmitting hydraulic fill pressures to the ground beneath the bulkhead through its own structural resistance.

It is idealized in Fig. 22, that the bulkhead is fixed against rotation at Elev. -38. Confinement due to the dike and rigidity of the natural ground tend to provide this situation. The statically indeterminate free body thus obtained has been analyzed according to conventional theory of flexure, and curves of shear, moment, and deflection are shown. The primary purpose of this structural analysis is to provide a common ground for comparison of the various phenomena measured during the filling operation. Thus it can be seen whether the soil pressures are consistent with the deflections and tie rod tensions.

Observed profiles of the deflected bulkhead at Sta. 27 + 30 are compared with computed profiles in Fig. 23. Here the shapes of the curves, insofar as

they correspond, are in fair agreement, but computed values are too small.

Most significant comparison is Fig. 24, where the results of Fig. 22, have been slightly amplified to give theoretical plots against vertical soil pressure at Elev. -10. Reasonable agreement among computed and measured tie rod tensions is indicated. The large tensions at Sta. 30 + 30 in the early stages are attributed to the high inside water level during that period (Table 4); this influence is also felt in the observed deflections at Sta. 30 + 30. The hinge at bottom of deflection reference beam (Elev. -9.5) deflects about 20% less in theory than in fact, as shown by the upper curves of Fig. 24. Shapes of both theoretical curves compare well with the observed.

PRESSURE DISTRIBUTIONS AFTER FILLING

During the filling operation the distribution of lateral soil pressure on the back of the bulkhead was, as nearly as could be determined, essentially in direct proportion to the weight of overlying fill. Beginning on about June 1st, the lateral pressure distribution curve at Sta. 27 + 30 began to assume a quite nonproportional shape, as indicated in Fig. 20. Pressures between wale and top of dike dropped sharply, while those above this region increased. Simultaneously the tie rod tension at Sta. 27 + 30 increased considerably. Tie rod tension at Sta. 30 + 30 did not increase correspondingly (see Fig. 24); this may be due to effects of the high inside water level during the early stages.

Explanation of this effect is believed to lie primarily in the settlement of the fill, evidence of which can be seen in Fig. 6. Measurements of movements of piezometer pipes showed settlements adjacent to the bulkhead ranging up to 0.6 ft., for H-6; this amount apparently occurred below Elev. -9 where the horizontal pipe to H-6 left the bulkhead. The silty clay layer between Elevs. -38 and -32 (Table 1) is very compressible. Usual experience of the Long Beach Harbor Department with fills obtained from Harbor soils has indicated settlements of the order of 2 to 3% over periods of 6 to 18 months; this would amount to perhaps one foot in 6 months in this case at locations away from bulkhead and anchor. The wale and

tie rods are contained in the fill and provide partial vertical support at Elev. +4. There is relative absence of opportunity for lateral deflection at this level. Therefore, it is deduced that settlement of fill below the wale was responsible for this change in lateral pressure distribution. Deflection of bulkhead is discounted as a cause, as no change in deflection was observed after completion of filling (Tables 3 and 4). Further investigation of this very new result is indicated.

The effect of a surcharge close to the bulkhead on pressure distribution is seen in the August 17, free body diagram, Fig. 20. Further increase in pressure above wale and in tie rod tension indicate that this surcharge has been carried essentially by the wale-and-tie-rod system; increase in tie rod tension due to this action of the tie rods as "cables" is the cause of the increase in lateral pressure.

Changes in bulkhead loading over a large range of tide (7.3 ft.) are given for a typical case in Fig. 20 (August 5 and 6). Hydrostatic excess, which acts inward on August 5, and outward on August 6, is not shown in this figure but may be obtained from data in Table 5. Tie rod tension increases about 15 kips with falling tide, while changes in hydrostatic excess roughly balance those in soil pressure. Total changes are relatively small.

PRINCIPAL FINDINGS

1. During the filling operation the pressure of fill against bulkhead was approximately in proportion to the weight of overlying fill. Proportionality constant, or coefficient of lateral pressure, was found to be about 0.7.

2. The portion of dike inside the bulkhead was effective in reducing outward pressures. The portion of dike outside the bulkhead provided some passive resistance and resulted in an effective point of fixity slightly below the original ground level.

3. Observed deflections and tie rod tensions at the two test stations agreed reasonably closely. Predictions of deflections, based on soil pressure

measurements and an assumption of fixity at Elev. -38, agreed qualitatively but were about 20% low; tie rod tensions agreed well with predictions.

4. Lateral pressure distribution not in proportion to weight of overlying fill developed after completion of filling. Pressures above wale increased sharply while those below decreased. This is attributed mainly to settlement of fill and accompanying partial support of upper part of fill on wale and tie rods.

5. Surcharge piled close to bulkhead after completion of filling was carried directly by the tieback system.

6. Maximum deflections were approximately 3.6 in., outward at top of dike and 3.9 in., inward at top of bulkhead, assuming no deflection of wale. No reversal in direction of the deflections occurred at any time. Deflection changes ceased upon completion of filling.

7. Maximum tie rod tension was about 200 kips. This occurred near the end of the tests, under maximum influence of pressure redistribution.

8. Effect of tide fluctuation was observed on all instruments. Tie rod tension increased about 15 kips in one case due to a 7-foot drop of tide.

9. Carlson stressmeters and strainmeters adapted themselves well to this problem.

DESIGN IMPLICATIONS

Several of the indications of the tests have major significance for design of hydraulically filled anchored flexible bulkheads, with or without dikes.

Maximum bending moment and tie rod tension probably do not occur simultaneously. The former occurs between wale and ground during filling and results from the high lateral pressure coefficient which is approximately uniform during the filling operation. The latter seems to occur after settlement of fill as a result of supporting of a portion of the fill weight on the tie back system (in the manner of relieving platform).

A surcharge should be studied principally for its effect on tie rod tension.

An inner dike is effective in transmitting part of the lateral fill pressure

into the ground but probably is not fully effective over its entire height (references 3, 5, and 6) unless constructed to the height of the wale.

"Arching in the vertical direction" due to bulkhead deflection (reference 8) is discounted as a design consideration. The lateral pressure redistribution at Pier C was due to another cause.

References Cited

1. Carlson, R. W. "Five Years Improvement of the Elastic Wire Strainmeter," Engr. News-Rec. Vol. 114, No. 2, May 16, 1935, pp. 696-697.

2. Carlson, Roy W. "Development and Analysis of a Device for Measuring Compressive Stress in Concrete." Thesis for Doctor of Science Degree, M. I. T., 1939.

3. Epstein, Harris. "Reduction of Lateral Cohesive Soil Pressure on Quaywalls by use of Sand Dikes." Proc. 2nd Int. Conf. Soil Mech., Vol. III, pp. 291-296. 1948.

4. Duke, C. Martin. "Pier C Bulkhead Tests." Report to Board of Harbor Commissioners, City of Long Beach, California, February, 1950, 34 pages, unpublished.

5. Tschebotarioff, Gregory P. and Phillip P. Brown. "Lateral Earth Pressure, a Problem of Deformation or of Rupture." Proc. 2nd Int. Conf. Soil Mech., Vol. II, pp. 81-86. 1948.

6. Tschebotarioff, Gregory P. "Large Scale Earth Pressure Tests with Model Flexible Bulkheads." Edwards Bros. Inc., Ann Arbor, Mich., 1949, 112 pp. 105 figs., $1.

7. War Department, Corps of Engineers. "Report on Instruments used on Test Tract at Hamilton Field." Report of Corps of Engineers, South Pacific Division, San Francisco District. December, 1946. $1.

8. "Normer for Vandbygnings-Konstruktioner." Udgivit of Dansk Ingeneoforeing. Kobenhaven. 1937. (Danish Engineering Society's, 1937 Bulkhead Regulations.)

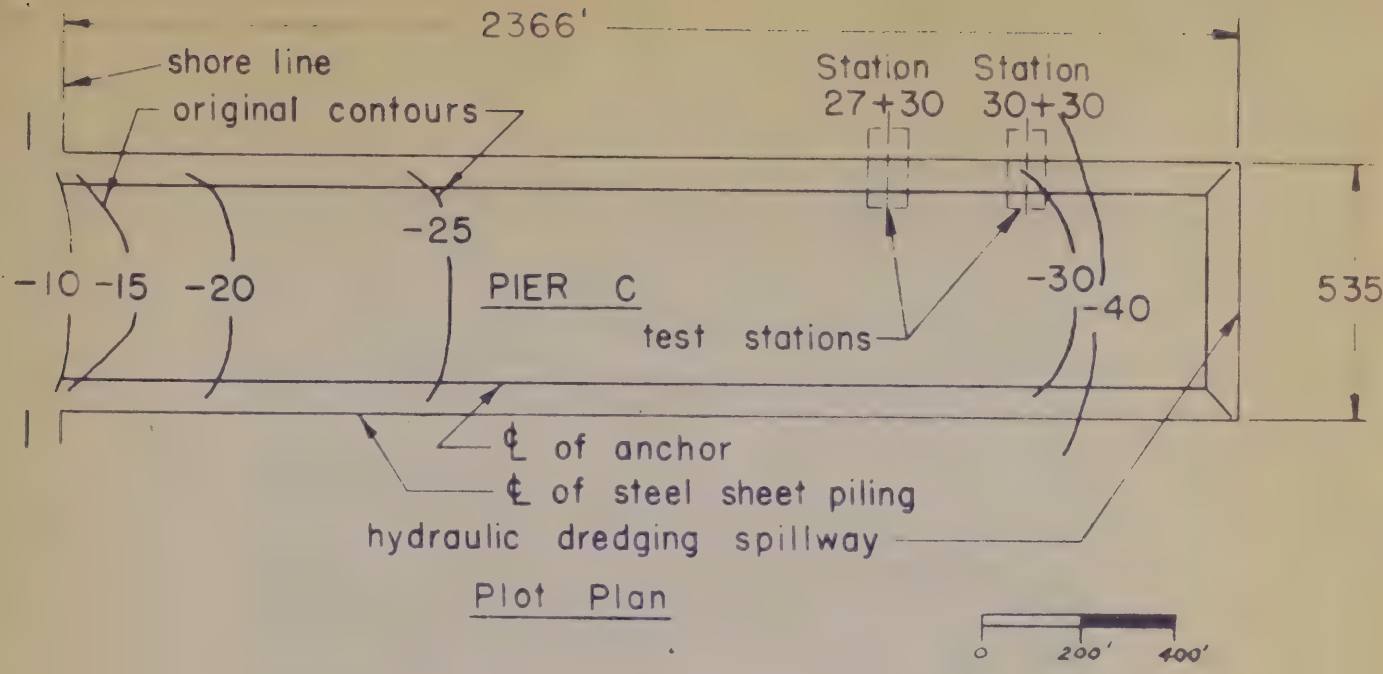

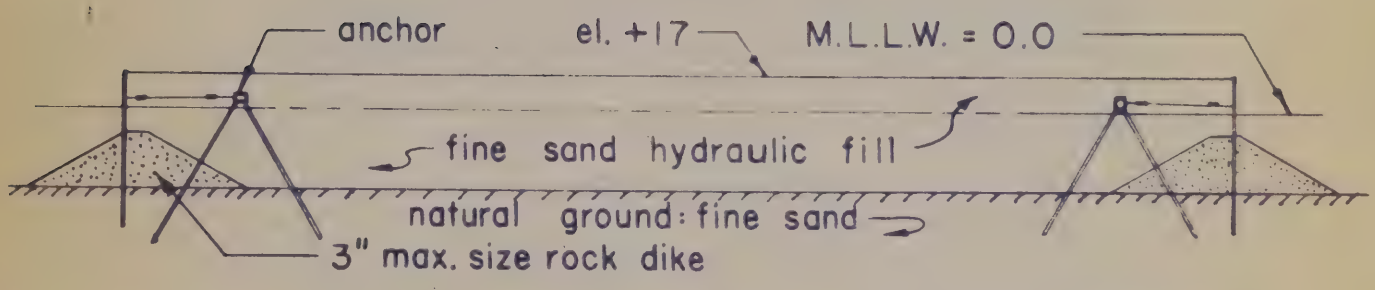

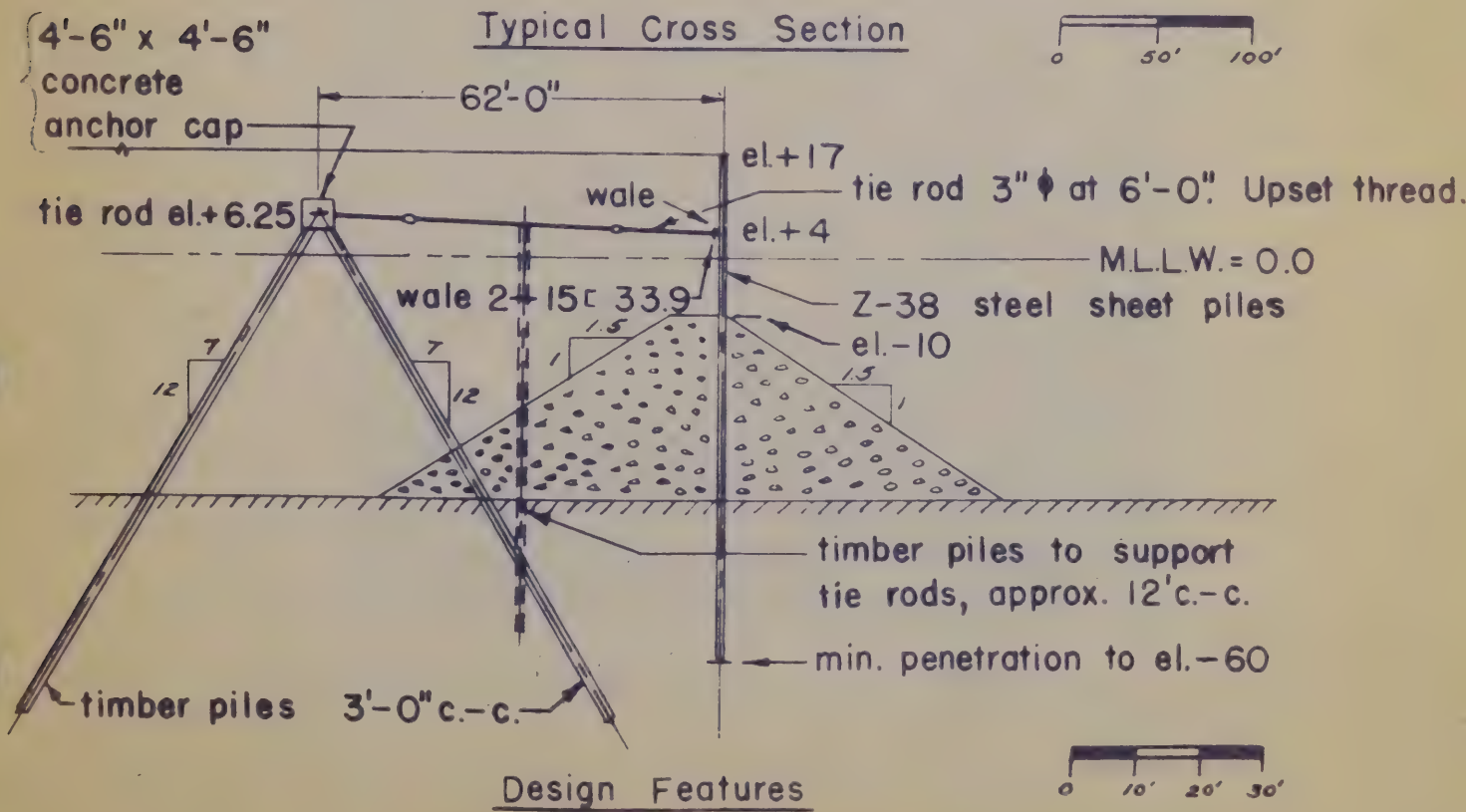

Fig 2. PIER C BULKHEAD - LONG BEACH HARBOR

Fig. 3. Interior View of Pier C, Looking South.

Feb. 17, 1949

Fig. 4. Placing Dike at Sta. 26 + 00 at East Bulkhead.

Feb. 17, 1949

Figs. 3 and 4.

Fig. 5. Fill at Sta. 27 + 30.

May 3, 1949

Fig. 6. Crack in Fill Over Anchor at Sta. 30 + 30.

June 3, 1949

Figs. 5 and 6.

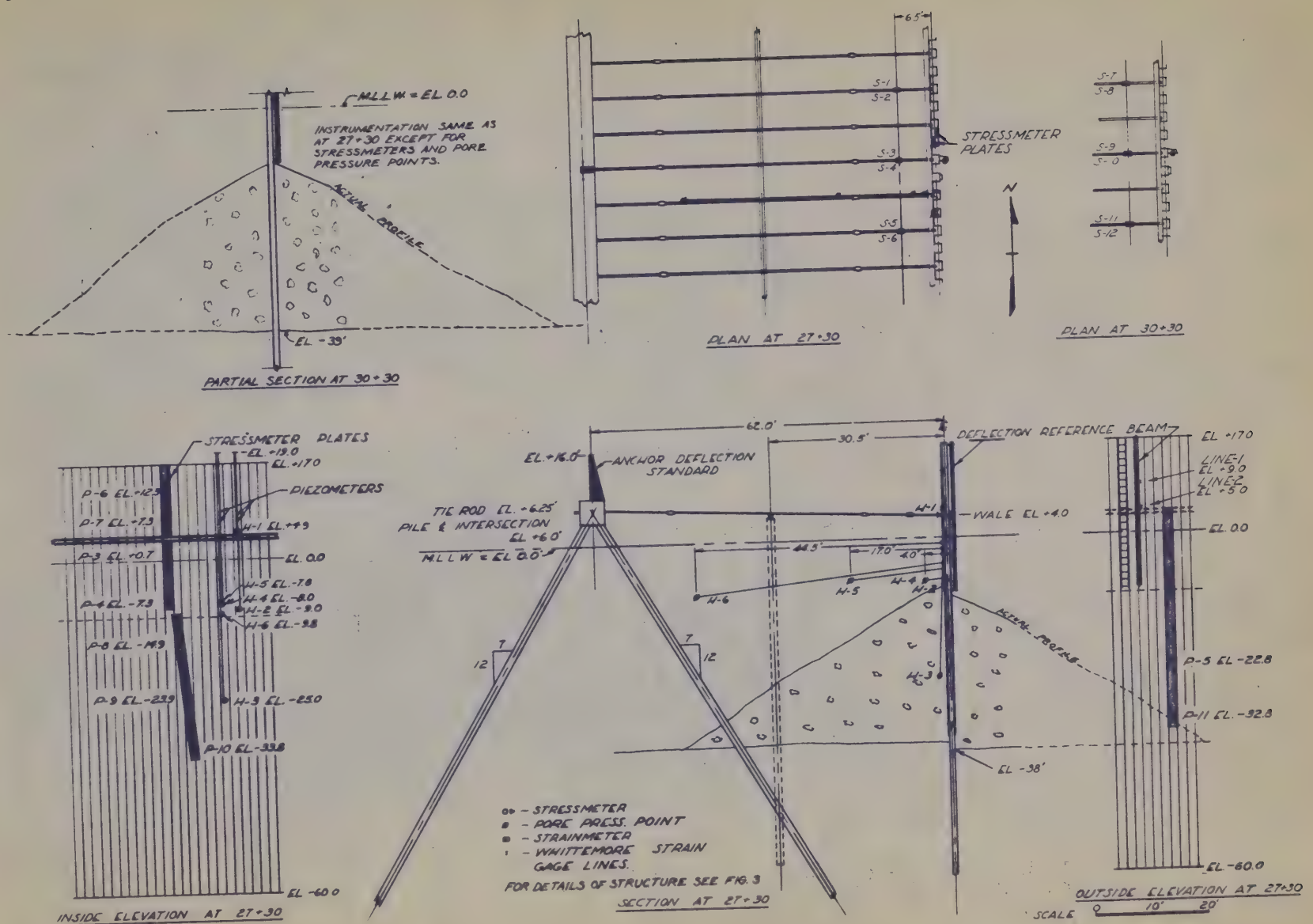

FIG. 7. INSTRUMENTATION LAYOUT

Fig. 8. Inside View of Finished Instrumentation, Sta. 27 + 30.

Mar. 17, 1949

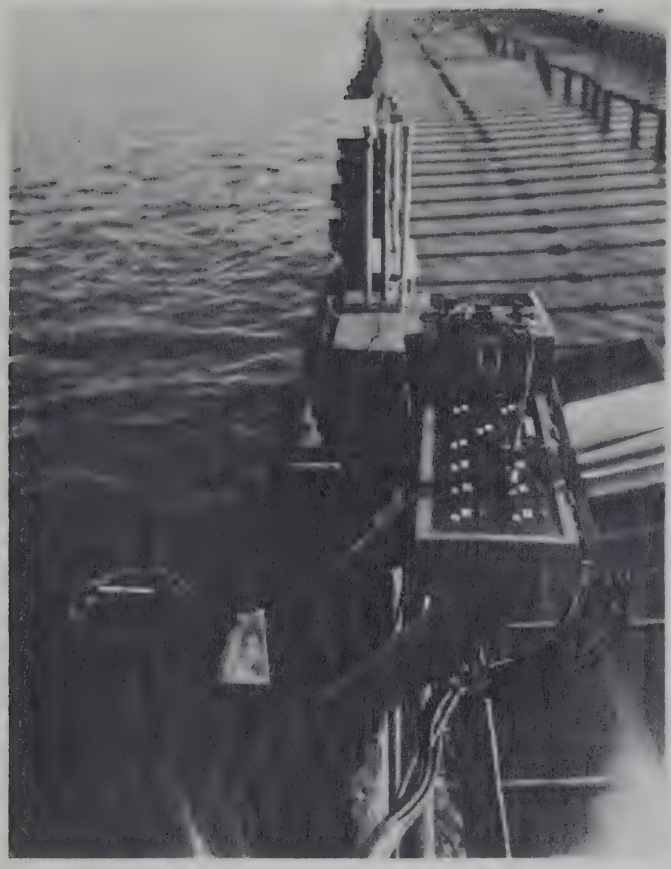

Fig. 9. Top View at Sta. 27 + 30.

Mar. 17, 1949

Fig. 10. Lower Inboard Stressmeter Plate.

Feb. 15, 1949

Figs. 9 and 10.

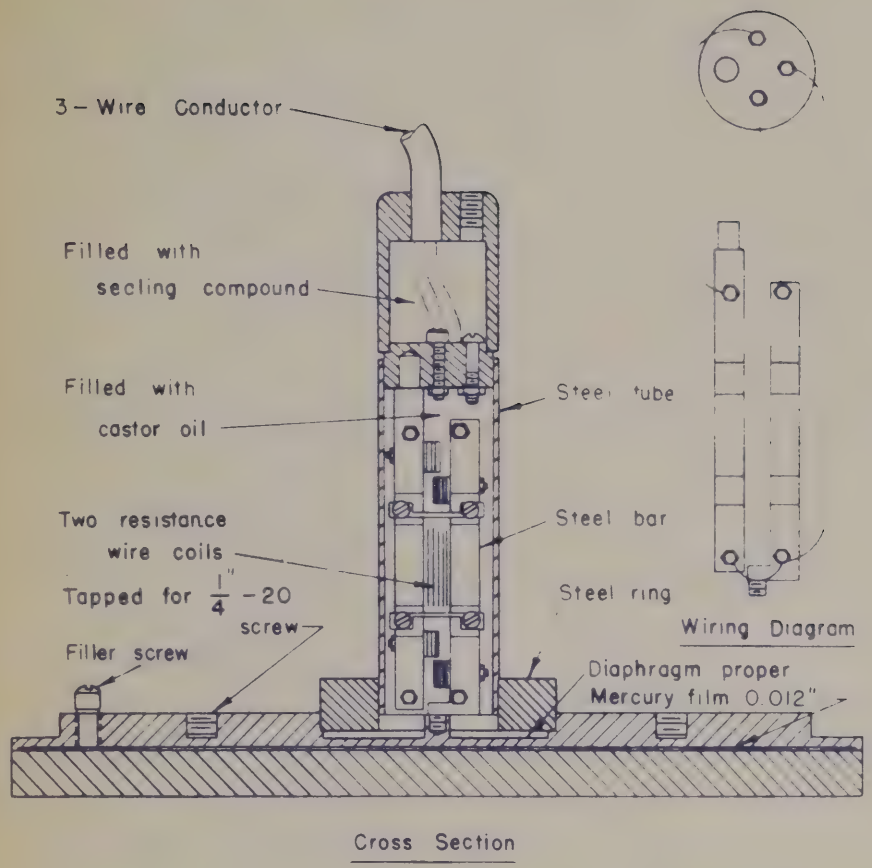

Fig. 11 CARLSON STRESSMETER FOR SOIL PRESSURE MEASUREMENT

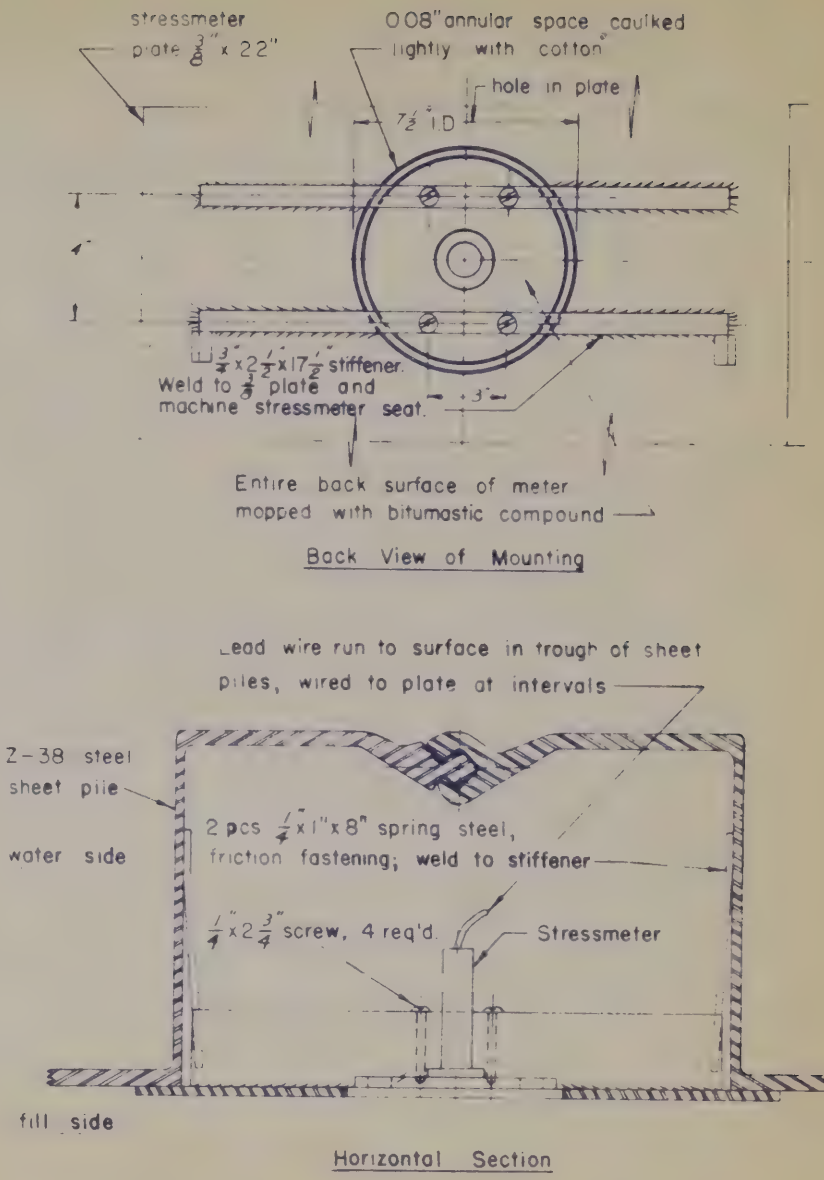
stressmeter plate 3/8" x 22"
0.08" annular space caulked lightly with cotton
hole in plate
7 1/2" I.D.
3/4" x 2 1/2" x 17 1/2" stiffener. Weld to 3/8" plate and machine stressmeter seat.
3"
Entire back surface of meter mopped with bitumastic compound
Back View of Mounting
Lead wire run to surface in trough of sheet piles, wired to plate at intervals
Z-38 steel sheet pile
water side
2 pcs 1/4" x 1" x 8" spring steel, friction fastening; weld to stiffener
1/4" x 2 3/4" screw, 4 req'd.
Stressmeter
fill side
Horizontal Section

Fig. 12. STRESSMETER INSTALLATION DETAIL

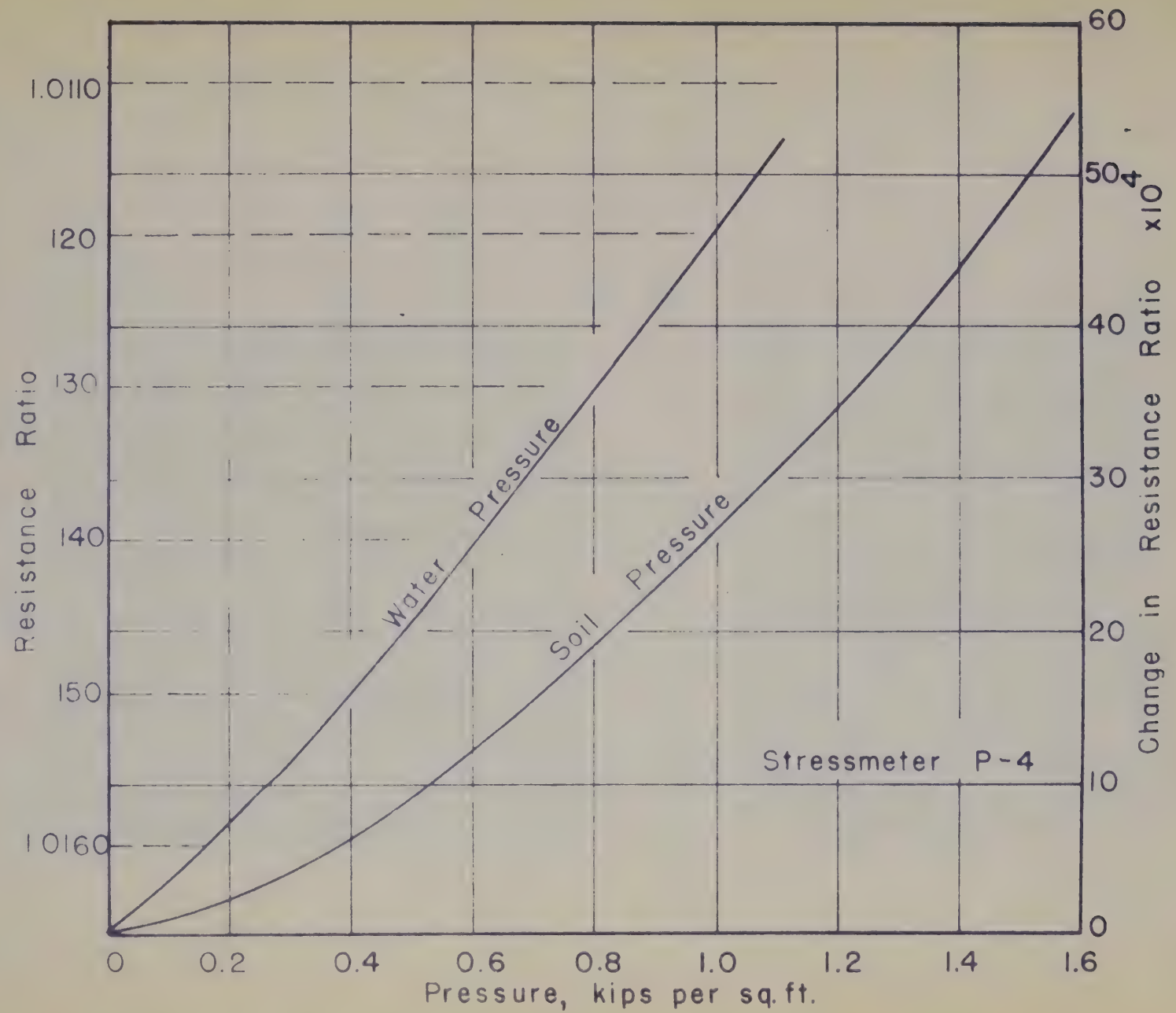

Fig. 13. TYPICAL STRESSMETER CALIBRATION CURVES

Fig. 14. Top of Lower Inboard Stressmeter Plate.

Feb. 16, 1949

Fig. 15. Detail of Piezometer H-1. Also shows Typical Dike Material on Wale.

Mar. 17, 1949

Figs. 14 and 15.

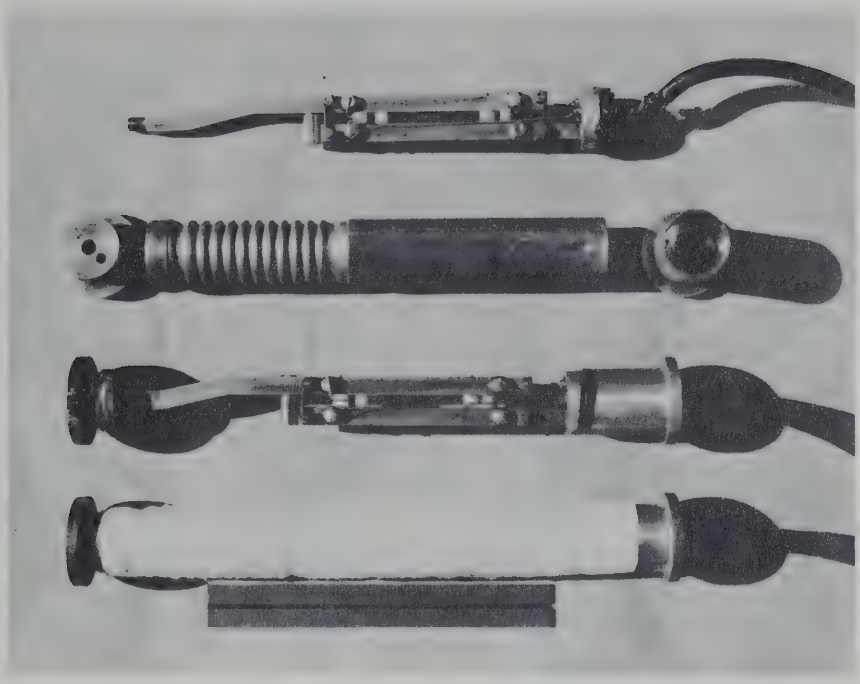

Fig. 16. Carlson Strainmeter.

(As Used in Concrete)

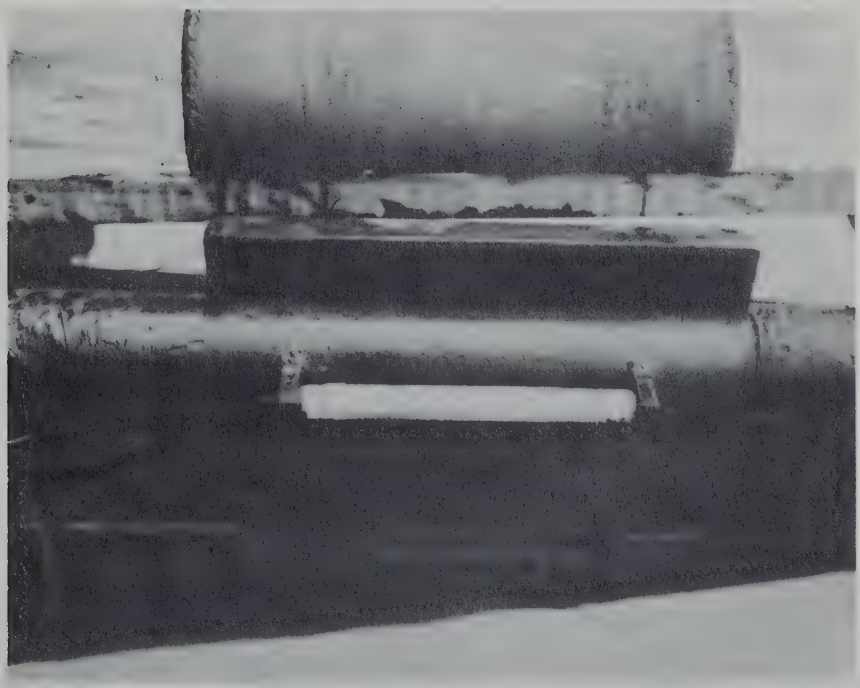

Fig. 17. Strainmeter Installation Detail.

Apr. 2, 1949

Figs. 16 and 17.

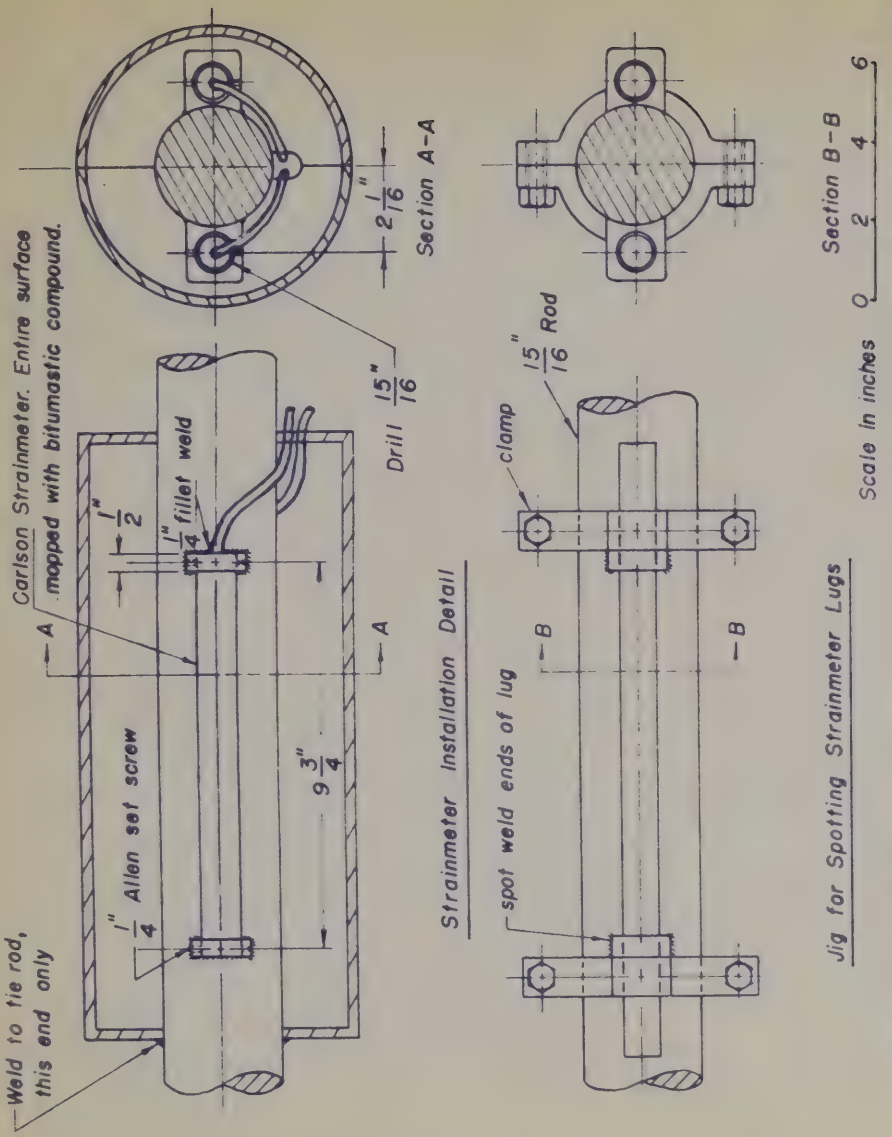

Fig. 18. STRAINMETER INSTALLATION

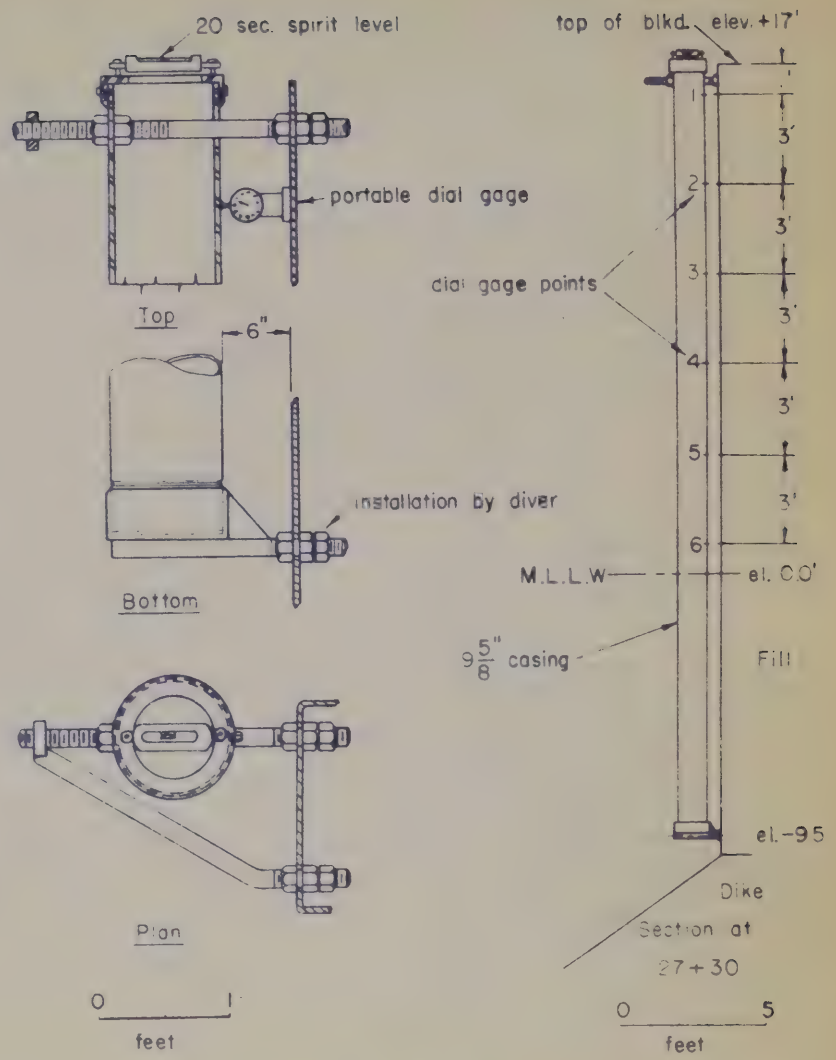

Fig. 9 REFERENCE BEAM DETAIL

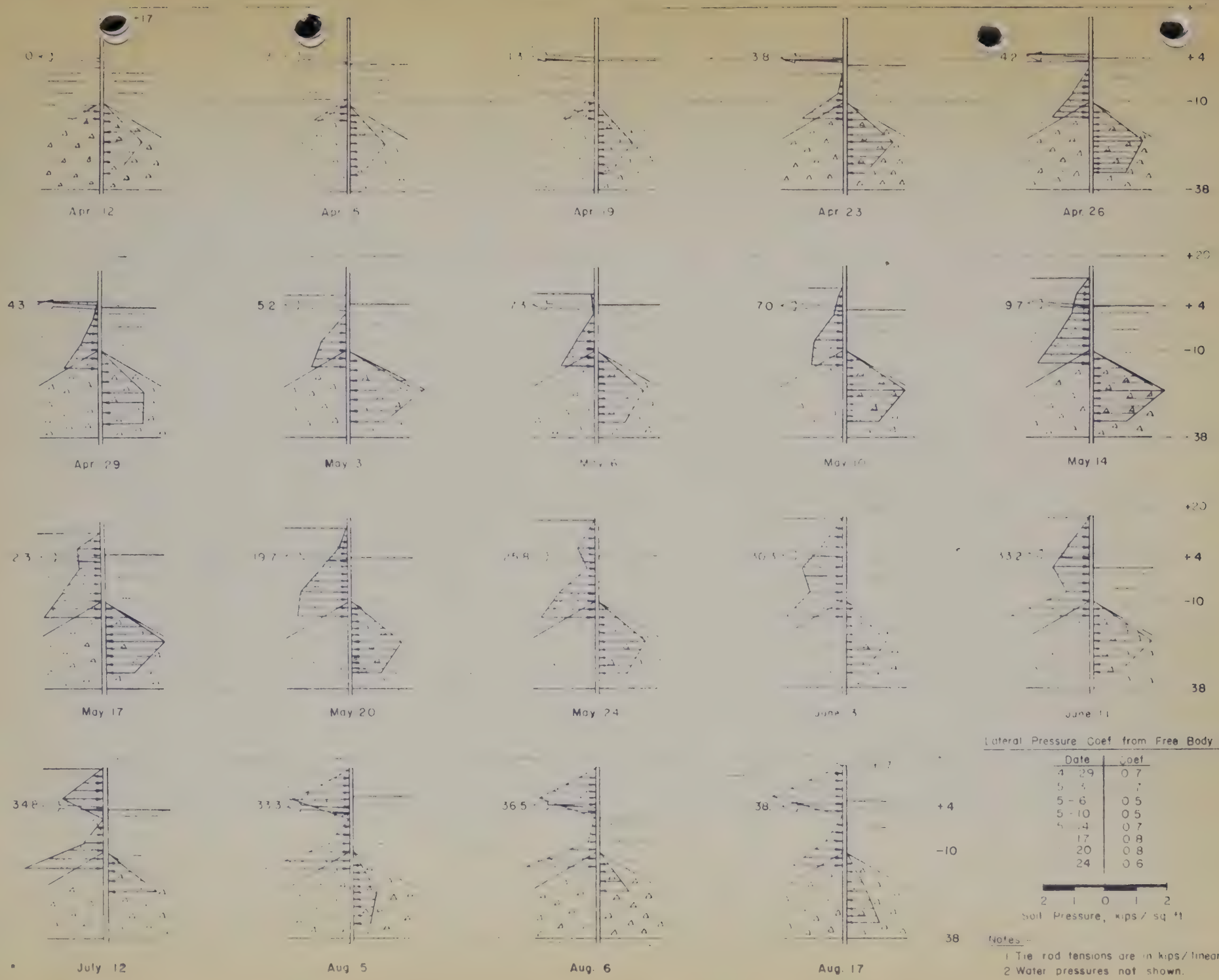

Lateral Pressure Coef from Free Body Diagrams

Date	Coef
4 29	0 7
5 - 6	0 5
5 - 10	0 5
5 - 14	0 7
17	0 8
20	0 8
24	0 6

2 1 0 1 2
Soil Pressure, kips / sq ft

Notes -
1 Tie rod tensions are in kips / linear foot
2 Water pressures not shown.

Fig 20. BULKHEAD FREE-BODY DIAGRAMS. STATION 27+30

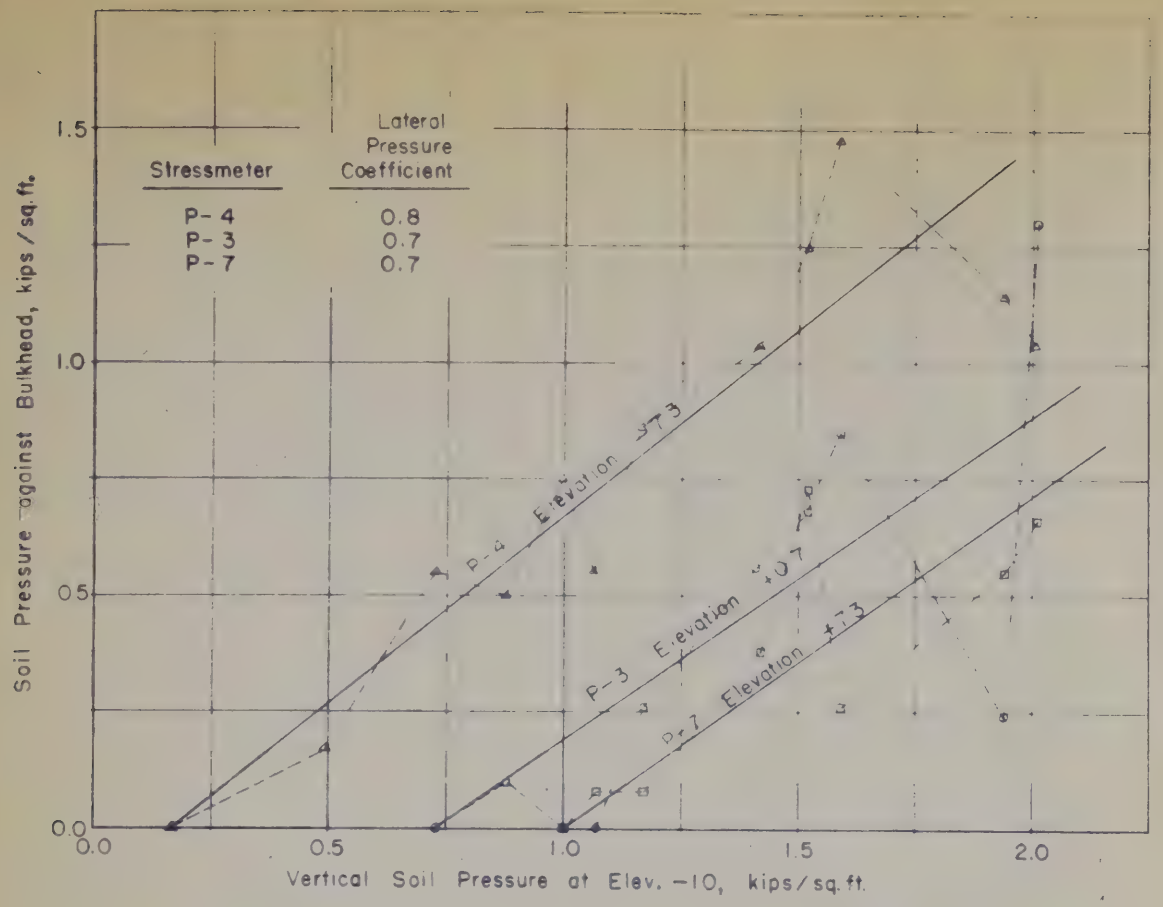

Fig. 21. Lateral Pressure Coefficients, During Filling, from Individual Stressmeters.

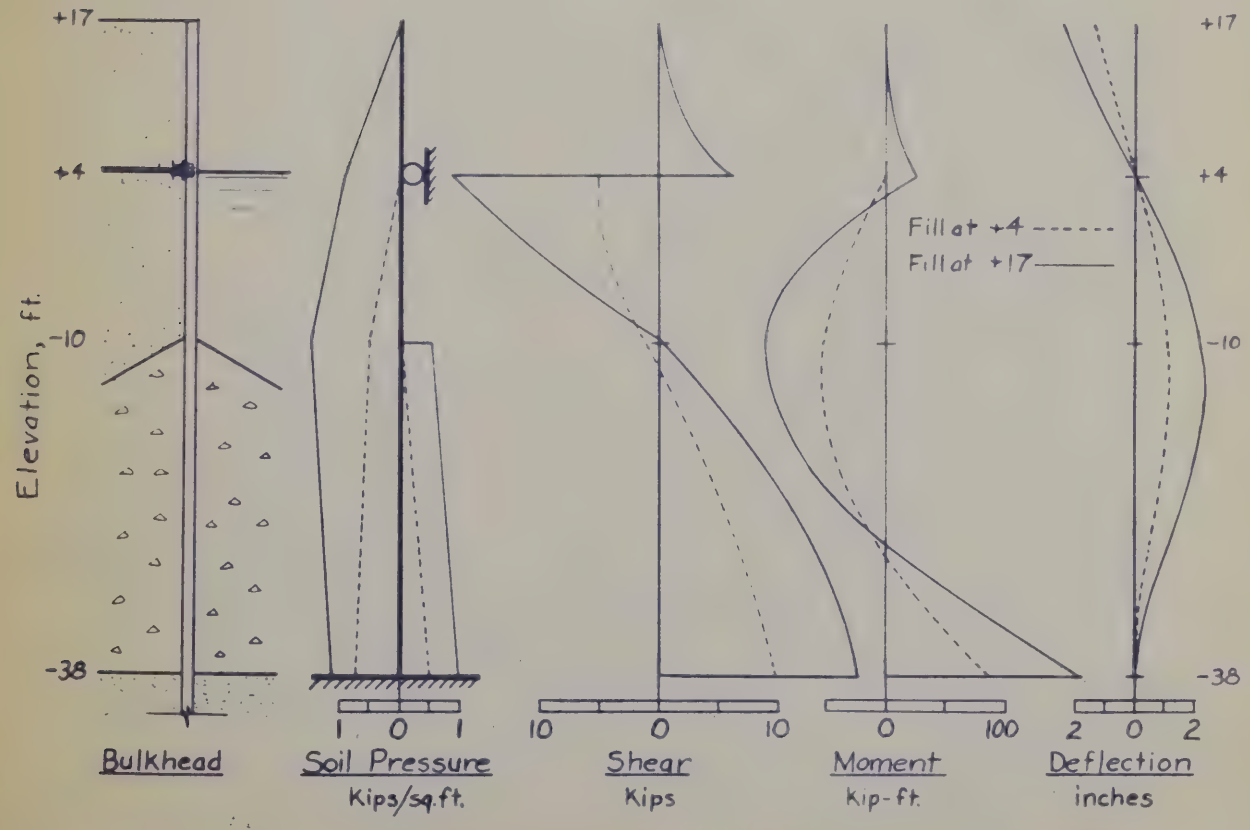

FIG. 22. BULKHEAD STRUCTURAL ANALYSIS

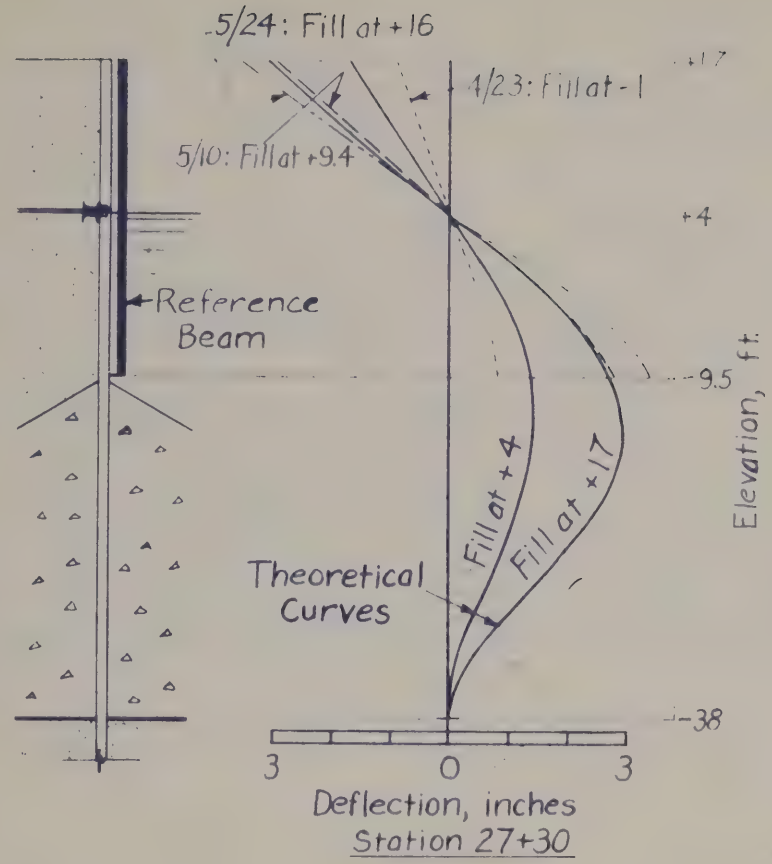

FIG. 23. DEFLECTION PROFILES

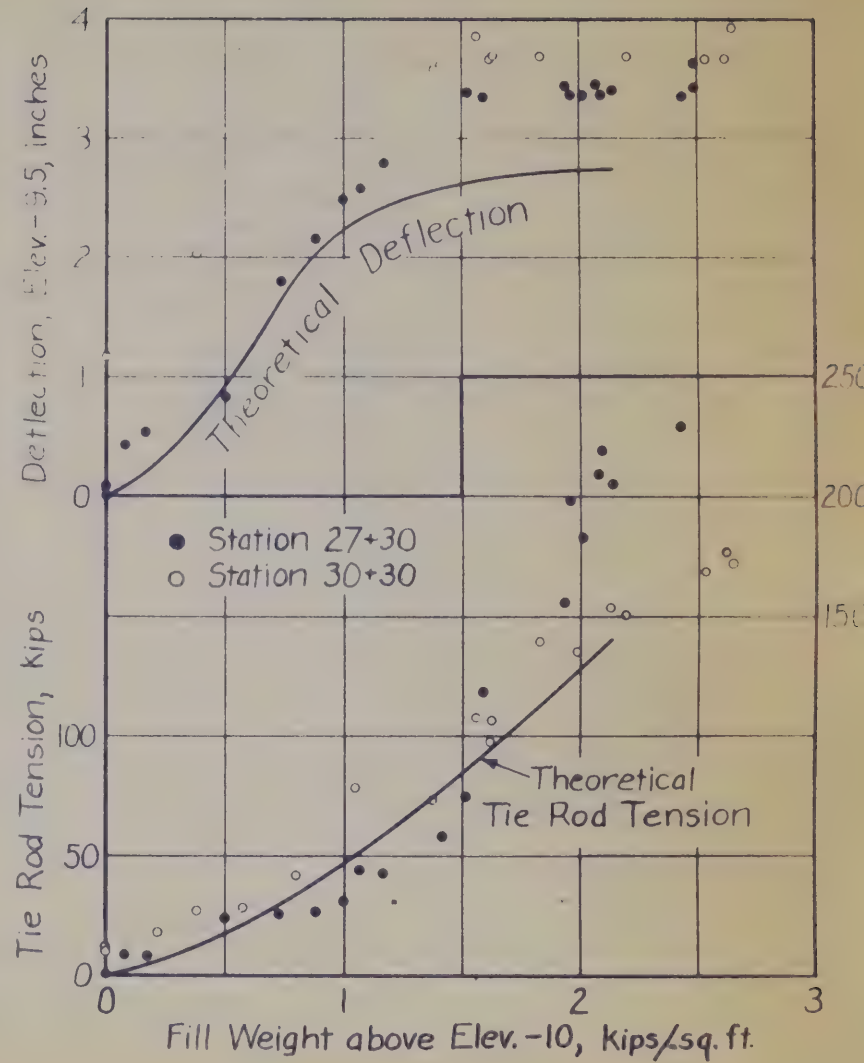

FIG. 24. THEORETICAL VERSUS OBSERVED PERFORMANCE

How Can Standards of Achievement by Students in Lower Division Work Be Made to Mean the Same to Junior and Senior Colleges?

HAROLD P. RODES

THERE seems to be little doubt in the educator's mind that the junior college is a firmly established institution. It therefore behooves those who are connected with higher education of the four-year college or university variety to take the initiative in achieving a mutually satisfactory understanding and working relationship with the junior colleges.

The subject of this article—"How can standards of achievement by students in lower division work be made to mean the same to junior and senior colleges?"—represents one of the major sources of misunderstanding and disagreement. Standards of achievement should be determined by educational objectives. The senior colleges, particularly in the areas of agriculture, business administration, and engineering, are concerned primarily with the preparation of students for entrance into their chosen profession. The junior college, on the other hand, if it is to fulfill its responsibilities as a community or regional institution, must be concerned with a wide variety of curricular and co-curricular services intended to meet the needs of many different students, most of whom will not continue with formal full time education beyond the lower-division level.

The statement of this basic difference in educational objectives is not intended to be an apology for the junior college. On the contrary, any junior college which includes among its educational objectives the preparation of a certain portion of its student body for upper division work, is obligated to require a sufficiently high standard of achievement to insure reasonable success on the part of its graduates.

The attainment of "reasonable success" of junior college transfer students in upper division work is dependent upon a thorough understanding on the part of junior college instructors of what is *actually* prerequisite to upper division courses in a given subject area, whether it be agriculture, business administration or engineering. The expression "actually prerequisite" is used to imply that all of the subject matter required in the lower division of a four-year college may not be actually prerequisite for upper division work. No one will question the right of a four-year college to specify the content of such subject matter for its own

lower division students. However, the right of the four-year college to specify similar content in nonprerequisite courses for junior college transfer students can be seriously questioned.

Experience has indicated, apparently to the satisfaction of junior college as well as senior college instructors, that at least a minimum lower division background in mathematics, physics, and chemistry is essential to success in the upper division engineering curriculum. This background can be specified in a variety of ways ranging from a general listing of topics to be covered, to instances where a given number of pages in a particular textbook have been listed as a prerequisite.

Over the years in California the former arrangement has proven more satisfactory than the latter. Practically all California University instructors, both upper division and lower division, are quite willing to provide their colleagues in the junior college with general outlines of topics which they cover in engineering and related courses, leaving to the discretion of the junior college instructor the manner in which these minimum essentials shall be covered.

As an illustration, there are several different lower division mathematics programs offered by the California junior colleges for preengineering students. The most common pattern is a series of four three-unit mathematics courses covering analytical geometry through integral calculus in the freshman and sophomore years. However, many other patterns may be found. One junior college which became concerned about the difficulty its graduates were encountering in upper division engineering mathematics, recently inaugurated a series of four four-unit mathematics courses which review comprehensively high school mathematics through trigonometry and then include in the last semester a thorough introduction to differential equations. The encouragement of such experimentation frequently leads to an improvement in student achievement whether at the junior or senior college level.

A second factor essential to the attainment of "reasonable success" by junior college students who transfer to a senior college is a continuous follow-up study. In other words, the most effective evaluation of standards of achievement at the lower division level is in terms of performance in upper division work. Each year the Office of Relations with Schools of the University of California makes a study of the grade-point averages attained at the University by junior colleges transfer students. Each junior college in the state is informed of the grades achieved by its students who have entered the University. In almost every case the only pressure needed to insure the maintenance of adequate standards of achievement in junior college transfer courses is

an examination of the facts. It is therefore possible for the University to place the major responsibility for the maintenance of adequate scholastic standards squarely upon the shoulders of the junior college. Recent studies have indicated that junior college transfer students who would have been eligible for admission to the University of California as freshmen, have done just as well in their upper division work as students who completed the freshman and sophomore years at the University. For these reasons, the University's Office of Admissions confidently follows the practice of accepting without question any course which a California junior college designates as a transfer course.

A third factor, pertinent to "standards of achievement" is the use of examinations for admission to upper division curricula. For several years the College of Engineering of the University of California has required a series of achievement examinations for admission to the junior year. These examinations have been required of lower division students in the University as well as of junior college transfer students. The examinations measure lower division achievement in the five subject areas of English, mathematics, engineering graphics, physics, and chemistry, and correlate rather highly with success in the upper division engineering curriculum. The tests are sufficiently general so that instead of standardizing the lower division engineering curriculum they have actually promoted greater flexibility, due to the fact that students who have completed a lower division engineering curriculum of a somewhat unconventional nature have an opportunity to indicate on the tests their readiness for upper division engineering courses.

It is interesting to note that the School of Business Administration at UCLA is currently developing a similar series of tests, but these tests will not be used as a criterion for admission until they have been validated sufficiently with the upper division curriculum.

No discussion of "standards of achievement" can proceed very far without the interjection of grades and grading systems. Senior college instructors and administrators are frequently disturbed by what they consider to be an inferior basis of assigning grades to students in the junior colleges. In dealing with this problem it is once again necessary to keep in mind the basic differences between the educational objectives and student characteristics of the junior college as contrasted with the four-year college and university. Since much of the grading done in institutions of higher learning is on a somewhat relative basis, it is not expected that the average junior college transfer student will receive as high grades in senior college as he did in junior college. Admittedly this differential for a given junior college should not be

too great. Studies in California, for example, indicate that student grades attained in junior college are, on the average, about one-half of a letter grade higher than subsequent grades received at the University. The important element, of course, is not the grades which a transfer student received in junior college, but rather the grades which he obtains in his upper division work. So long as junior college transfer students maintain grades in their upper division courses which compare favorably with grades obtained in the same courses by students who completed their lower division work at a four-year college, there need be no concern about any minor differences in grading standards between the junior and senior colleges.

INFLUENCE OF THE ELASTIC CONSTANTS ON THE PARTITION OF LOAD BETWEEN RIVETS

W. D. MITCHELL and D. ROSENTHAL, University of California, Los Angeles, California.

SUMMARY

Previous experiments have shown that the load is not evenly distributed between the rivets in a lap joint. The first and the last rivets in a line carry by far the greatest share of the load. The authors have attempted to improve this situation by making the rivets of a material which was less rigid than the plates. However, the experimental results did not show the expected improvement. The reason for this shortcoming was found in the limitation of deformation imposed on the rivets by the more rigid plates.

PURPOSE OF RESEARCH

The partition of load between rivets in a lap joint has been the subject of many studies both theoretical and experimental.(1)* The main conclusion of these studies is that the load in the elastic range is not equally divided between the rivets in a line. The end rivets carry by far the greatest share of the load, which then decreases rapidly as one approaches the center of the joint. Similar conclusions apply to the distribution of load along the side fillets of a fusion welded joint, or along a line of welded spots made by resistance welding.(2,3) In most experiments performed so far the joining elements, i.e. the rivet and the weld, were made of the same material as the members joined by those elements, and in those experiments where different materials were used, the rivet was made of the more rigid material.(4) But on the strength of theoretical studies(5) one would expect the load to be more evenly distributed among the rivets, if the latter were made of a less rigid material than the joined members. In order to check the validity of this assumption a series of tests were performed the results of which are briefly reported in this paper.

*Superiors in parentheses refer to bibliography.

EXPERIMENTAL PROCEDURES

Specimens. The type of specimen used in this investigation is represented in Fig. 1. It consisted of two cover plates and one middle plate made of mild steel, S.A.E., 1020.

In order to eliminate the effect of friction caused by riveting, the plates were joined by bolts which were machined to a close tolerance with respect to the diameter of the holes. The substitution of bolts for rivets was justified by the results of a previous investigation(6) which showed conclusively that at the working load the rivets behaved as ordinary pins. Also, by avoiding the effect of friction it was possible to obtain a load-displacement diagram which was essentially free from the hysteresis loop (found in previous work) and which was linear in the range of loads employed, see Figs. 4, 5, and 6. The bolts were made of the following materials: mild steel S.A.E. 1020, annealed aluminum alloy ST 24, brass 60/40, and lucite. Table 1 summarizes the elastic characteristics of these four materials.

Method of measurement. The load carried by an individual rivet in a line can be determined indirectly either from the stress gradient in the cover plate or from the value of the relative displacement of the joined elements in the neighborhood of the rivet.(7) In both cases the computation is based on certain assumptions and approximations, the validity of which can be verified to some extent by modifying the experimental conditions, for example, the number of rivets. A similar procedure has been followed in the present investigation. However, the experimental labor was greatly reduced by making one single measurement of displacement, namely at the end of the cover plates as shown in Figs. 1 and 2, and by varying the number of bolts in the joint. The partition of load between the bolts in any type of joint can then be computed as shown in Appendix, by assuming that the deformation of each element of the

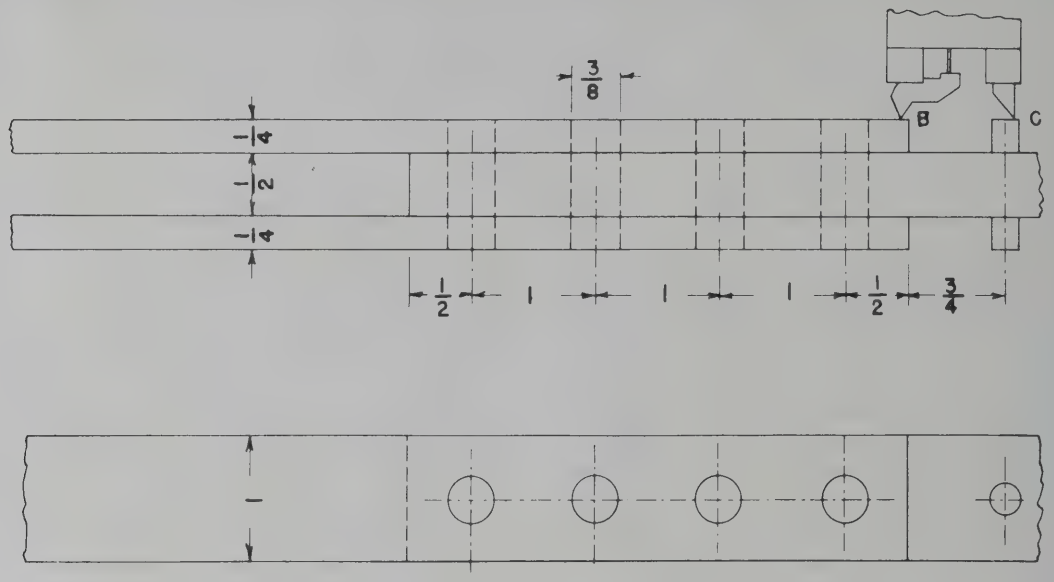

Fig. 1. Joint Test Section - Material: 1020 Steel.

TABLE I - ELASTIC CHARACTERISTICS OF THE MATERIALS

Material	Youngs Modulus E, psi	Poisson Ratio μ
Steel: SAE 1020	30×10^6	0.28
Aluminum Alloy: 24 ST	10.3×10^6	0.33
Brass: 60 / 40	12×10^6	0.30
Lucite	0.44×10^6	0.34

joint bears a constant relation to the load acting upon it, irrespective of the number and nature of bolts. This assumption is similar in nature to that made in a previous work,(5) and its validity can be checked experimentally as will appear in a later discussion. In this connection the recourse to an electric circuit analogy, developed in the Appendix, has proved particularly helpful.

The specimens were loaded in tension according to the schedule outlined in Table 2, and the range and value of load were adjusted to give about the same value of displacement for all types of joint.

The extensometer. The displacement between the cover plates and the middle plate was measured by means of a special extensometer* with one leg resting on the cover plate and the other on a small stud brazed to the middle plate, Figs. 1 and 2. The basic principle of operation is shown in Fig. 3. By displacing point B with respect to C the knife "a" is made to rotate around A, which imparts a vertical movement to the pin b. The latter forms a part of a non bonded resistance wire gage**, which translates the motion of the pin into a change of electric resistance. The gage is a self contained Wheatstone bridge with all four sides active. The output of the bridge is measured by means of a galvanometer using an input voltage of about 6 volts. The readings of the galvanometer are calibrated in terms of the displacement of the knife "a". Fig. 2 shows the strain-indicator unit*** containing the galvanometer, dry cells and various electric elements for the adjustment of input voltage, sensitivity, and zero.

The extensometer may also be operated by means of an SR-4 Strain indicator. In this case only two sides of the bridge are active.

*Built in the Mechanic Shop of the Department.

**Statham gage.

***We are indebted to M. G. Zizicas, graduate student in Engineering, for the construction of this indicator.

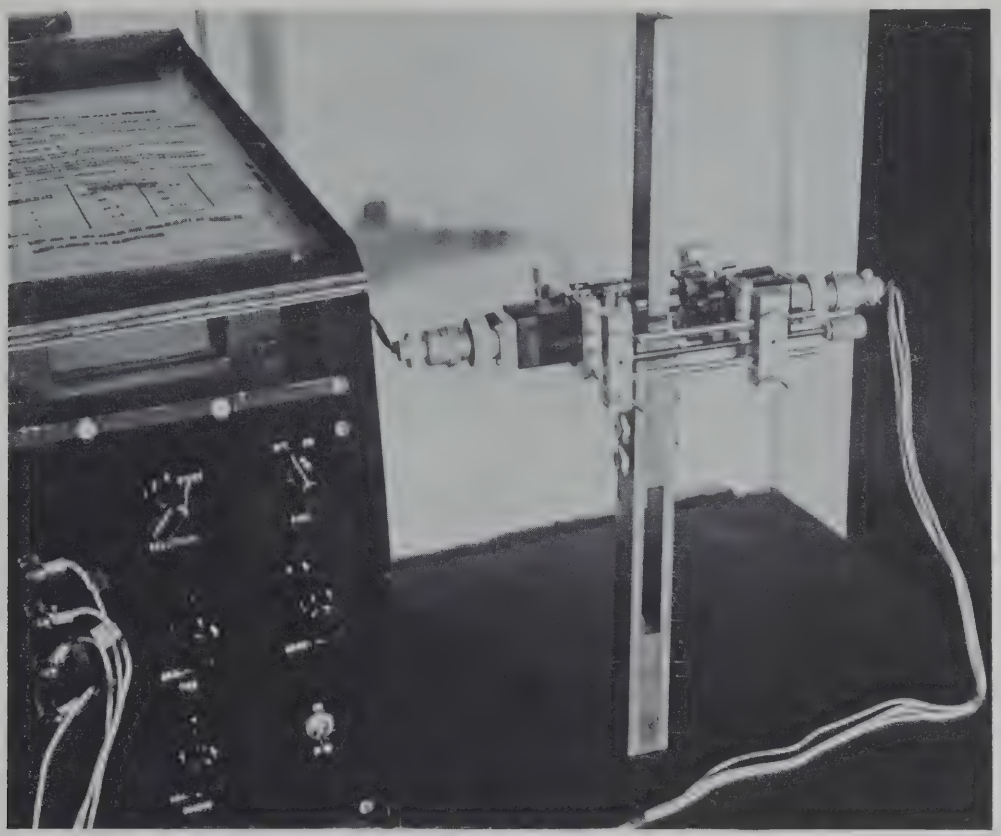

Fig. 2. Test apparatus.

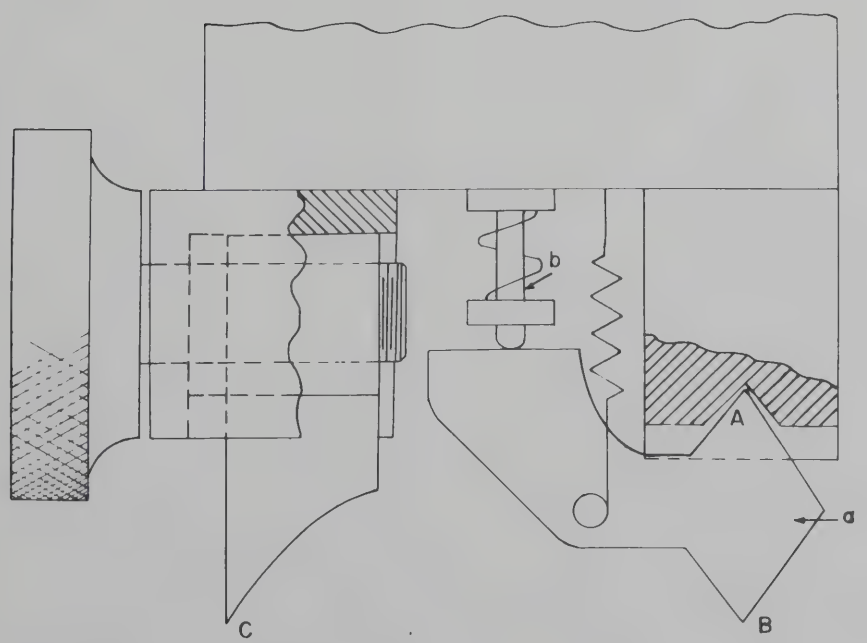

Fig. 3. Extensometer Details - Scale 4:1.

TABLE II - JOINT MODULI, J FOR VARIOUS JOINTS

Bolt Material	No. of Bolts	J, lbs. Experimental	Microinch Computed
STEEL: SAE 1020	1	1.25	--
	2	2.33	--
	3	3.00	--
	4	3.27	3.27
BRASS: 60 / 40	1	1.094	--
	2	2.06	2.055
	3	2.63	2.67
	4	2.97	3.02
ALUMINUM ALLOY: 24 ST	1	1.04	--
	2	2.00	1.98
	3	2.40	2.58
	4	2.65	2.92
LUCITE	1	0.106	--
	2	0.207	0.212
	3	0.312	0.310
	4	0.397	0.402

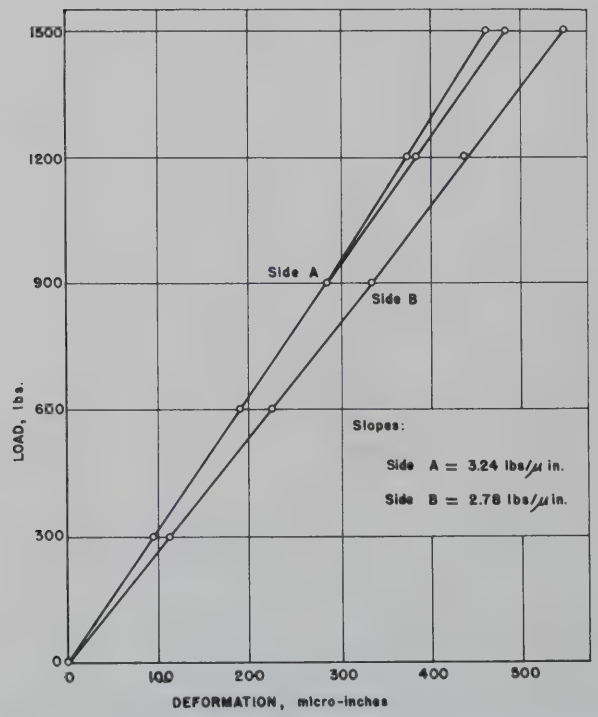

Fig. 4. Load vs. Deformation for 3 steel rivets.

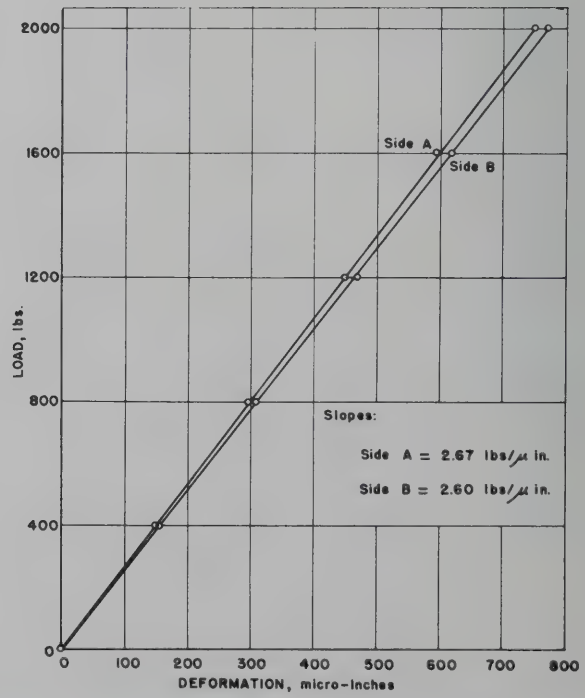

Fig. 5. Load vs. Deformation for 3 brass rivets.

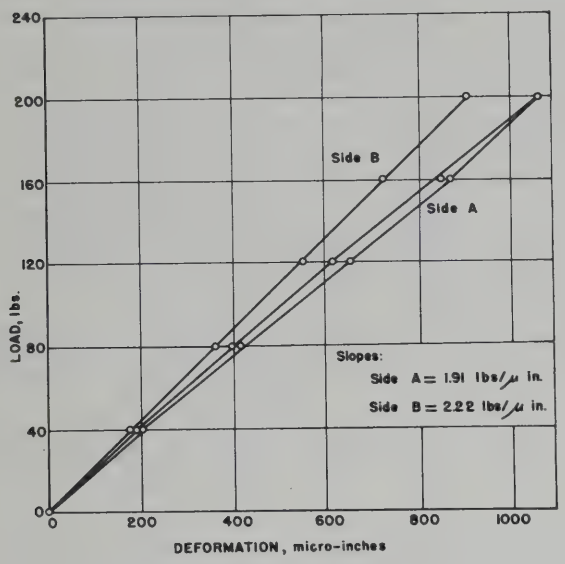

Fig. 6. Load vs. Deformation for 2 lucite rivets.

RESULTS

In order to correct any error due to bending, the displacement was measured on both sides of the joint by two extensometers mounted simultaneously as shown in Fig. 2. The two sets of readings were plotted separately as a function of applied load. Figs. 4, 5, and 6 are typical of the kind of plots obtained for all types of joints, except those made with three and four Aluminum Bolts. For these a slightly larger deviation from the straight line was noted on unloading, Figs. 7 and 8. The average deviation from the straight line was about 10% for the latter, while it was only about 3% for other types of joints. This circumstance may account in part for the discrepancies which appear in Table 2 and which will be discussed below.

Joint Modulus. From the results plotted in diagrams, Figs. 4, 5, etc., a value of load can be determined which will produce a displacement of one microinch (10^{-6} inch) between the points B and C, Fig. 1. When values from both sides of the joint are averaged to correct for the effect of bending they give a measure of what may be termed the rigidity of the joint. For this reason the above average has been called the joint modulus, J. In Fig. 9 the values of J have been plotted as a function of the number of bolts in the joint. It is seen that the joint modulus increases less rapidly than the

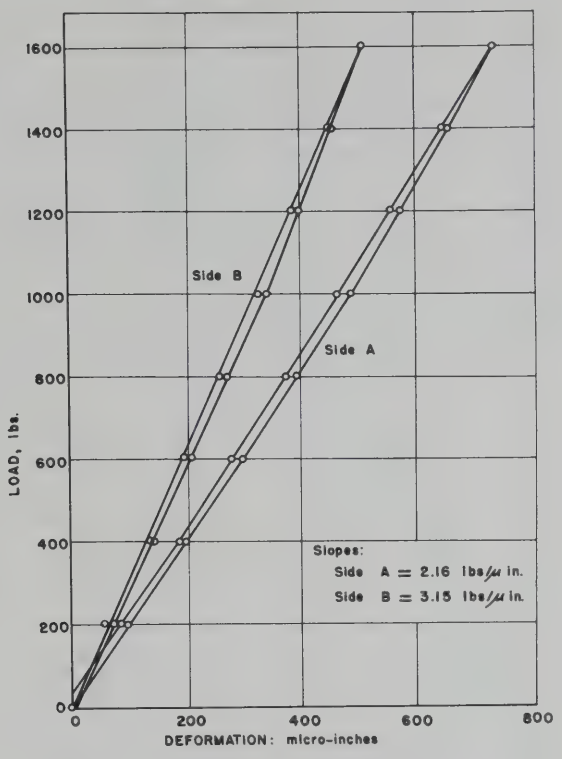

Fig. 7. Load vs. Deformation for 4 aluminum rivets.

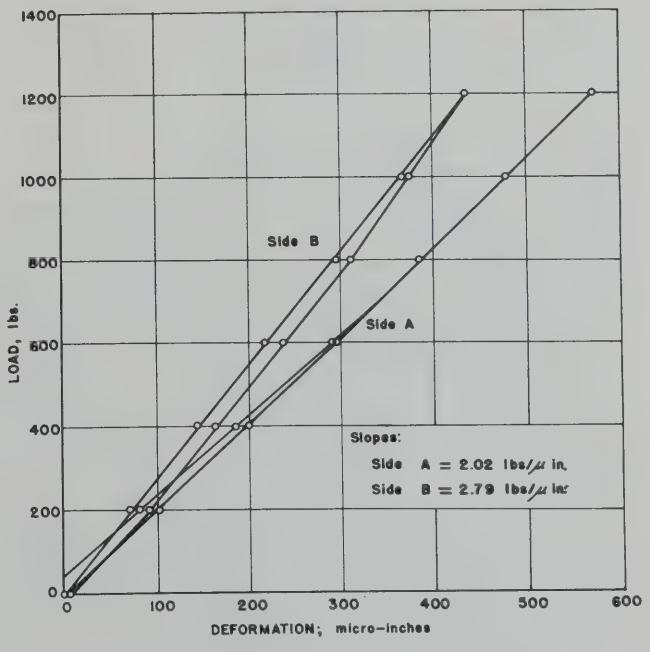

Fig. 8. Load vs. Deformation for 3 aluminum rivets.

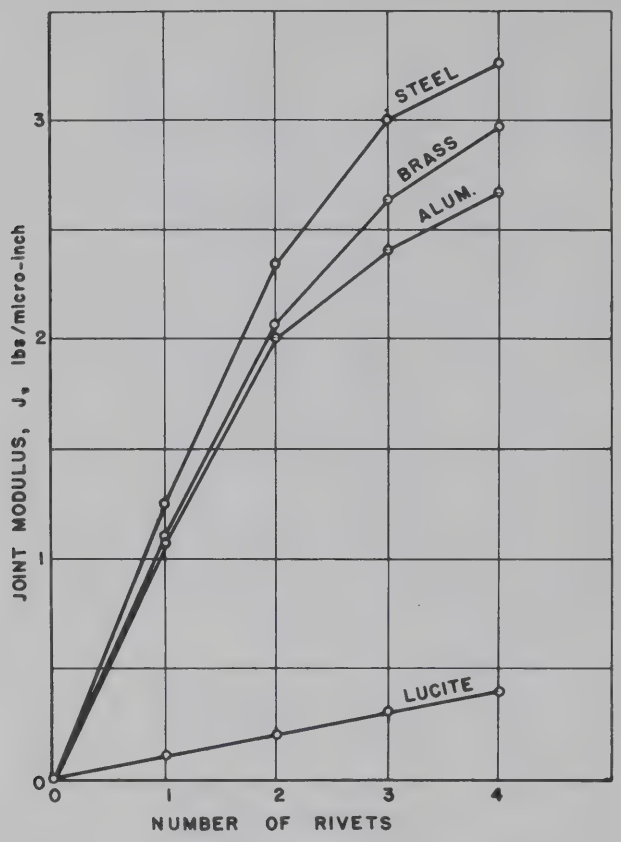

Fig. 9. Joint modulus as a function of the number of rivets.

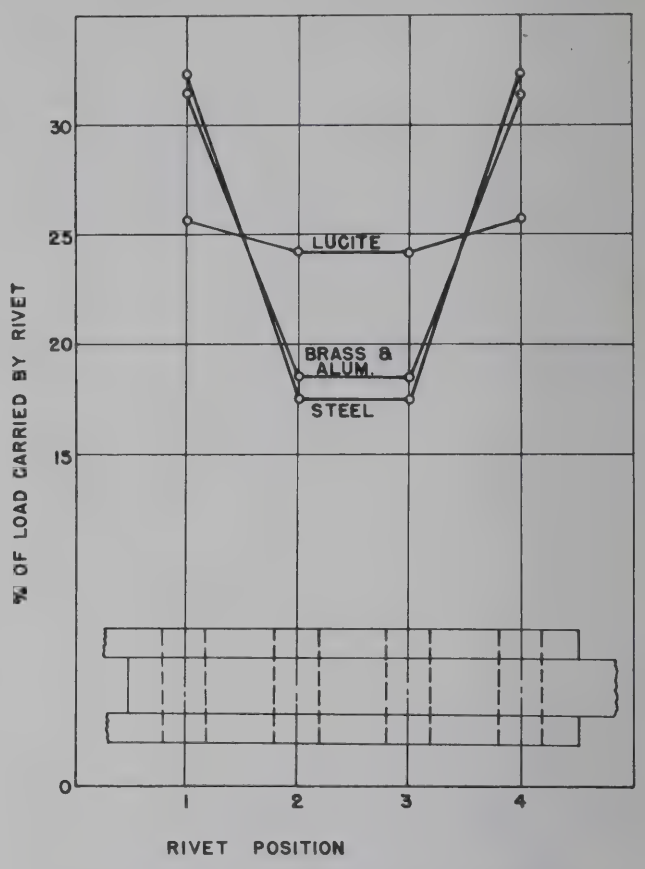

Fig. 10. % of load carried by each rivet for four rivets and four materials.

number of bolts. The lucite bolts are an exception. Here the relation is a straight line within the limits of experimental error.

Partition of load between the bolts. As shown in the Appendix the results of Fig. 9 afford a simple measure of the % of load carried by the individual bolts in a joint. If the computation is made for a "four bolt" joint, diagrams, Fig. 10 are obtained, from which it appears that only in the case of lucite bolts is there any significant improvement in the partition of load as compared to that of steel bolts. The change produced by the use of brass and aluminum bolts is quite small. It does not compare to the corresponding change of the moduli of elasticity and it is not in agreement with the theoretical considerations. In view of this discrepancy a more detailed discussion of the results appears necessary.

DISCUSSION OF THE RESULTS

Comparison between the computed and experimental joint moduli, J. In an earlier section it was pointed out that the partition of load between rivets could be determined indirectly by assuming a constant relation between load and deformation in each element of the joint, irrespective of the number and nature of rivets. In the elastic range the relation between load and deformation affects the form of a Hooke's law. Therefore, with the above assumption, the coefficient of proportionality in the corresponding Hooke's relation must depend solely on the geometry and nature of the particular element. This condition should apply to the rivets as well as to the plates. Because of symmetry, in the present case the elements of the plates are only of two kinds: (a) the portion of plate between two bolts, and (b) the end portion of the plate. The bolt is the third element of the joint, and this element bears a different relation to the load for each of the four materials of which it has been made. The number of independent variables for all 4 x 4 = 16 joints investigated is therefore 2 for the plates, plus

TABLE III - DEFORMATION OF BOLT, e_B: MICRO-INCHES/LB

Material	Experimental	Anticipated from Modulus Ratio	COMPUTED Shear Δ_s	COMPUTED Bending Δ_B
STEEL: SAE 1020	0.740	--	0.134	0.386
BRASS: 60 / 40	0.854	1.56	0.335	0.985
ALUMINUM: 24 ST	0.868	2.20	0.400	1.20
LUCITE	9.37	49.5	9.00	26.0

4 for the rivets, i.e. 6 total. In other words, 10 out of 16 results can be determined by computation and compared with the experimental ones. The computation has been carried out in the Appendix, and the results are shown in Column 4 Table II. On the basis of an experimental error of 3%, it is seen that the agreement between theory and experiment is good. The somewhat larger discrepancy for three and four aluminum bolts is believed to be due to the nature of the load-displacement diagrams, Figs. 7 and 8, discussed previously.

The deformation of bolts. From the above discussion it appears that the discrepancy between the expected and the true partition of load cannot be explained on the basis of an incorrect assumption. Attention therefore will be directed to the deformation of the bolts themselves. As pointed out previously this deformation can be determined experimentally for each of the bolts employed. When this is done, figures shown in Column 2, Table III, are obtained. On the other hand, Column 3 of the same table contains values for brass, aluminum and lucite which have been computed from the corresponding values for steel on the assumption that the modulus of elasticity is the only variable involved in the change of the material. It is seen that the actual deformation is of from two to five times smaller than the expected one. The discrepancy increases as the modulus of elasticity decreases. That is, in actual service the bolts made of a less rigid material are much stiffer than anticipated. Obviously, not only the modulus of elasticity but also the mode of deformation has undergone a change in this case.

The mode of deformation of a bolt or rivet is not readily amenable to an analysis. The current assumption of pure shear is much too over-simplified. As Talbot and Moore[6] have shown, rivets undergo considerable bending in a lap joint. However, this condition applies only to a homogenous joint. To the best of our knowledge the behavior of the rivet in a heterogenous joint has not been investigated.

Assuming a uniform pressure in the hole the deformation of the bolt due to shear and bending can be computed by means of the elementary beam theory. This computation has been carried out in the Appendix, and the results are shown in Columns 4 and 5, Table 3. By comparing the experimental and computed values it is found that:

(a) The steel bolts deform more than by assuming a combined action of shear and bending,
(b) The lucite bolts deform as though by assuming the action of shear alone, and
(c) The brass and aluminum bolts exhibit a behavior which is intermediate between shear and bending.

Thus, there is a gradual change in the mode of deformation as the material of the bolts becomes less rigid with respect to that of the plates. Apparently, whatever the deformation of the bolts, it is restricted in its nature and magnitude by the deformation of the holes in the steel plate. This circumstance explains why in a heterogenous joint the deformation of

the bolts increases less rapidly than the decrease of their moduli of elasticity.

CONCLUSION

From the above results and discussion the following conclusions may be drawn:

1. In order to improve substantially the partition of load between the rivets in a line, the latter must be made of a material which is at least ten times less rigid than the material of the joined members.
2. In heterogenous structures predictions based on the ratio of moduli of elasticity may be at fault because of restrictions imposed on the magnitude and nature of deformation of the less rigid elements by the more rigid ones.

APPENDIX I

COMPUTATION OF THE CHARACTERISTICS OF A LAP JOINT BY MEANS OF AN ELECTRIC ANALOGY

Principles of the analogy: According to the assumptions made in the main body of the report, the deformation, Δe, of any element of the joint is related to the force, F, acting on this element by the equation

$$\Delta e = kF \tag{1}$$

where k is the coefficient of deformability depending only on the geometry, size, and nature of the element. The word element implies any part of the joint: cover plate, middle plate, or rivet, considered between two points, A and B, of the joint. Under this assumption Δe is simply the displacement of point B with respect to point A. Now, the principle of continuity of deformation and the equilibrium of forces, applied to a structure made of various elements, states that:

1. The displacement between A and B in a given direction (in this case the axial direction) is independent of the path along which this displacement is measured, and
2. The forces acting on any point of the joint are in equilibrium.

Similar principles apply to an electrical circuit made of resistors, in which the voltage drop, V_{AB}, replaces the displacement between points A and B, and the current, i, the force acting on the element (A B). The analogy is completed by observing that equation (1) takes the form of Ohm's Law:

$$V_{AB} = Ri$$

in which the resistance, R, replaces the coefficient of deformability, k.

Equivalent networks: On the basis of the above analogy the computation of the displacements and forces in a lap joint is reduced to the solution of the following electric networks:

One bolt joint, fig. 11a.

$$V_{AB}^{I} = i(R_2 + R_3) \tag{3}$$

Two bolt joint, fig. 11b.

$$V_{AB}^{II} = i(\tfrac{1}{2}R_2 + R_3) \tag{4}$$

Three-bolt joint, fig. 11c.

$$V_{AB}^{III} = i\left\{R_3 + R_2\left(\frac{R_1 + R_2}{2R_1 + 3R_2}\right)\right\} \tag{5}$$

Four bolt joint, fig. 11d.

$$V_{AB}^{IV} = i\left\{R_3 + R_2\left(\frac{2R_1 + R_2}{4R_1 + 4R_2}\right)\right\} \tag{6}$$

3. Values of coefficients of deformability for plates and bolts.

From (3), (4) and (5) there follows:

$$R_1 = \frac{3\left(\frac{V_{AB}}{i}\right)^{III} - 4\left(\frac{V_{AB}}{i}\right)^{II} + \left(\frac{V_{AB}}{i}\right)^{I}}{1 - 2\left(\frac{V_{AB}}{i}\right)^{III} + 4\left(\frac{V_{AB}}{i}\right)^{II} - 2\left(\frac{V_{AB}}{i}\right)^{I}}$$

$$R_2 = 2\left(\frac{V_{AB}}{i}\right)^{I} - 2\left(\frac{V_{AB}}{i}\right)^{II}$$

$$R_3 = 2\left(\frac{V_{AB}}{i}\right)^{II} - \left(\frac{V_{AB}}{i}\right)^{I}$$

Or reverting to displacements and forces and relation (1):

$$k_1 = \frac{3\left(\frac{\Delta e}{F}\right)^{III} - 4\left(\frac{\Delta e}{F}\right)^{II} + \left(\frac{\Delta e}{F}\right)^{I}}{1 - 2\left(\frac{\Delta e}{F}\right)^{III} + 4\left(\frac{\Delta e}{F}\right)^{II} - 2\left(\frac{\Delta e}{F}\right)^{I}}$$

$$k_2 = 2\left(\frac{\Delta e}{F}\right)^{I} - 2\left(\frac{\Delta e}{F}\right)^{II}$$

$$k_3 = 2\left(\frac{\Delta e}{F}\right)^{II} - \left(\frac{\Delta e}{F}\right)^{I}$$

where k_1, k_2, and k_3 are the coefficients of deformability of the element of plate between holes, the bolt, and the end element of the plate, respectively.

Using the values of joint moduli, J_1, J_2, and J_3 compiled in table 2, the values of k_1 and k_3 and also the values of k_2 for various bolt materials, have been computed and entered in table 4.

TABLE IV

VALUES OF COEFFICIENTS OF DEFORMABILITY, k, FOR VARIOUS PARTS OF THE JOINT,

PART	k x 10^6 in/lb
End section of plate	0.059
Section of plate between holes	0.311
Steel bolt; SAE 1020	0.710
Brass bolt: 60 / 40	0.854
Aluminum bolt: 24 ST	0.868
Lucite	9.37

4. Joint Moduli for various joints: With the above values of k_1, k_2, and k_3, the joint modulus for any number of bolts may now be computed, using equations (4), (5), and (6). In the case of steel bolts only equation (6) will give a new result, since equations (3), (4), and (5) were used for the computation of k_1 and k_3. The computed values of J are presented in Column 4, Table 2.

5. Partition of load between bolts in the four bolt joint.

From Fig. 11 there follows that:

$$\frac{i_4}{I} = \frac{i_1}{I} = \frac{2R_1 + R_2}{4(R_1 + R_2)} \qquad (7)$$

$$\frac{i_3}{I} = \frac{i_2}{I} = \frac{R_2}{4(R_1 + R_2)} \qquad (8)$$

or

$$\frac{F_4}{F} = \frac{F_1}{F} = \frac{2k_1 + k_2}{4(k_1 + k_2)} \qquad (9)$$

$$\frac{F_3}{F} = \frac{F_2}{F} = \frac{k_2}{4(k_1 + k_2)} \qquad (10)$$

where F is the total load on the joint, and F_1, F_2, F_3, and F_4 the partial loads on each of the four bolts.

By substituting the values of k_1, k_2, and k_3 in equations (9) and (10) the partition of load between bolts for various bolt materials may be obtained. The results for the four materials employed in this work have been plotted in Fig. 10.

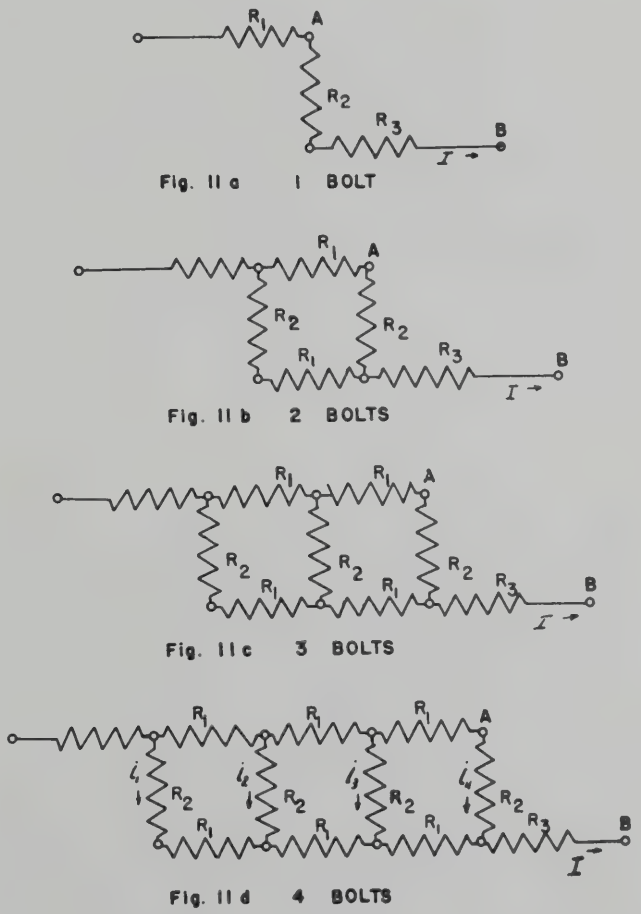

Fig. 11. Equivalent Networks.

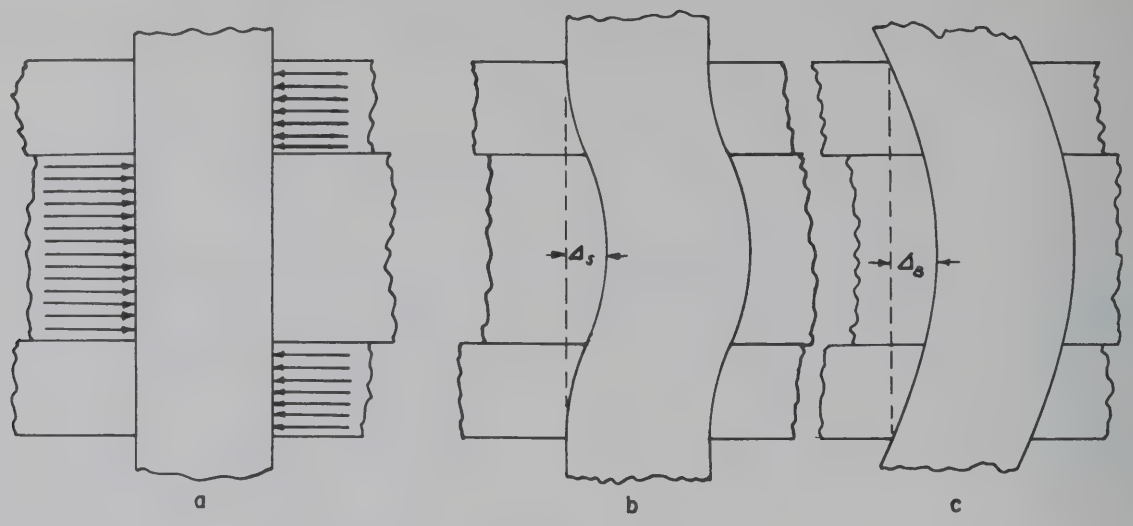

Fig. 12. Deflection of the bolt.

APPENDIX II

DEFLECTION OF THE BOLT

Assuming that the bolt is deformed as a freely supported beam loaded in the manner shown in Fig. 12, the deflection due to shear and bending may be computed by means of the usual equations of beam theory: viz. see Fig. 12 (b) and (c).

$$\frac{d^2y}{dx^2} = \frac{kp}{GA} \tag{11}$$

$$\frac{d^2y}{dx^2} = \frac{M}{EI} \tag{12}$$

where p is a distributed load $(p = F/2t)$; M, the bending moment; G and E, the shear and Young's moduli, respectively; A, the cross section area; I, the moment of inertia; and k, a distribution coefficient for shear, which in the case of a circular section is equal to 4/3.

Solving equations (11) and (12), there follows with reference to Fig. 12 (b) and (c)

$$\frac{\Delta_S}{F} = \frac{2.66t}{\pi d^2 G} \tag{13}$$

$$\frac{\Delta_B}{F} = \frac{45.2t^3}{\pi d^4 E} \tag{14}$$

where d is the diameter of the bolt. By substituting in these expressions t = 1/4, d = 3/8, and $G = \frac{E}{2(1+\mu)}$, where μ is the Poisson ratio, the values shown in Columns 4 and 5, Table 3, are obtained for the values of E and μ figuring in Table 1.

BIBLIOGRAPHY

1. For review of literature up to 1934 see: Discussion by A. E. R. de Jonge of the paper by A. Hrennikoff, Am. Soc. of Civil Engrs. Trans., Vol. 99, p. 474 (1934).

2. A. G. Solakian and G. E. Claussen "Stress Distribution in Fillet Welds" Review of Literature. Jour. of Am. Welding Soc., Vol. 26, May 1937.

3. D. Rosenthal and P. Levray, "Elastic Behavior and Strength of Side Fillet Welds". The Welding Journal, Vol. 28, Research Supplement, p. 140 (April 1939).

4. (a) Discussion by H. N. Hill and Marshall Holt of the paper by A. Hrennikoff, Am. Soc. of Civil Engrs. Trans., Vol. 99, p. 464 (1934).
(b) L. Moisseieff, E. C. Hartmann and R. L. Moore, "Riveted and Pin-connected Joints of Steel and Aluminum Alloys", Am. Soc. of Civil Engrs. Trans., Vol. 109, p. 1359 (1944).

5. See for example: C. Batho, "The Partition of the Load in Riveted Joints", Jour. of the Franklin Institute, Vol. 182, No. 5, p. 553-604 (Nov. 1916).

6. A. N. Talbot and H. F. Moore, "Tests of Ni-Steel Riveted Joints", Univ. of Ill. Bulletin, Vol. 8, No. 26 (February 27, 1911).

7. E. Hohn, "Nieten u Schweissen der Dampfkessel", Berlin, Julius Springer, 1925.

Made in United States of America

Reprinted from THE JOURNAL OF PHYSICAL AND COLLOID CHEMISTRY
Vol. 55, No. 3, March 9, 1951

THE INTERFACIAL TENSION OF SOME HYDROCARBONS AGAINST WATER

WILLIAM E. ROSE AND WILLIAM F. SEYER

Department of Engineering, University of California, Los Angeles, California

Received April 3, 1950

Numerous physical and chemical properties of the stereoisomers of decalin have been determined in the chemistry laboratories of the University of British Columbia during the past few years. It was to add to the knowledge already obtained about *cis*- and *trans*-decahydronaphthalenes that the present investigation into the interfacial tension of the compounds against water was undertaken. In particular, it was to determine whether the *cis* isomer gave any unusual values.

EXPERIMENTAL PROCEDURE

Many methods have been devised for the measurement of interfacial tension. After a detailed study of the most recent methods used, that of Hutchinson (3) was selected as the most appropriate for the material at hand. Hutchinson modified Sugden's original surface tension apparatus (6) for interfacial determinations. He further developed the following equation as it applied to his apparatus:

$$T = (h' - h'')gd\left(1 + \frac{0.6r}{dh}\right)A \qquad (1)$$

where T = interfacial tension in dynes per centimeter,
h' = height of meniscus in tube with small tip,
h'' = height of meniscus in tube with large tip,
d = density of phase inside tubes,
r = radius of larger tip,
h = $(h' - h'')$, and
A = an arbitrary constant for the apparatus.

This method is a relative one, i.e., it depends upon calibration with some interface of known value. One advantage in its use is that the apparatus can be readily constructed from laboratory glassware and is suited to temperature measurements. Another important feature is that only a small amount of material is needed for a determination.

The apparatus constructed was similar to that described by Hutchinson (3) (see figure 1). The essential part consisted of two Pyrex-glass bubbling tips of different radii for producing bubbles of one liquid inside the other. These tips were joined to a reservoir having side tubes in which the heights of the liquid could be read with a cathetometer. The side tubes were identical, so that no capillary corrections needed to be applied. The tubes were rigidly mounted in a rubber stopper and connected to a pressure system (figure 2). With the apparatus assembled, the faces of the tips were in a horizontal plane with respect to the side tubes.

The whole of this apparatus was enclosed in a Pyrex cell 5 cm. in diameter and about 8 cm. long. The cell was placed in a water bath and held firm by a brass collar. The entire apparatus was so arranged that the bubbling tips were as free from vibration as possible.

Water was chosen as the bath liquid, since it provides better visibility than oil. Agitation was supplied by a 4 cm. propellor driven by a variable-speed motor. A copper cooling coil through which water at 15°C. was circulated was inserted in the bath to provide suitable opposition to the heaters. The heaters were two 125-watt blade heaters which were connected with a thermoregulator at all times. A 200-watt heater was used to take the bath from one temperature range to another.

The temperatures were measured by a mercury thermometer over the range

from 20° to 70°C. The thermometer could be read to 0.1°C. and was calibrated against a Leeds & Northrup resistance thermometer previously standardized. With the help of this thermometer and a Cenco supersensitive relay it was possible to control the temperature of the water bath from 0.01° to 0.02°C.

The bath itself was a Pyrex-glass cylinder, 45 cm. high and 23 cm. in diameter. It was suitably lagged and covered with an insulated wooden lid. Since it was necessary to sight into the cell, its wall had to be tested for optical defects. This was done by immersing a brass meter scale inside the bath and measuring the distance between two points by means of a cathetometer through a window in

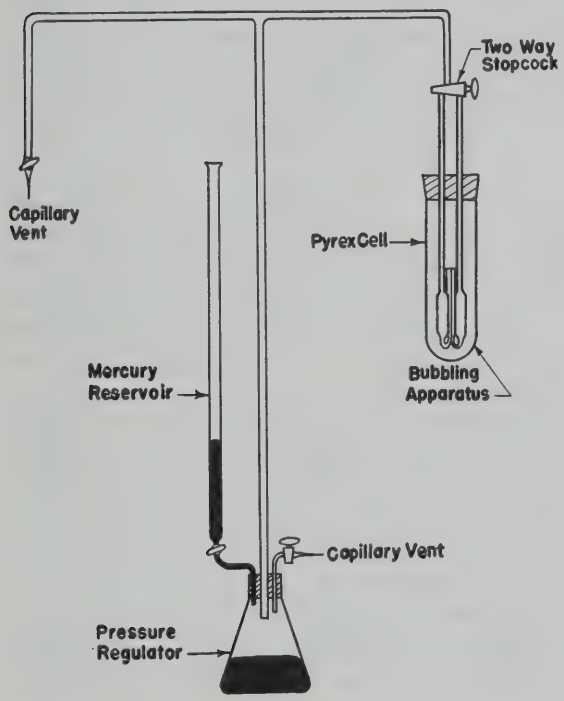

FIG. 1. Details of pressure system

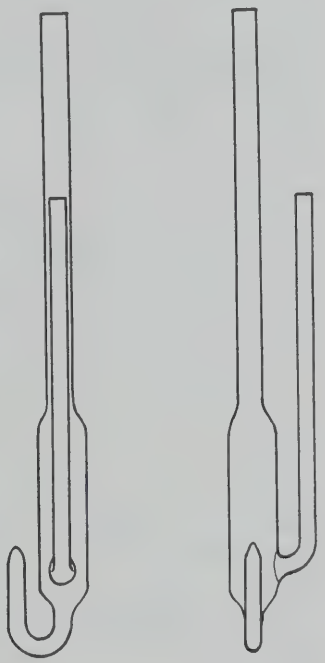

FIG. 2. Details of bubbling tube

the lagging. The measurement was then repeated with the scale outside of the bath. No difference was noted.

Since the heights of the liquids in the side tubes were all that one observed for a determination, it was necessary to make the cell of sufficient diameter so that the addition of one drop of liquid inside the tubes to the liquid in the cell would not substantially increase the pressure needed to produce a bubble.

The tips were drawn from 4 mm. Pyrex-glass tubing, marked with a diamond, then broken off. The tips thus made were found to break off very sharply and were not jagged as expected. They were examined with a low-power travelling microscope, and it was found that practically all of them were circular in cross section. Two tips were selected from a large number, and these were carefully

ground with fine emery powder until perfectly plane in cross section. The diameter of the larger tip was measured with the same microscope at 30° intervals of rotation.

The position of the side tubes proved somewhat critical, and after some experimenting it was found that the tube should be joined to the reservoir about 1 cm. below the level of the tips. This allowed the hydrocarbon to go up the side tubes and yet prevented water from backing up in the same tubes. The side tube and tip were placed at right angles to each other to facilitate reading the height of liquid and to check the level of the tips.

The method of producing the bubbles proved to be a problem in itself. Hutchinson (3) had a side tube on his cell and decreased the pressure above the cell liquid with an aspirator. This method was tried without success. It was found that the bubbles were produced too rapidly and could not be properly controlled. Since the meniscus could not be closely followed, the method was finally abandoned and another tried.

The tubes were next connected to a two-way stopcock so that the pressure could be raised in one tube without influencing the other. This was in turn connected to a pressure system consisting of a piece of pressure tubing which was placed in a vise so that it could be compressed, allowing the bubble of liquid to be produced very slowly. After some practice it was found that the pressure could be controlled very nicely and the height of the liquids in the side tubes could be reproduced without any great difficulty.

An alternate form of pressure device was also used, in which a buret dripped liquid slowly into a flask, displacing the air in the system and producing bubbles of liquid. This was found to be the best form of pressure device, since the investigator does not need to control any vise or in any way cause sudden increases in pressure. The operator merely sets the buret, which may be filled with mercury, sulfuric acid, or the liquid under investigation, so that the pressure is slowly increased. He then follows the rise of liquid in the side tube until the maximum height is reached. The meniscus can be followed easily with a cathetometer. The apparatus should be illuminated so that the meniscus can be read easily.

Before taking any readings it was necessary to calibrate the apparatus against a known interface and get the value of the arbitrary constant indicated in equation 1. The system benzene–water was selected because the value of the interfacial tension has been accurately determined at 20°C. and agreed upon by investigators. Furthermore, benzene can be obtained in reagent grade and readily purified by fractional crystallization. The pressure difference for the two tips was observed several times, and the mean constant for A in equation 1 calculated. The numerical value was 0.01813.

Extreme cleanliness was found to be necessary, so before each determination the bubbling tips and tubes were cleaned with hot sulfuric acid and dichromate solution, washed with alcohol, and rinsed with distilled water. The tubes were then dried for 20 min. at 110°C. After making a determination with *cis*-deca-

hydronaphthalene it was found necessary to heat the cleaning solution to about 120°C. before any satisfactory cleaning was observed. The criterion for cleanliness was that the liquid should not adhere to the glassware in droplets but should rather form a smooth continuous film over the glass surface. The same procedure was followed in cleaning the cell.

In making a run the cell was filled with distilled water to such a height that when the tubes were placed in the cell, the liquid would be about 1 cm. above the level of the tips. The cell was placed in the constant-temperature bath to allow the distilled water to come to the bath temperature. The tubes were filled in the following manner: Distilled water was poured into the side tubes until the tips were just filled and no more. This was to prevent the hydrocarbon from forming drops in the distilled water when the tubes were placed in the cell. The hydrocarbons were then poured into the side tubes until the liquid was 2 or 3 cm. above the face of the tip. The tubes were now placed in the cell and it was firmly bolted into position by tightening the brass collar, thereby holding the whole assembly together.

The whole assembly was kept in the bath for 20 min. before any readings were taken. This was not only to ensure thermal equilibrium but also to make it possible to neglect any aging effects at the interface. To check for interfacial equilibrium, the hydrocarbons were shaken with distilled water and left overnight. The organic phase was then used in place of the anhydrous hydrocarbon. No difference in the values of the interfacial tension was observed, however, and it was not deemed necessary to repeat this in subsequent determinations.

The tips were checked with the cathetometer to make certain that they were in the same horizontal plane and were adjusted if necessary. At the end of the 20-min. period, the pressure in the tube having the smaller tip was raised with the levelling bulb until the hydrocarbon was almost ready to leave the tip. The vise was now used to very slowly raise the pressure in the tube. The meniscus was followed with the telescope until the bubble had formed and the meniscus in the side tube suddenly fell. The maximum height of the meniscus was recorded and the pressure in the system reduced by means of the capillary stopcock. The two-way stopcock was now turned, and the maximum height of the meniscus for the tube with the larger tip was recorded.

This procedure was repeated at 10° intervals throughout the temperature range. Several readings were taken at each temperature interval and the mean used in the calculations. While no difficulty was encountered in holding the temperature constant at the lower end of the range, it was harder to control the temperature at the upper end.

As a check on the calibration constant, the interfacial tension of the system *n*-octane–water was measured at 20°C. and found to be 50.98 dynes per centimeter, as compared with a value of 50.8 recorded in the *International Critical Tables*. As a sample of the pressure differences encountered, the values for *trans*-decahydronaphthalene at 20°C. are listed in centimeters of height for that compound in table 1.

Using the densities of benzene, *n*-octane, and cyclohexane as given by the *International Critical Tables* and those given by Seyer and Davenport for *cis*- and *trans*-decahydronaphthalenes (5) the values of the interfacial tension were calculated and recorded in table 2.

TABLE 1

Pressure differences for trans-decahydronaphthalene at 20°C.

Trials	1	2	3	4
Height in cm	3.295	3.260	3.285	3.280

TABLE 2

Interfacial tension of trans-decahydronaphthalene, cis-decahydronaphthalene, cyclohexane, and n-decane

TEMPERATURE	INTERFACIAL TENSION			
	trans-Decahydronaphthalene	*cis*-Decahydronaphthalene	Cyclohexane	*n*-Decane
°C.	*dynes/cm.*	*dynes/cm.*	*dynes/cm.*	*dynes/cm.*
20	51.40	51.74	51.01	51.24
30	50.99	51.45	50.67	50.71
40	50.44	51.12	50.15	50.42
50	50.09	50.89	49.72	49.86
60	49.69	50.54	49.40	
70	49.40	50.40	49.09	

TABLE 3

Comparison of interfacial tension values

HYDROCARBON	TEMPERATURE	INTERFACIAL TENSION		
		Bubble pressure method	Others	Authority
	°C.	*dynes/cm.*	*dynes/cm.*	
Octane	20	50.98	50.8	*International Critical Tables*
trans-Decahydronaphthalene	20	51.18	50.98 at 25°C.	Guest and Lewis (1)
Cyclohexane	25	50.80	50.28	Mathews (4)

DISCUSSION OF RESULTS

The reliability of the differential bubble pressure method for interfacial measurements is shown by the close agreement of the present values and those made by others using different techniques. This agreement is illustrated in table 3. In the case of the first two values the deviation is less than 0.5 per cent, whereas with cyclohexane it is slightly over 1 per cent. The high value for cyclohexane might be due to impurities, since the substance had a slight yellow tinge, prob-

ably brought about by oxidation as the sample had been standing for some years after purification. It was also observed that the cleanliness of the tips was important, as values 10–15 per cent higher than those recorded were obtained when insufficient cleaning had taken place.

Hutchinson (3) makes no mention of how to correct for drops of the liquid in the tubes forming on the surface of the liquid in the cell. In the present investigation, the height of the meniscus in the tube with the small tip was recorded

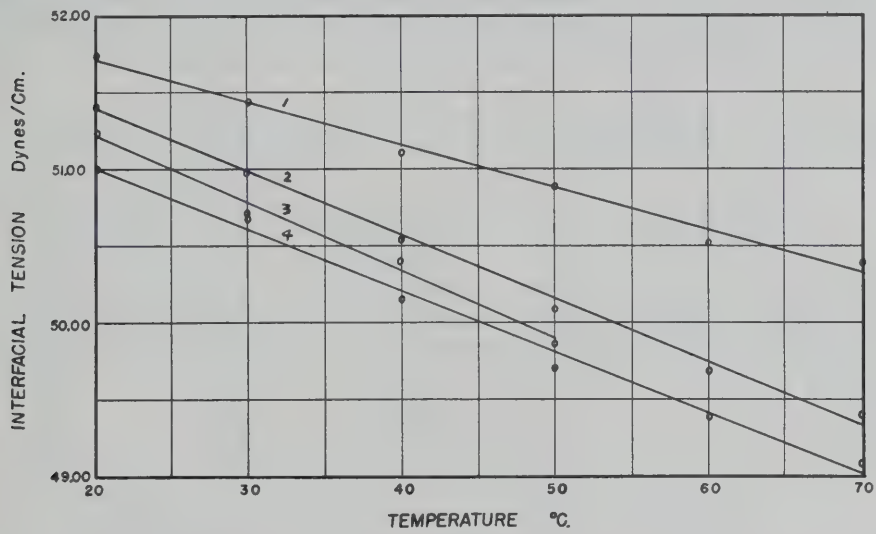

FIG. 3. Interfacial tension *vs.* temperature. Curve 1, *cis*-decahydronaphthalene and water curve 2, *trans*-decahydronaphthalene and water; curve 3, cyclohexane and water; curve 4, *n*-decane and water.

TABLE 4

Equations for calculating interfacial tension

HYDROCARBON	EQUATION
cis-Decahydronaphthalene	$y = 52.26 - 0.0275t$
trans-Decahydronaphthalene	$y = 52.20 - 0.0410t$
Cyclohexane	$y = 51.79 - 0.0395t$
n-Decane	$y = 52.11 - 0.0443t$

before reading the height of the meniscus for the large tip. This is not strictly correct and yet there seems to be no immediate way around the difficulty.

The results are shown graphically in figure 3. Assuming a linear relationship between temperature and interfacial tension and using the method of least squares the equations in table 4 were developed. Here y is the interfacial tension and t the temperature. At the critical solution temperature, if such were to exist, $y = 0$. In all cases this gives a value for the critical solution temperature well over 1000°C.; this value is obviously meaningless, since it is way above the critical

temperature of any of the compounds. It shows that there can be no critical solution temperatures for these systems, because complete miscibility can only occur in the gaseous phase. One would therefore expect that in the case of all the systems the solubility of one component in the others will be extremely low. However, it should be pointed out that in these systems absence of mutual solubility does not by itself explain the deviation from Antonoff's rule, as will be seen from table 5.

Table 5 brings out the influence of the steric factors in the formation of an interface. It would appear that in the case of the normal paraffin hydrocarbons a minimum is reached in the difference between the calculated and found values

TABLE 5

Calculated and found values of interfacial tension

SYSTEMS AT 20°C.	INTERFACIAL TENSION		
	Calculated from surface tensions of pure compounds*	Found	Difference
cis-Decahydronaphthalene + water	40.57	51.74	11.17
trans-Decahydronaphthalene + water	42.86	51.40	8.54
Cyclohexane + water	47.45	51.01	3.56
Decane + water	50.35	51.35	1.00
Octane + water	50.04	50.81	0.95
Hexane + water	53.94	51.25	2.69

* Mutual solubilities are so low that the effect on surface tension is negligible.

TABLE 6

Work of cohesion and work of adhesion for several hydrocarbons

HYDROCARBON	WORK OF COHESION	WORK OF ADHESION	DIFFERENCE
cis-Decahydronaphthalene	64.36	53.50	10.76
trans-Decahydronaphthalene	59.78	50.90	8.98
Cyclohexane	50.60	47.04	3.56
Decane	44.48	43.75	0.73
Octane	43.42	43.49	−0.98

of the interfacial tensions. A rather striking aspect of column 4 is that the interfacial tension value of all the hydrocarbons at 20°C. against water is nearly the same irrespective of molecular weight or configuration. One must conclude from this that all the hydrocarbons present a similar face to the water surface. This could occur if the molecules in the hydrocarbon surface were oriented and held in a position analogous to that which exists in their solid state. In such a case the cyclic compounds would rest edgewise in the surface layer so as to present one or possibly two —CH_2— groups to the water, while the normal hydrocarbons would lie with their long axis in a plane parallel to the water surface. It is interesting to note that the interfacial tension temperature coefficient, dy/dt, of *trans*-decahydronaphthalene and that of cyclohexane, which is now also con-

sidered to be in the *trans* form, are very nearly the same. The value of the *cis* form is very much smaller. In this case all that can be said is that, since dy/dt is a measure of the entropy of the surface, the interfacial tension coefficient of the *cis* isomer with water is lower than that of the *trans* isomer. It is of further interest to note that the work of cohesion and work of adhesion tend to approach each other in the case of decane and octane, as seen in table 6. The difference is very nearly equal to that between the values found and those calculated by Antonoff's rule. The exact significance of this is difficult to explain until reliable values of the actual solubilities of these hydrocarbons and water are known.

SUMMARY

1. The interfacial tensions of several cyclic and normal paraffins against water have been measured between 20° and 70°C. by the differential bubble pressure methods.

2. The interfacial tensions appear to be a linear function of temperature over the range investigated.

3. The interfacial temperature coefficients of the *trans* forms show a marked difference from that of the *cis* form of decahydronaphthalene.

4. Antonoff's rule is closely obeyed by octane and decane, for which the difference between the work of cohesion and that of adhesion approaches zero.

REFERENCES

(1) Guest, W., and Lewis, W.: Proc. Roy. Soc. (London) **A170,** 501 (1939).
(2) Harkins, W. D., and Humphrey, E. C.: J. Am. Chem. Soc. **38,** 228 (1916).
(3) Hutchinson, E.: Trans. Faraday Soc. **39,** 229 (1943).
(4) Mathews, J. B.: Trans. Faraday Soc. **35,** 1113 (1939).
(5) Seyer, W. F., and Davenport, C. H.: J. Am. Chem. Soc. **63,** 2425 (1941).
(6) Sugden, S.: J. Chem. Soc. **121,** 858 (1922).

INTERMITTENT HEATING FOR AIRCRAFT ICE PROTECTION WITH APPLICATION TO PROPELLERS AND JET ENGINES

MYRON TRIBUS, PhD *
Assistant Professor
University of California, Los Angeles

Consultant, Aircraft Gas Turbine Divisions,
General Electric Company, Lynn, Massachusetts

INTERMITTENT HEATING FOR AIRCRAFT ICE PROTECTION, WITH APPLICATION TO PROPELLERS AND JET ENGINES

Myron Tribus, Ph. D. *

SUMMARY

The equations for intermittent heat transfer during icing conditions are presented and solved by means of an electrical analogue. The results of the analogue investigation are compared favorably with measured time-temperature data previously reported in the literature. The analysis shows that contrary to the experience with steadily heated ice prevention systems, the energy requirements for ice prevention using intermittent heating decrease with increasing ice accretion rate. Corroborative evidence is found in the literature. The thermal analyzer is used to demonstrate how the protection afforded for propeller de-icing may be increased without an increase in the energy required from the airplane's electrical supply and without major redesign of existing propeller heaters. In the case of jet engine guide vane de-icing, for a typical installation the indicated power requirements are one kilowatt per engine. In each case the minimum energy requirements occur when large amounts of power are applied for very short intervals of time. Suggestions for further reductions in power are given.

SYMBOLS AND NOMENCLATURE

a	radius of droplet, ft
A	surface area, ft^2
b	dimensionless modulus,
B	barometric pressure, in. Hg.
C	chord length, ft
C_p	unit heat capacity of air, BTU/lb F
C_{p_i}	unit heat capacity of ice, BTU/lb F
C_{p_w}	unit heat capacity of water, BTU/lb F

*Member, ASME. Assistant Professor of Engineering, University of California, Los Angeles. Consultant in heat transfer to the General Electric Company, Aircraft Gas Turbine Division, West Lynn, Mass.

E	fractional catch, local. Dimensionless ratio of number of intercepted droplets to number of droplets directly ahead of surface.
E_M	fractional catch, total. Dimensionless.
$\Delta E/E_M$	dimensionless ratio of local water catch rate for an element of area to the catch rate of the entire airfoil.
f_c	unit thermal conductance for heat transfer, BTU/hr ft^2 F
g_c	conversion constant 32.2 ft/sec^2
J	conversion constant 778 ft lb/BTU
k	thermal conductivity BTU/hr ft^2 (F/ft)
L	heat of vaporization or sublimation, BTU/lb
p	vapor pressure of water or ice, in. Hg.
p_s	vapor pressure of water or ice at surface, in. Hg.
p	vapor pressure of water in free stream, in. Hg.
q	heat flux, BTU/hr
r	"recovery" factor, dimensionless
Ru	Reynolds Modulus, dimensionless $Ru = \frac{2 U_\infty a \rho_a}{\mu}$
R_w	rate of water impingement, lb/hr ft^2
s	distance measured along surface of airfoil from stagnation point, ft
t	temperature, F
t_s	surface temperature, F
T	temperature, R
U_∞	free stream velocity, ft/sec
w	liquid water content, $grams/meter^3$ (or lb/ft^3)
x	distance, ft
γ	density of air, lb/ft^3
θ	functions defined in equations 3, 4, 5 and 8, ^oF

τ_∞ free stream temperature, F

ψ scale modulus, dimensionless

$$\psi = \frac{9C\rho_a}{a\rho_d}$$

ρ_a mass density of air, slugs/ft^3

ρ_d mass density of the droplet, slugs/ft^3

μ viscosity of air, lb sec/ft^2

INTRODUCTION

Extensive analytical methods have been devised for the design of ice prevention equipment for surfaces utilizing continuous heating. (19, 28, 37, 39) No similar analysis has been made for the case of intermittent heating. By experiments with propellers it has been found that the periodic application of heat to propeller blades provides better ice protection than the continuous application of heat and requires less energy.

A literature search revealed few reports of significance in this regard. (1, 2, 3) Reference 1 treats the problem the most thoroughly, attempting to account for all the known factors. However, the analysis therein treats a propeller without regard for the heat transfer processes occurring in the blade. References (1) and (2) suggest the melting of specified thicknesses of ice at the ice-blade interface as a criterion for successful ice prevention. This criterion is not considered justified and the analysis which follows considers that the ice adhesion will be reduced to zero when the surface reaches the freezing point.

Considerable experimental data dealing with propellers have been reported, but little correlation has been attempted. (4, 5, 6, 7, 8)

EQUATIONS FOR ENERY TRANSFER AT THE ICE SURFACE

The energy balance at a point on the surface of a streamlined body where supercooled liquid water is impinging is expressed in words as:

The heat transfer from beneath the ice surface	EQUALS	The heat loss by convection
	Minus	the heat gain from the frictional heating of the air

Plus	the energy loss by sublimation (or evaporation)
Plus	the heat loss via sensible heating of the water
Minus	the gain from the heat of fusion
Minus	the gain from the kinetic energy of the droplets relative to the surface.

When the surface temperature is above the freezing point there will be no benefit from the heat of fusion of ice and the fifth term on the right side of the above equation will be absent.

In reference 32, the above equation was applied to the prediction of the energy required to maintain a small cylinder at the freezing point during icing conditions. As demonstrated in the above reference the energy balance may be written:

$$q = f_c A \left[t_s - \mathcal{T}_\infty - r \left(U_\infty^2 / 2_c J C_p \right) \right] + 2.29 f_c L A B^{-1} \left(p_s - p_\infty \right) + R_w \left[0.47\ t_s - \mathcal{T}_\infty - 127 - \frac{U_\infty^2}{2_c J} \right] \qquad t_s < 32\,^\circ F \tag{1}$$

For the purposes of calculation it is convenient to define the following functions:

$$b = \frac{R_w C_{p_w}}{f_c} \tag{2}$$

$$\theta_1 = \theta_1 \left(t_s, B, b \right) = t_s \left(1 + 0.47\, b \right) + 2.29\, L B^{-1} p_s \tag{3}$$

$$\theta_2 = \theta_2 \left(\mathcal{T}_\infty, B, b \right) = \mathcal{T}_\infty \left(1 + b \right) + 2.29\, L B^{-1} p_\infty \tag{4}$$

$$\theta_3 = \theta_3 \left(b, U_\infty \right) = \left[\frac{r}{C_{p_a}} + b \right] \left[U_\infty^2 / 2 g_c J \right] \tag{5}$$

The equation for the heat flow from the surface then is written:

$$q = f_c A \left(\theta_1 - \theta_2 - \theta_3 \right) \qquad t_s < 32\,^\circ F \tag{6}$$

When the surface is above the freezing point the term for the heat of fusion is absent and the equation for the energy balance becomes:

$$q = f_c A \left\{ \left[t_s (1+b) + 2.29\, L B^{-1} p_s \right] - \left[T_\infty (1+b) + 2.29\, L B^{-1} p_\infty \right] - \left[\eta / c_{p_a} + b \right] \left[\frac{U_\infty^2}{2 g J} \right] \right\} \quad (7)$$

Defining the function:

$$\theta_4 = \theta_4 (t, B, b) = t(1+b) + 2.29\, L B^{-1} p_s \quad (8)$$

the equation for the heat flow becomes:

$$q = f_c A \left[\theta_4 (t_s, B, b) - \theta_4 (T_\infty, B, b) - \theta_3 (b, U_\infty) \right] \quad (9)$$

The functions θ_1, θ_2, θ_3 and θ_4 are shown presented in figures 1a, 1b, 1c and 1d for B equal to atmospheric pressure.

A COMPARISON OF EQUATION 6 WITH EXPERIMENTAL DATA

If the heat flow term in equation 6 is set equal to zero, the solution of the equation for the surface temperature yields a prediction which may be compared directly with experimental data. Reference 34 gives measurements of the temperature on a propeller heated intermittently while subjected to icing conditions. During the "heat off" intervals the propeller temperatures approached a steady state temperature. These values may be used as a rather crude check upon equation 6 since the heat flow term was not equal to zero but was presumeably very small. The data are not considered accurate to better than 5° by the experimenters and certain necessary measurements for the evaluation of the terms which enter into equation 6 were not made. Nonetheless, tables I and II show the experimental data and the predictions are in fair agreement; all but a few of the cases showing agreement within the 5°F limit.

TABLE I

Case	T_∞	w‡	radius	rpm	x ++	Measured values of t_s	Figures in TN 1520
	°F	g/m³	ft		in	°F	
a	2	0.25	1.98	675	1.8	24	28a,29a
b	2	0.25	1.98	925	1.8	22,23,23	24a,24b,28b
c	11	0.46	1.98	675	1.8	27,24,34,34,33	25a,26a,27a, 30a,31a
d	11	0.46	1.98	925	1.8	32,32,33,34,31	25b,26b,27b, 30b,31b
e	2	0.20	3.02	675	1.2	25	29a
f	2	0.20	3.02	925	1.2	19,21,16	24a,24b,29b
g	11	0.40	3.02	675	1.2	24,24,27,29,26	25a,26a,27a, 30a,31a
h	11	0.40	3.02	9.25	1.2	25,32,33,32,28	25b,26b,27b, 30b,31b
i	2	0.15	4.22	675	1.3	22	29a*
j	2	0.15	4.22	925	1.3	25,27,29,27	24a,24b,28b,29b
k	11	0.30	4.22	675	1.3	28,30,32,33,32	25a,26a,27a, 30a,31a
l	11	0.30	4.22	925	1.3	30,35,36,36,34	25b,26b,27b, 30b,31b
n	2	0.30	1.15	925	1.2	28	28b
o	11	0.50	1.15	675	1.2	23,29,33,27	26a,27a,30a, 31a
p	11	0.50	1.15	925	1.2	28,30,32,28	26b,27b,30b,31b

TABLE I Temperature on propeller blades in icing conditions when the heat flow is very small. (Taken from figures 24 to 31 of NACA TN 1520.)

*This figure in TN 1520 must be in error. Points labeled △ should be ▽ as a study of the other curves will indicate.

‡ Values of the liquid water content, w, were corrected for uneven distribution of water across the tunnel section using figure 8b of TN 1520.

++ The distance, x, in column 6 is measured along the surface from the leading edge.

TABLE II

Case	r/R	rpm	T_∞	U_∞	ψ	Ru	E_M	LWC*	$\Delta E/E_M$	f_c	b	θ_2	θ_3	θ_1	t_s	t_{meas}
a	0.38	675	2	239	101	325	0.80	13.1	0.30	15.5	0.248	34.4	4.3	38.7	22	24
b	0.38	925	2	290	101	395	0.80	13.1	0.30	17.0	0.276	38.0	6.7	44.7	25	22 to 23
c	0.38	675	11	239	101	225	0.80	31.2	0.30	15.5	0.594	93.7	5.1	98.8	32	27 to 34
d	0.38	925	11	290	101	395	0.80	31.2	0.30	17.0	0.552	87.7	7.2	94.9	32	31 to 34
e	0.58	675	2	304	112	415	0.79	11.2	0.28	17.4	0.124	18.4	7.5	25.9	16	25
f	0.58	925	2	363	112	495	0.80	11.2	0.28	19.1	0.138	20.2	10.5	30.7	19	16 to 21
g	0.58	675	11	304	112	415	0.79	25.6	0.28	17.4	0.285	51.9	7.8	59.7	32	24 to 29
h	0.58	925	11	363	112	495	0.80	25.6	0.28	19.1	0.316	55.3	11.0	66.3	32	25 to 33
i	0.81	675	2	367	91	500	0.85	6.24	0.28	19.2	0.560	74.6	12.0	86.6	32	22
j	0.81	925	2	466	91	622	0.86	6.25	0.28	21.6	0.641	84.9	19.2	104.1	32	25 to 29
k	0.81	675	11	367	91	500	0.85	19.9	0.28	19.2	0.18	26.5	10.8	37.3	22	28 to 33
l	0.81	925	11	466	91	622	0.86	19.9	0.28	21.6	0.205	40.0	17.1	57.1	32	30 to 36
m	0.22	675	2	234	54	319	0.85	15.6	0.04	15.3	0.219	30.6	4.1	34.7	20	25
n	0.22	925	2	246	54	333	0.85	15.6	0.04	15.7	0.224	32.0	5.0	37.0	21.5	20 to 28
o	0.22	675	11	234	54	319	0.85	34.3	0.04	15.3	0.481	77.1	4.2	81.3	32	23 to 33
p	0.22	925	11	246	54	333	0.85	34.3	0.04	15.7	0.495	80.0	5.5	85.5	32	28 to 32

F ft/sec * $\frac{\text{BTU}}{\text{hr sq ft F}}$

TABLE II Comparison of measured and predicted temperatures on propeller blade during icing conditions.
*LWC denotes liquid water content in millionths of a pound of liquid water per cubic foot of air. The other columns are dimensionless or have their units given.

Additional data:

r/R	s/C	t/C	C
0.38	0.167	0.24	9"
0.58	0.150	0.12	10
0.81	0.186	0.10	8.1
0.22	0.10	0.75	4.8

R = 3.208 ft.

$$b \triangleq (R_w C_{p_w}) / (f_c)$$

$$b = \frac{(3600)(\Delta E/E_M)(E_M)(t/C)(LWC)(U_\infty)}{(\Delta_s/C)(f_c)}$$

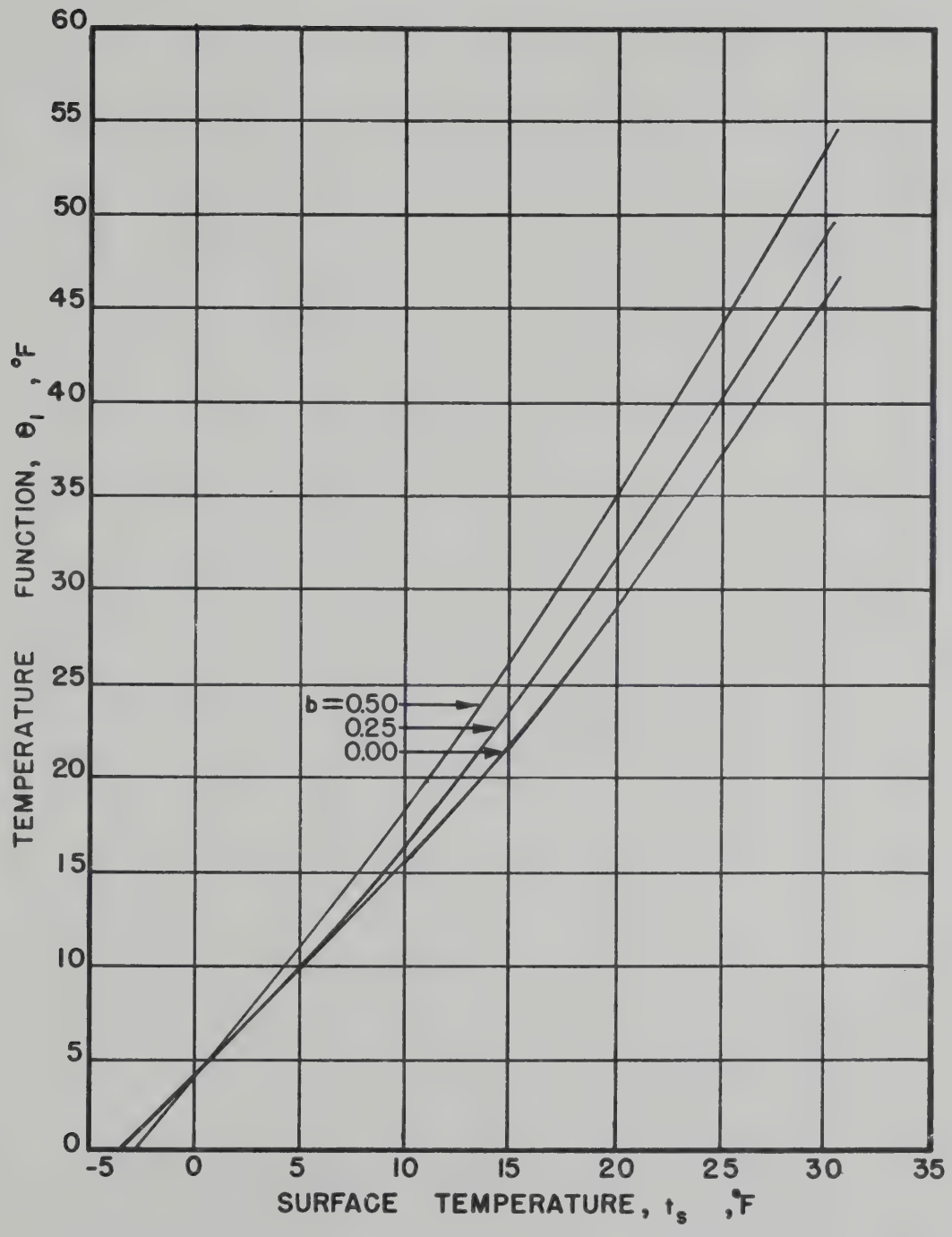

Fig. 1a Graph of $\theta_1 (t_s, B, b) = t_s (1 + 0.47b) + 2.29LB^{-1}p_s$ for the case, B = 29.9 inches of mercury, L = 1218 BTU/lb. (p_s corresponds to the saturation pressure over ice at temperature t_s)

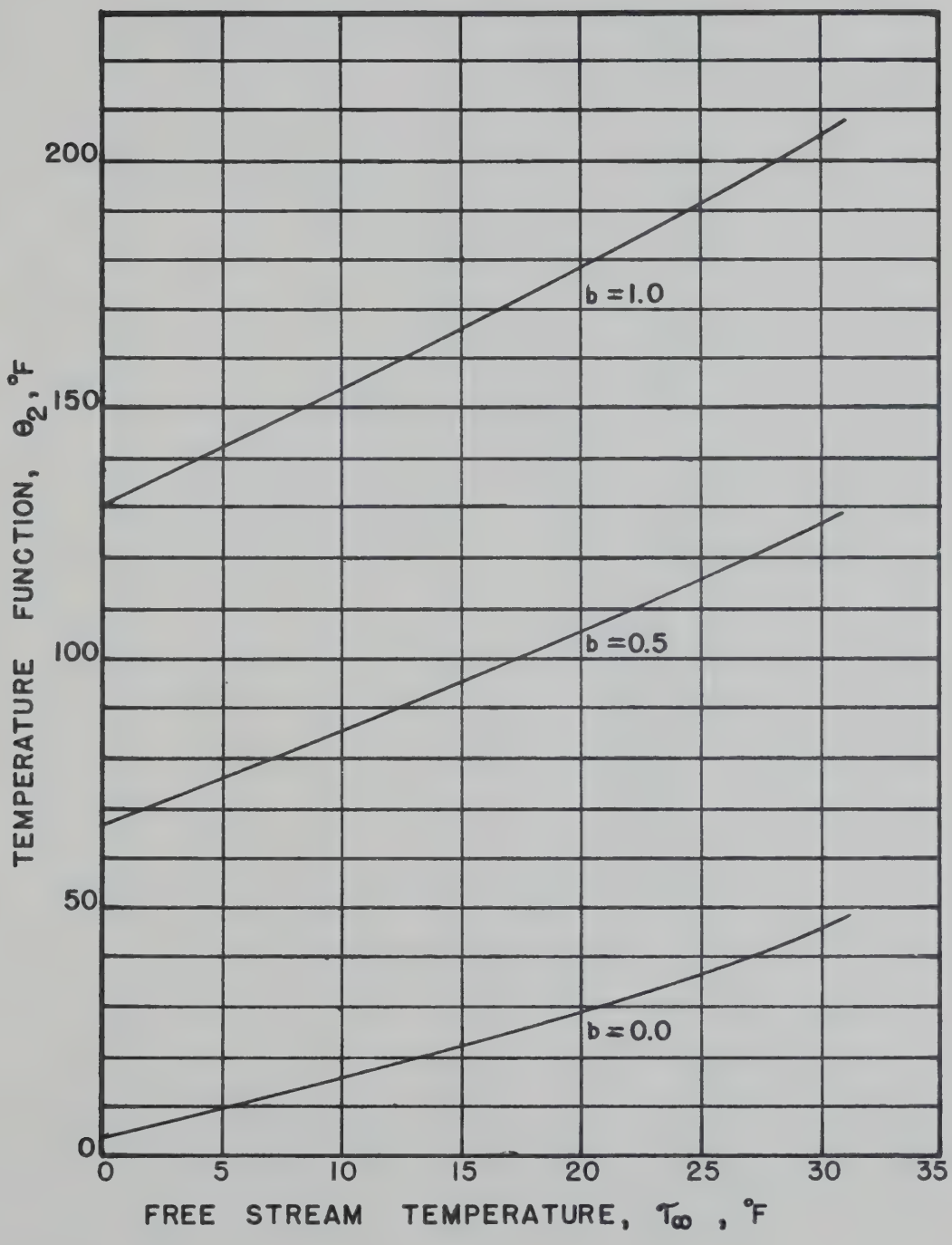

Fig. 1b Graph of $\theta_2 (T_\infty, B, b) = T_\infty (1 + b) + 127b + 2.29 LB^{-1} p_\infty$ for the case B = 29.9 inches of mercury, L = 1218 BTU/lb. (p_∞ corresponds to the vapor pressure of supercooled liquid water at temperature T_∞)

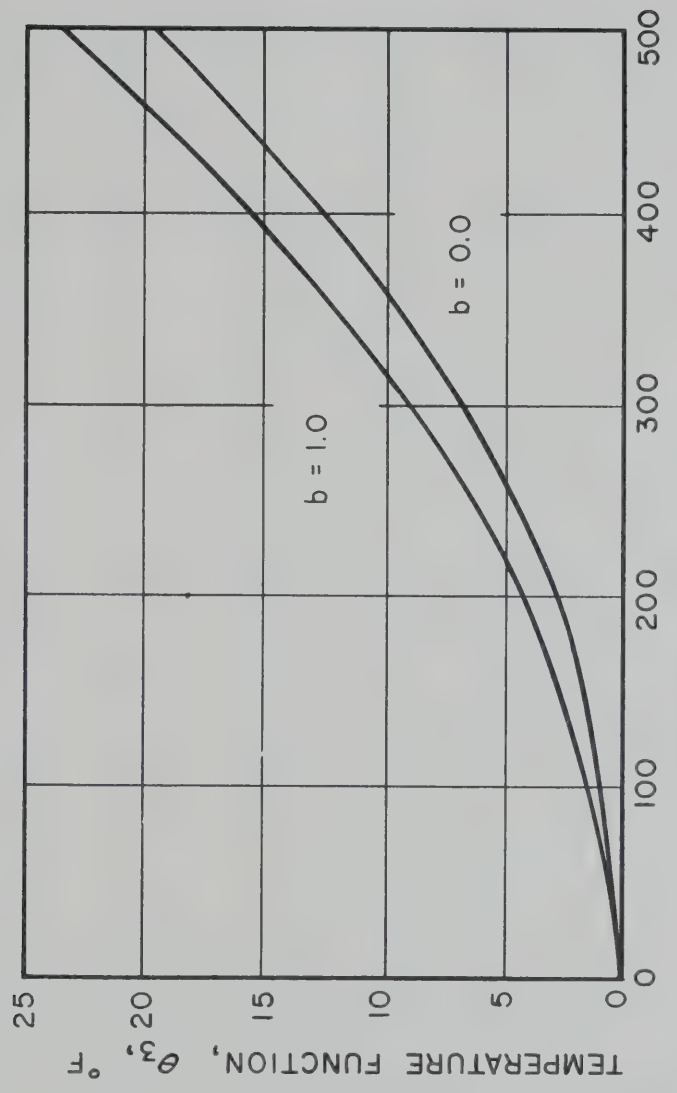
TEMPERATURE FUNCTION, θ_3, °F
25
20
15
10
5
0
0
100
200
300
400
500
STREAM VELOCITY, U_∞, FT / SEC.
b = 0.0
b = 1.0

Fig. 1C

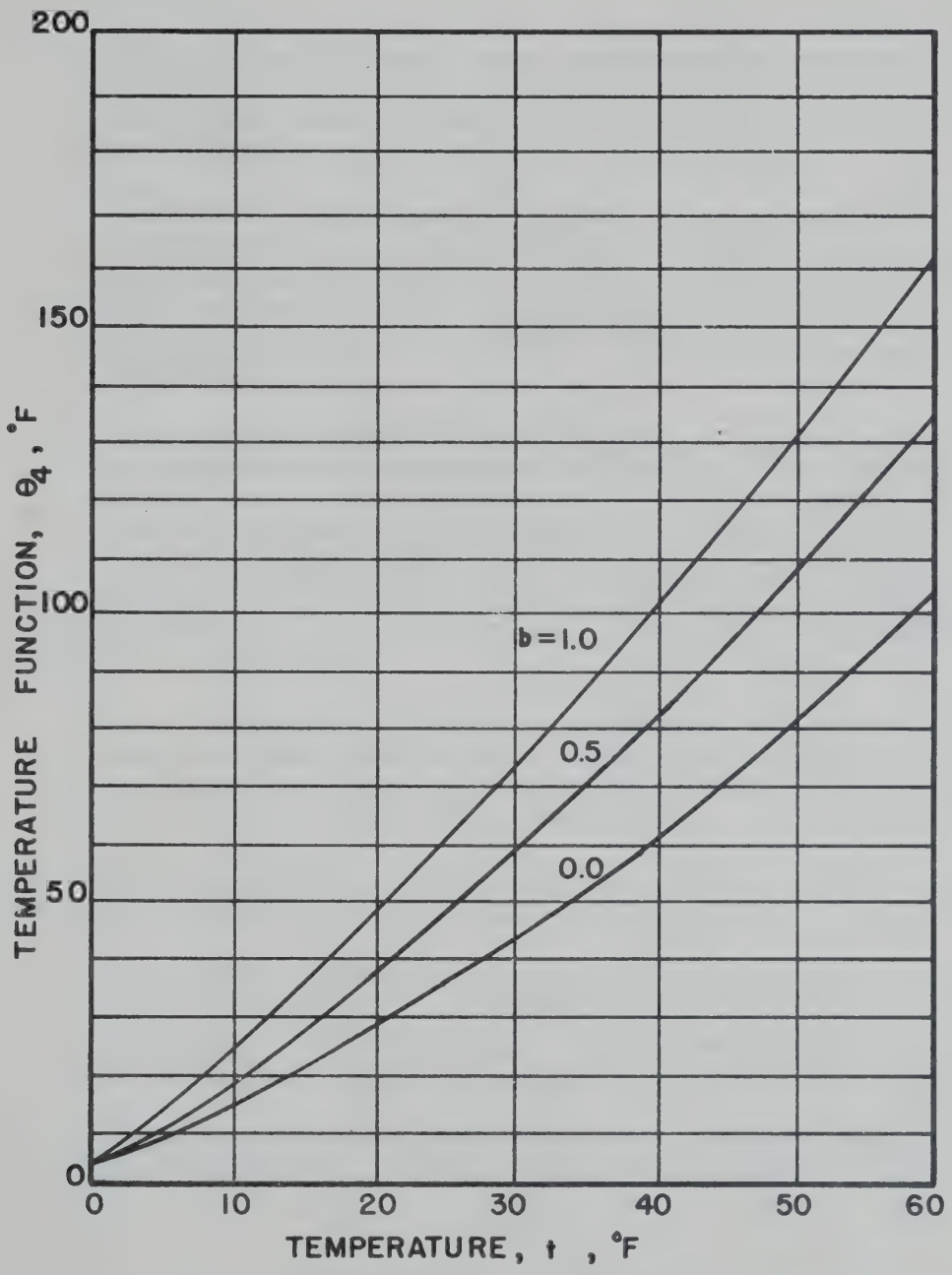

Fig. 1d Graph of θ_4 (t, B, b) = $t(1 + b) + 2.29LB^{-1}p$ for the case B = 29.9 inches of mercury, L = 1070 BTU/lb. (p corresponds to the vapor pressure of water at the temperature t)

The data of table II were obtained as follows:

A. From the given radius and rpm the tangential velocity in the propeller disc was calculated for each measuring station.

B. This velocity was added vectorially to the tunnel velocity which was reported as 120 mph for all tests, but which was not measured near the plane of the propeller during propeller operation.

C. The above resultant velocity, the blade profile data of reference 34, the average droplet size of 50 microns (approximate value) the tunnel air density and temperature were all used to compute the dimensionless moduli Ru and ψ (See nomenclature, also reference 36.)

D. Using the data of reference 31, a portion of which is reproduced in figure 2a and 2b, the rate of ice accretion on each measuring station was computed. The liquid water content of the tunnel at each radius was determined using the measured values reported in reference 34, figure 8b. (The spray devices did not produce uniform icing conditions in this portion of the tunnel.)

E. From equations given in reference 18 for laminar flow over streamlined bodies, the unit thermal conductance for heat transfer was computed. (The laminar flow values gave the best agreement.)

F. From the above values for f_c and R_w, the modulus b was computed. (See nomenclature.)

G. From the values of the resultant air velocity, free air temperature, barometric pressure and b, the functions θ_2 and θ_3 were computed using graphs similar to figures 1b and 1c.

H. Setting the heat flow equal to zero in equation 6 the function θ_1 may be computed from

$$\theta_1 = \theta_2 + \theta_3$$

I. Using this value of θ_1 and the value of b above, the value of t_s was computed using a figure similar to figure 1a.

A second test for equation 6 may also be made. Equation 6 predicts that the temperature of an unheated surface exposed to icing conditions should begin to rise when the ice begins to form.

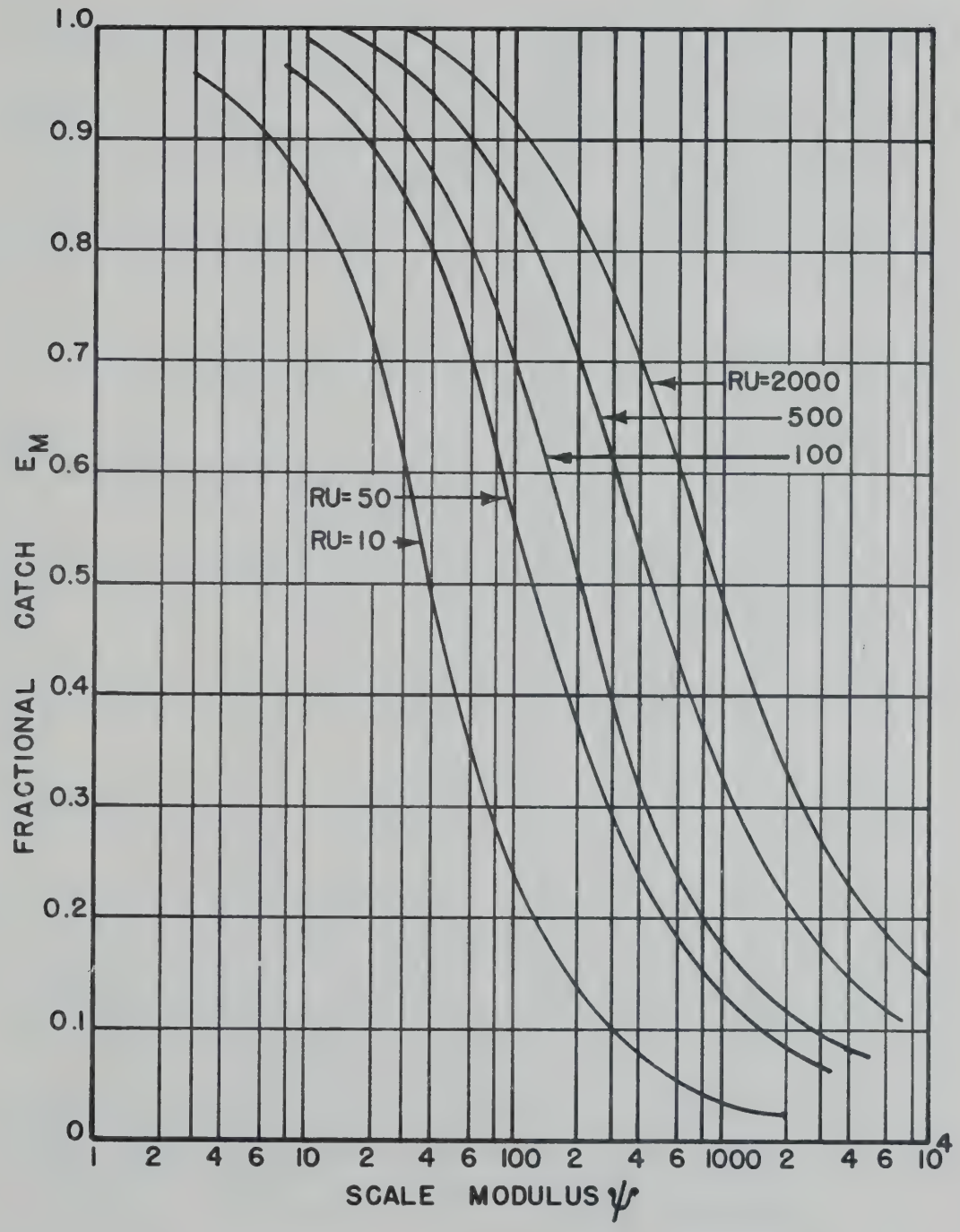
1.0
0.9
0.8
0.7
0.6
0.5
0.4
0.3
0.2
0.1
0
FRACTIONAL CATCH E_M
RU=2000
500
100
RU= 50
RU= 10
1 2 4 6 10 2 4 6 100 2 4 6 1000 2 4 6 10^4
SCALE MODULUS ψ

Fig. 2a

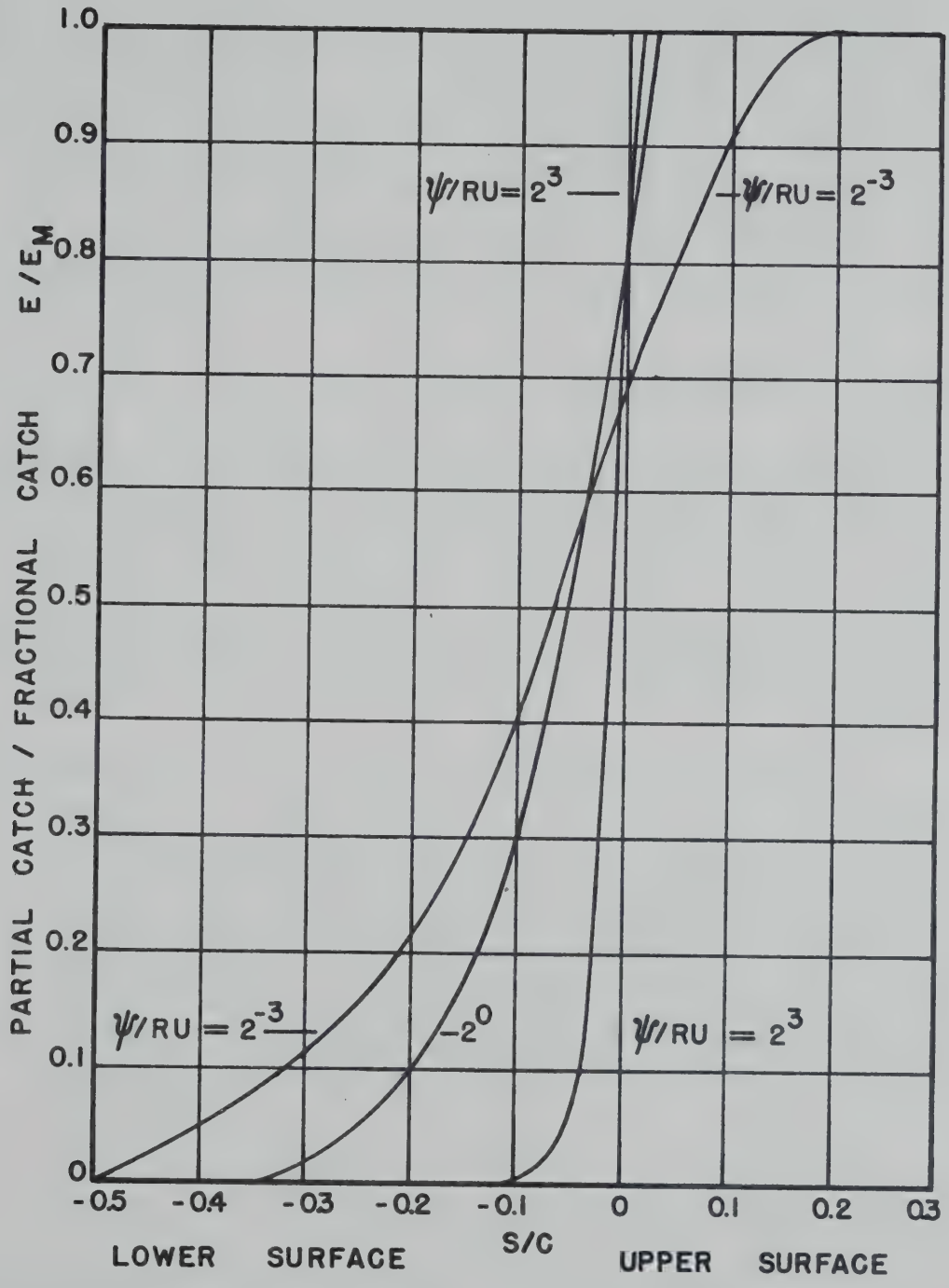
1.0
0.9
0.8
0.7
0.6
0.5
0.4
0.3
0.2
0.1
0
E/E_M
PARTIAL CATCH / FRACTIONAL CATCH
ψ/RU = 2^3
ψ/RU = 2^-3
ψ/RU = 2^-3
2^0
ψ/RU = 2^3
-0.5
-0.4
-0.3
-0.2
-0.1
0
0.1
0.2
0.3
S/C
LOWER SURFACE
UPPER SURFACE

Fig. 2b

If the rate of icing is great enough, the surface should reach 32F. Reference 9 reports data of this nature. Figures 3 and 4 are taken from reference 9 and show time temperature histories on the surface of propeller blades heated intermittently.* This interesting feature of these figures is that they show the temperature on the blade during the time the water sprays were turned on and before the heaters were energized. In figure 3 it can be seen that when the water sprays were turned on the temperature of the blade rose from 20F to 32F without the addition of heat from the heaters. This latter experiment was conducted with a relatively high liquid water content in the tunnel. Note that the temperature rise on the blade is larger than that produced by the electrical heaters. Figure 4 demonstrates a similar effect, only this time the liquid water content is much lower and the temperature does not rise to the freezing point.

TEMPERATURE VARIATIONS ON A PROPELLER WITH INTERMITTENT HEATING

Although insufficient data were available for a careful comparison between the predictions of the present analytical treatment and the temperature time measurements of Lewis (34), a few cases were considered in order to check whether the analysis would predict results yielding the same order of magnitude.

Figure 5 shows the type of heating system used by Lewis. The heating pads consisted of 0.048 inches of rubber cemented to the blades, nichrome heater wires and 0.024 inches of rubber as an outer layer.

The heat flow circuit was idealized as follows:

> Consider a small section of the blade, as in figure 6c, and note that the heat from the nichrome ribbons flows partially outward and partially inward towards the blade. The heat which flows inward flows along the steel blade to the cooler trailing edge. The heating is not steady and a good deal of energy is used in heating up the rubber and steel. For the calculations, the heat flow was postulated as occurring normal to the rubber layers in the rubber and parallel to the steel surface in the metal.

*A more detailed analysis of the data of reference 9 will be presented soon by Mr. Frederick Weiner of the Engineering Department, University of California, Los Angeles. Using the same methods as presented herein, excellent agreement between measured and predicted temperatures was obtained.

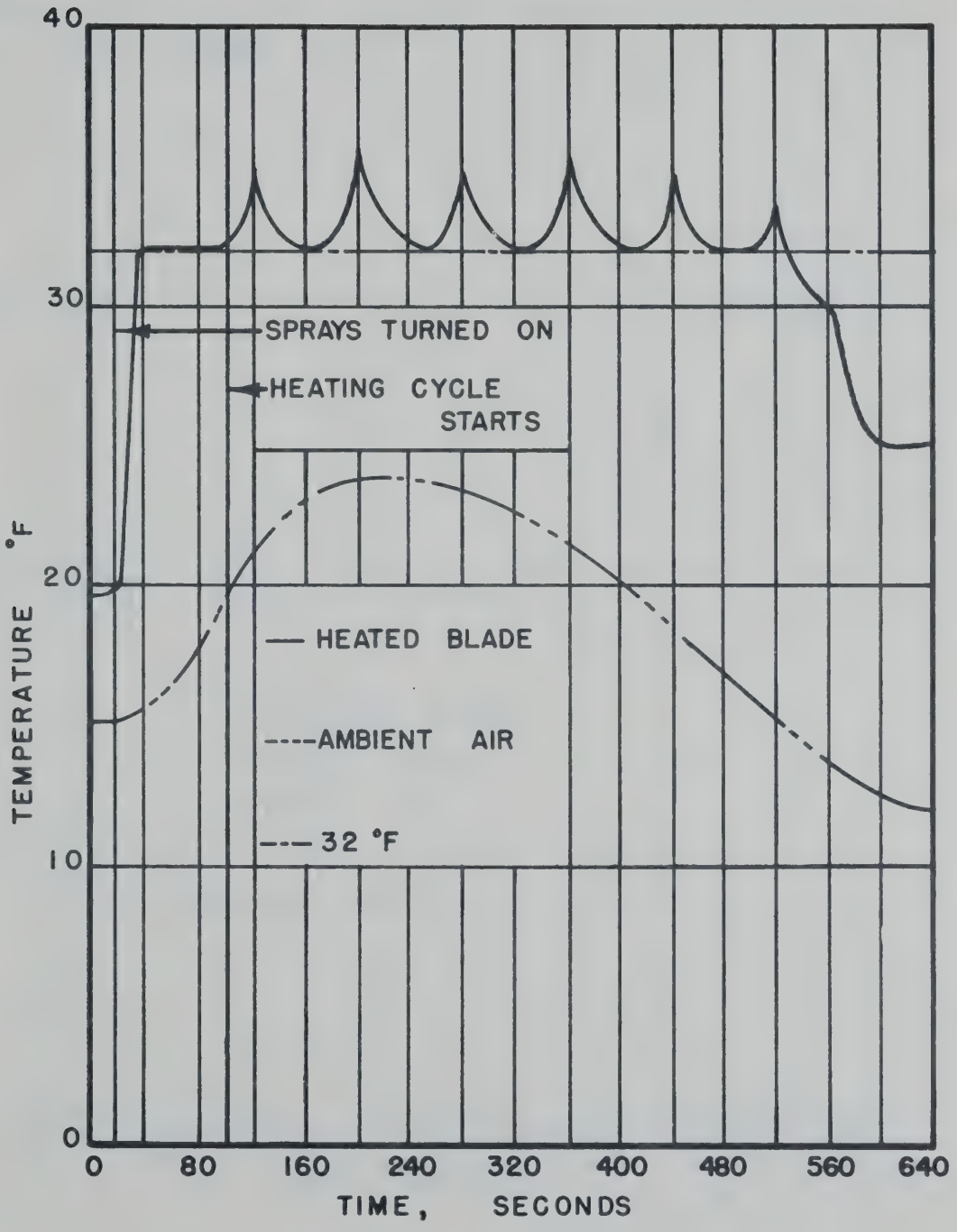

Fig. 3 Measurements by Lewis for internally heated blade. Liquid water content of air, 0.9 grams/meter^3. (From figure 10a ref. 9)

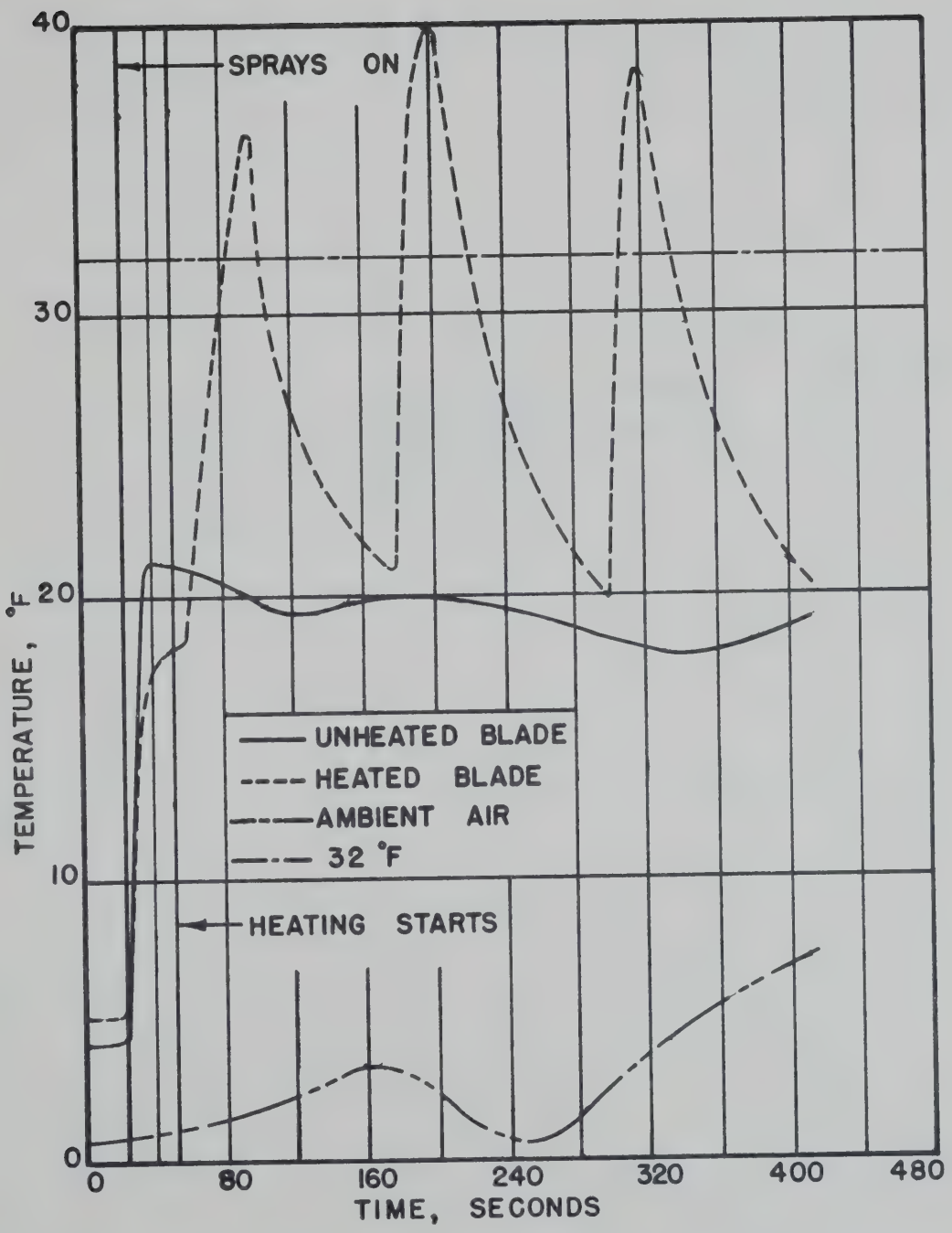

Fig. 4 Measurements by Lewis for internally heated blade. Liquid water content of air, 0.3 grams/meter^3 (From figure 10d ref. 9).

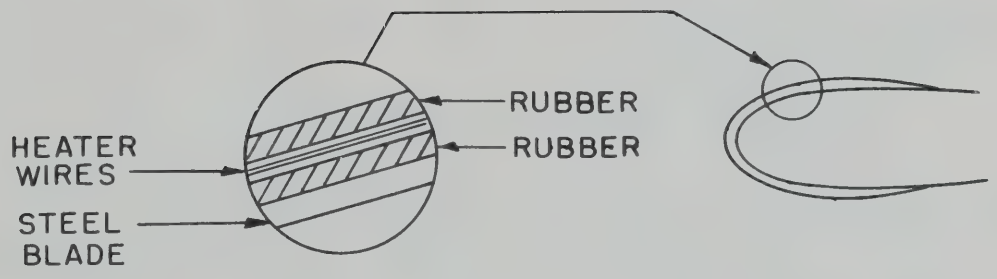

Fig. 5 Layer details of heaters used in propeller tests by Lewis. This construction is typical of presently used heaters.

The University of California Thermal Analyzer has been constructed for solving problems of the type represented by the network of figure 6. The thermal analyzer consists of a large number of resistors and capacitors conveniently arranged in a frame with terminals on a panel for ease of interconnections. The equivalent networks used in this investigation were constructed according to the relations given in Table III. A sample calculation of the values of the resistance and capacitance for one case is given in the appendix.

TABLE III

QUANTITY	ELECTRICAL	THERMAL
Flux	0.08 milliampere	3.413 BTU/hr (one watt)
Potential	4 volts	one degree Fahrenheit
Time	1/4 second	one second
Resistance	172 Kilo-ohm	one $^{o}F/(BTU/hr)$
Capacitance	5.2×10^{3} microfarad	one $BTU/^{o}F$

The heat flow from the surface of the rubber to the surroundings is not a linear function of the temperature, hence the linear elements of the thermal analyzer could not be combined to complete the network of figure 6. Figure 7 shows the rate of heat flow from various segments of a propeller blade calculated in accordance with equations 6 and 9 of this report. Figure 8 shows the non-linear network constructed to produce current-voltage characteristics analogous to figure 7. Figure 9 shows a comparison between the measured behaviour of the analogous network and the thermal system. Constant current sources and a timer were constructed to provide an analogy to the intermittently operated constant power heaters. Figure 10 shows a photograph of the thermal analyzer and the associated equipment.

The behaviour of the non-linear network was computed using equations 6 and 9 for each of the five segments of the propeller. Data for the segments were taken from drawings donated by the Curtiss Wright Corporation. A separate computation was required for each segment. The heat transfer resistance represented by the ice was omitted as small in comparison with the uncertainties in the thermal conductance due to convection.

The appendix gives the details of the computations required for one calculation.

Figures 11, 12 and 13 show comparisons between the analyzer predictions and the measurements of Lewis. Better agreement could be obtained by varying the value of the unit thermal conductance by 20% or by comparing the measured values with predicted temperatures just beneath the rubber surface, as in the case of a thermocouple imbedded in the rubber and partially insulated from

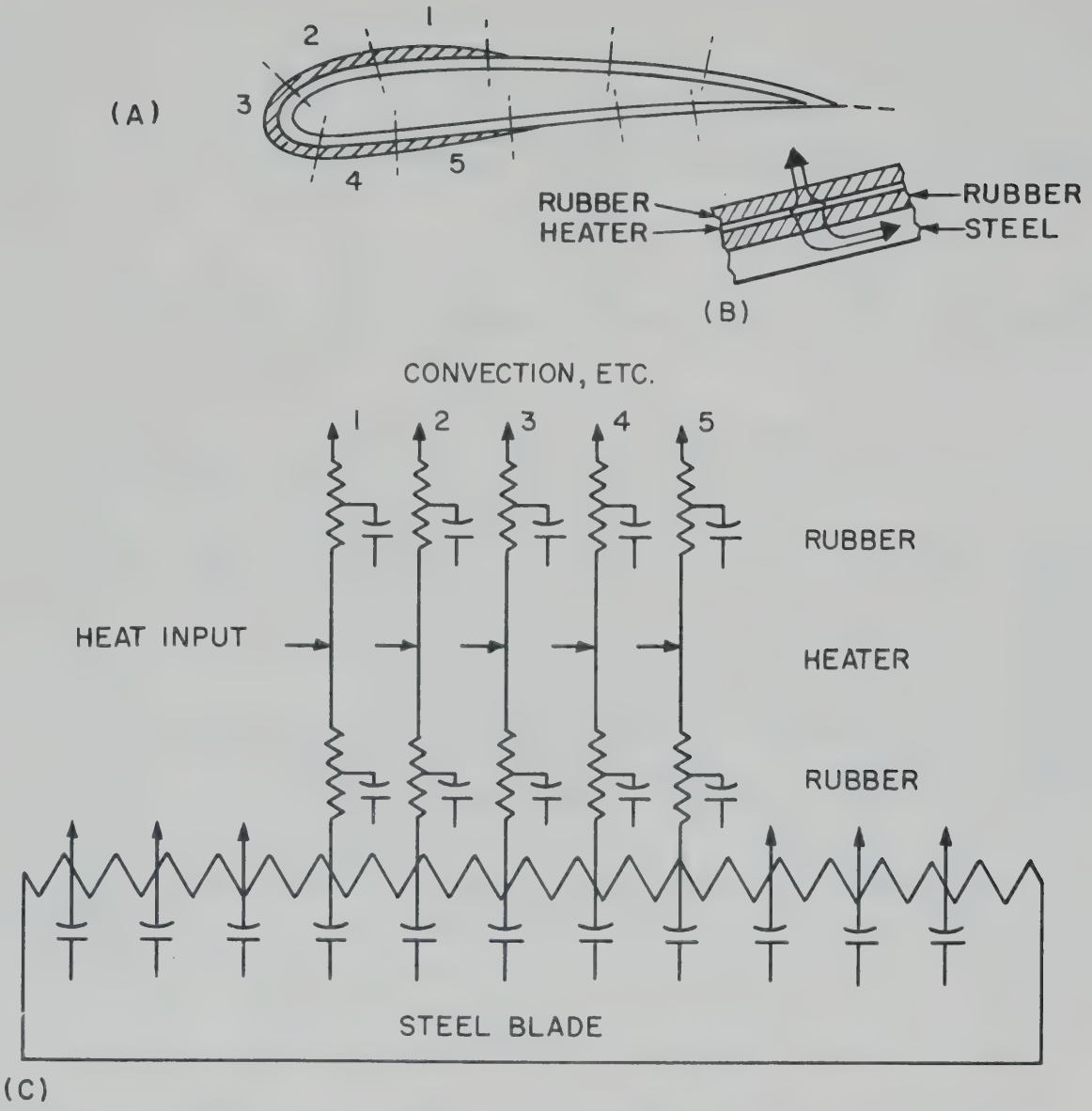

Fig. 6 Network representative of the idealized heat flow indicated by the arrows in (B) above.

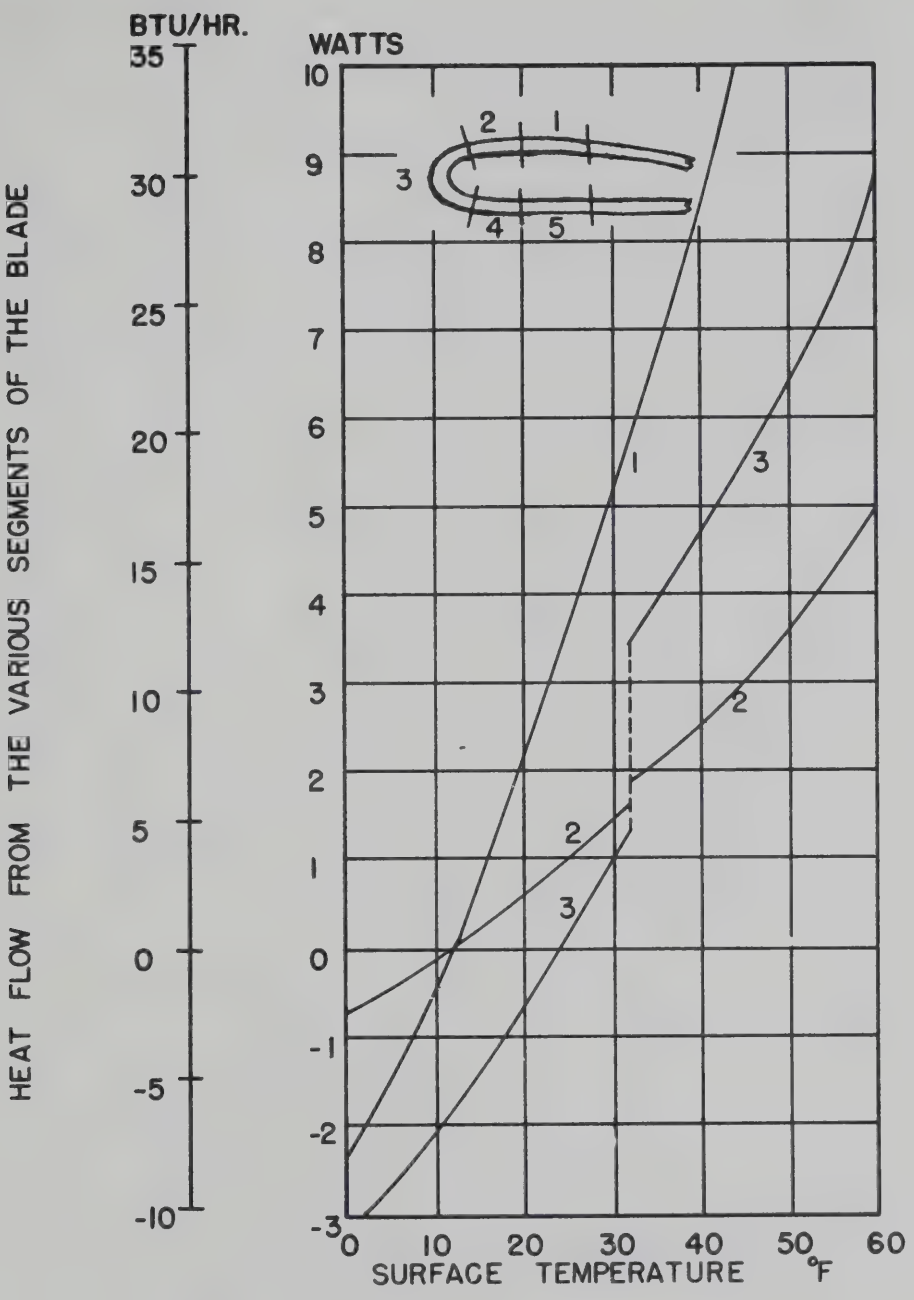

Fig. 7 Computed values for the heat flow from the segments of a propeller blade during icing conditions. (925 rpm, free stream temperature 2°F, radial station 3.02 ft, air velocity 120 mph, liquid water content 0.20 grams/cu. meter).

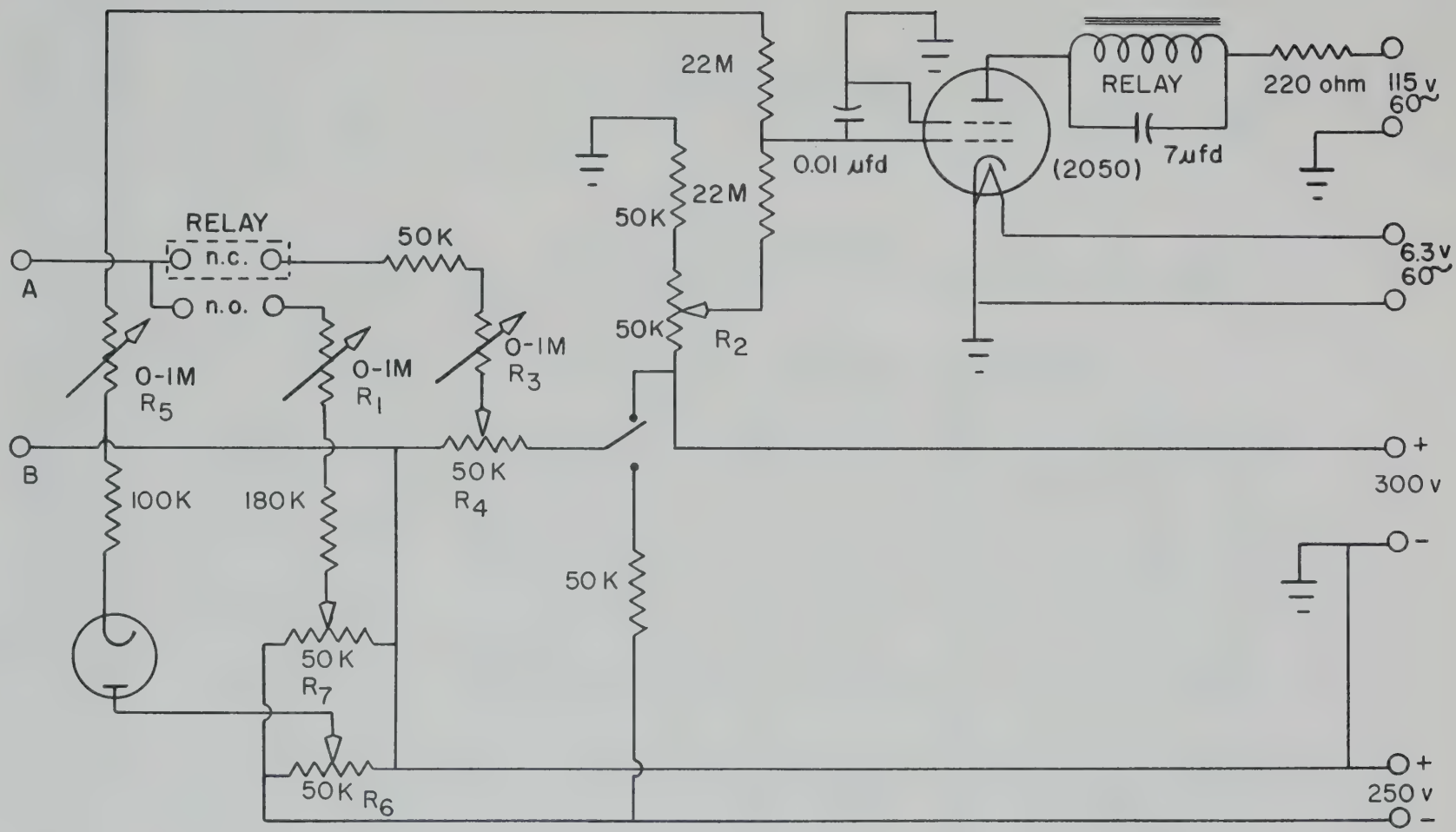

Fig. 8 Non-linear network used to represent energy flux at the ice surface.

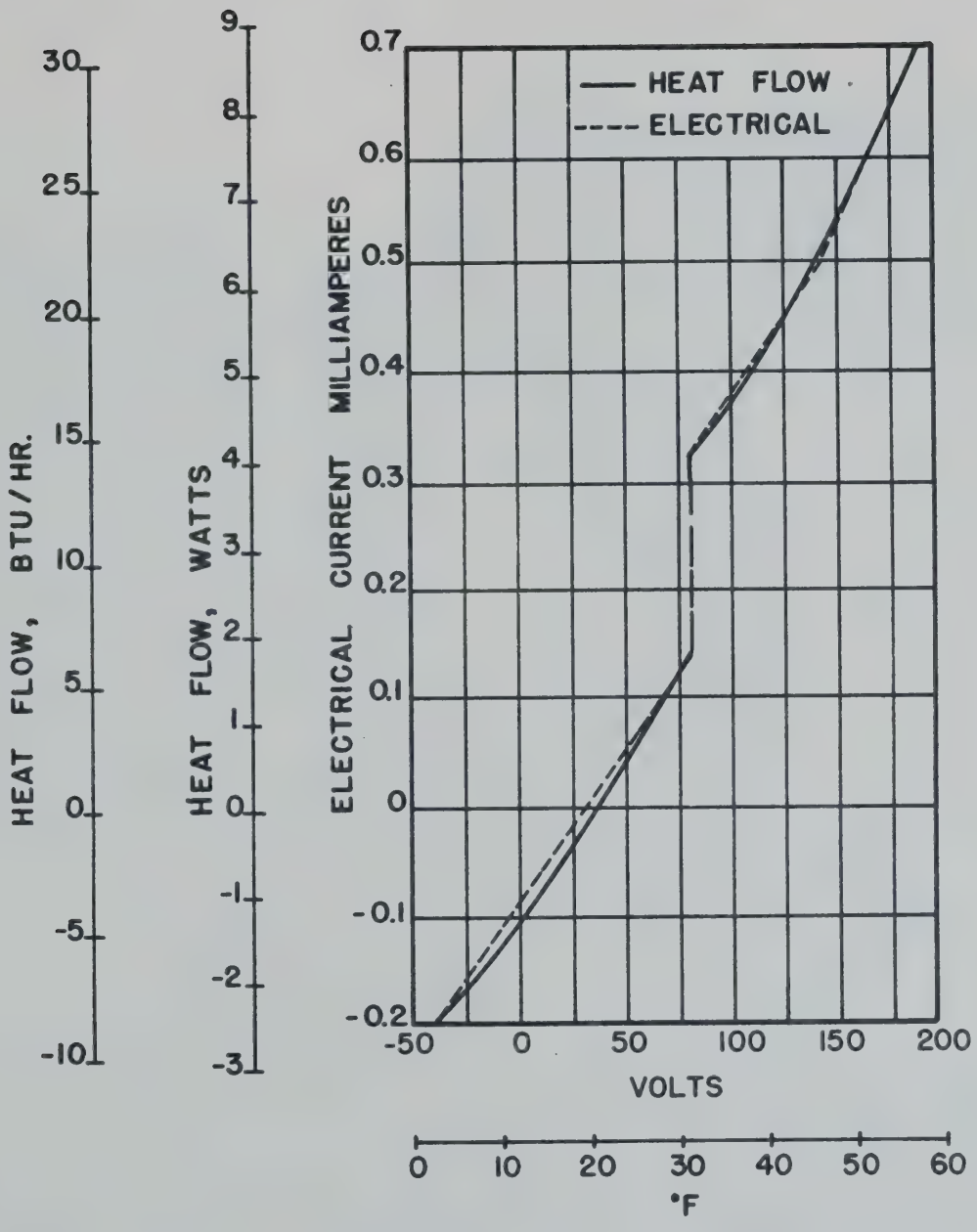

Fig. 9 Behavior or non-linear network shown in figure 8 when the parameters are adjusted to approximate the heat transfer characteristics of segment 3 of figure 7. The straight dashed line segments represent the electrical network current-voltage characteristics.

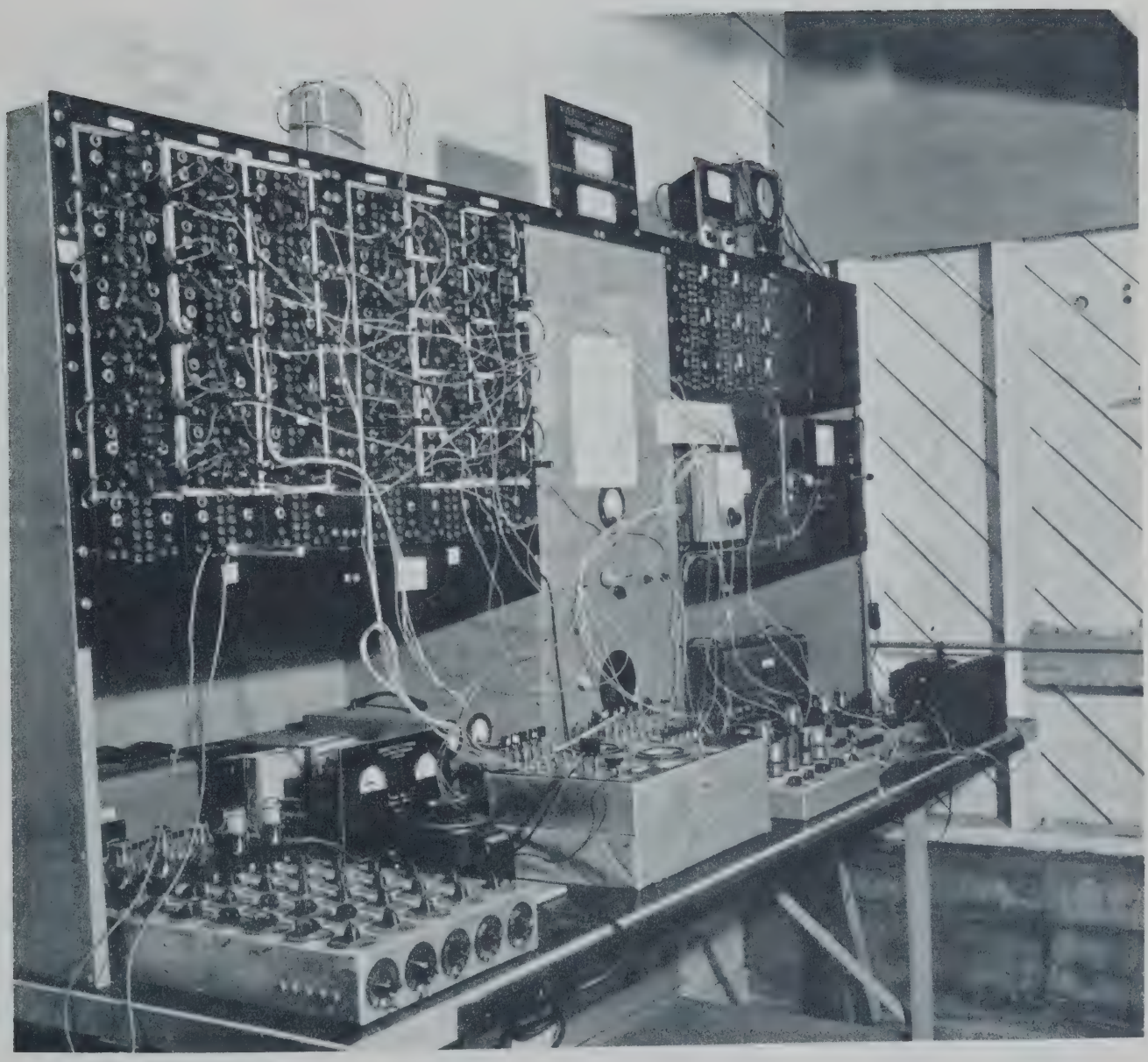

Fig. 10

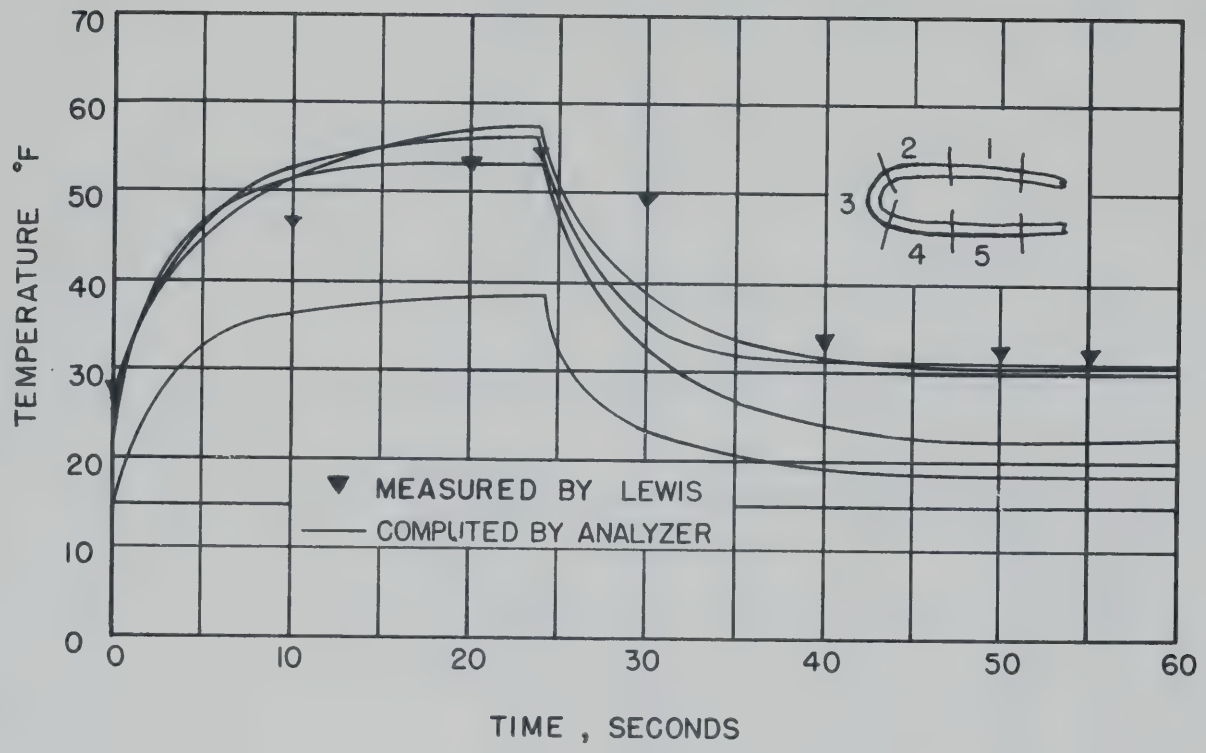

Fig. 11 Comparison between data of Lewis and Thermal Analyzer. (T_∞ = 2°F, 925 RPM, 9 watts/in^2 at seg 3, 8 watts/in^2 on 1, 2, 4, 5, r/R = 0.81) Points correspond to highest curve. See fig. 24, ref. 34.

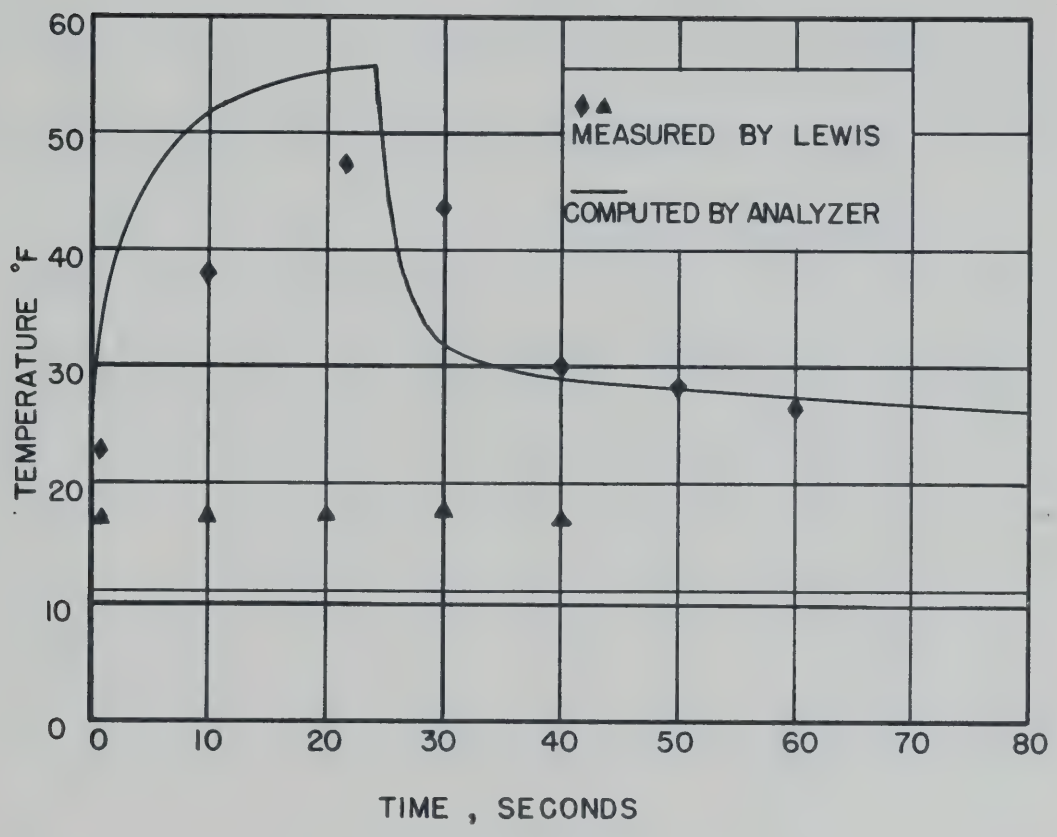

Fig. 12 Time temperature history on a propeller blade. Same conditions as figure 11 but with r/R = 0.58. The lower curve corresponds to the afterbody of the blade.

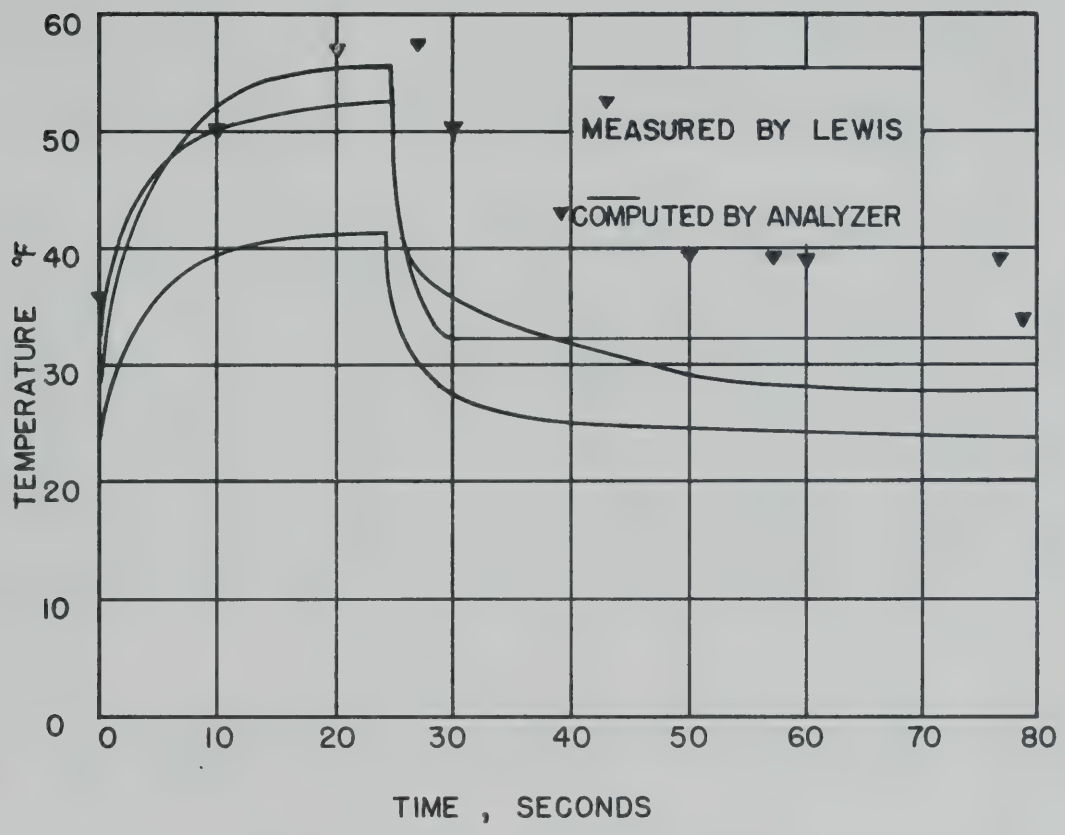

Fig. 13 Tunnel temperature 11°F, 925 rpm. See figure 30b of reference 34

the surface. Because of the many uncertainties mentioned before, no further analysis of these data was attempted.

The thermal analyzer permits easy measurement of some of the variables which are not readily determined in full scale tests on a rapidly whirling propeller. For example, figure 14 shows the rate of heat flow from the heating wires to the metal blade during one cycle. This figure is significant because it reveals that almost two-thirds of the energy put into the heating elements flows to the blade rather than the ice.

Since so much of the energy goes to heating up the blade metal, the equilibrium temperature of the blade when there is no heating assumes considerable importance. A conclusion to be drawn from this fact is that less energy should be required for ice protection as the ice accretion rate increases, all other conditions remaining the same. A search of the literature did not reveal corroborative evidence beyond the one experiment given below and taken from reference 9 since apparently this matter has not been considered important to other experimenters. Table IV demonstrates that the change in liquid water content in this test made a very great difference in the reported de-icing effectiveness. Unfortunately, these two runs are the only ones available for comparison.

TABLE IV

RUN	RPM	AIR TEMP	LIQUID WATER	HEAT ON	CYCLE TIME	HEATER POWER	DE-ICING EFFECTIVENESS
		^{o}F	$\frac{grams}{meter^3}$	seconds	seconds	watts/blade	% de-iced area
T	800	5	0.3	40	160	1,000	20-20
U	800	5	0.4	44	160	1,000	60-70

(reproduced from table II of reference 9)

This last result is of very great technical importance. The practice in testing de-icing equipment is to test under "severe" conditions. For example, reference 34 reports that the rates of icing in the tunnel were less than those recommended by the NACA. However, the recommended values are high liquid water contents in the air stream and the equipment would have shown up better in these "severe" conditions than it did in the tests as reported.

IMPROVEMENTS WHICH MAY BE MADE IN PRESENTLY OPERATING PROPELLER DE-ICERS.

Figure 15 shows a comparison of time temperature histories on a segment of a propeller blade wherein a constant energy input

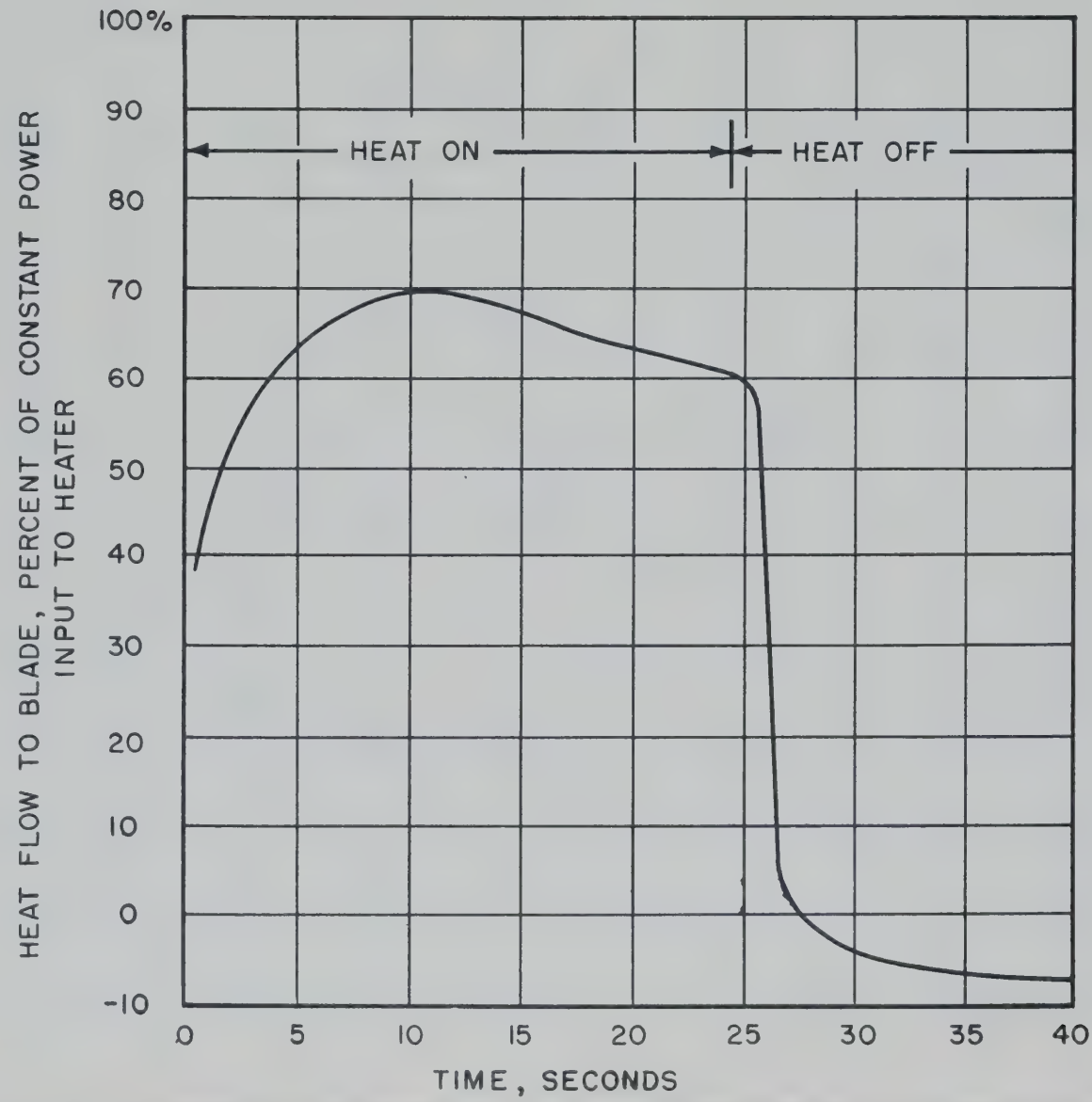

Fig. 14. Thermal analyzer data on heat flow inward to block during a cycle.

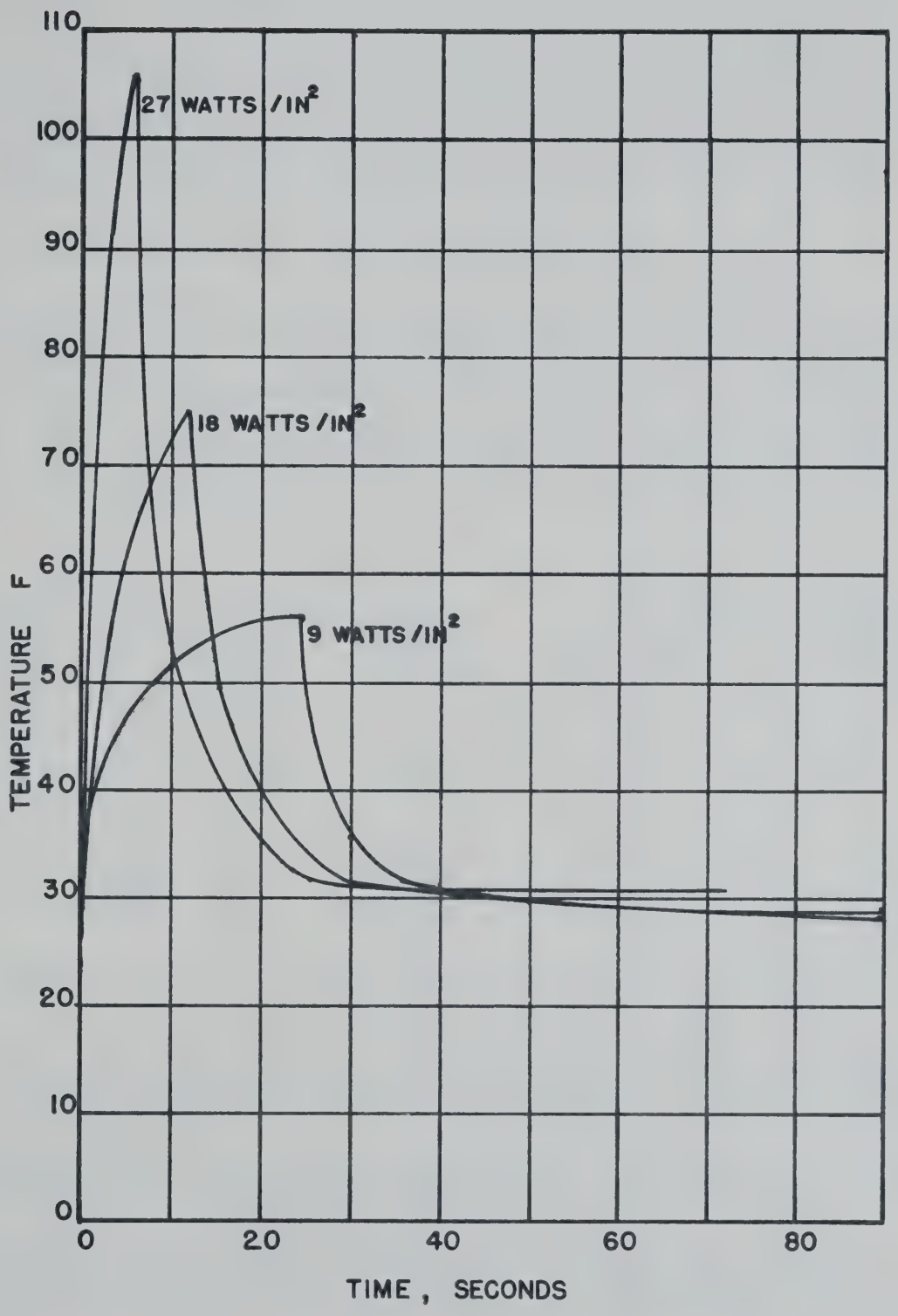

Fig. 15 Effect of varying power density at constant energy.

was maintained but the time of application was varied. If the time of application is decreased while the power is increased the surface temperatures rise to higher values. Considerable improvement in ice protection should result, then, if the propeller is divided into three sections and instead of being heated with 10 watts/ sq. inch for twenty seconds, is heated one section at a time with a power density of 30 watts/ sq. inch for 6.6 seconds. The airplane's electrical system would have to supply the same amount of power but the protection would be enhanced.

AN APPLICATION TO JET ENGINE GUIDE VANE DE-ICING.

Figures 16a and 16b show a jet engine guide vane and the method of constructing the analogous electrical circuit representing the heat flow paths when electrical heating is applied to the guide vane. The configuration chosen for detailed study on the analyzer was a guide vane with the heat applied uniformly to the leading edge only. (It turns out that this is not an efficient heat distribution). Table V indicates the cases chosen for study of the guide vane de-icing problems.

TABLE V*

CASE	AIR TEMP. AT BLADE	ICING RATE	AIR VELOCITY PAST BLADE	LIQUID WATER CONTENT	UNIT THERMAL CONDUCTANCE LEADING EDGE	TRAILING EDGE
	^{o}F	in/min	ft/sec	$\frac{\text{grams}}{(\text{meter})^3}$	BTU/hr sq ft ^{o}F	
I	2	0.035	463	0.10	50	92
II	2	0.14	463	0.38	50	92
III	11	0.042	175	0.30	30	42
IV	11	0.14	175	1.00	30	42

The surface area, both sides, for each segment, leading or trailing edge, was 7.63×10^{-3} sq ft.

Figure 17 shows the computed heat flow characteristics while Figure 18 shows the completed electrical network. Figures 19a and 19b, show typical data.

CONCLUSIONS CONCERNING THE ENERGY REQUIREMENTS FOR JET ENGINE GUIDE VANE DE-ICING.

The analysis of the data obtained from the thermal analyzer for the stainless steel guide vane indicates that the spanwise heat con-

*The peculiar mixture of units appearing in this table is the result of the present state of the art in ice prevention. The meteorologist reports data in the CGS system while the icing observers are habituated to measuring ice accretion in inches/minute.

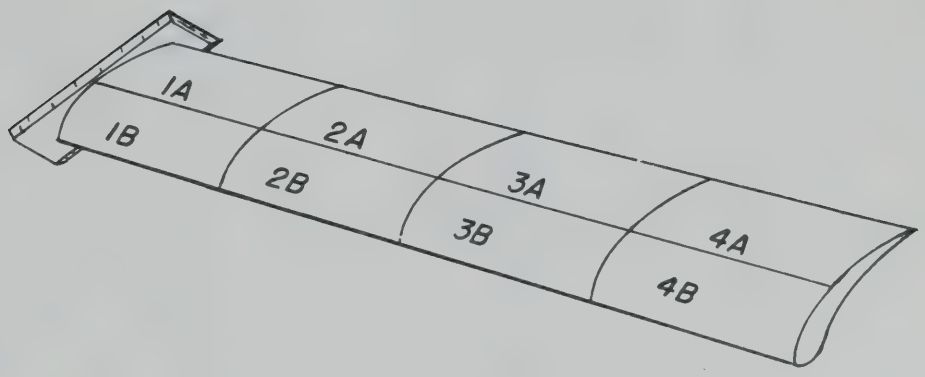

Fig. 16a

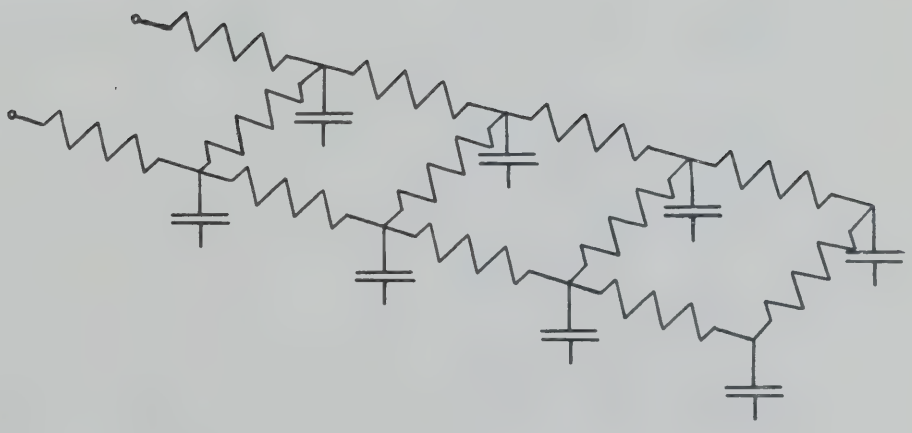

Fig. 16b

Fig. 16 Typical guide vane (A) and equivalent network (B).

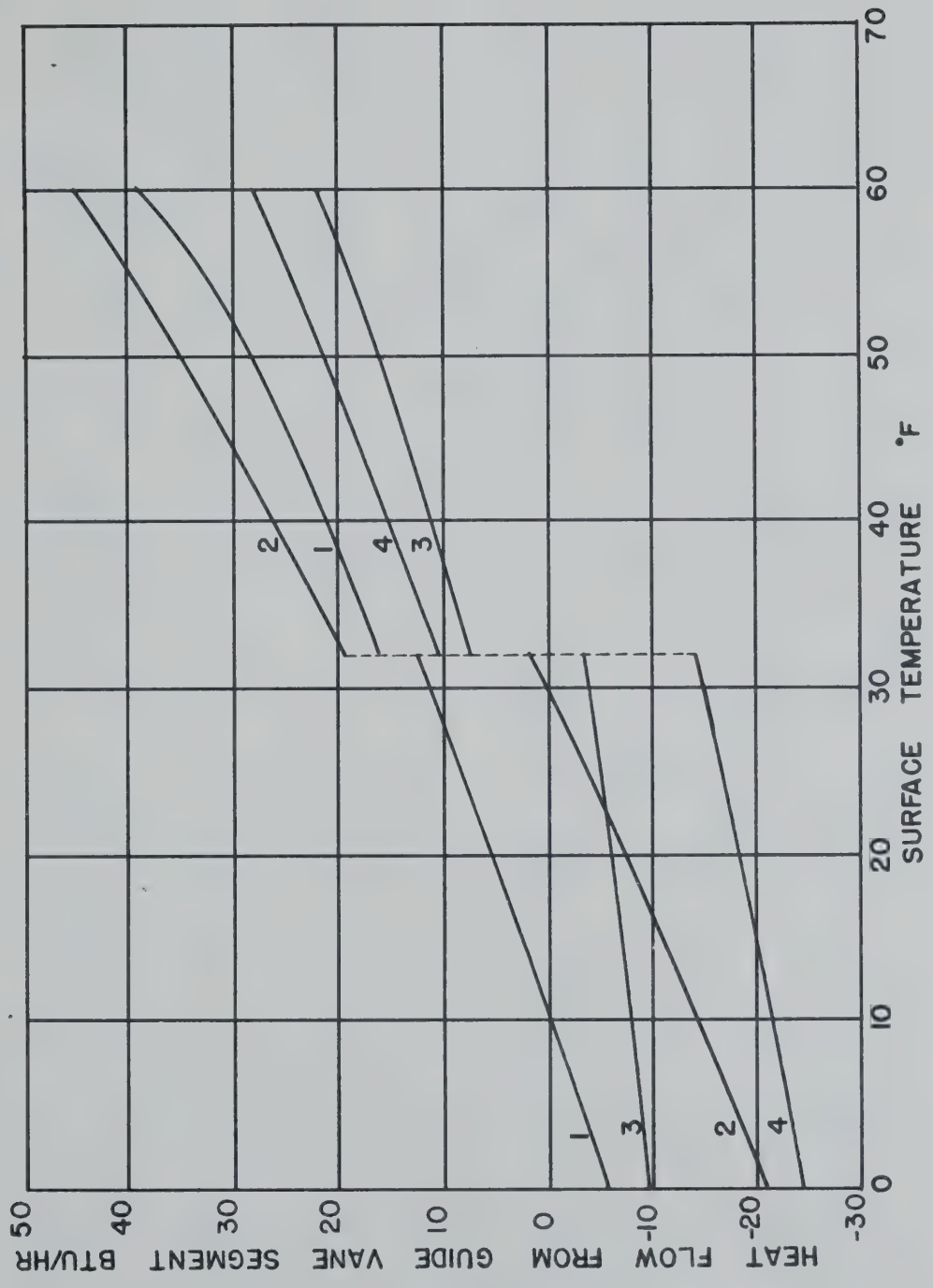

Fig. 17 Heat flow from guide vane leading edge half for conditions given in table V.

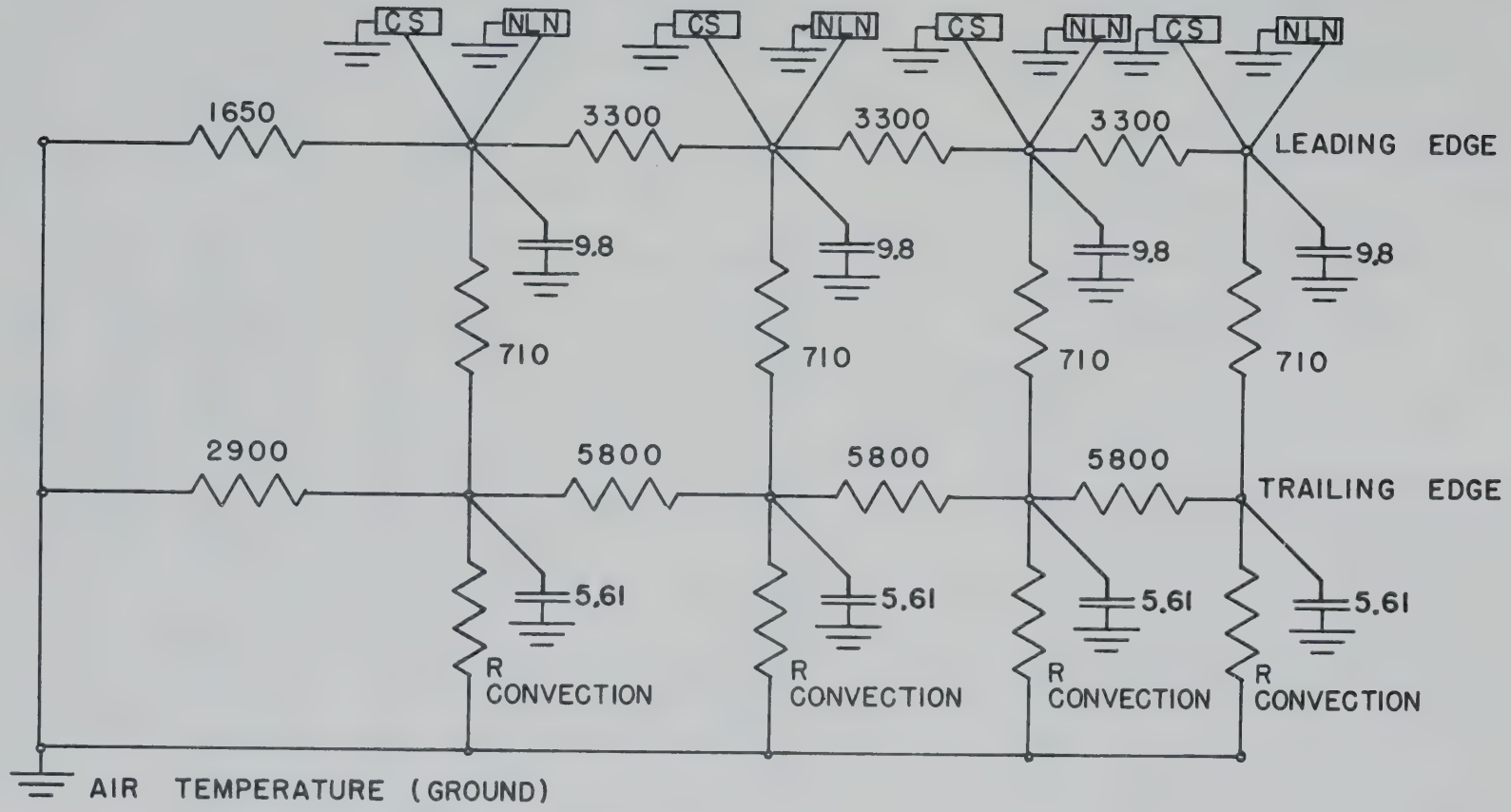

Fig. 18 Completed network for guide vane. Ice impingement was considered as occurring only over leading edge in the calculations.

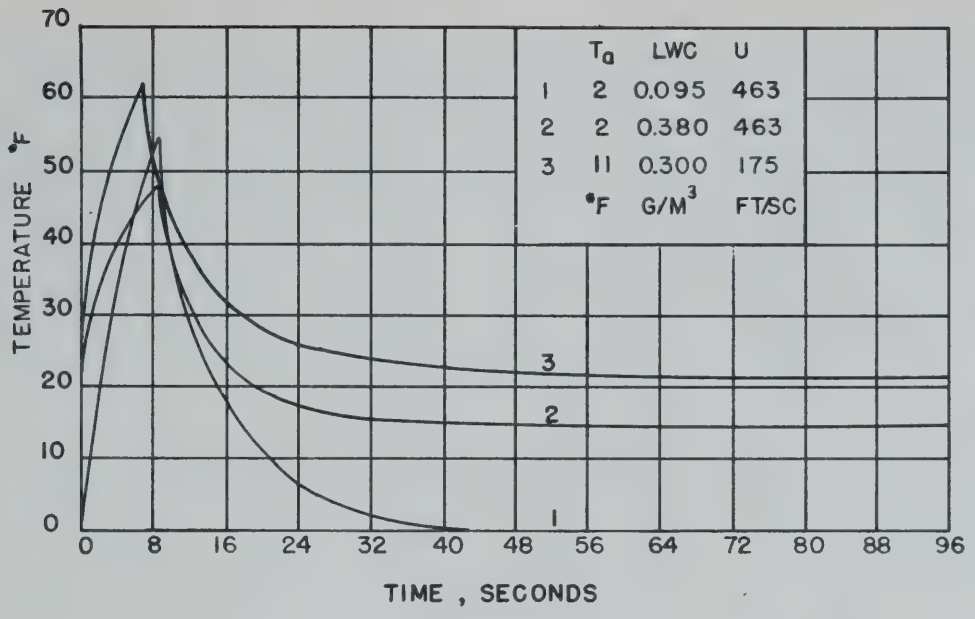

Fig. 19a

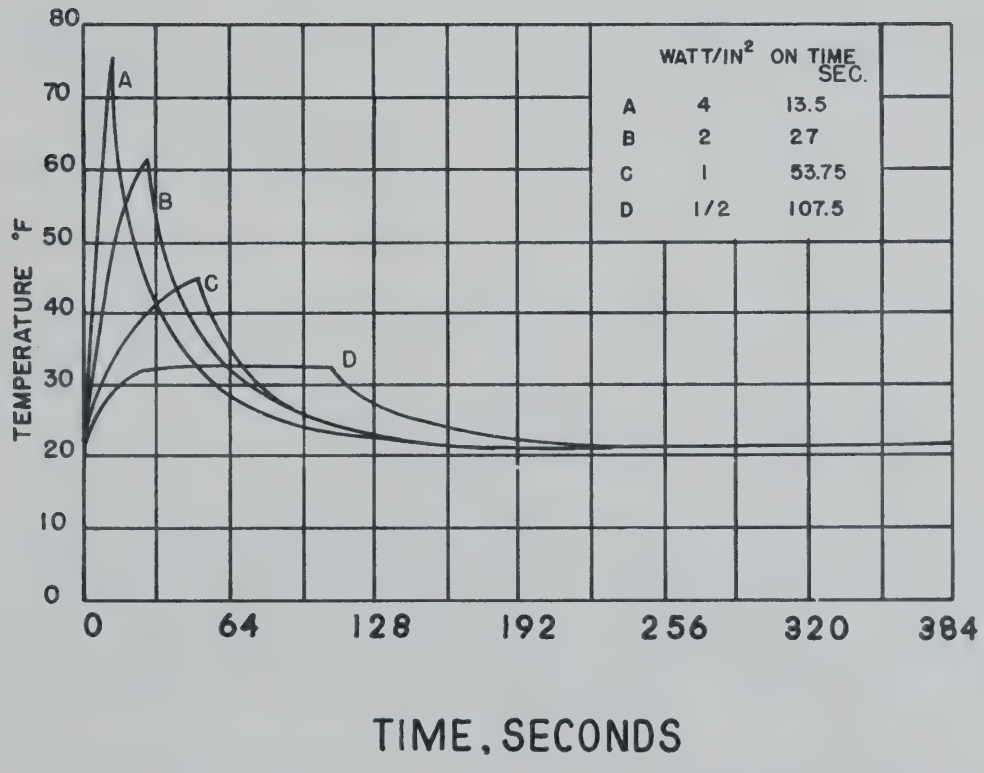

Fig. 19b

Fig. 19 Typical data obtained from analyzer. In fig. 19a, the power density was 4 watts/in^2. In figure 19b, T_∞ = 11°F, U_∞ = 175 ft/sec LWC = 0.300

duction is not very large and that if the entire vane is subjected to icing conditions, the entire vane must be heated. The most economical heating system will be one which does not heat any portion of the blade hotter than the average temperature. Such a system yields a very simple type of thermal network for the conduction of heat between the segments may then be put equal to zero. The circuit representation of figure 18 may then be simplified to the diagram figure 20. A conservative design results if the non-linear network is replaced by a linear element having an impedance equal to the lowest value occurring during the cycle. Figure 21 then shows the conservative simplified circuit.

The lowest value of the impedance occurs when the highest temperature is attained across the non-linear portion of the thermal network. In a good design the maximum surface temperature will be in the neighborhood of $32^{o}F$. Page 101 of reference 28 shows at this surface temperature that at sea level and low outside air temperature the evaporative term accounts for 30% as much heat transfer as the convective term in the energy flows at the surface of the ice. The benefits from the heat of fusion are zero at this temperature. The lowest resistance across the non-linear portion of the network is therefore taken equal to $(1/1.3)\ (1/f_c A)$. The maximum energy requirements for ice prevention will occur at low temperatures and when the rate of ice accretion is very low. In arriving at the conservative design, then, the contributions from the heat of fusion will be put equal to zero.

The time temperature variation in a circuit such as shown in figure 21 is given by:

$$\frac{\Delta t}{qR} = 1 - e^{-\theta/RC} \qquad (10)$$

Solving the above equation for q and multiplying both sides by time, θ, yields:

$$q\theta = C\Delta t \left[(\theta/RC) / (1 - e^{-\theta/RC}) \right] \qquad (11)$$

The total energy required, then, is proportional to the thermal capacitance of the vane multiplied by the temperature rise and multiplied by a function of the dimensionless heating time. Figure 22 shows the variation in energy required versus dimensionless heating time. The minimum energy required, of course, is the energy required to heat the guide vane through the stipulated temperature rise.

From figure 22 it is seen that the total energy required diminishes with decreasing heating periods. That is, short intervals of high power application are more effective than longer intervals at low powers. The graph indicates that little gain is

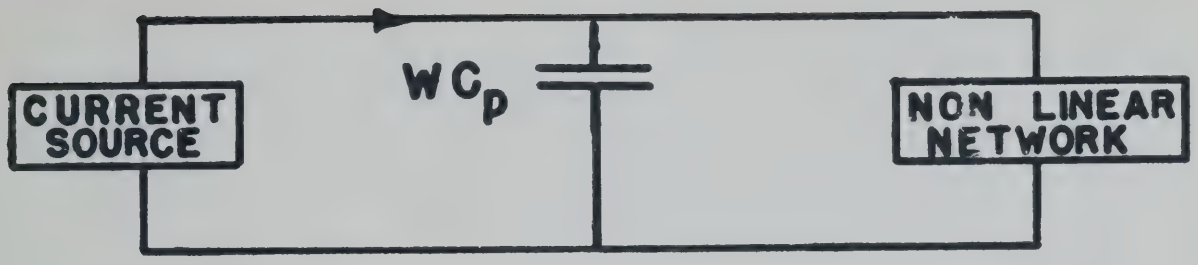

Fig. 20 Simplified representation of thermal circuit for efficiently heated guide vane.

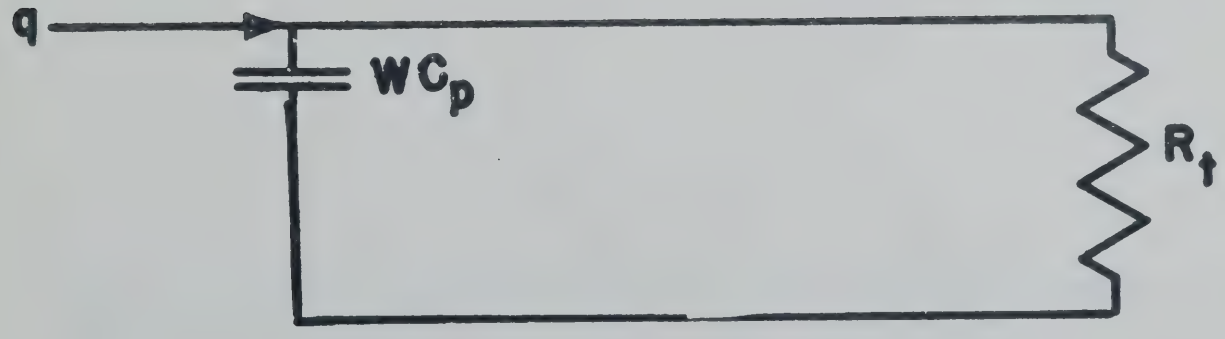

Fig. 21 A conservative simplified network for the efficiently heated guide vane.

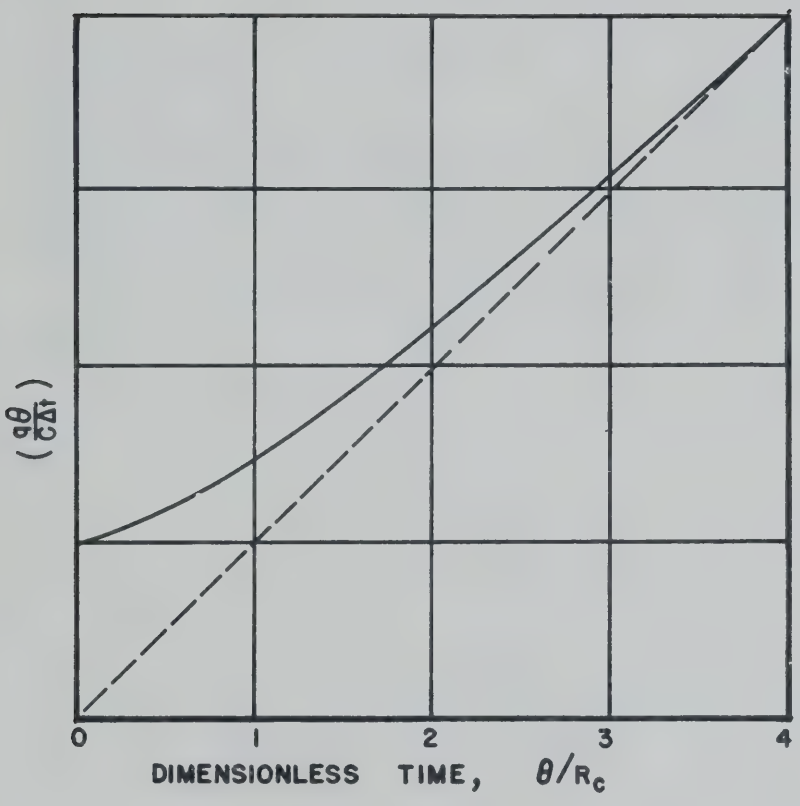

Fig. 22 Energy requirements for guide vane de-icing as a function of heating time.

had in taking the dimensionless time less than 0.10. For very short heating times, however, the correspondence between the distributed system behavior and the network approximation will be less close. The deviations, however, will be such as to yield a conservative design.

As an example of the application of the above results, consider a guide vane where the following conditions obtain (as in case I, table V.)

Unit thermal conductance	66 BTU/hr sq ft ^{o}F
Surface area	15.26×10^{-3} sq ft
Ambient temperature	-40^{o}F
Dimensionless heating time	0.1
(Thus requiring 1.05 times the minimum energy)	
Weight of guide vane	0.13 pounds
Unit Heat Capacity of guide vane	0.1 BTU/ lb ^{o}F
Design temperature rise (to 35^{o}F)	75^{o}F

Therefore,

$$q\theta = 1.05\ C\Delta t$$

$$= 1.05 \times 0.13 \times 0.1 \times 75$$

$$= 1.03 \text{ BTU/ blade cycle}$$

$$\theta = 0.1\ RC$$

$$R = (1/1.3)\ (1/66)\ (1/15.26)\ 10^{3} \quad {}^{\circ}F/(BTU/hr)$$

$$C = 0.13 \times 0.1 \text{ BTU/}{}^{\circ}F$$

$$\theta = \frac{0.1 \times 0.13 \times 0.1}{1.3 \times 66 \times 15.2}\ 10^{3}$$

$$= 1.02 \times 10^{-3} \text{ hr} = 3.6 \text{ seconds}$$

$$q = \frac{1.03}{1.02} \times 10^{3} = 1.01 \times 10^{3} \text{ BTU/hr} = 296 \text{ watts}$$

If each guide vane is to be unheated (and, therefore, permitted to gather ice) for a maximum time of one minute and there are 51 guide vanes per engine, they may be heated in groups of three with a continuous power required from the airplane of less than one kilowatt. It may be found more economical from the point of view of saving weight to use a greater amount of power than seventeen separate connections might permit. This is a matter of special consideration for each installation.

The power required for ice prevention may be further reduced by designing the blades in such a way as to diminish their thermal capacitance. Fewer blades, each blade of larger dimensions and possibly hollow blades might be utilized to diminish the energy requirements. The larger blades will have lower values of unit thermal conductance. The application of the heating elements in such a way as to partially insulate them thermally from the vane will also serve to reduce the energy requirements.

ACKNOWLEDGEMENTS

The writer wishes to acknowledge the many time saving suggestions made by Mr. H. R. Kaiser with regard to the design of the electrical equipment and the efforts of Mr. James DuBois in constructing the equipment. Thanks are due to the other members of the research staff of the Department of Engineering of the University of California for loan of equipment and to the Department of Engineering for sponsoring the project.

Professor L. M. K. Boelter and other members of my Doctoral Committee are to be thanked for suggestions concerning the research and presentation of the results.

The Curtiss Wright Corporation and the Hamilton Standard Propeller Company supplied reports and sample propellers with heaters for inspection and study.

Mr. Frederick Weiner, a graduate student at the University of California, kindly read and corrected the manuscript prior to publication. His own analysis of the internally heated propeller will be published shortly.

Special thanks are due Mrs. Tribus who patiently helped with the calculations, test runs, construction of equipment and proof reading of the report.

REFERENCES AND BIBLIOGRAPHY

1. Eder, Franz "Theory of Propeller De-Icing," AMC Translation F-TS-940-RE (From captured German document ZWB-FB-RE-11-5 S 123)

2. Eck, E. "Propeller Icing and Its Prevention," AAF Translation 517, October 21, 1944.

3. Scherrer, Richard "An Analytical Investigation of Thermal Electric Means of Preventing Ice Formation on a Propeller Blade," NACA ACR No. 4H31, 1944.

4. Scherrer, Richard and Rodert, Lewis A. "Tests of Thermal Electric De-Icing Equipment for Propellers," NACA ARR No. 4A20, 1944.

5. Sheets, J. H. "C633S-A Propeller De-Icing Tests," Curtiss Wright Corporation, Propeller Division, Caldwell, New Jersey, Company report C-1907, February 18, 1948.

6. Schulze, J. O. "Outrigger Flight Tests to Determine the De-Icing Power Requirements of Several Propeller Heating Elements Having Chosen Heat Distributions and Operated Cyclically," AAF Technical Report 5445. March 22, 1946.

7. Reaser, W. W. "Flight Tests of Hamilton Electrically Heated Propellers on DC 6 Number NX-37051," Douglas Aircraft Company Report, SM 12091, March 19, 1947.

8. Alford, W. M. "Flight Test of 50 Inch Blade Heaters (HSP 70101 on 23E50/6491A-0 Propeller)" Hamilton Standard Propeller Company, Report HSP 547, April 10, 1947.

9. Lewis, James P. and Stevens, H. C. Jr., "Icing and De-Icing of a Propeller with Internal Electric Blade Heaters," NACA TN 1691, August, 1948.

10. Eckert, E. "Heat Transmission of Bodies in Rapidly Flowing Gases," AAF Intelligence Report (T-2 Progress Report No. 46, Wright Field, February 28, 1946).

11. Wood, G. P. and Brevoort, M. J. "Design and Selection and Installation of Aircraft Heat Exchangers," NACA ARR 3G31, 1943.

12. Johnson, H. A. et al "Bibliography of Aerodynamic Heating and Related Subjects," AAF Tech Report 5633, Sept. 10, 1947.

13. Johnson, H. A. et al "A Design Manual for Determining the Thermal Characteristics of High Speed Aircraft," AAF TR 5632 Sept. 10, 1947.

14. "Elementary Heat Transfer," UC Syllabus 305, UC Press Berkeley 4, California.

15. McAdams, W. H. "Heat Transmission," McGraw Hill Book Company.

16. Frick, Charles W. and McCullough, George B. "A Method for Determining the Rate of Heat Transfer from a Wing or Streamline Body," NACA ACR December, 1942.

17. Allen, H. J. and Look, B. C. "A method for Calculating Heat Transfer in the Laminar Flow Region of Bodies," NACA ARR December, 1942.

18. Martinelli, R. C. et al., "An Investigation of Aircraft Heaters VIII A Simplified Method for the Calculation of the Unit Thermal Conductance over Wings," NACA ARR March, 1943.

19. Tribus, M. "Report on the Development and Application of Heated Wings," SAE Journal, June, 1946.

20. Boelter, L. M. K. et al., "An Investigation of Aircraft Heaters XVIII A Design Manual for Exhaust Gas and Air Heat Exchangers," NACA ARR 5A06 August, 1945.

21. Moore, Lyle L. "A Solution of the Laminar Boundary Layer Equations for a Compressible Fluid with Variable Properties Including Dissociation" Master's Thesis, University of California, Los Angeles, February, 1949.

22. Walker, W. H., Lewis, W. K., McAdams, W. H. and Gilliland, E. R., "Principles of Chemical Engineering," McGraw Hill Book Co. 1937 (p. 592).

23. Boelter, L.M.K., et al., "Heat Transfer Notes," University of California Press, Berkeley, 1946.

24. Schaefer, Vincent J. "Man Made Snow", Mech. Eng. January 47.

25. Marks, Lionel S. "Mechanical Engineers Handbook," McGraw Hill Co.

26. Langmuir, I. "The Cooling of Cylinders by Fog Moving at High Velocities," General Electric Company Report, March, 1945.

27. Langmuir, I. and Blodgett, K. "Mathematical Investigation of Water Droplet Trajectories," AAF TR 5418.

28. Tribus, M. and Tessman, J. "Report on the Development and Application of Heated Wings - Addendum I," AAF TR 4972 1946.

29. Bergrun, N. R. "A Method for Numerically Calculating the Area and Distribution of Water Impingement on the Leading Edge of an Airfoil in a Cloud," NACA TN 1937.

30. Glauert, Muriel, "A Method of Constructing the Paths of Raindrops of Different Diameters Moving in the Neighborhood of (1) a circular cylinder (2) and aerofoil, Placed in a Uniform stream of Air," R. and M. 2025, British ARC 1940.

31. Guibert, A. G. et al., "Impingement of Waterdrops on Various Airfoils from Trajectories obtained on Differential Analyzer," NACA RM 9A05 Feb. 16, 1949.

32. Tribus, Myron, et al., "Analysis of Heat Transfer over a Small Cylinder in Icing Conditions on Mount Washington," ASME Trans November 1948.

33. Tribus, Myron "A Review of Some German Developments in Airplane Anti-Icing," ASME Trans July 1947.

34. Lewis, J. P. "De-Icing Effectiveness of External Electric Heaters for Propeller Blades," NACA TN 1520 February 1948.

35. Drake, R. M. "Investigation of the Variation of Point Unit Heat Transfer Coefficients for Laminar Flow Over an Inclined Flat Plate," Jour. App. Mech. Paper 48-A-2.

36. Tribus, M., Young, G. and Boelter, L. M. K. "The Limitations and Mathematical Basis for Predicting Aircraft Icing Characteristics from Scale Model Studies," ASME Trans November 1948.

37. Bergrun, N. R. "General Results of NACA Flight Research in Natural Icing Conditions During the Winters of 1945 and 1946," Aero. Eng. Rev. January 1948.

38. North, David "Heat Anti Icing for the Airlines," ASME Paper 48SA 40.

39. Neel, Carr B. et al., "The Calculation of the Heat Required for Wing Thermal Ice Prevention in Specified Icing Conditions," NACA TN 1472 Dec. 1947.

APPENDIX

A SAMPLE CALCULATION FOR THE CASE SHOWN IN FIGURE 11.

The following will serve to outline the calculations required to permit adjustment of the thermal analyzer to produce the data shown in this report.

Briefly, from the geometrical data given in reference 34 the blade characteristics may be determined. Since the exact blade construction was not specified a blade donated by the Curtiss Wright Propeller Division was sectioned and measurements made directly. From these measurements and blueprints and the properties of steel and rubber the thermal circuit representative of the blade and its heater was constructed.

From the given rpm, blade station, liquid water content, tunnel temperature and wind velocity, the heat and mass transfer properties of the blades were determined. Knowledge of these heat and mass transfer characteristics permitted adjustment of the non-linear networks.

From the given data concerning the heat inputs to the various blade stations, the constant current sources were adjusted.

Figure A-1 shows a full scale view of the propeller section used for station $r/R = 0.58$.

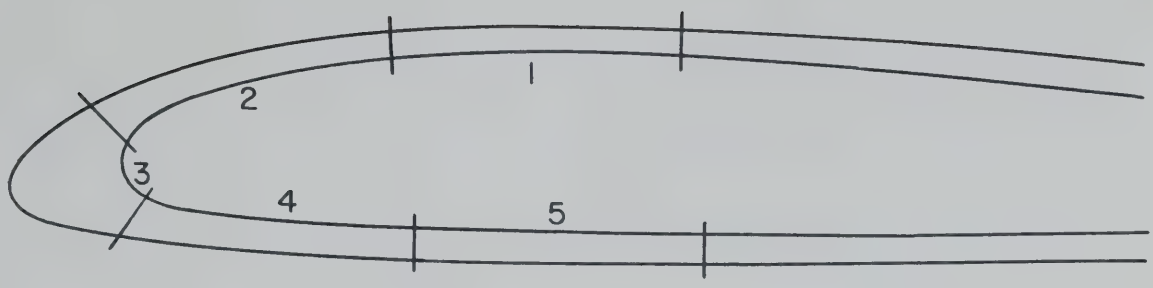

Figure A-2 shows the "equivalent" ideal lumped thermal circuit representative of the propeller section shown above.

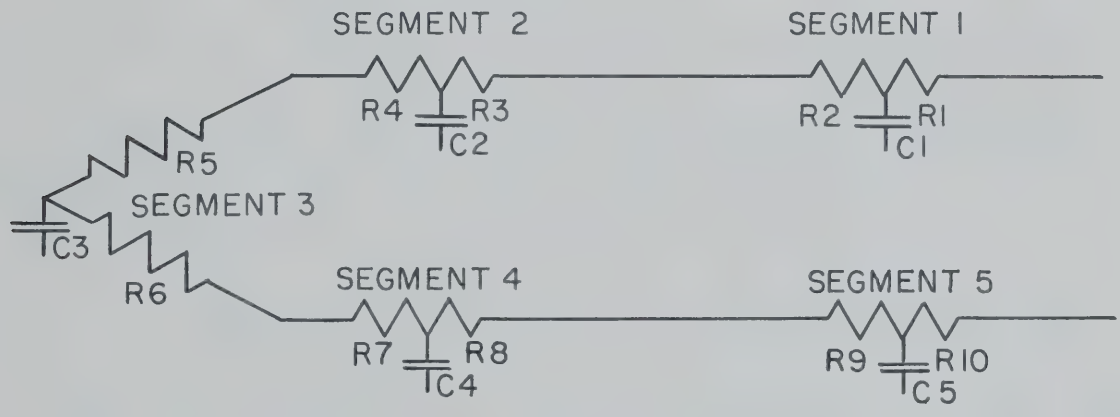

For example, the value of resistor R_4 of figure A-2 was calculated as follows: (See reference 14).

The thickness of the metal blade at the center of segment 2(d_2) and at the forward end (d_1) were measured. The length of the half segment was measured (x).

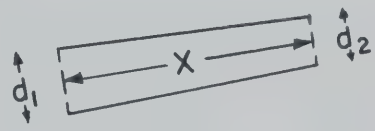

The resistance to heat transfer (per inch span) is given by:

$$R = \frac{12\ X}{k\frac{1}{2}(d_1+d_2)}$$

$X = (0.80 / 12)$ ft.

$\frac{(d_1 + d_2)}{2} = (0.15 / 12)$ ft.

$k = 14$ BTU / hr. ft.^{2} (°F / ft.)

HENCE

$R_4 = 4.57$ °F / (BTU / hr.)

The thermal capacity of segment 2 is obtained by measuring the cross sectional area and multiplying by the depth to obtain the volume. This volume when multiplied by the density and heat capacity of steel yields the thermal capacity.

$$C_t = (\text{volume}) \times (\text{density}) \times (\text{heat capacity}) \qquad (A\text{-}3)$$

$$C_t = 8.09 \text{ BTU} / {}^\circ\text{F} \ (\text{inch span}) \qquad (A\text{-}4)$$

Using the data of table III, the analogous electrical resistor and capacitor are found to have values of:

$$R_{electrical} = 805 \text{ K}\Omega \qquad (A\text{-}5)$$

$$C_{electrical} = 36.2 \ \mu\text{fd} \qquad (A\text{-}6)$$

Table A-1 shows the thermal properties used for the rubber and steel.

TABLE A-1

	Rubber	Steel
Thermal Conductivity, BTU/hr ft^2 ($^\circ$F/ft)	0.147	14
Density, pounds/cubic foot	91	492
Unit Heat Capacity at constant pressure BTU/lb $^\circ$F	0.406	0.12

The layer details of the rubber pads cemented to the blade are given in figure 5.

The completed lumped circuit, including elements representing the rubber pads and the blade, but not the non-linear networks, is shown in figure A-4.

Using the data on the propeller rpm, radius, etc. from reference 34, the unit thermal conductance and the icing rate for each segment of the propeller blade section were calculated. Table A-2 summarizes the given data and the results of the calculations.

TABLE A-2

GIVEN DATA

Propeller radius	5.208 feet
Radius ratio (r/R)	0.58
rpm	925
Free stream temperature	$2^{o}F$
Tunnel wind velocity	120 mph
Average droplet diameter	50 microns
Barometric pressure	29.9 in. Hg.
Chord Length	10.0 inches
Thickness ratio	0.12
Local Liquid Water Content	11.2×10^{-6} lb/ft^3

COMPUTED DATA

Relative velocity at this radius	363 ft/sec
Scale Modulus (ψ)	112
Reynolds Modulus of droplet	495
Fractional catch for airfoil, E_M	0.80

For each segmental area the ratio of water catch over that segment to the total water catch was computed using the data of figure 2b. This ratio is represented by the sumbol $\Delta E/E_M$. The unit thermal conductance was determined from reference 18. The length of the segment measured along the surface of the airfoil, expressed as fraction of chord length is given by the symbol $\Delta S/C$. The value of b was calculated from the equation:

$$b = \frac{E_M (\text{thickness / chord}) \, U \, (3600) \, (\text{Liq. water content}) \, (\Delta E / E_M)}{(\Delta S/C) \, f_c}$$

Laminar flow was taken for segments 2, 3, 4. Turbulent flow was taken for segments 1 and 2.

(Table A-2 cont'd.)

Segment	$\Delta S/C$	$\Delta E/E_M$	f_c	b
1	0.15	0.00	66	0.00
2	0.16	0.03	19	0.014

Segment	Δ S/C	$\Delta E/E_M$	f_c	b
3	0.12	0.56	41	0.159
4	0.16	0.29	19	0.133
5	0.15	0.12	66	0.017

The variation in heat flow with surface temperature was plotted as shown in figure 7 using equations 6 and 9. A separate calculation was required for each segment of the blade. Each of the five non-linear networks was then adjusted to match the calculated heat flow versus temperature curves as shown in figure 9. The equipment was allowed to cycle ten or more times under the control of an automatic timer adjusted to give six seconds on and eighteen seconds off. The current inputs to each of the five segments were as shown in table A-III.

TABLE A-III

Segment	Current (milliamperes)
1	0.00
2	0.96
3	1.08
4	0.96
5	1.10

These current inputs correspond to the heat inputs of figure 14b in reference 34. Figure A-5 shows a set of typical data obtained in this fashion.

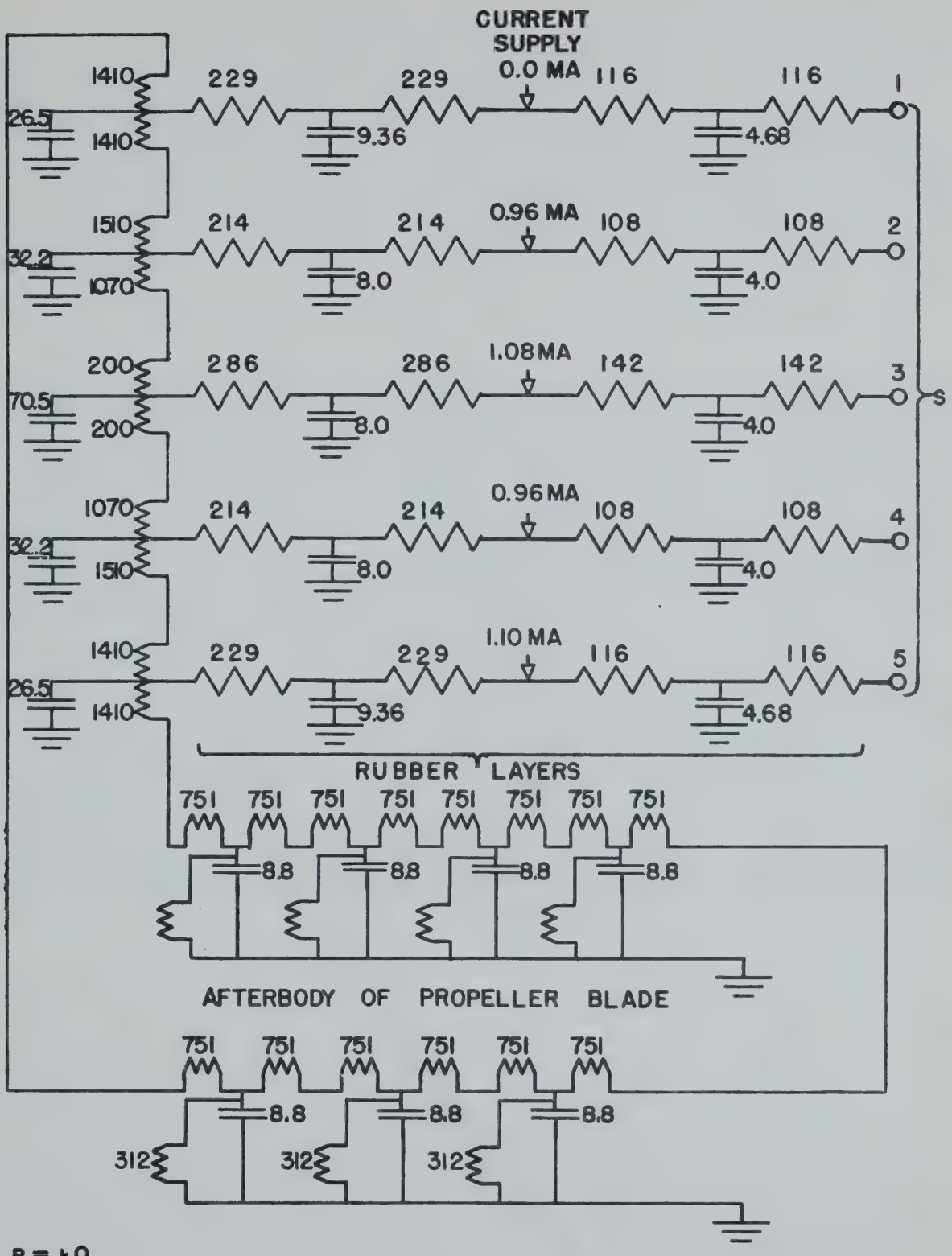

R = kΩ

C = μfd

S = SURFACE OF HEATERS EXPOSED TO ICING (NON LINEAR NETWORKS ATTACHED HERETO)

Fig. A-4

Figure A-5. A typical record obtained from the Brush recorder. The lower curve represents the variation in surface temperature on the rubber pad while the upper curve represents the variation in blade temperature under the rubber heating pad. The scale is two degrees Fahrenheit per division vertically and four seconds per division horizontally. The accuracy of the recording equipment is estimated as one whole division, or $2^{o}F$. The lowest line on the recording tape corresponds to $18^{o}F$ which is the sum of the tunnel temperature ($2^{o}F$) and the contribution of aerodynamic heating at this station ($16^{o}F$).

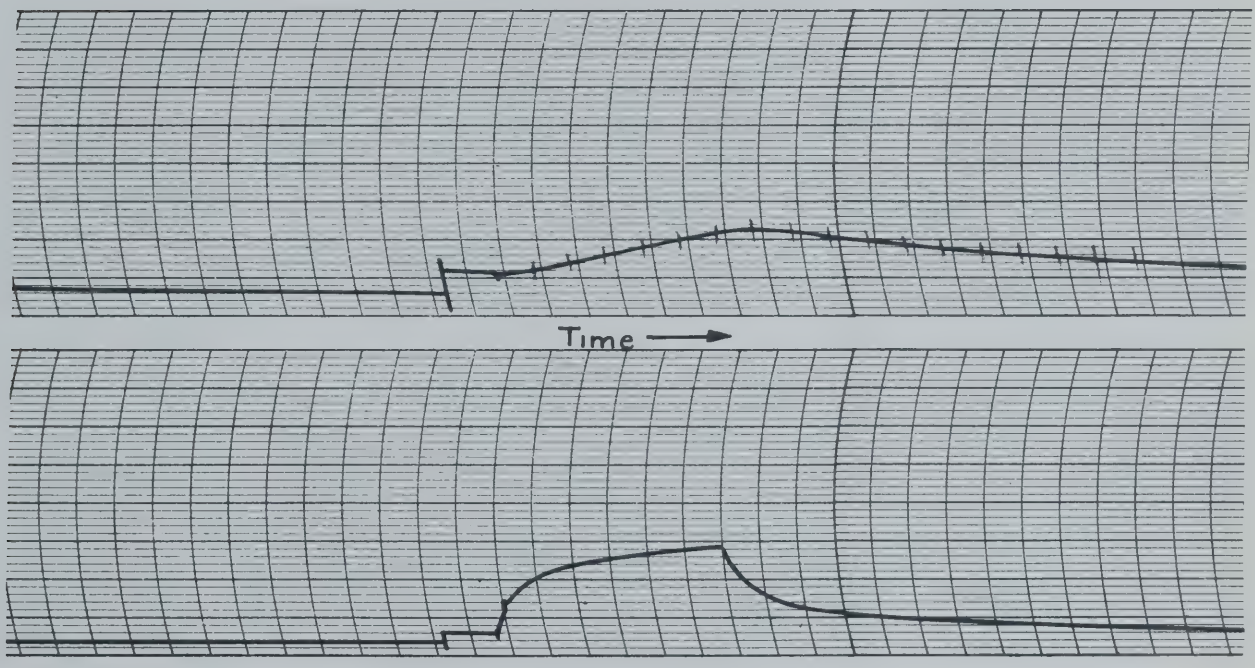

Reprinted from the JOURNAL OF ENGINEERING EDUCATION, Vol. 41, No. 3, November, 1950
Printed in U. S. A.

Laboratory Demonstration Experiment—A Link between "Fundamentals" and "Applications"

By D. ROSENTHAL and H. BAER

Department of Engineering, University of California, Los Angeles

1. *Introduction:* One of the avowed purposes of Engineering Education appears to be the teaching of the fundamental physical and chemical principles and laws as they apply to the engineering practice. In accordance with this purpose the student is first exposed (usually in the sophomore and junior years) to various courses, such as Mechanics, Strength of Materials, Thermodynamics, etc. in which the emphasis is on Fundamentals. To be sure the Fundamentals are slanted toward engineering applications, but the latter are generally treated as illustrations of methods of solution rather than as an aim in itself. The true applications come later. They are the subject of separate courses (usually in the senior year) known as: Structural Design, Machine Design, Unit Operation, etc. Not only are the Fundamentals and Applications taught separately, but as a rule they are taught by different instructors. This in itself is not a bad practice provided the two groups of instructors see eye to eye and work as a team. In the past the teamwork left much to be desired. In the cases in which the "Fundamentals" were treated with the necessary mathematical rigor they were entirely ignored in the "Applications," partly because the instructor in charge scorned at the "highbrow" mathematics, partly because he had more faith in his experience than in the underlying principles. As a result the student left the school under the impression that the "Fundamentals" were just a mental drill necessary for the attainment of the degree, but with no relation to the practice of the engineering profession. Under the impact of modern science this attitude no longer exists either with the instructor in charge of "Applications" or the student, but the necessary link between the "Fundamentals" and "Applications" is often missing in the instruction. A point in case is the relation between "Strength of Materials" and "Machine Design." It has been the authors' experience both as instructors and students that in the mind of the student only a tenuous link exists between these two subjects. To be sure the student

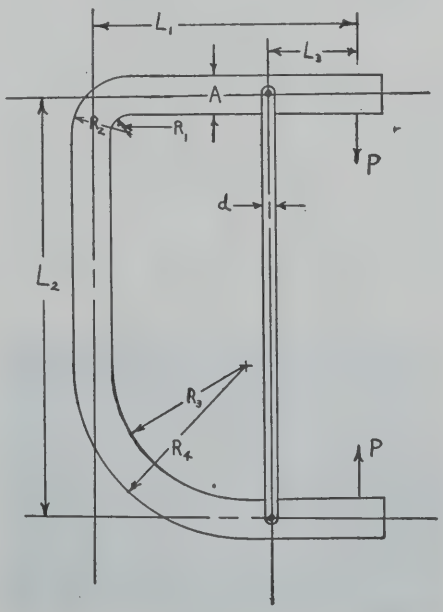

FIG. 1.

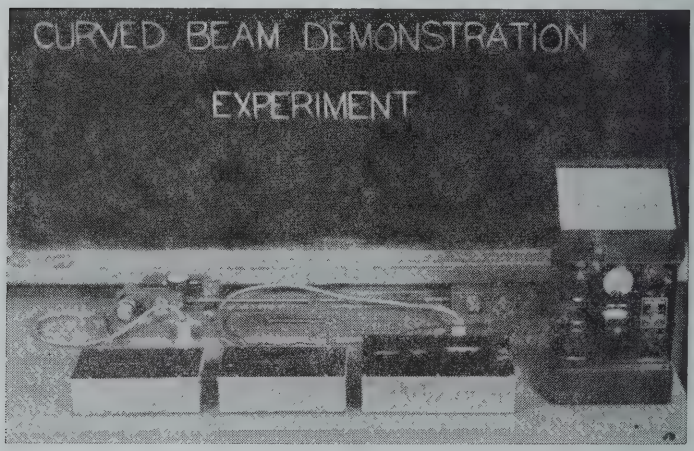

FIG. 2.

knows that the design of some of the machine parts is based on formulas of "Strength of Materials," but he is usually unaware of their limitations, and he is generally incapable to apply the methods which lead to these formulas. As a result, he is at a loss to explain the discrepancies between theory and experiment or assess the limits of the experimental error, when faced with the results of actual measurements. It is the authors' opinion that the cause of this deficiency lies in the lack of a proper transition between the "Fundamentals" (as taught in the sophomore and junior courses) and the "Applications" (as given later in the laboratory and senior courses). To correct this shortcoming an attempt has been made to provide the necessary transition by means of a scheme described below.

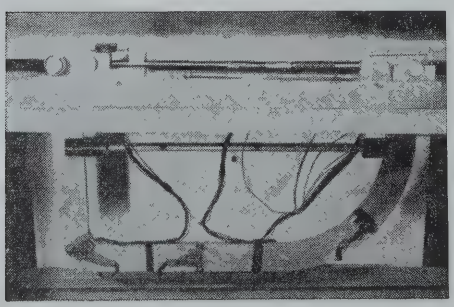

FIG. 3.

2. *The Laboratory-Demonstration Experiment:* The scheme consists of having the student solve a problem at various stages of idealization: from its theoretical inception to its industrial realization.

In the first stage the problem is in the nature of a computation. It is merely an application of principles and laws expounded in a theoretical course. In the second stage the analytical solution is obtained experimentally on a model reproducing all theoretical assumptions as closely as possible. In the third and final stage the experiment is carried out on an existing industrial system or machinery. This last step no longer forms a part of the "Fundamentals." It appears in a later year as a part of "Applications," and the experiment is performed not as a check of the theory, but as an inspection or test of the system or machinery.

The first and third stages of the scheme are not new. They have been improved continually. Thus, in the first stage classroom demonstrations, sometimes of remarkable simplicity,[1] and devices for visualization of great ingenuity [2, 3] have been

[1] R. S. Hartenberg, *J. of E. E.*, Vol. 40, p. 430.

[2] A. J. Durelli, C. H. Taso and R. H. Jacobson, *Ibid.*, p. 525.

[3] A. D. Moore, *Journal of Applied Physics*, Vol. 20, p. 790.

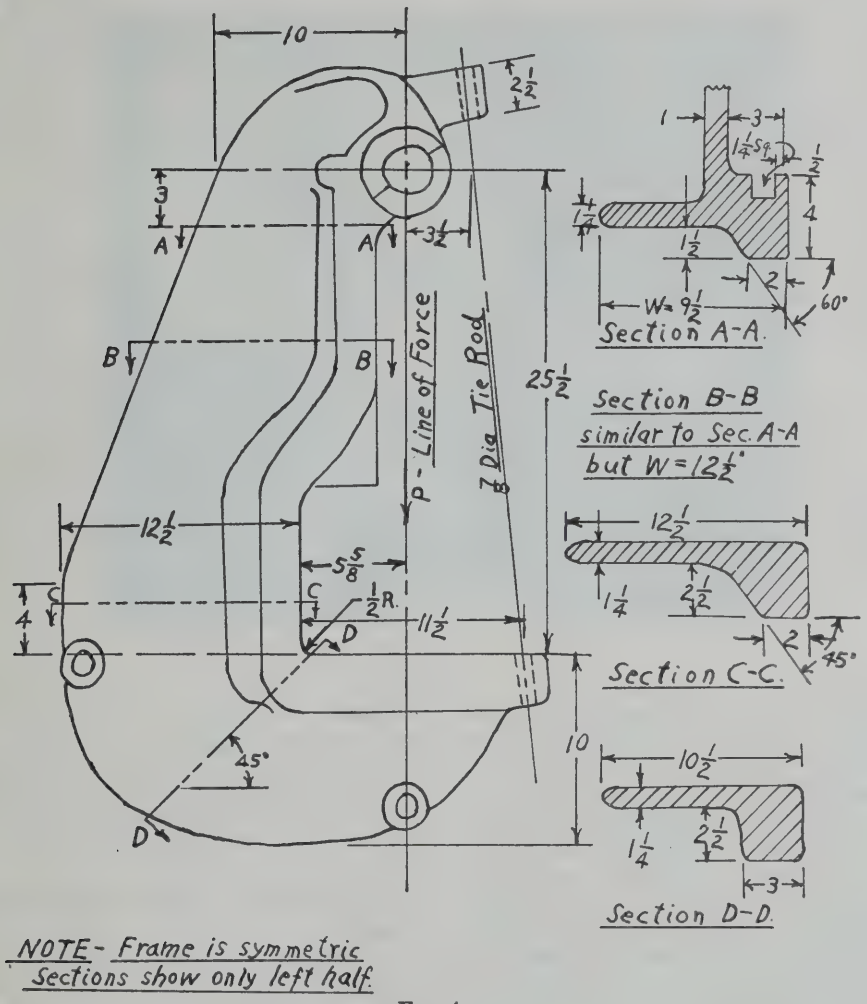

FIG. 4.

employed. The third stage was sometimes developed into highly complex and organized systems, e.g., in some power plant experiments.[4] But neither stage is believed to accomplish the aims of the second stage to which more specifically the name of "Laboratory-Demonstration Experiment" has been given. These aims are of a threefold nature:

1. From the experimental solution the student gets the real feeling of the quantities and methods involved in an otherwise abstract mathematical solution.

2. By comparing the computed and measured values on the basis of the experimental error he can assess for himself the validity of the principles and laws involved in the theory.

3. When dealing with an actual system or machinery he is in the position to account properly for the discrepancies resulting from the idealization of real conditions.

An example of the scheme just described

[4] M. J. Zucrow, *J. of E. E.*, Vol. 38 p. 482.

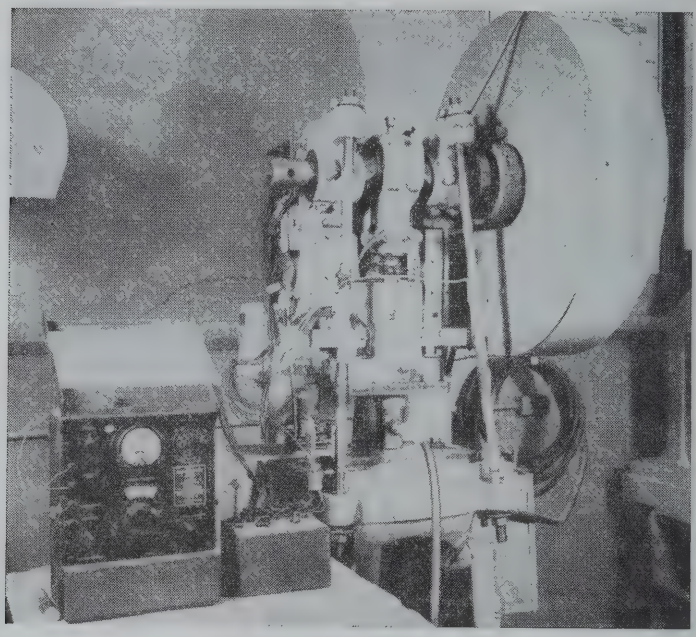

FIG. 5.

is given below. This example has been in use for about two years. It is still somewhat premature to speak of the results. That much appears certain: in order to serve its purpose the Demonstration-Laboratory Experiment must be conceived in such a way that it can be operated by the student at any time and without supervision. That is, the student must be given time and opportunity to make mistakes and to correct them himself, much the same as in his homework.

If it is agreed that the ability to idealize the real conditions forms a part of the engineering *thinking*, and the ability to account for the observed discrepancies a part of the engineering *judgment*, then the proposed scheme accomplishes its purpose.

3. *Example: Stress Analysis of a Punch Press Frame.*

First stage. Problem of strength of materials:

"Computation of Stresses Produced in the Frame Sketched, Figure 1."

Educational purpose: Application of the following principles and theories:

a) Equilibrium of forces and moments. Free body diagram. Method of section.

b) Principle of virtual work (or equivalent).

c) Beam theory (curved and straight beam).

d) Principle of elastic stability (column buckling).

Second Stage. Testing of an idealized system:

"Experimental Determination of Stresses Produced in the Frame, Figures 2 and 3."

Educational purpose: Verification of:

a) Hooke's Law. Establishment of linear relation between applied load and measured strain.

b) Bernouilli's Law. Establishment of linear and hyperbolic strain distribution in the straight and curved parts of the beam.

c) Analytical solution. Determination of the influence of sharp and mild corners.

d) Validity of the theory on the basis of the experimental error. Confidence in the experimental stress analysis.

Third Stage. Testing of actual machinery:

"Determination of Safe Operating Loads in the Punch Press, Figures 4 and 5."

Educational purpose:

a) Idealization of the behavior of the punch press frame for the purpose of a theoretical analysis.

b) Explanation of discrepancies between observed and computed values on the basis of

1) assumed idealizations,
2) assumed mechanical characteristics.

c) Use of Goodman-Johnson (or equivalent) fatigue diagram for the determination of safe operating loads with and without the tie rods.

d) Significance of stress raisers at sharp corners from the point of view of design.

e) Improvement of efficiency by:

1) residual stress (prestressing of tie rods),
2) modification of design (rounding of sharp corners),
3) substitution of a welded for cast frame.

f) Consideration of rigidity (influence of the deformation of the frame on the tolerances of the punching operation).

Reprinted from THE PHYSICAL REVIEW, Vol. 82, No. 1, 95–96, April 1, 1951
Printed in U. S. A.

Microwave Spectrum of Methyl Mercaptan

F. KENNETH HURD* AND W. D. HERSHBERGER†
University of California, Los Angeles, California
(Received February 9, 1951)

THE study of the K-Band microwave spectrum of CH_3SH is currently in progress. In the spectroscope, a 48-foot absorption cell is used with a double modulation method which employs both wide range saw-tooth 60 cycle/sec modulation and narrow range sinusoidal 87 kc/sec modulation. This technique in conjunction with a low noise input circuit described by Good[1] for the 87 kc/sec amplifier and a low pass filter gives a sensitivity of 1×10^{-7} nepers/cm as judged by the ability to detect all of the weak $N^{15}H_3$ lines tabulated by Kisliuk and Townes.[2]

TABLE I. Methyl mercaptan microwave spectra. Frequencies are known to an estimated 5 Mc/sec.

Frequency (Mc/sec)	Frequency (Mc/sec)	Frequency (Mc/sec)
19,909	22,414	24,485
19,996	22,558.0	24,995
20,052	22,561.2[a]	25,015
20,136	22,663	25,125
20,163	22,830	25,145.0
20,380	23,071.5	25,147.0[a]
20,645	23,075.0[a]	25,150.5
20,712.5	23,233[b]	25,152.0[a]
20,714.0[a]	23,260	25,210
21,058	23,340	25,225
21,522	23,500	25,290.0
21,735	23,525.0	25,290.4[a]
21,770	23,532.3[a]	25,565
21,866	23,565	25,660
21,878	23,622	
21,903	23,780	
21,945	23,805	
21,976	23,995	
22,270	24,072	
22,333	24,420	
	24,455	

[a] For each pair of lines so marked the separation of the two lines of the pair is known to an estimated 20 percent and the mean frequency of the pair to 5 Mc/sec.
[b] The accuracy of this frequency assignment is considered to be good to 0.5 Mc/sec. This is known by reference to an ammonia line at 23,232.20 Mc/sec.

The observed spectrum consists of some 55 lines extending from 19,940 Mc/sec to 25,656 Mc/sec with only a few scattered lines between 23,790 Mc/sec and 24,980 Mc/sec suggesting two groupings of lines. The region from 25,656 Mc/sec to 25,920 Mc/sec which is the present upper limit of our equipment is void of lines. The complete tabulation of lines is shown in Table I, where the frequencies are given to an estimated 5 Mc/sec as measured by a wavemeter calibrated against the known frequencies of the NH_3 lines.[2]

The interpretation of this spectrum has not yet been achieved. The CH_3SH molecule is a slightly asymmetric rotator with moments of inertia for the S^{32} isotope[3] consistent with a pure rotational transition $J_0=0\rightarrow J_0=1$ at approximately 24,600 Mc/sec. Because of the small Boltzmann factor for all vibrational levels other than $v_i=0$ this transition would be expected to yield a single strong line accompanied by a large number of extremely weak lines due to the excited vibrational levels. The 4.18 percent naturally occurring S^{34} would give a similar spectrum of intensity ratio 1 to 24 with respect to that of S^{32}. The observed spectrum does not fit this scheme. There exists, however, the splitting of the torsional vibration $v=0$ level into three levels as a result of hindered internal rotation. This splitting depends upon the quantum number K in a complex manner.[4] Transitions between these levels could easily yield the large number of lines observed.

* Physics Department.
† College of Engineering.
[1] W. E. Good, Westinghouse Research Paper 1538.
[2] P. Kisliuk and C. H. Townes, J. Research Natl. Bur. Standards **44**, 611 (1950).
[3] Russel, Osborne, and Yost, J. Am. Chem. Soc. **64**, 165 (1942).
[4] Koehler and Dennison, Phys. Rev. **57**, 1006 (1940).

Multiple-Output Predetermined Counter

By D. L. Gerlough and H. R. Kaiser*

Institute of Transportation and Traffic Engineering
University of California
Los Angeles, Calif.

In certain industrial applications, single-output predetermined counters[1,2] are not suitable and multiple-output predetermined counters must be used. In the multiple-output counter, output signals may occur at several predetermined points during the counting process whereas in single-output counters an output signal occurs only when a single predetermined count is reached.

The circuit of a counter having a counting capacity of 2^n and m predetermined outputs is shown in Fig. 1. This counter consists of two parts, a binary counter section and an interpretation section. The counter may have as many stages as necessary to give the desired counting capacity but with the component values shown there is a limit of about twelve stages.

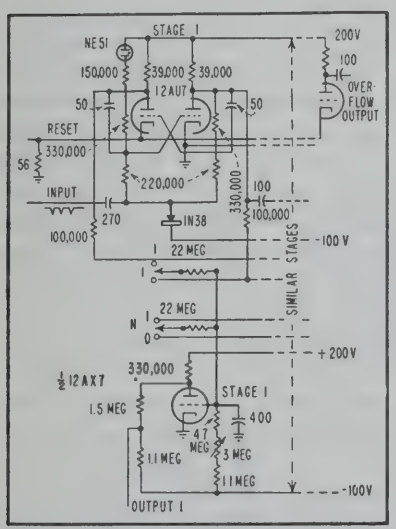

FIG. 1—Schematic diagram of a multiple-output predetermined counter having a capacity of 2^n and m predetermined outputs. Each NE51 socket contains a 50,000-ohm series resistor

The binary counter uses a standard circuit except for crystal diodes in the bias return of each stage to increase the ability of the stage to nected to the n 22-meg resistors are nonconducting, representing a total disagreement between the counter contents and the switch settings, the apparent grid voltage of the coincidence detector measured with the tube removed from the socket is approximately 77.5 volts. With the tube in the socket the actual grid voltage will go only slightly positive because of grid current flow.

When the contents of the binary counter are such that all plates connected to the n 22-meg resistors are conducting, representing total agreement between the counter contents and the switch settings, the apparent and actual grid voltages will be approximately −6.5 volts. Between total agreement and total disagreement the apparent grid voltages will change in increments of approximately 10.5 for a counter of eight stages.

Changing the grid voltage from a positive value to −6.5 volts will cause a 12AX7 to go from full conduction to cutoff, resulting in an output signal. This signal may be adjusted to the proper level for succeeding equipment by means of a voltage divider.

Because of the variations in the exact cutoff voltage of 12AX7's, a potentiometer is provided in the grid return to adjust the bias for maximum output signal.

In addition to the predetermined output signals, there is an output signal when the binary counter overflows. The multiple-output predetermined counter with the component values shown has been operated successfully at frequencies up to 50 kc.

In one application, an m-output predetermined counter has been used to distribute automatically counts into $m + 1$ class intervals of a statistical frequency distribution using a special recorder. This recorder, whose circuit is shown in Fig. 2, employs $m + 1$ electromechanical counters.

The electromechanical counter of stage 0 records the number of items having counts 0 or greater, but less than a_1; the counter of stage 1 records items having counts greater than a_m up to the maximum capacity of the binary counter, where a_1 to a_m are the predetermined output settings of the m-output counter. Thyratrons are used to "remember" the greatest class interval to which counting has progressed.

Sequence

Initially, in the operation of the predetermined counter and recorder circuits, the thyratron of stage 0 of the recorder is fired and the thyratrons of all other stages are extinguished. As counting takes place, stage 0 remains fired indicating class interval 0 to a_1, until stage 1 receives a signal from the first output of the predetermined counter. At this point the thyratron of stage 1 fires and extinguishes the thyratron of stage 0 by means of the 0.01-μf commutating capacitor.

The thyratron of stage 1 remains fired until the recorder receives a signal from the second output, a_2, of the predetermined counter through stage m. If counting continues after a_m, the memory thyratron of stage m remains fired indicating a count of a_m or greater.

The overflow signal from the

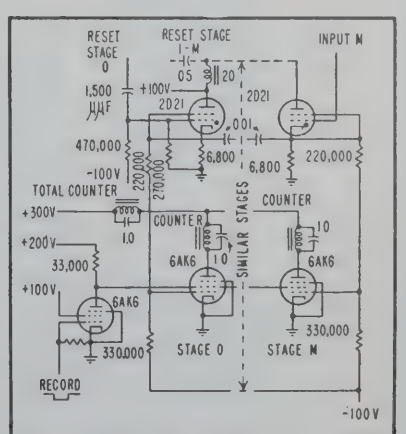

FIG. 2—Schematic diagram of statistical frequency-distribution recorder having m + 1 groups and m inputs

* H. R. Kaiser is now with Hughes Aircraft Co., Culvert City, Calif.

binary counter may be used to cut off the counter input so that recycling will not occur. When counting is completed, a 0.1-sec negative signal is applied to the grid of the 6AK6 at the left in Fig. 2, raising the screen potential on the 6AK6's of stages 0 to m. This allows any of these tubes not biased to cutoff to conduct.

The only tube not biased to cutoff will be the 6AK6 associated with the 2D21 thyratron which has remained fired. When this 6AK6 fires, its associated electromechanical counter in series with the electromechanical counter for totals is energized and a record of the count in the appropriate class interval and a cumulative record of the number of items in all class intervals is produced. After the recording operation is completed, resetting signals are sent to the binary counter, the thyratron of recorder stage 0 and the thyratrons of the other stages.

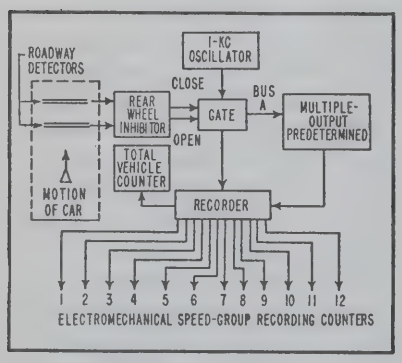

FIG. 3—Block diagram of vehicle speed-distribution recorder

The multiple-output predetermined counter and recorder described have been used as principal elements of a vehicle speed-distribution recorder.[3] In this instrument, block diagram in Fig. 3, the times required for vehicles to traverse a specified distance are translated into counts by means of a 1-kc gated oscillator.

Impulses from the roadway detectors pass through the rear-wheel inhibitor to open and close the gate. While the gate is open, pulses from the 1-kc oscillator pass through the gate into the multiple-output counter via bus A, as shown in Fig. 4. As the gate closes, counting is stopped and the recorder is set in operation. The recorder registers the counts, Fig. 5, on an electromechanical counter for the appropriate speed group.

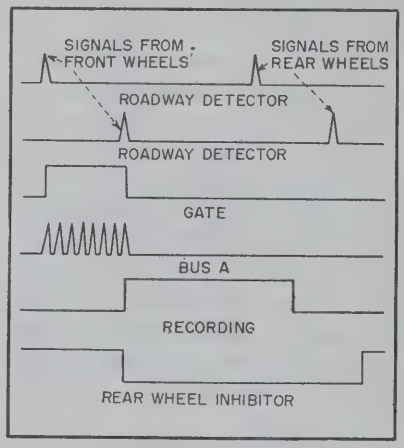

FIG. 4—Diagram showing sequence of operations within the speed-distribution recorder. The rear-wheel inhibitor blanks out signals from the roadway detectors long enough to permit the rear wheels to pass

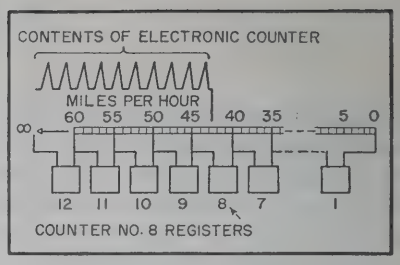

FIG. 5—Diagram showing typical electromechanical counter settings as set up by toggle switches on front panel of instrument

Speeds are divided into twelve class intervals by setting up the time equivalents of the desired speeds. The upper panel of the instrument contains the electromechanical counters for the twelve class intervals and the total. The center panel contains the toggle switches for setting up the predetermined counter and the neon indicators for the binary counter. The lower panel contains the power-supply controls and meters.

Credit is due J. Robert Hall for most of the construction of the vehicle speed-distribution recorder.

REFERENCES

(1) John J. Wild, Predetermined Counter, ELECTRONICS, p 121, March 1947.
(2) Richard J. Blume, Predetermined Counter for Process Control, ELECTRONICS, p 88, Feb. 1948.
(3) Robert Bromberg and D. L. Gerlough, Applications of Electronic Techniques to Traffic Instrumentation, *Proc. Highway Research Board*, **28**, p 348, 1948.

Reprinted from ELECTRONICS, February 1951
Copyrighted (all rights reserved) by McGraw-Hill Pub. Co., Inc.
330 W. 42nd St., New York 18, N. Y.

[Reprinted from the Journal of the American Chemical Society, 72, 3162 (1950).]
Copyright 1950 by the American Chemical Society and reprinted by permission of the copyright owner.

[Contribution from the Department of Engineering, University of California, Los Angeles]

Mutual Solubilities of Hydrocarbons. III. Systems *cis*-Decahydronaphthalene–*trans*-Decahydronaphthalene, *cis*-Dehydronaphthalene–Tetracosane, *cis*-Decahydronaphthalene–Dotriacontane

By William F. Seyer, Sun Yip and Gordon Pyle

This paper comprises a continuation of the studies dealing with the mutual solubilities of hydrocarbons by the freezing point method. The following systems were examined; *cis–trans* decahydronaphthalene, *cis*-decahydronaphthalene-tetracosane ($C_{24}H_{50}$), *cis*-decahydronaphthalene–dotriacontane ($C_{32}H_{66}$).

Experimental.—The bulb method was used for most of the determinations for two reasons. First, the effect of air and moisture could be avoided and, second, relatively small amounts of the materials were required. All the hydrocarbons used had been synthesized and purified by methods described previously. The m. ps. were as follows: *cis*-d. 43.27°, *trans*-d. 30.65°, tetradecane, 50.6°, and dotriacontane, 69.5°.[1]

The cyclic isomers were dried over sodium and then allowed to run into the dried glass bulbs whose capacities were about 20 cc., by means of a small glass funnel. The composition was established by weighing the bulbs before and after each addition of hydrocarbon. Next the contents of the bulbs were frozen by means of Dry Ice evacuated to 0.1 mm. and sealed. This was done by allowing the tube to collapse about 5 cm. above the liquid level. Hence, there was only a very small amount of material in the vapor phase at any time. Also the tube was long enough to serve as a handle for manipulating the bulb in the cold-bath.

Before measuring the f. p. the mixtures were shaken intermittently for several hours and then allowed to stand for at least twenty-four hours at room temperature to insure complete mixing. The mixture whose f. p. was to be determined was then frozen in an acetone-bath, cooled with a stream of carbon dioxide escaping from a reservoir of Dry Ice. Solidification having taken place, the temperature of the bath was then allowed to rise slowly until one or two small crystals remained. The temperature was now adjusted so that the crystals showed no signs of growing or disappearing. After this temperature had been found, it was then held constant for ninety minutes and if no change in crystal size was noted, this was taken as the f. p. This performance was repeated twenty-four hours later to ensure complete mixing and to be able to observe whether there was any reaction between the components. This latter point was checked by removing the bulb contents and measuring the refractive index in a Pulfrich refractometer. Comparison of the readings with those of a previously constructed chart showed no change in composition had taken place. All attempts to get consistent temperature readings at the first appearance of crystals on cooling were unsuccessful. This seemed to be due to the large amount of undercooling required to bring about crystallization.

The freezing point operations involving the two paraffin hydrocarbons below 30° were identical with that described. Above temperatures of 30°, the capillary tube method was used, as it was the most convenient. In this case, the solutions were made up in a weighing bottle. A sample of the solution was drawn into a weighed, thin-walled capillary tube, about 1 mm. in diameter, by merely placing it in the molten solution. The upper end was then sealed and the capillary tube inverted until the contents had drained to the bottom Upon solidification, the loaded tube was weighed. The length of solid in the tube was about 2 mm.

The capillary tube was then immersed into the bath with the sample adjacent to the thermometer and the whole heated until melting occurred. The rate of heating was regulated so that the temperature rise was less than 0.2° per minute in the vicinity of the melting point. The temperature where all the crystals disappeared was noted. The bath was next cooled until the white crystals of diacetyl appeared, upon which the bath was heated again slowly until the last trace of crystals in the tube just disappeared. The temperature at this point was taken as the freezing point of the mixture. The procedure was repeated with two other capillaries of the same mixture until the readings agreed with one another. The point of disappearance of the crystals was fairly sharp.

All temperatures were measured by a L. & N. platinum resistance thermometer, calibrated at the U. S. Bureau of Standards. The freezing points and mole fractions are given in the following tables: *cis–trans*-decahydronaphthalene Table I, *cis*-d.–tetracosane Table II and *cis*-d.–dotriacontane Table III.

Table I

Freezing Points of Mixtures of *cis*- and *trans*-Decahydronaphthalene

Mole fr. *trans*-D.	Temp., °C.
0.0000	−43.27
.0242	−44.22
.0536	−45.56
.0855	−47.04
.1752	−51.25
.2525	−55.12
.3478	−59.36
.382[a]	−61.1[a]
.4000	−57.71
.5023	−54.34
.5661	−50.07
.6199	−47.49
.6790	−45.29
.8000	−39.00
.8997	−34.05
.9688	−31.82
1.0000	−30.65

Table II

Freezing Points of System Tetracontane ($C_{24}H_{50}$)-*cis*-Decahydronaphthalene

Mole fr. tetracontane	F. p., °C.
1.0000	50.65
.8704	48.87
.7767	47.20
.7408	46.20
.7085	46.03
.7048	45.91
.5648	43.35
.4173	39.80
.3743	39.11
.3016	36.17
.2236	32.82
.1587	29.45
.1374	27.80
.0958	24.26
.0666	21.00
.0404	15.80
.0162	8.65

Table III

Freezing Points of *cis*-Dotriacontane ($C_{32}H_{66}$)

Mole fr. dotriacontane	F. p., °C.
1.0000	69.55
.9551	68.69
.8577	67.68
.7785	66.58
.7432	66.08
.6554	64.40
.5580	62.80
.5425	62.41
.4782	61.06
.3358	56.68
.2355	52.21
.1812	49.26
.1185	44.05
.0883	41.20
.0698	39.21
.0615	38.52
.0501	36.80
.0470	36.16

[a] Eutectic point from graph, Fig. 1.

Discussion of Results.—The results, when plotted, yielded Figs. 1, 2 and 3, indicating that all the systems approach the ideal state. Figure 1 gives a value of −61.2° for the eutectic temperature which agrees very closely with that calculated −61.55°, when the latent heats found by Parks and Hatton are used.[2]

A binary system such as is illustrated in Fig. 1 where there is a difference in the molecular volume

(1) Wm. F. Seyer, Ralph F. Patterson and John L. Keays, This Journal, 66, 179 (1944).

(2) Geo. S. Parks and John A. Hatton, *ibid*, 71, 2773 (1949).

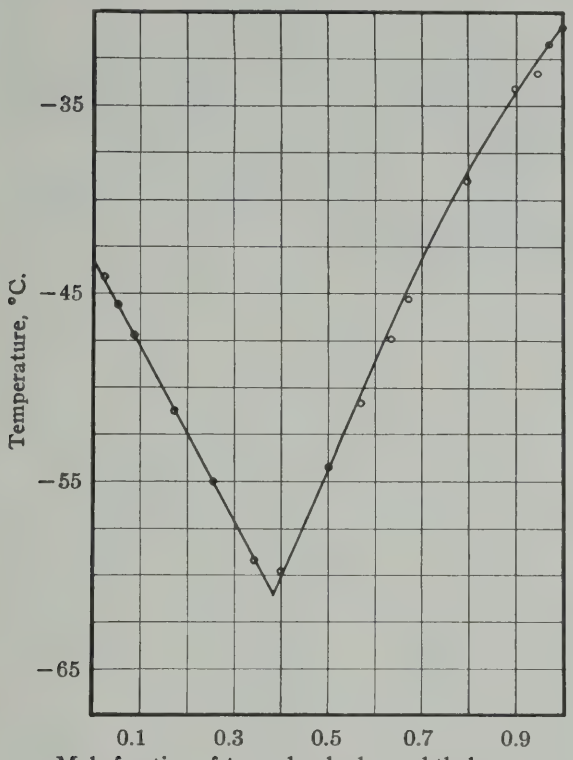

Fig. 1.—System *cis–trans*-decahydronaphthalene.

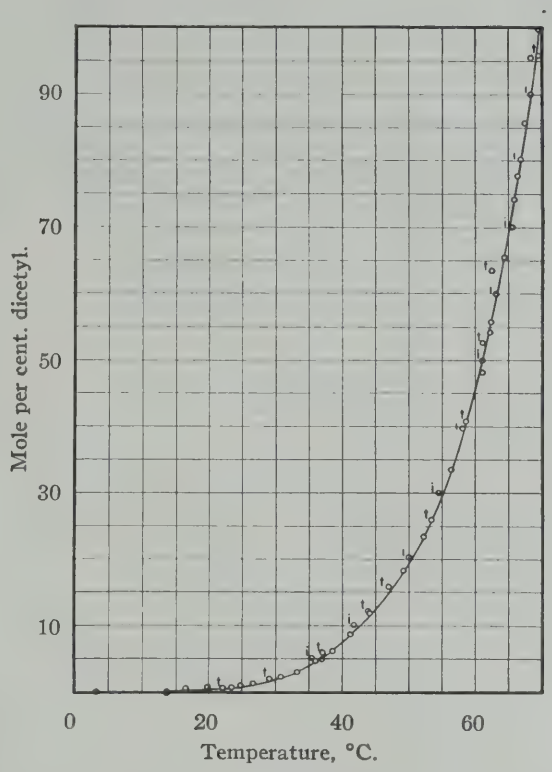

Fig. 3.—O, Mole per cent. dotriacontane; i_0, mole per cent. tetracosane; i_0, ideal system.

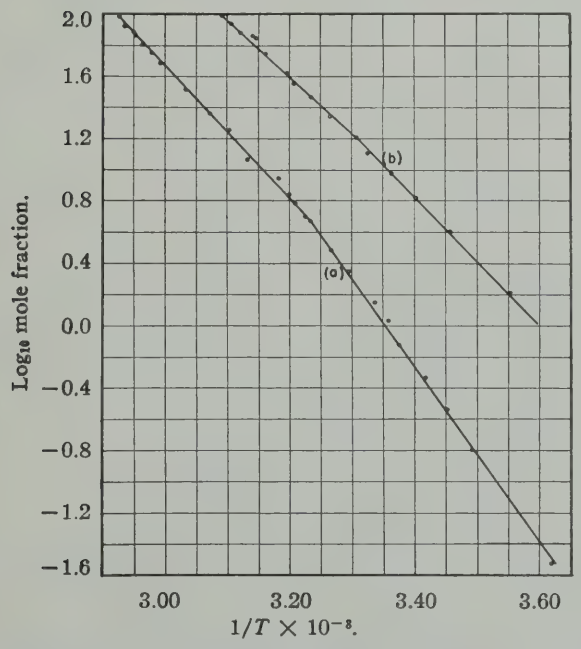

Fig. 2.—(a) Dotriacontane–*cis*-decahydronaphthalene; (b) tetracosane–*cis*-decahydronaphthalene.

of only 2.9% should be expected to give rise to some solid solution formation. Thus, Smittenberg, Hoog and Henkes reported that in the case of the system octane–nonane, where the molecular volume differed by 6.3%, a considerable amount of solid solution formed upon freezing a mixture of the two substances. However, they also found that in the case of mixtures of iso-paraffins and *n*-paraffins the systems behaved in an ideal manner with no solid solution forming.[3] Hence, it would appear that in mixtures where the components have different spatial configurations such that one species cannot enter the crystal lattice of the other, solid solution does not take place even if there is only a slight difference in their molecular columns. The behavior of the *cis–trans*-decahydronaphthalene mixture is then what one would expect on the basis of Hassel and Viervoll's spatial models of these two isomers. Assuming that Mohr's model for the *trans* form is correct, they have shown that then his model for the *cis* form cannot be so, but must have one of the rings almost at right angles to the other. This can occur, they point out, if one of the ring connecting bonds is of the χ-type and the other of the ϵ type.[4] This difference in structure appears to be sufficient to prevent either from occupying the crystal lattice of the other.

The systems depicted in Fig. 2 show both the effect of molecular volume and shape on the form of the freezing point curves. A transition point is clearly apparent at point (a) but less so at (b). As would be expected from the work of Piper

(3) J. Smittenberg, H. Hoog and R. A. Henkes, THIS JOURNAL, **60**, 17 (1938).

(4) O. Hassel and H. Viervoll, *Acta Chemica Scandinavia*, **1**, 194 (1947).

and his co-workers, the f.ps. of the solutions are depressed about 2.5° from that of the pure compounds.[5]

A comparison of the solubility of the cyclic hydrocarbon in the two *n*-paraffins as found, and as calculated on the basis of an ideal solution, is shown in Fig. 3. It also shows that the solubility of the cyclic hydrocarbon in the high molecular *n*-paraffins is very high, but the converse is not so.

(5) S. H. Piper, *et al.*, *Biochem. J.*, **25**, 2074 (1931).

Summary

1. The freezing points of the systems *cis*–*trans* decahydronaphthalene, dotriacontane–*cis*-decahydronaphthalene and tetracosane–*cis*-decahydronaphthalene have been examined and found to be very close to the ideal state.

2. The results indicate that the *cis* and *trans* isomers of decahydronaphthalene have different spacial configurations.

LOS ANGELES, CALIF. RECEIVED DECEMBER 17, 1949

UNIVERSITY OF CALIFORNIA

DEPARTMENT OF ENGINEERING

LOS ANGELES

A NEW LOW POWER PULSE TRANSFORMER

FOR

HIGH DUTY CYCLE OPERATION

ENGINEERING RESEARCH

REPORT

JUNE, 1950

ABSTRACT

A NEW LOW POWER PULSE TRANSFORMER FOR HIGH DUTY CYCLE OPERATION

by

William L. Martin

The following paper discusses a method of improving the operational characteristics of a transformer-coupled pulse repeater originally designed for general application in the National Bureau of Standards Interim Computer. The repeater stage is modified by redesigning the pulse transformer and changing the method of loading. An analysis of the equivalent circuit is made and predicted results are compared with those obtained experimentally. The resulting transformer and mode of operation have been incorporated into the latest assemblies of the NBS Interim Computer.

UNIVERSITY OF CALIFORNIA

LOS ANGELES

A NEW LOW POWER PULSE TRANSFORMER FOR HIGH DUTY CYCLE OPERATION

A thesis submitted in partial satisfaction
of the requirements for the degree
Master of Science
in
Engineering

by

William L. Martin

June, 1950

The thesis of William L. Martin is approved:

William D. Hershberger, Chairman

Thomas A. Rogers

Harold K. Ticho

S. N. Alexander

Committee

University of California

May 8, 1950

TABLE OF CONTENTS

	Page
Summary	1
Nomenclature	2
Acknowledgment	3
Introduction	4
Analysis and Evaluation of Equivalent Circuit	7
Experimental Results	27
Tables -- Table I Transformer Output Characteristics Rise and Fall Times and Pulse Width Times	28
Table II Effects of Varying Duty Cycle on Transformer Output Pulse Leading and Trailing Edge	30
Table III Stage Delay Characteristics 250-Turn Transformers Delays of Significant Points on Pulses in Microseconds	36
Table IV Stage Delay Characteristics 120-Turn Transformers Delays of Significant Points on Pulses in Microseconds	37
Table V Timing Characteristics	38
Conclusions	41
Bibliography	42

Index to Figures is given on the following pages

INDEX TO FIGURES

Fig. No.	Description	Page No.
1	Original NBS Interim Computer Pulse-Repeater Circuit	8
2	Idealized Equivalent Circuit of Pulse Transformer	9
3	Idealized Equivalent Circuit of Pulse Transformer Including Diode Loading	20
4	Load Circuits Tested Showing Cases of Overdamping, Underdamping and Critical Damping	27
5	Oscillogram - 1^{st} pulse from 250-turn transformer, overdamped case	31
6	Oscillogram - 1^{st} pulse from 120-turn transformer, underdamped case	31
7	Oscillogram - N^{th} pulse from 250-turn transformer, overdamped case	31
8	Oscillogram - N^{th} pulse from 120-turn transformer, underdamped case	31
9	Oscillogram - N^{th} pulse from 250-turn transformer, underdamped case 39% duty factor	32
10	Oscillogram - N^{th} pulse from 120-turn transformer, underdamped case 39% duty factor	32

Fig. No.	Description	Page No.
11	Oscillogram - N^{th} pulse from 100-turn transformer, underdamped case, 39% duty factor	32
12	Oscillogram - N^{th} pulse from 250-turn transformer, underdamped case, 51% duty factor	33
13	Oscillogram - N^{th} pulse from 120-turn transformer, underdamped case, 51% duty factor	33
14	Oscillogram - N^{th} pulse from 100-turn transformer, underdamped case, 51% duty factor	33
15	Oscillogram - N^{th} pulse from 250-turn transformer, underdamped case, 64% duty factor	34
16	Oscillogram - N^{th} pulse from 120-turn transformer, underdamped case, 64% duty factor	34
17	Oscillogram - N^{th} pulse from 100-turn transformer, underdamped case, 64% duty factor	34
18	Typical Gating Circuit Used in Testing Stage Delay Under Limiting Conditions	35
19	Oscillogram - Typical Stage Delay Data 1st pulse from three cascaded stages of 250-turn transformers superimposed	39
20	Oscillogram - Typical Stage Delay Data 1st pulse from three cascaded stages of 120-turn transformers superimposed	39
21	Oscillogram - Typical Stage Delay Data N^{th} pulse from three cascaded stages of 250-turn transformers superimposed	39

Fig. No.	Description	Page No
22	Oscillogram - Typical Stage Delay Data Nth pulse from three cascaded stages of 120-turn transformers superimposed	39
23	Inductance Data from Whirlwind Report	40

A NEW LOW POWER PULSE TRANSFORMER FOR HIGH DUTY CYCLE OPERATION

SUMMARY

The following paper discusses a method of improving the operational characteristics of a transformer-coupled pulse repeater originally designed for general application in the National Bureau of Standards Interim Computer. The repeater stage is modified by redesigning the pulse transformer and changing the method of loading. An analysis of the equivalent circuit is made and predicted results are compared with those obtained experimentally. The resulting transformer and mode of operation have been incorporated into the latest assemblies of the NBS Interim Computer.

NOMENCLATURE

BOTTOMING In a vacuum tube having the plate characteristic curve of a pentode, the steep portion of the characteristic below the point where the curve bends sharply is termed the "bottoming" region. If a load of high enough impedence is used, the tube operates on this portion of the curve at which time it is "bottoming".

SQUIRT INDUCTANCE Squirt inductance (Reference 2*) represents the effects of so called squirted flux which is due to currents charging the distributed capacitances in the windings of the transformer through the winding inductances.

LOW LIMIT TUBE For the purposes of the NBS Interim computer, a low limit tube is one for which the plate current, with 60 volts on the plate and screen and with the grid connected to the cathode, is as low as 25 milliamperes. Characteristically it is capable of less plate current than average tubes under similar operating conditions, and gives more distortion to a train of pulses.

HIGH LIMIT TUBE For the purposes of the NBS Interim computer, a high limit tube is one for which the plate current under the same conditions above exceeds 50 milliamperes or the screen current exceeds 20 milliamperes. Characteristically it passes more plate current than an average tube under similar conditions and gives higher amplitude pulses.

N^{th} PULSES N^{th} pulses are those occurring late in a sequence of pulses.

* References are listed in the bibliography.

ACKNOWLEDGMENT

The author wishes to thank the members of his committee for their aid in the preparation of this report. Particular thanks are due to Drs. William D. Hershberger and T. A. Rogers for their aid and helpful advice during the preparation and writing of this thesis.

The author also wishes to thank all the members of the Electronic Computers Section at the National Bureau of Standards in Washington, D.C. for their many valuable suggestions and their aid in making available the use of laboratory facilities. In particular, thanks are due to Drs. S. N. Alexander, C. H. Page, Samuel Lubkin, Ralph Slutz, and Mr. Robert Elbourn.

Special thanks are due to Mrs. Martin for her continuous encouragement and her aid in typing and proofreading preliminary copies.

INTRODUCTION

Since the advent of the first automatic control device, man has struggled to design machines to make simple decisions for him. Since the first World War, the pressure of development has centered strongly on such equipment. Automatic ranging equipment, automatic temperature control and automatic trouble indicators are only a few of the many devices now being used. Truly each device is a computer; that is, information reaching the device is processed and a decision is made which affects some other equipment. Today the word "computer" is generally applied to a piece of equipment designed and constructed to solve one or more types of complex problems.

Computers may be divided into two classes: analog and digital. Analog computers are those which, to some degree, simulate the system they are being used to analyze. That is, the computer is so assembled that the differential equations describing its operation are similar to those describing the system to be analyzed. The analog computer is operated by the controlled change of an independent variable representing time, distance or some appropriate quantity. Results appear as continuous curves and are interpreted accordingly.

Digital computers are machines capable of performing the arithmetical operation of addition, and in the more complex models, subtraction, multiplication and division. To analyze a system by use of digital machines, the differential equations must be solved in discrete steps with the degree of accuracy desired determining the precision of each step. However the degree of precision available in an analysis using digital computers is limited only be a knowledge of the system and the amount of time available for the analysis. Sometimes the accuracy available with analog computers (usually about three significant decimal digits) is not satisfactory for the problem to be solved. In such cases, digital computers are utilized and the resulting computations often require long periods of time for their completion. Desk type calculators are digital computers which are familiar to most scientists and the more complex punch-card machines perform similar operations, their main advantage being faster and more fully automatic operation.

High speed operation is of little advantage if the human operator must examine each result and make a decision, since then the speed of the operator will be the factor which limits the ultimate speed of the machine. This conclusion has resulted in the design of automatically sequenced computers in which a series of instructions and data are placed in the machine and the data are processed in ac-

cordance with the instructions. In this type of machine the instruction and numbers are held in some memory device readily accessible to the machine and a central control causes the instructions to be obeyed. Thus by making the machine more fully automatic, one may realize the advantages of higher speed operation. The use of vacuum tubes in a computer removes the speed limitation placed by the mechanical elements of such a machine. Thus the advent of electronic digital computers has become one more step in the direction of high speed operation.

In mechanical digital computers, data and instructions are represented by the position of a gear or a hole punched in a card or some other mechanical representation. In electronic digital computers the instruction and data are represented by the voltage upon some element, each element representing a digit. Since many electronic circuits are available which have two stable states, such as the familiar Eccles-Jordan flip-flop circuit, it seems reasonable that electronic digital computers should be designed to operate using binary arithmetic. This has the advantage of avoiding the reliability limitations of amplitude sensitive circuits, that might be necessary if the decimal system were used.

Two basic types of electronic digital computers under development at present are the parallel and the serial. In both parallel and serial computers the instructions and data are represented by voltage pulses traveling through the machine. Each pulse represents one binary digit position of a particular datum or a particular instruction. In serial computers the datum or instruction travels in sequential fashion, the first pulse position representing the first digit and the last pulse position representing the final digit, all pulses traveling over the same path. In parallel computers each digit has its own path and the first and last digits of a piece of information appear at the same time, or in other words, the information travels "broadside".

Unfortunately the pulses lose energy as they travel through the machine and it becomes necessary to replenish this energy at intervals. Various devices such as amplifiers and cathode-followers have been used for this purpose. Pulse transformers are particularly useful as they enable the designer to control the polarity and impedance of his amplifier stage output so as to obtain maximum efficiency from each tube. Pulse transformers, in the past however, have been used entirely in circuits where they are subject to low duty-cycles of 15% or less whereas some of the computers under development utilize duty-cycles as high as 50%. At higher duty-cycle operation, cumulative storage of energy takes place in pulse transformers causing a variety of undesirable effects.

In the design of the National Bureau of Standards Interim Computer, a serial electronic digital machine, a program was initiated to design a pulse transformer suitable for operation at duty-cycles as high as 50%. Due to the fact that the design of this computer was started in order to obtain a small-scale machine quickly, many phases of the component development program were discontinued when a working design was complete although further investigation might have yielded an improved model. In the case of the pulse transformer, no analytical investigation was made of its operation; the model used was designed by observing pulse output characteristics as the design parameters were varied. The resulting transformer is described in reference 1*, *Design of a Transformer-Coupled Pulse-Repeater for General Application in the NBS Interim Computer* by William L. Martin. The motive for the work described in this thesis was to analyze the operation of this latter transformer and design an improved model if possible.

* *References are listed in the bibliography.*

ANALYSIS AND EVALUATION OF EQUIVALENT CIRCUIT

In the NBS Interim Computer, the voltage pulses traveling in serial fashion through the machine are approximately square in shape, of about 0.5 microseconds duration and spaced at one microsecond intervals. Because intelligence is conveyed by the presence or absence of pulses in the various positions of a sequence, it is important that the effect of any device that replenishes lost energy be the same for all pulses regardless of their time position. It is also desirable that the device have a uniform delay to any pulse in order to enable the designer to predict the time-position of the pulse, before and after amplification, with respect to a time scale established by a central pulse generator. Since the machine responds satisfactorily only to a properly shaped pulse, it is important that the amplifier output be of correct form. If for some reason a particular pulse has been weakened more than others, it should be amplified to a standard level. Thus, the ideal function of such a device is that of a pulse-repeater rather than that of a conventional amplifier.

The repeater stage originally designed consisted of a tube-amplifier, a coupled pulse-transformer and the associated diode circuits. The diode circuits serve to establish a standard shape of input signal for each tube as well as to perform the logical functions necessary in a computer. To correct for tube variation and to obtain maximum output from a low-limit* tube, all tubes are operated on the steep portion of their plate characteristic curve in the region known as "bottoming".*

As a transformer is an a-c coupling element and the tube output has a large d-c component, in the presence of continuous pulses, the transformer stores energy during each succeeding pulse until the time integral

$$\int_{t}^{t + \Delta t} E \, dt \qquad \text{(where } \Delta t \text{ is the pulse period)}$$

of its output over one pulse period is equal to zero. Because energy storage causes current drawn by the tube to increase during

* *See nomenclature.*

a sequence of pulses, the tube must be bottomed further than would be otherwise necessary if one wishes to obtain uniform output above an initial voltage level, thus sacrificing some of its output capability. This mode of operation is described in more detail in reference 1.

If the energy stored in a transformer during a pulse could be dissipated before the next pulse occurs, the full output of the tube would be available on every pulse and each pulse would be subject to the same stage delay. Even if only a portion of this energy could be dissipated, an improvement in output would result and the variation in stage delay could be reduced.

In analyzing the operation of the transformer-coupled stage described in reference 1, the value of the energy stored in the transformer will be evaluated by determining the current in the primary inductance of an equivalent circuit after one pulse. Using this current as a new initial condition and an equivalent circuit appropriate for the transformer stage between pulses, the energy stored in the transformer at the time a second pulse might occur is evaluated by determining the current in the primary inductance at this time.

The circuit originally used as a result of the pulse transformer investigations at the National Bureau of Standards is shown in Figure 1. The transformer is a 250-50 turn unit with a core cross section 1/8" x 1/4". The core is grain-oriented silicon-iron, trade-named "Hipersil" by Westinghouse. The laminations are 0.001 inch thick; the core is formed of two "c's" and the window is ¼" x ½".

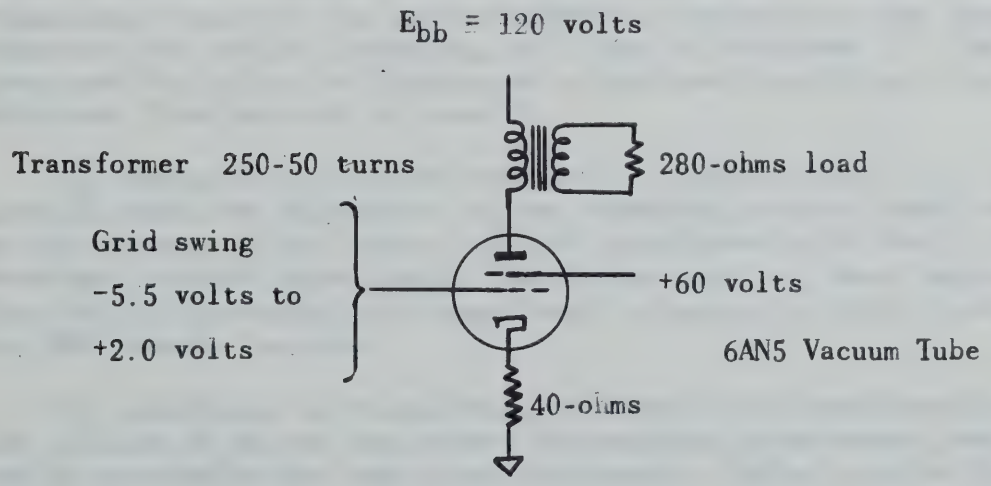

Figure 1

Transformer 250-30 turns
250-ohm load
-5.5 volts re

In order to calculate the circuit performance, the equivalent circuit of Figure 2 is derived from the basic transformer circuit as described in reference 2.

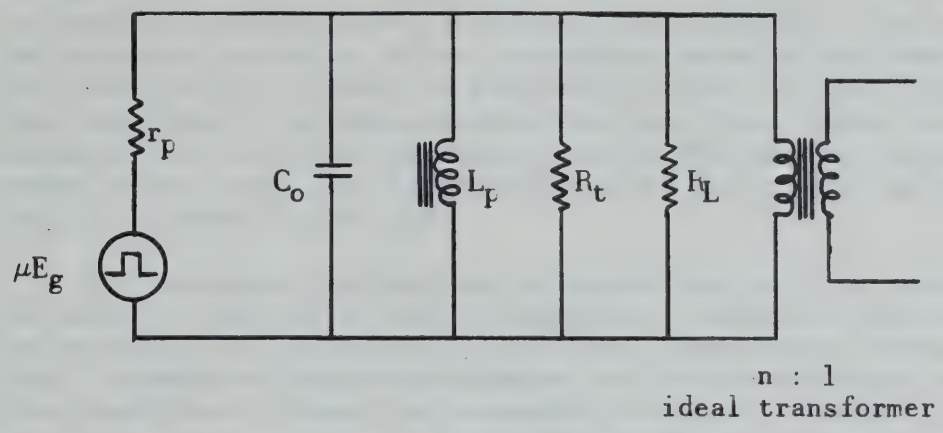

Figure 2

L_p represents the primary inductance of the transformer and is a function of pulse duration, duty cycle, primary turns, primary voltage and core material. In the presence of a pulse of current, the magnetic flux does not penetrate the iron core immediately because of eddy currents and the effective change in inductance that occurs during a pulse makes evaluation of the resulting circuit response difficult. For ease of calculation, average values of inductance during and between pulses are used. These values are consistent with the curves of primary inductance plotted against pulse duration which were obtained in the investigation of low-power pulse transformers made at the Servo-Mechanisms Laboratory at the Massachusetts Institute of Technology as listed in reference 2. The data used for effective inductance is obtained from Figure 11 of reference 2 and appears on page 40.

C_o represents the capacitance of the primary circuit, C_1, in parallel with the capacitance of the secondary circuit transformed to the primary, C_2/n^2, where n is the transformer ratio and C_2 the secondary circuit capacitance. The values used for these capacities are in agreement with those found in typical circuits used in the NBS Interim Computer.

R_L represents the transformer secondary load transferred to the primary; R_t is the resistance representing transformer loss; and r_p represents the tube plate resistance. During a pulse the

Figure 2

value of r_p will be far lower than its value between pulses because the tube will be operating in its bottoming region. Under these circumstances r_p will be only about 500 ohms. R_L is normally 7,000 ohms and R_t is about 24,000 ohms. (This value of R_t was obtained by examining oscillograms of voltages and currents in the primary and secondary circuits of the transformer under pulsed conditions. The losses were too small to observably affect the oscillograms but the precision of the measurements were such that losses would not appear if the equivalent resistor were 24,000 ohms or higher.) Between pulses, with the tube biased to -5.5 volts, from grid to cathode, r_p is about 60,000 ohms.

The equivalent circuit may be simplified if it is desired to emphasize a particular mode of operation. Factors which may be neglected in the equivalent circuit are, transformer leakage reactance, transformer squirt-inductance* and the capacitance between the transformer primary and secondary windings. However, noticeable pulse deterioration is caused by the leakage reactance which causes parasitic oscillations when resonating with the circuit capacitances and also acts to attenuate high frequency components of the pulse.

To obtain the value of the energy stored in L_p during a pulse it is necessary to solve the equations for the equivalent circuit of Figure 2 and evaluate the current in the primary inductance of the transformer at the end of a pulse. The generator in the equivalent circuit has a constant voltage output during this period due to the mode of operation of the tube. For ease of notation the resistance of R_L and R_t in parallel is called R_o.

$$R_o = \frac{R_L R_t}{R_L + R_t}$$

Writing the equations for the summation of the voltages around the loops in the equivalent circuit,

$$\mu E_g - i r_p = R_o i_{R_o} = L_p \frac{di_{L_p}}{dt} = \frac{1}{C_o} \int i_{C_o} dt, \qquad (1)$$

* *See nomenclature.*

and

$$i = i_{R_o} + i_{L_p} + i_{C_o}. \tag{2}$$

Also

$$i_{C_o} = R_o C_o \frac{di_{R_o}}{dt} \quad \text{and} \quad i_{L_p} = \frac{R_o}{L_p}\int i_{R_o}\,dt. \tag{3 and 4}$$

Substituting (2) into (1),

$$\mu E_g - \left(i_{R_o} + i_{L_p} + i_{C_o}\right) r_p - R_o i_{R_o} = 0.$$

Differentiating in respect to t,

$$0 - r_p \frac{di_{R_o}}{dt} - r_p \frac{di_{L_p}}{dt} - r_p \frac{di_{C_o}}{dt} - R_o \frac{di_{R_o}}{dt} = 0. \tag{5}$$

Substituting (3) and (4) into (5),

$$-\left(r_p + R_o\right)\frac{di_{R_o}}{dt} - \frac{r_p R_o}{L_p} i_{R_o} - r_p R_o C_o \frac{d^2 i_{R_o}}{dt^2} = 0$$

Dividing by $-R_o C_o r_p$,

$$\frac{d^2 i_{R_o}}{dt^2} + \frac{R_o + r_p}{R_o C_o r_p}\cdot\frac{di_{R_o}}{dt} + \frac{i_{R_o}}{L_p C_o} = 0 \tag{6}$$

Solving (6) in the form

$$i_{R_o} = C_1 \epsilon^{(\alpha + \beta)t} + C_2 \epsilon^{(\alpha - \beta)t} \tag{7}$$

where

$$\alpha \pm \beta = \frac{-b}{2a} \pm \frac{\sqrt{b^2 - 4ac}}{2a}$$

where $\alpha \pm \beta$ is the solution of

$$\frac{ad^2x}{dt^2} + \frac{bdx}{dt} + cx = 0,$$

and where

$$a = 1, \quad b = \frac{R_o + r_p}{R_o C_o r_p}, \quad c = \frac{1}{L_p C_o}.$$

C_1 and C_2 are integration constants to be evaluated using a knowledge of the initial conditions.

Thus

$$\alpha = -\frac{1}{2}\left[\frac{R_o + r_p}{R_o C_o r_p}\right], \tag{8}$$

and

$$\beta = \frac{1}{2}\sqrt{\left[\frac{R_o + r_p}{R_o C_o r_p}\right]^2 - \frac{4}{L_p C_o}}. \tag{9}$$

Initial conditions are as follows: at time t = 0, the equivalent circuit generator voltage has just become μEg. No voltage has been present until this time.

Thus at t = 0,

$$i_{R_o} = 0 \quad \text{or} \quad i_{C_o} = \frac{\mu Eg}{r_p}$$

Also at $t = 0$, $Q = C_o e$, that is, $e = \frac{Q}{C_o} = \frac{\int i_{C_o} dt}{C_o}$

where Q = charge in C_o, e = voltage across C_o.

Also

$$i_{R_o} = \frac{e}{R_o}, \quad \frac{di_{R_o}}{dt} = \frac{de}{dt}\frac{1}{R_o} = \frac{i_{C_o}}{C_o}\cdot\frac{1}{R_o} ,$$

but at $t = 0$, $i_{C_o} = \frac{\mu E g}{r_i}$,

therefore at $t = 0$, $\frac{di_{R_o}}{dt} = \frac{\mu E g}{R_o C_o r_i}$.

From (7), $\frac{di_{R_o}}{dt} = (\alpha + \beta)C_1 \epsilon^{(\alpha + \beta)t} + (\alpha - \beta)C_2 \epsilon^{(\alpha - \beta)t}$.(10)

Substituting the initial conditions in (7) and (10),

$$0 = C_1 + C_2, \text{ therefore, } C_2 = -C_1. \qquad (11)$$

$$\frac{\mu E g}{R_o C_o r_i} = (\alpha + \beta)C_1 + (\alpha - \beta)C_2 \qquad (12)$$

Substituting (11) in (12), $\frac{\mu E g}{R_o C_o r_i} = \alpha C_1 + \beta C_1 - \alpha C_1 + \beta C_1 = 2\beta C_1$,

$$C_1 = \frac{\mu E g}{R_o C_o r_p} \cdot \frac{1}{2\beta}, \quad C_2 = \frac{-\mu E g}{R_o C_o r_p} \cdot \frac{1}{2\beta},$$

therefore, $i_{R_o} = \frac{\mu E g}{R_o C_o r_p} \cdot \frac{1}{2\beta} \left[\epsilon^{(\alpha + \beta)t} - \epsilon^{(\alpha - \beta)t} \right]$.

From (1), $i_{L_p} = \frac{R_o}{L_p} \int i_{R_o} dt$,

therefore, $i_{L_p} = \frac{R_o}{L_p} \left\{ \frac{\mu E g}{R_o C_o r_p} \cdot \frac{1}{2\beta} \int \left[\epsilon^{(\alpha + \beta)t} - \epsilon^{(\alpha - \beta)t} \right] dt \right\}$

$$= \frac{\mu E g}{2 L_p C_o r_p \beta} \left\{ \frac{\epsilon^{(\alpha + \beta)t} - 1}{\alpha + \beta} + \frac{\epsilon^{(\alpha - \beta)t} - 1}{\alpha - \beta} \right\} \qquad (13)$$

To obtain an approximate value of the current in the primary inductance at the end of a pulse, it is necessary to evaluate equation (13) for the specific circuit constants involved.

An average value of L_p for a 0.5 microsecond pulse on a Hipersil core of the cross section stated above and having a 250-turn primary may be estimated from the Whirlwind data shown on page 40 to be about 7.5 millihenrys. R_L is 7,000-ohms, R_t is about 24,000-ohms and C_o may be taken to be about 12 micro-microfarads.

Thus $R_o = \frac{R_L R_t}{R_L + R_t} \approx 5{,}420$-ohms,

$C_o = 12 \cdot 10^{-12}$ farads,

$L_p = 7 \cdot 5 \cdot 10^{-3}$ henrys,

r_p = 500-ohms,

$\mu Eg \approx 100$ volts (measured),

$t \approx 0.5 \cdot 10^{-6}$ seconds (pulse duration),

$\alpha = -91.5 \cdot 10^6$ radians/sec.,

$\beta = 91.5 \cdot 10^6$ radians/sec.,

$\alpha + \beta \approx 0$ radians/sec,

$\alpha - \beta \approx -183 \cdot 10^6$ radians/sec.

$$i_{L_p} = (1.21 \cdot 10^4) \left[\frac{\epsilon^{(\alpha + \beta)t} - 1}{\alpha + \beta} + \frac{\epsilon^{(\alpha - \beta)t} - 1}{\alpha - \beta} \right],$$

but as $0 \leq \alpha + \beta << 1$, $(\alpha - \beta) << -1$, and $|\alpha - \beta| >> 10^6$,

an excellent approximation for the bracketed term above is

$$\left[\frac{\epsilon^{(\alpha + \beta)t} - 1}{\alpha + \beta} + \frac{\epsilon^{(\alpha - \beta)t} - 1}{\alpha - \beta} \right] = t.$$

Therefore,

$$i_{L_p} = 0.006 \text{ amperes.}$$

Hence, the current in L_p is increased by about 6 milliamperes during each pulse as long as the tube is operating in the bottoming region.

Figure 2 also represents an equivalent circuit of the transformer-coupled stage for the interval between pulses. During this time interval the generator has no output but a current in L_p initiated during the preceeding pulse or pulses is flowing.

To find the amount of energy present at the time the next pulse might occur or the energy dissipated between pulses, it is necessary to solve the equations for the circuit of Figure 2 with these new initial conditions and evaluate the current remaining in L_p at this new time. For ease of notation the resistance of r_p,

R_L and R_t in parallel is called R_z. $R_z = \dfrac{R_L r_f R_t}{R_L r_f + R_L R_t + r_f R_t}$

By Kirchoff's Law,

$$\frac{-L_f di_{L_f}}{dt} = (i_{R_z})R_z = \frac{1}{C_o}\int i_{C_o} dt \ , \tag{14}$$

and $i_{L_f} = i_{R_z} + i_{C_o}$; $i_{R_z} = i_{L_f} - i_{C_o}$. (15)

Also $i_{C_o} = \dfrac{-L_f C_o d^2 i_{L_f}}{dt^2}$ and $i_{R_z} = \dfrac{-L_f}{R_z} \cdot \dfrac{di_{L_f}}{dt}$. (16)

Combining (15) and (16), $\dfrac{-L_f di_{L_f}}{dt} = (i_{L_f} - i_{C_o})R_z$

$$= \frac{-L_f di_{L_f}}{dt} = (i_{L_f})R_z + \frac{R_z L_f C_o d^2 i_{L_f}}{dt^2} .$$

Dividing by $R_z L_f C_o$,

$$\frac{d^2 i_{L_f}}{dt^2} + \frac{1}{R_z C_o} \cdot \frac{di_{L_f}}{dt} + \frac{i_{L_f}}{L_f C_o} = 0 . \tag{17}$$

To solve for i_{L_f}, assume the solution is of the form,

$$i_{L_f} = C_1 \epsilon^{(\alpha + \beta)t} + C_2 \epsilon^{(\alpha - \beta)t} \tag{18}$$

where $\alpha = \frac{-1}{2R_zC_o}$ and $\beta = \frac{1}{2}\sqrt{\left(\frac{1}{R_zC_o}\right)^2 - \frac{4}{L_pC_o}}$.

α and β now have the new values shown and C_1 and C_2 are to be determined.

Setting initial conditions,

at $t = 0$, $i_{L_p} = \bar{\imath}$ where $\bar{\imath}$ is the current remaining in L_p after the preceding pulse.

At $t = 0$, $\frac{di_{L_p}}{dt} = 0$. This approximation is correct within 4% for each transformer considered due to the low capacitance of the circuits.

Differentiating (18), $\frac{di_{L_p}}{dt} = (\alpha + \beta)C_1\epsilon^{(\alpha + \beta)t} + (\alpha - \beta)C_2\epsilon^{(\alpha - \beta)t}$, (19)

therefore, from (18), at $t = 0$, $i_{L_p} = \bar{\imath} = C_1 + C_2$. $C_1 = \bar{\imath} - C_2$. (20)

From (19), at $t = 0$, $\frac{di_{L_p}}{dt} = 0 = \alpha C_1 + \beta C_1 + \alpha C_2 - \beta C_2$. (21)

Substituting (20) in (21),

$$\alpha\bar{\imath} - \alpha C_2 + \beta\bar{\imath} - \beta C_2 + \alpha C_2 - \beta C_2 = (\alpha + \beta)\bar{\imath} - C_2(2\beta) = 0 ,$$

therefore, $C_2 = \frac{(\alpha + \beta)}{2\beta}\bar{\imath}$.

$$C_1 = \bar{\imath} - \frac{(\alpha + \beta)\bar{\imath}}{2\beta} = \frac{2\beta\bar{\imath} - \alpha\bar{\imath} - \beta\bar{\imath}}{2\beta} = -\frac{(\alpha - \beta)\bar{\imath}}{2\beta} .$$

From (18), $i_{L_p} = \bar{i}\left\{\left[\frac{-(\alpha-\beta)}{2\beta}\right]\epsilon^{(\alpha+\beta)t} + \left[\frac{\alpha+\beta}{2\beta}\right]\epsilon^{(\alpha-\beta)t}\right\}$, (22)

or $\frac{i_{L_p}}{\bar{i}} = \left[\frac{-(\alpha-\beta)}{2\beta}\right]\epsilon^{(\alpha+\beta)t} + \left[\frac{\alpha+\beta}{2\beta}\right]\epsilon^{(\alpha-\beta)t}$. (23)

To determine the energy stored in the transformer 0.5 microsecond after the previous pulse has ended, (or just before the next pulse may occur) equation (23) for $^{1}L_{p}/\bar{i}$ must be evaluated using the appropriate values of circuit capacitance, inductance and resistance. A value of inductance higher than that just employed is now used due to the additional penetration of the core by the magnetic flux at this later time. The increased value of inductance is obtained from the curve on page 40. It represents the average value of inductance for a 250 primary turn transformer from 0.5 to 1 microsecond after the pulse was applied.

$L_p = (1.5)(10^{-3})(250/70)^2(2/3)$ henrys $= 12.8 \cdot 10^{-3}$ henrys.

As before, $C_o = 12.10^{-12}$ farads.

The relative portion of i_{L_p} remaining at time "t" $= \frac{i_{L_p}}{\bar{i}} =$

$$-\frac{(\alpha-\beta)}{2\beta}\epsilon^{(\alpha+\beta)t} + \frac{(\alpha+\beta)}{2\beta}\epsilon^{(\alpha-\beta)t}$$

where

$$\alpha = -\frac{1}{2R_zC_o} \quad \text{and} \quad \beta = \frac{1}{2}\sqrt{\left[\frac{1}{R_zC_o}\right]^2 - \frac{4}{L_pC_o}}$$

$$R_z = \frac{R_L R_t r_p}{R_L r_p + R_L R_t + r_p R_t}$$

where $r_p = 60{,}000$-ohms, $R_t = 24{,}000$-ohms, $R_L = 7{,}000$-ohms,

and $t = 0.5 \cdot 10^{-6}$ seconds.

Thus, $R_z = 4{,}970$-ohms,

$$\alpha = -\frac{1}{2R_zC_o} = -8.37 \cdot 10^6 \text{ radians/sec.}$$

$$\beta = 7.9 \cdot 10^6 \text{ radians/sec.}$$

$$\alpha + \beta = -0.47 \cdot 10^6 \text{ radians/sec.}$$

$$\alpha - \beta = -16.27 \cdot 10^6 \text{ radians/sec.}$$

Substituting the above values in equation (23),

$$\frac{i_{L_p}}{\bar{i}} = 0.815$$

Thus 81.5% of the current initially flowing in the primary inductance of the transformer is still flowing 0.5 microseconds after the pulse has ended.

The circuit is resonant but highly damped. If the damping were removed, the circuit would oscillate at a frequency,

$$f = \frac{1}{2\pi\sqrt{LC}} = 0.41 \cdot 10^6 \text{ cycles per second.}$$

As stated earlier, the goal of this investigation is to find a method of dissipating between pulses all or most of the energy stored in the transformer during a pulse so as to cause the circuit to return to its initial potential. If this latter condition could be attained without dissipating the stored energy, this would be just as satisfactory as long as the stored energy did not result

in some spurious signal. If the current in the transformer circuit could be made to oscillate at a suitable frequency between pulses, it would pass through a potential equal to that desired after one half period of oscillation. Any energy remaining in the circuit after this half period of oscillation would aid the tube to drive the transformer on the following pulse. However, if no following pulse occurred, this residual energy might cause a spurious signal. If less than one half period of such an oscillation (but more than one fourth period) took place in the interval between pulses, the transformer would possibly be closer to its initial potential than it was in the case of over-damping. One ready method of disconnecting the load at the desired time is to use germanium diodes in series with it; no more than one half period of oscillation can take place because, during the succeeding half period, the oscillation is heavily over-damped by the full load which is present when the diode conducts in its forward direction.

An equivalent circuit employing diode loading appears in Figure 3.

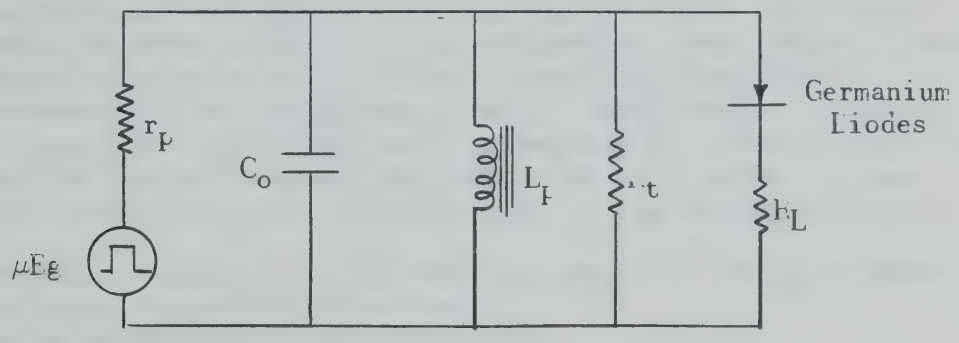

Figure 3

Although the present transformer will oscillate on the back-swing when operated into a non-linear load, the period of its oscillation is too large to allow it to return to its initial voltage state between pulses. In fact, it oscillates through less than one fourth period before the next pulse occurs.* As

---

** If a diode is connected in series with the load in a 250-turn transformer, it is connected in the secondary circuit. The back-*

(footnote continued on next page)

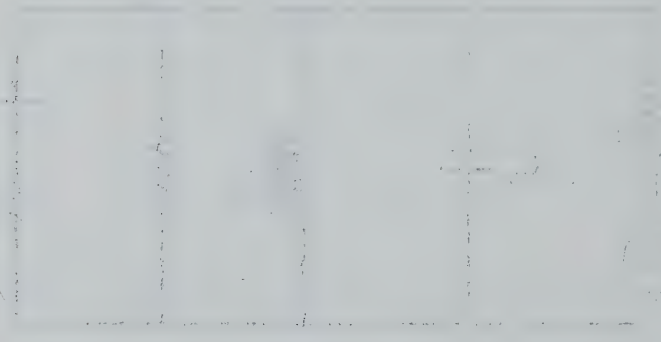

a result, the tube plate potential is made highly positive by the inductive backswing of the transformer at the time the next pulse may occur and the current through the tube must discharge this increased potential as well as the potential normally existing across the circuit capacitance. Therefore, the stage has an increased delay due to the time needed to discharge this additional potential and pulses occurring late in a sequence are delayed to an increased degree.

The problem of increasing the resonant frequency of the circuit may be solved by decreasing the primary inductance of the transformer; this is most easily done by using a smaller number of primary turns. The primary turns may not be decreased without limit, however, as current in the primary inductance (which increases the tube current) increases with decreasing inductance. The knee of the zero-bias plate characteristic curve of a low-limit 6AN5 tube occurs at approximately 25 milliamperes and the current in the transformer primary inductance added to the current in the primary load must not exceed this value if a low-limit tube is to remain bottomed and so give uniform output to all pulses. If the 250-turn transformer were redesigned so that the natural resonant frequency of the circuit were doubled, the period of oscillation would be near twice the interval between pulses since the current in the stage output would oscillate at approximately one megacycle per second. Decreasing the primary turns by a factor of two will reduce the inductance by a factor of four and thus cause the current to oscillate at the desired frequency.

Previous tests on transformers subjected to one pulse show

(footnote continued from previous page)

resistance of a germanium diode never is lower than 50,000-ohms and connecting three of them in parallel and the combination in series with the usual 280-ohms load will yield a secondary load of 50,000/3 + 280-ohms or 16,950-ohms. Transformed to the primary circuit this becomes $(16,950)n^2 = (16,950)(25) = 424,000$-ohms. Thus $R_z = 16,500$-ohms. The resulting frequency of oscillation is,

$$frequency = \frac{1}{2\pi} \cdot \sqrt{\frac{1}{L_p C_o} - \left[\frac{1}{2R_z C_o}\right]^2} = 0.0575 \cdot 10^6 \text{ cycles/sec.}$$

As before, $L_p = 12.8 \cdot 10^{-3}$ henrys, and $C_o = 12 \cdot 10^{-12}$ farads.

that with a low-limit tube, a decrease in the output pulse amplitude during the pulse does not occur for transformers with 120-primary turns; however if the turns are reduced to less than 120, this decrease occurs. As the mode of operation proposed would result in pulses which are relatively uninfluenced by the preceeding pulse, these early tests should be reliable in predicting a satisfactory transformer and a 120-turn primary might be suitable. Repeating the above calculations, this time for a 120-24-turn transformer, which would have a primary inductance reduced by the square of the ratios of the primary turns of the two units, (*i.e.*, $(120/250)^2$), i_{L_p} at the end of one pulse is,

$$i_{L_p} = \frac{\mu Eg}{2\beta L_p C_o r_p}\left[\frac{\epsilon^{(\alpha+\beta)t} - 1}{\alpha + \beta} + \frac{\epsilon^{(\alpha-\beta)t} - 1}{\alpha - \beta}\right] \quad \text{from (13)}$$

Where,

μEg = 100 volts as before,

L_p is reduced by $\left[\frac{120}{250}\right]^2$; $L_p = (7.5)\left[\frac{120}{250}\right]^2 \cdot 10^{-3}$

$= 1.73 \cdot 10^{-3}$ henrys

r_p = 500-ohms as before

$C_o = 12 \cdot 10^{-12}$ farads as before

$t = 0.5 \cdot 10^{-6}$ seconds " "

R_L = 7,000-ohms " "

R_t = 24,000-ohms " "

R_z = 16,500-ohms " "

Therefore, i_{L_p} after one pulse is 0.0264 amperes.

In evaluating $\frac{i_{L_p}}{\bar{i}}$ 0.5 microsecond after the first pulse has ended

the L_p existing at this later time is reduced by the square of the turns ratio for the two transformers as in the previous calculations and is $(12.8 \cdot 10^{-3})(120/250)^2 = 2.95 \cdot 10^{-3}$ henrys.

$C_o = 12 \cdot 10^{-12}$ farads as before.

$\alpha = -2.52 \cdot 10^6$ radians/sec.

$\beta = 4.7 \cdot 10^6 \sqrt{-1} = j4.7 \cdot 10^6$ radians/sec.

From the above,

$$\frac{i_{L_p}}{\bar{i}} = -\frac{(\alpha - \beta)}{2\beta}\epsilon^{(\alpha+\beta)t} + \frac{(\alpha + \beta)}{2\beta}\epsilon^{(\alpha-\beta)t} ,$$

but $\beta = j\delta$,

therefore,

$$\frac{i_{L_p}}{\bar{i}} = -\frac{(\alpha - j\delta)}{2j\delta}\epsilon^{(\alpha+j\delta)t} + \frac{(\alpha + j\delta)}{2j\delta}\epsilon^{(\alpha-j\delta)t}$$

$$= \epsilon^{\alpha t}\left[-\frac{(\alpha - j\delta)}{2j\delta}\epsilon^{j\delta t} + \frac{(\alpha + j\delta)}{2j\delta}\epsilon^{-j\delta t}\right] .$$

$$\frac{i_{L_p}}{\bar{i}} = \frac{\epsilon^{\alpha t}}{2j\delta}\left[-(\alpha - j\delta)(\cos \delta t + j \sin \delta t) + (\alpha + j\delta)(\cos \delta t - j \sin \delta t)\right]$$

$$= \epsilon^{\alpha t}\left(\cos \delta t - \frac{\alpha}{\delta} \sin \delta t\right) .$$

Substituting the above values in (24) and setting $\frac{i_{L_p}}{\bar{i}} = 0$,

$$0 = \epsilon^{-2.52 \cdot 10^6 t}(\cos 4.7 \cdot 10^6 t + 0.536 \sin 4.7 \cdot 10^6 t)$$

$t = 0.435$ microsecond.

Thus it takes 0.435 microsecond for the voltage across the capacitance to return to its initial value. If the time between pulses is as large as 0.435 microsecond, the transformer output voltage would return to its initial position if it were free to oscillate.

One problem which presents itself at this point is the effect of the energy in the inductance manifesting itself as a spurious signal at the end of one half cycle of oscillation if no second pulse is present. Because the load will result in heavy damping when the oscillation is in the phase to cause positive output, the oscillation should be almost quenched after one half period. If the noise signal is of sufficient amplitude to cause trouble, (a minimum signal to noise ratio of 10 has been set) it could be eliminated by operating the diode shunted by a resistor of the proper size to critically damp the circuit between pulses. Calculations for a resistor which is to be placed across the diode to cause critical damping for a 250-turn and 120-turn transformer appear below:

To cause critical damping the value of β must be equal to zero.

Therefore,

$$\beta = \frac{1}{2}\sqrt{\left[\frac{1}{R_z C_o}\right]^2 - \frac{4}{L_p C_o}} = 0$$

$$R_z = \frac{1}{2} \cdot \frac{L_p}{C_o}$$

For a 250-turn transformer,

$L_p = 12.8 \cdot 10^{-3}$ henrys

$C_o = 12 \cdot 10^{-12}$ farads

r_p = 60,000-ohms as before

R_t = 24,000-ohms as before

$$R_z = \frac{1}{2}\sqrt{\frac{L_p}{C_o}} = 16,300\text{-ohms}$$

If R_L is the resistance the secondary load circuit of the transformer reflects to the primary,

$$R_L = \frac{r_p R_t R_z}{r_p R_t - R_z r_p - R_t R_z} = 380,000\text{-ohms}$$

The secondary load is $\frac{R_L}{n^2}$ or 15,200-ohms as compared with the 17,000 ohms that is already present. Thus this transformer is very nearly critically damped if the circuit consists only of the diode-connected load.

A 120-turn transformer differs from the 250-turn unit in that a reduced L_p is used. L_p, as in the previous calculations for a 120-turn transformer is $2.95 \cdot 10^{-3}$ henrys.

$$R_z = \frac{1}{2}\sqrt{\frac{L_p}{C_o}} = 7,800\text{-ohms}$$

R_L = 143,000-ohms

The secondary load is $\frac{R_L}{n^2}$ or 5,730-ohms as compared with the 17,000-ohms that exists. The resistance of the paralleled germanium diodes and an accompanying shunt resistor must be equal to 5,730-ohms - 280-ohms or 5,450-ohms. The 5,450-ohm resistance will be called R_n. As the resistance of the three diodes in parallel is about 16,700-ohms, the resistance shunting these diodes should be

$$R_{shunt} = \frac{(R_n)(R_{diodes})}{R_{diodes} - R_n} = \frac{(5,450)(16,700)}{16,700 - 5,450} = 8,100\text{-ohms}$$

Because of the assumptions used in the previous evaluations, (50% duty cycle, vertical sided pulses and average inductances) actual operation with 50% duty cycle and sloped sided pulses may prevent the transformer from achieving the desired type of operation. However, as the transformer was satisfactory for single pulse operation, it may well be satisfactory for continuous pulses if the interval between pulses is not too short. With these limitations in mind, a test set-up for determining the relative outputs of 120-turn and 250-turn transformers was made.

EXPERIMENTAL RESULTS

To test the preceeding theory, oscillograms of transformer output for a 250-50-turn transformer and a 120-24-turn transformer were taken with a directly connected load (Figure 4A), diode loading (Figure 4B) and diodes in parallel with a resistor (Figure 4C)

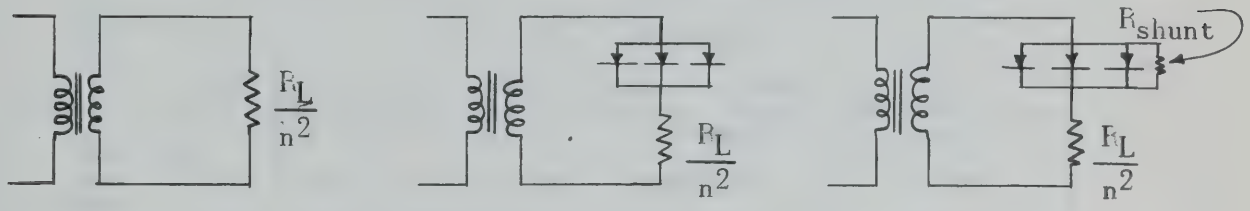

A
overdamping

B
underdamping

C
critical damping

Figure 4

With diode loading, the circuits oscillated between pulses at about the predicted frequencies. The largest spurious noise signal occurring for the circuit of Figure 4B after the half cycle of oscillation was less than 1/12 full signal amplitude and, therefore, because a minimum signal to noise ratio of 10 had been set, critical damping was not necessary. The response obtained with critically dampened circuits was almost identical with that for no damping. When tested with pulses having a duty cycle of about 40%, the output of the 120-turn transformer for any pulse in a train was of the same amplitude as the output of the 250-turn transformer. The worst rise and fall times were considerably less than those of the 250-turn transformer and this might be expected because of the reduced primary inductance and leakage reactance. Table I gives pulse characteristics taken from the test results. Pulse rise and fall times and top width time in microseconds for the first pulse in a sequence and for a pulse occurring late* in the sequence, are given.

**Pulses occurring late in a sequence will be referred to as "N^{th}" pulses throughout the remainder of this report.*

TABLE I

Transformer Output Characteristics

Output of 120 and 250-Turn Transformers Under Various Degrees of Damping

Transformer	Pulse Rise Time*		Pulse Fall Time*		Circuit Conditions	Output Amplitude (Nth Pulse)
	1st	Nth	1st	Nth		(volts)
120 Turn Trans.	0.07	0.08	0.09	0.07	Overdamped	14.6
	0.08	0.06	0.09	0.10	Underdamped	16.5
	0.08	0.06	0.09	0.10	Critically damped	16.5
250 Turn Trans.	0.06	0.10	0.20	0.10	Overdamped	16.8
	0.08	0 09	0.17	0.14	Underdamped	16.8
	0.06	0.09	0.20	0.14	Critically Damped	16.8

Transformer	Pulse Top Width Time* (Effective)		Circuit Conditions
	1st Pulse	Nth Pulse	
120 Turn Trans.	0.31	0.30	Overdamped
	0.29	0.32	Underdamped
	0.30	0.31	Critically damped
250 Turn Trans.	0.32	0.25	Overdamped
	0.28	0.26	Underdamped
	0.32	0.28	Critically damped

Note: The input pulse has a rise and fall time of 0.05 microsecond and an effective top of 0.3 microsecond.

The generated noise signal for the 250-turn transformer in the case of underdamping is less than 1/12 full signal level.

The generated noise signal for the 120-turn transformer in the case of underdamping is less than 1/10 full signal level.

* *All times are given in microseconds.*

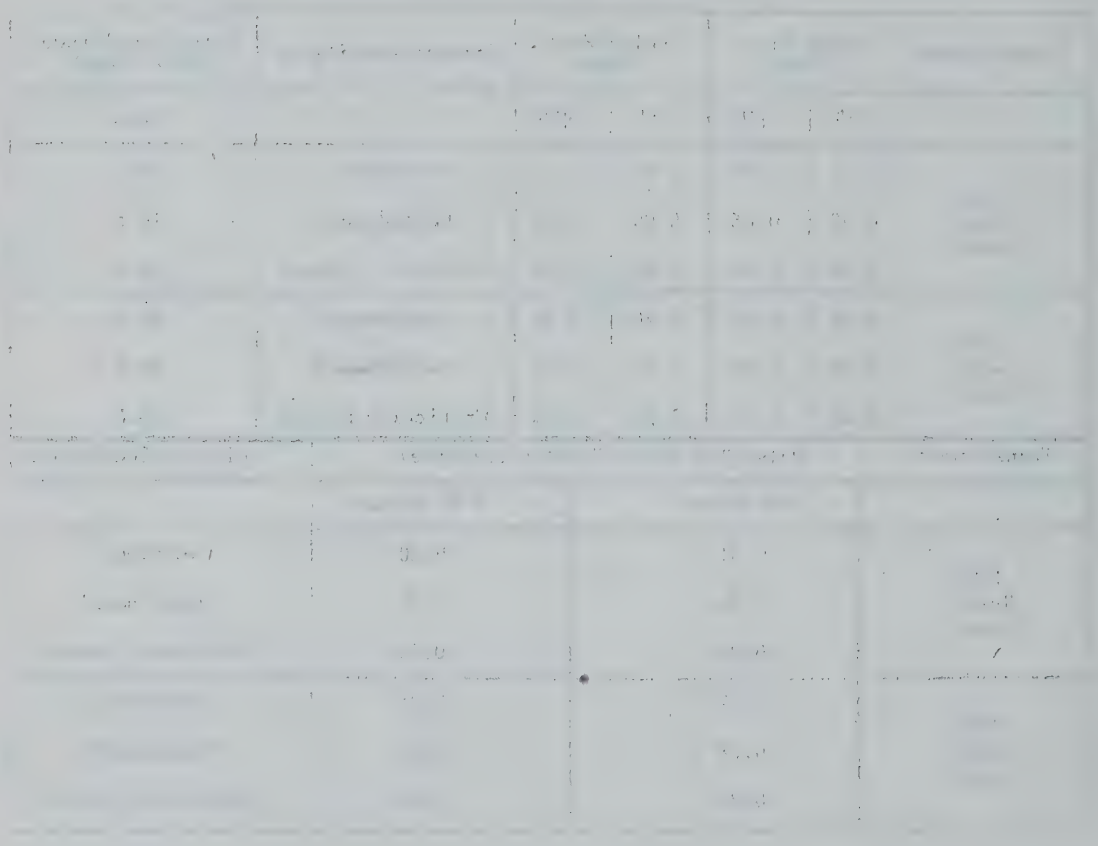

The data are repeated for the 120-turn and 250-turn transformers under conditions of overdamping, underdamping and critical damping.

Sample oscillograms of the output pulse characteristics for the case of underdamping for 250-turn and 120-turn transformers appear in Figures 5, 6, 7 and 8.

To obtain assurance that the use of 120-turn transformers would not result in an excessive reduction in pulse amplitude for pulses wider than those in the original tests, but required in some circuits of the machine, oscillograms were taken of transformer output for the two transformers previously tested. In these tests the pulse duration (pulse flat top) was varied from approximately 0.26 microseconds to 0.55 microseconds. A third transformer of 100-20-turns was also tested. Results of these tests appear in Table II. From the sample oscillograms in Figure 9 through 17, it can be seen that while the 250-turn transformer has little loss in pulse amplitude for long pulses, its top is impaired by the poor rise front. The 120-turn transformer has about 6% loss in amplitude for a pulse of about 0.41 microseconds duration but this loss increases to 25% for pulses as long as 0.52 microseconds. As the basic pulse lasts only 0.43 microseconds, the 120-turn transformer would probably be suitable for general application in the NES Interim Computer. The 100-turn transformer has about 25% loss in amplitude for pulses of about 0.41 microseconds duration and so would be unsuitable for general use. From Table II, the duty cycle in the case of the 0.41 microsecond pulse is about 51%. (That is, the base of the output pulse is 51% of a pulse period. It must be remembered that the transformer circuit can only oscillate, and so remove its stored energy, between pulse bases.)

As a further comparison of the characteristics of the two transformers, relative delay or timing tests for 120-turn and 250-turn transformers were made with stages containing all high or all low limit values of components that would affect pulse delay. The circuits used for these tests appear in Figure 18.

Three stages similar to the one shown in Figure 18 were used in series. Resistor values were as tabulated. Data were obtained of stage delay when both the resistors and the quality of tube in each stage were varied. For any given set of data, a high limit tube (designated H), a low limit tube (designated C) and an average tube (designated A) were used in the respective stages. Relative delays of the various significant points on the pulses passing

TABLE II

Amplitudes of Leading and Trailing Edges of Pulses from Test Transformers with Varying Duty Cycle of Operation

Pulse amplitude is in volts; repetition rate is one megacycle.

Pulse Top Width in Microseconds →	0.26		0.41		0.52		0.55	
Duty Factor →	39%		51%		59%		64%	
Transformer ↓	Lead	Trail	Lead	Trail	Lead	Trail	Lead	Trail
100-20	16.0	16.0	16.0	12.0	15.0	9.0	15.0	8.0
120-24	16.0	16.0	16.0	15.0	16.0	12.0	16.0	10.0
250-50	16.0	16.0	16.0	16.0	16.0	16.0	16.0	15.0
250-50 (Overdamped)	16.6	16.0	16.0	16.0	13.0	13.0	13.0	11.0

1^{st} pulses out of a
250-turn transformer

Figure 5

1^{st} pulses out of a
120-turn transformer

Figure 6

N^{th} pulses out of a
250-turn transformer

Figure 7

N^{th} pulses out of a
120-turn transformer

Figure 8

Note: In all the above cases, the load is three paralleled germanium diodes in series with a 280-ohm resistor. The vertical scale is 5.6 volts/small division and the horizontal scale is 0.08 microsecond/small division.

N^{th} pulses out of 250-turn
transformer on 280-ohm load.
Duty Factor -- 39%
Vertical scale -- 22 volts/small division
Horizontal scale -- 0.16 microsecond/small division

Figure 9

N^{th} pulses out of 120-turn
transformer on 280-ohm load.
Duty Factor -- 39%
Scales -- same

Figure 10

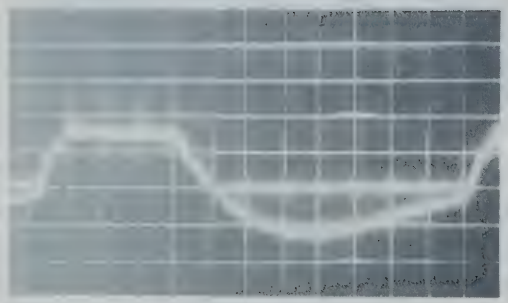

N^{th} pulses out of 100-turn
transformer on 280-ohm load.
Duty Factor -- 39%
Scales -- same

Figure 11

N^{th} pulses out of 250-turn
transformer on 280-ohm load.
Duty Factor -- 51%
Vertical scale -- 22 volts/small division
Horizontal scale -- 0.16 microsecond/small division

Figure 12

N^{th} pulses out of 120-turn
transformer on 280-ohm load.
Duty Factor -- 51%
Scales -- same

Figure 13

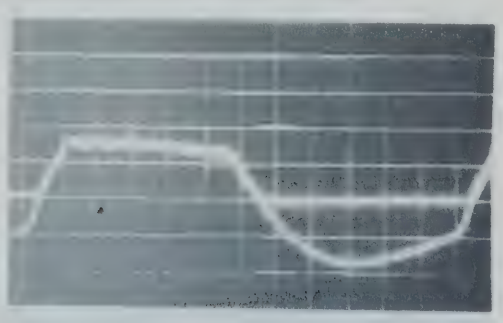

N^{th} pulses out of 100-turn
transformer on 280-ohm load.
Duty Factor -- 51%
Scales -- same

Figure 14

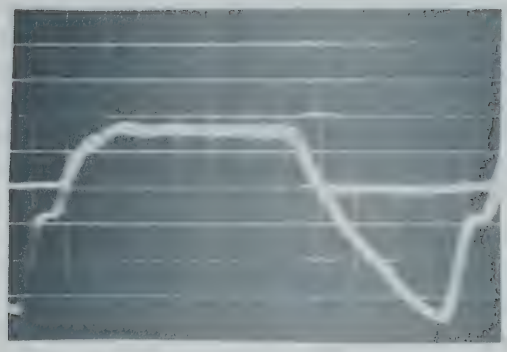

N^{th} pulses out of 250-turn
transformer on 280-ohm load.
Duty Factor -- 64%
Vertical scale -- 22 volts/small division
Horizontal scale -- 0.16 microsecond/small division

Figure 15

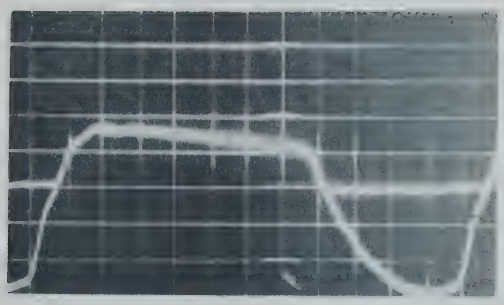

N^{th} pulses out of 120-turn
transformer on 280-ohm load.
Duty Factor -- 64%
Scales -- same

Figure 16

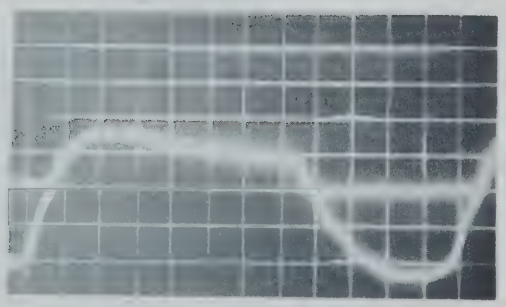

N^{th} pulses out of 100-turn
transformer on 280-ohm load.
Duty Factor -- 64%
Scales -- same

Figure 17

through the stage are recorded in Table III for the 250-turn transformer and Table IV for the 120-turn transformer. Table V gives an overall numerical representation of these results. Figures 19 through 22 are sample photographs of the data from which timing information was obtained. It can be seen in the latter figures that the decreased circuit Q caused by the smaller leakage reactances of the 120-turn transformer results in a cleaner wave form with less undesired oscillations on the leading edge of the pulse. These effects are more pronounced on gating loads (Figures 19 to 22) than on the resistor loads (Figures 5 to 8) that the first tests were made with.

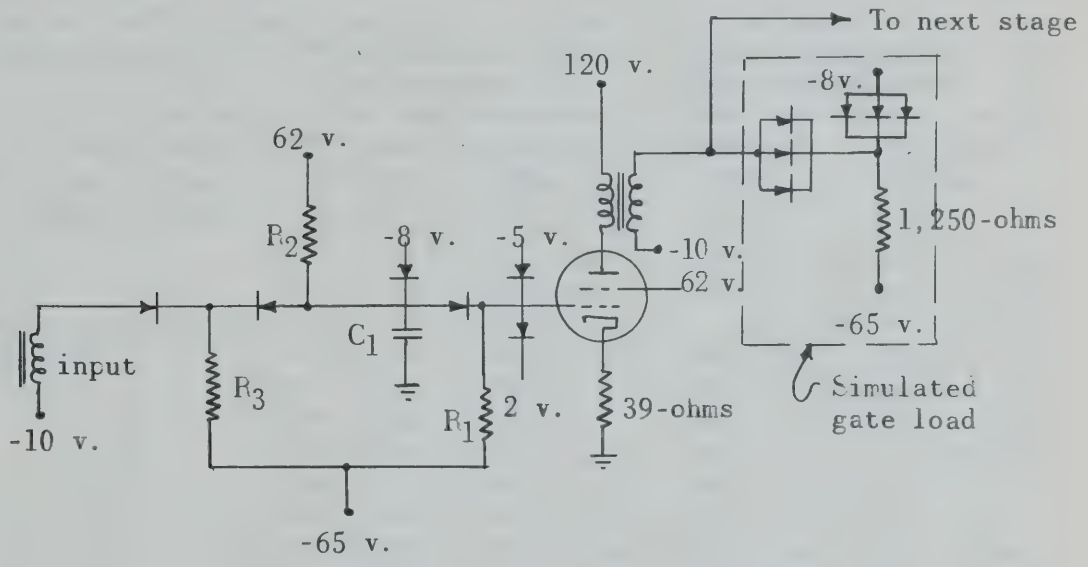

Typical Gating Circuit Used in Testing
Stage Delay Under Limiting Conditions

	Slow Gate	Fast Gate
R_1	= 39.6KΩ± 1%	32.4KΩ± 1%
R_2	= 14.3KΩ± 1%	11.7KΩ± 1%
R_3	= 8.25KΩ± 1%	6.75KΩ± 1%
C_1	= $5 \cdot 10^{-12}$ farads	0 farads

Figure 18

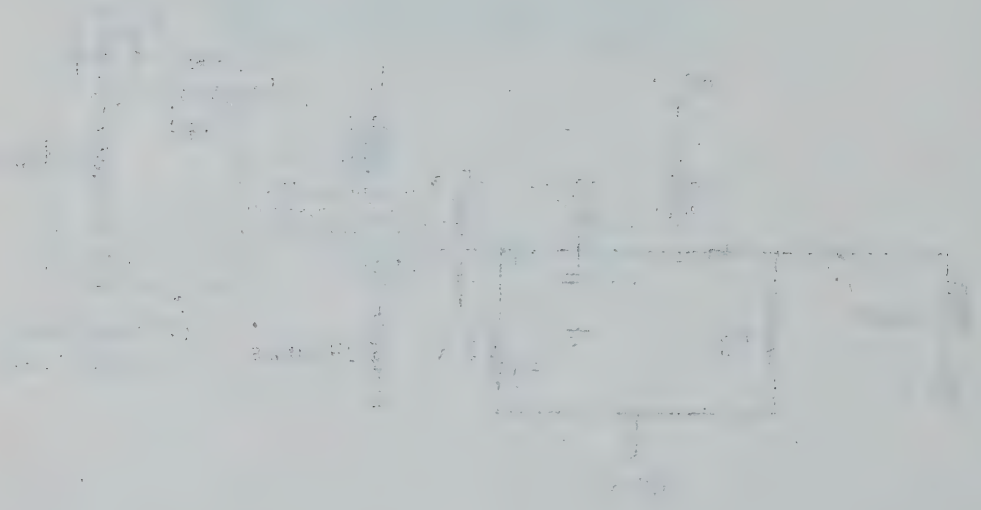

TABLE III

Pulse Delay Characteristics For A 250-Turn Transformer

Delay in microseconds is measured at two points on both the pulse leading edge and trailing edge with the circuit operating under the extreme conditions possible with limit components in each stage. The circuit used appears in Figure 18.

250-Turn Trans.			Pulse Leading Edge Delay Measured At:				Pulse Trailing Edge Delay Measured At:			
Gate	Tube in Stage	Delay over Stage	15% From Bottom Pulse		Effective Top Pulse		Effective Top Pulse		15% From Bottom Pulse	
			1st	Nth	1st	Nth	1st	Nth	1st	Nth
S	H	1	0.07	0.10	0.06	0.11	0.08	0.07	0.10	0.07
S	C	2	0.07	0.13	0.09	0.17	0.09	0.08	0.14	0.11
S	A	3	0.07	0.12	0.08	0.11	0.09	0.08	0 09	0.10
S	C	1	0.08	0.09	0.06	0.11	0.08	0.07	0.09	0.07
S	H	2	0.06	0.11	0.08	0.15	0.08	0.07	0.14	0.12
S	A	3	0.07	0 11	0.08	0.11	0.08	0.08	0 09	0.10
F	H	1	0.06	0.07	0.06	0.08	0.07	0.06	0.07	0.06
F	C	2	0.06	0.11	0.07	0.16	0.08	0.06	0.13	0.10
F	A	3	0.07	0.11	0.07	0.08	0.11	0.07	0.07	0.07
F	C	1	0.05	0.08	0.04	0 09	0.08	0 06	0.08	0.05
F	H	2	0.06	0.10	0.07	0.14	0.07	0.06	0.13	0.10
F	A	3	0.06	0.10	0.06	0.08	0.08	0.06	0.08	0.07
S	H	2	0.07	0.13	0.09	0.15	0.07	0.06	0.13	0.11
S	C	3	0.07	0.12	0.09	0.13	0.07	0.07	0.09	0.08
S	C	2	0.07	0.13	0.09	0.17	0.08	0.07	0.13	0.11
S	H	3	0.08	0.12	0.08	0.12	0.08	0.08	0.09	0.10
F	H	2	0.06	0 10	0.07	0.15	0.06	0 05	0.12	0.09
F	C	3	0.06	0.10	0.07	0.11	0.07	0 06	0 07	0.07
F	C	2	0.06	0 10	0.08	0.16	0.06	0.05	0.13	0.10
F	H	3	0.06	0.10	0.06	0.08	0.07	0.06	0.06	0.06

H designates a high-limit tube.
C designates a low-limit tube.
A designates an average tube.
F designates component tolerances such that the gate is relatively high speed.
S designates component tolerances such that the gate is relatively low speed.

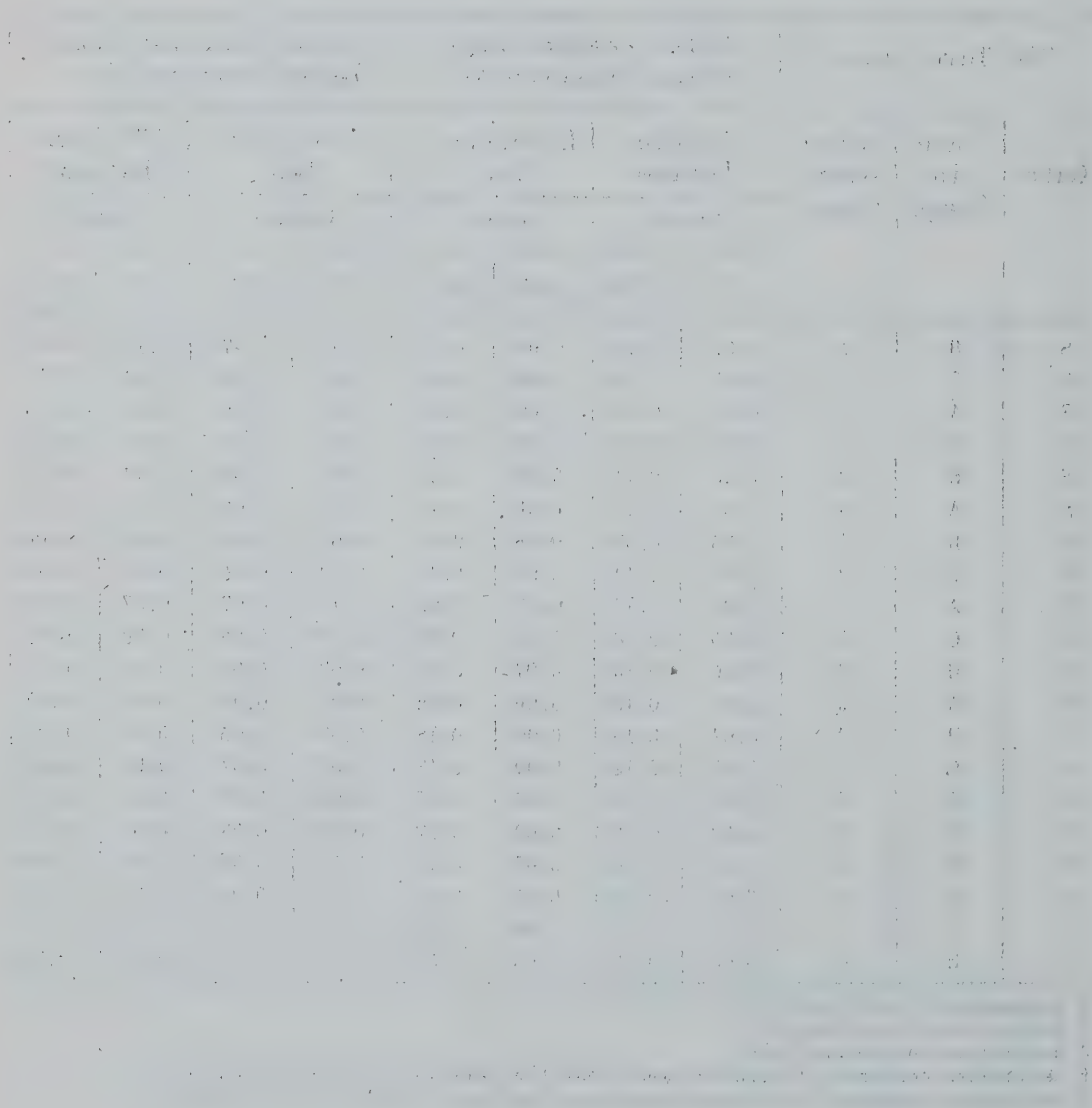

TABLE IV

Pulse Delay Characteristics For A 120-Turn Transformer

Delay in microseconds is measured at two points on both the pulse leading edge and trailing edge with the circuit operating under the extreme conditions possible with limit components in each stage. The circuit used appears in Figure 18.

120-Turn Trans.			Pulse Leading Edge Delay Measured At:				Pulse Trailing Edge Delay Measured At:			
Gate	Tube in Stage	Delay over Stage	15% From Bottom		Effective Top		Effective Top		15% From Bottom	
			Pulse		Pulse		Pulse		Pulse	
			1st	Nth	1st	Nth	1st	Nth	1st	Nth
S	H	1	0.05	0.05	0.03	0.06	0.07	0.05	0.06	0.06
S	C	2	0.06	0.09	0.08	0.10	0.04	0.04	0.07	0.07
S	A	3	0.06	0.06	0.07	0.07	0.04	0.04	0.06	0.06
S	C	1	0.06	0.06	0.04	0.06	0.03	0 04	0.04	0.04
S	H	2	0.06	0.08	0.08	0.10	0.03	0 03	0.08	0.08
S	A	3	0.06	0.07	0.07	0.07	0.03	0.03	0.05	0.05
F	H	1	0.07	0.05	0.03	0.06	0.04	0.04	0.03	0.03
F	C	2	0.06	0.08	0.07	0.09	0.03	0.04	0.06	0.07
F	A	3	0.06	0.06	0.05	0.06	0.04	0.04	0.05	0.06
F	C	1	0.07	0.05	0.03	0.05	0.04	0.03	0.02	0.04
F	H	2	0.05	0.06	0.07	0.08	0.03	0.06	0.06	0.03
F	A	3	0.05	0.06	0.05	0.06	0.03	0.05	0.05	0 03
S	H	2	0.06	0.09	0.08	0.10	0.04	0.05	0.08	0.08
S	C	3	0.07	0.07	0.08	0.08	0.03	0.04	0.04	0.04
S	C	2	0.07	0.09	0.08	0.10	0.04	0.05	0.06	0.08
S	H	3	0.06	0.06	0.06	0.07	0.03	0.03	0.05	0.06
F	H	2	0.05	0.07	0.06	0.08	0.03	0.03	0.06	0.06
F	C	3	0.06	0.06	0.06	0.06	0.03	0.03	0.04	0.05
F	C	2	0.05	0.07	0.07	0.09	0.04	0.04	0.06	0.06
F	H	3	0.06	0.06	0.06	0.06	0.03	0.04	0.05	0.05

H designates a high-limit tube.
C designates a low-limit tube.
A designates an average tube.
F designates component tolerances such that the gate is relatively high speed.
S designates component tolerances such that the gate is relatively low speed.

TABLE V

Timing Characteristics

Relative Delays at Two Critical Points on Pulse Leading and Trailing Edges

The values* listed are those selected from Tables III and IV which indicated the worst pulse deterioration. The points referred to are coded as in the sketch at the bottom of this table.

Stage	1st Pulse	Nth Pulse	Any Pulse
120-Turn Transformer			
1st Stage Only	0.04 | 0.03 / 0.05 | 0.06	0.06 | 0.04 / 0.05 | 0.06	0.06 | 0.03 / 0.05 | 0.06
2nd or 3rd Stage	0.08 | 0.03 / 0.05 | 0.08	0.10 | 0.03 / 0.06 | 0.08	0.10 | 0.03 / 0.05 | 0.08
Any Stage	0.08 | 0.03 / 0.05 | 0.08	0.10 | 0.03 / 0.05 | 0.08	0.10 | 0.03 / 0.05 | 0.08
250-Turn Transformer			
1st Stage Only	0.06 | 0.07 / 0.05 | 0.10	0.11 | 0.08 / 0.07 | 0.07	0.11 | 0.07 / 0.05 | 0.10
2nd or 3rd Stage	0.09 | 0.06 / 0.06 | 0.14	0.17 | 0.05 / 0.10 | 0.12	0.17 | 0.05 / 0.06 | 0.14
Any Stage	0.09 | 0.06 / 0.05 | 0.14	0.17 | 0.05 / 0.07 | 0.12	0.17 | 0.05 / 0.05 | 0.14

Delay at the effective top of the leading edge of each pulse.	Delay at the effective top of the trailing edge of each pulse.
Delay 15% from the bottom of the leading edge of each pulse.	Delay 15% from the bottom of the trailing edge of each pulse.

* *All times are given in microseconds.*

250-Turn Transformer

The 1st pulse out of three cascaded stages is superimposed.

Figure 19

120-Turn Transformer

The 1st pulse out of three cascaded stages is superimposed.

Figure 20

250-Turn Transformer

The Nth pulse out of three cascaded stages is superimposed.

Figure 21

120-Turn Transformer

The Nth pulse out of three cascaded stages is superimposed.

Figure 22

Note: Gate components adjusted to bend high speed range. An average tube is in stage #1, a high-limit tube in stage #2 and a low-limit tube in stage #3. The vertical scale is 5.6 volts/small division and the horizontal scale is 0.08 microsecond/small division.

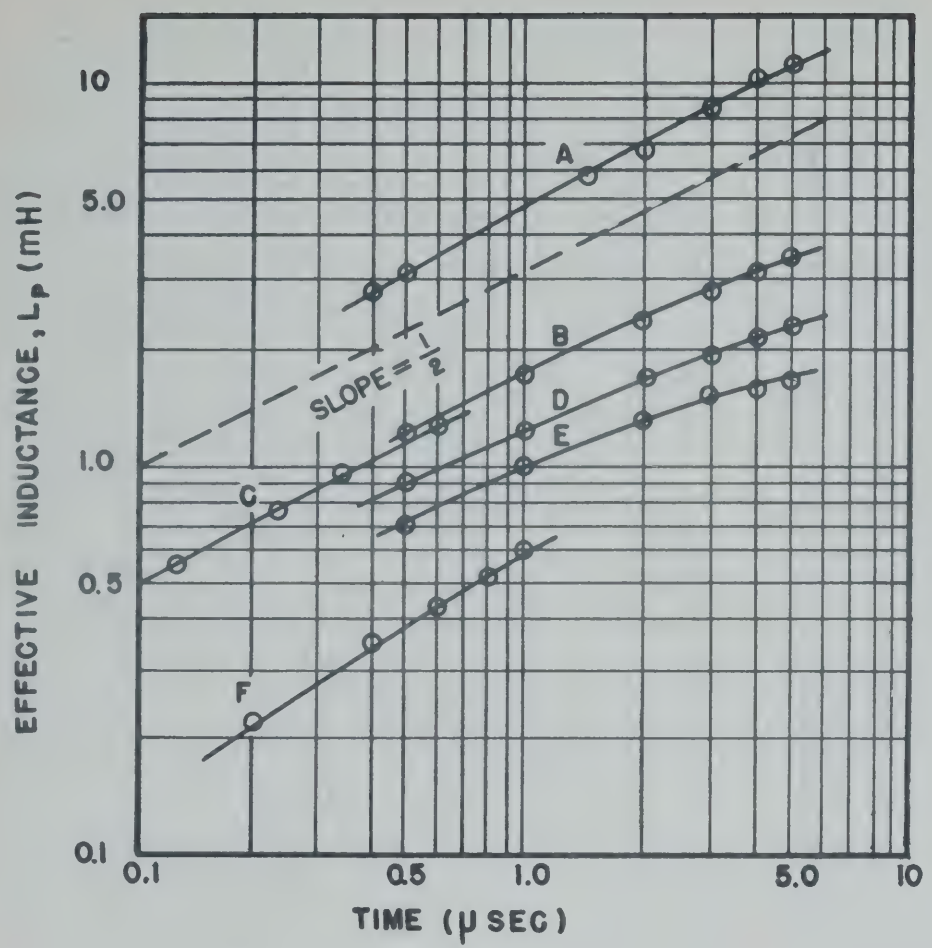

(A) 2-MIL HIPERSIL, N=80, R_p=3000 OHMS
CROSS SECTION $\frac{1}{4}$" X $\frac{1}{4}$". DATA-2TFW 76.

(B) 1-MIL HIPERSIL, N=70, R_p=2600 OHMS
CROSS SECTION $\frac{1}{4}$" X $\frac{3}{16}$". DATA-2TFW 136.

(C) 1-MIL HIPERSIL, N=70, R_p=1050 OHMS
CROSS SECTION $\frac{1}{4}$" X $\frac{3}{16}$". DATA-2TFW 142.

(D) 1-MIL HIPERSIL, N=70, R_p=530 OHMS
CROSS SECTION $\frac{1}{4}$" X $\frac{3}{16}$". DATA-2TFW 136.

(E) BACKSWING DECAY FOR 5 μ SEC PULSE OF (D).
DATA-2TFW 136.

(F) 2-MIL HIPERSIL, N=48, R_p=430 OHMS
CROSS SECTION $\frac{1}{4}$" X $\frac{1}{8}$". DATA-2TFW 105.

FIG. 11 EFFECTIVE INDUCTANCE VS. TIME FOR WINDINGS ON HIPERSIL CORES.

CONCLUSIONS

From the timing test results tabulated in Tables III and IV, it is seen that by using a transformer with 120 primary turns the variation in stage delay for various pulses in a sequence may be reduced. Also, the pulse rise and fall times are decreased and the total stage delay is reduced.

The results described in this report are derived for a single tube and transformer. If more load current is necessary than can be supplied by one tube, additional tubes may be used in parallel, all operating into a single transformer. To cause this transformer to oscillate at the desired frequency on the backswing, it is necessary to reduce its primary inductance to compensate for the increased circuit capacitance. This objective may be accomplished by decreasing the number of primary turns by the square root of the number of tubes added (assuming all tubes add equal capacity).

If pulses of duration greater than 0.5 microseconds are desired, or if a duty cycle higher than 50% is used, a 250-turn transformer will be more satisfactory than the 120-turn unit.

A full load, equivalent to 7,000 ohms on the primary, must be used to prevent the oscillation from giving a spurious signal after a train of pulses. If this full load is not required in the load circuit, additional resistive loading must be used.

BIBLIOGRAPHY

1. Martin, William L., *Design of a Transformer-Coupled Pulse-Repeater for General Application in the NBS Interim Computer.* Report No. 8952 of the Electronic Computers Section, Electronics Division, National Bureau of Standards, Washington 25, D.C. May 27, 1949.
(This report was for the internal circulation of the Electronics Division of the National Bureau of Standards. Copies might possibly be obtained by writing to Dr. S. N. Alexander in care of this section. Copies are on file in Engineering Research of the Engineering Department of the University of California, Los Angeles, California.)

2. Wimett, Thomas F., *Low Power Pulse Transformers.* Report R-122 of Project Whirlwind, Servomechanisms Laboratory, Massachusetts Institute of Technology, Cambridge 39, Massachusetts. December, 1947.
(This report is an unrestricted publication from Project Whirlwind. A copy is on file in Engineering Research of the Engineering Department of the University of California, Los Angeles, California.)

3. E. E. Staff, M. I. T., *Magnetic Circuits and Transformers.* New York: John Wiley and Sons, 1943.

4. Bostick, W. H., in *Radiation Laboratory Technical Series,* Vol. 5, "Pulse Generators", New York: McGraw-Hill Book Company, Inc. 1948.

5. Terman, F. E., *Radio Engineers Handbook,* New York: McGraw-Hill Book Company, Inc. 1943.

[*Reprinted from* The Aeronautical Quarterly, Vol. 2, *May* 1950]

Published by The Royal Aeronautical Society

A Note on Subsonic Aerofoil Theory

by

JOHN W. MILES, Ph.D.

A NOTE ON SUBSONIC AEROFOIL THEORY

by

JOHN W. MILES, Ph.D.
(Department of Engineering, University of California, Los Angeles)

SUMMARY

A linearised theory for the subsonic, lifting surface problem is formulated in terms of Fourier integral solutions to Laplace's equation. The symmetric and anti-symmetric problems of the first kind are solved explicitly, while the problems of the second kind depend on the solution of dual integral equations. The anti-symmetric problem of the second kind is cast in a variational form, from which certain well-known theorems may be deduced.

1. INTRODUCTION

The following development of linearised, subsonic aerofoil theory is derived from a recent analysis given for the supersonic problem[1] which in turn was motivated by Schwinger's variational approach to diffraction problems[2, 3]. While the majority of the end results to be obtained are not new, their formulation, in certain respects, is rather novel, and the analysis is felt to be of interest *per se*.

Earlier formulations of linearised, lifting surface theories are discussed by von Kármán[4], and rather general approaches have been given more recently by Kussner[5] and Reissner[6]. A Fourier transform approach of lifting line theory has been discussed by von Kármán[7] and Fuchs[8].

Notation

a	x co-ordinate of axis of rotation in pitch
b	wing span
c	reference value of chord
C_D	drag coefficient
C_L	lift coefficient
C_l	rolling moment coefficient
C_M	pitching moment coefficient

Paper received April 1949.
[The Aeronautical Quarterly, Vol. II, May 1950]

G	*see* equation (7)
g	*see* equation (9)
G^*	*see* equation (12)
g^*	*see* equation (13)
$\mathscr{F}$	"the imaginary part of"
$\mathbf{i}, \mathbf{j}, \mathbf{k}$	unit vectors along x, y, z
K_0	MacDonald's function of order zero[12]
K_1	MacDonald's function of order one[12]
p	perturbation pressure
$\mathbf{q}$	vector perturbation velocity
R	integration operator. *See* equation (8)
T	transform operator. *See* equation (4*a*)
$\overline{T}$	inverse of T
u, v, w	x, y, z components of perturbation velocity
U	Fourier transform of u. *See* equation (4)
V	free stream velocity
x, y, z	Cartesian co-ordinates (Fig. 1)
α	wing incidence ($\alpha = -w$ in σ)
$\partial(\mu)$	Dirac delta function; $\int_{-\infty}^{\infty} \delta(\mu)=1;\ \delta(\mu)=0,\ \mu \neq 0.$
η	y co-ordinate of integration
μ, ν	spectrum co-ordinates
ξ	x co-ordinate of integration
ρ	air mass density
σ	projection of aerofoil on $z=0$
τ	remainder of plane $z=0$
ϕ	velocity potential

2. STATEMENT OF PROBLEM

A thin wing is located near the xy ($z=0$) plane, its projection there being denoted by σ (the remainder of the plane being denoted by τ). The theory is linearised in the sense that the boundary conditions are applied in σ rather than at the aerofoil, and all perturbation velocities are assumed small compared to the free

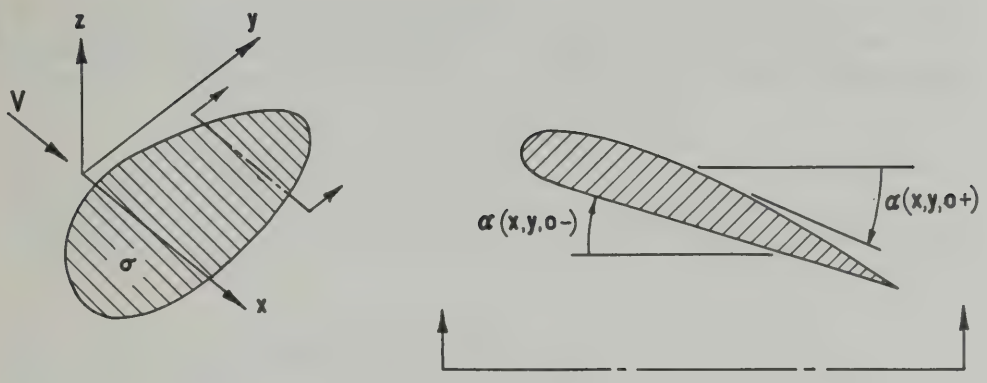

Fig. 1.
Plan and section views of aerofoil.

stream velocity, V, which is in the positive x direction. The perturbation velocity may be written

$$\mathbf{q}=(\mathbf{i}u+\mathbf{j}v+\mathbf{k}w)\,V=V\nabla\phi \quad . \quad . \quad . \quad . \quad . \quad (1)$$

$$\nabla^2\phi=0 \quad . \quad . \quad . \quad . \quad . \quad . \quad (2)$$

and the (linearised) perturbation (relative to free stream) pressure is given by

$$p=-\rho V^2u \quad . \quad . \quad . \quad . \quad . \quad . \quad (3)$$

where ρ is the mass density. It is required to find $\phi\,(x,\,y,\,z)$ from a knowledge of the boundary conditions in the plane $z=0$ and at infinity.

The boundary conditions require that the flow be tangent to the aerofoil and that the pressure be continuous except across the aerofoil. The top and bottom surfaces of the aerofoil will generally have different slopes, but the linearisation permits separate consideration of two problems consisting of the symmetrical and anti-symmetrical distributions of the incidence (measured in a section of constant y), corresponding to the thickness and camber (and twist) distributions, respectively. Hence, it suffices to consider only the half space $z>0$, the boundary conditions being applied to $u\,(x,\,y,\,0+)$ or $w\,(x,\,y,\,0+)$ (the case whose $v\,(x,\,y,\,0+)$ is specified is not generally of technical interest).

In addition to the explicit boundary conditions in the plane $z=0$, it is required that the solutions be chosen such that ϕ will vanish far upstream, reduce to a

two-dimensional flow far downstream (the Trefftz plane)[9] and vanish as $y, z \longrightarrow \infty$. Moreover, the Kutta condition must be satisfied, *i.e.* $u(x, y, 0+)$ must vanish continuously at the trailing edge of σ.

3. SOLUTION

Let lower and upper case letters represent functions of the co-ordinates (x, y) and their double, complex, Fourier transforms in the (μ, ν) spectrum, respectively, *e.g.*

$$u(x, y)=T\{U(\mu, \nu)\}=\frac{1}{2\pi}\int_{-\infty}^{\infty} d\mu \int_{-\infty}^{\infty} d\nu\, U(\mu, \nu)\exp\,[i(\mu x+\nu y)]\ . \qquad (4a)$$

$$U(\mu, \nu)=T\{u(x, y)\}=\frac{1}{2\pi}\int_{-\infty}^{\infty} d\xi \int_{-\infty}^{\infty} d\eta\, u(\xi, \eta)\exp\,[-i(\mu\xi+\nu\eta)]\ . \qquad (4b)$$

Then a solution to Laplace's equation (2) which exhibits the desired behaviour at infinity (in the half space $z>0$) and whose x derivative reduces to $u(x, y)$ at $z=0+$ may be established as

$$\phi(x, y, z)=T\{[(i\mu)^{-1}+\pi\delta(\mu)]\exp\,[-(\mu^2+\nu^2)^{\frac{1}{2}}z]\,U(\mu, \nu)\}\ . \qquad (5)$$

The branch cuts in the complex ν plane are taken from $\pm i|\mu|$ to $\pm i\infty$, respectively, and the path of integration in the complex ν plane may be taken anywhere in the strip $|\mathscr{I}(\nu)|<|\mathscr{I}(\mu)|$, provided $z\geqslant 0$, as assumed. Proper behaviour for large values of y is guaranteed by giving $\mathscr{I}(\nu)$ the same sign as y, with the real axis admissible for all y. The path in the μ plane is taken along $\mathscr{I}(\mu)\leqslant 0$, and the contour may be closed in the upper or lower half of the μ plane for large positive or negative x, respectively, giving a vanishing solution far upstream and a potential solution (the contribution of the pole) far downstream. If the path is taken along the real axis in the μ plane, the indentation *under* the pole $\mu=0$ yields equal and opposite contributions upstream and downstream, which are then matched by the contribution from the term $\pi\delta(\mu)$[10] in such a way as to give the correct solutions both upstream and downstream. These choices determine essentially the arbitrary function of (x, y) introduced when $u(x, y, z)$ is integrated with respect to x to determine $\phi(x, y, z)$. The Kutta condition does not enter the solution explicitly at this point since it is implicit in the specification of $u(x, y)$.

The upwash corresponding to equation (5) may be written,

$$w(x, y)=\phi_z(x, y, 0+)=-T\{G(\mu, \nu)U(\mu, \nu)\exp\,[-(\mu^2+\nu^2)^{\frac{1}{2}}(0+)]\}\ . \qquad (6)$$

$$G(\mu, \nu)=(i\mu)^{-1}(\mu^2+\nu^2)^{\frac{1}{2}}+\pi\delta(\mu)|\nu| \qquad . \quad . \quad . \qquad (7)$$

The requirement $z=0+$ in equation (6) guarantees absolute convergence of the integrals in the limits $\mathcal{F}(\mu)=\mathcal{F}(\nu)=0$, but in the following the results will be formally interpreted for $z=0$ (*cf.* footnote †). Applying the Faltung theorem[11] to equation (6) yields

$$w(x, y)=-(2\pi)^{-1} R\{g(x-\xi, y-\eta)\, u(\xi, \eta)\}$$

$$=-(2\pi)^{-1}\int_{-\infty}^{\infty} d\xi \int_{-\infty}^{\infty} d\eta\, g(x-\xi, y-\eta)\, u(\xi, \eta) \quad . \quad . \quad (8)$$

where R is an operator denoting double integration over all (ξ, η), and $g(x, y)$ is the inverse transform of $G(\mu, \nu)$. Carrying out the integrations required for the

$$g(x, y)=-(i\pi \mid y \mid)^{-1}\int_{-\infty}^{\infty} d\mu\, K_1(\mu \mid y \mid)\exp(i\mu x)-y^{-2} \quad . \quad . \quad (9a)$$

$$=-2(\pi \mid y \mid)^{-1}\int_{0}^{\infty} d\mu\, K_1(\mu \mid y \mid)\sin(\mu x)-y^{-2} \quad . \quad . \quad (9b)$$

$$=-y^{-2}[1+x(x^2+y^2)^{-\frac{1}{2}}] \quad . \quad . \quad . \quad . \quad . \quad . \quad (9c)$$

where the path of integration for equation (9*a*) is indented under the pole $\mu=0$, and K_1 is a modified Bessel function of the second kind in the notation of Watson[12].

The result obtained by substituting equation (9*c*) in equation (8) evidently has a direct interpretation in terms of a source distribution over $z=0+$, and, after integration by parts to give integrals possessing Cauchy principal values†, it is in agreement with results obtained by rather more direct approaches.

4. INVERSION OF INTEGRAL EQUATION

Equations (6) and (8) represent a direct, closed form solution for $w(x, y)$ if $u(x, y)$ is known everywhere for $z=0+$. Conversely, if $w(x, y)$ is known these results are integral equations of the first kind for $U(\mu, \nu)$ and $u(x, y)$, respectively. The integral equation may be inverted by taking the inverse transform‡ of

---

† If z is kept finite (>0), it is found that

$$g(x, y)=-\frac{\partial}{\partial z}\left\{z(z^2+y^2)^{-1}[1+x(x^2+y^2+z^2)^{-1/2}]\right\}$$

and no difficulties occur at $z=0$, after integration by parts.

‡In taking the reciprocal of $G(\mu, \nu)$, *cf.* equation (7), the delta function drops out since, in any event, $G^*(\mu, \nu)$ has a first order zero at $\mu=0$. *See,* for example, Ref. 10, p. 21.

equation (6) and applying the Faltung theorem, namely

$$u(x, y) = -T\{G^*(\mu, \nu) W(\mu, \nu)\} \quad . \quad . \quad . \quad . \quad . \quad (10)$$

$$u(x, y) = -(2\pi)^{-1} T\{g^*(x-\xi, y-\eta) w(\xi, \eta)\} \quad . \quad . \quad (11)$$

$$G^*(\mu, \nu) = G^{-1}(\mu, \nu) = i\mu(\mu^2+\nu^2)^{-\frac{1}{2}} \quad . \quad . \quad . \quad . \quad . \quad (12)$$

Taking the inverse transform of equation (12) yields

$$g^*(x, y) = (i/\pi) \int_{-\infty}^{\infty} \mu\, d\mu\, K_0(\mu\,|\,y\,|) \exp(i\mu x) \quad . \quad . \quad . \quad (13a)$$

$$= -(2/\pi) \int_{0}^{\infty} \mu\, d\mu\, K_0(\mu\,|\,y\,|) \sin(\mu x) \quad . \quad . \quad (13b)$$

$$= -x(x^2+y^2)^{-3/2} \quad . \quad . \quad . \quad . \quad . \quad . \quad (13c)$$

Here again, the results are formal, convergence being obtained through an appropriate choice of paths in the transform planes and interpretation at $z=0+$, followed by integration by parts in (x, y).

5. PROBLEMS OF FIRST AND SECOND KIND

In a problem of the first kind either u or w is known over the entire plane $z=0+$, and the results of the last two sections therefore furnish exact solutions. In a problem of the second kind u and w are specified over different (but compatible) portions of the plane, and it is necessary to solve a "dual" integral equation†.

Referring to the symmetric (s) and anti-symmetric (a) problems previously mentioned, w_s and u_a vanish over that portion of the plane (τ) not occupied by the aerofoil (σ); hence, the determinations of either u_s or w_a from a knowledge of w_s or u_a, respectively, in σ leads to a problem of the first kind, while the determination of u_a or w_s from w_a or u_s, respectively, in σ leads to a problem of the second kind. The only exact solutions known for cases of interest in the latter category are the solutions for the circular[16] and elliptic[17] plan forms.

6. UNIQUENESS

While no adequate treatment of dual integral equations of the first kind appears to exist in the literature, they may be expected to exhibit characteristics similar to

† *See* Ref. 11, pp. 334-342, for discussion of this type of integral equation.

other Fredholm integral equations arising in mathematical physics. (*See*, for example, Ref. 15.) In particular, eigensolutions may be expected for any given plan form, and these will generally possess singularities at the plan form edges. Various singularities are possible, but only singularities which are integrable, in the sense that they yield finite forces on the wing, can be admitted in the present problem, namely logarithmic and $(-\frac{1}{2})$ power singularities, in the symmetric and anti-symmetric problems, respectively[16]. Now the particular solution to the integral equation may also be expected to exhibit a $(-\frac{1}{2})$ power singularity (in the anti-symmetric problem) at the plan form edges, so that the eigensolution may be chosen in such a way as just to cancel this singularity along the trailing edge, thus satisfying the Kutta condition and establishing the solution as unique.† The singularity along the leading edge remains and indeed is required (on the assumption of an ideal fluid) to eliminate drag (other than induced).

The question of uniqueness is a recondite one, both mathematically and physically (no physical answer to the question can be given without considering the effects of viscosity in some detail), and it cannot be said that the question has been answered in any completely satisfactory way. It is, therefore, of some interest to remark that the same situation exists in other fields, *e.g.* diffraction[17], and has often been ignored. An interesting, if laconic, discussion of the supersonic case has been given recently by Hayes[18].

7. VARIATIONAL FORMULATION

A variational formulation of the dual integral equation of the first kind has been given by Schwinger[1, 2]. Such a formulation of the present problem leads to a variational expression for the drag and is of interest only for the lifting surface problem of the second kind (angle of attack, *i.e.* downwash, distribution prescribed over aerofoil), since it is known, *a priori*, that the drag for a symmetrical aerofoil must vanish (ideal, irrotational flow).

The drag is obtained by integrating the product of pressure, *cf.* equation (3), and downwash ($w_a(x, y) = -\alpha_a(x, y)$) over the aerofoil ($\sigma$). The result is‡

$$C_D = (\rho V^2 \sigma/2)^{-1} R \{ [p(x, y, 0-) - p(x, y, 0+)] \alpha_a(x, y) \}$$
$$= (4/\sigma) R \{ u_a(x, y) \alpha_a(x, y) \} \quad . \quad . \quad . \quad . \quad . \quad . \quad (14)$$

†It is also of interest to note that the discontinuity across the vortex sheet behind the wing is uniquely determined by the Kutta condition, or by any other uniqueness condition which might be formulated.

‡The matter of leading edge thrust (*see*, for example, Ref. 4, pp. 26-29) is passed over in silence here, except to state that the end results require no correction for such a thrust. It is not necessary to restrict the integration to σ, since u_a vanishes off σ.

It follows from Parseval's theorem† that equation (14) may also be written

$$C_D=(4/\sigma)R\{U(\mu,\nu)\overline{A(\mu,\nu)}\}$$
$$=(4/\sigma)R\{\overline{U(\mu,\nu)}A(\mu,\nu)\} \quad . \quad . \quad . \quad . \quad (15)$$

where the bar denotes the complex conjugate. Alternative forms are given by substituting $\alpha(x, y)$ or $A(\mu, \nu)$ from the integral equations (6) or (8), respectively, to obtain

$$C_D=(2/\pi\sigma)R^2\{u(x, y)g(x-\xi, y-\eta)u(\xi, \eta)\} \quad . \quad . \quad . \quad . \quad (16)$$

$$C_D=(4/\sigma)R\{U(\mu, \nu)G(\mu, \nu)\overline{U(\mu, \nu)}\} \quad . \quad . \quad . \quad . \quad . \quad (17)$$

where R^2 indicates integration over both (x, y) and (ξ, η). If equations (16) and (17) are divided by the squares of equations (14) and (15), respectively, the results are

$$C_D^{-1}=(\sigma/8\pi)[R\{u(x, y)\alpha(x, y)\}]^{-2}\times R^2\{u(x, y)g(x-\xi, y-\eta)u(\xi, \eta)\} \quad (18)$$

$$C_D^{-1}=(\sigma/4)[R\{U(\mu, \nu)\overline{A(\mu, \nu)}\}]^{-2}\times R\{G(\mu, \nu)|U(\mu, \nu)|^2\} \quad . \quad . \quad (19)$$

Equations (18) and (19) are variational in the sense that they are absolute minima (not merely stationary) with respect to arbitrary (not merely first order) variations of u or U about the exact solutions to the integral equations (6) and (8), respectively. A proof of this assertion, due to Schwinger, has been given elsewhere‡, it being specifically remarked that the present kernel is symmetric and positive definite.

To prove the assertion that the kernel is positive definite, it may be observed that, since $u(x, y)$ is real, its transform satisfies the relation

$$U(-\mu, -\nu)=\overline{U(\mu, \nu)} \quad . \quad . \quad . \quad . \quad . \quad (20)$$

whence $U(\mu, \nu)\overline{U(\mu, \nu)}$ is an even function of μ and ν, and only that part of $G(\mu, \nu)$ which is even in μ, *i.e.* $\pi\delta(\mu)|\nu|$, *cf.* equation (7), contributes to the result. In particular, equation (17) reduces to

$$C_D=\left(\frac{8\pi}{\sigma}\right)\int_0^\infty \nu d\nu\,|U(0, \nu)|^2 \quad . \quad . \quad . \quad . \quad (21)$$

---

†Ref. 11, p. 51 (2.1.8).

‡*See* Appendix IV of Ref. 19, the proof being for a vector integral equation with dyadic kernel.

as obtained (essentially) by von Kármán[7]. This result corresponds to the calculation of the induced drag in the Trefftz plane ($x=\infty$ or $\mu=0$). It may be remarked further that

$$U(0,\ \nu)=(2\pi)^{-1}\int_{-\infty}^{\infty} d\eta \exp(-i\nu\eta)\int_{-\infty}^{\infty} d\xi\, u(\xi,\ \eta) \quad . \quad . \quad . \quad (22)$$

and is therefore essentially the Fourier transform of the circulation about the "lifting line." The result that the induced drag is independent of chordwise distribution of pressure (for fixed circulation) is of course the well-known Munk stagger theorem. (Ref. 4, p. 132.)

The variational equivalent of equation (21) is deduced from equation (19) as

$$C_D^{-1}=\left(\frac{\pi\sigma}{2}\right)\int_0^{\infty} \nu d\nu \left|\frac{U(0,\ \nu)}{R\{U(\mu,\ \nu)\overline{A(\mu,\ \nu)}\}}\right|^2 \quad . \quad . \quad . \quad (23)$$

The result that the reciprocal of C_D is a minimum, so that C_D is a maximum, with respect to variations about the true solution for the circulation is not new, for the usual (Fourier series) method of solving the Prandtl, lifting line, integral equation generally exhibits C_D in a positive definite, quadratic (in the expansion coefficients) form. *See*, for example, the work of Hildebrand[20].

8. LIFT AND MOMENT COEFFICIENTS

To complete the specification of the forces acting on the wing, the lift and moment coefficients will be expressed in terms of the transforms.

The lift coefficient is defined by

$$C_L=(\rho V^2\sigma/2)^{-1} R\{p(x,\ y,\ 0-)-p(x,\ y,\ 0+)\}$$
$$=\left(\frac{4}{\sigma}\right)R\{u_a(x,\ y)\} \quad . \quad . \quad . \quad . \quad . \quad . \quad . \quad (24)$$

Similarly, the pitching moment about $x=a$ and the rolling moment about the line $y=0$ are referred to the coefficients

$$C_M=\left(\frac{4}{\sigma c}\right)R\{(a-x)u_a(x,\ y)\} \quad . \quad . \quad . \quad . \quad (25)$$

$$C_l=-\left(\frac{4}{\sigma b}\right)R\{yu_a(x,\ y)\} \quad . \quad . \quad . \quad . \quad . \quad (26)$$

where c is a reference wing chord, and b is the wing span. These integrals may be expressed in terms of $U(\mu, \nu)$, just as in the case of the circulation, *cf.* equation (22), since u_a vanishes off the wing. The results are

$$C_L = \left(\frac{8\pi}{\sigma}\right) U(0, 0) \quad . \quad . \quad . \quad . \quad . \quad . \quad . \quad (27)$$

$$C_M = \left(\frac{8\pi}{\sigma}\right)\left\{\left(\frac{a}{c}\right) U(0, 0) - \left(\frac{i}{c}\right)\left[\frac{\partial U}{\partial \mu}(\mu, 0)\right]_{\mu=0}\right\} \quad . \quad . \quad . \quad (28)$$

$$C_l = -\left(\frac{8\pi i}{\sigma b}\right)\left[\frac{\partial U}{\partial \nu}(0, \nu)\right]_{\nu=0} \quad . \quad . \quad . \quad . \quad . \quad . \quad (29)$$

REFERENCES

1. Miles, J. W. (1948). On Linearized Supersonic Airfoil Theory. North American Aviation Company, Aerophysics Lab. Report AL-801, 1948.
2. Schwinger, J. S. (1944). Seminar on the Theory of Guided Waves. Radiation Laboratory, Massachusetts Institute of Technology, Cambridge, Mass., 1944.
3. Levine, H., and Schwinger, J. (1948). On the Theory of Diffraction by an Aperture in an Infinite Plane Screen, I. *Physical Review* 74, 958-974, 1948.
4. Durand, W. F. (1942). *Aerodynamic Theory,* Part II, Div. E. Durand Reprinting Committee, Pasadena, 1942.
5. Kussner, H. G. (1940). Allgemeine Tragflachentheorie. *Luftfahrtforschung,* 17, 370-378, 1940; translated in N.A.C.A. Technical Memorandum 979, 1941.
6. Reissner, E. (1944). On the General Theory of Thin Airfoils for Non-Uniform Motion. N.A.C.A. Technical Note 946, 1944.
7. von Karman, Th. (1935). Neue Darstellung der Tragflügeltheorie. *Zeitschrift für Angewandte Mathematik und Mechanik* 15, 56-61, 1935.
8. Fuchs, R. (1939). Neue Behandlung der Tragflügeltheorie. *Ingenuieur Archiv.* 10, 48-63, 1939.
9. Trefftz, E. (1921). Zur Prandtlschen Tragflächentheorie. *Math. Annal.* 82, 306-319, 1921.
10. Dirac, P. (1935). *Quantum Mechanics,* Oxford, pp. 21 *et seq.,* 1935,
11. Titchmarsh, E. C. (1937). *Theory of Fourier Integrals,* Oxford, p. 50 (2.1.2), 1937.
12. Watson, G. N. (1947). *Bessel Functions,* MacMillan & Co., New York, 1947.
13. Kinner, W. (1937). Die kriesförmige Tragfläche auf potential-theoretischer Grundlage. *Ingenieur Archiv.* 8, 47-80, 1937.
14. Krienes, K. (1940). Die elliptische Tragfläche auf potential-theoretischer Grundlage. *Zeitschrift für Angewandte Mathematik und Mechanik* 20, 65-68, 1940; translated in N.A.C.A. Technical Memorandum 971, 1941.
15. Courant, R., and Hilbert, D. (1937). *Methoden der Mathematischen Physik,* Julius Springer, Berlin, Vol. II, p. 269 *et seq.,* 1937.

16. LAGERSTROM, P. A. (1948). Linearized Supersonic Theory of Conical Wings. N.A.C.A. Technical Note 1685, pp. 12-14, 71, 1948.

17. BOUWKAMP, C. J. (1947). (In reviewing E. T. Copson's *An Integral Equation Method of Solving Plane Diffraction Problems*), Mathematical Reviews 8, 180, 1947.

18. HAYES, W. D. (1947). Linearized Supersonic Flow. California Institute of Technology. Ph. D. Thesis 1947; also distributed as North American Aviation Company AL-222, pp. 66-75, 1947.

19. MILES, J. W. (1946). The Equivalent Circuit for a Plane Discontinuity in a Cylindrical Wave Guide. *Proceedings of the Institute of Radio Engineers* 10, 728-742, 1946.

20. HILDEBRAND, F. B. (1944). A Least Squares Procedure for the Solution of the Lifting Line Integral Equation. N.A.C.A. Technical Note 925, 1944.

THE LEWES PRESS (Wightman & Co. Ltd.), Friars Walk, Lewes, Sussex.

Reprinted from JOURNAL OF THE AERONAUTICAL SCIENCES
Copyright, 1950, by the Institute of the Aeronautical Sciences and reprinted by permission of the copyright owner
APRIL, 1950 VOLUME 17, NO. 4

On Downwash Corrections in Unsteady Flow*

John W. Miles
Department of Engineering, University of California at Los Angeles
December 16, 1949

STATLER[1] HAS STATED that the most important unsteady flow effect in the calculation of dynamic stability derivatives generally may be identified as the "complex downwash lag" factor, which will enter in the determination of wing-tail interference. While we have taken exception to the generality of his conclusions,[2] it does appear that the downwash lag will be important, and we wish to advance here a simple method for its calculation.

Assuming the harmonic time dependence exp ($i\omega t$), the velocity potential (ϕ) at the upper and lower surfaces of the vortex sheet behind a plane wing must exhibit a dependence on the streamwise coordinate (x, positive downstream) which will ensure continuity of the pressure. If we assume that the vortex sheet remains in the plane of the wing ($z = 0$), this requirement is satisfied by taking

$$\phi(x, y, 0 \pm) = \pm\phi_1(y) \exp\left\{-ik\left[\frac{x - x_1(y)}{b}\right]\right\} \quad (1)$$

$$k = \omega b/U \quad (2)$$

where U is the freestream velocity, b is a reference length, y is the spanwise coordinate, $x_1(y)$ is the coordinate of the trailing edge, $\phi(x, y, z)$ is the velocity potential, and $\phi_1(y)$ is the value of this potential at the trailing edge of the upper surface. Calculating the pressure at the wing and evaluating the section lift and moment (about $x = 0$) coefficients (c_l and c_m), we find

$$\phi_1(y) \exp\left[ikx_1(y)/b\right] = \frac{1}{4} U\left[c_l(y) - \frac{ikc(y)c_m(y)}{b}\right] \quad (3)$$

c_l and c_m are referred to c and c^2, respectively, where c is the chord. Now, if $c_{l_k}(y)$ represents the lift coefficient calculated in the absence of unsteady flow effects and $\phi_0(y, 0 \pm)$ the corresponding velocity potential at the vortex sheet, we may write (assuming k to be small)

$$c_l(y) - (ikc(y)c_m(y)/b) = c_{l_0}(y) \exp\left[ik\delta(y)\right] \quad (4)$$

$$\phi(x, y, 0 \pm) = \phi_0(y, 0 \pm) \exp\left\{ik[\delta(y) - (x/b)]\right\} \quad (5)$$

Having the potential $\phi(x, y, 0 \pm)$, the calculation of $\phi(x, y, z)$ is reduced to a classical boundary value problem. In principle, the solution of this problem is straightforward, but, in practice, it is likely to prove cumbersome; moreover, the introduction of such important factors as viscosity and warping of the vortex sheet leads to even more serious complications. However, if $\epsilon_0(x, y, z)$ represents the downwash field in the absence of unsteady flow effects but including experimentally or empirically determined corrections, it appears reasonable to assume that the downwash field in unsteady flow, at locations not too remote from the vortex sheet, may be approximated by

$$\epsilon(x, y, z) = \epsilon_0(x, y, z) \exp\left\{ik[\delta(y) - (x/b)]\right\} \quad (6)$$

Consider now the application of the result (6) to a pitching oscillation of amplitude α_0 about the axis $x = ab$. The local angle of flow at the tail then may be written

$$\alpha_{\text{eff.}} = \alpha_0\left\{1 + ik[(x/b) - a]\right\} - \epsilon_T \quad (7)$$

where ϵ_T is the wing downwash at the tail. Substituting ϵ from Eq. (6) and differentiating with respect to α_0, we have

$$\frac{d\alpha_{\text{eff.}}}{d\alpha_0} = \left(1 - \frac{d\epsilon_{T_0}}{d\alpha_0}\right) + ik\left[\left(1 + \frac{d\epsilon_{T_0}}{d\alpha_0}\right)\left(\frac{x}{b} - a\right) + (a - \delta)\left(\frac{d\epsilon_{T_0}}{d\alpha_0}\right)\right] + 0(k^2) \quad (8)$$

where ϵ_{T_0} is implicitly dependent on the coordinates of a point on the tail and δ on y. Now, in the absence of downwash interference, the term α_0 in $\alpha_{\text{eff.}}$ would lead to a moment derivative $C_{M_{\alpha_0}} + ikC_{M_{\dot{\alpha}}}$, the latter term being due to unsteady flow effects, while the term $ik\alpha_0[(x/b) - a]$ would lead to the derivative C_{M_q}. Hence, in the presence of interference, we write

$$\frac{dC_{M_{\text{eff.}}}}{d\alpha_0} = \left(1 - \frac{d\epsilon_{T_0}}{d\alpha_0}\right) C_{M_{\alpha_0}} + ik\left[\left(1 + \frac{d\epsilon_{T_0}}{d\alpha_0}\right) C_{M_q} + \left(1 - \frac{d\epsilon_{T_0}}{d\alpha_0}\right) C_{M_{\dot{\alpha}}} + (a - \delta)\left(\frac{d\epsilon_{T_0}}{d\alpha_0}\right) C_{M_{\alpha_0}}\right] + 0(k^2) \quad (9)$$

where ϵ_{T_0} and δ now are assumed to have been appropriately averaged over the tail. A similar result holds for the lift derivative, and entirely analogous results may be obtained for the derivatives with respect to angle of yaw. We remark that the corrections $[1 - (d\epsilon_{T_0}/d\alpha_0)]$ and $[1 + (d\epsilon_{T_0}/d\alpha_0)]$ applied to $C_{M_{\alpha_0}}$ and C_{M_q}, respectively, are standard, but the introduction of the term $C_{M_{\dot{\alpha}}}$, together with its downwash correction and the term $(a - \delta)C_{M_{\alpha_0}}$, generally is neglected. The last term is presumably the "downwash lag" term referred to by Statler. It would appear that the usual analysis of downwash in unsteady flow[3] implicitly assumes $\delta = a$.

In applying the result (9), the derivative $(d\epsilon_{T_0}/d\alpha_0)$ may be calculated from steady flow theory or measured in the wind tunnel, so that it only remains to calculate an appropriately averaged value of $\delta(y)$. If we take this average as

$$\delta = \frac{1}{S}\int_{-l/2}^{l/2} c(y)\delta(y)dy \quad (10)$$

where S, c, and l are the area, chord, and span of the *wing*, and substitute $\delta(y)$ from Eq. (4), retaining only the first power of k, we have

$$\delta = \frac{1}{S}\int_{-l/2}^{l/2} c(y)\left\{\frac{c_{l_q}(y) + c_{l_{\dot{\alpha}}}(y) + [c(y)c_{m_{\alpha_0}}(y)/b]}{c_{l_{\alpha_0}}(y)}\right\} dy \quad (11)$$

Assuming $c_{l_{\alpha_0}}$ to be constant across the wing and taking $x = 0$ at the aerodynamic center of the wing, we obtain

$$\delta = [(C_{L_q} + C_{L_{\dot{\alpha}}})/C_{L_{\alpha_0}}]_{\text{wing}} \quad (12)$$

For conventional wing-tail configurations, δ will be negative. While it would have been a better approximation to have carried out the integration of Eq. (10) over the tail rather than the wing, it appears that the result (12) should be reasonably accurate in those cases where $\delta(y)$ does not exhibit large variations across the wing span. Thus, the results should not be applied to heavily swept wings without further investigation.

* This work was carried out at the Aerophysics Laboratory, North American Aviation, Inc., during the summer of 1949.

REFERENCES

[1] Statler, I. C., *Dynamic Stability at High Speeds from Unsteady Flow Theory*, I.A.S. Preprint 187 (New York I.A.S. meeting, January, 1949).

[2] Miles, J. W., *Unsteady Flow Theory in Dynamic Stability*, Journal of the Aeronautical Sciences, Vol. 17, No. 1, pp. 62–63, January, 1950.

[3] Durand, W. F., *Aerodynamic Theory*, Durand Reprinting Committee, Pasadena, Calif., Vol. V, pages 49–51, 1943.

Reprinted from JOURNAL OF THE AERONAUTICAL SCIENCES
Copyright, 1950, by the Institute of the Aeronautical Sciences and reprinted by permission of the copyright owner
DECEMBER, 1950 VOLUME 17, No. 12

On the Equations of Longitudinal Stability

John W. Miles
Associate Professor of Engineering, University of California at Los Angeles
September 18, 1950

RECENTLY, THERE HAS BEEN some speculation as to which of the unsteady flow terms arising in the calculation of aerodynamic forces on an oscillating aircraft should be retained. The classical procedure[1] includes, in addition to the "quasi-stationary" terms, only that term arising from the effect of wing downwash on the tail. Nevertheless, it has been demonstrated that the calculation of pitch (or yaw) damping on a quasi-stationary basis may lead to serious errors,[2] and Statler has shown that unsteady flow effects may be important in other respects.[3] However, an order analysis of the problem in terms of its (dimensionless) characteristic parameters seems never to have been set forth, and it is to that end that the following is submitted.

Let x, y, z be a set of right-handed axes *fixed in direction* and with origin at the center of gravity of the aircraft, being positive in the direction of undisturbed flight, to starboard and down, respectively; Uu and Uw, perturbation velocities (U is the flight velocity) along x and z and θ a rotation about y; m, the total mass; B, the centroidal moment of inertia in pitch; and δX, δZ, δM the perturbation forces due to the deviations u, w, θ. The equations of motion are

$$m(\partial/\partial t)(Uu) = \delta X \tag{1a}$$
$$m(\partial/\partial t)(Uw) = \delta Z \tag{1b}$$
$$B(\partial^2/\partial t^2)\theta = \delta M \tag{1c}$$

Then, introducing the notation of Durand (reference 1, pp. 130–135; however, Durand uses axes fixed in the body), we have the following dimensionless notation:

$$\mu = m/(\rho S l) \tag{2}$$
$$k_B = B/(\mu\rho S l^3) = B/(ml^2) \tag{3}$$
$$\lambda = (\mu l/U)(\partial/\partial t) \tag{4}$$
$$\delta X = -\rho U^2 S x \tag{5a}$$
$$\delta Z = -\rho U^2 S z \tag{5b}$$
$$\delta M = -\rho U^2 S l k_B m \tag{5c}$$
$$x = (1/2)\delta C_D = [x_{u_0} + (\lambda/\mu)x_{u_1}]u + [x_{w_0} + (\lambda/\mu)x_{w_1}]w + [x_{\theta_0} + (\lambda/\mu)x_{\theta_1}]\theta \tag{6a}$$
$$z = (1/2)\delta C_L = [z_{u_0} + (\lambda/\mu)z_{u_1}]u + [z_{w_0} + (\lambda/\mu)z_{w_1}]_w + [z_{\theta_0} + (\lambda/\mu)z_{\theta_1}]\theta \tag{6b}$$
$$m = -(1/2)(\delta C_M/k_B) = [m_{u_0} + (\lambda/\mu)m_{u_1}]u + [m_{w_0} + (\lambda/\mu)m_{w_1}]w + [m_{\theta_0} + (\lambda/\mu)m_{\theta_1}]\theta \tag{6c}$$

where l is a characteristic length. Eqs. (1a)–(1c) then read

$$\lambda u + x = 0 \tag{7a}$$
$$\lambda w + z = 0 \tag{7b}$$
$$\lambda^2\theta + \mu m = 0 \tag{7c}$$

To obtain the stability quartic, we require the determinant, $F(\lambda, \mu)$, of Eqs. (7a)–(7c) to vanish. Arranging this determinant in powers of λ and μ, we have terms of order $\mu^{1,\ 0,\ -1,\ -2}$ and $\lambda^{4,\ 3,\ 2,\ 1,\ 0}$. Now the order of magnitude considerations that distinguish dynamic stability from flutter, where such distinction is possible, require μ to be large and λ to be of order one. (In this connection, we remark that, for harmonic motion, $\lambda = \mu k$, where k is the reduced frequency introduced in flutter work.) Thus, if μ is sufficiently large to justify the original neglect of terms of order $(\lambda/\mu)^2$ in Eqs. (6a)–(6c), which would have contributed terms of order μ^{-1} to the end result, we may consistently retain only terms of order μ^1 and μ^0 in the determinant of Eqs. (7a)–(7c), whence we obtain

$$F(\lambda, \mu) = A\lambda^4 + B\lambda^3 + C\lambda^2 + D\lambda + E \tag{8}$$
$$A = 1 + 0(\mu^{-1}) \tag{9a}$$
$$B = (x_{u_0} + z_{w_0} + m_{\theta_1}) + 0(\mu^{-1}) \tag{9b}$$
$$C = \mu m_{\theta_0} + \left[\begin{pmatrix} x & z \\ u_0 & w_0 \end{pmatrix} + \begin{pmatrix} z & m \\ w_0 & \theta_1 \end{pmatrix} + \begin{pmatrix} z & m \\ w_1 & \theta_0 \end{pmatrix} + \begin{pmatrix} x & m \\ u_0 & \theta_1 \end{pmatrix} + \begin{pmatrix} x & m \\ u_1 & \theta_0 \end{pmatrix}\right] + 0(\mu^{-1}) \tag{9c}$$
$$D = \mu\left[\begin{pmatrix} x & m \\ u_0 & \theta_0 \end{pmatrix} + \begin{pmatrix} z & m \\ w_0 & \theta_0 \end{pmatrix}\right] + \left[\begin{pmatrix} x & z & m \\ u_0 & w_0 & \theta_1 \end{pmatrix} + \begin{pmatrix} x & z & m \\ u_0 & w_1 & \theta_0 \end{pmatrix} + \begin{pmatrix} x & z & m \\ u_1 & w_0 & \theta_0 \end{pmatrix}\right] \tag{9d}$$
$$E = \mu \begin{pmatrix} x & z & m \\ u_0 & w_0 & \theta_0 \end{pmatrix} \tag{9e}$$

where the parenthetic sets of four and six variables denote Jacobians; e.g.,

$$\begin{pmatrix} x & z & m \\ u_0 & w_0 & \theta_0 \end{pmatrix} = \begin{vmatrix} x_{u_0} & x_{w_0} & x_{\theta_0} \\ z_{u_0} & z_{w_0} & z_{\theta_0} \\ m_{u_0} & m_{w_0} & m_{\theta_0} \end{vmatrix} \tag{10}$$

Eqs. (9a)–(9e) simplify considerably for the case of free (power-off, no autopilot) flight at small angles of attack (α), in which case (due to our choice of axes fixed in direction)

$$(\partial/\partial w)_0 = (\partial/\partial\theta)_0 = (\partial/\partial\alpha) \tag{11}$$

Also, we may prove that

$$(\partial/\partial\theta)_1 = (\partial/\partial q) + (\partial/\partial\dot{\alpha}) \tag{12}$$
$$(\partial/\partial w)_1 = (\partial/\partial\dot{\alpha}) \tag{13}$$

where $(\partial/\partial q)$ implies steady flight at constant angular velocity (e.g., along a curved flight path, as in a pull out) and $\dot{\alpha}$ denotes a vertical acceleration, positive down. In view of the assumption of small angle of attack, we also may neglect drag terms relative to lift and moment terms, and Eqs. (9a)–(9e) reduce to

$$A = 1 \tag{14a}$$
$$B = (z_\alpha + m_q + m_{\dot{\alpha}}) \tag{14b}$$
$$C = \mu m_\alpha + \begin{pmatrix} z & m \\ \alpha & q \end{pmatrix} \tag{14c}$$
$$D = \mu \begin{pmatrix} x & m \\ u_0 & \alpha \end{pmatrix} + \begin{pmatrix} x & z & m \\ u_0 & \alpha & q \end{pmatrix} \tag{14d}$$
$$E = 0 \tag{14e}$$

It follows that, in this case at least, the only unsteady flow term of importance is $m_{\dot{\alpha}}$.

We should expect this last conclusion to be equally valid, insofar as aerodynamic (as opposed to autopilot) terms alone are concerned, for power-on flight, but the neighborhood of stalled flight may not be included without further investigation. Moreover, in interpreting Eqs. (14a)–(14e), it should be remarked that z_q, $z_{\dot{\alpha}}$, m_q, and $m_{\dot{\alpha}}$, when properly calculated, all include downwash effects of wing on tail.[4]

A similar analysis of the equations of lateral stability could be carried out, although it would be necessary to use axes fixed in the body and to discuss the effects of yawing the wake.

REFERENCES

[1] Durand, W. F., *Aerodynamic Theory*, Vol. V; Durand Reprinting Committee, Pasadena, Calif., 1943.

[2] Miles, John W., *Unsteady Flow Theory in Dynamic Stability*, Readers' Forum, Journal of the Aeronautical Sciences, Vol. 17, No. 1, p. 62, January, 1950.

[3] Statler, I. C., *Dynamic Stability at High Speeds from Unsteady Flow Theory*, Journal of the Aeronautical Sciences, Vol. 17, No. 4, pp. 232–242, April, 1950.

[4] Miles, John W., *On Downwash Corrections in Unsteady Flow*, Readers' Forum, Journal of the Aeronautical Sciences, Vol. 17, No. 4, p. 253, April, 1950.

Reprinted from JOURNAL OF THE AERONAUTICAL SCIENCES
Copyright, 1951, by the Institute of the Aeronautical Sciences and reprinted by permission of the copyright owner
MARCH, 1951 VOLUME 18, No. 3

On the Equations of Longitudinal Stability—II

John W. Miles
Associate Professor of Engineering, University of California at Los Angeles
December 22, 1950

DR. NEUMARK (R.A.E., FARNBOROUGH, ENGLAND) has pointed out that the result $E = 0$ in Eq. (14e) of a recent note[1] on this subject is at variance with the usual result for free, power-off flight. This was due to an incorrect assumption that $x_{\theta_0} = x_{u_0} = x_\alpha$, whereas we can state correctly only $x_{\theta_0} = x_\alpha$, and Eqs. (14) should read

$$A = 1 \tag{14a}$$

$$B = (z_\alpha + m_q + m_{\dot\alpha}^{\cdot}) \tag{14b}$$

$$C = \mu m_\alpha + \begin{pmatrix} z & m \\ \alpha & q \end{pmatrix} \tag{14c}$$

$$D = \mu \begin{pmatrix} x & m \\ u_0 & \alpha \end{pmatrix} + \begin{pmatrix} x & z & m \\ u_0 & \alpha & q \end{pmatrix} + (x_{\theta_0} - x_{w_0}) \left[\begin{pmatrix} z & m \\ u_0 & \theta_1 \end{pmatrix} + \begin{pmatrix} z & m \\ u_1 & \alpha \end{pmatrix} \right] \tag{14d}$$

$$E = \mu (x_{\theta_0} - x_{w_0}) \begin{pmatrix} z & m \\ u_0 & \alpha \end{pmatrix} \tag{14e}$$

the notation being that of reference 1.

Further, the derivatives with respect to u_1, representing virtual inertia in the direction of flight, may be established as small by direct dimensional considerations, and m_{w_0} generally is small, vanishing for trimmed flight at low speeds. With these approximations, Eq. (14d) reduces to

$$D = \mu \begin{pmatrix} x & m \\ u_0 & \alpha \end{pmatrix} + \begin{pmatrix} x & z & m \\ u_0 & \alpha & q \end{pmatrix} + z_{u_0} (x_{\theta_0} - x_{w_0}) (m_q + m_{\dot\alpha}^{\cdot}) \tag{14d'}$$

Hence, the conclusion that $m_{\dot\alpha}^{\cdot}$ is the only unsteady flow term that need be included in the longitudinal stability equations remains unchanged.

REFERENCE

[1] Miles, John W., *On the Equations of Longitudinal Stability*, Readers Forum, Journal of the Aeronautical Sciences, Vol. 17, No. 12, pp. 815–816, December, 1950.

[*Reprinted from* The Aeronautical Quarterly, Vol. II, *November* 1950]

Published by The Royal Aeronautical Society

On Non-Steady Motion of Slender Bodies

by

JOHN W. MILES

ON NON-STEADY MOTION OF SLENDER BODIES

by

JOHN W. MILES

(*Associate Professor of Engineering, University of California, Los Angeles*)

SUMMARY

Following the original work of Munk, Jones, and Ward for steady flow, a solution is given for unsteady, supersonic flow over very slender bodies of revolution and wings. The results are subject to the restriction $(M^2-1)\,\delta^2 \log_e [(M^2-1)^{\frac{1}{2}}\delta] << 1$ where δ is the slenderness ratio, M is the Mach number and, in addition, to the usual restrictions imposed by linearisation. As examples, the lifts and pitching moments on flat wings and bodies of revolution executing pitching motion and the damping moment on a rolling wing are calculated.

It is shown that the order of approximation is consistent with the limitations already imposed by linearisation, at least in supersonic flow, where no Kutta condition is required.

Notation

A	wing aspect ratio (*see* equation (28))
C_L	lift coefficient
C_M	pitching moment coefficient
C_l	rolling moment coefficient
D/Dt	differential operator with respect to time
I_n	*see* equation (24)
L	lift (transverse) force
M	Mach number
R	radius of cross section of body of revolution
S	area of wing plan form
S_1	base area for body of revolution
$S(x)$	area of cross section of body of revolution
U	free stream velocity

Paper received January 1950.

[The Aeronautical Quarterly, Vol. II, November 1950]

a	fraction of body length of axis of pitch aft of nose
b	span at x
c	sonic velocity in free stream
k	reduced frequency (*see* equation (9))
l	body length
m	apparent mass of cross section
p	angular velocity in roll
r	polar co-ordinate
t	time
w	downwash, *i.e.* velocity transverse to free stream
x, y, z	Cartesian co-ordinates
α	amplitude of pitch displacement (*see* equation (19))
β	$(M^2-1)^{\frac{1}{2}}$
γ	semi-apex angle of triangular wing
δ	slenderness ratio (maximum width/length)
θ	polar co-ordinate
ρ	density
ϕ	velocity potential
τ	dimensionless time (Ut/l)
ω	angular frequency

1. INTRODUCTION

The solutions for steady flow past slender bodies of revolution and narrow wings were first given by Munk[1] and Jones[2] respectively. More recently, a critical treatment has been given by Ward[3]. An extension of their work to the problem of unsteady flow is presented here, treating only the lifting forces. While the results of the slender body analysis are independent, in a restricted sense, of Mach number, the supersonic case will be treated primarily since the effect of the wake may then be disregarded.

It is assumed that the body lies in the immediate vicinity of the x axis, its most forward point projecting on the origin and its length being l. The free stream of velocity U is directed along the positive x axis, and the theory is linearised in the usual manner. The velocity potential then satisfies the linearised equation

$$\nabla^2\phi(x, y, z, t) = \frac{1}{c^2}\left(U\frac{\partial}{\partial x} + \frac{\partial}{\partial t}\right)^2 \phi(x, y, z, t), \quad . \quad . \quad (1)$$

where c is the sonic velocity in the undisturbed medium. It is convenient to assume the co-ordinates (x, y, z) to be dimensionless, with l as the unit of length, and to introduce the dimensionless time

$$\tau = Ut/l. \quad . \quad . \quad . \quad . \quad . \quad . \quad (2)$$

Expanding the Laplacian and introducing τ, equation (1) reads

$$\phi_{yy} + \phi_{zz} = \beta^2 \phi_{xx} + 2M^2 \phi_{x\tau} + M^2 \phi_{\tau\tau}, \quad . \quad . \quad . \quad . \quad (3)$$

where

$$M = U/c, \quad \beta = (M^2 - 1)^{\frac{1}{2}}. \quad . \quad . \quad . \quad . \quad . \quad (4)$$

The slender body approximation in steady flow assumes the flow to be essentially two-dimensional at every cross section, thereby implicitly neglecting the term $\beta^2 \phi_{xx}$. In the case of a steady flow past a body of revolution, Lighthill[4] has shown that this is the best approximation which is consistently allowed within the framework of the linearised theory. This approximation naturally breaks down for sufficiently large values of β^2, *i.e.* in the hypersonic régime but, since the linearised theory itself is invalid for large M, this does not represent an entirely new limitation. More precisely, if δ is the slenderness ratio, the slender body approximation (in steady flow) requires

$$(\beta\delta)^2 \log_e (\beta\delta) << 1 \quad . \quad . \quad . \quad . \quad . \quad (5)$$

whereas the hypersonic limitation requires $M\delta$ to be small, so that the two restrictions are not exactly equivalent. For a more critical discussion of the slender body approximation in steady flow, the reader is referred to the work of Lighthill[4, 5, 6] and Ward[3].

Turning to the case of unsteady flow, reference is made to a general discussion of the linearising process for the two-dimensional case which has been given recently by Lin, Reissner, and Tsien[7]. They conclude that necessary conditions for the validity of the linearised theory are

$$M\delta << 1 \quad . \quad . \quad . \quad . \quad . \quad . \quad (6)$$

$$kM\delta << 1, \quad . \quad . \quad . \quad . \quad . \quad . \quad (7)$$

where δ is the thickness or amplitude of oscillation, whichever is larger, referred to l, and $1/k$ is a characteristic time, *cf.* equation (9). They also conclude that if M is not large and either $|1 - M|$ or $k >> \delta^{\frac{2}{3}}$ the linearised theory for unsteady flow is valid even in the transonic range. In this connection $\beta\delta$ is the important parameter in the slender body approximation in steady flow, *cf.* equation (5), whereas Ward[3] evidently assumes $\beta = O(1)$ and uses δ alone.

No attempt will be made to discuss here the sufficiency of the foregoing conditions for linearisation of the three-dimensional, unsteady flow problem, other than to point out that, in the case of the body of revolution, there is the additional complication of possible singularities on the axis, as a result of which logarithmic terms are introduced in the order of magnitude approximations. However, a very cursory examination of the analysis of Ref. 7 makes it evident that the restrictions (6) and (7) also will be necessary in the three-dimensional case. Accordingly a two-dimensional cross flow will be assumed and the result examined *a posteriori*, in the light of the restrictions.

2. THE SLENDER BODY SOLUTION

The transverse oscillations, exhibiting the harmonic time dependence $\exp(i\omega t)$, of a pointed body of revolution, described in cylindrical polar co-ordinates by $r=R(x)$, will be considered. The (linearised) boundary condition, to be satisfied at the mean position, is given by

$$\phi_r(x, r, \theta, \tau)\,|_{r=R(x)} = -w(x)\cos\theta\exp(ik\tau) \quad . \quad . \quad . \quad (8)$$

$$k=\omega l/U, \quad . \quad . \quad . \quad . \quad . \quad . \quad (9)$$

where k is the reduced frequency parameter, and $w(x)$ is the prescribed downwash. There is also the implicit condition that the disturbance vanish at infinity in the proper manner (the Sommerfeld "radiation" condition).

If two-dimensional flow is now assumed at any cross section by neglecting the x derivatives in equation (3),

$$\phi_{rr}+\frac{1}{r}\phi_r+\frac{1}{r^2}\phi_{\theta\theta}=M^2\phi_{\tau\tau}. \quad . \quad . \quad . \quad . \quad (10)$$

A solution to equations (8) and (10), which represents an outgoing disturbance at infinity, is given by

$$\phi(x, r, \theta, \tau)=-\frac{w(x)H_{1(2)}(kMr)\cos\theta\exp(ik\tau)}{kM[H_{1(2)}'(kMr)]_{r=R(x)}} \quad . \quad . \quad . \quad (11)$$

where $H_{1(2)}$ is Hankel's function of the second kind and order one. In the vicinity of the body, where $r\sim R=O(\delta)$, equation (11) reduces to

$$\phi(x, r, \theta, \tau)=w(x)R^2(x)\left(\frac{\cos\theta}{r}\right)\exp(ik\tau)\{1+O[(kM\delta)^2\log_e(kM\delta)]\} \quad (12)$$

Moreover,

$$O\left[\frac{2M^2\phi_{xr}}{\frac{1}{r}\phi_r}\right]=(kM\delta)(M\delta) \quad . \quad . \quad . \quad . \quad (13)$$

$$O\left[\frac{\beta^2\phi_{xx}}{\frac{1}{r}\phi_r}\right]=(M\delta)^2. \quad . \quad . \quad . \quad . \quad . \quad (14)$$

It follows that, in view of the restrictions of equations (6), (7), the approximate solution of equation (12) is all that is justified by the linearised theory.

While the foregoing discussion has been limited to a body of revolution, a more general analysis could have been given, following that of Ward. Thus it is found that the linearised flow about any slender body may be approximated as a solution to Laplace's equation provided that, in addition to the restrictions imposed by linearisation, both the maximum angle between any tangent plane to the body and the free stream direction and the rate of change of this angle are $O(\delta)$ and the curvature of any section is $O(1/d)$, where d is the maximum section diameter, at all points where the section is convex outwards (there being no similar restriction at points where the section is concave outwards). The last restriction guarantees small disturbance velocities, relative to U. If it is not satisfied, as in the case of thin flat wings, it can no longer be asserted that equation (12) correctly describes the order of the approximation, but this difficulty is present whenever the linearised theory is applied to thin wings, and the resultant errors in integrated results (such as lifts and moments) generally are acceptable.

In considering bodies of arbitrary cross section, generally it is necessary to consider the interaction of the axial flow, which will introduce a logarithmic term in the potential, and the cross flow, as done by Ward[3]. In the special case of a body of revolution the axial flow has no net effect on the transverse forces, by virtue of symmetry, although naturally it must be included in the calculation of the drag. Thus, the concept of virtual mass may be introduced in the calculation of the transverse forces acting on a body of revolution and, also, on a slender, flat wing, since the axial flow introduces no disturbance in the latter case. (The application of the virtual mass concept to such problems is due to Jones[2].) In the case of a winged body of revolution, on the other hand, the axial flow due to wing-body interference must be considered, and the concept of virtual mass is no longer sufficient for a complete analysis.

Since the solution to equation (3) for unsteady flow is identical with that for steady flow, the difference between the two cases manifests itself entirely in the linearised Bernouilli equation, namely:—

$$\text{pressure}=-\rho\frac{D}{Dt}\phi=-\rho U(\phi_x+ik\phi). \quad . \quad . \quad . \quad . \quad (15)$$

Thus, if $m(x)$ is the virtual mass of a cross section at x, the transverse (lift) force may be calculated directly from Newton's law, namely:—

$$\frac{\partial}{\partial x} L(x) = \frac{D}{Dt}[m(x) w(x) \exp(ik\tau)]$$

$$= U\left(\frac{\partial}{\partial x} + ik\right)[m(x) w(x)] \exp(ik\tau) \quad . \quad . \quad . \quad (16)$$

3. BODY OF REVOLUTION

The potential for this problem has already been obtained, *cf.* equation (12), and equation (16) is applied directly. The virtual mass of a circular cross section is given by

$$m(x) = \rho S(x) = \pi \rho R^2(x) \quad . \quad . \quad . \quad . \quad . \quad (17)$$

whence equation (16) reads

$$\frac{\partial}{\partial x} L(x) = \rho U^2 \left(\frac{\partial}{\partial x} + ik\right)\left[S(x) \frac{w(x)}{U}\right] \exp(ik\tau) \quad . \quad . \quad . \quad (18)$$

The case of principal interest is that of a pitching oscillation of amplitude α about $x = a$, for which

$$w(x) = U\alpha[1 + ik(x-a)] \quad . \quad . \quad . \quad . \quad . \quad (19)$$

If the lift and moment (with respect to $x = a$) coefficients are defiined by

$$C_L = [\tfrac{1}{2}\rho U^2 S_1 \exp(ik\tau)]^{-1} \int_0^1 L'(x)\, dx \quad . \quad . \quad . \quad . \quad (20)$$

$$C_M = [\tfrac{1}{2}\rho U^2 S_1 l \exp(ik\tau)]^{-1} \int_0^1 (a-x) L'(x)\, dx \quad . \quad . \quad (21)$$

where $S_1 = S(1)$ is the base area, equations (18) and (19) yield

$$C_{L\alpha} = 2[1 + ik(1 - a + I_0) + k^2(aI_0 - I_1)] \quad . \quad . \quad . \quad . \quad (22)$$

$$C_{M\alpha} = 2[-(1 - a - I_0) - ik(1-a)^2 + k^2(I_2 - 2aI_1 + a^2 I_0)] \quad . \quad . \quad (23)$$

$$I_n = \int_0^1 x^n \frac{S(x)}{S_1} dx. \quad . \quad . \quad . \quad . \quad . \quad . \quad . \quad (24)$$

It is of particular interest that the imaginary part of $C_{M\alpha}$, *i.e.* the damping moment, vanishes for an axis through the base ($a = 1$).

4. LOW ASPECT RATIO WINGS

In this section low aspect ratio, pointed wings, are considered, of span $b(x)$, subject to the restriction

$$b'(x) \geqslant 0. \quad . \quad . \quad . \quad . \quad . \quad . \quad (25)$$

In the more general case, where equation (25) is not invoked, it would be necessary to impose the boundary condition

$$\phi(x, y, 0\pm) = \exp[ik(x_1(y) - x)]\,\phi[x_1(y), y, 0\pm] \quad . \quad . \quad . \quad (26)$$

at points in the wake aft of the maximum cross section, $x_1(y)$ denoting the trailing edge. Equation (26) ensures continuity of the pressure across the wake, even though the potential itself is discontinuous there. Effectively the imposition of equation (26) spoils the assumption of a two-dimensional cross flow, since the boundary conditions at sections aft of the maximum span are no longer independent.

In the case of steady flow over a flat wing with constant incidence, Jones[2] and Ward[3] have shown that this boundary condition is satisfied by making the cross flow about all cross sections aft of the maximum span identical, so that no lift force arises (*i.e.* $D/Dt = U\partial/\partial x = 0$). Unfortunately this neat state of affairs does not prevail in the case under consideration, both due to the phase factor in equation (26) and the dependence of the local incidence, $w(x)/U$, on x.

Despite the restriction of equation (25), continuity of the pressure also would have to be required at the trailing edge if the flow were subsonic, in satisfaction of the so-called Kutta condition. From the mathematical viewpoint, the Kutta condition, as applied in conventional aerofoil theory, is essentially a uniqueness condition and is required because of the existence of eigensolutions to the boundary value problem. In the case of the slender body solution, however, the solution for the two-dimensional cross flow is already unique for the boundary conditions stated, and no eigensolutions exist. The answer to the apparent paradox lies in the violation of the initial assumptions on which the slender body approximation rests, for if the potential is discontinuous at the trailing edge its x derivatives most certainly cannot be assumed small. Thus, while it has sometimes been stated that the slender body approximation is valid for subsonic, as well as supersonic, flow, this may be asserted with certainty only in those special cases* where the Kutta condition is satisfied automatically. While it may furnish acceptable results in other cases, the order of the error can be established only by a more thorough investigation or by comparison with experiment. Similar objections may be

*Such as the elliptic wing used by Jones[2] as a basis of comparison between the slender body approximation and a known exact result.

levelled at the application of the slender body approximation to the analysis of subsonic flow about a body of revolution having a base of finite area, but in this case no satisfactory theory exists to describe the actual phenomena, which must be heavily influenced by viscous effects. Accordingly this investigation is restricted to supersonic flow over wings with monotonically increasing span (which implies a straight trailing edge, transverse to the flow), so that no section is influenced by events occurring downstream.

Returning to the special category of wings described by equation (25), the approach of equation (16) is used. The virtual mass of a flat plate is identical with that of the circumscribed, circular cylinder, whence

$$m(x)=(\pi/4)\rho b^2(x). \quad . \quad . \quad . \quad . \quad . \quad (27)$$

If the lift and moment coefficients are referred to the plan form area S, and the aspect ratio is introduced

$$A=b_1{}^2/S, \quad . \quad . \quad . \quad . \quad . \quad . \quad (28)$$

where b_1 is the maximum span (in this case, the span at the trailing edge), the results may be taken over from those for the body of revolution by multiplying the latter by $(\pi A/4)$ and replacing $S(x)$ by $b^2(x)$ in equation (24).

The simplest, pointed, low aspect ratio wing, and perhaps the only one of any practical importance, is the triangular wing, for which

$$b(x)/b_1=x, \quad \mathrm{I}_n=(n+3)^{-1}. \quad . \quad . \quad . \quad . \quad (29)$$

In this case

$$C_{L\alpha}=(\pi A/2)\left[1+ik\left(\frac{4}{3}-a\right)+k^2\left(\frac{a}{3}-\frac{1}{4}\right)\right] \quad . \quad . \quad . \quad . \quad (30)$$

$$C_{M\alpha}=(\pi A/2)\left[-\left(\frac{2}{3}-a\right)-ik(1-a)^2+k^2\left(\frac{1}{5}-\frac{a}{2}+\frac{a^2}{3}\right)\right]. \quad . \quad (31)$$

5. NON-PLANAR MOTION

Consider now the more general case, where the motion of the wing is not plane. The problem is one in potential flow (because of the slender body approximation) and, in principle, is straightforward.

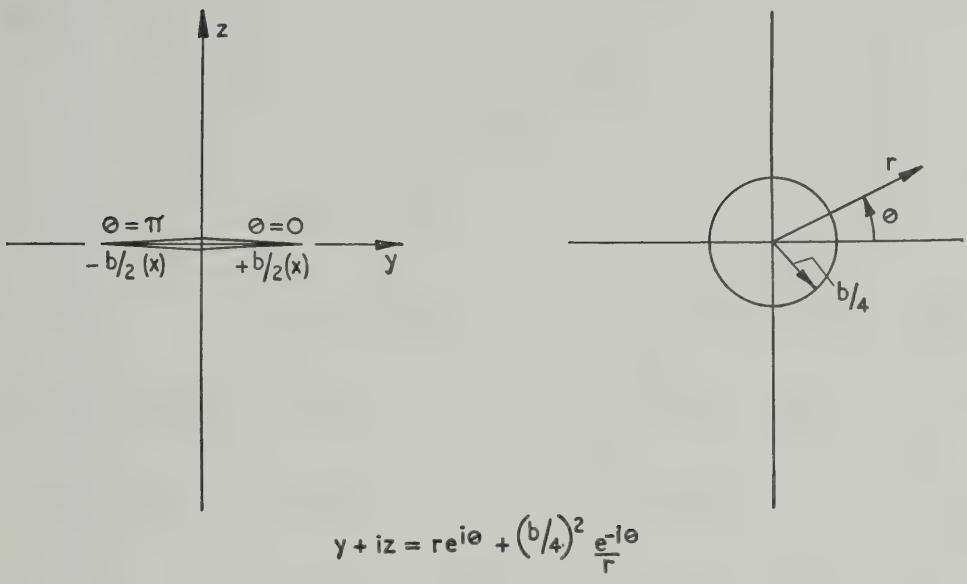

Fig. 1.

Mapping of wing section on circle.

A section of the wing is shown in Fig. 1. The (linearised) boundary conditions are

$$\phi_z(x, y, z)\,|_{z=0+} = -w(x, y), \quad |y| < \tfrac{1}{2}b(x) \qquad . \quad . \quad . \quad (32)$$

$$\phi(x, y, 0) = 0, \quad |y| > \tfrac{1}{2}b(x) \qquad . \quad . \quad . \quad (33)$$

$$\phi(x, y, z) \longrightarrow 0, \quad |y|, |z| \longrightarrow \infty \qquad . \quad . \quad . \quad (34)$$

while ϕ is required to satisfy Laplace's equation

$$\phi_{yy} + \phi_{zz} = 0. \qquad . \quad . \quad . \quad . \quad . \quad . \quad (35)$$

The harmonic time dependence factor has been suppressed.

The desired solution is obtained by mapping the wing ($z=0$, $|y| < b/2$) on the circle $r=(b/4)$ with the aid of the Joukowsky transformation

$$y + iz = re^{i\theta} + \left(\frac{b}{4}\right)^2 \frac{e^{-i\theta}}{r}, \qquad . \quad . \quad . \quad . \quad (36)$$

as shown in Fig. 1.

Proceeding in the usual manner, a solution to equations (32) to (35) is given by

$$\phi\left(x, \frac{b}{2}\cos\theta, z\right) = \frac{b(x)}{\pi} \sum_1^\infty \left[\frac{b(x)}{4r}\right]^n \frac{\sin n\theta}{n} \int_0^\pi w\left(x, \frac{b}{2}\cos\varphi\right) \sin n\varphi \sin\varphi \, d\varphi \quad . \quad (37a)$$

$$= \frac{b(x)}{2\pi} \int_0^\pi w\left(x, \frac{b}{2}\cos\varphi\right) \sin\varphi \log_e \left[\frac{1+(4r/b)^2 - 2(4r/b)\cos(\theta+\varphi)}{1+(4r/b)^2 - 2(4r/b)\cos(\theta-\varphi)}\right] d\varphi. \quad . \quad (37b)$$

On the aerofoil ($r=b/4$), equation (37) reduces to

$$\phi\left(x, \frac{b}{2}\cos\theta, 0+\right) = \frac{b(x)}{\pi} \sum_1^\infty \frac{\sin n\theta}{n} \int_0^\pi w\left(x, \frac{b}{2}\cos\varphi\right) \sin n\varphi \sin\varphi \, d\varphi \quad . \quad (38a)$$

$$= \frac{b(x)}{2\pi} \int_0^\pi w\left(x, \frac{b}{2}\cos\varphi\right) \sin\varphi \log_e \left[\frac{1-\cos(\theta+\varphi)}{1-\cos(\theta-\varphi)}\right] d\varphi. \quad . \quad (38b)$$

For the lift and rolling moment on the wing section at x, the following integrals are required

$$\psi_0(x) = \int_{-\frac{1}{2}b(x)}^{\frac{1}{2}b(x)} \phi(x, y, 0+)\, dy \quad . \quad . \quad . \quad . \quad . \quad . \quad (39a)$$

$$= \frac{b(x)}{2} \int_0^\pi \phi\left(x, \frac{b}{2}\cos\theta, 0+\right) \sin\theta \, d\theta \quad . \quad . \quad . \quad (39b)$$

$$= \frac{b^2(x)}{4} \int_0^\pi w\left(x, \frac{b}{2}\cos\theta\right) \sin^2\theta \, d\theta \quad . \quad . \quad . \quad . \quad (39c)$$

$$\psi_1(x) = \int_{-\frac{1}{2}b(x)}^{\frac{1}{2}b(x)} \phi(x, y, 0+)\, y dy. \quad . \quad . \quad . \quad . \quad . \quad (40a)$$

$$= \frac{b^2(x)}{4} \int_0^\pi \phi\left(x, \frac{b}{2}\cos\theta, 0+\right) \sin\theta\cos\theta \, d\theta \quad . \quad . \quad (40b)$$

$$= \frac{b^3(x)}{32} \int_0^\pi w\left(x, \frac{b}{2}\cos\theta\right) \sin 2\theta \sin\theta \, d\theta \quad . \quad . \quad (40c)$$

As an example the damping due to roll (angular velocity p) is considered.

The downwash is given by

$$w(x, y) = py = p[b(x)/2]\cos\theta \quad . \quad . \quad . \quad . \quad (41)$$

and the rolling moment coefficient by

$$C_l = -[\tfrac{1}{2}\rho U^2 S b_1]^{-1} \int_0^1 dx \int_{-\frac{1}{2}b(x)}^{\frac{1}{2}b(x)} [-2p(x, y, 0+)]\, y dy \quad . \quad . \quad (42a)$$

$$= -\frac{4}{Sb_1}\int_0^1 \left(\frac{\partial}{\partial x} + \frac{\partial}{\partial \tau}\right)\frac{\psi_1(x)}{U} dx \quad . \quad . \quad . \quad . \quad . \quad (42b)$$

Substituting the distribution (41) in (40*c*) and the latter in equation (42*b*),

$$C_{lp} = \frac{\partial C_l}{\partial\left(\frac{pb}{2U}\right)} = -(\pi A/32)\left[1 + ik\int_0^1 \frac{b^4(x)}{b_1^4} dx\right] \quad . \quad . \quad (43)$$

The real and (negative) imaginary parts correspond to the damping and inertia respectively. For a triangular wing of semi-apex angle γ, the aspect ratio $A = 4\tan\gamma$, and equation (43) then gives $-(\pi/8)\tan\gamma$ for the damping moment coefficient. The exact (linearised) result for the damping in roll of a triangular wing in supersonic flow has been calculated by Robinson[8] and, in the limit of small γ, yields

$$C_{lp} = -(\pi\tan\gamma)/8 + O[(\beta\tan\gamma)^3 \log_e(\beta\tan\gamma)] \; . \quad . \quad . \quad (44)$$

in agreement with the result above for small γ. The comparison reveals that the accuracy of the slender body approximation in predicting integrated force coefficients, relative to the three-dimensional, linearised theory, is correctly indicated by equation (5), despite the violation of the restriction on curvature of convex sections. Similar comparisons also have been made for the results (30), (31) with the limiting forms of the complete longitudinal, stability derivatives[9] (Robinson[8] gives only the quasi-stationary results, neglecting the time derivatives in the Bernoulli equation and the continuity equation).

REFERENCES

1. Munk, M. M. (1923). The Aerodynamic Forces on Airship Hulls. N.A.C.A. Report 184, 1923.

2. Jones, R. T. (1946). Properties of Low-Aspect-Ratio Pointed Wings at Speeds Below and Above the Speed of Sound. N.A.C.A. Tech. Note 1032, 1946.

3. Ward, G. N. (1949). Supersonic Flow Past Slender Bodies. *Quarterly Journal of Mechanics and Applied Mathematics*, 2, 75-97, 1949.

4. LIGHTHILL, M. J. (1945). Supersonic Flow Past Bodies of Revolution. R. & M. 2003, 17-21, 1945.

5. LIGHTHILL, M. J. (1948). Supersonic Flow Past Slender Pointed Bodies of Revolution at Yaw. *Quarterly Journal of Mechanics and Applied Mathematics,* 1, 76-89, 1948.

6. LIGHTHILL, M. J. (1949). Methods for Predicting Phenomena in High Speed Flow of Gases. *Journal Aeronautical Sciences,* 16, 69-83, 1949.

7. LIN, C. C., REISSNER, E. and TSIEN, H. S. (1949). On Two-Dimensional Non-Steady Motion of a Slender Body in a Compressible Fluid. *Journal Mathematics and Physics,* 27, 220-231, 1949.

8. ROBINSON, A. (1948). Rotary Derivatives of a Delta Wing at Supersonic Speeds. *Journal Royal Aeronautical Society,* 52, 735-752, Nov. 1948.

9. MILES, J. W. (1949). On Damping in Pitch for Delta Wings. *Journal Aeronautical Sciences,* 16, 574-575, 1949.

Made and Printed in Great Britain by The Lewes Press
(Wightman & Co. Ltd.), Friars Walk, Lewes, Sussex.

On the Response of a Directive Antenna to Incoherent Radiation*

FREDERICK W. SCHOTT†, MEMBER, IRE

Summary—The relative response of directive antennas is dependent on the mechanism whereby the energy is conveyed. This fact, which often seems to be neglected, is of particular importance when the energy arriving at a receiving antenna can be represented in terms of a spectrum of incoherent plane-wave components. Such may be true frequently in the extraoptical propagation of microwaves.

A study of an idealized situation is presented which compares the behavior of several pencil-beam antennas of varying aperture. A brief comparison with some recent observations is made.

Introduction

THE CONCEPT of antenna gain is a useful tool for computing the power received by an antenna when the incident radiation consists of a single, substantially plane, wave. However, when the incoming radiation is of a more complex nature as, for example, when due to an aggregate of scattering elements randomly located, the gain concept must be applied with some caution.

The purpose of this paper is to indicate the manner in which the power received by a directive antenna depends upon the distribution of the incident radiation and to illustrate the result with an application to a pencil-beam antenna.

The Weighted Antenna Gain

A directive antenna whose axis is chosen as the reference direction is shown in Fig. 1. A parabolic antenna is shown; however, the form of the antenna is immaterial

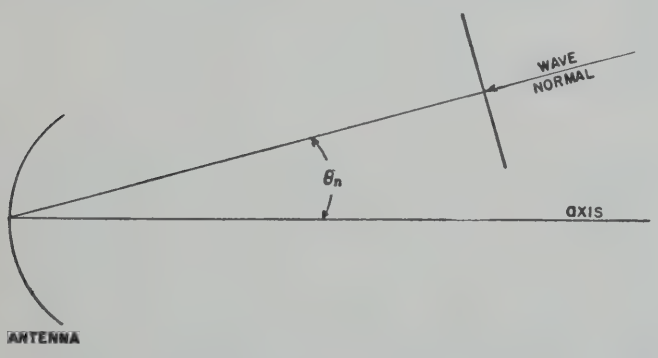

Fig. 1—Directive antenna and associated notation.

at this point. It is supposed that the incident radiation consists of many plane-wave components, and it is assumed that the nth component is arriving from the direction θ_n, ϕ_n, where θ_n represents the colatitude and ϕ_n the azimuth. Because of the directive characteristics of the antenna, this wave produces a component of voltage of relative amplitude a_n at the antenna output, i.e.,

$$a_n = a(\theta_n, \phi_n).$$

The resultant amplitude (voltage) at the antenna output due to the many plane waves is then

$$E = \sum_{n=1}^{N} a_n e^{j\alpha_n}, \tag{1}$$

where α_n represents the phase of the nth component relative to some arbitrary reference and is assumed to be *random*.

The power associated with this resultant voltage (except for a constant of proportonality) is then

$$S = |E|^2 = \left| \sum_{n=1}^{N} a_n e^{j\alpha_n} \right|^2 \tag{2}$$

and the average power

$$\overline{S} = \sum_{n=1}^{N} a_n^2 \tag{3}$$

because of the random nature of the α's. If the plane-wave components are sufficiently numerous, the above summation over n can be represented by a corresponding integration over the appropriate directions. Since the element of area is proportional to $\sin \theta d\theta d\phi$, the average is given by[1]

$$\overline{S} = C \int_0^{2\pi} \int_0^{\pi} a^2(\theta, \phi) \sin \theta d\theta d\phi, \tag{4}$$

where C is a constant and $a(\theta, \phi)$ now represents the probability per unit area that the component of amplitude a is associated with the direction θ, ϕ.

Because $a(\theta, \phi)$ is a measure of the relative amplitude at the antenna output, it represents the effect of antenna directivity as well as the directional character of the radiation itself. Hence

$$a^2(\theta, \phi) = a_1^2(\theta, \phi) G(\theta, \phi),$$

where $a_1(\theta, \phi)$ is the relative amplitude of the plane-wave component in the direction of polarization of the antenna arriving from the direction θ, ϕ, and $G(\theta, \phi)$ is the gain function[2] of the antenna in a homogeneous medium.

If an isotropic antenna were used, the average received power would be given by

* Decimal classification: R125×R326.8. Original manuscript received by the Institute, May 9, 1950; revised manuscript received, October 2, 1950. Presented, IRE-URSI Symposium on Antennas and Propagation, San Diego, Calif., April 3, 1950.

† University of California, Los Angeles, Calif.

[1] See P. M. Morse, "Vibration and Sound," McGraw-Hill Book Co., New York, N. Y., p. 383; 1948.

[2] As defined, for example, by S. Silver, "Microwave Antenna Theory and Design," Radiation Laboratory Series, McGraw-Hill Book Co., New York, N. Y., vol. 12, p. 3; 1949.

$$\overline{S}_I = C \int_0^{2\pi} \int_0^{\pi} a_1^2(\theta, \phi) \sin \theta d\theta d\phi. \quad (5)$$

Thus, the power received by the directive antenna relative to that received by an isotropic antenna is

$$\frac{\overline{S}}{\overline{S}_I} = \frac{\int_0^{2\pi} \int_0^{\pi} a_1^2(\theta, \phi) G(\theta, \phi) \sin \theta d\theta d\phi}{\int_0^{2\pi} \int_0^{\pi} a_1^2(\theta, \phi) \sin \theta d\theta d\phi}, \quad (6)$$

which might be termed the "weighted" gain. This rather general result must include, as a special case, that of radiation arriving from a single direction, θ_1, ϕ_1. In the latter case the directivity of the incident radiation may be represented by the delta function, i.e., $a_1(\theta, \phi) = \delta(\theta - \theta_1, \phi - \phi_1)$, giving

$$\frac{S}{\overline{S}_I} = G(\theta_1, \phi_1),$$

as required.

It should be noted that the result using (6) is determined by the method used to illuminate the scattering elements as well as their own directivity characteristics, since this determines $a_1(\theta, \phi)$. An analysis by Booker and Gordon,[3] based on the work of Pekeris,[4] has given explicit results for certain cases of forward scattering due to atmospheric inhomogeneities.

Examples

As an illustration of the use of (6), the following case will be considered: It will be assumed that the antenna is viewing the "center" of a scattering region such that $a_1(\theta, \phi) = a_1(\theta)$ only, and furthermore that the incident plane-wave components arrive uniformly from all directions within the cone semiangle θ_0, and that no radiation is arriving from outside this region. This is indicated in Fig. 2. In addition, it will be assumed that

$$G(\theta, \phi) = G(\theta)$$

only. Thus (6) becomes

$$\frac{\overline{S}}{\overline{S}_I} = \frac{\int_0^{\theta_0} G(\theta) \sin \theta d\theta}{\int_0^{\theta_0} \sin \theta d\theta}. \quad (7)$$

The assumptions leading to (7) would be, in general quite severe; however, there are instances where highly directive antennas are used in which such restricted results may be of value.

To obtain specific results, four parabolic antennas having apertures of 12, 18, 30, and 48 inches, respectively, have been studied, using (7). For each antenna the gain function in the E and H planes was measured at 9,375 mc and the average used as $G(\theta)$. This procedure is appropriate[5] inasmuch as the significant portion of the pattern is nearly identical in the two planes.

The results, expressed as a function of θ_0, are shown in Fig. 3.

Fig. 2—A theoretical distribution of incident radiation.

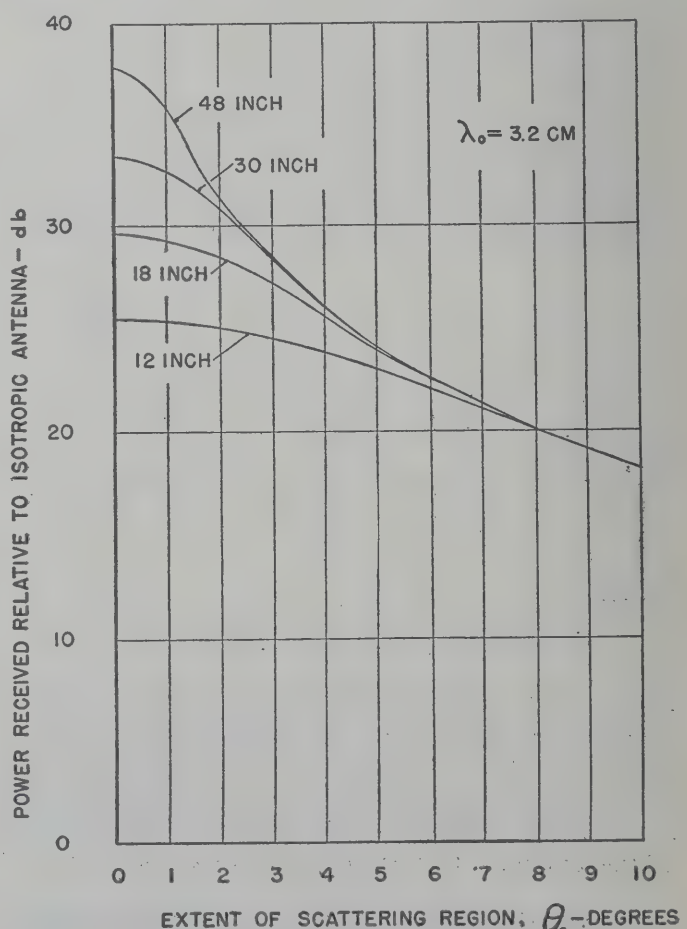

Fig. 3—The response of parabolic antennas to scattered radiation.

[3] H. G. Booker and W. E. Gordon, "A theory of radio scattering in the troposphere," Proc. I.R.E., vol. 38, pp. 401–413; April, 1950.

[4] C. L. Pekeris, "Note on scattering in an inhomogeneous medium," *Phys. Rev.*, vol. 71, p. 268; February, 1947.

[5] See page 413 of footnote reference 2.

It may be seen that if the radiation is arriving from a region which is sufficiently large, i.e., if θ_0 is large relative to the beam width, the received power is independent of the antenna aperture. Furthermore, in a case such as this, where the minor lobe pattern is insignificant, the incident radiation could vary in any manner outside the main portion of the beam, such as indicated by the dotted curve of Fig. 2, for example, without invalidating the above observation.

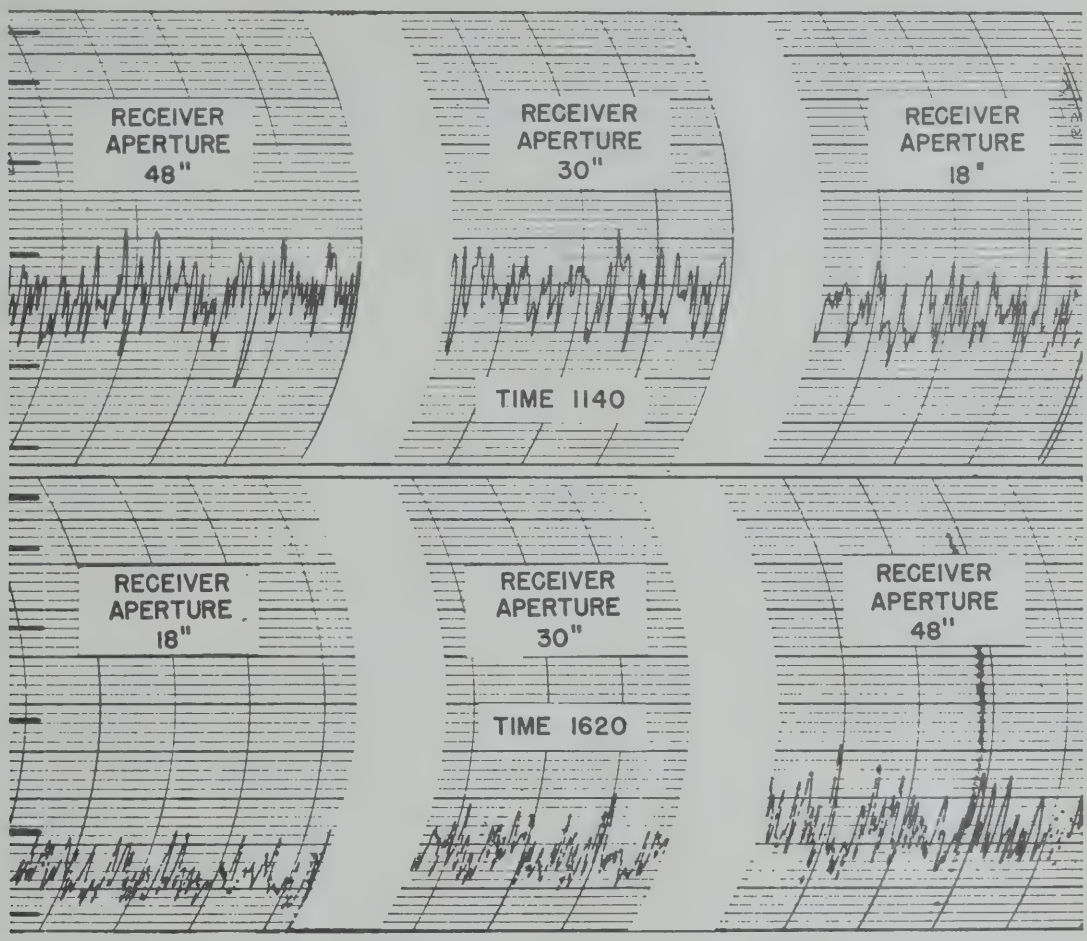

Fig. 4—Relative response of directive antennas. (March 6, 1950; 9,340 mc; transmitter aperture, 18 inches; transmitter and receiver cab elevation, 0 foot; separation, 46.2 miles.)

Microwave propagation experiments in the Arizona Desert have indicated that in many cases scattering may have been the dominant mechanism involved, and recent studies have been made to learn more of the nature of these scattered fields. Although a complete analysis of these data will follow in a later paper, two preliminary observations may be noted:

1. Only during the evening, under conditions of a strong temperature inversion, or during the day when high in the diffracted region, was the average received power proportional to the gain of the receiving antenna. At these times the fields did not fluctuate greatly.

2. During the daytime with low antenna heights, when rapid scintillations of large amplitude were noted, the average received power would usually increase when a higher gain antenna was used, but never in proportion to the gain increase. In a typical situation, changing the aperture from 18 to 30 and from 30 to 48 inches corresponded to measured gain increments of 3.7 and 4.5 db. whereas the observed power increased in steps of 2.1 and 2.4 db, respectively. This is illustrated in the lower portion of Fig. 4. The upper data represent a less common but more striking example of this phenomenon. (The markers at the left indicate 10-db intervals.)

Conclusions

There are many situations where an arriving wave can be represented only by a spatial spectrum of essentially incoherent plane wave components. This seems to be true often in the extraoptical propagation of microwaves,[6] and it is felt to be of significance in the optical range in the presence of appreciable rain attenuation.

[6] Recent experimental results presented by A. W. Straiton and D. F. Metcalf at the IRE-URSI Symposium on Antennas and Propagation held in San Diego, during April 3–5, 1950, suggest that extra-optical propagation at FM frequencies may also be due to atmospheric scattering.

When it is desired to predict the manner in which a particular receiving antenna will perform under such circumstances, considerations of the type indicated may be appropriate.

In this connection it must be emphasized that the frequently used engineering procedure for expressing the power associated with an incident field may be misleading and erroneous. It is quite common to find fields expressed in decibels relative to a particular microvolt-per-meter level.[7] This is accomplished by the use of a calibration which is appropriate when the wave front is essentially plane; however, this same calibration is then used *regardless of whether or not the radiation is known to be of this type.*

If the distribution of the incident radiation is unknown, one can only state the power received by the particular antenna configuration used.

[7] E. W. Allen, W. C. Boese, and H. Fine, "Summary of Tropospheric Propagation Measurements and the Development of Empirical VHF Propagation Charts (Revised)," Federal Communications Commission, T.I.D. Report No. 2.4.6.; May 26, 1949.

Reprinted from the PROCEEDINGS OF THE I.R.E.
VOL. 39, NO. 6, JUNE, 1951

PRINTED IN THE U.S.A.

Reprinted from JOURNAL OF THE AERONAUTICAL SCIENCES
Copyright, 1950, by the Institute of the Aeronautical Sciences and reprinted by permission of the copyright owner
OCTOBER, 1950 VOLUME 17, No. 10

On Virtual Mass and Wave Drag at Subsonic Speeds

John W. Miles
Associate Professor, Department of Engineering, University of California at Los Angeles
June 20, 1950

THE PROBLEM OF IMPULSIVE MOTION of a body in an ideal, incompressible fluid has been discussed by Lamb, Larmor, Kelvin, and others.[1] As might be expected from the concept of virtual mass,[2] an impulsive force is required to generate impulsive motion, insofar as the fluid is assumed to be incompressible. However, if the compressibility of the fluid is taken into account, the force required to generate impulsive motion may be expected to remain bounded and to vanish only asymptotically with time. Moreover, the concept of virtual mass, while still valid for the description of the energy and momentum of the fluid flow in the steady state, is of no direct aid in computing the transient response. In particular, we find that the work required to generate impulsive motion is not entirely recoverable, so that the process is irreversible, and some part of the starting force must be regarded as "wave drag." (Indeed, the present remarks were motivated by a brief discussion of just this question with Prof. Th. von Kármán, who raised the question of the validity of the virtual mass concept in a compressible fluid. Our thanks also are due to Prof. H. K. Forster, with whom we discussed the same question. Professor Forster pointed out the similarity between the present situation and the acceleration of an electron, with which is associated radiation.)

As a simple example, we consider certain aspects of the sudden acquisition of a velocity v by a body in an ideal, nearly incompressible fluid. First, after equilibrium is attained, the flow will be potential, and there will be no resultant force on the body. Second, if m is the virtual mass of the body in this potential flow, the final momentum of the associated flow will be mv, whence the total impulse required to impart the motion is given by

$$I = \int_0^\infty F(t)\,dt = mv \tag{1}$$

(Of course, if the fluid is truly incompressible, the time required is zero and the force infinite, but this indeterminacy does not affect the integrated results.) Third, since this force acts at a constant velocity, the total work done is given by

$$W = \int_0^\infty F(t)v\,dt = mv^2 \tag{2}$$

Fourth, the kinetic energy of the associated flow, after equilibrium has been established, is given by

$$\text{K.E.} = (1/2)mv^2 \tag{3}$$

It follows that an equal amount of energy $[(1/2)\,mv^2]$ has become unavailable during the period of transient motion. Moreover, if the body were to be stopped suddenly, the remaining $(1/2)mv^2$ also would be rendered unavailable. The agency of dissipation, in both cases, is radiation, and the associated force is appropriately designated as "wave drag," although this term generally is applied only to supersonic configurations.

We remark that a result somewhat analogous to the foregoing arises in the rather more transparent problem of a linear system of one degree of freedom. Thus, if an ideal capacitor is charged by a suddenly applied constant voltage source, the final energy stored in the capacitor is only half that delivered by the source, even though there is no (ohmic) resistance in the circuit. In both cases, we have irreversibilities, albeit without *direct* degradation of energy.

In seeking an explicit solution to the foregoing problem, dimensional consideration leads us to write

$$F(t) = mv(c/l)f(ct/l) \tag{4}$$

where l is a characteristic length and (l/c) is a characteristic time, the characteristic velocity being chosen as the sonic velocity c. Similarly, if a constant force F is suddenly applied to a body, we write for the resulting acceleration

$$(d/dt)v(t) = (F/m)g(ct/l) \tag{5}$$

In the case of a circular cylinder of radius a, moving normal to its axis, we find on the basis of the acoustic approximation $(v/c \ll 1)$

$$f(x) = 1 - \frac{1}{2}x - \frac{1}{16}x^2 + \frac{5}{48}x^3 + 0(x^4) \tag{6a}$$

$$= -2x^{-3} - [62 - 24\ln(2x)]x^{-5} + 0(x^{-7}\ln^2 x) \tag{6b}$$

$$g(x) = \delta(x) + \frac{1}{2} + \frac{3}{8}x + 0(x^2) \tag{7a}$$

$$= 1 - x^{-2} + [4.232 - 3\ln(4x)]x^{-4} + 0(x^{-6}\ln^2 x) \tag{7b}$$

where $\delta(x)$ is the Dirac delta function, and the characteristic length is a. It is of particular interest that $f(x)$ changes sign. In connection with $g(x)$, we remark that the actual apparent mass is initially zero, jumps immediately to $2m$, decreases in accordance with $2m[1 - (3\tau/4)]$ and is asymptotic to m as $(1 + \tau^{-2})$, where $\tau = ct/a$. More detailed calculations are in progress but await the availability of certain tabulated integrals, to which we have been referred by Prof. A. Erdelyi.

If a constant force acts for time t_1 on a circular cylinder, we find that the work done for small and large values of τ_1 is given by

$$W = \frac{mv^2}{2}\left[2\tau_1^{-1} + \frac{1}{2} + \frac{1}{8}\tau_1 + 0(\tau_1^2)\right] \tag{8a}$$

$$= \frac{mv^2}{2}\left[1 + 2\tau_1^{-2}\ln(2\tau_1) + \tau_1^{-4} - 2\tau_1^{-4}\ln(4\tau_1) + 0(\tau_1^{-6}\ln^2\tau_1)\right] \tag{8b}$$

where v is the *final* velocity. Hence, if a body is accelerated rapidly, the starting efficiency is vanishingly small; while, if it is accelerated slowly, the efficiency approaches unity.

REFERENCES

[1] Lamb, H., *Hydrodynamics*, pp. 10, 11, 160–167; Dover Press, New York, 1945.

[2] Lamb, H., *loc. cit.*, pp. 77, 160–180.

Reprinted from the JOURNAL OF THE AERONAUTICAL SCIENCES
Copyright, 1949, by the Institute of the Aeronautical Sciences and reprinted by permission of the copyright owner
UNE, 1949 VOLUME 16, No. 6

On the Oscillating Rectangular Airfoil at Supersonic Speeds

John W. Miles
Department of Engineering, University of California at Los Angeles
March 4, 1949

THE PRESSURE DISTRIBUTION on a quarter infinite, zero thickness supersonic airfoil, having an arbitrarily prescribed distribution of down-wash which exhibits the harmonic time dependence $\exp(i\omega t)$ can be found by using Fourier transforms to formulate the boundary value problem as a Wiener-Hopf type integral equation,[1] for which an exact solution may be given. The result is valid for a rectangular wing where the Mach lines from the leading edge wing tips do not intersect on the wing.

The expression for the pressure distribution due to an arbitrary distribution of down-wash over the wing is rather complicated, but the integration of the pressure over a spanwise strip of a rectangular airfoil effects a considerable simplification. Thus, if the down-wash is constant over the span, the lift coefficient for a spanwise strip x on a rectangular airfoil of leading edge $x = 0$, trailing edge $x = 2$, and aspect ratio A.R. is given by

$$c_p(x, t) = \left(\frac{2}{\rho U^2}\right) \frac{\partial L(x, t)}{\partial x} = 4(M^2 - 1)^{-1/2} \times \left\{\alpha(x, t) + \int_0^x g(x - \xi)\alpha(\xi, t)d\xi\right\} \quad (1)$$

$$g(x) = \left(\frac{\partial}{\partial x} + ik\right)\{[J_0(\kappa x) - (2\kappa \text{A.R.}_e)^{-1} \sin(\kappa x)]\exp \times (-2i\kappa M x)\} \quad (2)$$

$$k = (\omega b/U) \quad (3)$$

$$\kappa = [kM/(M^2 - 1)] \quad (4)$$

$$\text{A.R.}_e = (M^2 - 1)^{1/2} \text{A.R.} \quad (5)$$

$$\alpha(x, t) = -\frac{1}{U}\left(\frac{\partial}{\partial x} + ik\right) z(x, t) \quad (6)$$

where U is the free-stream velocity, M is the free-stream Mach Number, k is the usual reduced frequency parameter (based on the semichord b), A.R.$_e$ is the "effective aspect ratio," and z is the displacement of the airfoil above its equilibrium position. This result differs from the two-dimensional solution only in the addition of the sin (κx) term, so that the three-dimensional correction of the two-dimensional results[2] is a relatively simple matter. For the limiting case of steady flow ($k = 0$) and constant α, Eq. (1) reduces to

$$c_p(x) = 4\alpha (M^2 - 1)^{-1/2} [1 - (2\text{A.R.})^{-1}x] \quad (7)$$

in agreement with the well-known Busemann result.[3]

Similar results for down-wash distributions with other spanwise weighting factors may be obtained, and it appears that the required integrals will generally be elementary, with the exception of the integrals of $J_0(\kappa x)$, which have already been evaluated.[2] It is also of interest to remark that, whereas the results (1) and (2) are valid only for A.R.$_e \geq 2$, the various lift and moment coefficients obtained by integration are valid for A.R.$_e \geq 1$.

Numerical computations based on the above results (including flutter derivatives and gust response) are being undertaken in the Ballistics Division of the U.S. Naval Ordnance Test Station, Inyokern, Calif., and will be published, together with details of the analysis, in the near future.

---

[1] Miles, J. W., *Transform and Variational Methods in Supersonic Aerodynamics*, Journal of the Aeronautical Sciences, Readers' Forum, Vol. 16, No. 4, pp. 252–253, April, 1949.

[2] For a complete résumé of the two-dimensional results see Karp, J. N., Shu, S. S., Weil, H., Biot, M. A., *Aerodynamics of the Oscillating Airfoil in Compressible Flow*, F-TR-1167-ND, HQ, AMC, Wright Field, Dayton, Ohio, 1947; also F-TR-1195-ND, 1948.

[3] Busemann, A., *Infinitesimale kegelige Uberschallstromung*, Jahrbuch der Luftfahrtforschung, Vol. 7B, pp. 105–121, 1943.

Reprinted from the JOURNAL OF ENGINEERING EDUCATION, Vol. 41, No. 8, April, 1951
Printed in U. S. A.

Promotional System Variables for Engineering Faculties*

By HARRY W. CASE

Associate Professor of Engineering and Psychology, University of California, Los Angeles

Recognizing the pitfalls and sources of error in the "scientific method" of employee evaluation, many college administrators have shown extreme caution in applying evaluatory techniques in appraising their faculties. Expanding student enrollments, with equivalent growth of academic, non-academic, and research employees in engineering colleges, have however increased the need for adequate information on existent promotional policies in engineering schools. Information compiled in this survey on current promotional practices may prove of benefit to administrators.

Questionnaires were sent to universities, state colleges, colleges, and technical institutes, in care of their respective deans as indicated by the Directory of the American Society for Engineering Education. Replies were received from fifty-three universities, twenty-six colleges and state colleges, and ten technical institutes, all of whom had a curriculum in engineering.

The questions and the percentages of replies received are shown in Table 1. In each instance the percentages indicate the proportion of the total of that type institution which replied to the question. The percentages indicated for each question do not equal 100 per cent because of omissions of various questions by different schools. Questions 6, 10, 13, and 14 are not included in this table because the nature of the questions does not lend itself to percentage compilation. Tables 2, 3, and 4 present graphically questions 6, 13, and 14, respectively.

Question 10 which read: "If a written evaluation system is used, please list the qualities evaluated, such as:

a. Teaching ability
b. Attitude, etc.

OR, PREFERABLY, ATTACH A SAMPLE COPY OF THE RATING SHEET."—

was not compiled into tabular form since no technical institutes and only five of the colleges replied listing factors or enclosing a sample rating form. Four universities sent copies of their formal rating sheet, while seven listed qualities used in the written evaluation system. In schools sending copies of their evaluation system, there was little similarity in the mechanics of the systems used. They ranged in type from a linear continuum, with provision made to place a point on a line indicating the degree of the quality possessed, to a simple alphabetical system in which a descriptive phrase of the quality was associated with a letter ranking. One of the scales used a simple numerical system, and still another used a straight subjective essay covering each of the points on which the individual was being evaluated. In terms of complexity they varied from a simple rating scale with very little explanatory material to a complex and detailed scale, accompanied

* Presented at a meeting of the Educational Methods Division at the ASEE Annual Meeting, Seattle, Washington, June 22, 1950.

TABLE 1

ANSWERS TO QUESTIONS 1 THROUGH 5, 7 THROUGH 9, 11, 12, AND 15

The percentages indicate the proportion of the answers received from the specific type institution. Various institutions omitted various questions.

Questions	Universities		Colleges and State Colleges		Technical Institutes	
	Yes	No	Yes	No	Yes	No
1. Does your university have a standard promotional procedure?	34%	53%	35%	54%	50%	50%
a. For academic personnel?	36%	30%	38%	19%	30%	10%
b. For non-academic personnel? (Excluding research)	15%	45%	31%	23%	10%	30%
c. For personnel engaged solely in research?	15%	42%	12%	34%	10%	20%
2. If your university does have a standard promotional procedure, is it in effect in the College of Engineering?	34%	—	42%	8%	30%	—
a. For academic personnel?	34%	—	42%	4%	30%	—
b. For non-academic personnel?	15%	13%	31%	11%	10%	20%
c. For personnel engaged solely in research?	13%	9%	12%	23%	10%	10%
3. If your university does not have a standard promotional procedure, does the College of Engineering have one?	4%	45%	12%	45%	10%	50%
a. For academic personnel?	—	24%	12%	11%	—	10%
b. For non-academic personnel?	—	24%	—	15%	—	10%
c. For personnel engaged solely in research?	—	24%	4%	19%	—	10%
4. Is this promotional procedure administered by:						
a. An administrative officer in the university?	26%	8%	23%	4%	20%	—
b. An administrative officer of the College of Engineering?	21%	9%	27%	—	10%	—
c. By a committee?	11%	15%	4%	11%	10%	—
d. By a committee making recommendations which are acted upon by an administrative officer?	19%	11%	15%	12%	10%	10%
5. If you use a committee, is it composed of:						
a. Joint membership of Engineering and other academic departments?	11%	13%	12%	3%	10%	—
b. Solely membership of College of Engineering?	6%	13%	12%	3%	—	—
c. Solely Engineering Department membership?	8%	16%	4%	4%	—	—
d. Solely other academic membership?	2%	17%	4%	4%	—	—

TABLE 1—*Continued*

Questions	Universities		Colleges and State Colleges		Technical Institutes	
	Yes	No	Yes	No	Yes	No
7. In ascertaining the eligibility of an individual for promotion, what type of written evidence is accepted?						
a. Publications?	58%	6%	35%	11%	30%	—
b. Written recommendations?	43%	14%	50%	12%	30%	—
c. Some form of rating evaluation?	23%	20%	23%	15%	20%	20%
8. If an evaluation system is used, is it?						
a. A method of rating individuals from best to poorest by overall ability? I.e., 1. Scott—best; 2. Jones—next best; 3. Smith—next best.	9%	25%	4%	15%	10%	10%
b. A rating system in which the individual is placed on a continuum or scale? I.e., rated on certain qualities and the totals obtained?	11%	21%	12%	11%	10%	—
c. A short written description of his activities is prepared or written statements made to certain questions?	23%	13%	27%	8%	10%	—
9. If an evaluation system is used, does it result in:						
a. A score for the individual?	8%	24%	8%	15%	10%	—
b. A letter grade?	—	26%	—	19%	—	—
c. A series of marked descriptions?	8%	20%	—	19%	10%	—
d. A written statement?	23%	13%	27%	8%	—	—
11. Are the faculty required to utilize an analysis of their teaching:						
a. Filled out by themselves?	2%	51%	—	57%	—	10%
b. Filled out by the students?	13%	45%	15%	54%	20%	—
c. Filled out by an administrator?	13%	44%	—	54%	10%	10%
12. Are the results of the evaluation made known to the faculty member?	13%	30%	23%	15%	20%	10%
15. Do promotions within the Engineering Department occur:						
a. More frequently than in other academic departments?	6%	30%	12%	23%	10%	20%
b. Less frequently than in other academic departments?	2%	26%	—	19%	—	20%
c. Approximately the same as in other academic departments?	70%	2%	62%	—	40%	—

TABLE 2

6. In recommending promotions, the factors taken into consideration are: (Indicate percentage of total.)

	Universities												Colleges and State Colleges								Tech. Inst.
	A	B*	B†	C	D	E	F	G	H	I	J	K	A	B	C	D	E	F	G	H	A
a. Teaching ability	25			35	30–45	70	70		25	50	15	52	50					50	20		60
b. Teaching load	5			5					15	25			10								
Sub-Total	30	50	30	40	30–45	70	70	65	40	75	15	52	60	50	25	60	50	50	20	70	60
c. Research ability	5			15	5– 5	5	5		10	5	5	8	15						10		5
d. Research load	5			3		5						8									
e. Research publications				7	15–15		5			5	10	8									
Sub-Total	10	15	15	25	20–20	10	10		10	10	15	24	15			5	20		10	5	5
f. Development ability				1					5		5	2						25	10		10
g. Development load				1					5			2									
h. Development publications				3																	
Sub-Total	5	10	15	5				5	10		5					5		25	10		10
i. Administrative ability	5			3	15– 0	5			5		5	2							10		
j. Administrative load	10			1					5		5	2							5		
k. Administrative publications				1																	
Sub-Total	15		7½	5	15– 0	5		20	10		10	4		20	5	5			15		
l. Committee ability	15			3	5– 5					5	5	2									5
m. Committee load	5			1					↓	5		2									
n. Committee publications				1					↓												
Sub-Total	20	10	7½	5	5– 5				5	10	5	4			10	10				5	5
o. Student counseling and guidance ability	10			2		5	10		4		5	2						15	10		10
p. Student counseling and guidance load				1					3			2									
q. Students' reports on counseling and guidance				2					3		5										
Sub-Total	10			5		5	10	5	10		10	4		20	10	5		15	10	15	10
r. Public service ability				1	5– 5				5		5	2						10	10		
s. Public service load				4					5			2									
Sub-Total				5	5– 5				10		5	4		10	10		10	10	10		
t. Writings—texts				5						5	5	2				5					5
u. Writings—research publications				4	↓	↓			↓		10	2									5
v. Writings—other			↓	1	↓	↓			↓												
Sub-Total			10	10	10–10			5	5	5	15	4			15	5	20		10	5	10
w. Other	10	15	15		15–15	10	10				20		25		25				15		
Total												11								8	1
Percentage of returned questionnaires												21								31	10

* Junior appointments.
† Senior appointments.
Note: Arrows refer to distribution of sub-total.

by comprehensive instructions, designed to cover many job qualifications of the individual being evaluated. From the limited sample it would appear that the scales developed for evaluation purposes in the universities and colleges have a surface validity comparing favorably with those used in private industry.

Schools which listed the qualities shown on their evaluation forms, but failed to enclose an evaluation sheet, included the following factors:

Teaching ability
Personality
Use to the institution
Academic training
Experience
Supervision exercised
Public service
Interest in students in school

TABLE 3

13. At what time intervals are the faculty members evaluated?

PERCENTAGE OF RETURNED QUESTIONAIRES

Time Intervals	Universities	Colleges and State Colleges	Technical Institutes
Twice a year		4	
Yearly	36	54	60
Two years	2		
Three years		4	
Irregular	11	4	
Continuously	4		

Responsibility for methods and policy
Responsibility for records, reports, and schedules
Responsibility for machinery, equipment, and safety
Responsibility for public relations
Responsibility for non-academic duties and committee work
Professional activity outside of classroom
Ability and activity in research
Acceptance by students and colleagues
Attitude
Writings
Student counseling ability
Administrative ability
Professional standards
Laboratory ability.

The factors utilized in the evaluation systems of different institutions differ greatly. However, six institutions listed teaching ability, five attitude, four personality, and two research ability. The remaining factors occurred only once in each of the listings.

Table 2 (in which the specific weights assigned promotional factors are indicated for twelve universities, eight colleges, and one technical institute) emphasizes the difference of opinion existing as to the importance assigned to various tasks in the determination of promotions. It is interesting that the institutions answering this question assigned weights ranging from 15 to 75% to the general area related to teaching in determining promotions in the universities, while the range was from 20 to 70% for the colleges and state colleges. Unlike the popular conception that research is the sole criterion, the weight assigned ranged from 10 to 25% for the universities and from 5 to 20% for the colleges. Seventeen institutions reported they had no specific percentages but considered all the factors listed, while others stated that they had not determined percentages but considered specific items. Of eleven schools which answered the question but said they used no specific percentage, *teaching ability* was listed eleven times; *research ability* nine; *research load* eight; *student counseling and guidance ability* seven; *administrative ability* six; *committee ability* five; *research publications, writings—texts,* and *writings—research publications* four each; *teaching load,* and *writings—other* three each; *development ability,*

TABLE 4

14. What is the usual length of time elapsing between promotion from one academic rank to the next?

PERCENTAGE OF RETURNED QUESTIONNAIRES

Yearly Intervals	Universities	Colleges and State Colleges	Technical Institutes
1– 5	2		
2– 3		4	
2– 5	2		
2–10	2		
3	6	4	
3– 4	2		
3– 5	4	4	10
3– 6	2	8	
3– 7	2		
3– 8	2		
3–10	4		
4	2	4	
4– 5		15	
4– 6			10
4–10	2		
5	2	4	
5– 6			10
5– 7			10
5– 8	2		
5–10		4	10
Irregular	30	23	10

committee load, and *public service ability* two each; and *reports from students* and *other* one each. Nine wrote in their covering letter that they did not believe in any system which considered specific factors or assigned weights to specific areas, but preferred to judge the individual on the basis of his "merit", but unfortunately they did not indicate how this was determined.

Table 3 tabulates the percentages of replies received to the question: "At what time intervals are faculty members evaluated?" While yearly evaluation of the faculty member is the most common, a surprisingly large number of universities (11) and colleges (4) indicated that they had no fixed time interval for evaluation. This may be reflected in one of the replies which read in part: "Practically all the promotions that I have seen since my stay here have been more or less accidental and not due to any plan."

Question 14, "What is the usual length of time elapsing between promotion from one academic rank to another?", is tabulated in Table 4. The poor wording of the question, which did not allow for a sliding time period for promotion from different ranks, is no doubt partly responsible for the fairly wide ranges indicated by some of the schools furnishing data. The explanations that accompanied many of the returned questionnaires indicated that in some instances a three-year period was observed for promotions from one rank to the next for all academic grades, while in other instances the time elapsing was greater if the individual being promoted was of a higher rank. In one case the reverse was true and the longest elapsed time was from instructor to assistant professor. Almost half of the institutions appear to have no formal or customary length of elapsed time between promotions.

An examination of the questions tabulated in Table 1 reveals certain trends. With the exception of the technical institutes, less than half of the institutions replying have a standard promotional procedure, and the chances of an institution's having one for research personnel is less than for academic personnel.

Question 2 seems to show that if the university has a standard promotional procedure, it is also used in the college of engineering for engineering academic personnel. Other personnel do not appear to fare quite so well. In relatively few instances is the college of engineering pioneering in the field of promotional procedures, for the percentages shown in the answers to question 3 indicate that if the university does not have a standard promotional procedure, the engineering college has not attempted to institute one.

The answers to question 4 show that the promotional procedure is administered by an administrative officer of the university or of the college of engineering, and to a much lesser degree by the action of a committee, although in a fairly large number of cases a committee makes recommendations which are acted on by an administrative officer.

When a committee system for promotion is used, it would appear common practice to have the committee formed of members selected from engineering and other academic departments. Surprisingly enough 2% indicated that the committee was entirely composed of members of departments other than engineering.

Question 7 reveals that while publications are the most common type of accepted promotional evidence, written recommendations are also heavily favored and approximately one-fifth to one-fourth of the schools accept some form of rating evaluation. Question 8 indicates that although the short written statement is used in many institutions, the rating continuum is acceptable, and in some instances the method of absolute ranking is followed. In terms of the evaluation system it appears that the most common form is the type which results in a written statement. A series of marked descriptions and a score for the individual remains in second order of frequency.

Roughly 26% of the universities re-

plying to the questionnaire require the faculty to utilize an analysis of their teaching, either filled out by an administrator or by the students.

Finally, question 15 shows that in the majority of instances promotions occur within the engineering department in approximately the same time sequence as in other departments.

Many helpful replies were received in the form of letters that accompanied the returned questionnaire. It is unfortunate that they must be treated as confidential. In general it may be said that the reception to the questionnaire ranged all the way from indignation on the part of some of the smaller institutions, who appeared to be irritated at what they felt was a suggestion that they needed a system for promotions, to outright request for copies of the data as soon as it could be compiled. Many institutions were in the process of investigating the promotional policy with a view toward attempting to correct many of the evils which appeared to have existed in the past. One thing that stood out clearly was that there is relatively little current knowledge concerning the factors or the systems in use in other institutions.

Reprinted from the JOURNAL OF THE AERONAUTICAL SCIENCES
Copyright, 1949, by the Institute of the Aeronautical Sciences and reprinted by permission of the copyright owner
AUGUST, 1949 VOLUME 16, No. 8

Quasi-Stationary Airfoil Theory in Compressible Flow

John W. Miles
Department of Engineering, University of California at Los Angeles
April 29, 1949

IT WAS RECENTLY POINTED OUT that the use of steady flow theory could lead to erroneous results in the calculation of stability derivatives, and the correct results for quasi-stationary incompressible flow over a thin airfoil were obtained as limiting results of the previously known flutter results.[1] These results have now been extended to the case of subsonic, compressible flow by obtaining a solution to the Possio integral equation,[2] considering only terms which are first order in frequency.

The lift and quarter-chord moment coefficients on a thin airfoil with leading edge at $x = -1$ and trailing edge at $x = +1$ in a subsonic flow of velocity U and Mach Number M with downwash distribution $w(x)$ exp $(i\omega t)$ are given by

$$C_l = 2(1 - M^2)^{-1/2} \int_0^\pi \left\{ (1 - \cos\varphi) + ik(1 - M^2)^{-1} \sin^2\varphi + ik(1 - M^2)^{-1}(1 - \cos\varphi)\left[\gamma + \frac{i\pi}{2} + \log_e\left(\frac{k}{2}\right) - F(M)\right]\right\} \frac{w(-\cos\varphi)}{U}\, d\varphi + 0(k^2 \log k) \quad (1)$$

$$C_m = \frac{1}{2}(1 - M^2)^{-1/2} \int_0^\pi [(\cos\varphi - \cos 2\varphi) - ik(1 - M^2)^{-1} \times (1 - \cos\varphi)\sin^2\varphi] \frac{w(-\cos\varphi)}{U}\, d\varphi + 0(k^2 \log k) \quad (2)$$

$$F(M) = M^2 + \log_e\left[\frac{2(1 - M^2)}{M}\right] - (1 - M^2)^{1/2} \log_e \times \left[\frac{1 + (1 - M^2)^{1/2}}{M}\right] \quad (3)$$

$$k = \omega c/2U \quad (4)$$

where k is the reduced frequency, based on the semichord $(c/2)$, and γ is Euler's constant. These results reduce to the well-known Munk formulas,[3] together with the Prandtl-Glauert factor $(1 - M^2)^{-1/2}$, for $k = 0$.

For the important case of pitching about the quarter chord—

$$W_\alpha(x) = U\{1 + [(1/2) + (2x/c)]ik\} \quad (5)$$

Eqs. (1) and (2) reduce to

$$C_{l\alpha} = 2\pi(1 - M^2)^{-1/2}\left\{(1 + ik) + ik(1 - M^2)^{-1} \times \left[\frac{1}{2} + \gamma + \log_e\left(\frac{k}{2}\right) - F(M)\right]\right\} \quad (6)$$

$$C_{m\alpha} = -(i\pi k/4)(1 - M^2)^{-3/2}(2 - M^2) \quad (7)$$

For plunging of the airfoil—i.e.,

$$w_h(x) = ikU \quad (8)$$

the results are

$$C_{l_h} = 2\pi ik(1 - M^2)^{-1/} \quad (9)$$

$$C_{m_h} = 0 \quad (10)$$

In interpreting these results, it may be remarked that nonstationary effects need be considered only when the downwash includes a term that is zero order in frequency. In this case, however, the term introduced is logarithmic and will be increasingly important for small k, corresponding to high-speed flight. Moreover, the compressibility correction of this term is approximately $(1 - M^2)^{-3/2}$ rather than $(1 - M^2)^{-1/2}$. It follows that the effects under consideration will be particularly important at high speeds.

As an example, consider the calculation of the damping of a rotary motion of a tail surface about a center five chord lengths ahead of its quarter-chord. Carrying out the calculations with the aid of the above results and also with the results obtained by setting $k = 0$ in Eqs. (1) and (2) and designating the damping derivatives as C_{m_q} and $C^0_{m_q}$, respectively, it is found that the latter calculation overestimates the damping by a considerable margin. Typical numbers are

$$\frac{C_{m_q}}{C^0_{m_q}} = \begin{array}{|c|c|c|} \hline M^k & 0.1 & 0.01 \\ \hline 0 & 0.828 & 0.618 \\ \hline 0.7 & 0.662 & 0.342 \\ \hline \end{array} \quad (11)$$

While these ratios neglect induction effects and wing interference, they are indicative of the errors that may be expected when steady flow theory is used for the calculation of tail stability derivatives. Similar results may be expected for the damping in pitch of a swept wing.

REFERENCES

[1] Miles, J. W., *Quasi-Stationary Thin Airfoil Theory*, Journal of the Aeronautical Sciences, Vol. 16, No. 7, p. 440, July, 1949.

[2] Possio, C., *L'azione Aerodinamica sul Profilo Oscillante in un Fluido Compressibile a Velocita Iposonora*, L'Aerotechnica, Vol. 18, pp. 441–458, 1938.

[3] Munk, M., *General Theory of Thin Wing Sections*, N.A.C.A. T.R. No. 142, 1922.

Residual Stress and Fatigue Strength

Los Angeles

The articles by A. L. Boegehold in the February and March issues and by E. W. P. Smith in the April issue of *Metal Progress* emphasize the importance of residual stress in the fatigue behavior of heat treated steel parts. They also point to the need for more quantitative data so that a better prediction of the actual performance can be made. Two major difficulties exist when such a prediction is attempted.

1. Along with the residual stress other changes, structural or physico-chemical, are generally induced in the heat treated parts.
2. Under service conditions a redistribution of the residual stress is possible due to the applied load.

At the University of California at Los Angeles, tests have been conducted in which the above two

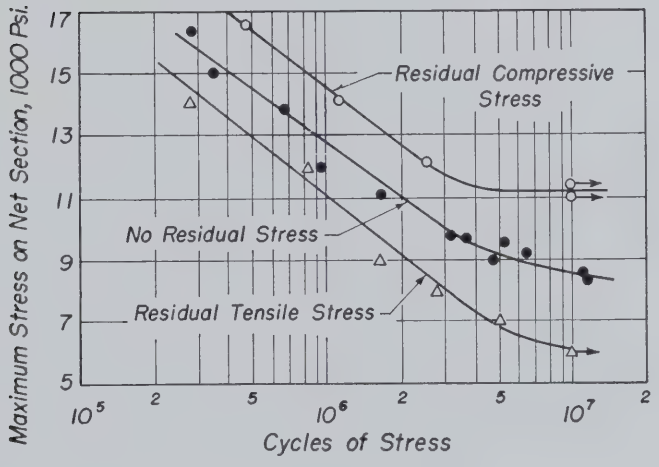

factors have been controlled and the stresses measured locally by means of the X-ray diffraction technique. Notched specimens (stress concentration of 2.5) made from ⅜-in. 61S-T6 aluminum plate have been tested. Both residual compressive and tensile stresses were induced at the notch by means of a small amount of overstressing which was believed to be insufficient to produce any marked cold working. The stresses induced were 14,000 psi. as measured by the X-ray diffraction method, and their magnitude was not significantly altered during cycling.

It may be seen from the accompanying fatigue curves that an improvement of almost 100% in permissible stress and a fatigue life increased by 10 times can be realized by changing the residual stress from tension to compression.

D. Rosenthal and George Sines
Department of Engineering
University of California

Made in United States of America

Reprinted from Proceedings of the Twenty-Ninth Annual Meeting of the Highway Research Board, December, 1949

A SEGMENTED ELECTRICAL ELEMENT FOR DETECTING VEHICULAR TRAFFIC

J. H. Mathewson, R. Brenner, and R. J. Reiss, *Institute of Transportation and Traffic Engineering, University of California, Los Angeles*

SYNOPSIS

Most vehicle detecting mechanisms or systems in use today have a serious limitation in that they cannot accurately determine the transverse location of a vehicle. This deficiency is serious inasmuch as many important traffic problems cannot be properly studied or satisfactorily solved to the exclusion of data on lane traffic patterns and transverse placement. To facilitate the study of such problems, the Institute of Transportation and Traffic Engineering of the University of California initiated a research program to develop a more universally applicable detecting unit. In addition to sensitivity to transverse placement, other important design criteria included inexpensive manufacture, inexpensive installation and maintenance, portability, rugged construction for field use, reliability of operation, concealment from the driver, and weather resistant qualities. The detecting unit which was designed is believed to embody the various qualities specified.

The detector is of the so-called metallic contact type in which two metallic elements, normally held open by some form of a spacer, are closed by a wheel passing over them. In this design, the bottom contact extends throughout the entire length of the unit and serves as a common contact for all the circuits. The top contact is made up of one-foot metal segments which, together with the common bottom contact, constitute the elements for the individual circuits. Lead wires are attached to each segment so that, with appropriate jumper connections,

any desired segment width can be readily obtained. The entire unit is attached to the road surface by means of a quick drying rubber cement and a covering of industrial adhesive tape. The tape also serves to protect the unit from abrasive tire action.

In order to evaluate the design a test program was set up wherein the detecting unit would be subjected to both severe and ordinary driving conditions as well as to a series of controlled conditions involving rapid acceleration, deceleration and skidding. The results of these tests indicate that the design is basically sound and also practical.

An integral part of almost all traffic instrumentation systems is a detecting medium which impresses the presence of a vehicle at a specific point on the road into the system. The system, in turn, utilizes this information to determine the particular traffic variable being measured, such as speed, volume, density or transverse placement. In the past, the detecting function has been performed in a number of ways which can be conveniently grouped in three categories, namely; visual, photographic and vehicle-actuated.

In visual detecting systems, the position of a vehicle relative to a fixed landmark is determined by an observer watching the road. An example would be an observer counting the vehicles that went past him. Telescopes and various surveying instruments have been used as a refinement for sighting the vehicle from a distance, but the general principle is the same.

In the photographic method, motion pictures are taken of a given landmark and show each vehicle approaching and reaching the landmark. Since the camera is usually operated at a constant speed, the time-location of the vehicle is given by the particular frame in which the vehicle is shown as having reached the predetermined position (*5*).

The vehicle-actuated system, which has been the most widely used method of the three, operates on the principle of automatically giving a signal at the instant a vehicle moves across a fixed line on the road. A vehicle actuated system which does not operate on this principle is the Electro-matic Speed Meter (*1*)[1] which indicates the instantaneous speed of a moving vehicle on the basis of the change in frequency of a radio wave reflected from the moving vehicle. This principle of operation is quite different from the other, but since there is only the one system based upon it, it will not be considered in this paper.

[1] Italicized figures in parentheses refer to the list of references at the end of the paper.

Probably the most commonly used vehicle- or wheel-actuated detecting device, other than the permanently installed treadle-type detector used in traffic control systems, is the pneumatic detector in which a length of rubber tube is placed across the road perpendicular to the direction of vehicular travel and is secured in place by clamps spiked to the road. The tire rolling over the tube sets up an air pulse which actuates some form of switch or counter which is attached to one end of the tube (*3*).

Another vehicle-actuated detecting system utilizes photo-electric tube circuits. Here, a light beam is directed across a roadway into either a phototube or photoelectric cell. When the beam is interrupted by a passing vehicle, an electrical circuit is either energized, or degenerized (*4*) (*7*). In another class of vehicle-actuated detecting systems, metallic contacts, normally held open, are pressed together as the wheels pass over them, thereby closing an electrical circuit. These are usually referred to as the direct contact type of detectors.

Each of these three systems has some very desirable characteristics. The pneumatic detector is portable, relatively easy to install, inexpensive, and stands up well under field conditions. The photoelectric systems subject no parts to traffic wear, can be used on all types of roads and can be effectively camouflaged so that the driver does not know that the road is instrumented. In the metallic contact detector, the operation is the most positive and, at the same time, simple. At the present stage of development all of these detectors are so limited in application that transverse placement cannot be measured, although some phototube systems can differentiate direction. The seriousness of this limitation will be evident if consideration is given to the many important problems in which lane traffic patterns and transverse position are significant.

To overcome the deficiency, the Institute of

Transportation and Traffic Engineering of the University of California initiated a program for the development of an appropriate type of vehicle-actuated detector. Design criteria were established with the aim that the final design would embody, in addition to the transverse placement measuring quality, the most desirable characteristics of the other vehicle-actuated detecting systems to the greatest extent feasible. Desired characteristics included:

1. Sensitivity to transverse placement
2. Inexpensive manufacture
3. Inexpensive installation and maintenance
4. Portability
5. No impedance to traffic

traffic pick-up element known as a "Transverse Placement Detector," was made available for study.

This unit had several of the desired characteristics, including sensitivity to transverse placement, rugged construction and direct electrical contacts. However, on the basis of examination of the sample, it was believed that the unit was not sufficiently portable, that it would be expensive to manufacture, and that it would be readily distinguished by a driver. Notwithstanding these apparent drawbacks, the design served as an excellent guide and materially facilitated the subsequent development program.

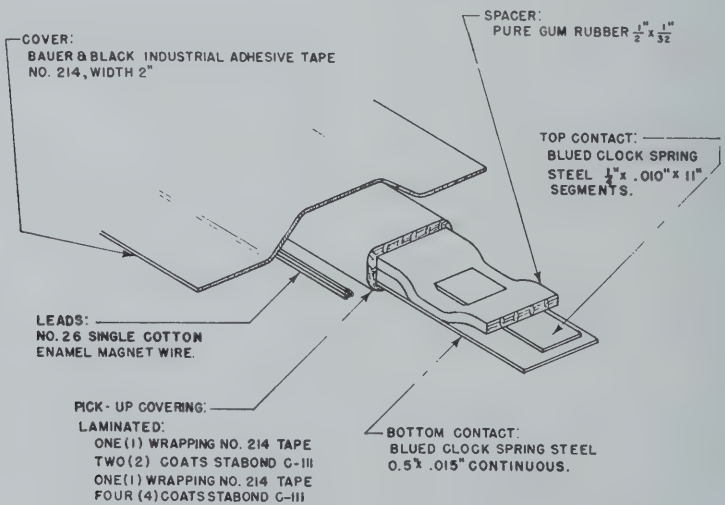

Figure 1. Design Details of the Segmented Traffic Tape

6. Rugged construction for field use
7. Reliability of performance
8. Not readily distinguishable by the driver
9. Weather resistant

The most practical approach appeared to center around the use of some form of the direct contact system since neither the pneumatic detector nor the photoelectric system was considered to be adaptable to the transverse placement measuring requirement. Moreover, direct contact systems had been successfully used in previous transverse location studies (*6*). Through the cooperation of Mr. O. K. Normann, Chief, Section of Traffic Operations, U. S. Bureau of Public Roads and Chairman, Committee on Highway Capacity, Highway Research Board, a sample of such a

DESIGN DETAILS

The design details of the unit which was developed are shown in Figure 1. Segments of blued clock spring steel $\frac{1}{4}$-in. wide, 0.01-in. thick and 11-in. long are laced through a continuous spacer of pure gum rubber- $\frac{1}{2}$in. wide, $\frac{1}{32}$-in. thick. The lacing is placed against a continuous strip of blued clock spring steel, $\frac{1}{2}$-in. wide, .015-in. thick. A separate electrical lead is attached to each steel segment and one lead is attached to the continuous bottom segment. The bottom steel strip serves as a common contact for all of the circuits, while the separate top segments are the other contacts for the individual circuits. The gum rubber serves as the spacer separating the

contacts until pressure on the top forces them together.

The lacing, made up of the top contacts and the spacer, and the continuous bottom contact are bound together by a laminated covering made up of three wrappings of industrial adhesive tape[2] and six coats of rubber cement.[3] Terminal lugs, which are soldered to the steel segments, extend outside the wrapping thus providing a means for connecting the lead wires. The wrapped assembly is referred to as the pick-up element, while the wires attached to the lugs are referred to as the harness. The whole is referred to as the detecting unit. This unit is secured in place on the roadway by a cover of industrial adhesive tape which also serves to protect the unit from the abrasive wearing action of traffic. To ensure a strong bond between the cover tape and the roadway, a strip of the latter is brush coated with rubber cement immediately preceding the placing of the detecting unit. The protective cover and harness are considered expendable, but the pick-up element is not. However, the cost of fabricating the pick-up element, as will be demonstrated later, is so low that possibly it too could be considered expendable.

When installed on the roadway, the complete detecting unit measures 2 in. in width and varies in thickness from .010 in. at the edges to a maximum of $\frac{3}{16}$ in. at the center. Accordingly, on a concrete pavement, the driver cannot easily distinguish it from an asphaltic-type expansion joint.

TEST PROGRAM—FIRST PHASE

In order to evaluate the design, a test program was devised whereby the detecting element would be subjected to both severe and ordinary driving conditions.

The objective of the first phase of the test program was to determine how long an installation would operate under traffic conditions without any major malfunction. A detecting unit 10 ft. long was installed 75 ft. ahead of a traffic signal, this location being selected so that the unit would be subjected to accelerating and decelerating vehicle movements in addition to movements at higher speeds at night when the signal was not operating. An electro-mechanical counter was connected to the unit to indicate the total number of wheels which passed over the detecting unit. No attempt was made to evaluate other characteristics of the traffic flow at this point. Relative to determining if the unit picked up all vehicles passing over it, the assumption was made that if the unit was operating satisfactorily at a given time, it had been operating satisfactorily up to that time. Actually this assumption can be criticized although repeated observations indicated that all vehicles were being recorded.

The unit operated satisfactorily for a continuous period of 47 days during which time there was a total rainfall of 0.13 in., the maximum for one 24 hour period being 0.08 in. A total of 555,973 wheels were registered which could have represented anywhere from 138,000 to 276,000 vehicles since there would be four wheel counts for some vehicles and two for others depending upon the transverse placement of the vehicle. There were four broken lead connections at the lugs, but there were no signs of wear or deterioration in the pick-up element which was cut open for study at the end of the test period.

TEST PROGRAM—SECOND PHASE

There were three objectives in the second phase of the testing program; namely;

1. Observation of the performance of the complete segmented element and assembly under severe driving conditions.
2. Determination of the effectiveness of the unit as a pick-up element when actuated by a vehicle traveling at high speeds.
3. Determination of any possible hazard in the event of physical failure of the unit.

The site selected for these tests was at the City of Santa Monica (California) Municipal Airport. A non-traffic situation was selected because it was desired to conduct the tests under controlled conditions which could not be achieved on a public thoroughfare without hazard to the test drivers, other drivers, or pedestrians.

A ten-segment unit was installed on the test course, part of the surface of which was very soft asphalt and the remainder bituminous concrete. Each segment was electrically connected to a separate light bulb so that when a wheel passed over the segment the specific circuit would be closed and that bulb would

[2] Industrial Adhesive Tape: Bauer and Black No. 214, 2 in. width.

[3] Rubber Cement: "Stabond C-111", The Latex Company, Los Angeles, California.

light. This, of course, served only to indicate that the circuit had been closed.

The first tests made were high, but constant, speed tests in which a test car was driven over the detecting unit at a speed of 60 mi. per hr. as indicated by the speedometer of the vehicle. The initial test run was made immediately after the installation was completed, that is, without allowing the rubber cement to set. Successive passes were made until each segment had been actuated at least four times. The detecting unit operated satisfactorily on every trial, and there were no signs of wear or displacement of the tape.

The second series of tests were conducted with the test car being driven over the unit under various accelerating and decelerating conditions which roughly simulated actual driving conditions. Acceleration and deceleration rates were not measured inasmuch as it was believed that these data, although interesting, would not contribute enough to the performance evaluation of the detecting unit to justify the work involved in making such measurements. Procedures for the various acceleration and deceleration tests were specified in order to insure that each segment of the detecting unit would be subjected to approximately the same wear. This was done so that in the event of a single failure, the segment at which the failure occurred could be compared with the other segments for possible delineation of desirable as well as undesirable characteristics of the design. The conditions of the various tests along with the number of actuations of each segment under those conditions are as follows:

Acceleration from Stop Test (20 actuations of each segment)—The test car, at complete rest 1 ft. from the detecting unit, is fully accelerated in first gear.

Low Acceleration Test (20 actuations of each segment)—The test car, in second gear, approaches at a speed of 25 mi. per hr. The accelerator is fully depressed when the vehicle reaches a point 15 ft. in front of the detecting unit.

High Acceleration Test (6 actuations of each segment)—The test car, in second gear approaches at a speed of 15 mi. per hr. The accelerator is fully depressed when the vehicle reaches a point 10 ft. in front of the detecting unit.

Deceleration Tests (6 actuations of each segment)—The test car approaches the detecting unit at a speed of 40 mi. per hr. The brakes are firmly applied, but not locked, just as the front wheels reach the unit.

As was the case in the high, but constant, speed tests the detecting unit operated satisfactorily on every accelerating and decelerating trial and there were no signs of wear.

The third series of tests were designed to subject the detecting unit to the grinding action of a wheel slipping on the road surface.

In these tests, the test car was at rest with the rear wheels almost touching the tape. With the engine of the car "racing," the clutch was quickly engaged causing the wheels to spin while passing over the detecting unit. Each segment was actuated four times under these conditions. The detecting unit operated satisfactorily on each trial, but the protective adhesive tape covering was torn where it was attached to the soft asphalt surface as shown in Figure 2, or was pushed back where it was attached to the bituminous concrete. There was no apparent damage to either the harness or the pick-up element.

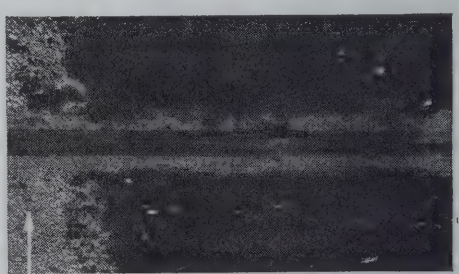

Figure 2. The Effect of a Grinding Action of a Tire on the Protective Covering

The final series of tests in this phase of the testing program were the locked-wheel braking tests in which the test car approached the detecting unit at speeds varying from 30 to 35 mi. per hr. The brakes of the vehicle were locked when it was about 10 ft. in front of the unit, all wheels accordingly skidding over the detecting unit. In order to eliminate side thrust during skidding, the brakes of the test car had been carefully adjusted beforehand. Each segment was actuated an average of five times in this manner, the operation and appearance of the unit being carefully observed after each trial. After the first skidding trial,

abrasions were noted on the adhesive tape covering and after repeated skids the covering was split along the aft edge. This was the entire extent of the damage. There were no electrical malfunctions and the harness and pick-up element showed no apparent damage. This was verified by high-speed tests which were repeated (two actuations of each segment) at the conclusion of the skidding tests and during which all circuits operated satisfactorily. The slide marks at the conclusion of the skidding tests are shown in Figure 3.

At the conclusion of the tests, the pick-up element, harness, and almost all of the adhesive tape covering were still firmly fixed in place on both the asphalt and bituminous concrete surfaces. Although there were no apparent indications that the bond with the pavement was breaking down, the possibility

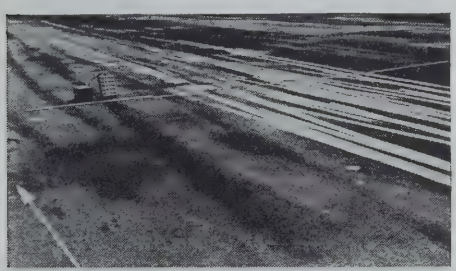

Figure 3. Slide Marks at the Conclusion of the Skidding Tests
(Arrow indicates direction of travel)

of its breaking at a later time could not, of course, be eliminated entirely. However, in the light of the severity of the tests, it appeared that the bond would be maintained under normal traffic conditions almost indefinitely. This was interpreted as a desirable safety factor in that little hazard can be associated with an installation that remains firmly secured to the road.

TEST PROGRAM—THIRD PHASE

There were four primary objectives in the third phase of the test program including:

1. Observation of the performance of the detecting unit under heavy traffic conditions.
2. Determination of the effect of repeated installations of the unit upon its performance.
3. Observation of the performance of the unit under traffic conditions in rainy weather (simulated).
4. Development of techniques for repairing the unit without removing it from its installed position on the roadway.

The site selected for these tests was on the south side of Sunset Boulevard adjacent to the University Nursery School, Los Angeles, California.

Two detecting units were installed on the test course, the first being made up of a new adhesive covering along with the pick-up element and harness which had been subjected to the previously described severe driving tests of the second phase of the test program. This will be referred to as the "A" unit. The other unit was completely new and will be referred to as the "B" unit. In order to roughly quantify the speed characteristics of the vehicles involved, the units were used as the detecting elements for the Vehicle Speed Distribution Recorder which was developed by the Institute of Transportation and Traffic Engineering and reported at the 28th Annual Meeting of the Highway Research Board in December 1948 (*2*).

Fourteen installations of the "A" unit were made, each being maintained for approximately three hours either in the morning or afternoon. These installations were made at one of three adjacent locations so that there was no more than one installation on any one location within any 24-hr. period. This was done to minimize any positive effects of previous installations on the adhesive properties of the later installations. The "B" unit served as the control for the "A" unit with respect to the effect of repeated installations. Although the "B" unit should have been installed only once, it actually was removed and reinstalled a second time to facilitate the making of several changes in the electrical circuits. However, this additional installation was not considered to have invalidated its use as this control.

The tests extended over an 11-day period with measurements being taken on 9 days. On seven of these days the road was dry. During the last 2 days of measurements, rainy conditions were simulated by directing a stream of water from a garden hose on both units. The entire area extending approximately 30 ft. in front of the units was also kept wet with the garden hose.

During the test period, 11,789 vehicles were registered and an additional 3000 vehicles are estimated as having passed over the de-

tecting units while the counting equipment was not operating. Therefore, a total of approximately 15,000 vehicles passed over the two units.

The mean speed of the vehicles counted was 34.9 mi. per hr., with the distribution of the speeds as shown in Figure 4. Segment counts were simultaneously maintained on the "A" unit to establish the effectiveness of the design in measuring transverse placement while serving also as a detecting element in speed measurement. The operation was entirely sat-

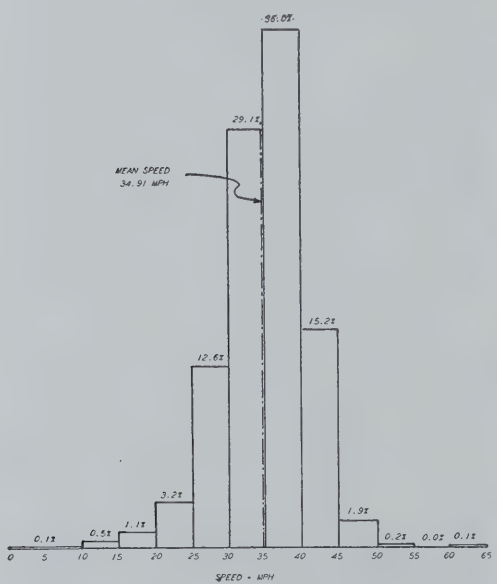

Figure 4. Percent of Eastbound Vehicles vs. Speed—Weekday Forenoon and Afternoon Traffic—Third Phase of Test Program

Dates of Test: August 3rd to 11th, 1949
Test Site: Sunset Blvd., 250 yards East of Westwood Blvd.
Total Vehicles Represented: 11,789

isfactory, although quantitative results were not obtained since the road was 35 ft. wide and only a 10-ft. length of the detecting unit was used.

During the simulated rainy weather tests, both units operated satisfactorily for 45 min. For approximately one-half of this period both units were completely submerged. Short circuits between different segments and the ground lead began to occur intermittently during the next hour, but persisted only for a few minutes. After 2 hr. of wetting all segments were shorted.

The units were left on the site for 16 hr. (overnight) during which time no water was applied. All segments except one were again operating satisfactorily the next morning although short circuit resistances ranging from 10,000 to 500,000 ohms existed. The units were subjected to an additional 5 hr. of wetting during which the operation became progressively worse. At the end of this period, four of the ten segments of unit "A" were still operating satisfactorily. Unit "B" was inoperative. Both units were still firmly attached to the road which demonstrated the adequacy of the bond (Figure 5). Since no attempt was made to control the amount of water, setting up analogies as to rates of rainfall to which the units had been subjected was impossible.

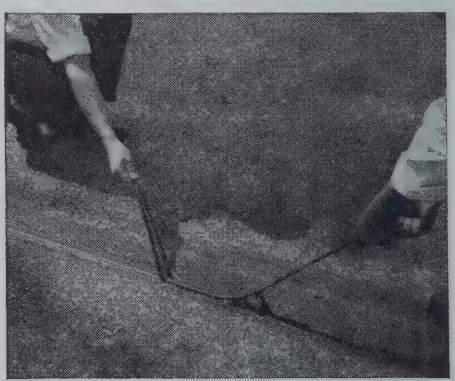

Figure 5. Taking Up a Detecting Unit After the Simulated Rainy Weather Tests

At the conclusion of the tests, the pick-up elements of both units were split open for examination. A very small amount of rust was found inside each. This indicated that the elements could have continued to "recover," that is, dry out and continue to operate satisfactorily. The fact that there was no appreciable difference in the amount of rust in the two elements was believed to be significant. Assuming that the amount of rust present at a specific point in the pick-up element is an indication of the amount of moisture which was present at that point, it follows that the amount of moisture which seeped into the pick-up elements was approximately the same in both units. The "A" unit, however, had been installed and re-installed 15 times as compared to two for the "B". The "A" unit had also been subjected to the severe grinding

and skidding tests while unit "B" was new. It can be inferred, therefore, that the severe grinding and skidding tests, as well as the repeated installations of the "A" unit, apparently did not affect the moisture resistant properties of this pick-up element. It is assumed that the "A" and "B" pick-up elements were identical when new, which was the case as nearly as could be determined. If the moisture resistant properties can be extrapolated to be an indication of wear, then the grinding, skidding, and repeated installations did not noticeably affect the wearing properties of the element.

During the entire test period there were a total of three breaks among the eleven leads which made up the harness of the "A" unit. Each of these breaks was repaired without taking the unit up by a technique in which the protective adhesive cover was cut open at the location of the break. After the break was spliced, the cover was flattened back over the pick-up element and harness assembly, and a patch of new tape placed over the old tape at that point. The maximum time required for a complete repair was ten minutes.

DISCUSSION OF THE DESIGN

The following interesting design features are worthy of note. First, the unit is completely portable weighing approximately 0.1 lb. per lin. ft. of pick-up element and harness for a 40-segment unit. The adhesive tape covering is supplied in compact 60-yd. rolls. The pick-up element and harness assembly can be easily coiled without harmful effects. The coil shown in Figure 6 is 40 ft. long and is segmented at 1-ft. intervals.

Another very desirable characteristic of the design is the general nature of the transverse placement problems which can be readily instrumented. The lugs are spaced at 1-ft. intervals and by connecting any number of lugs together in any desired arrangement a wide range of placement problems can be efficiently attacked. For example, suppose total counts in each of two adjacent 10-ft. lanes were desired, the five center segments in each lane would be jumpered together which would leave an inactive length of 2.5 ft. on each side of the active portion of the detecting unit. The two adjacent inactive sections together would be 5 ft. long and would minimize the double counting of lane straddling vehicles. In the event that counts of the number of lane "straddlers" were desired, the appropriate connection could also be made. The detecting unit can be made sensitive to transverse placement from 1-ft. intervals up to full lane widths over a multi-lane highway merely by connecting the appropriate harness to the same pick-up element. Actually, one harness can be used for the same variety of applications by making the necessary jumper connections at the instrument end. However, it is desirable to have a minimum number of wires stretched across the road even though they are relatively well protected by the adhesive tape covering.

The water resistant properties of the unit tested were not up to the standard desired, although there were indications that under actual weather conditions the performance might be better. The covering of the pick-up element which was tested was laminated of adhesive tape and rubber cement. Since the time of that test, a dipped rubber cover over the pick-up element in place of the laminated wrapping has been developed. A specimen pick-up element of this type was soaked in a barrel of water for two weeks at the end of which high resistance short circuits, 15,000 ohms minimum, had developed. These were not considered excessive since the element was still completely operative. It is believed that the weather resistant properties will be bettered.

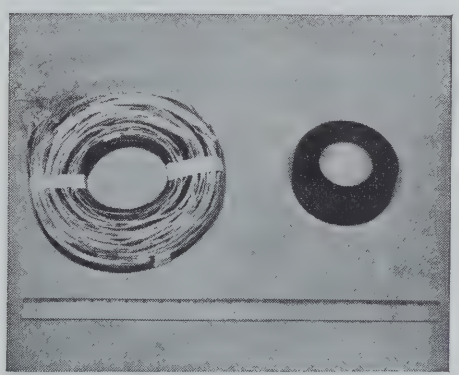

Figure 6. Forty Foot Length of Pick-up Element and Harness Segmented at One Foot Intervals and a Sixty Yard Roll of the Protective Adhesive Tape Covering

An important consideration in the design of any instrumentation is the cost involved in

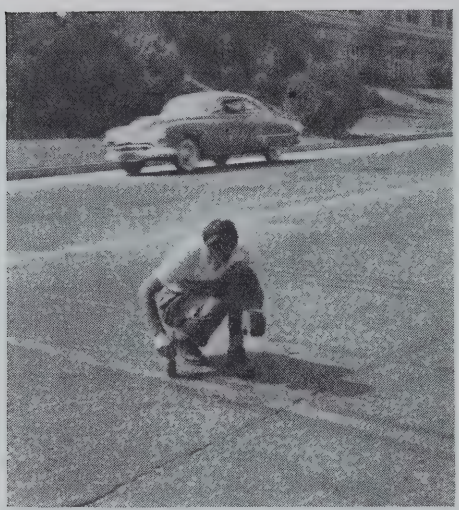

Figure 7. Installation Procedure: Applying Rubber Cement to Roadway Immediately Preceding the Placing of the Detecting Unit

Figure 8. Installation Procedure: Locating the Detecting Unit for Speed Measurements

Figure 9. Installation Procedure: Applying the Protective Adhesive Tape Covering Over the Detecting Unit

both manufacture and use. Designs can be directed toward precision and top quality materials in order to lengthen the effective life or they can be directed toward low cost and complete expendability. The design under discussion was developed with the latter objective in mind, namely toward inexpensive manufacture and expendability. However, as demonstrated in the testing program, the inexpensive materials used were entirely satisfactory so that in all probability very little would have been gained by using more costly materials. The following breakdown is an estimate of the unit cost of a 1-ft. length including labor and material:

Detecting Unit

Pick-up element	$.52
Harness	.04
Protective Cover	.02
Installation	.02
	$.60

The above estimates are believed to be conservative inasmuch as the design lends itself to mass production techniques, while the cost picture set forth is based on the manufacture of a single 40-ft. length.

One of the factors in the design of a detecting unit with which the traffic engineer is concerned is the time required to complete an installation under traffic conditions. The time must be a minimum, not only to minimize traffic delay but, of even greater importance, to minimize the exposure to danger of personnel making the installation. Repeated measurements indicated that a 35-ft. unit could be installed by one man in 7 min. and that traffic could move over the unit immediately after the installation was completed. It is believed that this time compares favorably with the time required for installing any detecting unit which is attached to the road. Installation procedures are shown in Figures 7, 8, 9.

CONCLUSIONS

This new type of segmented element is an effective, practical device for detecting vehicular traffic. It is entirely portable, positive in action and can be inexpensively manufactured. It is particularly well adapted to a wide variety of transverse placement studies in addition to usual speed, volume and other traffic

studies which require comprehensive data on vehicular movements. It is not necessarily the solution for all vehicle detecting problems since there are situations where such a unit should not be used. For example, there would certainly be little point in using such a unit to perform functions which could just as easily be performed by a pneumatic tape. On the other hand, the unit could hardly be considered as more than a temporary substitute for any permanent installation, although the basic principle of operation could be used for the design of a permanent installation. Each of the various detecting systems has specific uses for which it is best suited and it is the responsibility of the traffic engineer to select the system most appropriate for the particular measurement involved.

ACKNOWLEDGMENTS

The writers are indebted to the members of the staff of the Institute of Transportation and Traffic Engineering, University of California, Los Angeles, for their material assistance and many constructive suggestions which greatly facilitated the development program of this detecting unit.

The writers also wish to express their appreciation to Mr. O. K. Normann, Chief, Section of Traffic Operations, Bureau of Public Roads, and Chairman, Committee on Highway Capacity, Highway Research Board, who criticized the detecting unit at an early point in its development and suggested several of the test procedures, and to Mr. Ralph T. Dorsey, Principal Street Traffic Engineer, Department of Traffic Engineering, City of Los Angeles, with whose cooperation the third phase of the testing program was performed.

REFERENCES

1. Barker, J. L. "New Developments in Traffic Actuated Control", *Proceedings*, First California Traffic Engineering Conference, University of California, Los Angeles, July 1948, pp. 76–80.
2. Bromberg, R. and D. L. Gerlough. "Applications of Electronic Techniques to Traffic Instrumentation", *Proceedings*, Highway Research Board, National Research Council, Vol. 28, pp. 348–353 (1948).
3. Craig, R. E. and Reymer, S. E. "A Simple Portable Automatic Traffic Counter", *Public Roads*, Vol. 19, pp. 213–221 (Jan. 1939).
4. Dana, H. J. and Clarke, H. F. "A New Photo-Electric Speed Recorder and Its Adaptation for Two-way Traffic Counting", Engineering Bulletin, No. 66, Washington State College, Engineering Experiment Station, Vol. 2 (October 1941).
5. Gourlay, S. M. "Merging Traffic Characteristics", Technical Report No. 4, Bureau of Highway Traffic, Yale University, pp. 61–77 (1948).
6. Holmes, E. H. and Reymer, S. E. "New Techniques in Traffic Behavior Studies", *Public Roads*, Vol. 21, pp. 29–45 (April 1940).
7. "Phototubes for Catching Speeders", *Electronics*, Vol. 8, p. 59 (February 1935).

SERVO THEORY APPLIED TO FREQUENCY STABILIZATION WITH SPECTRAL LINES

by

W. D. HERSHBERGER AND L. E. NORTON

REPRINTED FROM JOURNAL OF THE FRANKLIN INSTITUTE
VOL. 249, NO. 5, MAY, 1950

Reprinted from JOURNAL OF THE FRANKLIN INSTITUTE.
Vol. 249, No. 5, May, 1950
Printed in U. S. A.

SERVO THEORY APPLIED TO FREQUENCY STABILIZATION WITH SPECTRAL LINES [1]

BY

W. D. HERSHBERGER [2] AND L. E. NORTON [3]

In an earlier paper (1)[4] the writers described work in which stabilization of frequency was accomplished using the absorption lines of ammonia which occur in the 24,000 megacycle frequency region. The advantages which arise from the use of such lines, namely, high inherent Q of 100,000 or more, and high long term stability which results from the use of a natural and universal standard of frequency were discussed in some detail. A long term stability of better than 1 part in 10^6 was reported in the paper, but no upper limit could then be placed on this stability due to inadequacy of monitoring equipment. Applications to television relay work, to radar beacons, and to frequency multiplier chains to control a clock were also outlined. Obviously much work, developmental in character, based on the servo-search principle employed in the work reported remains to be done. The purpose of the present paper is to discuss the applicable servo theory, to describe some of the circuits in fuller detail, and to report the present status of the work.

In essence, in this method a cyclic comparison is made between two frequencies: one the fixed frequency of a gas-absorption line, and the second a frequency to be stabilized or related to that to be stabilized in the simplest case by the relationship

$$f = \frac{f_{\text{gas}} \pm f_i}{n}, \tag{1}$$

where n is a whole number and is the order of a harmonic, while f_i is an off-set frequency. Conventional methods of frequency multiplication and addition may be used to make accessible for stabilization any one of a wide range of frequencies, by choice of n and f_i, both of which are at the disposal of the circuit designer. These techniques are of course old, hence need not be described. The comparison is made by means of a sweeping technique. A pulse is generated each time the frequency of a swept oscillator passes through the frequency of the gas line and also

[1] Much of the material in the present paper was presented before a conference sponsored jointly by the AIEE, the Institute of Radio Engineers, and the National Bureau of Standards, in Washington, D. C. on January 10, 1949. An abstract was printed in *Electrical Engineering*, Vol. 68, pp. 251–252, March, 1949.

[2] Professor of Engineering, University of California, Los Angeles, Calif.

[3] RCA Laboratories, Princeton, N. J.

[4] The boldface numbers in parentheses refer to the references appended to this paper.

each time one passes through a frequency defined by Eq. 1. The two wave forms carrying this frequency information are fed to a detector whose output is zero when the two sets of pulses or wave forms are in time coincidence but the sign of the output of the detector is such as to correct for frequency drift of the oscillator to be stabilized when the servo loop is closed by a connection to an element which controls frequency, as for example the reflector of a klystron tube or the grid of a reactance tube.

The discriminator itself may take a variety of forms. Figure 1

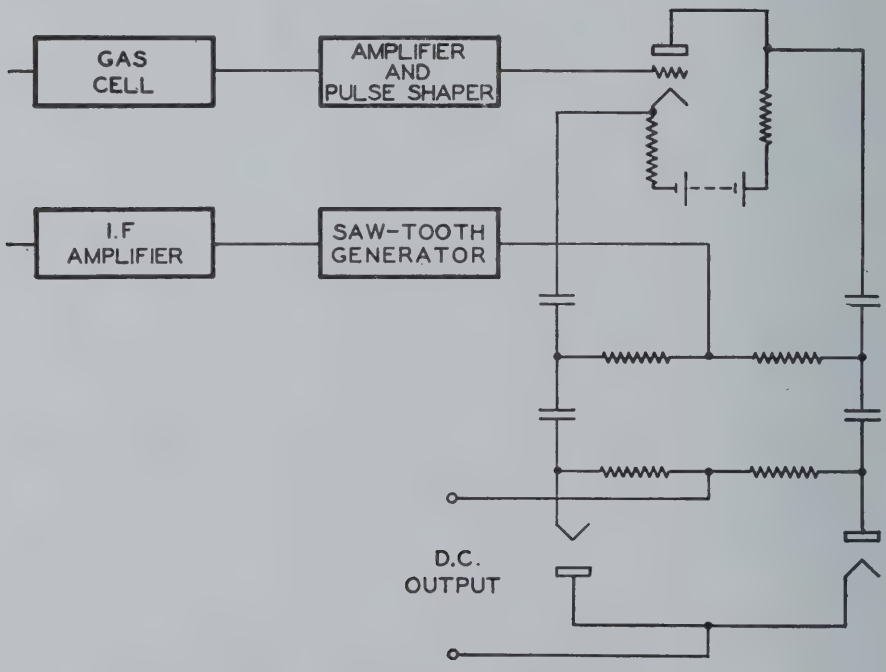

FIG. 1. Frequency discriminator using pulse coincidence.

shows a form in which one starts with two sets of similiar pulses. The pulses from the gas cell after amplification are differentiated, clipped, and shaped and both positive and negative pulses coincident in time appear in the output of a final stage. These pulses convey or carry precise frequency information. Pulses from the i.f. amplifier channel of reference (1) are converted to a saw tooth wave. This saw tooth wave and the positive and negative pulses are fed to a pair of diodes whose output is the desired control voltage. A discriminator sensitivity of 200 volts per megacycle is readily realized with the above arrangement. Pulse coincidence detectors are also described in a number of U. S. Patents (2). The operating point of the discriminator is the mid-point of the steepest part on the saw tooth wave.

Figure 2 shows the essential features of the servo loop used in an analysis of the method of frequency stabilization.

The critical element is the error detector or frequency discriminator E. The output of the discriminator is proportional to an error frequency, which is the difference $(F_s - F_o)$ between a reference or set-point frequency F_s and the oscillator frequency F_o. In the discriminator, two distinct functions are performed. In the first place, the reference frequency is established, namely, that frequency for which the discrim-

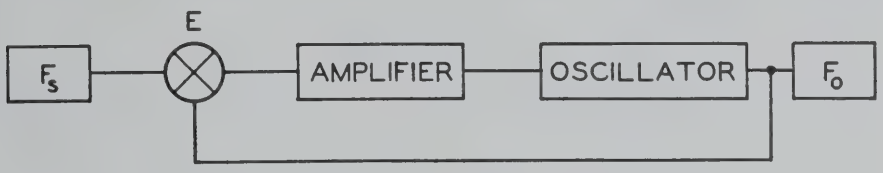

FIG. 2. Servo-loop used in analysis of frequency stabilizer.

inator output changes sign. The long term stability of the oscillator depends upon how well and with what degree of permanence the discriminator performs this first function. In the second place, the discriminator is characterized by a sensitivity—volts per megacycle—which among other factors determines loop gain μ. The ability of a stabilizer to protect output frequency against transient or short term disturbances depends upon loop gain. For the circuit of Fig. 2, the loop gain is given by

$$\mu = \frac{K}{1 + j\omega CR} \tag{2}$$

where K is a dimensionless constant and is the product of discriminator sensitivity, oscillator frequency sensitivity per control volt, and the amplifier gain. The manner in which μ varies with frequency is determined by a capacity C and resistance R used to limit gain at high frequencies. A servo pass characteristic of the type shown in Fig. 1 of course meets the Nyquist criterion for stability.

Two functions of μ, namely, $\frac{1}{1+\mu}$ and $\frac{\mu}{1+\mu}$, play a critical part in a description of the performance of the stabilizing system. If Δf_o represents a frequency change experienced by an unstabilized oscillator or oscillator followed by a multiplier due to an impressed disturbance such as a change in supply voltage, or to changes in temperature, the actual change which results with the feed back loop closed is

$$\Delta f_o' = \frac{1}{1+\mu}\Delta f_o = \frac{\Delta f_o}{S}, \tag{3}$$

where S is the stabilization factor.

The factor $\frac{\mu}{1+\mu}$ is used to calculate how well changes in the "set point" or reference frequency Δf_s are reproduced in the output frequency. The set point frequency is varied in resonant cavity methods by varying the resonant frequency of the cavity itself, or in the present method by varying the pass frequency of an intermediate frequency amplifier, or the gas frequency by use of a Stark field. For an impressed change in reference frequency Δf_s the resulting change in oscillator frequency is

$$\Delta f_s' = \frac{\mu}{1+\mu}\Delta f_s. \tag{4}$$

Thus the function $\frac{1}{1+\mu}$ is a measure of the performance of the stabilizer as a regulator assuming a fixed reference frequency, while the function $\frac{\mu}{1+\mu}$ is a measure of its performance as a "follow-up" system to changes introduced in the reference frequency.

Substituting Eq. 2 in (4) we obtain

$$\Delta f_s' = \frac{K}{1+K}\frac{1}{1+j\omega\frac{CR}{1+K}}\Delta f_s \simeq \frac{1}{1+j\omega\frac{CR}{1+K}}\Delta f_s. \tag{5}$$

Equation 5 shows that the speed of response of output frequency to changes in the reference frequency is determined by the time constant CR divided by loop gain rather than by the CR product itself. In general, the speed with which frequency is corrected is set by the effective time constant of the filter used with the discriminator and by the sampling rate. In the present system, the sampling rate is the limiting factor.

Here we encounter an interesting application of the uncertainty principle. The rate at which it is possible to elicit precise frequency information from a spectral line is limited by its band width. Thus in the present system, line width sets an upper limit to the interrogation rate, while in Pound's (3) cavity method the band-width of the cavity sets an upper limit to the frequency of the side bands which accompany an intermediate frequency to convey the error information. If we wish to increase interrogation rate and obtain information at a more rapid rate we may do so by increasing the gas pressure thereby increasing the line width, but as a result the mid-frequency of the line is now poorly defined. On the contrary, if we could increase Q so line width is say 10 cycles per second, the optimum interrogation rate is of the order of 10 per second, but the information obtained on line mid-frequency is exceedingly precise. Thus we cannot at once have both a high interrogation rate and highly precise information on the mid-frequency of a line.

It is sometimes desirable to modulate a stabilized oscillator. A method of wide band modulation may be based on simultaneous "set-point" and oscillator modulation. If we add Eqs. 3 and 4 we obtain a net frequency modulation Δf_n.

$$\Delta f_n = \frac{1}{1+\mu}\Delta f_o + \frac{\mu}{1+\mu}\Delta f_s. \tag{6}$$

Δf_o makes the dominant contribution to Δf_n at high modulating frequencies above the range for which the stabilizer acts degeneratively on frequency modulation impressed directly on the oscillator, while Δf_s is the dominating term at frequencies low enough for faithful reproduction in the output frequency of changes introduced in the set-point frequency.

If we now impose the restriction

$$\Delta f_o = \Delta f_s \tag{7}$$

Eq. 5 becomes

$$\Delta f_n = \Delta f_o = \Delta f_s. \tag{8}$$

The restriction in Eq. 7 may be satisfied by way of example in the present instance by introducing a change in some voltage which varies oscillator frequency such that in an unstablized oscillator the frequency change would be Δf_o, and *simultaneously* introducing an equal change in "set-point" frequency Δf_s by varying the tuning of the intermediate frequency amplifier by use of an appropriate reactance tube, or by use of a Stark shift in line position. Under these circumstances, no change in error frequency arises and hence no correction voltage, yet we have shifted frequency by the amount Δf_n to effect frequency modulation.

The performance of the present stabilizer, both short term and long term, may now be analyzed in terms of criteria used in discussing the behavior of servo-mechanisms. In the present equipment, K, the loop gain at frequencies such that $\omega < \frac{1}{CR}$, is somewhat greater than 10^5. The discriminator sensitivity itself is of the order of 200 volts per megacycle, which incidentally is approximately 1000 times as great as that of microwave discriminators which employ some form of microwave bridge (3), energized by power from a microwave oscillator, and using opposed crystal detectors. In contrast, the present discriminator employs a moderate amount of amplification at intermediate and audio frequencies before the frequency comparison is made. With K equal to 10^5, a disturbance which would give rise to a 10 megacycle shift in an unstabilized oscillator is reduced by feed-back to less than 100 cycles. Short term stability of a stabilized oscillator may be kept high by two means: first, the use of adequate shielding, electrical, thermal, and other, to reduce to a minimum any disturbances which tend to cause a frequency shift and, second, the use of high gain in the feed-back loop.

Short term stability of 1 part in 10^8 or better has been reported for a number of stabilizing systems presently in use. The difference in performance between a stabilizer using a spectral line and one using a resonant cavity resides not in a significant improvement in short term stability as much as in realizable improvements in long term stability.

The long term stability of a stabilized oscillator depends on a number of factors which merit discussion. Of primary importance is the use of a standard which is reproducible, may be set up without referring to any other standard, is not subject to human "tinkering," and whose frequency is not affected by aging, and mechanical mishaps or deformation to which resonant cavities and quartz crystals are subject. However, the full advantages available by the use of a spectral line as a frequency standard may be lost in part in an ineffective discriminator. Discriminators whose "zero" is determined in a microwave bridge, itself frequency selective, or which employ opposing "matched" crystals are rather vulnerable on this score. In the present discriminator, the zero is set when we have time coincidence between two wave forms. Such coincidence owes its significance to the fact that the same spectrum analyzer—whose essential part is a swept microwave frequency—is used to compare two spectra, one characteristic of the gas line itself, and the second of the frequency being stabilized, or a frequency derived from the stabilized frequency by multiplication and addition. As a result the characteristics of the spectrum analyzer—power output, sweep width, and sweep rate—play a minor role in determining the zero of the discriminator.

Ultimate performance now depends on the ability of a coincidence or phase detector, together with the closed feed-back loop, to hold two wave forms in coincidence. When a narrow range sweep is used, as well as the same band width in the intermediate frequency amplifier as in the gas line, the two wave forms begin to resemble sine waves, and after filtering are sine waves in fact. The phase detector now in use is certainly able to distinguish phase differences which correspond to $\frac{1}{100}$ the width of a resonance curve which when taken in conjunction with line Q of 10^5, means that at present a long term stability of 1 part in 10^7 is realized. It should of course be pointed out that if n independent tuned L-C circuits determine the response of the intermediate frequency amplifier, the output voltage as a function of frequency is given by an expression of the form

$$\left(\frac{1}{\sqrt{1+\gamma^2}}\right)^n,$$

where γ is zero at resonance and is a measure of the frequency deviation from resonance. If the resonance curve is of the Lorentz type the cor-

responding expression is

$$\frac{1}{1+\gamma^2},$$

while if line shape is determined in part by collisions and in part by Doppler effect we have a line shape intermediate in form between one

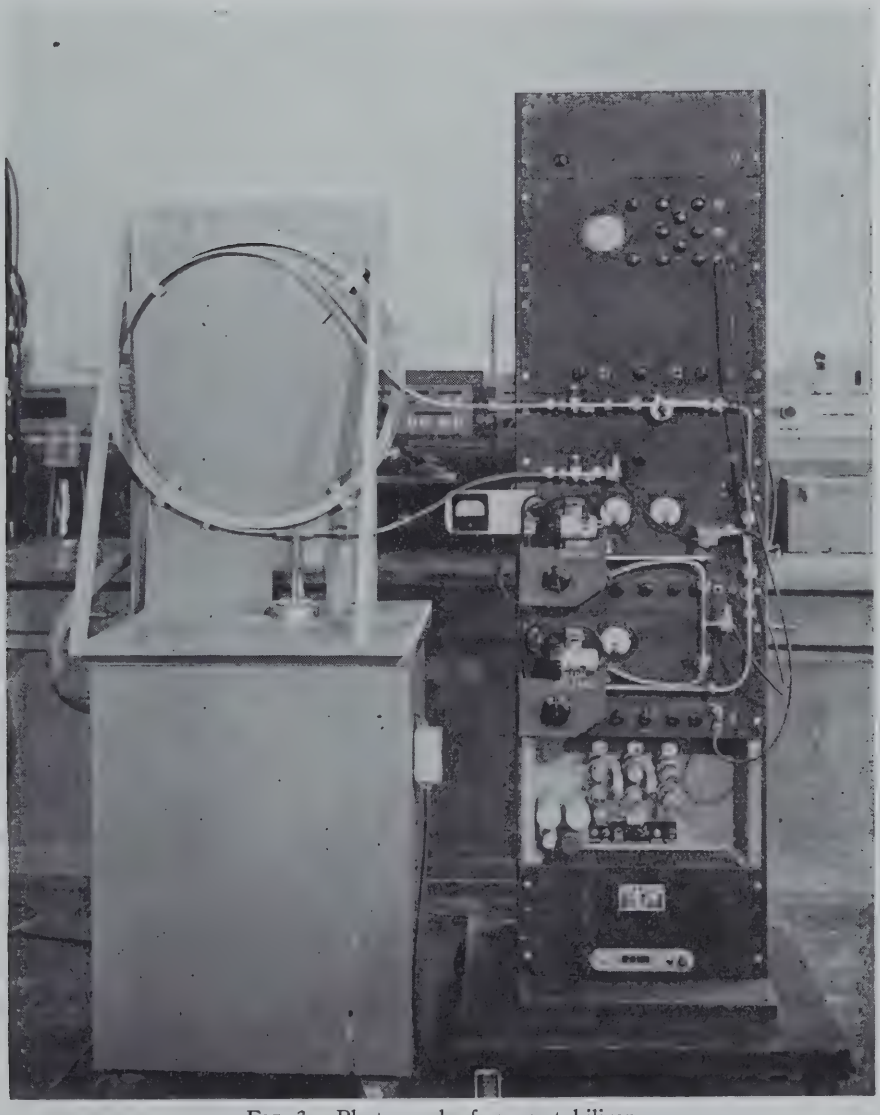

FIG. 3. Photograph of servo-stabilizer.

that is purely "Gaussian" and one that is "Lorentzian." These considerations serve to emphasize the advantages that arise in operating the system so "coincidence" is made to depend on the maxima of the response curves.

If at any point in a servo system for controlling frequency, such as in setting up a bridge balance, or determining a time coincidence, we are able to make an adjustment which shifts the zero of the discriminator, we have found a vulnerable point in the system such that inadvertent changes in this adjustment or noise at this point will adversely affect the frequency stability. Moreover, the more nearly the factor $\frac{\mu}{1+\mu}$ of Eq. 4 approaches unity over a wide frequency range, the more faithfully these disturbances appear in the output frequency. High loop gain is not an unmixed blessing as an examination of Eq. 5 will show since with increasing gain the discriminator becomes more and more sensitive to noise over an increasing band width.

A stabilizer is shown in the photograph of Fig. 3. At present a 30-ft. section of wave guide is employed as a gas cell and the pressure used is approximately 2×10^{-2} mm. of mercury. The stabilizer has been in use at K band with a variety of ammonia lines using either 2K33 or 2K50 tubes while 2K46 tubes have been stabilized at 7100 megacycles using a tripler and off-setting its third harmonic 15 megacycles from the (5, 3) ammonia line at 21,285.30 megacycles. Conclusive experiments or long term stability of course will require long term experiments while a variety of short term stability experiments are now possible with the equipments in use.

The question of long term stability of spectral lines is of more than academic interest. In the present state of the art, one need not differentiate between "dynamical" time (4) kept by aggregations of matter such as a pendulum, quartz crystals, or planetary systems and "kinematic" time kept by radiating molecules and atoms. However it is not unlikely that data from molecular clocks will play an important role in testing current hypotheses on the origin of the red shift of astronomy.

REFERENCES

(1) W. D. HERSHBERGER AND L. E. NORTON, "Frequency Stabilization with Spectral Lines," *RCA Review*, Vol. 9, No. 1, pp. 38–49, March, 1948.

(2) See for example, U. S. Patent No. 2,250,284 issued July 22, 1941.

(3) R. V. POUND, "Electronic Frequency Stabilization of Microwave Oscillators," *Review of Scientific Instruments*, Vol. 17, No. 11, pp. 490–505.

(4) J. B. S. HALDANE, "A New Theory of the Past," *American Scientist*, Vol. 33, No. 3, pp. 129–145, July, 1945.

PRINTED IN U. S. A.

LANCASTER PRESS, INC., LANCASTER, PA.

Reprinted from JOURNAL OF THE AERONAUTICAL SCIENCES
Copyright, 1950, by the Institute of the Aeronautical Sciences and reprinted by permission of the copyright owner
OCTOBER, 1950 VOLUME 17, No. 10

Some Relations Between Harmonic and Transient Loading of Airfoils

John W. Miles
Associate Professor, Department of Engineering, University of California at Los Angeles
June 20, 1950

THE WELL-KNOWN DUALITY between the responses of a linear system to harmonic and step function excitations and the associated duality between the Fourier and Duhamel methods of superposition, respectively, can be used to establish some rather useful theorems relative to the transient loading of a thin airfoil. Let $f_{0,\,1,\,2}$ denote (operationally) the responses to the normal (at the airfoil) velocity distributions $w_{0,\,1,\,2}$ in accordance with

$$w_0(x, y) = \alpha(x, y) \rightarrow f_0\{\alpha(x, y)\} \tag{1}$$

$$w_1(x, y) = \alpha(x, y) \exp(ikt) \rightarrow f_1\{k, \alpha(x, y)\} \exp(ikt) \tag{2}$$

$$w_2(x, y) = \alpha(x, y)\mathbf{1}[t - t_0(x, y)] \rightarrow f_2\{t, t_0(x, y), \alpha(x, y)\}\mathbf{1}(t) \tag{3}$$

where t is a dimensionless time obtained by multiplying the true time by the quotient of a characteristic velocity and a characteristic length, k is a dimensionless frequency obtained by dividing the true (angular) frequency by this same quotient, (x, y) are coordinates in the plane of the airfoil, and t_0 is the time at which the normal velocity arises at (x, y). We assume t_0 to be positive, definite and bounded. Then, it follows directly from the aforementioned duality that

$$\lim_{t\to\infty} f_2\{t, t_0, \alpha\} = f_1\{0, \alpha\} = f_0\{\alpha\} \tag{4}$$

$$f_2\{0, t_0, \alpha\} = \lim_{k\to\infty} f_1\{k, \exp(-ikt_0)\alpha\} \tag{5}$$

In connection with Eq. (5), we remark that linearized theory is not reliable for large k, since terms of order $(kM\delta)^2$ are neglected, δ being the airfoil thickness parameter.[1]

$$\int_0^\infty f_2\{t, t_0, \alpha\}\, dt = \lim_{k\to 0} (ik)^{-1} f_1\{k, \exp(-ikt_0)\alpha\} \tag{6a}$$

$$\int_0^\infty [f_2\{t, t_0, \alpha\} - f_0\{\alpha\}]\, dt = \left[\frac{\partial}{\partial(ik)} f_1\{k, \alpha\}\right]_{k=0} - f_0\{t_0\alpha\} \tag{6b}$$

The integral in Eq. (6a) exists only if $f_0\{\alpha\} = 0$; otherwise, Eq. (6b) is to be used. In connection with Eq. (6), we remark that the time required to attain the steady state after a suddenly imposed disturbance is $M(M-1)^{-1}$ for a supersonic airfoil if the maximum chord is taken as the characteristic length.

Eq. (5) may be used to establish the initial lift coefficient (referred to the product of dynamic pressure and wing area) of an airfoil under transient loading as

$$(C_{L_2})_{t=0} = (4/M)\,\overline{(\alpha)}_{t_0=0} \tag{7}$$

where M is the free-stream Mach Number, and $\bar{\alpha}$ is the average value of α over that portion of the airfoil for which $t_0 = 0$. This is a generalization of a result obtained by Heaslet and Lomax[2] and is valid at both subsonic and supersonic speeds. Also, the initial lift acts through the centroid of the initial distribution of α.

A result that is useful in connection with Eq. (6) is[3]

$$\phi_1\{k, \alpha\} = \phi_0\{\alpha\} + ikM^2(M^2-1)^{-1} \times [\phi_0\{x\alpha\} - x\phi_0\{\alpha\}] + 0(k^2) \tag{8}$$

where ϕ is the velocity potential for an airfoil whose trailing edge is everywhere supersonic.

If the results of Eqs. (6) and (8) are applied to the penetration of a uniform, sharp-edged gust by a supersonic, rectangular airfoil of effective aspect A, we find

$$\overline{C_{L_2}} = \left[1 - \frac{1}{3}\left(\frac{M}{M+1}\right)\left(\frac{3A-2}{2A-1}\right)\right] C_{L_0} \tag{9}$$

$$C_{L_0} = 4(M^2-1)^{-1/2}\,[1 - (2A)^{-1}] \tag{10}$$

$$\overline{C_{M_2}} = \left(\frac{M}{M+1}\right)\left[\frac{6A^2 - 6A + 1}{9(M^2-1)^{1/2}A(2A-1)}\right] \tag{11}$$

$$A = (M^2-1)^{1/2}\ \text{A.R.} \geq 1 \tag{12}$$

where $\overline{C_{L_2}}$ and $\overline{C_{M_2}}$ are the average (incremental) lift and moment (with respect to the *final* center of pressure) coefficients over the transient period, C_{L_0} is the final lift coefficient (increment), and the chord is chosen as the characteristic length. Similarly, for a delta airfoil of apex angle 2γ entering a sharp-edged gust we find

$$\overline{C_{L_2}} = \left\{1 - \left[\frac{(2M^2+1) - 2(f_1/f_0)}{3M(M+1)}\right]\right\} C_{L_0} \tag{13}$$

$$C_{L_0} = 4(M^2-1)^{-1/2} f_0 \tag{14}$$

$$\overline{C_{M_2}} = \frac{(2M^2+1)f_0 - 2f_1}{9M(M+1)\,(M^2-1)^{1/2}} \tag{15}$$

$$f_0 = \pi\sigma/2E'(\sigma), \quad \sigma \leq 1 \tag{16a}$$

$$\equiv 1, \quad \sigma \geq 1 \tag{16b}$$

$$f_1 = (3\pi/4)\,\sigma(1-\sigma^2)[(1-2\sigma^2)E'(\sigma) + \sigma^2 K'(\sigma)]^{-1}, \quad \sigma \leq 1 \tag{17a}$$

$$\equiv 1, \quad \sigma \geq 1 \tag{17b}$$

$$\sigma = (M^2-1)^{1/2} \tan\gamma \tag{18}$$

where $K'(\sigma)$ and $E'(\sigma)$ are *complementary*, complete, elliptic integrals of the first and second kinds, respectively.

Similar results may be established concerning the response of an airfoil to an impulsive (delta function) gust, since this response may be represented as the time derivative of the response to a uniform, sharp-edged gust.

All of the foregoing results are, of course, subject to the usual restrictions imposed in the linearization of the hydrodynamical equations.[1]

REFERENCES

[1] Lin, C. C., Reissner, E., and Tsien, H. S., *On Two-Dimensional Non-Steady Motion of a Slender Body in a Compressible Fluid*, J. Ma. and Ph., Vol. 27, pp. 220–231, 1948.

[2] Heaslit, M. A., and Lomax, H., *Two-Dimensional Unsteady Lift Problems in Supersonic Flight*, N.A.C.A. T.N. No. 1621, 1948.

[3] Miles, John W., *On Harmonic Motion at Supersonic Speeds*, Readers' Forum, Journal of the Aeronautical Sciences, Vol. 16, No. 6, pp. 378-379, June, 1949.

(*Reprinted from Journal of the American Rocket Society, December, 1950*)

SOME STATISTICAL CONSIDERATIONS OF THE JET ALIGNMENT OF ROCKET-POWERED VEHICLES

By A. L. Stanly

Assistant Professor of Engineering, University of California, Los Angeles, Calif., and Research Physicist, Hughes Aircraft Company

JET misalignment can be defined as the perpendicular distance from the line of thrust of the rocket motor to the center of gravity of the vehicle.

Jet misalignment is of interest because the thrust of the rocket motor, acting over the misalignment distance as a lever arm, sets up a pitching (or yawing) moment about the center of gravity which tends to swing the vehicle off its prescribed trajectory. Since the thrust of a given rocket motor is established by the application in which it is to be used, the magnitude of

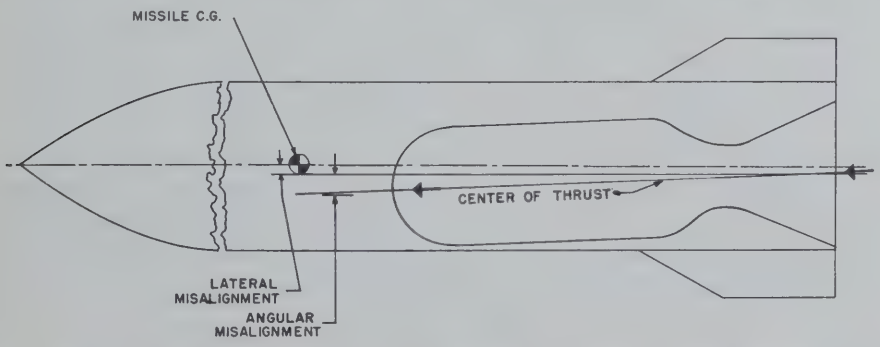

FIG. 1 LATERAL AND ANGULAR MISALIGNMENT OF ROCKET-POWERED VEHICLE

this undesirable pitching moment is determined in practice solely by the magnitude of the misalignment. This misalignment is dependent mainly upon the precision of positioning of the thrust vector and is thus a function of the thermodynamic process producing thrust and the statistical relationships involved in establishing a position by the assembly of numerous nonexact parts.

Presented before the Southern California Section of the AMERICAN ROCKET SOCIETY on June 28, 1950.

Copyright 1950, by the American Rocket Society, Inc., and reprinted by permission of the copyright owner.

Basic Principles of Jet Misalignment

Types of Misalignment: Two types of misalignment are common. This is shown in Fig. 1 by the thrust vector which exemplifies the following two components of misalignment: (1) Lateral misalignment, when the thrust vector remains parallel to the center line of the vehicle, but is displaced laterally; and (2) angular misalignment, when the thrust vector is at an angle to the center line of the missile. In general, both types of misalignment will be present.

Location of Thrust Vector, Ideal Rocket: Before the variables which affect the position of the thrust vector can be explored, it is necessary to understand the mechanism of the rocket that produces the thrust vector. These principles are already well known. However, a brief review of the broad aspects will insure common agreement of the terminology, assumptions, and limitations of the remainder of this paper.

Postulate an ideal rocket motor as in Fig. 2 consisting of a combustion chamber and a nozzle. The combustion chamber contains an infinite reservoir of gas at a constant pressure P_c and zero velocity.

For the purposes at hand it is sufficient to note that the thermodynamics of the system result in the gas leaving the rocket system via the nozzle at a lower pressure P_e and a finite exit velocity V_e. The analysis will be simplified if it is also postulated that across any cross section of the nozzle, the gas is at uniform pressure, density, and speed. In general, the ambient atmospheric pressure P_a, will differ from P_e, the nozzle exit pressure and, for the sake of simplicity, can be postulated as bearing over the outer face of the nozzle exit section. Two distinct components of thrust can be recognized intuitively from this oversimplified idealization: (1) Thrust due to the change in momentum of the gas; and (2) thrust attributable to the difference in pressure over the exit face of the nozzle.

This intuitive approach yields the familiar equation,

$$T = \frac{W}{g} V_e + (P_e - P_a) A_e \quad \ldots\ldots [1]$$

where

T = thrust, lb
V_e = exit velocity, fps
W = weight rate of propellant, lb per sec
A_e = nozzle exit area, sq in.
P_e = nozzle exit pressure, psia
P_a = atmospheric pressure, psia

From the foregoing approach it can be seen that the thrust due to the change in momentum, which is normally by far the major proportion of the total thrust, will be in exactly the oppo-

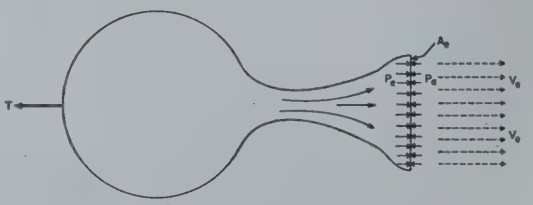

FIG. 2 IDEAL ROCKET MOTOR

site direction to the mean velocity of the exit gases—i.e., perpendicular to the plane of the nozzle exit section. Since uniform density and speed across the nozzle have been postulated, the center of thrust will be at the geometric center of the nozzle exit area—i.e., along what can be defined as the perpendicular center line of the nozzle exit section. With uniform pressure across the nozzle exit area, the thrust resulting from the pressure differential at exit will also act along the perpendicular center line of the nozzle exit area.

Accordingly, for this ideal rocket, the location and direction of center of thrust are determined by the location and direction of the nozzle exit section, and by nothing else. The tolerances of the misalignment of thrust are therefore a direct function, for the ideal rocket, of the mechanical misalignments resulting from the manufacturing tolerances of those parts which locate the nozzle exit face.

Location of Thrust Vector, Real Rocket: Of the many ways in which a real rocket differs from this ideal rocket only those that influence the orientation of the thrust vector are relevant to this paper. Two types of variables merit consideration.

The first group of variables are those (other than the exhaust gas) which produce a net nonaxial thrust on the combustion chamber. These variables consist largely of the momentum and pressure-differential thrust of any entering propellants, and the momentum thrust of the nonaxial motion of the burning propellants within the combustion chamber. The misalignment moments from these variables are normally negligible because: (1) The magnitude of thrusts involved are very small relative to the exhaust jet thrust; and (2) the position of the injection nozzles, if any, and the direction of burning gases are normally designed to be symmetrical with respect to the design axial center line of the nozzle.

The second group of variables are those resulting in gaseous misalignment which, for the purpose at hand, can be defined as consisting of non-

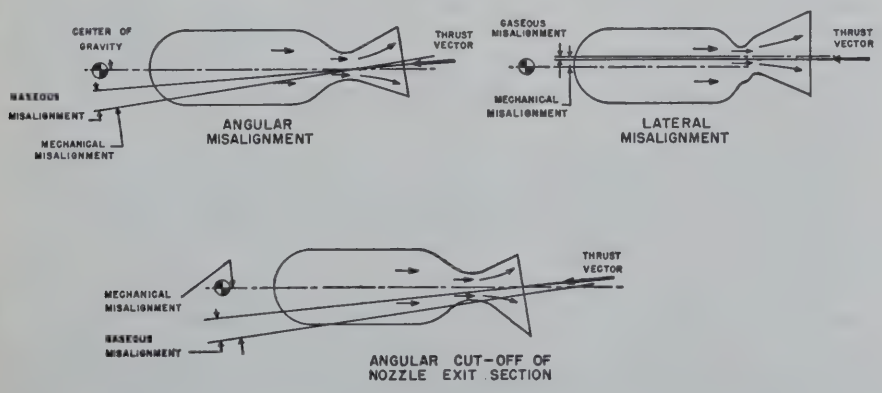

FIG. 3 GASEOUS MISALIGNMENT RESULTING FROM MECHANICAL MISALIGNMENT

uniform pressure, density, or speed of the exhaust gas at the exit section of the nozzle, and therefore a thrust vector which does not coincide with the perpendicular center line of the nozzle exit section. These variables are composed of: (1) Mechanical misalignment (nonaxial assembly) of the mechanical parts of the rocket motor; and (2) nonsymmetry of either the distribution of gases leaving the combustion chamber or of the mechanical parts of the rocket motor by such eccentricities as bulges and dents.

The first of these items, mechanical (nonaxial) misalignments, directly result in gaseous misalignments, as shown in Fig. 3. The relationship between these mechanical and gaseous misalignments depends upon the type of misalignments, the relationship of consecutive misalignments, the dimensions of the rocket parts, the degree of nozzle expansion (under or over expansion), and a good many other factors.

From the inertia properties of gases, however, it appears that these gaseous misalignments are normally in the opposite direction and of lower magnitude than the mechanical misalignments that originate them (Fig. 3). Thus, the effect of each mechanical misalignment in general is partially decreased by the effect of its resultant gaseous misalignment.

This conclusion permits measuring mechanical misalignments and taking their concomitant gaseous misalignments into account by simply recognizing that the combined mechanical-gaseous misalignment is less on the average (although not invariably) than the mechanical misalignment alone.

An estimate of the reduction could probably be made in each individual case at the expense of considerable detailed measurement and calculation, but does not appear merited.

The second source of gaseous misalignments—nonsymmetry of manufacture—can be expected to have a small effect since most rocket motors are designed to have radial symmetry, which is comparatively easy to maintain with conventional manufacturing procedures. However, an additional nonsymmetry can be introduced during firing by irregular burning or warpage. Misalignments from this latter source cannot be predicted for a given rocket type except by extrapolations of experimental data.

In summary, it appears that the significant sources of misalignment are (1) mechanical misalignments, including their subsidiary, partially-compensating gaseous misalignments, and (2) gaseous misalignments from nonsymmetry.

The latter are not predictable except from experimental data, and are frequently relatively small. Accordingly, the remainder of this paper is devoted to consideration of mechanical misalignments which are dependent upon specified production tolerances, and the means for predicting and reducing such misalignments.

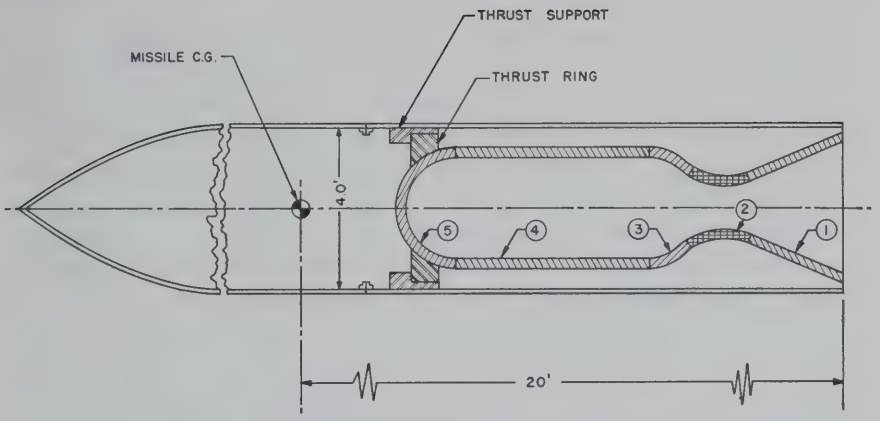

FIG. 4 LARGE ROCKET-POWERED MISSILE (SIMPLIFIED)

Mechanical Misalignments

The rocket missile is normally symmetrical with its center of gravity designed to lie on the center line of the missile. This center line is defined as the center line of the missile skin surrounding the center of gravity. A lack of coincidence of either the perpendicular center line of the nozzle exit section or the actual missile center of gravity with the design position of the missile center of gravity is therefore a direct measure of mechanical misalignment.

As noted earlier, mechanical misalignments result from manufacturing tolerances. A representative picture of the type of items to be considered can be gained from Fig. 4 showing a fictitious large rocket.

The mounting of the motor has been portrayed in simple fashion in order to reduce the number of details under discussion. The rocket motor is made of five sections. At the forward section of the motor, a thrust ring is mounted. This ring is supported and aligned by the thrust support carried by the missile skin and frame.

In counting the total possible sources of mechanical misalignment, it may be noted that the tolerances of each metal part in the chain between the nozzle exit section and the missile skin at the thrust support provide several sources of misalignment. If the parts of the rocket motor are assembled by using jigs to align the internal surfaces during a welding process, then there will be a minimum of misalignments. Three sources of misalignment will still be present for each part: (1) Lateral displacement of adjacent parts after welding; (2) angular displacement of adjacent parts after welding; and (3) lateral displacement of the center of the fore end of each part with the center of its aft end.

It should be noted that other techniques of assembly such as threaded joints would have involved other tolerances such as the external dimensions

of each part, or the relative angularity of the fore and aft surfaces of each part.

In addition to the roughly 21 misalignment possibilities for the seven parts between the nozzle exit and the missile skin at the thrust support, it is also possible for the missile skin at the center of gravity to be laterally and angularly misaligned with the missile skin at the thrust support. The missile center of gravity in turn may be misaligned with its adjacent missile skin. A total of approximately 24 misalignments is therefore possible. An instance where these misalignments all add arithmetically is shown in Fig. 5.

The possibility of a rocket such as that of Fig. 5 is evident. The question of how worrisome this situation is depends upon how probable it is. Obviously, if it happens only once in 1,000,000 motors, it will not merit concern. Accordingly, the probability of a given magnitude of misalignment must be determined before its undesirability can be judged. This is where statistical theory enters the picture.

Statistical Treatment

Ideal Statistical System: It will again be helpful to confine attention initially to an idealized system. Accordingly, it will be postulated for the sake of the initial statistical analysis that: (1) The dimensions of the various reproductions of each part follow a Gaussian—that is, a normal—distribution in magnitude and uniform distribution in angle; and (2) the specified production tolerances of each part denote the three standard deviation (3σ) limits of the distribution of sizes of that part.

In order to translate these concepts into conventional language, consider the distribution of the dimensions of a single part such as the diameters of 1000 reproductions of the thrust ring. Suppose that the diameter of this ring is specified as 34.000 ± 0.007 in. Since machining operations, particularly with human operators, are not exact but are influenced by

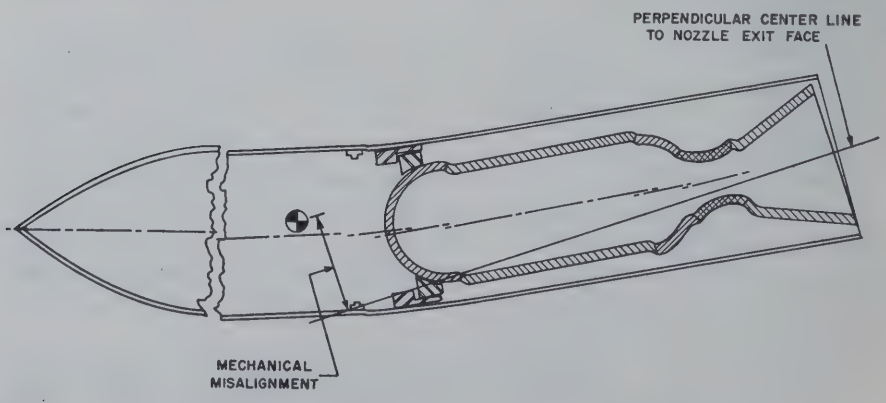

FIG. 5 ROCKET-POWERED MISSILE WITH ADDITIVE MISALIGNMENTS

random or chance effects, some variation in the diameter of the rings can be expected. If the diameters are measured to the nearest 0.0005 in., then the number of rings at each measured diameter will be something like that shown by the frequency bar chart in Fig. 6.

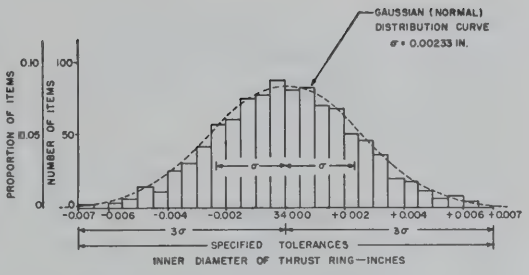

FIG. 6 FREQUENCY DISTRIBUTION FOR 1000 THRUST RINGS WHEN SPECIFIED TOLERANCES ARE EQUAL TO THE 3σ RANGE

Most of the items center around the specified mean dimension. The number of items of each dimension decreases rapidly as the distance from the mean increases, and soon approaches zero. Experience with mass-produced parts, and statistical theory both indicate that, if the variations are due solely to random effects, the envelope of the frequency bar chart usually approaches a normal or Gaussian distribution as shown by the dotted line. For both the frequency chart and the normal distribution curve, the included area between the horizontal axis and the upper limits over a given range of the horizontal scale represents the proportion of the total number of items. It thus represents the probability that an item chosen at random will fall within the corresponding range of values.

The mean of a distribution is defined as the arithmetic average.

$$m = \frac{\sum_{i=1}^{n} x_i}{n} \qquad [2]$$

where

m = mean of the distribution
x = value of each observation
n = total number of observations

The standard deviation, termed σ, is defined as the root-mean-square of the deviations from the mean

$$\sigma = \frac{\sqrt{\sum_{i=1}^{n} (x - m)^2}}{n} \qquad [3]$$

The standard deviation is a measure of the spread or scatter of the observations. For example, if great

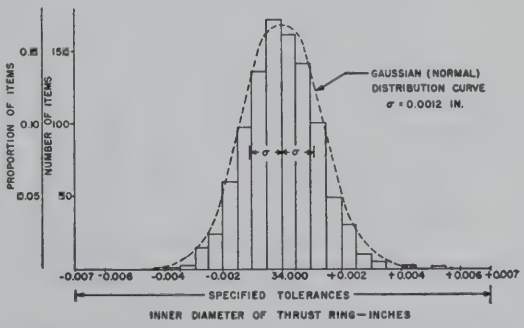

FIG. 7 FREQUENCY DISTRIBUTION FOR 1000 RINGS WHEN THE 3σ RANGE IS LESS THAN THE SPECIFIED TOLERANCES

care is taken in the manufacture of the thrust rings, then the distribution diagram would approximate that of Fig. 7. The distribution would have virtually the same mean as before, but less scatter and therefore a smaller standard deviation.

The great advantage of a normal distribution is that it is completely defined in terms of its mean and its standard deviation. For example, the probability that a random point will fall within 1σ of the mean is 68.2 per cent for all normal distributions. For a 3σ range on either side of the mean, the probability is 99.7 per cent. The 3σ range has received common acceptance among production quality control engineers as the range which, in the words of Gilbert and Sullivan, is "Never—well, hardly ever" exceeded by chance effects alone.

The successful experience with this practice is the reason that the 3σ range was chosen in the ideal system to coincide with the specified production tolerances. The 3σ range is undoubtedly not exactly correct for any one manufacturing situation but conforms in a broad sense to economical practice which dictates that just enough care be taken in production to insure that the specified tolerances are literally "hardly ever" exceeded.

Now that the distribution of dimensions for reproductions of a given part has been reviewed, it may be informative to see what happens when parts are combined. Consider for the sake of example the total misalignment obtained from the combination of parts containing four components of misalignment. The misalignment of each component can be represented by a vector (see Fig. 8) which varies in magnitude according to a normal probability distribution and which varies in angle according to a uniform probability distribution. The total misalignment is the vector sum and is represented by the closing vector from the origin representing the center line of the missile. For simplicity it will be postulated that

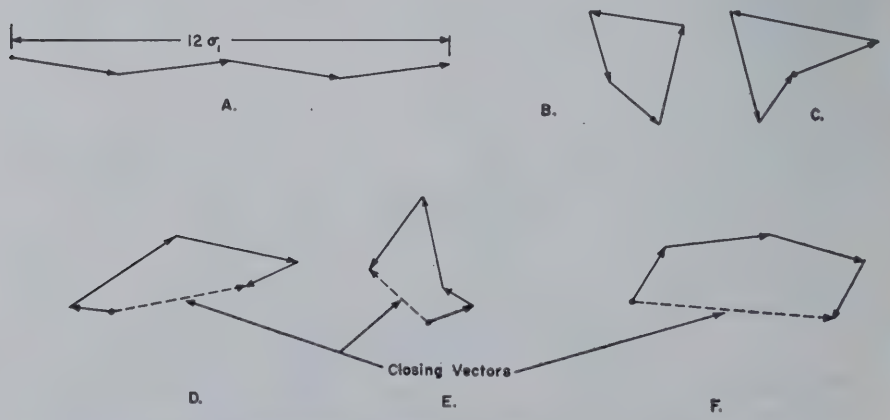

FIG. 8 EXAMPLES OF THE SUM OF FOUR RANDOM VECTORS
[Properties of the vectors: (1) Normal probability distribution in magnitude with equal σ's; (2) uniform random probability distribution in angle]

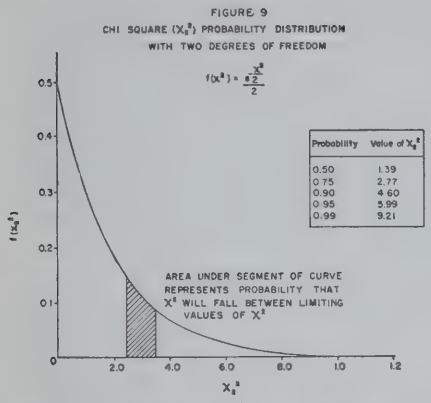

FIG. 9 CHI-SQUARE (χ_2^2) PROBABILITY DISTRIBUTION WITH TWO DEGREES OF FREEDOM

each of the component vectors has the same σ or production tolerance in terms of misalignment.

The component vectors can be of such magnitude and direction as to add up to a closing vector equal in size to the arithmetic sum of 3σ magnitudes for all four component vectors. The resulting closing vector would be an extremely rare occurrence since it would occur one time in 100,000,000 on the average. Less rare but still highly improbable is the possibility that the vectors add to virtually zero as in Fig. 8b and 8c. Most of the time, such as in cases 8d, 8e, and 8f, the closing vector will have a magnitude in the intermediate range. The problem thus resolves down to determining what proportion of the time—i.e., with what probability—each range of closing-vector values can be expected.

Fortunately, the complete probability distribution of the vector sum for the general case of n components can be derived by invoking some theorems from mathematical statistics. The proof is involved and only incidental to the purpose here. Accordingly, it will merely be demonstrated that the results are reasonable. The theoretical derivation is appended for those who are interested.

The statistical theory indicates that the probability distribution of the net misalignment $p(M)$, is given by

$$p(M) = \sigma_T(\chi_2^2)^{1/2} \quad [4]$$

where $\sigma_T^2 = \sigma_1^2 + \sigma_2^2 + \ldots \sigma_n^2$ and $\sigma_1, \sigma_2, \ldots, \sigma_n$ are the respective standard deviations for the n component misalignments, and χ_2^2 represents the chi-square probability distribution with two degrees of freedom.

That is, the magnitude of a misalignment at a given probability level is equal to σ_T times the square root of χ_2^2 at the same probability level. For example, χ^2 has a 99 per cent probability of being equal to or less than 9.21. Then the magnitude of the misalignment has a 99 per cent probability of being equal to or less than $\sigma_T\sqrt{9.21}$.

The values of χ^2 at various probability levels are available from conventional statistical tables and are shown in Fig. 9 and Table 1. The nature of the probability distribution of net misalignment is shown in Fig. 10 for a σ_T equal to 1.0. It may be noted

TABLE 1

Probability of inclusion	χ_2^2
0.99	9.21
0.95	5.99
0.90	4.61
0.75	2.77
0.50	1.39

that the distribution of net misalignments agrees in principle with the earlier reasoning from Fig. 8.

Real Statistical System, Sample Problem: Recall that the prior statistical analysis is based upon an ideal system and is not exact for real systems. Perhaps the usefulness and the limitations of the analysis can best be appreciated if it is applied to an actual misalignment problem.

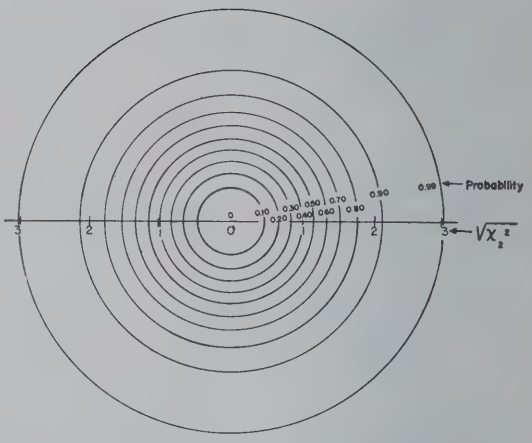

FIG. 10 PROBABILITY DISTRIBUTION OF NET MISALIGNMENT VECTOR, $\sigma_T = 1.00$

Ideal Statistical Model: Consider the large rocket of Fig. 4 in the light of the theory proposed thus far to see what can be said about the probability distribution of the total mechanical misalignment if it has a simplified set of specified mechanical tolerances as in Table 2.

The table also shows the corresponding standard deviation σ for each misalignment when its corresponding specified tolerance is taken equal to the 3σ range. Recall that the standard deviation of the total misalignment is given by $\sigma_T^2 = \sigma_1^2 + \sigma_2^2 + \ldots, \sigma_n^2$.

TABLE 2 SPECIFIED TOLERANCES AND CORRESPONDING STANDARD DEVIATIONS OF THE RESULTING POSSIBLE MISALIGNMENTS

No.	Item	Tolerances		
		Lateral, in.	Angular, deg	σ, in.
1	Lateral location of missile center of gravity relative to the center line of the missile	±0.060	...	0.02
2	Lateral location of center line of missile skin at center of gravity relative to the center line at the rocket thrust ring	±0.050	...	0.017
3	Angularity of center line of missile skin at center of gravity with the center line at the rocket thrust ring	...	±0.020	0.028[a]
4–10	Lateral alignment of the center line of the fore face of each part with the center line of the aft face	±0.010	...	0.0033
11–17	Lateral alignment of adjacent sections after being welded together or otherwise joined	±0.010	...	0.0033
18–24	Angularity of adjacent sections after being welded together or otherwise joined	...	±0.010	0.014[a]

[a] Calculated for a distance of 20 ft between nozzle exit face and missile center of gravity.

TABLE 3 STANDARD DEVIATION OF GROUPED MECHANICAL MISALIGNMENTS

Items in Group (From Table 2)	Grouped Misalignment	σ, in.
1–3	Location of missile center of gravity relative to the center line of missile at the rocket thrust ring	0.0387
4–17	Lateral alignment after assembly of center of nozzle exit face with missile center line at rocket thrust ring	0.00466
18–24	Angular alignment after assembly of perpendicular center line of nozzle exit face with missile center line at rocket thrust ring	0.014
A11	Over-all grand total, σ_T	0.0412

Incidentally, this relationship also holds true if component σ's are grouped according to type to obtain a measure of the relative importance of the various types of variables. This is shown in Table 3.

It may be noted from Table 3 in passing that because of the root-mean-square relationships, small misalignments tend to have a negligible effect. For the tolerances under consideration, the influences of the lateral tolerances of the motor itself are completely insignificant. Angular tolerances of the motor have a minor effect, while the location of the missile center of gravity relative to the missile center line at the point of rocket attachment is dominant.

Hence, on the basis of this information alone, the lateral tolerances on the motor could be relaxed appreciably without noticeable penalty. In addition, if it is concluded that mechanical misalignments should be reduced, emphasis would be concentrated on the production practices which determine the position of the missile center of gravity with respect to the motor mount. A more thorough approach would be to devise some method of controlling over-all misalignment of groups of parts, or better still, of the entire missile.

However, to resume the quest for the probability distribution of the total mechanical misalignment, only the over-all standard deviation, 0.0412 in., in the probability relationship stated earlier need be considered:

$$P(M) = \sigma_T(\chi_2^2)^{1/2} \ldots\ldots\ldots\ldots [5]$$

By using values of χ_2^2 from Table 1, Table 4 can be constructed to the desired relationships. The maximum possible mechanical misalignment based upon simple arithmetic addition of all tolerances has been included for comparison.

TABLE 4 PROBABILITY OF TOTAL MISALIGNMENTS

Probability of not exceeding maximum misalignment	χ_2^2	Maximum misalignment, in.
$1-10^{-27}$	...	0.628[a]
0.99	9.21	0.125
0.95	5.99	0.10
0.90	4.61	0.088
0.75	2.77	0.069
0.50	1.39	0.048

[a] By simple arithmetic addition of all tolerances.

It can therefore be concluded that although a total mechanical misalignment of 0.628 in. is possible within specifications, 99 per cent of the time the mechanical misalignment would not exceed 0.125 in. Similarly, 90 per cent of the time, the misalignment will remain below 0.088 in., 50 per cent of the time, below 0.048 in., etc.

Modifications Required for a Real Statistical Model: Thus far, the analysis of the real rocket has been based upon the ideal statistical model. It is now appropriate to examine the conclusions reached thus far to see how they should be modified in view of the deviations of the real rocket from the ideal statistical model. The following deviations from the ideal statistical model deserve consideration:

1 The distribution of the critical dimension of each component part may not be exactly Gaussian (normal). This fact conceivably threatens the validity of the root-mean-square addition of σ's.

In actuality, however, a small deviation from normality, as is probable, will introduce only a small error. Moreover, it is a theorem of theoretical statistics that the distribution of the sum of several nonnormal distributions approaches the properties of the sum of normal distributions. Since the situation at hand involves the sum of many distributions, it may be safely concluded that the principle of root-mean-square addition of σ's is applicable.

2 The specified tolerances may not correspond exactly to the 3σ range of the distribution of dimensions of each part. If this deviation from theory is consistent throughout, it will introduce a directly proportional error in the conclusions.

If the deviations from 3σ are randomly inconsistent they will tend to cancel. As was noted earlier, there is a strong economical incentive for the tolerance limits to mark the "hardly ever" range of production parts. Whether this range in any given situation corresponds to the 3σ range can only be determined by measurements of the parts from the actual production situation.

3 The distribution of the component parts may not have a uniform distribution in angle—i.e., may not be radially symmetrical. This possibility threatens the validity of the χ^2 distribution of the total distributions.

It is possible that certain types of assembly jigs will introduce misalignments in the assembly of radially symmetrical parts which are not random in angle, but which consistently occur along certain angles. Fortunately this effect like the lack of normality is washed out when several sources of deviation are present. It can therefore be safely concluded that application of the χ^2 distribution is valid. All in all, it appears that consideration of the deviations of the real system from the ideal statistical model does not disclose significant inaccuracies and does not change conclusions in principle or in order of magnitude. It does indicate that without data on manufacturing precision of each individual manufacturing process, the

conclusions from the ideal statistical model may not be assumed to be highly precise.

Over-all Evaluation: Thus far, the analysis of the sample rocket has led to the conclusions that the probability distribution of the mechanical misalignment will be on the order of the values discussed earlier, and shown in Table 4. The total mechanical-plus-gaseous misalignment will be larger or smaller than the mechanical misalignment depending upon whether or not the additive gaseous misalignments from nonsymmetry exceed the compensating gaseous misalignments originating from the mechanical misalignments.

The probability distribution of gaseous misalignments can be determined for a given rocket vehicle only by experiment. In general it is expected that the net gaseous misalignment will be of the same order of magnitude or smaller than the mechanical misalignment. In accordance with the theory presented earlier, the standard deviation for the distribution of the total misalignment is the root-mean-square sum of the σ's for the mechanical and gaseous misalignment distributions.

When the distribution of the total misalignment has been determined, some decisions must be reached about (1) the maximum permissible misalignment, and (2) the probability (relative frequency of occurrence) that is acceptable for the maximum permissible misalignment.

The maximum permissible misalignment will depend upon the design and application of the rocket vehicle. Variables such as aerodynamic stability, size of target, roll rate of vehicle, type of guidance, total time of flight, and total rocket impulse, will dictate permissible misalignment.

The acceptable probability of permissible misalignment is largely dependent upon the application and the manufacturing difficulties involved. Thus, a short range bazooka missile might be quite satisfactory under production conditions which resulted in a 90 per cent probability of satisfactory alignment. On the other hand, a large, extremely expensive sounding rocket might require the added manufacturing expense of insuring better than 99 per cent probability of a satisfactory alignment. In some cases, the probability of a successful flight will vary with the magnitude of the misalignment, which in itself follows a probability distribution. Determination of the optimum values of the permissible misalignment in such instance would therefore depend upon the analysis of a joint or three-dimensional probability function.

Conclusions

The foregoing analysis has led to the following major conclusions:

1 Jet misalignment arises from mechanical and gaseous misalignments which stem from nonaxial and nonsymmetrical manufacture.

2 The relative effect of individual sources of mechanical misalignment can be estimated by adding their specified tolerances according to root-

mean-square sums. This results in numerous small tolerances having a negligible effect while a few large tolerances can have a relatively predominant effect.

3 Over-all misalignments are reduced when assembly alignments are controlled for groups of parts, rather than for individual parts. Lowest misalignment is obtained if direct control of over-all misalignment is incorporated in the manufacturing assembly procedure.

4 The proposed statistical method of assessing the probability distributions of total jet misalignment yields values at the various probability levels which are probably correct in relation to each other. For more precise conclusions, experimental observations on the probability distributions of dimensions of the manufactured parts and on the average order of magnitude of gaseous misalignments are required.

Appendix

Theoretical Deviation of the Probability Distribution of the Vector Sum of n Random Vectors:

Given n random vectors $r_1, r_2, \ldots, r_n$ with probability distributions such that:

1 The lengths of the vectors follow Gaussian distributions with means $m_1 = m_2 = \ldots, m_n = 0$, and variances $\sigma_1, \sigma_2, \ldots, \sigma_n$.

2 The angles of the vectors follow uniform, random distributions. Then, from the generalized central limit theorem, the vector sum R of the n vectors will be a random variable such that its projections, x and y, on any two arbitrary, mutually perpendicular planes, X and Y, respectively, will follow independent Gaussian distributions defined by

$$m_x = m_y = 0 \quad [6]$$

$$\sigma_x^2 = \sigma_y^2 = \sigma_1^2 + \sigma_2^2 + \ldots, \sigma_n^2 \quad [7]$$

From geometry, $x^2 + y^2 = R^2$.

Hence the distribution of R^2 is the sum of the squares of two independent Gaussian distributions. However, the sum of the squares of two standard normal deviates is a chi-square (χ_2^2) distribution with two degrees of freedom.

By definition, x/σ_x and y/σ_y are standard normal deviates. Hence

$$\left(\frac{x}{\sigma_x}\right)^2 + \left(\frac{y}{\sigma_y}\right)^2 = \chi_2^2$$

But $\sigma_x = \sigma_y$. Hence,

$$\left(\frac{R}{\sigma_x}\right)^2 = \left(\frac{x}{\sigma_x}\right)^2 + \left(\frac{y}{\sigma_x}\right)^2 = \chi_2^2$$

and

$$R^2 = \sigma_x^2 \chi_2^2$$

whence

$$R = \sigma_x(\chi_2^2)^{1/2}.$$

UNIVERSITY OF CALIFORNIA

SPECIAL ABILITIES IN PRE-ENGINEERING STUDIES

HARVEY S. MOREDOCK, JR.

APRIL 1950

An Analysis of the Complex of Special Abilities Necessary for Successful Achievement in the Pre-Engineering Curriculum

By

Harvey Stewart Moredock, Jr.
B.S. (United States Naval Academy) 1939
M.A. (University of California) 1949

DISSERTATION

Submitted in partial satisfaction of the requirements
for the degree of

DOCTOR OF PHILOSOPHY

in

EDUCATION

in the

GRADUATE DIVISION

of the

UNIVERSITY OF CALIFORNIA

TABLE OF CONTENTS

CHAPTER		Page
I.	INTRODUCTION	1
	Statement of the Problem	2
	Justification for Study	3
	Purposes of the Study	6
	Limitations and Assumptions	6
	Definition of Terms	7
	Procedure	9
II.	MEASURES OF SCHOLASTIC ABILITY IN ENGINEERING PART I	11
	A Perspective	11
	Previous Scholastic Records	14
	Tests of General Scholastic and Primary Mental Abilities	19
	Scholastic Achievement Tests	25
	Chapter Summary	34
III.	MEASURES OF SCHOLASTIC ABILITY IN ENGINEERING PART II	38
	Yale Educational Aptitude Battery	41
	Pre-Engineering Inventory	43
	Mechanical Ability	45
	Spatial Visualizing Ability	51
	Special Verbal Abilities	54
	Quantitative Reasoning and Interpretation	59
	Differential Predictive Value	63
	Chapter Summary	73
IV.	DIFFERENTIAL ANALYSIS OF THE PRE-ENGINEERING INVENTORY	77
	Experimental Groups	77
	Criteria	82
	Differential Analysis	89
	Chapter Summary	98

CHAPTER Page

V. FACTOR ANALYSIS OF THE PRE-ENGINEERING INVENTORY 101

Intercorrelations 101
Item Analysis 113
Chapter Summary and Identification of Factors 127

VI. SUMMARY AND CONCLUSIONS 133

Summary of Findings and Conclusions 133
Suggestions for Further Development 141

BIBLIOGRAPHY 147

List of Tables iv

LIST OF TABLES

TABLE		Page
I.	Summary of Correlations Found by Various Studies between High School Record and Achievement in First Semester and Second Semester Freshman Engineering	15
II.	Summary of Correlations Found by Various Studies between American Council Psychological Examination and Freshman First and Second Semester Average Grades in Engineering	21
III.	Correlations of Thurstone's Primary Abilities Tests with First Semester Averages of Various Schools and Colleges at the University of Pennsylvania	23
IV.	Summary of Correlations Found by Various Studies between Scholastic Achievement Tests in Mathematics and Freshman First and Second Semester Average Grades in Engineering	26
V.	Summary of Correlations Found by Various Studies between Physics and Chemistry Scholastic Achievement Tests and Freshman First and Second Semester Average Grades in Engineering Training	29
VI.	Summary of Correlations Found by Various Studies between Scholastic Achievement Tests in English and Freshman First and Second Semester Average Grades in Engineering	32
VII.	Comparison of Median Correlations for Engineering Scholarship and General College Scholarship Relative to Three Predictive Measures	35
VIII.	Summary of Correlations between Various Tests of Mechanical Ability and Academic Success in Freshman Engineering Obtained by Four Predictive Studies	46

TABLE Page

IX. Summary of Correlations between Various Tests of Spatial Visualizing Ability and Academic Success in Freshman Engineering Obtained by Four Predictive Studies..... 52

X. Summary of Correlations between Tests of Special Verbal Abilities and Academic Success in Freshman Engineering..... 55

XI. Summary of Correlations Found by Various Studies between Tests of Quantitative Reasoning and Interpretation and Academic Success in Freshman Engineering..... 61

XII. Summary of Certain Validity Correlations for Aptitude Tests Administered to Yale Freshman Classes of 1944 and 1945..... 66

XIII. Summary of Correlations of Yale Aptitude Tests with Achievement in Freshman Courses..... 69

XIV. Summary of Means and Standard Deviations of Scores on Three Pre-Engineering Inventory Tests for Four Groups of Freshmen at an Unidentified University..... 72

XV. Means and Standard Deviations on the Seven Sub-Tests of the Pre-Engineering Inventory for Beginning Freshman and Sophomore Engineering Students in September 1946..... 81

XVI. Means and Standard Deviations of Grade Point Averages in Five Subject Areas for Two Groups of Beginning Freshman Engineering Students from 1946 to 1948..... 86

XVII. Intercorrelations among the Five Subject Areas of the Pre-Engineering Curriculum for Beginning Freshman Engineering Students after Two Years of Study, 1946-1948..... 87

XVIII. Correlations between the Seven Sub-Tests of the Pre-Engineering Inventory and the Five Subject Areas of the Pre-Engineering Curriculum for Freshman and Sophomore Groups, 1946-48..... 91

TABLE Page

XIX. Correlations between Ten Sections of Sub-Tests in the Pre-Engineering Inventory and the Five Subject Areas of the Pre-Engineering Curriculum for the Freshman Group 1A, 1946-48..... 95

XX. Intercorrelations among the Seven Sub-Tests of the Pre-Engineering Inventory for the Freshman Engineering Groups 1A and 1C..... 102

XXI. Intercorrelations among the Seven Sub-Tests of the Pre-Engineering Inventory for the Sophomore Group 2A, N = 227..... 106

XXII. Intercorrelations among the Sections of Sub-Tests of the Pre-Engineering Inventory for the Freshman Group 1A, N = 190..... 110

CHAPTER I

INTRODUCTION

Although the fundamental issues in higher education have to a large extent remained the same in the past and will probably remain the same in the future, the recent surge in college enrollments has brought into sharp relief the many problems involved in counseling and guidance at the college level. In particular, attention has been directed to the problems of how many students should be educated beyond the high school level and what range of talents should be served by higher education. Examination of the literature in higher education reveals a marked increase in studies being made by college faculties concerning the aims and objectives of their institutions and the relation of the curriculum and the students to these aims. National interest in these problems has resulted in the establishment of the President's Commission on Higher Education, which has already published one of a series of reports on the critical issues in higher education.[1] A further indication of concern for the problems of guidance of college students has been the widespread

---

1. Report of the President's Commission on Higher Education, Vol. I, Establishing the Goals (Washington: Government Printing Office, 1947).

development of qualifying examinations for the several schools and colleges in each of the professions.

Statement of the Problem

As a part of the overall problem of counseling and guidance at the college level, this study proposes to make a critical analysis of the complex of special abilities necessary for successful achievement in the pre-engineering curriculum. Specifically, the problem is:

1. To determine the extent to which certain special ability measures are involved in the general area of engineering study and in the following subject areas of the pre-engineering curriculum:

   a. Mathematics - through integral calculus.

   b. Chemistry - general inorganic and organic.

   c. Physics - mechanics, electricity, magnetism, heat, light, sound.

   d. Engineering - pre-professional subjects.

   e. Cultural - English, history, economics, speech.

2. To investigate the interrelationships among these special ability measures and to determine the relative independence of these measures.

3. To seek clues for the further development of special ability tests to be used for the counseling and guidance of engineering students.

Justification for Study

Immediately following the close of the recent war, the engineering colleges throughout the country were suddenly faced with enrollment problems never before experienced. A national survey made in 1946 by a committee of the American Society of Engineering Education found that in a single year, from the fall of 1945 to the fall of 1946, engineering enrollments had more than trebled the previous year's total enrollment and at the same time had exceeded the maximum capacity of the engineering colleges by 50 per cent.[2] In commenting on the future trend of engineering enrollment, this committee has the following to say:

> Because of the growth of interest in scientific and technical pursuits one student out of every nine students of the country, including both men and women, is now enrolled in engineering (not including related fields of physical science), and no abatement of this trend is in immediate prospect. Thus it seems clear that a rapid rate of increase of enrollments will continue during the coming year and that the resources of engineering schools already seriously overtaxed, will be loaded still further.[3]

Thus the increasing demand for engineering study and the limited facilities of the colleges of engineering make necessary the careful scrutiny of the special abilities of the incoming students to determine those students who are

---

2. Report of the Committee on Transfer Students from Emergency Institutions, in The Journal of Engineering Education, 38:31-38, September, 1947.
3. Ibid., p. 31.

most likely to profit by engineering training.

The President's Commission on Higher Education found that the recent increase in engineering enrollment has another implication for engineering education. In estimating the occupational needs of the nation, the Commission reports that "the supply of engineering graduates may exceed immediately available engineering positions by June 1950, or perhaps 1949, and that if enrollments continue at their present level, this condition might continue in later years."[4] Fortunately, according to the Commission, engineering education has for some time been recognized as having great value as general education. Nevertheless, the possible future surplus of engineering graduates over immediately available engineering positions "emphasizes the imperative need of a thorough-going program of guidance and selection of prospective college students, especially prospective engineering students. ...."[5]

Another indication of the need for ascertaining the level of abilities necessary for engineering study is the high rate of engineering student mortality as evidenced by the drop in number. One of the more prominent studies in student mortality was that by McNeely, in which he found that the percentage of engineering students leaving the twenty-five institutions

---

4. Report of the President's Commission on Higher Education, op. cit., p. 81.
5. Loc. cit.

studied during the four-year period without obtaining a degree was 61.7 per cent.[6] Feder and Adler were particularly concerned about the guidance implications involved in the fact that of the group they were studying who completed the first semester in engineering, only 25 per cent remained in college to graduate.[7] Sackett points out the fact that national surveys made in 1929 and 1939 reveal the same percentage, 50 per cent, of entering freshmen engineering students failing to graduate because of "deficient scholarship, indefinite interest, or lack of fundamental aptitudes and other factors." Sackett further observes that "apparently no marked progress has been made in the counseling and selection of applicants for the purpose of eliminating those who are such obvious failures in their first year of collegiate experience."[8]

Such studies as those listed above and many others could be cited which point to the fact that there is a definite need for a more thorough analysis of the special abilities involved in engineering study.

---

6. John H. McNeely, College Student Mortality. Office of Education Bulletin 1937, No. 11 (Washington: Government Printing Office, 1937), pp. 26-29.
7. D. D. Feder, and D. L. Adler, "Predicting the Scholastic Achievement of Engineering Students," The Journal of Engineering Education, 29:380-85, January, 1939.
8. R. L. Sackett, "Selection of Engineering Students--Discussion," The Journal of Engineering Education, 30:595-600, March, 1940.

Purposes of the Study

The primary purpose of this study is to analyze the special abilities involved in the successful pursuit of pre-engineering training. In order to accomplish this major purpose, the following specific objectives, which comprise the large subdivisions of the study, are necessary:

1. To determine the theory of special ability measurement and to trace and evaluate the development of special ability tests for engineering study.

2. To determine which special abilities, as measured by the tests used, are seemingly necessary for the general pre-engineering curriculum and for certain sections of the curriculum.

3. To determine the separate abilities which are measured by the group of special ability tests used in this study.

4. To find clues from the above analyses for the further development of special ability tests to be used in the guidance and selection of engineering students.

Limitations and Assumptions

The investigation and analysis of the proposed problem is restricted to the study of a certain group of students in the College of Engineering, University of California at Berkeley, who come under the following classifications:

1. Students who entered the College of Engineering in the fall semester 1946 and who took the Pre-Engineering Inventory on September 14, 1946.

2. Students who had no college level courses on their records upon entering the College of Engineering.

3. Students who had one year of previous college experience prior to entering the College of Engineering at Berkeley and who could be classified as having sophomore standing in engineering.

The study is further limited to the students' academic records and the test results which are on file at the College of Engineering. Likewise, the special abilities analyzed in this study are limited to those abilities measured by the Pre-Engineering Inventory.

In order to proceed with the problem outlined in this study, it must be assumed that:

1. Pre-engineering study requires certain skills and abilities apart from those required for other areas of study.

2. Those abilities whose measures show the highest correlation with average marks in all or any part of the pre-engineering curriculum are the ones most necessary for successful achievement in the curriculum.

Definition of Terms

In order to establish common meanings of certain terms used in this study, the following definitions are given.

Complex.--A whole made up of complicated or interrelated parts. The term is used in this study in connection with a

combination of special abilities believed necessary for engineering study.

Special Ability.--Proficiency in performing a certain type of work. The primary concern here is academic work in engineering and the performance in certain scholastic work samples. Skills and abilities are used synonymously in this study since skills are considered to be developed or acquired abilities.

Successful Achievement.--Measured by instructors' marks and averaged by giving certain weights to these marks. The grade point average is a ratio of the number of grade points received to the number of units undertaken. The following grade points are assigned to each mark at the University of California at Berkeley:

For each unit of A grade	3 grade points
For each unit of B grade	2 grade points
For each unit of C grade	1 grade point
For each unit of D grade	0 grade point
For each unit of F grade	0 grade point and the units are not counted toward fulfilling degree requirements.

Pre-Engineering.--Refers to the first two years of engineering training at the college level, i.e., the freshman and sophomore years at a college of engineering.

Differential Prediction.--The prediction of relative achievement in different subject areas. A test having

differential value would be one that has a distinctly higher correlation with its appropriate criterion than with other criteria.

Procedure

An investigation will be made first into the literature dealing with special ability measurement in order to determine the development of the theory involved. Several studies using various predictive measures for engineering study will be examined and an attempt will be made to evaluate the various types used and to point out the promising trends in special ability measurement on the basis of the findings reported in the studies.

Using the average marks made by the groups of students used in this study, intercorrelations among the subject areas of the pre-engineering curriculum are computed to determine the relative independence of the criteria. Correlation coefficients between the sub-tests of the Pre-Engineering Inventory and the subject areas are computed, and on the basis of these validity coefficients a differential analysis is made to determine the tests which are particularly identified with certain subject areas.

Intercorrelations are computed next among the sub-tests of the Pre-Engineering Inventory to determine the amount of overlapping and the relative independence of the tests. A

factor analysis is made of these intercorrelations to determine which tests seem to be measuring a common factor. In order to examine more closely the nature of the special abilities measured by the test battery, an item analysis is made on the basis of grade point averages earned in the College of Engineering. The items found to be the most discriminating between good achievers and poor achievers are picked out from the context of the test and analyzed as to the various types of skills and abilities required. On the basis of the factor analysis and item analysis, the independent special abilities measured by the Pre-Engineering Inventory are identified.

The findings of the various analyses made of the data are then summarized and the special abilities which are particularly involved in pre-engineering study are noted. Likewise, clues are sought from the findings which will aid in the further development of ability tests to be used in the guidance and selection of engineering students.

CHAPTER II

MEASURES OF SCHOLASTIC ABILITY IN ENGINEERING - PART I

As outlined in the procedure of Chapter I, the first step in this study is to determine those factors which have been found by various studies to be especially operative in successful engineering achievement. Each type of ability measure will first be described as to its nature and theoretical basis and then evaluated on the basis of its particular application to engineering study. This first step is necessary to provide a background for an intelligent analysis of the nature of the special abilities which seem to exert a prominent influence upon academic achievement in engineering.

A Perspective

Numerous studies have been made on the prediction of success in college, most of which have made limited contributions to this field of knowledge. Occasionally there appears a significant study which gives direction and meaning for research in scholastic prediction. One of these significant studies is that conducted by the University of Minnesota which extended over a period of six years and was completed in

1942.[1] As reported by Douglas, the following factors were employed in this study:

1. General ability or intelligence tests
2. Achievement test scores in various subjects
3. Special ability tests
4. Average marks in high school
5. Average marks in college
6. Marks in certain subjects
7. Interest analysis inventories
8. Age, sex, living conditions[2]

This list of factors used in predicting college success covers in scope most of those factors which have been developed in predictive studies to date.

Since an exhaustive predictive study was made in each of the schools and colleges of the University of Minnesota, it was possible to get an advantageous perspective not usually obtained in most predictive studies. One significant finding of this study was the fact that variables found especially useful in predicting success in one school or college were not found to be equally prognostic for any other school or

---

1. University of Minnesota, Studies in the Prediction of Scholastic Achievement, Parts I and II (Minneapolis: University of Minnesota Press, 1942).
2. H. R. Douglass, "Different Levels and Patterns of Ability Necessary for Success in College," Occupations, 22:183, December, 1946.

college.[3] A prediction study made on a student body in the College of Business Administration, according to this finding, would not be particularly significant for the College of Engineering since different types of abilities are required for success in each college. This would detract somewhat from the significance of such studies as those made by Durflinger[4] and Segel[5] where an extensive summary was made of college prediction in general. No attempt was made in these studies to differentiate between types of colleges involved in their predictive summaries.

Since the University of Minnesota studies have indicated that the Colleges of Engineering seem to require certain special abilities to a greater degree than do other schools and colleges, the search for significant factors in the prediction of scholastic success in engineering should be limited to studies which are concerned with engineering colleges. In spite of the fact that there are wide variations among the different colleges of engineering due to differences in types of students attending and in standards maintained, the similarity in the programs of study in the engineering colleges

---

3. Douglass, "Different Levels and Patterns of Ability Necessary for Success in College," op. cit., p. 183.
4. G. W. Durflinger, "Prediction of College Success--A Summary of Recent Findings," Journal of the American Association of Collegiate Registrars, 19:68-78, October, 1943.
5. D. Segel, Prediction of Success in College. U. S. Office of Education Bulletin, No. 15 (Washington: Government Printing Office, 1934.

is sufficient to warrant a study of the measures of certain abilities which are persistently required for success in the various engineering colleges. The subsequent evaluation of the various ability measures therefore should be made not only on the basis of predictive value but also on the basis of the ability of the measures to differentiate engineering students from other students.

Previous Scholastic Records

In determining the academic ability of a student, attention is generally directed first to the student's previous scholastic record. This is based upon the generally accepted assumption that performance in the past is a good predictor of performance in the future in a similar type of activity. Counselors and administrators at the college level are fortunate in having access to students' academic records covering a number of years of secondary school work. The various techniques used in connection with previous scholastic records will not be discussed here since the topic is not within the scope of this study and has been fully investigated in another study by the writer.[6]

Table I presents a summary of correlations between high school achievement and first and second semester freshman engineering achievement reported by Bartlett, Berdie, Butsch,

---

6. H. S. Moredock, Techniques in the Selection of Engineering Students (Master's thesis, University of California, 1949).

Cohen, and Laycock and Hutcheon.[7]

TABLE I

SUMMARY OF CORRELATIONS FOUND BY VARIOUS STUDIES BETWEEN HIGH SCHOOL RECORD AND ACHIEVEMENT IN FIRST SEMESTER AND SECOND SEMESTER FRESHMAN ENGINEERING

Author	First Semester r	Second Semester r	No. of Cases	Date
Bartlett	.46	.48	--	1943
Bartlett	.39	.45	--	1943
Berdie		.56	154	1944
Butsch	.553		333	1934-37
Cohen	.51		156	1941
Cohen	.48		180	1942
Laycock and Hutcheon		.61	144	1939

Table I shows that the correlations between high school achievement and success in freshman engineering range from .39 to .61 with the median correlation being .48. The correlation of .61 found by Laycock and Hutcheon might be misleading due to the fact that the final high school marks were based on achievement test scores. If this study were not taken into consideration because of the additional factor of achievements test scores being entered, the range of correlations would extend from .39 to .56 with the median remaining

7. R. S. Bartlett, "Guidance and Placement of Engineering Students, "The Journal of Engineering Education, 33:549, March, 1943.
R. L. C. Butsch, "Improving the Prediction of Academic Success through Differential Weighting," The Journal of Educational Psychology, 30:407-15, September, 1939.

the same at .48.

Comparison of these results with those obtained by studies of the prediction of general college achievement from high school records shows that the median correlation reported in Table I is slightly lower. Segel finds a median correlation of .55 and a range of .29 to .77 in his summary of studies in the prediction of college scholarship from high school average marks.[8] This would indicate that average marks in high school predict about the same for all colleges and do not differentiate particularly among the various academic fields.

In searching for measures of special abilities, marks received in certain high school courses have been considered as indicative of special abilities for specialized college training. Studies have consistently shown that there is little or no relation between specific patterns of high school subjects and college scholarship in the various fields of study.[9]

---

7. (Continued)
L. Cohen, "Predicting Academic Success in an Engineering College and Suggestions for an Objective Evaluation of High School Marks," The Journal of Educational Psychology, 37:384, September, 1946.
S. R. Laycock, and S. B. Hutcheon, "Preliminary Investigation into the Problem of Engineering Aptitude," The Journal of Educational Psychology, 30:284, April, 1939.

8. As reported by A. C. Eurich, and L. F. Cain, "Prognosis," in Encyclopedia of Educational Research (New York: The Macmillan Co., 1941), pp. 848-49.

9. H. R. Douglass, "Relation of Pattern of High School Credits to Scholastic Success in College," North Central Association Quarterly, 6:283-97, December, 1931.

Bartlett points out the following reasons why the scrutiny of scholastic performance in high school, with special attention to contrasting achievement in different subjects is an unfruitful one:

1. Only rarely is a student's record consistent; generally it is erratic due to maturing growth.

2. Motivation may vary from year to year and from subject to subject.

3. Schools differ widely in emphasis on different studies and standards maintained.[10]

Prediction studies in engineering have shown that when early achievement in engineering colleges is compared with scholarship at the advanced levels of engineering, the correlations are sizably increased. Bartlett reported a correlation of .65 between the first semester freshman grades in engineering and marks achieved in the senior year.[11] Brush found a correlation of .837 between first semester average marks and total grades made in engineering.[12] When the average grades made during the first year in engineering were compared with the average marks obtained in the subsequent

---

10. R. S. Bartlett, "Guidance and Placement of Engineering Students," The Journal of Engineering Education, 33:537, March, 1943.
11. Ibid., p. 549.
12. E. N. Brush, "Mechanical Ability as a Factor in Engineering Aptitude," The Journal of Applied Psychology, 25:307 June, 1941.

Bartlett points out the following reasons why the accuracy of scholastic performance in Mr. Asbury, with special attention to contrasting achievement in different subjects is an

1. Only recently is a student's record permanently kept so easily it is available due to modern process.

2. Motivation may vary from year to year and from person to person to another.

3. Schools differ widely in [illegible] and standards maintained.

Predictive studies in engineering have given rise [illegible] early attempts to accurately relate a [illegible] scholarship to the advanced [illegible] Correlations are usually [illegible] Bartlett reports a correlation of .65 between the first semester freshman grades engineering and marks obtained in the senior year.[1] Brumbaugh found a correlation of .577 between [illegible]

---

1. R. Bartlett, Unpublished [illegible] Engineering Education, Vol. Journal of Engineering Education, March, 1940.

three years, Wilson and Hodges reported a correlation coefficient of .584, which is somewhat lower than the others.[13] Siemens likewise compared the freshman year grade point average with the upper division average in each of the three major branches of engineering--electrical, mechanical, and civil engineering, and he obtained correlations ranging from .67 to .74.[14] These studies bear out the obvious fact that predictive efficiency increases when the data upon which the prediction is based approach in kind the data forecasted.

In general, high school records cannot be considered as having differential predictive value. This does not mean that high school records have no value whatever for guidance and selection of engineering students. Table I clearly shows that high school achievement has predictive value for engineering study but not for engineering study alone. In the guidance and selection of engineering students, high school records should be considered as indicative of general scholastic ability and not as indicators of certain special abilities.

---

13. M. O. Wilson, and J. H. Hodges, "Predicting Success in the Engineering College," The Journal of Applied Psychology, 16:349, August, 1932.
14. C. H. Siemens, Prognosis of the Achievement of Engineering Students (Ph.D. dissertation, University of California, 1939), p. 25.

Tests of General Scholastic and Primary Mental Abilities

Out of the belief that intelligence is the primary determiner of scholastic success, several tests have been developed which propose to measure general intelligence. More recently these tests have been called general scholastic aptitude tests since validation is made on the basis of scholastic achievement. According to the theory underlying the construction of these tests every individual is believed to possess, in greater or lesser extent, a certain amount of generalized learning power or scholastic efficiency. A test which measures this learning power is considered to have equal significance for any field of intellectual endeavor, and gross scores on these tests are therefore interpreted to be measures of academic promise.

Originally the general scholastic aptitude tests were of the "omnibus" type, consisting of items with the sole purpose of measuring intellectual capacity without regard to any components of aptitude. Recently, these tests such as the American Council Psychological Examination and the College Board Scholastic Aptitude Test have been revised to yield verbal or linguistic and mathematical or quantitative scores. The subject matter of these tests, however, is secondary to the types of abstract thinking which are believed to be basic to scholastic aptitude.

A number of studies were found which used the American Council Psychological Examination in connection with the prediction of scholastic success in engineering. Table II summarizes the results of the studies made by Bartlett, Berdie, Brush, Butsch, Holcomb and Laslett, McGehee, Remmers and Gage, and Vaughn.[15]

---

15. R. S. Bartlett, "Guidance and Placement of Engineering Students," The Journal of Engineering Education, 33:549, March, 1943.
R. F. Berdie, "Prediction of College Achievement and Satisfaction," The Journal of Applied Psychology, 28:242, June, 1944.
E. N. Brush, "Mechanical Ability as a Factor in Engineering Aptitude," The Journal of Applied Psychology, 25:307, June, 1941.
R. L. C. Butsch, "Improving the Prediction of Academic Success through Differential Weighting," The Journal of Educational Psychology, 30:407-15, September, 1939.
G. W. Holcomb, and H. R. Laslett, "A Prognostic Study of Engineering Aptitude," The Journal of Applied Psychology, 16:112, April, 1932.
W. McGehee, "The Prediction of Differential Achievement in a Technological College," The Journal of Applied Psychology, 27:89, February, 1943.
H. H. Remmers, and H. E. Geiger, "Predicting Success and Failure of Engineering Students in the School of Engineering in Purdue University," Purdue University Studies in Higher Education, 38:17, May, 1940.
K. W. Vaughn, "Basic Consideration in a Program of Freshman Evaluation," The Journal of Engineering Education, 35:178, November, 1944.

TABLE II

SUMMARY OF CORRELATIONS FOUND BY VARIOUS STUDIES BETWEEN AMERICAN COUNCIL PSYCHOLOGICAL EXAMINATION AND FRESHMAN FIRST AND SECOND SEMESTER AVERAGE GRADES IN ENGINEERING

	American Council Psychological Examination			
Author	First Semester	Second Semester	No. of Cases	Date
Bartlett	.35	.25	--	1941
Bartlett	.44	.41	--	1941
Bartlett	.46	.55	--	1938
Berdie		.21	154	1944
Brush	.47		160	1932
Butsch	.585		333	1934-37
Holcomb and Laslett		.55	--	1932
McGehee		.48	383	1942
Remmers and Geiger	.624		1089	1933-34
Vaughn		.43	428	1944
Vaughn		.47	600	1944

The zero order correlation coefficients range from .21 to .624 for the American Council Psychological Examination with the median being .46. Only one study was found which used the College Board Scholastic Aptitude Test in connection with predicting engineering academic success. This study was based on one hundred freshman engineering students at Cornell College of Engineering and reported a correlation of .46 with the verbal section and .52 with the mathematical section of the test.[16] In Segel's summary of the correlations between

16. N. Frederiksen, "Prediction of Academic Success in Engineering Schools" (a pamphlet distributed by the College Entrance Examination Board), 1947.

tests of general scholastic aptitude and college scholarship, the median correlation found was .44.[17] These data indicate that the scholastic aptitude tests predict general college scholarship about as well as engineering achievement and therefore have no particular differential value. Table II indicates, however, that the predictive value of these tests is sufficient to conclude that general scholastic ability is a factor in engineering academic achievement.

A further development in scholastic aptitude tests is the Thurstone Primary Mental Abilities Test which attempts to measure the separate factors in scholastic aptitude. This test is discussed in connection with general scholastic tests because its construction is similar to that of other scholastic tests except for the feature of having more component factors. In the attempt to get at primary mental abilities, the subject matter of the items is secondary to the nature of the intellectual activity required. Only the simplest of materials is used but the level of thinking required runs up into adult levels.

Goodman reports the results of a number of studies made on Thurstone's Primary Mental Abilities Tests in connection with predicting college success at the University of Penn-

---

17. As reported by A. C. Eurich, and L. F. Cain, op. cit., p. 847.

sylvania.[18] Table III presents some of the data found in Goodman's study and organized in a manner which will permit an analysis of the predictive value for engineering and the differential value of the primary abilities tests.

TABLE III[a]

CORRELATIONS OF THURSTONE'S PRIMARY ABILITIES TESTS WITH FIRST SEMESTER AVERAGES OF VARIOUS SCHOOLS AND COLLEGES AT THE UNIVERSITY OF PENNSYLVANIA

	School			
Ability Test	Engineering N = 170	Chemistry and Physics N = 147	Home Economics N = 113	Liberal Arts N = 306
P	.04	-.008	.28	.15
N	.32	.23	.41	.24
V	.33	.44	.51	.35
S	.23	.08	.28	.04
M	.10	.36	.20	.28
I	.34	.25	.40	.28
D	.38	.40	.42	.27

Key: P - Perception
N - Number
V - Verbal
S - Space
M - Memory
I - Induction
D - Deduction

a Adapted from C. H. Goodman, "Prediction of College Success by Means of Thurstone's Primary Abilities Tests," Educational and Psychological Measurement, 4:125-140, Summer 1944.

18. C. H. Goodman, "Prediction of College Success by Means of Thurstone's Primary Abilities Tests," Educational and Psychological Measurement, 4:125-140, Summer 1944.

A multiple correlation combining the various abilities tests was found to be .48 for engineering students. This compares favorably with the correlations found for other scholastic aptitude tests. Inspection of Table III reveals, however, that the primary abilities tests have no particular differential value. The tests seem to predict about the same for all colleges and schools reported, particularly the number, verbal, and reasoning tests.

Another study which was made by Stuitt and Hudson administered the Thurstone Primary Mental Abilities Test to students in various academic fields.[19] The number of cases used in the study is so small that the results are highly unreliable. Therefore the study is mentioned only in passing.

Crawford and Burnham point out the following construction defects found in the Primary Mental Abilities Test:

1. Failure to make adequate item-analysis of the individual questions.

2. Excessive influence of sheer response-speed.

3. Rather high probable errors of the basic intercorrelations.

Not only have doubts arisen as to the validity of the test but also of the primary factors themselves. There is evidence that these factors are variable in nature for different

---

19. D. B. Stuitt, and H. H. Hudson, "The Relation of Primary Mental Abilities to Scholastic Success in Professional Schools," The Journal of Experimental Education, 10:179-182, December, 1941.

tests was found to be 43 for engineering students. This
compares favorably with the correlations found for other
scholastic aptitude tests. Inspection of Table III, however, that the primary abilities tests have no partial
differentiating value. The tests seem to stand or about the same
for all colleges and so can be dispensed, particularly the
number, verbal, and reasoning tests.

Another study which was made by Pyle[19] and others
consists in various academic [illegible] the
used in the study to an email from the [illegible]
[illegible]. Therefore the effect [illegible]

Thurstone and Ruckman point out the following
tion defects found in the Primary Mental Abilities Test:

2. Inconclusive indication of what [illegible]
[illegible] high correlate criteria of the [illegible]

test but also of the primary functions themselves. There is a

---

19. T. H. Pyle, Harold E. Kelly, and R. E. Pinkerton, "The Relation of Primary Mental Abilities to Scholastic Success in Freshman"

age levels or populations, and therefore are not primary in a realistic sense.[20]

Scholastic Achievement Tests

The scholastic achievement tests are primarily factual in nature. The emphasis in these tests is upon knowledge acquired or "achieved" by the student in certain specialized subject areas. An achievement test is therefore administered after a student has taken a particular course or series of courses to find out how much has been learned. These tests are retrospective in outlook and their content is largely determined by standard curricula.

A number of prognostic studies have been made in engineering using achievement tests in various subject areas. Since engineering study draws heavily from the subject content of mathematics and natural science, the achievement tests studied in connection with engineering have been limited mainly to these subjects.

Table IV indicates in a general way how well certain scholastic achievement tests in high school mathematics correlates with average marks in freshman engineering. For comparative purposes, the names of the different achievement

---

20. A B. Crawford, and P. S. Burnham, Forecasting College Achievement (New Haven: Yale University Press, 1946), pp. 213-14.

tests are given along with their validity coefficients. The data for Table IV are drawn from the studies of Bartlett, Berdie, Brush, McGehee, and Sackett.[21]

TABLE IV

SUMMARY OF CORRELATIONS FOUND BY VARIOUS STUDIES BETWEEN SCHOLASTIC ACHIEVEMENT TESTS IN MATHEMATICS AND FRESHMAN FIRST AND SECOND SEMESTER AVERAGE GRADES IN ENGINEERING

Author	Name of Test Used	1st Sem. r	2nd Sem. r	No. of Cases
Bartlett	Cooperative Math Test	.69	.64	--
Bartlett	Cooperative Math Test	.54	.43	--
Berdie	Cooperative Math Test		.45	154
Brush	CRB* Algebra	.529		77-160
Brush	CRB* Plane Geometry	.323		77-160
McGehee	Cooperative Math Test		.50	383
Sackett	Cooperative Math Test		.554**	1738

*Columbia Research Bureau.
**Average of eight colleges of engineering.

21. R. S. Bartlett, "Guidance and Placement of Engineering Students," The Journal of Engineering Education, 33:549, March, 1943.
R. F. Berdie, "Prediction of College Achievement and Satisfaction," The Journal of Applied Psychology, 28:242, June, 1944.
E. N. Brush, "Mechanical Ability as a Factor in Engineering Aptitude," The Journal of Applied Psychology, 25:307
W. McGehee, "The Prediction of Differential Achievement in a Technological College," The Journal of Applied Psychology, 27:89, February, 1943.
R. L. Sackett, "Discovery of Engineering Talent," The Journal of Engineering Education, 35:180, November, 1944.

The predictive measures for the mathematics achievement tests studied in Table IV range from .32 to .69 with the median correlation being .52. Probably more weight should be given the correlation of .554 obtained by Sackett when he averaged the results of eight different colleges of engineering. Sackett found a smaller range of correlations from .44 to .645 in his study.

The Cooperative Mathematics Test is comprehensive in nature, covering all the subject matter of high school mathematics. The study by Brush provides an interesting comparison between achievement tests in algebra and plane geometry. His results, as shown in Table IV, indicate that for the particular group studied the algebra test has a substantially higher validity coefficient than that of the plane geometry test. Further comparisons would be needed before the results are conclusive.

Considering the results summarized in Table IV, there is clear evidence that proficiency in mathematics as measured by the scholastic achievement tests in mathematics is an important factor in engineering achievement. The wide range of correlations obtained by the different studies would indicate that the degree of importance to be attached to these tests in mathematics achievement should be determined by each individual college of engineering.

Turning now to the predictive value of scholastic achievement tests in the natural sciences for engineering, a similar tabulation in Table V has been made of the results obtained from the same group of studies used in previous tables with the addition of Dvorak and Salyer.[22]

The range of correlations presented in Table V extends from .30 to .59 and the median is computed to be .54. This median corresponds closely to the median correlation of .52 and the average correlation of .55 for mathematics achievement reported in Table IV, which would indicate that the two types of achievement tests have about the same predictive value for the engineering colleges included in these studies. Further comparison of Tables IV and V shows that Bartlett and Berdie report higher validity coefficients for the Cooperative Mathematics Tests than the Cooperative Chemistry Tests for their particular experimental groups. On the other hand, Brush finds that the CRB Physics Test has a higher correlation coefficient than the CRB Algebra, Plane Geometry, and Chemistry Tests. No general conclusions can be drawn from these data because there are too many unknown variables. The relative value of these tests will need to be determined for

---

22. A.Dvorak, and R. C. Salyer, "Significance of Entrance Requirements for the Engineering College at the University of Washington," The Journal of Engineering Education, 23:620, April, 1933.

TABLE V

SUMMARY OF CORRELATIONS FOUND BY VARIOUS STUDIES BETWEEN PHYSICS AND CHEMISTRY SCHOLASTIC ACHIEVEMENT TESTS AND FRESHMAN FIRST AND SECOND SEMESTER AVERAGE GRADES IN ENGINEERING TRAINING

Author	Name of Test Used	1st Sem. r	2nd Sem. r	No. of Cases
Bartlett	Cooperative Chemistry Test	.57	.56	--
Bartlett	Cooperative Chemistry Test	.53	.30	--
Berdie	Cooperative Chemistry Test		.34	154
Brush	CRB* Chemistry	.43		77-160
Brush	CRB* Physics	.589		77-160
Dvorak and Salyer	Iowa Physics Placement		.546	--

*Columbia Research Bureau.

each separate college of engineering in accordance with the type of student drawn there and the nature of the learning experiences provided. Generally, speaking, however, achievement in chemistry and physics as measured by these tests is a factor to be considered in predicting average marks made in engineering.

Durflinger affords an excellent opportunity to compare the results of Tables IV and V with studies that have made a summary of correlations between content examinations in general and college scholarship. He found that summary studies made by Douglass, Segel, and Wagner obtained median correlations between achievement tests and college scholarship ranging from .545 to .560.[23] Their findings closely correspond to the median correlations found in Tables IV and V, which would indicate that content examinations have about the same predictive value for all the specialized programs in colleges and universities, including engineering. These summary studies, however, do not indicate which parts of the content examinations have particular value for each of the various specialized programs of study.

Further examination of the engineering prognostic studies reveals that achievement in English is a factor in engineering

---

23. G. W. Durflinger, "The Prediction of College Success--A Summary of Recent Findings," Journal of the American Association of Collegiate Registrars, 19:73, October, 1943.

scholastic success not to be overlooked. Although English as a subject is stressed very little in engineering programs of study, there is a growing realization that the engineering student must be able to understand and handle verbal symbols in order fully to understand the technical reading material that he meets and adequately to express the results of his own thinking in engineering study. Drawing from the same source of studies previously used, with the addition of Feder and Adler,[24] a summary has been made in Table VI of the correlations obtained by the studies using certain achievement tests in English.

For this particular group of studies, a median correlation of .47 was computed, and the correlations ranged from .28 to .62. At the outset it is evident that the predictive value of achievement tests in English is generally somewhat less than that of achievement tests in mathematics, or physics and chemistry, which is to be expected. Butsch administered the Iowa High School Content Examination to a group of 333 entering freshman engineering students and found that the relative contribution of the English and history sections to

---

24. D. D. Feder, and D. L. Adler, "Predicting the Scholastic Achievement of Engineering Students," The Journal of Engineering Education, 29:381, January, 1939.

TABLE VI

SUMMARY OF CORRELATIONS FOUND BY VARIOUS STUDIES BETWEEN SCHOLASTIC ACHIEVEMENT TESTS IN ENGLISH AND FRESHMAN FIRST AND SECOND SEMESTER AVERAGE GRADES IN ENGINEERING

Author	Name of Test Used	1st Sem. r	2nd Sem. r	No. of Cases
Bartlett	Cooperative English Test	.47	.35	--
Bartlett	Cooperative English Test	.48	.44	--
Bartlett	Cooperative English Test	.53	.43	--
Berdie	Cooperative English Test		.28	154
Feder and Adler	Iowa English Training Test	.62	.60	84-99
McGehee	Comparative English Test		.46	383
Remmers and Geiger	Purdue English Placement	.52		1087
Sackett	Cooperative English Test		.402*	1738

*Average correlations of eight colleges of engineering.

the predictive value of the content examination as a whole was negligible.[25]

In analyzing the special abilities required for engineering study, consideration should not be given only to the predictive value of the special ability measures but should also include diagnostic and guidance values as well. In line with this point of view, the factor of achievement in English needs closer analysis in the light of criteria other than predictive ability. Feder and Adler showed that the Iowa English Training Test had diagnostic value for their group. They found that no student who stood below the 30th percentile rank on this test graduated in engineering.[26] Vaughn likewise points out that "students who do very well on verbal tests may or may not succeed in engineering, but students who do very poorly on such tests rarely succeed in any college curriculum, engineering or otherwise."[27] Achievement in English is an important factor to be considered in engineering scholastic success primarily because of its diagnostic value.

---

25. R. L. C. Butsch, "Improving the Prediction of Academic Success through Differential Weighting," The Journal of Educational Psychology, 30:417, September, 1939.
26. D. D. Feder, and D. L. Adler, "Predicting the Scholastic Achievement of Engineering Students," The Journal of Engineering Education, 29:385, January, 1939.
27. K. W. Vaughn, "The Yale Scholastic Aptitude Tests as Predictors of Success in the College of Engineering," The Journal of Engineering Education, 34:578, April, 1944.

In analyzing the special abilities required for engineering study, consideration should not be given only to the predictive value of the special ability measure but should also include diagnostic and guidance values as well. In line with this point of view, the factor of achievement in engineering classes analysis in the light of orthogonal [illegible] predictive ability. Moore and Miller showed that the Iowa Psychological Testing Test had diagnostic value for their group. They [illegible] that no student was alone making the 30th percentile mark on this test proceeded to graduate.[26] Weldon Dilworth points out that "students who do very well on verbal tests may or may not succeed in engineering, but students who do very poorly on such tests rarely succeed in any college curriculum, engineering or otherwise."[27] Achievement in [illegible] is an important factor to be considered in engineering [illegible] success primarily because of its diagnostic value.

---

26. D. G. Paterson, and G. L. Adler, "Predicting the Industrial Performance of Engineering Students," [illegible]

27. W. Weldon, "The Role Scholastic Aptitude Tests Predictions of Success in the College Curriculum,"

The Iowa English Training Test which Feder and Adler found to have such high validity coefficients consists of four parts: spelling, punctuation, grammatical construction, and sentence meaning. In each part, examples are given and the student is required to select the correct ones and wrong ones. The Cooperative English Test, which is widely used at the freshman college level, consists of six parts of multiple choice items: spelling, vocabulary, punctuation, grammar and diction, capitalization, and sentence structure. The scope and content of these tests are typical of the English achievement tests. Other types of verbal tests will be subsequently discussed.

Chapter Summary

A six-year study made by the University of Minnesota has confirmed the fact that colleges of engineering require certain special abilities to a greater degree than do other schools and colleges, and therefore the search for significant factors in the prediction of scholastic success is justified and is properly limited to studies which are concerned with engineering colleges.

Up to this point, an analysis has been made of prognostic studies in engineering which have used the predictive measures of previous academic records, certain achievement tests, and general scholastic aptitude tests. Each of these predictive

measures was first described as to its theoretical basis for determining certain abilities and then evaluated on the basis of its predictive value and differential value for engineering study as far as could be determined by the studies analyzed. Such an analysis has its limitations. Not all studies are equally significant, and therefore care should be taken in interpreting the results of a summary of a group of studies. Nevertheless, in spite of these limitations, certain trends in results can be noted.

Median correlations for each of the three factors were computed from summaries of engineering prognostic studies in order to determine the predictive value of each measure. The median correlations found in this study were then compared with median correlations for the same predictive measures relative to general college scholarship as reported by other summary studies. Table VII presents this comparison.

TABLE VII

COMPARISON OF MEDIAN CORRELATIONS FOR ENGINEERING SCHOLARSHIP AND GENERAL COLLEGE SCHOLARSHIP RELATIVE TO THREE PREDICTIVE MEASURES

Predictive Measure	Engineering Scholarship	General College Scholarship
High School Record	.48	.55
General Scholastic Tests	.46	.44
Achievement Tests		.545-.560
Mathematics	.52	
Science	.54	
English	.47	

Inspection of Table VII reveals that each of the measures has predictive value for engineering but also has about the same predictive value for other types of colleges as well. This would indicate that the differential value of these measures for engineering is limited and therefore the search for special abilities in these measures would be unprofitable.

Further evidence of the unlikelihood of these measures defining special abilities is found in examining the nature of the measures. The use of marks in certain courses to determine special abilities is highly unreliable because a student's record is rarely consistent, and schools differ widely in emphasis on different studies and standards maintained. Achievement tests add a certain amount of definiteness to the picture, but their use as special ability measures is limited because they emphasize facts or knowledge acquired and because only a few areas of study are covered. By nature of construction, the general scholastic aptitude tests attempt to measure a certain scholastic ability which is applicable to all fields of study, and consequently it is unlikely that special abilities for certain fields of study are to be found in this type of measure. Thurstone's Primary Mental Abilities Test attempts to measure specific components of scholastic ability, but studies have indicated that this test still measures general scholastic ability and does not differentiate for the various fields of study.

It is necessary, therefore, to investigate other types of measures for special abilities in engineering study. The next chapter continues the analysis of prognostic studies in engineering for these other measures.

CHAPTER III

MEASURES OF SCHOLASTIC ABILITY IN ENGINEERING PART II

Continuing the search for special abilities that have been defined by engineering prognostic studies, attention is now directed to measures of specialized abilities. Since this is a relatively new field, the number of studies investigating the predictive value of these measures for engineering study is somewhat limited, but the results so far achieved are significant in that they point toward future possibilities in special ability measurement.

First presented in this chapter will be a brief outline of the theory of special ability measurement. Following this will be a description of two test batteries recently developed to measure a group of special abilities, parts of which will be compared with other similar special abilities tests throughout the chapter. The remainder of the chapter will be devoted to an analysis of special ability measures for engineering.

Theory of Special Ability Measurement

In this section it is evident that the search for engineering special abilities becomes involved in educational aptitude testing, and the reason for this is found in the

nature of the construction of specialized educational aptitude tests. In the previous chapter it was noted that general scholastic aptitude tests were developed to measure a scholastic ability believed to be necessary for academic achievement in all the fields of learning. Parallel to this development was the construction of specialized aptitude tests which were designed for the purpose of predicting achievement in the specific fields of learning. Instead of being "omnibus tests" with the purpose of measuring general learning power, specialized aptitude tests have been constructed to measure the specific abilities requisite for learning in certain areas of study. As Carter points out, "Academic abilities are somewhat specialized; the modern trend is toward analyzing them into their specialized components."[1]

The basic technique in the construction of these specialized aptitude tests might be called the "miniature-task" technique, or "task-simulation" technique, as suggested by Crawford and Burnham.[2] Essentially, this method consists of presenting a sampling of situations or tasks which are similar to the type of activity which will be confronted in

---

1. H. D. Carter, "Measurement and Prediction of Special Abilities," Review of Educational Research, 17:34, February, 1947.
2. A. B. Crawford, and P. S. Burnham, Forecasting College Achievement (New Haven: Yale University Press, 1946), pp. 6-7.

the future. This technique has been in use over a period of years, particularly in the field of industrial psychology, and great progress was made in the use of the technique for the construction of the specialized aptitude tests for the Armed Services. Only recently has the technique been used for specialized aptitude tests in education.

The specialized aptitude tests in education which use the "miniature-task" technique provide a fruitful source for analyzing special abilities since certain special abilities are required in the performance of the miniature tasks presented in the tests. Carter suggests that the criteria for defining these special abilities include "evidence regarding the reliability and validity of measurement as well as independence from 'general intelligence'."[3] This study therefore intends to investigate the various specialized aptitude tests in the first place to determine what special abilities are measured and in the second, to determine the predictive value of these tests for engineering in order to ascertain the degree to which these abilities are necessary for engineering study.

---

3. H. D. Carter, "Measurement and Prediction of Special Abilities," Review of Educational Research, 17:33, February, 1947.

Yale Educational Aptitude Battery

One of the first test batteries developed to measure a certain group of special abilities was the Yale Educational Aptitude Battery. The theoretical considerations in the development of this test battery and a more complete description of the battery can be found in Crawford and Burnham.[4] Since parts of the Yale Battery will be referred to throughout the rest of the study, a description of each section will be given at this time.

Test I. Verbal Comprehension

a. Paragraph comprehension - Consists of a series of paragraphs in which one word destroys the meaning of the paragraph. The student is required to select this word. Determines indirectly the student's comprehension of the central thought.

b. Word-relations section - Student is required to recognize antonyms and parts of speech applying to words whose parts of speech are given.

c. A test of the student's ability to recognize synonyms of given words.

Test II. Artificial Language

Student is supplied with a set of language rules and an artificial language vocabulary. In Parts I and II, student refers to given rules and vocabulary.

Part I - Student is required to translate English words and sentences into the artificial language.

---

4. A. B. Crawford, and P. S. Burnham, Forecasting College Achievement (New Haven: Yale University Press, 1946).

Part II - Student translates sentences in artificial language into English.

Part III - Student must rely on memory of rules and vocabulary previously presented. It is a good test of the student's ability to remember and apply what he has recently studied.

Test III. Verbal Reasoning

Part I. Logical Inferences. Student is presented with a statement of fact and a conclusion from the statement of fact. Student is then required to select one of five possible judgments which applies to the conclusion.

Part II. Interpretation of Experiments. Student is presented with the data of an experiment and an interpretation of the experiment. Student is required to select one of five possible judgments which applies to the interpretation.

Test IV. Quantitative Reasoning

Part I - Student is presented with a series of paragraphs containing sets of data illustrating mathematical principles. Student is required to discover and apply the principle underlying each set of data.

Part II - Student is presented with various number series and is required to select from a given set of numbers the one which applies to each series.

Part III - Student is given symbolic relationships and is required to draw conclusions from them.

Test V. Mathematical Ingenuity

Part I - Student is presented with an algebraic expression or series of expressions, and is required to solve for one unknown quantity.

Part II - Student is required to translate a verbal statement into an algebraic equation.

Test VI. Spatial Visualizing

Part I - Student is presented with various sets of cubes and is required to count the cubes which fulfill certain specifications.

Part II - Student is presented with drawings of two orthographic views of an object and is required to select from four suggested views the one which applies to the given set of two.

Part III - A number of irregularly shaped figures are presented and the student is required to recognize combinations of various patterns.

Test VII. Mechanical Ingeuity

Part I - Drawings of mechanical devices are presented and the student is required to recognize and apply the principles involved.

Part II - Student is required to solve a number of elementary problems in kinematics.

Pre-Engineering Inventory

Another special abilities test battery using the "task-simulation" technique is the Pre-Engineering Inventory, which was developed as a joint project of the Engineers' Council for Professional Development, The American Society of Engineering Education, and the Carnegie Foundation for the Advancement of Teaching. Parts of this test battery will be referred to throughout the rest of this study, and therefore a description of the battery will be given at this time.

Test I. General Verbal Ability

I A - Student is presented with words used in phrases and is required to select the correct synonym for each given word.

II B - Reading passages are given and the student is required to determine the meaning of words in a particular context, comprehend the central thought of a paragraph, and draw conclusions from a paragraph.

Test II. Technical Verbal Ability

Student is presented with words found in the reading material of science and mathematics and is required to recognize the meanings of these words.

Test III. Comprehension of Scientific Materials

III A - Several technical reading passages are presented and the student is required to comprehend the meaning of the passage and to interpret the passage in the light of previous training in science and mathematics.

III B - Student is required to interpret the meaning of given tables, graphs, and drawings of a technical nature.

Test IV. General Mathematical Ability

IV A - Student is required to solve algebraic formulas, solve verbal problems, translate verbal expressions into algebraic formulas, interpret geometric figures, and perform indicated mathematical operations.

IV B - Student is required to use his mathematical ingenuity in interpreting certain dimensioned drawings, tables, reading passages, and graphs.

Test V. Comprehension of Mechanical Principles

Various mechanical devices are presented and the student is required to comprehend the principles in the operation of these devices.

Test VI. Spatial Visualizing Ability

VI A - Two orthographic views of an object are given and the student is required to select the third view.

VI B - Student is presented with a drawing of a cube having markings on the visible faces and is required to identify the same cube turned in a different position among a set of cubes.

Test VII. Understanding of Modern Society

VII A - Student is required to answer questions of a general nature concerning various institutions, business, labor, and governmental functions in American democracy.

VII B - Student is required to determine the meaning and implications of certain reading passages on current topics.

Mechanical Ability

The first of the special abilities considered is mechanical ability. This ability has long been closely associated with the field of engineering and has been considered an important factor in engineering academic success. As a result, several tests have been developed to measure this particular ability, and a number of studies have investigated the relationship between these tests and engineering scholarship. Table VIII summarizes the relationships between scholastic achievement in engineering and various tests of mechanical ability which were determined by the following four studies:

TABLE VIII

SUMMARY OF CORRELATIONS BETWEEN VARIOUS TESTS OF MECHANICAL ABILITY AND ACADEMIC SUCCESS IN FRESHMAN ENGINEERING OBTAINED BY FOUR PREDICTIVE STUDIES

Author	Name of Test Used	1st Sem. r	2nd Sem. r	No. of Cases
Brush	Minn. Assembly Test**		.278	104
Brush	O'Connor No.5(Wiggly Block)**		.281	104
Brush	O'Connor No. 72 (Dividers)**		.154	104
Brush	Cox Mechanical Explanation		.323	104
Brush	Cox Mechanical Completion		.390	104
Brush	Cox Mechanical Models		.425	104
Brush	MacQuarrie Mechanical Ability		.249	104
Brush	Cox Mechanical Completion	.364		77-160
Brush	Cox Mechanical Models	.403		77-160
Holcomb & Laslett	MacQuarrie Mechanical Ability		.48	--
Holcomb & Laslett	Steinquist Mechanical Aptitude No. 1		.15	--
Holcomb & Laslett	Steinquist Mechanical Aptitude No. 2		.43	--
Holcomb & Laslett	Steinquist Assembly Test No. 1		.16	--
Laycock & Hutcheon	Cox Mechanical Models		.16	--
Laycock & Hutcheon	Cox Mechanical Diagrams		.14	--
Vaughn	PEI* Mechanical Principles	.39***		--
Vaughn	Yale Mechanical Ingenuity		.307	643

*Pre-Engineering Inventory
**Individual tests
***Median correlation of ten colleges of engineering

Brush, Holcomb and Laslett, Laycock and Hutcheon, and Vaughn.[5]

An analysis of the tests listed in Table VIII indicates that they may be classified into two broad categories according to the nature of abilities required. Such tests as the Minnesota Assembly Test, O'Connor No. 5 (Wiggly Block), O'Connor No. 72 (Dividers), and Steinquist Assembly Test may be considered as manipulative tests because they require the handling of certain objects. Tests such as the Cox Mechanical Explanation, Cox Mechanical Completion, Steinquist Mechanical Aptitude No. 2, PEI Mechanical Principles, and Yale Mechanical Ingenuity may be classified as mechanical comprehension tests. Comparing the correlations obtained by the studies in Table VIII for these two groups of tests, it is found that the median correlation for the manipulative tests is .22 and for the mechanical comprehension tests, .39. This would indicate that tests which attempt to measure the

---

5. E. N. Brush, "Mechanical Ability as a Factor in Engineering Aptitude," The Journal of Applied Psychology, 25:306-07, June, 1941.
G. W. Holcomb, and H. R. Laslett, "A Prognostic Study of Engineering Aptitude," The Journal of Applied Psychology, 16:112, April, 1932.
S. R. Laycock, and N. B. Hutcheon, "A Preliminary Investigation into the Problem of Measuring Engineering Aptitude," The Journal of Educational Psychology, 30:284, April, 1939.
K. W. Vaughn, "The Yale Scholastic Aptitude Tests as Predictors of Success in the College of Engineering," The Journal of Engineering Education, 34:576, April, 1944.
K. W. Vaughn, "A Proposed Engineering Aptitude Test for High School Students," The Journal of Engineering Education, 38:119, October, 1947.

ability to comprehend mechanical principles and relationships show definite promise of becoming an important factor in engineering academic success. Scores on the manipulative tests would tend to have lower correlations with scholastic achievement in engineering since these tests measure manual dexterity as well as mechanical insight.

Three of the tests included in Table VIII were not classified into the two groups just discussed. One of these is the MacQuarrie Test for Mechanical Ability. In the strict sense of the word, this test is not a manipulative test since it is a paper and pencil test and no objects are handled. However, the test does give an indication of a person's aptitude for acquiring manipulative skills and it measures to some extent the ability to recognize space relations, speed of decision and of movement, hand and eye coordination, muscular control, and visual acuity.[6] There are seven subtests which consist of such tasks as tracing, tapping, dotting, copying, location, blocks, and pursuit. It is interesting to note the discrepancy in the results obtained by Holcomb and Laslett ($r = .48$) and Brush ($r = .249$) with the MacQuarrie Mechanical Ability Test. From the nature of the test it would seem that the result obtained by Brush is

---

6. W. V. Bingham, Aptitudes and Aptitude Testing (New York: Harper and Bros., 1937), pp. 314-15.

closer to being true.

The exact nature of the Cox Mechanical Models Test could not be determined by the writer from various reports on this test. Ten wooden models are involved in this test, and it is believed that the proctor handles each wooden object. If such is the case, this test could be classified as a mechanical comprehension test. There is doubt as to the validity of the Cox Mechanical Models Test since Brush obtained a correlation of .403 and Laycock and Hutcheon found a correlation of .16. The small number of cases involved in each of these studies may account for some of the discrepancy. Most reports on the Cox Mechanical Models Test agree that the instructions for administering this test are quite complicated, and this fact may also contribute to the wide discrepancy found in the results of these two studies.

Another unclassified test is the Steinquist Mechanical Aptitude Test No. 1, one of the pioneer tests in this field. This test is not a manipulative test, nor does it attempt to measure comprehension of mechanical principles and relationships. The test consists of ninety-five problems in which the task is to match pictures of common tools and mechanical contrivances. This would measure the ability to preceive the operational uses of certain tools and mechanical devices, and this ability would depend to a certain extent on familiarity with these tools and devices. It is interesting to note the

comparison of the Stenquist Mechanical Aptitude Tests No. 1 (r = .15) and No. 2 (r = .43) made by Holcomb and Laslett. The Stenquist Mechanical Aptitude Test No. 2 contains questions about pcitures and diagrams of machines and machine parts which presumably call for keen perception of mechanical relations and ability to reason about them.[7] This test would be classified as a mechanical comprehension test and understandably would have a higher validity coefficient than the Stenquist Mechanical Aptitude Test No. 1.

The results of the studies on mechanical ability show that tests which measure this ability are a factor in engineering academic achievement although the validity coefficients are low. Tests which purport to measure the ability to preceive mechanical relationships and understand mechanical principles show the best promise. Since the predictive value of these tests are limited, there is need for study of the diagnostic value of these tests of mechanical insight to determine the minimum degree of understanding necessary for engineering study and to determine which courses in the engineering curriculum are best predicted by measures of mechanical ability.

---

7. W. V. Bingham, Aptitudes and Aptitude Testing (New York: Harper and Bros., 1937, p. 320.

Spatial Visualizing Ability

Ordinarily, aptitude for dealing with spatial relations is considered a factor of mechanical intelligence. In most of the tests of mechanical ability just discussed, some degree of spatial visualizing ability is measured. However, a number of tests have been developed for the specific purpose of measuring this special ability, and therefore these tests deserve consideration as a separate factor in engineering academic success.

In Table IX are the results of validity coefficients obtained by four studies using various spatial relations tests. The studies summarized in this table are those by Berdie, Brush, Laycock and Hutcheon, and Vaughn.[8]

Of the above group of tests, the Minnesota Spatial Relations Test shows the lowest correlation. This test is administered individually, and consists of four standard form-boards, out of each of which have been cut fifty-eight pieces

---

8. R. F. Berdie, "The Prediction of College Achievement and Satisfaction," The Journal of Applied Psychology, 28: 242, June, 1944.
E. N. Brush, "Mechanical Ability as a Factor in Engineering Aptitude," The Journal of Applied Psychology, 25:306-07.
S. R. Laycock, and N. B. Hutcheon, "A Preliminary Investigation into the Problem of Measuring Engineering Aptitude," The Journal of Educational Psychology, 30:284, April, 1939.
K. W. Vaughn, "The Yale Scholastic Aptitude Tests as Predictors of Success in the College of Engineering," The Journal of Engineering Education, 38:284, 576, October, 1947.

TABLE IX

SUMMARY OF CORRELATIONS BETWEEN VARIOUS TESTS OF SPATIAL VISUALIZING ABILITY AND ACADEMIC SUCCESS IN FRESHMAN ENGINEERING OBTAINED BY FOUR PREDICTIVE STUDIES

Author	Name of Test Used	1st Sem. r	2nd Sem. r	No. of Cases
Berdie	Minn. Paper Form Bd.		.22	154
Brush	Minn. Paper Form Bd.*		.420	104
Brush	Minn. Spatial Relations*		.064	104
Brush	Minn. Paper Form Bd.	.175		77-160
Laycock & Hutcheon	British Form Relations		.25	144
Vaughn	PEI Spatial Visualizing	.35**		--
Vaughn	Yale Spatial Visualizing		.385	643

*Individual Test.

**Median correlation of ten colleges of engineering.

of different forms and sizes. The task is to put each of these pieces in its proper space. The test therefore proposes to measure speed and accuracy in discriminating sizes and shapes. Since the test is a manipulative one, the factor of manual dexterity is inherent and the test would naturally have a low correlation with scholastic achievement for reasons just previously discussed in connection with mechanical ability.

The Minnesota Paper Form-Board Test and the British Form Relations Test are of the same variety of space relations tests. The Minnesota Paper Form-Board Test consists of problems in which irregular figures are presented and the student is required to select from a group of accompanying figures the one which embodies the original irregular figures. The British Form Relations Test consists of drawings of squares or cubes with certain portions cut out and the student is required to select from a number of drawings the ones which will fit into the missing portions of the squares or cubes. In Table IX the validity coefficients of Berdie, Brush, and Laycock and Hutcheon are in the neighborhood of .20, which is rather low. In addition, Brush found that the individual form of the Minnesota Paper Form-Board Test had a substantially higher validity coefficient.

The spatial visualizing tests of the Yale Scholastic Aptitude Tests and the Pre-Engineering Inventory have been previously described, and it should be pointed out here that

they are a departure from the paper form-board type. Both of these tests contain a section in which the student is required to visualize in terms of orthographic representation of an object. It is evident that an effort has been made to measure those spatial visualizing abilities which more closely correspond to those actually used in certain engineering subjects as engineering drawing and descriptive geometry. The result of this effort is shown in the fact that the validity coefficients of these two tests are markedly higher than other spatial relations tests.

Special Verbal Abilities

At first consideration it may seem that a discussion of special verbal abilities overlaps the previous discussion of achievement tests in English. The English achievement tests studied in the previous chapter and summarized in Table VI were limited primarily to the mechanics of English usage, such as spelling, vocabulary, punctuation, grammar and diction, capitalization, and sentence structure. Attempts have been made recently to construct verbal tests which emphasize such special abilities as comprehension, reasoning, and interpretation of certain reading material. The validity coefficients of some of these special verbal abilities tests are summarized in Table X. The studies used in this table are those made by Feder and Adler, Holcomb and Laslett, and

TABLE X

SUMMARY OF CORRELATIONS BETWEEN TESTS OF SPECIAL VERBAL ABILITIES AND ACADEMIC SUCCESS IN FRESHMAN ENGINEERING

Author	Name of Test Used	1st Sem. r	2nd Sem. r	No. of Cases
Feder & Adler	Iowa Silent Reading	.57	.50	99
Holcomb & Laslett	Iowa Silent Reading		.40	--
Vaughn	Yale Verbal Comprehension		.310	120
Vaughn	PEI General Verbal	.38*		--
Vaughn	PEI Technical Verbal	.47*		--
Vaughn	PEI Scientific Materials	.55*		--

*Median correlations of ten colleges of engineering.

Vaughn.[9]

For the particular group of special verbal abilities tests in the above table, the median correlation was computed to be .47, which exactly corresponds to the median correlation computed for the achievement tests in English summarized in the previous chapter. This might be construed to mean that the special verbal abilities tests are no improvement over the English achievement tests. Further analysis of these verbal abilities tests might produce results that show promise.

The test having the lowest validity coefficient in Table X is the Yale Verbal Comprehension Test. Close analysis of the nature of this test reveals certain possible weaknesses which could explain its low validity coefficient with engineering achievement. In the first section of this test, the student's comprehension of the central thought of a paragraph is determined indirectly by the choice of one word which destroys the meaning of the paragraph. In such a situation

---

9. D. D. Feder, and D. L. Adler, "Predicting the Scholastic Achievement of Engineering Students," The Journal of Engineering Education, 29:381, January, 1939.
G. W. Holcomb, and H. R. Laslett, "A Prognostic Study of Engineering Aptitude," The Journal of Applied Psychology, 16:112, April, 1932.
K. W. Vaughn, "The Yale Scholastic Aptitude Tests as Predictors of Success in the College of Engineering," The Journal of Engineering Education, 34:576, April, 1944.
K. W. Vaughn, "A Proposed Engineering Aptitude Test for High School Students," The Journal of Engineering Education, 38:119, October, 1947.

the student is required to determine a certain consistency of thought in a paragraph which may not indicate the student's ability to comprehend and interpret the meaning of the paragraph. The remaining two sections of the test consist of verbal analogies and word recognitions which are types of items found in general scholastic aptitude tests or general intelligence tests. This would weight the Yale Verbal Comprehension Test heavily with general scholastic ability items, and would tend to make the correlation low with engineering academic success, as previously discussed in connection with general scholastic ability tests.

The General Verbal Ability Test of the Pre-Engineering Inventory shows the next lowest validity coefficient in Table X. As previously noted, this test contains a section on recognition of word meanings and another section on comprehension of selected reading passages. Eighty-one per cent of this test consists of word meanings and the rest of it is verbal comprehension. Therefore this test is heavily weighted with general vocabulary items and would tend to have a low validity coefficient with engineering scholastic achievement.

The Technical Verbal Ability Test of the Pre-Engineering Inventory is likewise a vocabulary test, but it attempts to measure the student's ability to recognize meanings of technical words found in the reading material of science and mathematics. This test combined with the Comprehension of

Scientific Materials Test of the Pre-Engineering Inventory indicates a different approach to measuring verbal abilities in engineering. In these two tests, verbal abilities are considered to be specifically related to the nature of the content material used, and therefore the material for these tests is drawn from the course content in engineering. The increase of the validity coefficients for these two tests over the General Verbal Test would tend to validate their approach to measuring verbal abilities in engineering, and further study of their approach might lead to more significant results.

Table X also shows that relatively high validity coefficients are obtained through use of the Iowa Silent Reading Test although there is a discrepancy in the results obtained by Feder and Adler ($r = .57, .50$) and Holcomb and Laslett ($r = .40$). This discrepancy is probably due to the small samplings involved and to the variations found prevalent among various colleges and universities. This test consists of five parts. Part I contains items involving the meaning of paragraphs taken from science and literature. Part II is a vocabulary test consisting of words drawn from the subject areas of social science, science, mathematics, and English. In Part III the student is required to select the central idea of a paragraph and to outline the paragraph organization. Part IV is a sentence meaning test. Part V measures the student's ability to locate information, to use an index, and

to select key words. It is evident from this brief description that the Iowa Silent Reading Test attempts to measure certain functional verbal abilities in specific kinds of reading material.

A further interesting analysis may be made by comparing the validity coefficients of the PEI Comprehension of Scientific Materials Test ($r = .55$) and the achievement tests in physics and chemistry summarized in Table V of the previous chapter (median $r = .54$). Practically the same subject matter is covered by these tests, but a different approach is used by the PEI test. It is evident that there is very little difference in the predictive value of these two types of tests. The value of the PEI Comprehension of Scientific Materials Test over the science achievement tests will have to be determined on the basis of differential prediction, which will be discussed later in this chapter.

Quantitative Reasoning and Interpretation

There have been recent attempts to measure aspects of mathematical ability other than the ability to solve the usual textbook exercises which comprise the majority of items found in mathematics achievement tests. The more recent mathematical ability tests attempt to measure the student's ability to reason and interpret quantitatively in given problem situations rather than to measure only the student's skill in manipulating

mathematical symbols and numbers. Studies using tests of quantitative reasoning and interpretation in connection with predicting engineering academic success are few in number, and their results are summarized in Table XI.[10]

The Iowa Mathematics Placement Test was one of the first to break away from the straight achievement-type of test in mathematics. The first section of this test, called Mathematics Training, is an achievement type of test containing items in arithmetic, algebra, geometry, and algebraic formulation. The Mathematics Aptitude section of this test, however, consists of the following parts:

Part I - Student is presented with various number series and is required to determine the principle involved and apply it.

Part II - Student is required to solve verbal exercises of various types.

Part III - Student is asked to determine the true and false conclusions from given hypotheses.

Part IV - Student is required to match bracketed phrases of a given passage in mathematics with questions on the passage.

---

10. Results in this table are drawn from the following studies: A. Dvorak, and R. C. Salyer, "Significance of Entrance Requirements for the Engineering College at the University of Washington," The Journal of Engineering Education, 23:620, April, 1933; D. D. Feder, and D. L. Adler, op. cit., p. 381; H. H. Remmers, and H. E. Geiger, "Predicting Success and Failure of Engineering Students in the School of Engineering in Purdue University," Purdue University Studies in Higher Education, 38:17, May, 1940; Vaughn, op. cit., pp. 284, 576.

TABLE XI

SUMMARY OF CORRELATIONS FOUND BY VARIOUS STUDIES BETWEEN TESTS OF QUANTITATIVE REASONING AND INTERPRETATION AND ACADEMIC SUCCESS IN FRESHMAN ENGINEERING

Author	Name of Test Used	1st Sem. r	2nd Sem. r	No. of Cases
Dvorak & Salyer	Iowa Math. Placement		.577	--
Feder & Adler	Iowa Math. Placement	.72	.69	84-99
Remmers & Geiger	Iowa Math. Placement	.687		1087
Vaughn	PEI General Math. Ability	.62*		--
Vaughn	Yale Quantitative Reasoning		.504	643
Vaughn	Yale Math. Aptitude		.513	643

* Median correlation of ten colleges of engineering.

The Mathematics Aptitude section of the Iowa Mathematics Placement Test is an early attempt to explore various factors in mathematical ability, and the validity coefficients of this test are among the highest reported in Table XI. If the studies using this test had reported separate validity coefficients for each section, a more significant analysis could have been made.

The two Yale Tests of Quantitative Reasoning and Mathematics Aptitude afford an interesting comparison. The Yale Mathematics Aptitude Test is primarily an algebraic achievement test since it consists of solving for unknowns in algebraic equations and writing formulas from verbal statements. The Yale Quantitative Reasoning Tests consist of tasks requiring the discovery of principles in mathematical data and the drawing of conclusions from given quantitative relationships. These tasks are quite similar to those required in the Mathematics Aptitude section of the Iowa Mathematics Placement Examination. The achievement-type test shows a validity coefficient of .513 and the quantitative reasoning type of test has a validity coefficient of .504. These two types of test have about the same predictive value and their validity coefficients are the lowest reported in Table XI when considered separately. The combination of the two Yale tests which would result in a similar type test as the Iowa Mathematics Placement Examination would probably have a

validity coefficient about the same as that of the Iowa test.

The previous description of the General Mathematical Ability Test of the Pre-Engineering Inventory reveals that this test contains a section of achievement-type items and a section of quantitative reasoning and interpretive type of items. Combination of the two sections results in a validity coefficient of .62, which is only slightly lower than that generally obtained for the Iowa Mathematics Placement Examination.

The median of the correlations listed in Table XI is found to be .62, which is somewhat higher than the median correlation ($r = .52$) obtained in Table IV for the mathematics achievement tests. This would indicate that the inclusion of items which measure the ability to reason and interpret quantitatively results in an increase in predictive value of mathematics tests.

Differential Predictive Value

Differential prediction is primarily the prediction of relative achievement in different subjects or groups of subjects. In addition to predicting general achievement in college, differential prediction attempts to determine in what subject area a student is most likely to do his best work. According to Crawford and Burnham, differential prediction implies two basic assumptions: (1) That different

types of thinking ability are required for successful achievement in different subject areas; (2) that there is usually variation in the levels of these abilities for each individual.[11]

Certain difficulties have been encountered in differential prediction including the unreliability of college marks, differences in departmental standards and procedures and varying levels of ability of students who are attracted by different departments.[12] In spite of these and other difficulties, a certain amount of progress has been made in differential prognosis.

In general, two methods have been used to determine the differential predictive value of a test. The first method is by correlation analysis. Coefficients of correlation are computed for the test in the various subject areas. If the test has a high validity coefficient for one subject area and markedly lower validity coefficients for the other areas, then the test has differential predictive value for that subject area.

The second method may be called a bi-modal distribution

---

11. A. B. Crawford, and P. S. Burnham, Forecasting College Achievement (New Haven: Yale University Press, 1946), p. 5.
12. A. C. Eurich, and L. F. Cain, "Prognosis," Encyclopedia of Educational Research (New York: The Macmillan Co., 1941), p. 852.

analysis. The test is administered to groups of students who have demonstrated successful achievement in their subject area major; for example, engineering majors and liberal arts majors. If the average test score for the engineering group is significantly different from the average score of the liberal arts students or other groups of students, then the distribution of test scores would be bi-modal in nature and the test would be differentiating engineering students from the rest of the students.

A differential predictive analysis has been made for the two test batteries described earlier in this chapter, the Yale Educational Aptitude Battery and the Pre-Engineering Inventory. Crawford and Burnham made a correlation analysis to determine the differential value of the Yale tests, and their results are summarized in Table XII.

Underlined in Table XII are the validity coefficients for the tests with appropriate criteria. The verbal section of the Scholastic Aptitude Test has higher validity coefficients for English and history whereas the Verbal Reasoning Test has higher validity correlations for physics. Both tests therefore have differential value. The Mathematical Aptitude Test tends to differentiate both physics and mathematics from the other subjects. Since physics is differentiated by two tests, this would indicate that physics requires certain special abilities measured by the Verbal

TABLE XII[a]

SUMMARY OF CERTAIN VALIDITY CORRELATIONS FOR APTITUDE TESTS ADMINISTERED TO YALE FRESHMAN CLASSES OF 1944 AND 1945

1st Term Course	Class	No. of Students	I SAT	II ALT	III VRT	IV QRT	V MAT	VI SVT	VII MIT
General Average	1944	829	.38	.33	.37	.31	.29	.20	.22
	1945	969	.49	.39	.39	.29	.28	.19	.19
English & History	1944	290	.49	.34	.40	.23	.16	.22	.17
	1945	286	.44	.25	.30	.22	.18	.11	-.01
Physics	1944	55	.40	.37	.52	.36	.45	.40	.24
	1945	62	.31	.43	.45	.40	.51	.35	.40
Mathematics	1944	291	.08	.21	.10	.23	.32	.11	.07
	1945	394	.23	.38	.35	.39	.49	.26	.30
Engr. Draw.	1944	202	.11	.07	.23	.41	.15	.55	.42
	1945	293	.19	.22	.24	.30	.37	.56	.47

[a] Adapted from Crawford and Burnham, Forecasting College Achievement, p. 268.

SAT - Scholastic Aptitude (verbal)
ALT - Artificial Language
VRT - Verbal Reasoning
QRT - Quantitative Reasoning
MAT - Mathematical Aptitude
SVT - Spatial Visual
MIT - Mechanical Ingenuity

Reasoning Test and Mathematical Aptitude Test. Engineering Drawing is likewise differentiated from the other subject areas by two tests, the Spatial Visual Test and the Mechanical Ingenuity Test. In this type of analysis, it is soon evident that the important consideration is the relative differences in validity coefficients for each test with the various subject areas. If a test has an outstanding validity coefficient with a certain subject area while the coefficients are relatively low for the other areas, then the test has differential value.

Table XII also reveals that two tests of the Yale Battery failed to differentiate for the subject areas considered. The Artificial Language Test understandably does not discriminate among the subjects listed because the nature of its construction would indicate that the test has possible differentiating value for foreign language which is not included in the table. Not so clear is the reason why the Quantitative Reasoning Test does not discriminate among the subjects listed. Crawford and Burnham found that this test had a somewhat higher correlation with mathematics and engineering drawing combined.[13] This would indicate that certain quantitative-spatial factors are being measured by this test. The test

---

13. A. B. Crawford, and P. S. Burnham, Forecasting College Achievement (New Haven: Yale University Press, 1946), p. 161.

also contains items which are found in tests of general scholastic ability, such as number series and symbolic relationships. Further study and analysis are needed to determine the type of items which would increase the discriminating power of the test.

Vaughn made a further correlation anaylsis of the Yale Educational Aptitude Battery in connection with engineering students from four institutions of higher learning.[14] Three classifications of courses were adopted:

1. Cultural subjects - English, history, social science, economics, speech, and other socio-humanistic courses.
2. Scientific subjects - Mathematics, physics, and chemistry.
3. Engineering subjects - Engineering drawing, descriptive geometry, engineering problems, and similar preprofessional subjects.

Table XIII summarizes the results found in this study.

Underlined in this table are the validity coefficients which indicate the discriminatory power of the tests. Comparison of the verbal section of the Scholastic Aptitude Test with the Quantitative Reasoning Test relative to cultural courses is an excellent example of how a differential analysis works. Table XIII reveals that the Quantitative Reasoning

---

14. K. W. Vaughn, "The Yale Scholastic Aptitude Tests as Predictors of Success in the College of Engineering," The Journal of Engineering Education, 34:572-82, April, 1944.

TEST XIII[a]

SUMMARY OF CORRELATIONS OF YALE APTITUDE TESTS
WITH ACHIEVEMENT IN FRESHMAN COURSES

		Cultural Courses		Scientific Courses		Engineering Courses		Freshman Average	
Tests		N	r	N	r	N	r	N	r
I.	SAT	105	.398	120	.299	116	.059	120	.310
II.	ALT	595	.356	641	.353	610	.238	643	.363
III.	QRT	595	.434	641	.483	610	.353	643	.504
IV.	SVT	595	.236	641	.364	610	.411	643	.385
V.	MAT	595	.373	641	.509	610	.387	643	.513
VI.	MIT	595	.189	641	.312	610	.269	643	.307

[a]Adapted from Vaughn, "The Yale Scholastic Aptitude Tests as Predictors of Success in the College of Engineering," p. 577.

SAT -- Scholastic Aptitude (verbal)
ALT -- Artificial Language
QRT -- Quantitative Reasoning
SVT -- Spatial Visual
MAT -- Mathematical Aptitude
MIT -- Mechanical Ingenuity

Test has a higher validity correlation (r = .434) with cultural courses than does the Scholastic Aptitude Tests (r = .398). It is further revealed, however, that the Quantitative Reasoning Test has an equally high validity coefficient for scientific courses, and therefore this test has no particular differential value. Although the Scholastic Aptitude Test (Verbal) has a relatively lower validity correlation with cultural courses, the correlation is higher than the corresponding correlations for the other subject areas, and therefore this test has discriminating value for cultural courses.

The fact that the Scholastic Aptitude Test (Verbal), Spatial Visual Test, and Mathematical Aptitude Test have differential value is in accord with the results found earlier in Table XII. Likewise, the fact that the Artificial Language Test and the Quantitative Reasoning Test have no differential value in Vaughn's study agrees with the results of Crawford and Burnham. The one discrepancy between the two studies is the fact that Vaughn's study reveals no differential value for the Mechanical Ingenuity Test. This might be due to the addition of engineering courses other than engineering drawing. The combination of the various subjects in Vaughn's study is open to question, particularly the combination of mathematics, physics, and chemistry. A more significant study would have been made had these subject areas been considered separately.

Vaughn illustrates the method of bi-modal distribution analysis in determining the differential value of the Pre-Engineering Inventory.[15] The first three tests of the Pre-Engineering Inventory were administered to 1,175 freshman students entering in the fall of 1943 at an unidentified university. This class was divided into the following groups: engineering students, science students, liberal arts students, and business or commerical students. Table XIV presents the results found by Vaughn.

The General Verbal Test fails to differentiate one group of students from the other groups. The liberal arts students have the highest average on this test, but the chances are 50 out of 100 that a significant difference exists between the engineering students and liberal arts students.

Table XIV reveals, however, that the engineering students are differentiated from the other groups to some extent on the basis of the Technical Verbal and Scientific Materials Tests. These tests do not discriminate very well between engineering students and science students since there are only 60 chances in 100 that the differences are significant. Likewise the chances are 79 out of 100 that a significant difference exists between engineering students and liberal

---

15. K. W. Vaughn, "Basic Consideration in a Program of Freshman Evaluation," The Journal of Engineering Education, 35:161-179, November, 1944.

TABLE XIV[a]

SUMMARY OF MEANS AND STANDARD DEVIATIONS OF SCORES ON THREE PRE-ENGINEERING INVENTORY TESTS FOR FOUR GROUPS OF FRESHMEN AT AN UNIDENTIFIED UNIVERSITY

		I. General Verbal		II. Technical Verbal		III. Scientific Materials	
Group	N	M	S.D.	M	S.D.	M	S.D.
Engineering	428	39.46	16.22	47.89	16.29	47.97	15.31
Science	167	41.43	16.02	43.14	15.48	42.96	15.14
Liberal Arts	162	42.94	15.91	29.54	16.93	31.75	16.16
Business	418	33.20	15.46	19.00	11.47	24.10	12.84

[a] K. W. Vaughn, "The Yale Scholastic Aptitude Tests as Predictors of Success in the College of Engineering," p. 577.

arts students on the basis of these tests. The critical ratios do show, however, that there is a significant difference at the 5 per cent level between engineering students and business students on these tests.

One weakness in Vaughn's study can be found in the fact that the groups of students are formed solely on the basis of enrollment in certain schools or colleges within the university studied. A more significant analysis could have been made if the groups were made on the basis of successful achievers in the various areas of study.

Chapter Summary

In this chapter, the search for special ability measures in engineering is taken into studies using specialized educational aptitude tests. The construction of these tests is based upon the belief that aptitudes are specific as well as general, and therefore the content of these tests is primarily items which simulate specifically the kinds of tasks likely to be met in the pursuit of a certain area of study. By nature of their construction, these tests provide fruitful sources for special ability analysis. Two aptitude test batteries, the Yale Educational Aptitude Battery and the Pre-Engineering Inventory, were described fully in order to indicate the scope of these specialized aptitude tests.

Measures of mechanical ability were discussed first in connection with engineering achievement. Results showed that tests which tend to measure comprehension of mechanical principles and relationships were superior to tests involving the manipulation of certain mechanical objects. The correlations for these tests with engineering scholastic achievement were low, which points to the need for further study of the diagnostic value of these mechanical ability measures.

Various tests of spatial visualizing ability were analyzed and found to be a factor in engineering study. Tests which require visualization in terms of graphic representation were found to be somewhat superior to the paper formboard type of test. This is probably due to the fact that engineering students are called upon to work with graphic representations of objects in their courses.

Next considered were tests of special verbal abilities which emphasize certain special abilities, such as comprehension, reasoning, and interpretation of specific kinds of reading material. No particular increase in predictive value was found for these tests over the English achievement tests. It was later shown, however, that these special verbal abilities tests have distinct differential value. In the analysis of these test, it was found that the tests which contained items of a general nature tend to have lower validity coefficients. Tests which attempt to measure verbal reasoning and

interpretation of technical reading material found in engineering courses have greater predictive and differential value.

Tests of quantitative reasoning and interpretation have been a fairly recent development in the field of mathematical aptitude tests. In connection with engineering study, it was found that single tests of achievement and of interpretation in mathematics have lower correlations than do tests which combine the two types of approach. An analysis of the quantitative reasoning tests showed that the ones containing items of a general nature such as number series and symbolic relationships tend to have lower validity coefficients than do the tests which require mathematical ingenuity and reasoning in technical data found in engineering study.

A differential analysis of the Yale Educational Aptitude Battery and the Pre-Engineering Inventory indicates that specialized aptitude tests have definite possibilities of being able to discriminate among the various subject areas and groups of students. This analysis also indicates that tests which are more specific in their content have greater differential value. On the other hand, it was indicated that specialized aptitude tests showed no particular gain in predictive value over the other types of tests. This might be due to the fact that this type of test is relatively new in the field of measurement and has not been fully developed as yet.

Studies that have been investigated up to this point have been primarily concerned with the predictive value of special ability measures and only a few have explored the discriminating value and diagnostic value of these tests. There is a definite need for a more searching analysis of these tests to determine more exactly the nature of the special abilities measured by these tests and to derive certain principles of test construction which have proven effective in order to consolidate the gains already made. Furthermore, there is need for a more thorough investigation of the relationship between these tests and certain sections of the engineering curriculum rather than the whole engineering curriculum. The rest of this study will attempt to make such an anlysis of the Pre-Engineering Inventory in connection with engineering scholastic achievement.

CHAPTER IV

DIFFERENTIAL ANALYSIS OF THE PRE-ENGINEERING INVENTORY

The previous chapter has indicated the nature of differential analysis and how it is used in connection with special abilities tests. The type of differential analysis made here in this study will be the correlation type in which correlation coefficients are computed between various ability measures and different criteria in the engineering curriculum.

Experimental Groups

On September 14, 1946 the Pre-Engineering Inventory was administered to 1,356 students who enrolled in the College of Engineering, University of California at Berkeley, for the fall semester, 1946 at the freshman and sophomore levels. Of this group, records were obtained on 1,191 students, and for purposes of this study the students are classified as follows:

1 A Freshmen N = 190

This group consists of students who finished high school in June, 1946 and enrolled in the College of Engineering for the fall semester, 1946. Median age, eighteen years.

1 B Freshmen N = 466

Included in this group are students who had finished high school prior to June, 1946 and had taken courses at the college level but were still classed as freshmen in engineering. In most cases, their schooling was interrupted by service in the armed forces; however, there were some students who took college level training while in the armed forces. Median age, twenty-two years.

1 C Freshmen N = 284

This group had graduated from high school prior to June, 1946 but had no previous college experience. Interruption due to the recent war is also an important factor for this group. Median age, twenty-two years.

1 D Freshmen N = 24

These are foreign students who registered as freshmen in engineering.

2 A Sophmores N = 227

This group consists of students taking the examination who had previously achieved sophomore standing in engineering either prior to or during the war, or both. Median age, twenty-three years.

This study is primarily concerned with the 474 students which comprise the 1 A and 1 C groups. These students may be

considered as beginning freshmen in engineering without any previous college background. The two groups are kept separate because the 1 C group is an older and more mature group than the 1 A group. In order to compare the beginning freshmen with a more advanced group, this study will also consider the sophomore group 2 A. The 1 B freshmen students are a nebulous in-between group and therefore will receive little consideration in this study. For obvious reasons, the small group of foreign students is eliminated.

In addition to the previous academic records which served as a basis for the classification of the students, records were obtained which indicated the scholastic achievement of the students in engineering during the two academic years of 1946-47 and 1947-48. The following is a summary of the academic status of these students at the end of the second academic year, June, 1948:

Group	Continuing	Withdrew in Good Standing	Withdrew in Poor Standing	Dismissed	Total
	%	%	%	%	%
1 A	48.4	23.0	11.2	17.4	100.0
1 C	58.0	18.0	9.4	14.6	100.0
2 A	71.4	8.2	10.0	10.4	100.0

These results indicate what is generally found to be true, that the more mature and advanced students tend to be more stable. Previous selective factors which have operated

in the sophomore group 2 A would insure the fact that a higher percentage of this group would still be continuing their studies in engineering at the end of two academic years. A combination of the continuing students with those who withdrew in good standing shows that there is very little difference between the 1 A group (71.4 per cent) and the 1 C group (76 per cent). This would indicate that there is only a slight scholastic difference between these two groups. The 1 A group is less sure of what area of study to pursue.

Comparison of the means and standard deviations for the 1 A, 1 C, and 2 A groups on the seven sub-tests of the Pre-Engineering Inventory is provided for in Table XV.

There is not much difference in average scores between the two freshmen groups and they have about the same variability. Therefore these two groups may be said to have about the same average level of certain abilities as measured by the Pre-Engineering Inventory. The sophomore group 2 A shows consistently higher average scores than the freshmen groups. Critical ratios indicate, however, that none of the differences in means between the freshman and sophomore groups are statistically significant. The greatest difference in means between the freshman and sophomore groups is found on the General Mathematics Test, and the chances that the true difference is greater than zero are 79 out of 100. The

TABLE XV

MEANS AND STANDARD DEVIATIONS ON THE SEVEN SUB-TESTS OF THE PRE-ENGINEERING INVENTORY FOR BEGINNING FRESHMAN AND SOPHOMORE ENGINEERING STUDENTS IN SEPTEMBER 1946

Tests	1A Freshmen		1C Freshmen		2A Sophomores	
	Mean	S.D.	Mean	S.D.	Mean	S.D.
I. General Verbal	44.02	21.24	46.87	20.76	53.08	23.24
II. Technical Verbal	52.33	15.06	49.74	14.82	65.00	14.30
III. Scientific Materials	55.46	15.96	54.36	14.56	64.70	15.60
IV. General Mathematics	45.96	13.80	44.84	15.05	59.07	13.58
V. Mechanical Principles	23.30	10.24	23.86	9.32	26.27	18.86
VI. Spatial Visualization	33.48	11.28	34.02	11.20	42.17	18.76
VII. Modern Society	32.75	11.60	34.07	10.85	37.09	16.52

variability of the groups is about the same except for the last three tests of Mechanical Principles, Spatial Visualization, and Modern Society where the sophomore group shows greater variability.

Criteria

As indicated in the introductory chapter, the criterion of scholastic achievement is measured by the weighted average of instructors' marks known at the University of California as the grade point average. The limitations in using this measure of academic success are widely recognized, and predictive studies are quick to point out the fact that a marking system employing only five intervals has a very definite effect in lowering their validity coefficients. Such factors as low criterion reliabilities, coarse grouping measures, and self-selection among students in their choice of courses are definite limitations to mental measurement and are roughly analogous to such factors as friction, weight, observation errors, and uncertain calibration, which serve to complicate physical measurement. These limitations need to be recognized and accounted for in any attempt to validate special ability measures against certain academic criteria. In light of these limitations, Crawford and Burnham believe that it seems reasonable to regard validity coefficients of .40 or more for specialized aptitude tests as being encouraging

with .60 as perhaps maximal.[1]

In order to make a differential analysis of the special ability measures in the Pre-Engineering Inventory, the pre-engineering curriculum is divided into the following five subject areas: mathematics, chemistry, physics, engineering, and cultural. An analysis of the catalogues of eighteen engineering colleges throughout the country shows that these areas comprise the pre-engineering curriculum of all the colleges studied.[2] For purposes of this study, these five subject areas are more specifically defined as follows:

Mathematics.--Includes analytical geometry, differential calculus, and integral calculus. Does not include intermediate algebra, trigonometry, and college algebra.

Chemistry.--Consists of courses in general introductory chemistry, inorganic chemistry, and organic chemistry taken at the freshman-sophomore level.

Physics.--Includes mechanics, heat, light, sound, electricity, and magnetism.

Engineering.--Includes the pre-professional engineering courses such as plane surveying, engineering drawing, descriptive geometry, advanced engineering drawing, engineering statics, manufacturing processes, and strength of materials.

---

1. A. B. Crawford, and P. S. Burnham, Forecasting College Achievement (New Haven: Yale University Press, 1946), p. 162.
2. Made by the writer in preparation of a report for the Southwestern Sectional Meeting of the American Society for Engineering Education, December, 1947.

and culture). An analysis of the catalogues of eighteen

areas comprise the pre-engineering curriculum of all the

colleges studied.[2] The purposes of this study, these five

subject areas are more specifically defined as follows:

calculus, and integral calculus. Does not include intermediate

algebra, trigonometry, and college algebra.

Chemistry.--Courses of courses in general introductory

at the freshman-sophomore level.

Physics.--Includes mechanics, heat, light, sound, elec-

tricity, and magnetism.

---

1. D. Crawford, and P. E. Burton, Preparing for College

Mathematics (New Haven: Yale University Press, 1941), p. 341.

2. Made by this writer in connection of a report for the

Southwestern Sectional Meeting of the American Society for

Does not include an orientation course in engineering.

Cultural.--Consists of courses in elementary economics, public speaking, history, English, political science, philosophy. Does not include courses in statistics, accounting, art, music, physical or life sciences, foreign language, and military science.

The definition of these five subject areas which will serve as criteria in the differential analysis of the Pre-Engineering Inventory is an important step. The subject areas of mathematics, chemistry, physics, and engineering are fairly well defined by the nature of the courses that are given in those areas. Not so clearly defined is the cultural area. The above definition indicates a heavy emphasis in the social studies area. This is the result of an attempt to define a homogeneous group of courses for this area on the basis of nature of content and nature of instruction. It was found for the experimental group that each student had at least one or more of the courses included in the cultural area on his record. The reasons for excluding certain subjects from the cultural area as defined above were: That the subjects overlapped too much with the areas already defined in the pre-engineering curriculum, e.g., statistics, accounting, and physical science courses; that the courses were a part of other areas of study such as foreign languages and life science courses; that the courses were only taken by an

Does not include an orientation course in engineering.

Optional.--Consists of courses in elementary economics, social sciences, literature, speech, modern languages, fine and applied art, music, physical or life sciences, foreign languages, and military science.

The definition of these five curriculum areas will serve as criteria in the differential analysis of the Engineering Inventory in an important step. The various areas of mathematics, chemistry, drafting, and engineering are fairly well defined by the nature of the courses that are given in these areas. But no clearcut method is the ordinal area. The second definition introduces a very vagueness in the ordinal studies area. This is the result of an attempt to define a large general group of courses for which there is basis of nature or content and methods of instruction. It was found for the experimental group that each student had at least one or more of the courses included in the curriculum from the cultural area as given above were. Even the subjects overlapped too much with the areas already defined in the physical sciences to mean that the courses were a part of

occasional engineering student; for example, art and music.

With the five subject areas now defined, it is possible to compare the grade point averages in each area obtained by the freshman groups 1 A and 1 C for the period of two academic years, 1946-1948. Table XVI presents a summary of these grade point averages.

The freshman group 1 C consistently obtained somewhat higher mean grade point averages in each of the subject areas and for the over-all average. Comparison of the results on the Pre-Engineering Inventory in Table XVI shows that the two groups had about equal level of ability at the beginning of their engineering study, yet the freshman group 1 C was able to obtain somewhat higher grades. The greatest difference is in the subject area of chemistry and is found to be significant. On the other hand, the differences in means for the remaining subject areas are not statistically significant and are too small to warrant any general interpretation. The standard deviations indicate that there is almost equal variation for the two freshman groups in the subject areas listed.

The interrelationships among the criteria of subject areas is another important factor in differential analysis because one of the basic assumptions previously mentioned in differential prediction is that different types of thinking ability are required for successful achievement in different subject areas. If the criteria are highly interrelated as shown by intercorrelations, then one ability measure will

TABLE XVI

MEANS AND STANDARD DEVIATIONS OF GRADE POINT AVERAGES IN FIVE SUBJECT AREAS FOR TWO GROUPS OF BEGINNING FRESHMAN ENGINEERING STUDENTS FROM 1946 TO 1948

	1A. Freshmen N-190		1C. Freshmen N-284	
Subject Area	Mean	S.D.	Mean	S.D.
Mathematics	1.143	.744	1.202	.736
Chemistry	1.201	.732	1.537	.642
Physics	1.393	.696	1.502	.696
Engineering	1.209	.704	1.254	.612
Cultural	1.273	.688	1.319	.664
Over-all GPA '46-'48	1.289	.596	1.349	.514

tend to predict equally well for all the criteria and it would be impossible to differentiate among the criteria.

Table XVII presents the intercorrelations among the five subject areas of the pre-engineering curriculum for the combined freshman groups 1 A and 1 C.

Probably the average intercorrelation for Table XVII is somewhat misleading because the correlations between the cultural subjects area and the other four subject areas are relatively low, whereas the intercorrelations among the four subject areas of mathematics, chemistry, physics, and mathematics are markedly higher. The average correlation between the cultural area and the other areas listed is .37. The average intercorrelation among four subject areas of mathematics, physics, chemistry, and engineering is .57. Crawford and Burnham obtained similar data on 1,634 Yale freshmen of 1934-36, and the average correlations found by them for the same relationships were .38 and .57 respectively, which are almost identical to those obtained in Table XVII.[3] No special significance can be attached to this close similarity except that the results of Table XVII are not likely to be out of line with results obtained elsewhere.

---

3. A. B. Crawford, and P. S. Burnham, Forecasting College Achievement (New Haven: Yale University Press, 1946), p. 98.

TABLE XVII

INTERCORRELATIONS AMONG THE FIVE SUBJECT AREAS OF THE PRE-ENGINEERING CURRICULUM FOR BEGINNING FRESHMAN ENGINEERING STUDENTS AFTER TWO YEARS OF STUDY, 1946 - 1948

Subject Areas	Freshman Groups 1A and 1C, N = 474				
	Mathematics	Chemistry	Physics	Engineering	Cultural
Mathematics	--	.570	.715	.565	.384
Chemistry	.570	--	.595	.418	.324
Physics	.715	.595	--	.530	.438
Engineering	.565	.418	.530	--	.332
Cultural	.384	.324	.438	.332	--

Range of intercorrelations .324-.715

Average .487

Median .438

Siemens obtained data on 497 engineering students who took their pre-engineering work at the College of Engineering, University of California at Berkeley, during the ten-year interval from 1928 to 1938. He computed intercorrelations among the subject areas of mathematics, physics, and chemistry for these students. The intercorrelations ranged from .69 to .87 and the average was found to be .75.[4] These results are considerably higher than those found in Table XVII. An explanation for this discrepancy can be found in the fact that Siemens used in his study only those students who had completed their two years of pre-engineering training and had continued at least one semester of junior level work.

In light of the forthcoming differential analysis which will use the five subject areas listed in Table XVII as criteria, there will probably be little difficulty in differentiating the cultural area from the other areas due to the low intercorrelations that have been obtained. For the other four areas, the intercorrelations range from .40 to .60 with the exception of the correlation .715 between mathematics and

---

4. C. H. Siemens, Prognosis of the Achievement of Engineering Students (Ph.D. dissertation, University of California, 1939), pp. 34, 38, 40.

physics. It is reasonable to assume, therefore, that there are distinguishing features in each subject area of the pre-engineering curriculum which warrant a differential analysis made on the basis of various special ability measures. The results of Table XVII certainly do not justify the combination of mathematics, physics, and chemistry into one subject area as was done by Vaughn.[5]

Differential Analysis

Product-moment coefficients of correlation were computed between the seven sub-tests of the Pre-Engineering Inventory and the five subject areas of the pre-engineering curriculum, by use of scattergram plots. Separate correlations were computed for the freshman groups 1 A and 1 C. Only the correlations between the sub-tests and the over-all grade point average were computed for the sophomore group 2 A since the subject areas for this group are not comparable to those of the freshman groups.

Predictive studies have consistently shown that validity coefficients for predictive measures tend to decrease as the length of time for the criteria increases.[6] Since the criteria

---

5. K. W. Vaughn, "The Yale Scholastic Aptitude Tests as Predictors of Success in the College of Engineering," The Journal of Engineering Education, 34:577, April, 1944.
6. See H. R. Douglass, "Different Levels and Patterns of Ability Necessary for Success in College," Occupations, 22:183, December, 1943.

for this study extend over a period of two academic years, it is reasonable to expect that the validity coefficients of the tests will be low. In a differential analysis, however, the general predictive value of a test is not the most important factor.

Table XVIII presents a summary of validity coefficients for the sub-tests of the Pre-Engineering Inventory.

Comparing the general predictive value of the tests for the freshman and sophomore groups, the over-all average is predicted somewhat better for the sophomore group than for the freshman groups, particularly by the General Mathematics Test where the validity coefficient is .590. As previously indicated, the nature of the academic work for these groups is different and may account for the discrepancy. Comparison of the two freshman groups shows that the general predictive value of these tests is about the same.

Turning now to the subject areas, where the particularly differentiating coefficients are underlined, Table XVIII reveals that the General Verbal Test (I) and the Modern Society Test (VII) discriminate well for the cultural subject area. These two tests have about equal predictive value for the cultural subjects, but the General Verbal Test does a better job of differentiating because its validity coefficients with the other subject areas are lower than those of the Modern Society Test. The discriminatory value of these two tests applies to both freshman groups.

TABLE XVIII

CORRELATIONS BETWEEN THE SEVEN SUB-TESTS OF THE PRE-ENGINEERING INVENTORY AND THE FIVE SUBJECT AREAS OF THE PRE-ENGINEERING CURRICULUM FOR FRESHMAN AND SOPHOMORE GROUPS, 1946-48

Subject Areas	Student Group	Pre-Engineering Inventory Sub-tests I	II	III	IV	V	VI	VII
General Average 1946-48	1A	.150	.344	.403	.416	.367	.288	.252
	1C	.241	.405	.436	.384	.322	.174	.329
	2A	.338	.447	.521	.590	.388	.210	.396
Mathematics	1A	.079	.289	.370	.519	.355	.350	.169
	1C	.179	.314	.349	.398	.269	.206	.221
Chemistry	1A	.192	.391	.417	.409	.357	.273	.306
	1C	.021	.323	.285	.290	.129	.035	.200
Physics	1A	.129	.244	.306	.257	.340	.304	.234
	1C	.144	.374	.316	.303	.216	.099	.172
Engineering	1A	-.039	.184	.333	.358	.385	.461	.095
	1C	.139	.232	.354	.302	.360	.285	.196
Cultural	1A	.340	.153	.200	.071	.094	.025	.329
	1C	.488	.323	.307	.172	.106	-.023	.499

Student groups:
- 1A - Beginning Freshmen, uninterrupted
- 1C - Beginning Freshmen, interrupted
- 2A - Entering Sophomores

Pre-Engineering Inventory Sub-tests:
- I - General Verbal
- II - Technical Verbal
- III - Scientific Materials
- IV - General Mathematics
- V - Mechanical Principles
- VI - Spatial Visual
- VII - Modern Society

The validity coefficients for the Technical Verbal Test (II) do not present a clear-cut picture. This test differentiates the chemistry area for the 1 A group and the physics area for the 1 C group. However, the validity coefficients relative to the over-all average are as high or higher than the validity coefficients relative to the subject areas for this test. The discriminatory value of the Technical Verbal Test is rather doubtful and needs further analysis.

The Scientific Materials Test (III) likewise presents a confusing picture from a differential standpoint. This test discriminates the chemistry area for the freshman group 1 A but has no discriminatory value for the 1 C group. However, for both groups this test has a high validity coefficient for the over-all average. This would indicate that the Scientific Materials Test has better predictive value for the general area of pre-engineering study than for any particular subject area within the curriculum.

The Mathematics Test (IV) definitely has differential value for the subject area of mathematics for both groups. Likewise the Spatial Visual Test (VI) discriminates well for the two freshman groups in the engineering subject area. The Mechanical Principles Test (V) differentiates the engineering subject area for the 1 C group but has no discriminatory value for the 1 A group. In both freshman groups this test has about equal predictive value for the general area of

engineering study and for the subject areas.

Generally speaking, Table XVIII reveals that the mathematics engineering, and cultural subjects areas are differentiated by one sub-test of the Pre-Engineering Inventory for both freshman groups. The chemistry and physics subject areas are not clearly differentiated by any of the sub-tests for both freshman groups, although the chemistry area seems to be differentiated for the 1 A group and the physics area for the 1 C group.

Five of the seven sub-tests of the Pre-Engineering Inventory contain two sections which use different approaches to measure the same special ability. In the anticipation of finding further significant results, scores were obtained for the freshman group 1 A for each section of the sub-tests and correlations were computed between these section scores and the subject areas of the pre-engineering curriculum.

In further subdividing the Pre-Engineering Inventory, the number of items in each section becomes important because the reliability of the section is affected by this factor. If the number of items becomes too small, the reliability of the test is questionable and the validity coefficients tend to be lower. The following is a list of the sections which are identified by a brief descriptive title and the number of items contained in each section.

Test I - General Verbal Ability

I A - Word meanings, 75 items
I B - General reading comprehension, 25 items

Test III - Comprehension of Scientific Materials

III A - Technical reading comprehension, 75 items
III B - Interpretation of technical data, 25 items

Test IV - General Mathematical Ability

IV A - Mathematical Computation, 60 items
IV B - Mathematical interpretation, 30 items

Test VI - Spatial Visualizing Ability

VI A - Graphic representation, 24 items
VI B - Cube identification, 32 items

Test VII - Understanding of Modern Society

VII A - Knowledge of American institutions, 40 items
VII B - Comprehension of social issues, 30 items

From the above list, the nature of what is measured by each section can be determined from the titles. The reliability of some of the sections is certainly open to question, particularly the ones containing only twenty-five items, and this would be an important factor in explaining any low validity coefficients obtained for these sections.

Table XIX presents the validity coefficients for the sections of the Pre-Engineering Inventory.

This table provides for a differential analysis of each section of the Pre-Engineering Inventory. The vertical

VI A - Graphic representation, 2b items
VI B - Cross tie diffusion, 52 items

Item VII - Threatening of Modern Society

VII A - Emergence of American Institutions, 90 items
VII B - Consolidation of Social Issues, 31 items

TABLE XIX

CORRELATIONS BETWEEN TEN SECTIONS OF SUB-TESTS IN THE PRE-ENGINEERING INVENTORY AND THE FIVE SUBJECT AREAS OF THE PRE-ENGINEERING CURRICULUM FOR THE FRESHMAN GROUP 1A, 1946-48

	Sub-test Scetions of Pre-Engineering Inventory									
Subject Areas	IA	IB	IIIA	IIIB	IVA	IVB	VIA	VIB	VIIA	VIIB
General Average	.124	.203	.353	.369	.367	.311	.333	.164	.305	.128
Mathematics	.052	.151	.323	.383	.452	.411	.375	.226	.178	.074
Chemistry	.163	.222	.382	.386	.430	.222	.308	.127	.325	.188
Physics	.107	.175	.192	.216	.255	.258	.274	.224	.280	.164
Engineering	-.058	.013	.321	.293	.328	.312	.531	.272	.088	.034
Cultural	.336	.311	.190	.129	.084	.060	.055	-.029	.344	.258

columns of the table are examined to determine any validity coefficients which are markedly higher than the remaining coefficients in the vertical column. Such validity coefficients are underlined which denote differentiation among the subject areas listed.

Table XIX reveals that both sections of the General Verbal Test (I A and I B) continue to differentiate the cultural area from the other subject areas. The Word Meanings section (I A) shows better differentiation, but this may be due in part to a greater number of items contained in this section than in the Comprehension section (I B). When these sections are combined, there is greater differentiation and increased predictive value for the cultural area as shown in Table XVIII.

The two sections of the Scientific Materials Test (III A and III B) failed to differentiate for any particular subject area. It was previously pointed out that the test as a whole shows better predictive value for the general area of pre-engineering study than for any particular subject area within the curriculum. Since neither section of the Scientific Materials Test showed any differential promise, further study of what abilities are measured is needed.

Previous analysis showed that the General Mathematics Test (IV) discriminated well for the mathematics subject area. Table XIX reveals that the Mathematical Interpretation

section (IV B) of this test is a much better discriminator than the Mathematical Computation section (IV A), although section IV A has a somewhat higher predictive value. This fact becomes even more significant when it is realized that section IV B contains only thirty items, whereas section IV A contains sixty items. Combination of the two sections results in an increased predictive value for the mathematics subject area and about the same differential value as for the Mathematical Interpretation section (IV A).

Table XIX likewise reveals that the Graphic Representation section (VI A) has much greater differential power for the engineering subject area than the Cube Identification section (VI B). Furthermore, it is revealed that section VI A has greater predictive value for the engineering subject area than either section VI B or the combination of sections VI A and VI B. The fact that the Graphic Representation section (VI A) has both predictive value and differential value for the engineering subject area would make whatever special ability is measured by this section particularly significant.

No particularly discriminatory value was found for the two sections VII A and VII B of the Understanding of Modern Society Test. The combination of these two sections did result in differentiation for the cultural area as was indicated previously in Table XVIII. The reason for this is due

in part to the small number of items in each section when considered separately.

Chapter Summary

The Pre-Engineering Inventory was administered to 1,356 freshman and sophomore engineering students in September, 1946. Excluding the advanced standing freshmen, a differential analysis was made for the sub-tests of the Pre-Engineering Inventory on the basis of 474 beginning freshman students and 227 sophomore engineering students. The beginning freshman students were divided into two groups: those who came direct from high school (1 A) and those whose schooling was interrupted between high school and college for a year or more (1 C).

Comparison of the means and standard deviations on the sub-tests of the Pre-Engineering Inventory showed that the two freshman groups were of approximately the same level of average ability and equal variation. The sophomore group 2 A consistently obtained higher average scores than the freshman groups, although the differences in means were not statistically significant.

The criteria used in the differential analysis of the Pre-Engineering Inventory are the following five subject areas of the pre-engineering curriculum: mathematics, chemistry, physics, engineering, and cultural subjects. These subject

areas were specifically defined by the courses included. Comparison of the grade point averages made in these subject areas by the two freshman groups revealed that the freshman group 1 C made slightly better average grades, although the differences were not statistically significant.

Intercorrelations among the five subject areas showed the cultural area to be unrelated to the other subject areas. The intercorrelations among the mathematics, physics, chemistry, and engineering subject areas were higher but still low enough to indicate that each subject area had distinguishing features for making worth-while a differential analysis.

Correlations between the various sub-tests of the Pre-Engineering Inventory and the pre-engineering subject areas served as a basis for the differential analysis. The General Verbal Test I was shown to have differential value for the cultural area. Likewise each of the two sections of this test showed differential power for the cultural area. The Technical Verbal Test II and the Mechanical Principles Test V had better predictive value for the general area of the pre-engineering curriculum than differential value for any particular subject area within the curriculum. Likewise the Scientific Materials Test III failed to show differentiation for the subject areas, but the test did have general predictive value. Further analysis indicated that neither section of this test showed differential promise.

The General Mathematics Test IV differentiated the mathematics subject area, and it was further shown that the Mathematical Interpretation section IV B had greater differential power than the Mathematical Computation section IV A of this test. The Spatial Visual Test VI had discriminatory value for the engineering subject area; however, it was later shown that all of the discriminating was done by the Graphic Representation section VI A, whereas the Cube Identification section VI B of this test had negligible differential value.

None of the sub-tests or sections of the Pre-Engineering Inventory had definite discriminatory value for the physics or chemistry subject areas. Further analysis is therefore needed to determine what ability measures are most likely to differentiate for these areas and to investigate the factors that caused certain measures of the Pre-Engineering Inventory to be especially differentiating while other measures failed. Such an analysis will be made in the following chapter.

CHAPTER V

FACTOR ANALYSIS OF THE PRE-ENGINEERING INVENTORY

In the previous chapter, the various sections of the Pre-Engineering Inventory have been identified with certain subject areas of the pre-engineering curriculum. It is now the purpose of this chapter to determine the nature of the special abilities measured in each of the sections of the Pre-Engineering Inventory. This analysis is made through use of intercorrelations among the sub-tests and sections of the Pre-Engineering Inventory and an item analysis of the test battery.

Intercorrelations

Intercorrelations among the sections of the Pre-Engineering Inventory give an indication of what measures are distinct and separate from the other measures. Also indicated is the amount of overlapping among the tests or what group of tests seem to be measuring the same factors.

First presented will be the intercorrelations among the seven sub-tests of the Pre-Engineering Inventory for the two freshman groups 1 A and 1 C. The intercorrelations listed in Table XX are computed from scattergram plots as was done for

TABLE XX

INTERCORRELATIONS AMONG THE SEVEN SUB-TESTS OF THE PRE-ENGINEERING INVENTORY FOR THE FRESHMAN ENGINEERING GROUPS 1A AND 1C

Tests	Fresh. Group	I*	II	III	IV	V	VI	VII
I. General	1A	--	.580	.680	.376	.465	.323	.738
Verbal	1C	--	.560	.601	.313	.287	.269	.714
II. Technical	1A	.580	--	.717	.551	.548	.500	.569
Verbal	1C	.560	--	.715	.534	.516	.364	.398
III. Scientific	1A	.680	.717	--	.729	.788	.670	.743
Materials	1C	.601	.715	--	.656	.698	.524	.536
IV. General	1A	.376	.551	.729	--	.686	.669	.452
Mathematics	1C	.313	.534	.656	--	.642	.448	.314
V. Mechanical	1A	.465	.548	.788	.686	--	.675	.580
Principles	1C	.287	.516	.698	.642	--	.603	.332
VI. Spatial	1A	.323	.500	.670	.669	.675	--	.378
Visual	1C	.269	.364	.524	.448	.603	--	.234
VII. Modern	1A	.738	.569	.743	.452	.580	.378	--
Society	1C	.714	.398	.536	.314	.332	.232	--

Range of intercorrelations: .234-.788
Median intercorrelation: .551
Average intercorrelation: .540

Freshman Groups: 1A, beginning freshmen uninterrupted N = 190
1C, beginning freshmen interrupted N = 284

the correlations previously reported in this study.

The freshman group 1 A consistently has higher intercorrelations than the freshman group 1 C. The largest difference is shown in the intercorrelations between Test V, Mechanical Principles, and Test VII, Modern Society, where the intercorrelation for the 1 A group is .580 and for the 1 C group, .332. However, the differences are generally small and no special significance can be placed upon these results. Considering Table XX as a whole, the intercorrelations among the tests are about the same for the two freshman groups 1 A and 1 C.

Test III, Scientific Materials, definitely has the highest intercorrelations with the other tests. These intercorrelations range from .788 with Test V, Mechanical Principles, to .525 with Test VI, Spatial Visualization. The average intercorrelation for the Scientific Materials Test III is .671. This would indicate that Test III measures factors that are included in the other tests and that this test does not particularly measure independent abilities. Therefore Test III could be excluded from the test battery without much loss as to the number of specific abilities measured by the battery. On the other hand, the test battery could be replaced by the Scientific Materials Test if a shorter form were needed. In the previous chapter it was shown that the Scientific Materials Test III had more general predictive value for pre-engineering

study than differential value for any of the subject areas of the curriculum. The reason for this is now found in the fact that Test III measures certain general factors that are found in the other special abilities tests.

Excluding Test III which has such high intercorrelations with the other tests, the following list presents the average of intercorrelations for each of the sub-tests of the Pre-Engineering Inventory:

Test	Average of Inter-correlations
I General Verbal	.463
II Technical Verbal	.512
IV General Mathematics	.501
V Mechanical Principles	.533
VI Spatial Visualization	.446
VII Modern Society	.470

The range of average intercorrelations is relatively small, from .446 for Test VI, to .533 for Test V, Mechanical Principles. These intercorrelations indicate certain general factors are present in all the tests. A certain amount of overlapping is to be expected because "the more complex the measures correlated, the greater are the chances that they will have common elements and the higher will their intercorrelations tend to be."[1] However, these intercorrelations

---

1. A. Anastasi, Differential Psychology (New York: The Macmillan Company, 1937), p. 110.

VII Orders Quickly 170

are sufficiently low to warrant the belief that separate abilities are being measured by these tests.

Table XXI next presents the intercorrelations for the sophomore group 2 A.

Comparing the intercorrelations of the above sophomore group with those of the freshman groups, the range and average of intercorrelations are practically identical. The average of intercorrelations for the sophomore group 2 A ($r = .544$) is somewhat lower than the average of intercorrelations for the freshman group 1 A ($r = .591$) although the difference is small. Comparison of the corresponding intercorrelations for the 1 A and 2 A groups reveals that in seven cases out of twenty-one, the intercorrelations for the sophomore group 2 A are higher than the corresponding intercorrelations for the freshman group 1 A. Generally speaking, studies have shown that as students progress in their educational development, their special abilities become more differentiated and intercorrelations among special ability measures for these students tend to decrease.[2] In this study no clear-cut trend has been noted in the comparison of the intercorrelations for the beginning freshman group 1 A and the entering sophomore group 2 A.

---

2. A. B. Crawford, and P. S. Burnham, Forecasting College Achievement (New Haven: Yale University Press, 1946), p. 157.

TABLE XXI

INTERCORRELATIONS AMONG THE SEVEN SUB-TESTS OF THE PRE-ENGINEERING INVENTORY FOR THE SOPHOMORE GROUP 2A, N = 227

Tests		I	II	III	IV	V	VI	VII
I.	General Verbal	--	.705	.703	.480	.396	.246	.718
II.	Technical Verbal	.705	--	.696	.573	.442	.212	.565
III.	Scientific Materials	.703	.696	--	.798	.740	.513	.711
IV.	General Mathematics	.480	.573	.798	--	.701	.466	.508
V.	Mechanical Principles	.396	.442	.740	.701	--	.560	.476
VI.	Spatial Visual	.246	.212	.513	.466	.560	--	.216
VII.	Modern Society	.718	.565	.711	.508	.476	.216	--

Range of intercorrelations: .212-.798

Median intercorrelation: .560

Average intercorrelation: .544

Once again the Scientific Materials Test III has the highest intercorrelations with the other tests in the battery. The average of intercorrelations for this test is .694 for the sophomore group as compared to .671 for the freshman groups. Excluding the Scientific Materials, Test III, the following are the average intercorrelations for each of the Pre-Engineering Inventory sub-tests as determined from Table XXI.

Test		Average of Inter-correlations
I	General Verbal	.509
II	Technical Verbal	.599
IV	General Mathematics.	.546
V	Mechanical Principles	.515
VI	Spatial Visualization	.340
VII	Modern Society	.497

The intercorrelation averages for the sophomore group are somewhat higher than the freshman groups for Tests I, IV, and VII, somewhat lower for Tests II and V, and markedly lower for Test VI, Spatial Visualization. Still no clear-cut trend can be noted in the comparison of intercorrelations for the freshman and sophomore groups. The intercorrelations of the tests for the sophomore group indicate that these tests measure separate special abilities at the sophomore level as well as at the freshman level.

I Power [Verbs]	[V]
II [Verbal] Terms	[Vn]
IV Powers [Nouns] [Adv.]	[Nv]
V Uncharacterized Items, [Adj.]	[Adj]
VII Indoor Country	[Adv]

The use of average intercorrelations to obtain a generalized picture of the amount of overlapping of the tests has definite limitations. Garrett points out that an arithmetic mean can be used if the range of correlations is relatively small. If the range is great, Fisher's "squared r" method should be used.[3] For purposes of this study, however, the arithmetic mean of the correlations will be sufficient in view of the restricted range of correlations and of the fact that only relative comparisons are made in which true values of the average correlations are not so important.

With the intercorrelations among the seven sub-tests of the Pre-Engineering Inventory available for the three groups 1 A, 1 C, and 2 A, it is possible to make a factorial analysis* of the test battery by determining which sub-tests seem to form natural groups as indicated by high intercorrelations. Such an analysis shows that Test I, General Verbal, and Test VII, Modern Society, form a natural group since their average correlation for the three groups of students is .710. Another group is formed by Test III, Comprehension of Scientific Materials, Test IV, General Mathematical Ability, and Test V, Mechanical Principles. The average intercorrelation between Test III and Test IV is .728, between Test III and

---

3. H. E. Garrett, Statistics in Psychology and Education (New York: Longmans, Green and Co., 1937), p. 283.

* Factorial analysis means in this study an informal inspectional analysis of the intercorrelations rather than a specific technique such as Thurstone's centroid method.

Test IV and Test V is .676. Test II, Technical Verbal, may be considered as peripheral to the latter group since its intercorrelation with Test III is high (average r = .704), but the intercorrelations between Test II and Test IV (average r = .553) and between Test II and Test V (average r = .502) are relatively low. The Spatial Visualization Test VI is shown to be relatively independent of the other tests.

In a factor analysis, it is generally customary to name the factors thus obtained. However, the identification of these factors will be withheld in this study until all the data have been completely presented.

Further intercorrelations for the freshman group 1 A are presented in Table XXII showing the relationships among the sections of sub-tests in the Pre-Engineering Inventory. These intercorrelations are machine computed and therefore tend to be somewhat higher than similar correlations computed from scattergram plots. Although Tests II and V do not contain sections, they are included to Table XXII for analysis.

In order to aid in the interpretation of the above intercorrelations, the means and standard deviations of the twelve subdivisions in the Pre-Engineering Inventory are listed below.

TABLE XXII

INTERCORRELATIONS AMONG THE SECTIONS OF SUB-TESTS OF THE PRE-ENGINEERING INVENTORY FOR THE FRESHMAN GROUP 1A, N = 190

Sections	IA	IB	II	IIIA	IIIB	IVA	IVB	V	VIA	VIB	VIIA	VIIB
IA	--	.906	.577	.423	.398	.292	.330	.509	.166	.294	.819	.627
IB	.906	--	.565	.791	.541	.512	.502	.724	.282	.398	.870	.773
II	.577	.565	--	.697	.539	.799	.337	.675	.452	.375	.707	.464
IIIA	.423	.791	.697	--	.678	.568	.606	.878	.521	.467	.865	.681
IIIB	.398	.541	.539	.678	--	.630	.587	.883	.503	.520	.560	.476
IVA	.292	.512	.799	.568	.630	--	.634	.793	.515	.495	.426	.429
IVB	.330	.502	.337	.606	.587	.634	--	.567	.407	.396	.324	.346
V	.509	.724	.675	.878	.883	.793	.567	--	.708	.695	.805	.645
VIA	.166	.282	.452	.521	.503	.515	.407	.708	--	.531	.347	.246
VIB	.294	.398	.375	.467	.520	.495	.396	.695	.531	--	.294	.330
VIIA	.819	.870	.707	.865	.560	.426	.324	.805	.347	.294	--	.881
VIIB	.627	.773	.464	.681	.476	.429	.346	.645	.246	.330	.881	--

IA - Word Meanings
IB - Reading Comprehension
II - Technical Word Meanings
IIIA - Technical Reading Comprehension
IIIB - Interpretation of Technical Data
IVA - Mathematical Computation
IVB - Mathematical Interpretation
V - Comprehension of Mechanical Principles
VIA - Graphic Representation
VIB - Cube Identification
VIIA - Knowledge of American Institutions
VIIB - Comprehension of Social Issues

Section	Mean	S.D.
I A Word Meanings	33.8	17.10
I B General Reading Comprehension	10.3	4.68
II Technical Word Meanings	52.3	15.06
III A Technical Reading Comprehension	40.3	12.68
III B Interpretation of Technical Data	15.1	4.00
IV A Mathematical Computation	31.5	9.76
IV B Mathematical Interpretation	14.1	4.98
V Comprehension of Mechanical Principles	23.3	10.24
VI A Graphic Representation	15.9	6.21
VI B Cube Identification	14.7	8.16
VII A American Institutions	21.7	4.88
VII B Social Issues	11.1	6.15

In the above list, the tests having particularly small standard deviations are Tests I B, III B, IV B, and VII A.

Examination of Table XXII reveals that the General Word Meanings section I A, General Reading Comprehension section I B, American Institutions section VII A, and Comprehension of Social Issues section VII B, all seem to be measuring a common factor as judged by their relatively high intercorrelations. This is in general agreement with the results previously found in the intercorrelations of the sub-tests.

I A Word Problems	33.3	17.10
I B General Reading Comprehension	10.3	4.68
III A Technical Reading Comprehension		
III E Interpretation of Technical Data	11.1	4.30
IV A Mathematical Computation	31.5	9.76
IV B Mathematical Interpretation	14.1	4.98
V Comprehension of Mechanical Principles	23.3	10.24
VI A Graphic Representation	15.9	6.21
VI B Code Identification	14.7	8.16
VII A American Inventions	12.7	4.80
VII B Social Issues	11.1	6.15

In the above list, the tests having particularly small standard deviations are Tests I B, III B, IV B, and VII A.

Examination of Table VIII reveals that the General Word of Social Issues section VII B, all seem to be measuring a

Another cluster indicated in Table XXII consists of the Technical Reading Comprehension section III A, Interpretation of Technical Data section III B, and Comprehension of Mechanical Principles Test V. Previous results in Tables XX and XXI showed that the General Mathematical Ability Test IV should be included in this group, but Table XXII does not indicate this to be true. This later table reveals that the Mathematical Computation section IV A has a high intercorrelation with Test II, Technical Word Meanings, and therefore these two measures combine to form a separate cluster.

The remaining sections IV B, Mathematical Interpretation, VI A, Graphic Representation, and VI B, Cube Identification, are shown to be relatively independent in Table XXII. It should be pointed out further that the section VII A, Knowledge of American Institutions, could very well be included in the second cluster of measures consisting of sections III A, III B, and Test V because the intercorrelations of section VII A with this group of measures are high. Previous results indicated that Test VII as a whole did not have very high intercorrelations with Tests III and V, and therefore section VII A is not included in the second cluster of measures because of this discrepancy.

Now that the sections and sub-tests of the Pre-Engineering Inventory which seem to be measuring the same special abilities have been determined through an analysis of

intercorrelations, the purpose of the remainder of this chapter will be to identify the separate special abilities measured by the Pre-Engineering Inventory.

Item Analysis

The Pre-Engineering Inventory contains a total of 558 items. The item analysis made in this study is relatively simple. On the basis of grade point averages made in engineering study, students in the beginning freshman group 1 A were selected to form the upper 25 per cent group in scholastic standing and the lower 25 per cent group. Answer sheets were obtained for students in these two groups and were hand-scored. For each item in the Pre-Engineering Inventory, the following information was obtained: the number of students in the upper group who answered the item correctly, the number of students in the lower group who answered the item correctly, the difference in number of students in each group who answered the item correctly, and the total number of students in both groups who answered the item correctly.

The difference in number of students in the upper and lower groups who answered an item correctly is an indication of the value that the item has in discriminating between the upper and lower groups of students. The total number of students in each group who answered an item correctly is an indication of the difficulty level for that item. Frequency

distributions were made of the differences and the sums. Items which showed about average difficulty and whose discriminatory value was in the upper 20 per cent for the entire group of items were then selected for further analysis.

These items showing high discrimination between the upper and lower groups of students can be considered as being particularly pertinent for engineering study and likewise the abilities measured by these items can be considered as having important for successful achievement in the pre-engineering curriculum. Therefore a careful study will be made to determine the nature of the abilities measured by these items.

In making an analysis to determine the special abilities measured by these highly discriminatory items, certain limitations are involved which need to be pointed out at this time. It is entirely possible that certain items are not measuring the abilities which are obviously intended to be measured. This may be due to the presence of certain underlying factors such as the location of the item in the test, the wording of the question, the nature of the multiple choices for the item, the peculiar previous experience of the student taking the test, and others too numerous to mention. In order to provide for these discrepancies, it will be necessary to assume that the Pre-Engineering Inventory has been carefully constructed and that it is highly probable that the test items measure the special abilities which are intended to be

measured.

Another limitation involved in the determining of special abilities measured by these test items concerns the subjective character of such an analysis. To some extent, the nature of the abilities measured by these items is quite obvious. In a number of cases, however, the nature of the abilities measured is subtle and obscure. The nomenclature of these abilities is arbitrary and usually attempts to give clues as to what is being measured. In any case the clarity in the definition of these abilities is dependent to a large extent upon the ability of the author to give an accurate description of what specific abilities are involved.

With these limitations in mind, attention will now be directed to the items showing high discrimination in each of the sub-tests of the Pre-Engineering Inventory. In Test I. General Verbal Ability, an attempt is made to measure the student's ability to recognize word meanings and to measure the extent of the student's general vocabulary. This type of test tends to measure general scholastic ability; however, previous analysis showed that this test differentiated for the cultural subjects area. The item showing the greatest discrimination consist of determining the word meanings for pecuniary, cajole, poignant, and manifestly. In Part II of this test where the ability to comprehend general reading materials is measured, no items of significant discriminatory

value were found.

Test II, Technical Verbal Ability, is a similar type of test as Test I where an attempt is made to measure the student's ability to recognize word meanings. In Test II, however, the words are drawn from reading materials in science and mathematics. The mathematical terms having high discriminatory value are: abscissa, a mathematical function, radian, and helix. Scientific terms having similar discriminatory value are: Hertzian waves, synthesis, achromatic, coulombs, sublimination process, and Wheatstone bridge. From the nature of these items, it can be readily seen that a working knowledge of certain mathematical and scientific terms is necessary for engineering study. The fact that this test contains both scientific and mathematical concepts may account for the fact that the test did not differentiate any particular subject area.

Unlike Tests I and II, which are primarily word recognition or vocabulary tests, Test III makes use of the "miniature task" technique previously described and therefore would be classified as a specialized aptitude test. Test III attempts to measure the ability to comprehend scientific materials. An item analysis of this test should reveal more exactly the nature of the abilities involved.

The content of Test III consists of descriptive reading materials in the field of physical science accompanied by

Test II, Reasoning Ability, is a similar type of test as Test I where an attempt is made to measure the student's ability to recognize word meanings. In Test II, however, the words are drawn from reading materials in science and mathematics. The mathematical terms having high discriminatory value were [illegible], [illegible], [illegible], and [illegible]. From the scores of these items, it can be readily seen that a working knowledge of certain mathematical and scientific terms is necessary for examining ability. The fact that this test contains both scientific and mathematical concepts may account for the fact that the test did not differentiate any particular [illegible].

Unlike Tests I and II, which are primarily word recognition or vocabulary tests, Test III places more of the "mathematical test" technique previously described and therefore would be classified as a specialized aptitude test. Test III attempts to measure the ability to comprehend relationships. An item analysis of this test should reveal more exactly the nature of the abilities involved.

The content of Test III consists of descriptive reading

tables, graphs, and diagrams of a quantitative nature. Each reading passage is followed by a number of questions on the given passage. The items having the greatest discriminatory value are carefully analyzed to determine what is required of the student, and these items are grouped according to similarity in the abilities required. Parts I and II of this test are quite similar in nature and are therefore not discussed separately.

The following are the special abilities measured by the items in Test III which show particularly high discriminatory value.

1. The ability to distinguish between the cause of a situation and the symptoms or indications of that situation.
   a. The student is given a description of a disease called polycythemia and its treatment. Student is asked to note if the cause of the disease is given and if the treatment applies to the cause or to the symptoms of the disease.
2. The ability to apply a principle or relationship expressed in a table or formula to a specific situation or to infer what would happen in a given situation.
   a. A Brinell hardness table and an explanation of it is given. Student is asked to determine which of

four steels with different carbon content would be the hardest under certain conditions.

b. Student is asked to determine certain dimensions of bolt heads and nuts from a formula in one instance and from a table in another instance.

c. The operation of a spherometer is explained and the student is asked to determine what would happen if the scale were set to zero and if the spherometer were used to determine the radius of a sphere.

d. The principle of a differential chain block-hoist is explained. The student is first asked to compute the mechanical advantage of the chain block from a given formula and then to determine the effect upon the operation of the chain hoist if certain conditions were imposed.

3. The ability to determine the reason for certain phenomena and results described in the reading passages.

a. Certain properties of an element X are given, and the student is asked to explain the behavior of the element under certain conditions.

b. Bode's law for determining the mean distance of the various planets from the sun is explained. The student is asked to determine why certain omissions were present.

c. The operation of a spherometer is described and the student is asked to determine why the spherometer could be used equally well on concave or convex surfaces.

4. The ability to perceive certain relationships or principles implicit in given data.

a. A table showing the application of Bode's law is given, and the student is asked to determine the unit of measure used in the table.

b. An explanation of the method of finding the resultant of two coplaner concurrent forces is given. The student is asked to determine the condition when the Pythagorean theorem may be used.

5. The ability to interpolate a graph.

a. A curved line graph is presented, and the student is asked to determine certain between-interval values, a task which requires a certain amount of judgment and carefulness.

6. The ability to determine the writer's purpose in explaining certain data.

a. A reading passage on some technical subject is given, and the student is asked to determine the writer's purpose in a certain paragraph.

From the above list, it can be seen that certain specific abilities are called for in the "miniature tasks" contained

in Test III. These abilities are not mutually exclusive, and together they are part of the student's ability to interpret and comprehend technical data.

In attempting to determine the reason why a number of items failed to discriminate between the upper and lower groups of students, it was found that some of these items called for previous knowledge and experience which only a few graduating high school seniors would have. A speed factor was also indicated by the small number of students who attempted the last ten items in Part I of the test. This would make useless an item analysis for these items.

Test IV attempts to measure general mathematical ability. An analysis of the discriminating items in Test IV reveals the following special abilities which are called for by these items and which are a part of general mathematical ability.

1. The ability to solve formulas

   a. Given $V = \sqrt{at}$, solve for a

   b. Given $S = NC$ and $C = \pi D$, solve for N

   c. Given $T = 2\pi\sqrt{\frac{L}{g}}$ and $T = 2$, solve for L

   d. Given V and h of a circular cylinder, find radius of the base

2. Ability to express given written relationships in terms of formulas. This is also known as algebraic formulation.

a. Given the written relationship of the volume of water in a cylindrical tank to the diameter height, determine the formula.

b. Given the written relationship of the pressure of a weight to the dimensions of the steel post, determine the formula.

c. Determine the formula for weight in terms of density and volume.

d. Given the relationship between horsepower and watts, and of watts in terms of voltage and amperes, determine the formula for horsepower in terms of volts and amperes.

e. Given the relationship of Force in terms of Mass, Velocity, and Radius of rotation, determine the formula.

f. Given the relationship of Force to Weight, Height of inclined plane, and length of inclined plane, determine the formula.

3. Ability to express geometric relationships in terms of formulas.

a. Given the figure, determine the formula for the circumference of a circle.

b. Given the figure, determine the formula for the area of a circle.

c. Determine the area of a right triangle from a given figure.

d. Determine the formula for the sides of a given right triangle.

4. Ability to apply previous knowledge of basic geometric relationships to given situations.
   a. From a given diagram, select equal angles.
   b. Given two similar triangles, find the unknown side.
   c. Given the numerical value of an angle, find the value of its complementary angle.
5. Ability to apply newly learned mathematical procedures and principles.
   a. In a reading passage, the method of computing means, medians, and modes is given. The student is then asked to compute a mean and median in a given situation.
   b. The system of rectangular coordinates is explained, and the student is asked to determine which of a list of points identified by coordinates lies in the fourth quadrant.
6. Ability to perceive certain relationships implied in given formulas.
   a. A formula is given which expresses a relationship between two variables. The student is asked to determine what would happen to the value of one variable if the other one is doubled.
   b. In a given formula, the student is asked to determine how one variable varies in relation to the other.

d. Determine the formula for the sides of a given

4. Ability to apply previous knowledge of basic geometric

a. From a given diagram, select equal angles.

b. Given two similar triangles, find the unknown sides.

c. Given the numerical value of an angle, find the

value of its complementary angle.

5. Ability to apply newly learned mathematical procedures

and principles.

a. In a reading passage, the method of computing

means, medians, and modes is given. The student is

then asked to compute a mean and median in a given

b. The system of rectangular coordinates is explained,

and the student is asked to determine which of a

list of points identified by coordinates lies in

6. Ability to perceive certain relationships implied in

a. A formula is given which expresses a relationship

two variables. The student is asked to

determine what would happen to the value of one

able if the other one is doubled.

a given formula, the student is asked to deter-

variable varies in relation to the

Other discriminating items not included in the above list consist of problems involving fractional exponents and interpolation in a table of trigonometric functions. One outstanding feature of the above list is the fact that most of the items are concerned with formulas in some way or another.

Test V proposes to measure the student's ability to comprehend mechanical principles. Several diagrams of mechanical devices followed by questions on each of these devices are presented. In some cases the student is asked to determine the principle involved in the operation of the mechanical device and then apply that principle to a particular situation. In most cases, however, the principle of operation is given along with the mechanical device, and the student is asked to demonstrate his understanding of the principle by applying to given situations.

The following problem situations in Test V showed significant discrimination between the higher scholastic group and the lower scholastic group of students in the beginning freshman group 1 A.

a. Given two pistons connected to a rocker arm on the same side of the fulcrum and acting in opposite directions. Determine the force exerted by one of the pistons when a certain force is acting upon the other.

b. Given a diagram of a system of wheels interconnected by belts and the principle that the speeds of the

Other discriminating items not included in the above
comparat of problems involving fundamental equations and
interpolation in a table of trigonometric functions. One out-
standing feature of the above list is the fact that most of
the items are concerned with formulas in some way or other.

Test V proposes to measure the student's ability to
comprehend mechanical principles. Several
test devices followed by questions on each of these devices
are presented. In some cases the student is asked to determine
the principle involved in the operation of the mechanical
device and then apply that principle to a particular situation.
In most cases, however, the principle of operation is given
along with the mechanical device, and the student is asked to
demonstrate his understanding of the principle by applying
to given situations.

The following problem situations in Test V showed signif-

the lower achievement group of students in the beginning
freshman group I A.

a. Given two platens connected to a rocker arm on the
same side of the fulcrum and acting in opposite
directions. Determine the force exerted by one of
the platens when a certain force is acting upon the

b. Given a diagram of a system of wheels interconnected
by belts and the principle that the speeds of the

wheels are inversely proportional to their diameters. Determine which wheels make the same number of revolutions per minute as a given wheel. Also determine how many complete turns are made by a wheel when another wheel makes a certain number of revolutions.

c. Given diagrams of four separate pulley arrangements and the principle of mechanical advantage involved. Determine the pull necessary to lift a certain weight in one of the arrangements, the tension on certain parts of the pulley arrangements, the mechanical advantage for each pulley arrangement. These questions had particularly high discriminatory value.

d. Given a system of gears that can be shifted and the principle that the speed of the gears varies inversely to the number of teeth on the gears. Determine what speeds result from certain gear combinations, what gear combination will give a desired speed, and what change will result from one combination being changed to another.

e. Given a hydraulic system containing two cylindrical pistons of known cross-sectional areas. Determine the effect of a force on one of the pistons and the effect of a certain movement of one of the pistons.

f. Given a crank and sliding block linkage. Determine the position of the tip of the crank for a given position of the sliding block.

Throughout the test on mechanical principles, the student is required to deal with ratios. This test is quite similar to Text III in that the student is asked to apply certain principles to specific situations. The only difference is that in Test III the principles apply to reading material and quantitative data. In Test V the principles apply to diagrams of mechanical devices. This may account for the high intercorrelations previously obtained between these tests.

Test VI, Spatial Visualizing Ability, contains two parts. Since Part I showed superior predictive value and differential value, and since almost all of the discriminating items are contained in Part I, only the nature of the special abilities as measured in the first part of this test will be discussed.

In Part I of Test VI, the ability to think in terms of orthographic representation is measured. Two orthographic views of an object as presented, and the student is asked to select from a group of suggested views the missing third orthographic view which completes the picture. Previous training in high school mechanical drawing would be a definite asset for this type of test. Mechanical drawing is a prerequisite subject for entrance into the College of Engineering at Berkeley, and a check of the high school records showed that each student in the beginning freshman

group 1 A had taken at least one year of mechanical drawing. Also a full explanation of what is expected of the student is given at the beginning of the test. Therefore the students should be about equally prepared for this type of test.

In determining the third missing orthogonal view, the student may use one of two approaches. One method consists of trying out each of the suggested views to see if it fits the specifications. In the other method, the student visualizes the whole object from the two given views and then visualizes what the missing view should be. The student then selects the proper view from the suggested list. The latter method is faster; however, both methods require visualizing ability.

All of the items in Part I of Test VI are of the same nature and therefore measure the same ability to visualize in terms of orthographic representation. The difference between the discriminating items and the non-discriminating items lies in the fact that more oblique surfaces and hidden lines were involved in the discriminating items.

Test VII attempts to measure the student's understanding of modern society. This test is a general information type of test and consists of questions of a general nature on American institutions and social issues. The discriminating questions in this test are as follows:

a. Why is universal education particularly important in a democracy?

b. What was the original purpose of the system of checks and balances in our government?

c. What best described business conditions in this country after 1918?

d. What is characteristic of modern industry?

e. What group gains the greatest benefit when the United States levies a high protective tariff on an article?

f. In its commonest meaning, the term "collective bargaining" refers to bargaining between what types of political or economic groups?

From the nature of the above questions, it can be seen that the test measures general information concerning American institutions. Part II of this test which contains reading passages on current social issues did not have any discriminating items.

Chapter Summary and Identification of Factors

The purpose of this chapter was to determine the nature of the special abilities measured in each of the sections of the Pre-Engineering Inventory. First considered were the intercorrelations among the ability measures in order to determine which ones are measuring separate abilities. The intercorrelations for the freshman group 1 A were consistently somewhat higher than those for the freshman group 1 C.

However, some of the intercorrelations between similar sub-tests for the freshman group 2 A were higher than those for the 1 A group and therefore no trend was indicated.

A factorial analysis of the Pre-Engineering Inventory sub-test intercorrelations for the three groups of students showed definite tendencies for certain tests to group themselves together. One group was formed by Test I, General Verbal, and Test VII, Understanding of Modern Society. Also indicated was a close relationship among Test III, Scientific Materials; Test IV, General Mathematics; and Test V, Mechanical Principles. Test II, Technical Verbal, was considered peripheral to this group since its intercorrelations with the tests of this group were inconsistent. The Spatial Visualization Test VI was shown to be relatively independent of the other tests.

A further factorial analysis was made of the intercorrelations among the sections of sub-tests in the Pre-Engineering Inventory for the freshman group 1 A. This analysis revealed that the General Word Meanings section I A, General Reading Comprehension section I B, American Institutions section VII A, and Comprehension of Social Issues section VII B formed a group which seemed to be measuring a common factor. Another group consisted of section III A, Technical Reading Comprehension; section III B, Interpretation of Technical Data; and Test V, Comprehension of Mechanical

Principles. Unlike the previous analysis, the Mathematical Computation section IV A and Technical Word Meanings Test II formed a separate group. The remaining sections IV B, Mathematical Interpretation; VI A, Graphic Representation; and VI B, Cube Identification, were shown to be relatively independent.

In order to determine more accurately the nature of the abilities measured, an item analysis was made of the Pre-Engineering Inventory on the basis of the freshman group 1 A. The items in each of the sub-tests showing particularly high discrimination were grouped according to similarity in abilities measured.

Tests I and II were found to measure the student's ability to recognize word meanings. In Test I, the discriminating words were found to be pecuniary, cajole, poignant, and manifestly. In Test II, the technical terms having significant discriminating value were abscissa, a mathematical function. radian, halix, Hertzian waves, synthesis, achromatic, coulombs, sublimation process, and Wheatstone bridge. The discriminatory items of Tests I and II indicate that a working knowledge of both general and technical vocabulary is needed for engineering study.

Test III was found to contain "miniature tasks" involving scientific reading materials. The following special abilities were measured by the discriminatory items in this test:

a. The ability to distinguish between the cause of a situation and the symptoms or indications of that situation.

b. The ability to apply a principle or relationship expressed in a table or formula to a specific situation or to infer what would happen in a given situation.

c. The ability to determine the reason for certain results and phenomena described in the reading passages.

d. The ability to perceive certain relationships or principles implicit in given data.

e. The ability to interpolate a graph.

f. The ability to determine the writer's purpose in explaining certain data.

Test IV attempted to measure general mathematical ability which consisted of the following specific abilities as measured by the discriminating items of the test.

a. The ability to solve formulas.

b. The ability to express given written relationships in terms of formulas (algebraic formulation).

c. The ability to express geometric relationships in terms of formulas.

d. The ability to apply previous knowledge of basic geometric relationships to given situations.

e. The ability to apply newly learned mathematical procedures and principles.

f. The ability to perceive certain relationships implied in given formulas.

In Test V, all the problem situations involved a diagram of some simple mechanical device followed by questions. These items measured the student's ability to comprehend the mechanical principle involved in the operation of the mechanical device and to demonstrate his understanding by applying the principle to specific situations.

Nearly all of the discriminating items in Test VI were contained in Part I. This section of the test measured the student's ability to think in terms of orthographic representation. Likewise in Test VII, all of the discriminating items were found in Part I of the test. This section of the test measured general information concerning American institutions.

On the basis of the factor analysis and item analysis just completed, the following separate abilities are believed to be measured by the Pre-Engineering Inventory:

a. Ability to demonstrate a working knowledge of general vocabulary and general information concerning American Democracy (Tests I and VII).

b. Ability to comprehend basic principles involved in technical reading passages, quantitative data, and diagrams of mechanical devices, and to apply these principles to specific situations. (Tests III, V, and part of II.)

c. Ability to perceive quantitative relationships and to work effectively with mathematical symbols and concepts. (Test IV and part of II.)

d. Ability to visualize in terms of orthographic representation. (Test VI.)

CHAPTER VI

SUMMARY AND CONCLUSIONS

The purpose of this final chapter is to summarize briefly the findings of the previous chapters and to point up conclusions that will serve as clues for the further development of special ability tests in engineering.

Summary of Findings and Conclusions

1. The basic assumption in this study that pre-engineering study requires certain skills and abilities apart from other areas of study and that the main subject areas within the pre-engineering curriculum further require separate abilities seems to be warranted. The six-year study made by the University of Minnesota indicated that variables found especially useful in predicting success in one school or college were not found to be equally prognostic for any other school or college. Vaughn presented data which indicated that engineering students tend to make higher average scores on certain ability measures than do other students. Crawford and Burnham further indicate in their data that certain subject areas require separate abilities.

2. The predictive measures of the high school record, general scholastic tests, primary or basic mental abilities

tests, and achievement tests are not particularly useful in defining special abilities. An analysis of engineering prognostic studies which used these measures revealed that these measures had predictive value for engineering study, but they also had equal predictive value for the other areas of the study. The use of high school marks in certain courses to determine special abilities has been highly unreliable because a student's record is rarely consistent and schools differ widely in emphasis in different studies and standards maintained. By nature of construction, general scholastic aptitude tests have equal predictive value for all areas of scholarship and are therefore unfruitful sources for special ability analysis. Thurstone's Primary Mental Abilities Test has attempted to measure specific components of scholastic abilities, but studies indicated that the test still measured general scholastic ability and had no differential value. Achievement tests added a certain amount of definiteness to the picture and had some differential value, but they were still unfruitful sources for special ability analysis because they have emphasized facts or knowledge acquired.

3. The content of recently developed specialized educational aptitude tests has definite possibilities for special ability analysis. These tests contain items which simulate specifically the kinds of tasks likely to be met in the study

of a particular subject area, and certain special abilities are required in the solution of these "miniature tasks." The specialized aptitude tests used by the engineering prognostic studies were classified into the following categories according to the nature of what was measured:

a. Mechanical ability

b. Spatial visualization

c. Reading comprehension and interpretation

d. Quantitative reasoning and interpretation

Most of the studies using these tests attempted to determine the predictive value of these tests for the general area of pre-engineering study. These studies revealed that the specialized aptitude tests had about the same predictive value for engineering study as did the other measures of high school record, general scholastic aptitude tests, and achievement tests. These studies, however, did indicate the superiority of certain types of specialized aptitude tests over other types of specialized aptitude tests in predictive value. They are summarized as follows:

a. Tests measuring comprehension of mechanical principles and relationships were found to be superior to tests involving the manipulation of certain mechanical objects.

b. Tests requiring visualization in terms of graphic representation were found to be superior to the paper form-board type of test.

c. Reading comprehension tests which contained items of a general nature were found to be inferior to tests which attempted to measure verbal reasoning and interpretation of technical reading material found in engineering courses.

d. Aptitude tests in mathematics which contained only reasoning and interpretative type of items were found to be inferior to mathematics tests which contained both achievement-type and interpretative-type of items.

Only a few studies attempted to determine the differential value of these specialized aptitude tests, but their findings were unanimous that these tests have definite possibilities of being able to discriminate among various subject areas and groups of students. Particularly noteworthy was the fact that the Pre-Engineering Inventory had differential value for distinguishing engineering students from other students, and that most of the sub-tests of this battery had incorporated the best features of specialized aptitude tests.

4. In determining the special abilities necessary for successful achievement in the general area of pre-engineering study and in the subject areas of the pre-engineering curriculum, the following analyses were made:

a. A differential analysis was made of the Pre-Engineering Inventory to determine which tests were particularly significant for each of the areas of study.

b. An item analysis was made of the Pre-Engineering

Inventory to determine the special abilities significantly measured by the discriminating items in each of the tests.

The following are the results of these analyses which apply to the beginning freshman groups used in this study:

General Area of Engineering Study.- The differential analysis indicated that Test II Technical Verbal Ability; Test III Comprehension of Scientific Materials; and Test V Comprehension of Mechanical Principles, all predicted the general average marks made in engineering as well as if not better than average marks made in the subject areas. These tests therefore had no particular differential value for the subject areas and yet had a significant predictive value for the general area of engineering study. The special abilities measured by these tests have significance for engineering study in general and these special abilities are listed as follows:

Test II, Technical Verbal Ability - Measures the ability to recognize technical word meanings found in the reading material of science and mathematics. The discriminating items in this test indicate that the engineering student needs to have a working knowledge of certain scientific and mathematical terms.

Test III, Comprehension of Scientific Materials - Measures significantly the ability to comprehend the scientific principles presented in technical reading materials and to

interpret these principles when faced with specific instances.

Test V, Comprehension of Mechanical Principles - Measures according to the discriminating items in the test the student's ability to comprehend the mechanical principle invovled in the operation of a mechanical device and to demonstrate his understanding by applying the principle to specific situations.

Mathematics.--The differential analysis clearly showed that this subject area was differentiated by Test IV, General Mathematical Ability. The abilities measured by this test as shown by the discriminating items in this test are as follows:

a. The ability to solve formulas.

b. The ability to express given written relationships in terms of formulas (algebraic formulation).

c. The ability to express geometric relationships in terms of formulas.

d. The ability to apply previous knowledge of basic geometric relationships to given situations.

e. The ability to apply newly learned mathematical procedures and principles.

f. The ability to perceive certain relationships implied in given formulas.

Chemistry.--No tests of the Pre-Engineering Inventory had definite differential value for this subject area. Test II, Technical Verbal Ability, and Test III, Comprehension of Scientific Materials, had some differential value for the uninterrupted freshman group 1 A but no differential value for the interrupted freshman group 1 C.

Physics.--No tests of the Pre-Engineering Inventory were found to have differential value for the subject of physics. Test II, Technical Verbal Ability, had slight differential value for this subject area for the freshman group 1 C but none for the freshman group 1 A.

Engineering.--The differential analysis of the Pre-Engineering Inventory indicated that this subject area was clearly differentiated by Test VI, Spatial Visualizing Ability. Nearly all the discriminating items were contained in Part I of Test VI. All of the items in this section of the test are of the same nature and they measure the student's ability to visualize in terms of orthographic representation.

Cultural.--This subject area was found to be discriminated by Test I, General Verbal Ability, and Test VII, Understanding of Modern Society. Test I measured the student's ability to recognize word meanings found in general reading material and attempted to determine the student's general vocabulary. All of the discriminating items in Test VII were contained in Part I. This section of the test measured

general information concerning American democracy.

5. In order to determine the amount of overlapping and the relative independence of the sub-tests of the Pre-Engineering Inventory, intercorrelations among the tests were computed and a factorial analysis was made. On the basis of the factor analysis, the following relatively independent special abilities were found to be measured in the Pre-Engineering Inventory.

a. Ability to demonstrate an extensive background of knowledge concerning general vocabulary and general information on the American democratic society (measured by Tests I and VII).

b. Ability to comprehend basic scientifc principles and concepts involved in technical reading passages quantitative data, and diagrams of mechanical devices, and to apply these principles to specific instances (measured by Tests III and V, and part of II).

c. Ability to perceive quantitative relationships and to work effectively with mathematical symbols and concepts (measured by Test IV and part of Test II).

d. Ability to visualize in terms of orthographic representation (measured by Test VI).

Suggestions for Further Development

On the basis of the findings and conclusions determined in this study, some suggestions are made to serve as guide for the further development of special ability tests in engineering.

1. The test battery should use various approaches in measuring special abilities and should experiment with new techniques. Some of the approaches which can be used are as follows:

   a. Miniature-task technique.--This technique has been explained previously and has been shown to have definite possibilities in special ability testing. The tasks should be specific and care should be taken that the background of the student is not over-extended. This technique is well adapted to technical reading material, diagrams, and quantitative data.

   b. Exercise-type of test item.--This approach consists of presenting the student with certain exercises which measure specific skills. This type is particularly useful in measuring computational skills in mathematics where the student is asked to solve mathematical exercises.

   c. Information-type of test item.--This type of approach calls for factual knowledge and general information, and can be used when measuring the general background knowledge of the student.

d. Projective technique.--This technique was not used in any of the tests or prognostic studies covered in this study; however, it is suggested here as an experimental technique. Test items using this approach are of an ambiguous nature to allow each student to project himself into various situations. Such a technique could be used in determining what activities the students imagine themselves to be doing in the future when they finish their training. This information along with other data could be useful in differentiating between students best fitted for terminal type or technical institute type of engineering training and students most likely to succeed in the theoretical type of engineering training.

2. The test battery should contain one test which predicts well for the general area of engineering study and does not necessarily discriminate for any of the subject areas within the pre-engineering curriculum. Each of the remaining tests should be highly discriminatory for at least one subject area if possible. Tests have been found in this study which differentiate for the mathematics, engineering, and cultural subjects areas. A study needs to be made to determine the distinguishing characteristics of the subject areas of physics and chemistry. These characteristics would serve as

a basis for developing discriminating tests in these areas. In the meantime, the results of this study indicate that measures of certain scientific terms and comprehension of certain reading material in these subjects have possibilities of discriminating for these subject areas.

3. Regardless of content, the items in the test battery should require the following abilities:

a. Perceive certain implicit relationships and principles.

b. Give logical inferences and use good judgment.

c. See the implications involved.

d. Draw on previous background in giving reasons for certain happenings.

e. Distinguish between cause and symptom.

f. Readily grasp new procedures and principles and apply them.

g. Visualize movements and manipulate objects imaginatively in three dimensions.

h. Read carefully and accurately.

Other abilities could be mentioned, but the ones listed above were found to be particularly significant in this study.

4. The following is a suggested organization of a test battery for use in the counseling and guidance of engineering students. The nature of the abilities to be measured have been listed above. Only the nature of content and validation will be listed below.

Special Abilities Test for Engineering

I. General Cultural Background

Content:

a. General vocabulary.
b. General information on social issues and affairs of society.
c. Reading materials in social studies.

Validation:

Average marks made in cultural subjects and differential value for the cultural subject area.

II. Interpretation of Technical Data

Content:

a. General technical reading material.
b. Mechanical diagrams.
c. Quantitative data.

Validation:

Average marks made in the pre-engineering curriculum and differential value for the general area of pre-engineering study.

III. Mathematical Ability

Content:

a. Formulas and algebraic formulation.
b. Mathematical concepts.
c. Geometrical relationships.

Validation:

Average marks made in mathematics and differential value for the mathematics subject area.

IV. Spatial Visualization

Content:

a. Orthographic projections.

Validation:

Average marks made in engineering and differential value for the engineering subject area.

a. General vocabulary.
b. General information on initial issues and status
   of report.
c. Meeting materials in general binders.

V. Physics Aptitude

Content:

a. Physics concepts.
b. Reading materials in physics.
c. Physical laws and relationships.

Validation:

Average marks in physics and differential value for the physics subject area.

VI. Chemistry Aptitude

Content:

a. Chemistry concepts.
b. Reading materials in chemistry.
c. Chemical relationships and principles.

Validation:

Average marks in chemistry and differential value for the chemistry subject area.

VII. The Engineering Profession

Content:

a. Activities involved.
b. Clearly defined purposes.
c. Motivation and interest.

Validation:

Differential value between successful achievers in the academic engineering program and successful achievers in the terminal or technical engineering program.

The development of the first four tests can be made on the basis of the results found in this study. The remaining three tests would have to wait upon further studies made to determine the distinguishing characteristics of the physics

and chemistry subject areas, and of the groups of successful achievers in the two areas of engineering study. It is quite possible that these studies might reveal the impossibility or the infeasibility of such tests.

BIBLIOGRAPHY

BIBLIOGRAPHY

Adams, W. M. "Prediction of Scholastic Success in Colleges of Law," Educational and Psychological Measurement, 4:13-19; 1944.

Bartlett, R. S. "Guidance and Placement of Engineering Students," The Journal of Engineering Education, 33: 535-51, March, 1943.

_____. "Re-appraisal of Values in the Selection of Engineering Students," The Journal of Engineering Education, 32:227-38, November, 1941.

Bennett, G. K., and Cruikshank, R. M. A Summary of Manual and Mechanical Ability Tests (Preliminary Form). New York: The Psychological Corporation, 1942.

Berdie, R. F. "Prediction of College Achievement and Satisfaction," Journal of Applied Psychology, 28:239-45, June, 1944.

Bingham, W. V. Aptitudes and Aptitude Testing. New York: Harper and Bros., 1937.

Bittner, R. H., and Wilder, C. E. "Expectancy Tables: A Method of Interpreting Correlation Coefficients," The Journal of Experimental Education, 14:245-52, March, 1946.

Blommers, P. "Statistical Theory: Some Recent Developments," Review of Educational Research, 15:423-40, December, 1945.

Boardman, C. W., and Finch, F. H. "Relation of Secondary School Preparation to Success in the College of Engineering," The Journal of Engineering Education, 24:466-75, March, 1934.

Borow, H. "Current Problems in the Prediction of College Performance," Journal of the American Association of Collegiate Registrars, 22:14-26, October, 1946.

Brogden, H. E. "On the Interpretation of the Correlation Coefficient as a Measure of Predictive Efficiency," The Journal of Educational Psychology, 37:65-76, February, 1946.

Brush, E. N. "Mechanical Ability as a Factor in Engineering, Aptitude," Journal of Applied Psychology, 25:300-12, June, 1941.

Bunker, J. W. "Challenge to American Educators," School and Society, 64:33-4, July 20, 1946.

Buros, O. K. Second Yearbook of Research and Statistical Methodology. Highland Park, New Jersey: Gryphon Press, 1941.

Butsch, R. L. C. "Improving the Prediction of Academic Success through Differential Weighting," The Journal of Educational Psychology, 30:401-20, September, 1939.

Campbell, R. K. The Relationships of Interest to Achievement in Engineering and Social Science Courses. (Ph.D. Dissertation, Stanford University, 1940).

Carrothers, G. E. "Criteria for Selecting College Students," National Association of Secondary School Principals Bulletin, 30:85-91, April, 1946.

Carter, H. D. "Measurement and Prediction of Special Abilities," Review of Educational Research, 17:33-52, February, 1947.

Chambers, W. M. "Four Steps to Improve U.S. Educations," School Executive, 66:46-7, May, 1947.

Cohen, L. "Predicting Academic Success in an Engineering College and Suggestions for an Objective Evaluation of High School Marks," The Journal of Educational Psychology, 37:381-84, September, 1946.

Conant, J. B. "Selective Principle in American Colleges," The Harvard Educational Review, 7:165-75, March, 1937.

_____. "Selective Process in Education," School and Society 47:155-58, January 29, 1938.

Crawford, A. B., and Burnham, P. S. Forecasting College Achievement. New Haven: Yale University Press, 1946. 291 pp.

Curtis, G. B., and Stoughton, B. "Control and Stabilization of Enrollment," The Journal of Engineering Education, 29:591-610, April, 1939.

Douglass, H. R. "Different Levels and Patterns of Ability Necessary for Success in College," Occupations, 22: 182-6, December, 1943.

Durflinger, G. W. "Prediction of College Success - A Summary of Recent Findings," Journal of the American Association of Collegiate Registrars, 19:68-78, October, 1943.

Dvorak, A., and Salyer, R. C. "Significance of Entrance Requirements for the Engineering College at the University of Washington," The Journal of Engineering Education, 23:618-23, April, 1933.

Embler, W. "Higher Education for American Democracy," The Journal of Engineering Education, 38:705-10, June, 1948.

Engineers Council for Professional Development. Report of the Committee on Student Selection and Guidance. Eleventh Annual Report, 1943.

Eurich, A. C., and Cain, T. F. "Prognosis," Encyclopedia of Educational Research. New York: The Macmillan Company, 1941. Pages 838-860.

Eysenck, H. G. "Student Selection by Means of Psychological Tests: A Critical Survey," British Journal of Educational Psychology, 17:20-39, February, 1947.

Feder, D. D., and Adler, D. C. "Predicting the Scholastic Achievement of Engineering Students," The Journal of Engineering Education, 29:380-85, January, 1939.

Freund, C. J. "Veterans Turned Scholars," The Journal of Engineering Education, 37:762-64, June, 1947.

Froelich, G. J. Prediction of Academic Success at the University of Wisconsin. Madison: University Press, 1941.

Garrett, W. S. "The Ohio State Psychological Examination - An Instrument for Predicting Success in College," Occupations, 22:489-95, May, 1944.

Geiger, H. E., and Remmers, H. H. "Predicting Success and Failure of Engineering Students in the Schools of Engineering in Purdue University," Purdue University Studies in Higher Education, 38:10-19, May, 1940.

Gerberich, J. R. "Factors Related to the College Achievement of High-Aptitude Students Who Fail of Expectation and Low-Aptitude Students Who Exceed Expectation," The Journal of Educational Psychology, 32:253-65, April, 1941.

Goodman, C. "Prediction of College Success by Means of Thurstone's Mental Abilities Tests," Educational and Psychological Measurement, 4:125-40; 1944.

Goodman, C. H. "A Comparison of the Interests and Personality Traits of Engineers and Liberal Arts Students," Journal of Applied Psychology, 26:721-27, December, 1942.

Gould, G. "Predictive Value of Certain Selective Measures," Educational Administration and Supervision, 33:208-12, April, 1947.

Gowdy, R. C. "Selection and Guidance Aspects of Cooperative Engineering Education," The Journal of Engineering Education, 35:187-91, November, 1944.

Griffin, C. H., and Borow, H. "An Engineering and Physical Science Aptitude Test," Journal of Applied Psychology, 28:376-87, October, 1944.

Harding, G. H. "Correlation of Freshman Placement Tests with Scholastic Achievement," The Journal of Engineering Education, 28:735-38, June, 1938.

Higgins, T. J. "Study of Mathematical Ability in Relation to Success in Engineering Studies," The Journal of Engineering Education, 23:743-46, June, 1933.

Holcomb, G. W., and Laslett, H. R. "A Prognostic Study of Engineering Aptitude," Journal of Applied Psychology, 16:107-115, April, 1932.

Honeywell, R. J. The Educational Work of Thomas Jefferson. Boston: Harvard University Press, 1931.

Hurd, A. W. "Problem of the Prediction of College Success," Journal of Educational Research, 38:217-19, November, 1944.

Johnson, H. G. "Certain Properties of the Correlation Coeffcient," The Journal of Experimental Education, 14:263-6, March, 1946.

Kandel, I. T. Professional Aptitude Tests in Medicine, Law, and Engineering. New York: Teachers College, Columbia University, 1940.

Krathwohl, W. C. "3 by 3 Analysis of Predictive Value of Test Scores," Journal of Applied Psychology, 28:318-22, August, 1944.

Kurani, H. A. "Re-thinking Selection," The Harvard Educational Review, 12:259-68, May, 1942.

Lawshe, C. H., and Mills, W. B. "Further Studies in the Development of Test Batteries for Identifying Potentially Successful Naval Electrical Trainees," Journal of Psychology, 21:97-105, January, 1946.

Laycock, S. R., and Hutcheon, S. B. "Preliminary Investgation into the Problem of Engineering Aptitude," The Journal of Eucational Psychology, 30:280-88, April, 1939.

Mann, C. V. "Engineering Aptitudes: Their Definition, Measurement, and Use," The Journal of Engineering Education, 32:673-86, April, 1942.

Mathewson, R. H. "Educational Problems of Veterans - and Other Civilians," Journal of the American Association of Collegiate Registrars, 21:462-74, July, 1946.

McGehee, W. "Prediction of Differential Achievement in a Technological College," Journal of Applied Psychology, 27:88-92, February, 1943.

Moore, M. F. "Evaluation of Certain Factors for Predicting the Success of Students Entering the College of Pharmacy of the University of Minnesota from 1933 through 1943," The Journal of Experimental Education, 14:207-24, March, 1946.

National Education Association, Educational Policies Commission. Learning the Ways of Democracy. Washington, D. C.: National Education Association, 1940.

Nelson, L. W. "Schoolmaster Looks at the College," National Association of Secondary School Principles Bulletin, 31:69-73, October, 1947.

Nemzek, C. L. "Direct and Differential Prediction of Academic Success as Measured by the Stanford Achievement Test; from a Thesis," Journal of Social Psychology, 13:71-87, February, 1941.

Nemzek, C. L. "Note Concerning Direct and Differential Prediction of Academic Success," Journal of Social Psychology, 15:325-30, May, 1942.

Prator, R. "Essential Elements in a Sound Plan of Selecting and Counseling College Entrants," College and University 23:268-73, January, 1948.

Pierson, G. A. "School Marks and Success in Engineering," Educational and Psychological Measurement, 2:612-14; 1947.

Pressey, S. L. "Efficiency Engineering in the Educational Emergency," School and Society, 65:425-28, June 7, 1947.

Prior, J. A. "What Curriculum and Procedure for the Returned Service Man with Partial Undergraduate Education?," The Journal of Engineering Education, 35:125-27, October, 1944.

Report of the Pacific Coast Committee. College-Age Population Study, 1947-64; Arizona, California, Nevada, Oregon, Washington. Washington, D. C.: American Council on Education, November, 1947.

Russell, J. D. "Critical Issues in Higher Education," The North Central Association Quarterly, 22:149-61, October, 1947.

_____. "Enrollment Trends in Higher Education," Journal of the American Association of Collegiate Registrars, 22:413-31, July, 1947.

Sabine, G. H. "Are State Universities Different?," School and Society, 34:349-57, September 12, 1931.

Sackett, R. L. "College Hurdles," The Journal of Engineering Education, 27:286-89, December, 1936.

_____. "Discovery of Engineering Talent," The Journal of Engineering Education, 35:180-83, November, 1944.

_____. "Engineering Colleges Help Returning Veterans," The Journal of Engineering Education, 35:425-27, March, 1945.

_____. "Selection of Engineering Students - Discussion," The Journal of Engineering Education, 30:595-600, March, 1940.

Scates, D. E. "Correlation Coefficients and Other Constants for Combined and Separated Distributions," The Journal of Experimental Education, 9:275-84, March, 1941.

Scott, C. M. "Background and Personal Data as Factors in the Prediction of Scholastic Success in College," Journal of Applied Psychology, 22:42-9, February, 1938.

Segel, D. Prediction of Success in College. U. S. Office of Education Bulletin No. 15. Washington: Government Printing Office, 1934.

Segel, D., and Brintle, S. L. "The Relation of Occupational Interest Scores as Measured by the Strong Interest Blank to Achievement Test Results and College Marks in Certain College Subject Groups," The Journal of Educational Research, 27:442-45, February, 1934.

Siemens, C. H. "Forecasting the Academic Achievement of Engineering Students," The Journal of Engineering Education, 32:617-21, April, 1942.

_____. "Note on a Technique in the Application of the Tolley-Ezekiel Method of Handling Multiple Correlation Problems," The Journal of Experimental Education, 12:242-43, March, 1944.

_____. "Predicting Success of Transfer Students," Junior College Journal, 14:24-8, September, 1943.

_____. Prognosis of the Achievement of Engineering Students, (Ph.D. Dissertation, University of California, 1939).

Slaymaker, R. R. "Admission Test Procedure," The Journal of Engineering Education, 37:402-13, January, 1947.

Smith, F. F. "Use of Previous Record in Estimating College Success," The Journal of Educational Psychology, 36:167-76, March, 1945.

Society for the Promotion of Engineering Education, "Report of the Committee on Student Selection and Orientation," The Journal of Engineering Education, 32:2247-27, November, 1941.

_____. "Report of the Committee on Transfer Students from Emergency Institutions," The Journal of Engineering Education, 38:31-8, September, 1947.

Strong, E. K. "Predictive Value of the Vocational Interest Test," The Journal of Educational Psychology, 26:331-49, May, 1935.

Stright, I. L. "Some Factors Affecting College Success," The Journal of Educational Psychology, 38:232-40, April, 1947.

Stuit, D. B., and Hudson, H. H. "Relation of Primary Mental Abilities to Scholastic Success in Professional Schools," The Journal of Experimental Education, 10:179-82, December, 1941.

_____, and Lapp, C. J. "Some Factors in Physics Achievement at the College Level," The Journal of Experimental Education, 9:251-53, March, 1941.

Swineford, F., and Holzinger, K. J. "Selected References on Statistics, the Theory of Test Construction, and Factor Analysis," School Review, 55:363-68, June, 1947.

Thompson, R. B. "Predictive Criteria for Selecting AST Students," Journal of the American Association of Collegiate Registrars, 19:492-500, July, 1944.

Tiegs, E. W. Tests and Measurements for the Improvement of Learning. Boston: Houghton Mifflin Company, 1939.

Traxler, A. E. "Some Comments on 'The Prediction of Differential Achievement in a Technological College,'" Journal of Applied Psychology, 27:176-79, April, 1943.

University of Minnesota. Studies in the Prediction of Scholastic Achievement, Parts I and II. Minneapolis: University of Minnesota Press, 1942.

Vaughn, K. W. "Basic Consideration in a Program of Freshman Evaluation," The Journal of Engineering Education, 35:161 79, November, 1944.

_____. "Measurement and Guidance Project in Engineering Education," Carnegie Foundation for Advancement of Teaching, 39th Annual Report, 1943-44, pp. 37-43.

_____. "Pre-Engineering Inventory," The Journal of Engineering Education, 34:615-25, May, 1944.

_____. "Proposed Engineering Aptitude Test for High School Students," The Journal of Engineering Education, 38:114-21, October, 1947.

Vaughn, K. W. "Selecting Engineering Students," Occupations, 25:186, December, 1946.

_____. "Yale Scholastic Aptitude Tests as Predictors of Success in the College of Engineering," The Journal of Engineering Education, 34:572-82, April, 1944.

Veterans Administration. Predicting Success in Engineering Training, Bulletin TB 7-11. Washington: Government Printing Office, December 11, 1946.

Votaw, D. F. "Comparison of Test Scores of Entering College Freshmen as Instruments for Predicting Subsequent Scholarship," Journal of Educational Research, 40:215-18, November, 1946.

Warner, W. L.; Havighurst, R. J.; and Loeb, M. B. Who Shall Be Educated? New York: Harper and Bros., 1944.

Williamson, E. G. How to Counsel Students. New York: McGraw-Hill, 1939.

Wilson, M. O., and Hodges, J. H. "Predicting Success in the Engineering College," Journal of Applied Psychology, 16:343-57, August, 1932.

Reprinted from JOURNAL OF THE AERONAUTICAL SCIENCES
Copyright, 1950, by the Institute of the Aeronautical Sciences and reprinted by permission of the copyright owner
DECEMBER, 1950 VOLUME 17, NO. 12

A Study of the Response of an Airplane Landing Gear Using the Differential Analyzer*

WALTER C. HURTY†

University of California at Los Angeles

SUMMARY

The response of a conventional airplane landing gear is studied by deriving and solving the differential equations of motion for the system. The resistance of the air-oil shock strut depends upon an orifice damping coefficient and an exponent, γ, which determines the air pressure as a function of volume. A study of experimental "drop-test" results on similar systems is made to determine these constants. The nonlinear equations of motion are solved by means of the differential analyzer for (1) the landing condition as simulated by a drop test and (2) the taxiing condition in which a periodic ground contour function is assumed. The differential analyzer solutions for the landing condition are compared with drop-test results on the same system.

SYMBOLS

x, $\dot{x}$, $\ddot{x}$	= horizontal components of displacement, velocity, and acceleration, respectively; positive if directed in direction of motion of the airplane
z, $\dot{z}$, $\ddot{z}$	= vertical components of displacement, velocity, and acceleration, respectively; positive if directed up
φ	= angle included between the shock-strut centerline and the vertical
α	= angle included between a tangent to the ground contour at the point of contact and the horizontal
M	= one-half of total airplane mass less m
m	= mass of "unsprung system" including wheel, tire, axle, and shock-strut piston
F_s	= axial force applied to shock strut
$G(y_2)$	= normal ground force applied to tire
z_C', z_C''	= derivatives of the ground contour function taken with respect to x_C
L	= one-half of total aerodynamic lift on airplane
g	= acceleration of gravity
λ	= wave length of ground sinusoid
a	= amplitude of ground sinusoid
ω	= angular frequency of excitation
p_a	= air pressure in shock-strut cylinder
Δp_o	= pressure drop across orifice
p_f	= fluid pressure in shock strut below orifice
d_c, d_f, d_p	= diameters, respectively, of shock air chamber, fluid chamber at orifice, and piston
a_c, a_f, a_p	= cross-section areas corresponding to diameters d_c, d_f, and d_p
y_1	= displacement of shock-strut piston measured from fully extended position
y_2	= tire deflection
$F(y_1)$	= force due to air pressure; function of y_1
$R(y_1)$	= damping function due to flow through orifice
V_a	= air volume in strut cylinder; function of y_1
V_o	= air volume when piston is fully extended
γ	= constant for polytropic compression and expansion of air
y_{1i}, y_{2i}	= initial values of y_1 and y_2 at beginning of motion
Q	= quantity of fluid flow through orifice
A_o	= orifice area
c_d	= orifice discharge coefficient
c_p	= orifice pressure coefficient
k_p	= shock-strut constant $= a_p/V_o$
h	= height of free drop in drop test

Subscripts A, B, and C refer, respectively, to the airplane center of gravity, the center of the wheel, and the point of contact of wheel with ground. Subscript so refers to snubber orifices.

INTRODUCTION

IN THE DESIGN OF AIRPLANE STRUCTURES, it is becoming increasingly important to take into consideration transient states of stress, as well as steady-state stresses resulting from periodic forces applied to the airplane. An example of the emphasis placed upon the determination of such dynamic stresses may be seen in the many efforts that have been made in recent years to determine stresses in the wings of an airplane resulting from the landing impact.[1, 2] The growing urgency of this problem has been brought about by two trends in airplane design: first, the use of thin wings demanded by aerodynamic considerations connected with high-speed flight; second, the disposition of items of considerable mass along the wing span outboard of the landing gear attachment points. Both factors reduce the natural frequencies of the wing in both bending and torsion and, hence, increase the likelihood of exciting large amplitude vibrations by means of ground forces.

The calculation of bending and torsional vibrations of an elastic wing can be made by well-established methods of analysis provided the forces applied by the landing gear are known as functions of time. It is the purpose of this paper to outline a method of determining such force functions in specific cases rather than to investigate the wing vibrations. Strictly speaking, the problem cannot thus be separated into two parts, since the motions of the shock-absorbing system and those of the vibrating wing are coupled. However, it has been shown[2] that the landing-gear forces can be determined with but a small error on the conservative

Received January 3, 1950.

* The author is indebted to Northrop Aircraft, Inc., and, in particular, to A. M. Schwartz and Dr. A. T. Zahorski of that company for the data used in this analysis. He also wishes to thank Prof. L. M. K. Boelter, Dean of the College of Engineering, University of California at Los Angeles, for making available the use of the differential analyzer for the solution of the equations.

† Assistant Professor, College of Engineering.

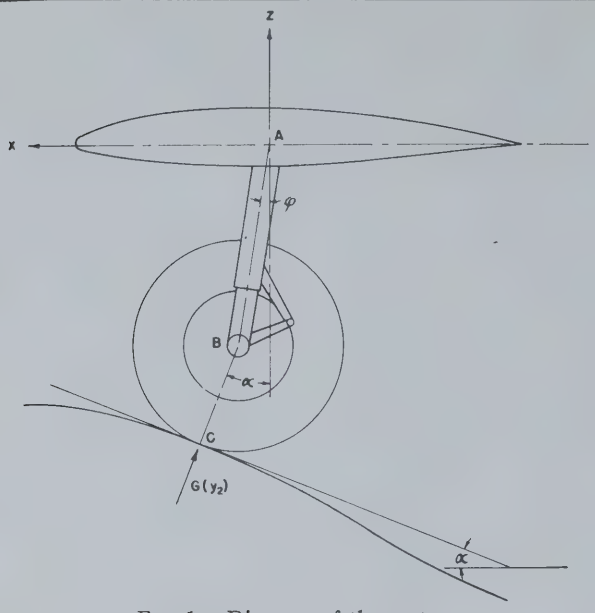

FIG. 1. Diagram of the system.

side by considering the airplane as a rigid body, and this procedure is followed in the present investigation.

The work reported here was carried out as part of a general analysis made in connection with the design of a particular airplane. In scope, the problem consisted of the determination, by analytical means, of the forces imposed on the wing by the landing-gear strut in landing and taxiing the airplane. Since the bending modes of vibration were of particular interest, only the vertical forces transmitted to the wing were found. The equations of motion derived for the two degree of freedom system are nonlinear and require for their solution the use of numerical analysis techniques or an analog computer. In this case, use was made of the mechanical differential analyzer located on the campus of the University of California at Los Angeles and operated by the College of Engineering. This machine is extremely versatile and well adapted to the solution of nonlinear differential equations.

EQUATIONS OF MOTION

The system, shown in Fig. 1, consists of a mass M, representing the airplane; a conventional air-oil shock strut; and a mass, m, representing the wheel, tire, axle, and shock-strut piston. Equations are derived for the motion of the system as the airplane rolls over an uneven ground surface at a constant velocity. From these equations we may write those pertinent to the landing case without difficulty. Energy dissipated by the tire is neglected, inasmuch as it will be small compared with that dissipated by the shock strut. Referring to Fig. 1, we may obtain the following velocity relationships useful in the derivation:

$$\left.\begin{aligned} \dot{x}_A &= \dot{x}_C + \dot{y}_1 \sin\varphi + \dot{y}_2 \sin\alpha \\ \dot{z}_A &= \dot{z}_C - \dot{y}_1 \cos\varphi - \dot{y}_2 \cos\alpha \\ \dot{x}_B &= \dot{x}_C + \dot{y}_2 \sin\alpha \\ \dot{z}_B &= \dot{z}_C - \dot{y}_2 \cos\alpha \end{aligned}\right\} \tag{1}$$

Differentiating with respect to time, the following acceleration equations are written:

$$\left.\begin{aligned} \ddot{x}_A &= \ddot{x}_C + \ddot{y}_1 \sin\varphi + \ddot{y}_2 \sin\alpha + \dot{y}_2\dot{\alpha}\cos\alpha \\ \ddot{z}_A &= \ddot{z}_C - \ddot{y}_1 \cos\varphi - \ddot{y}_2 \cos\alpha + \dot{y}_2\dot{\alpha}\sin\alpha \\ \ddot{x}_B &= \ddot{x}_C + \ddot{y}_2 \sin\alpha + \dot{y}_2\dot{\alpha}\cos\alpha \\ \ddot{z}_B &= \ddot{z}_C - \ddot{y}_2 \cos\alpha + \dot{y}_2\dot{\alpha}\sin\alpha \end{aligned}\right\} \tag{2}$$

The equations of equilibrium of the vertical components of the forces at points A and B are

$$-M\ddot{z}_A - Mg + L + F_s \cos\varphi = 0 \tag{3}$$

$$-m\ddot{z}_B - mg + G(y_2)\cos\alpha - F_s \cos\varphi = 0 \tag{4}$$

We substitute for $\ddot{z}_A$ and $\ddot{z}_B$ their equivalents given by equations and express the equilibrium equations in terms of the vertical components of the accelerations at the ground contact point C. This, in turn, may be calculated if we know the velocity of the airplane and the ground contour function.

$$\dot{z}_C = \dot{x}_C \tan\alpha \tag{5}$$

$$\ddot{z}_C = \ddot{x}_C \tan\alpha + \dot{x}_C\dot{\alpha}\sec^2\alpha \tag{6}$$

$$\left.\begin{aligned} \tan\alpha &= z_C', \quad \sec^2\alpha = 1 + z_C'^2 \\ \dot{\alpha} &= [z_C''/(1 + z_C'^2)]\dot{x}_C \end{aligned}\right\} \tag{7}$$

Finally, expressing $\dot{x}_C$ in terms of $\dot{x}_A$ from Eqs. (1) we can write the two equations of equilibrium as follows:

$$\ddot{y}_1(\cos\varphi + z_C' \sin\varphi) + \ddot{y}_2\sqrt{1 + z_C'^2} = \ddot{x}_A z_C' + z_C''\left(\dot{x}_A - \dot{y}_1 \sin\varphi - \dot{y}_2 \frac{z_C'}{\sqrt{1 + z_C'^2}}\right)^2 + g\left(1 - \frac{L}{Mg}\right) - \frac{F_s}{M}\cos\varphi \tag{8}$$

$$\ddot{y}_1 z_C' \sin\varphi + \ddot{y}_2\sqrt{1 + z_C'^2} = \ddot{x}_A z_C' + z_C''\left(\dot{x}_A - \dot{y}_1 \sin\varphi - \dot{y}_2 \frac{z_C'}{\sqrt{1 + z_C'^2}}\right)^2 + g - \frac{G(y_2)}{m\sqrt{1 + z_C'^2}} + \frac{F_s}{m}\cos\varphi \tag{9}$$

These equations are perfectly general in that they apply for any ground contour function we may choose as long as the tire is tangent to the ground at not more than one point. Although no fundamental difficulty is encountered in attempting to solve the equations by the differential analyzer, they may be simplified for most practical cases without appreciable loss of accuracy. In the present problem, the strut angle φ is small for the taxiing attitude of the airplane. Also, the ground slope z_C' is usually small compared with unity. Thus, Eqs. (8) and (9) may be simplified to the following form:

$$\ddot{y}_1 + \ddot{y}_2 = \ddot{x}_A z_C' + \dot{x}_A{}^2 z_C'' + g[1 - (L/Mg)] - (F_s/M) \quad (10)$$

$$\ddot{y}_2 = \ddot{x}_A z_C' + \dot{x}_A{}^2 z_C'' + g - \{[G(y_2) - F_s]/m\} \quad (11)$$

Considering the airplane velocity to be constant, the equations are finally arranged in the following dimensionless form:

$$\frac{\ddot{y}_1}{g} = \frac{G(y_2)}{mg} - \frac{F_s}{mg}\left(1 + \frac{m}{M}\right) - \frac{L}{Mg} \quad (12)$$

$$\frac{\ddot{y}_2}{g} = \frac{\dot{x}_A{}^2 z_C''}{g} - \frac{G(y_2)}{mg} + \frac{F_s}{mg} + 1 \quad (13)$$

It can easily be verified that Eqs. (12) and (13) apply to the landing condition on a level surface if we make z_C'' zero and apply the proper initial conditions.

It was of particular interest in this investigation to study the response of the system to excitation produced by a periodic ground function. Therefore, the simplest periodic function, the sinusoidal wave, was chosen.

$$z_C = (a/2)\,[1 - \cos(2\pi x_C/\lambda)] \quad (14)$$

This may be written as a function of time, and the dimensionless acceleration term may be expressed as

$$\dot{x}_A{}^2 z_C''/g = (a\omega^2/2g)\cos\omega t \quad (15)$$

It can be shown that the quantity $a\omega^2/2g$ is proportional to the ground reaction that would be developed if the system were rigid.

The Shock-Absorbing System

The shock-absorbing system consists of a conventional air-oil shock strut, such as used on most military and commercial airplanes, and a low-volume high load-capacity tire designed for airplanes having limited space for landing-gear retraction. The static and impact load-deflection characteristics are shown in Fig. 2. Fig. 3 shows the shock-strut design with the working parts essential to this discussion. The main orifice is metered as shown so that its area is a function of piston position. Snubber orifices are provided for rebound control and are effective only during the expansion stroke.

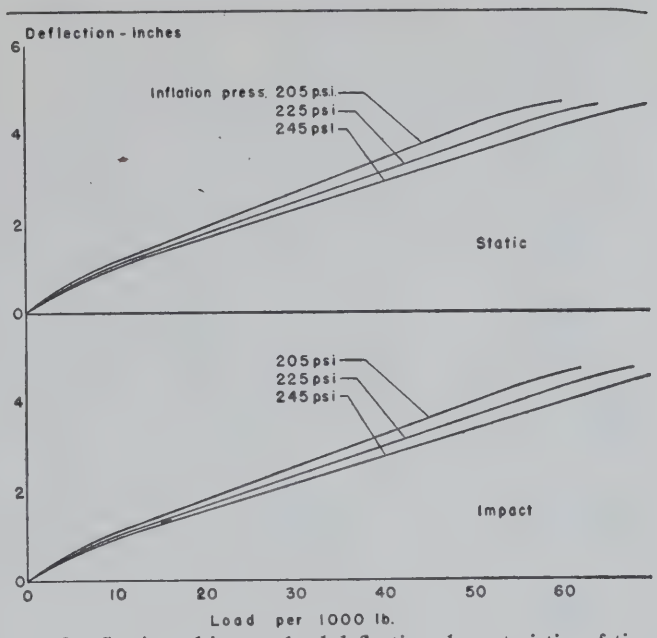

Fig. 2. Static and impact load-deflection characteristics of tire.

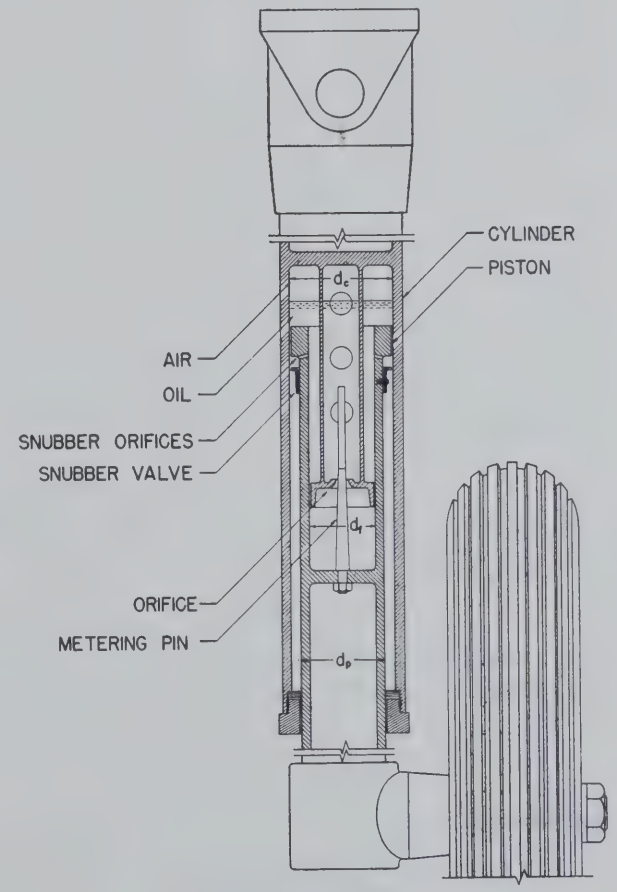

Fig. 3. Shock-strut design.

During the compression stroke, the fluid pressure below the orifice is equal to the pressure p_a and the pressure drop across the orifice Δp_o.

$$p_f = p_a + \Delta p_o \quad (16)$$

The compressive force on the piston is found by multiplying these pressures by corresponding piston areas.

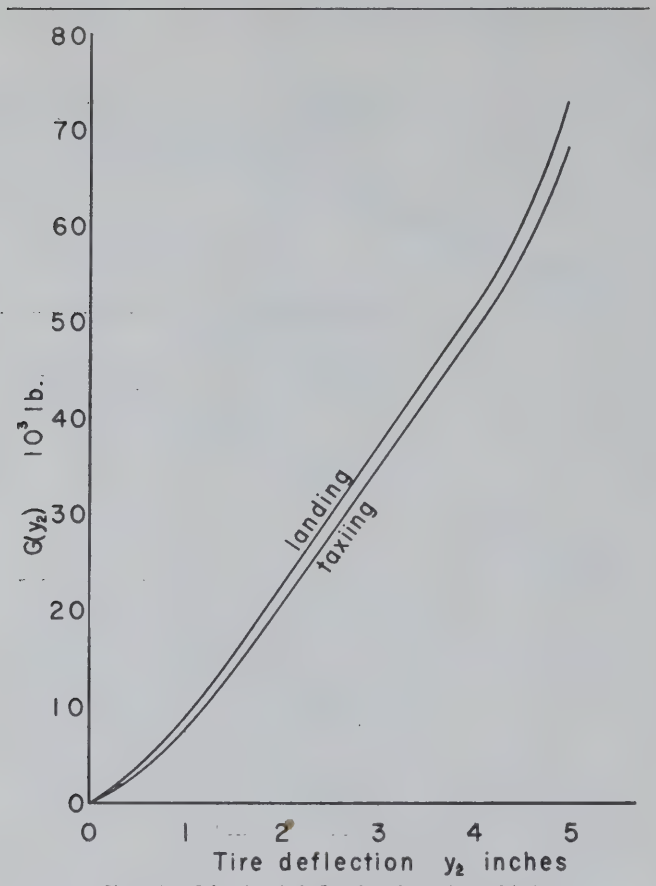

FIG. 4. Tire load-deflection function, $G(y_2)$.

$$F_s = p_a(a_c - a_f) + p_f a_f - p_a(a_c - a_p) = p_a a_p + \Delta p_o a_f \quad (17)$$

The air pressure p_a is a function of piston position only while Δp_o is a function of both position and velocity. We may write

$$F_s = F(y_1) + R(y_1)\dot{y}_1^2 \quad (18)$$

To determine $F(y_1)$, it is assumed that the air pressure may be found from

$$p_a V_a^\gamma = \text{constant} \quad (19)$$

where γ is a suitably chosen constant. We may write V_a in terms of the air volume when the piston is fully extended.

$$V_a = V_o - a_p y_1 \quad (20)$$

Substituting in Eq. (19), the force $F(y_1)$ is obtained.

$$F(y_1) = \text{constant} \times [a_p/(V_o - a_p y_1)^\gamma] \quad (21)$$

The constant depends upon the position of the piston and the force applied to it at the beginning of the motion. Assuming that the air is initially at ambient temperature, we may consider the initial piston position to have been reached by an isothermal compression from the fully extended position. This permits us to express $F(y_1)$ in terms of the initial piston position and the force F_o which holds the piston against the stops when extended.

$$F(y_1) = (1 - k_p y_{1i})^{\gamma-1} [F_o/(1 - K_p y_1)^\gamma] \quad (22)$$

To determine the orifice function $R(y_1)$, we use the equation for turbulent flow through orifices or other restrictions.

$$Q = C_d A_o \sqrt{2gh'} \quad (23)^6$$

This equation may be used to give the pressure drop across the orifice in terms of orifice area and piston velocity.

$$\Delta p_o = (3.9 \times 10^{-5})/c_d^2)\ (a_f/A_o)^2 \dot{y}_1^2 \quad (24)$$

From this, $R(y_1)$ can be determined. For the compression stroke it is given by the equation

$$R(y_1) = (3.9 \times 10^{-5}/c_d^2)\ (a_f^3/A_o^2) \quad (25)$$

During the expansion stroke, the flow conditions are more complex because of the behavior of the return flow through the main orifice and flow through the snubber orifices. As the piston moves outward, oil in the chamber above the orifice is forced by air pressure to flow downward through the main orifice. The pressure conditions are

$$p_f = p_a - \Delta p_o$$
$$p_s = p_a + \Delta p_{so}$$

Under these conditions the force on the piston is given by

$$F_s = p_a(a_c - a_f) + p_f a_f - p_s(a_c - a_p) = p_a a_p - \Delta p_o a_f - \Delta p_{so}(a_c - a_p) \quad (26)$$

and the expression for $R(y_1)$ is

$$R(y_1) = -\frac{3.9 \times 10^{-5}}{c_d^2}\frac{a_f^3}{A_o^2} - \frac{3.9 \times 10^{-5}}{c_{dso}^2}\frac{(a_c - a_p)^3}{A_{so}^2} \quad (27)$$

If the outward velocity of the piston becomes great enough, a critical velocity would be reached at which the resistance to flow through the main orifice would become equal to the pressure causing it. This condition would be characterized by the equation

$$\Delta p_o = p_a \quad (28)$$

At this velocity and beyond, the pressure p_f would drop to zero, and Eq. (26) would become

$$F_s = p_a(a_p - a_f) - \Delta p_{so}(a_c - a_p) \quad (29)$$

In this event we choose to continue to use Eq. (18), with suitable modification of R, which now becomes a function of velocity as well as displacement. We obtain it by letting $\Delta p_o = p_a$ in Eq. (26) and substituting p_a from Eq. (22).

$$R = -\frac{a_f}{a_p}\frac{(1 - k_p y_{1i})^{\gamma-1}}{(1 - k_p y_1)^\gamma}\frac{F_o}{\dot{y}_1^2} - \frac{3.9 \times 10^{-5}}{c_{dso}^2}\frac{(a_c - a_p)^3}{A_{so}^2} \quad (30)$$

Numerical Data

Because Eqs. (12), (13), and (18), which make up the system of equations to be solved, are nonlinear, their solution is sought in numerical form. Therefore, it is necessary to introduce the numerical data to be used in the specific example to be considered.

The tire function $G(y_2)$ is obtained from the tire manufacturer's data shown in Fig. 2. The impact characteristics are used in the analysis. However, the static characteristics are used to establish initial conditions; hence, a rigorous treatment would require the use of a different load curve for each initial tire deflection considered. These, in turn, depend upon the weight of the airplane and the aerodynamic lift. Actually, the differences involved are small and are accounted for by using two curves—one for the landing condition and one for the taxiing conditions. These curves are plotted in Fig. 4.

At the present time, it appears that the constants γ and c_d can only be obtained by direct experiment. As a part of this general investigation, a number of landing-gear drop-test oscillograph records were analyzed in an attempt to determine them. These records were obtained from drop tests on shock struts similar in size and design to the one considered in this problem. Although many such drop tests have been made, not many include the direct measurement of air pressures throughout the compression and expansion strokes. Eight records in which air-pressure records were made were available for study, and the values of γ and c_d were based on results of the analysis of these records. Pressure-volume points from one of the records are plotted on logarithmic coordinates in Fig. 5. It is seen that these points group fairly closely about the straight line representing $\gamma = 1.1$, although in some of the records the scatter is somewhat greater than in the one shown. In all cases, the compression stroke begins with a γ close to the adiabatic constant for air, decreasing in value as the compression stroke progresses and then dropping still further at the end of the stroke and during the expansion stroke. The loop thus formed probably represents the heat loss through the walls of the strut during the process. From the records studied, it is concluded that γ is not a constant but that the heat transfer characteristics should be included in a rigorous study of such a system. However, from an energy standpoint, the error involved in taking γ as a constant is not great, and this simplification of the problem seems to be justified. For the solution of the present problem, a value of 1.1 was chosen.

The determination of c_d from the records is more difficult, and the values found show considerable scatter when plotted. It was found convenient to use an orifice pressure coefficient, c_p, defined by

$$\Delta p_o = c_p V_o^2 \tag{31}$$

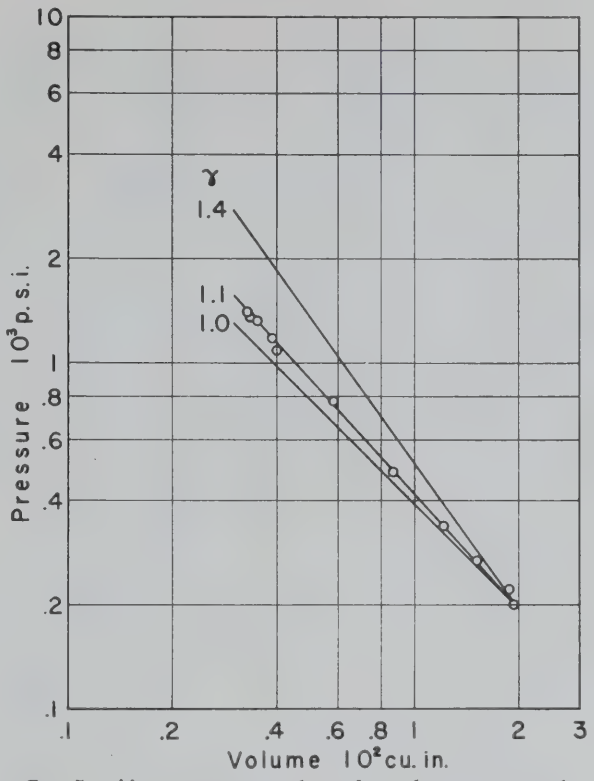

Fig. 5. Air pressure vs. volume from drop-test record.

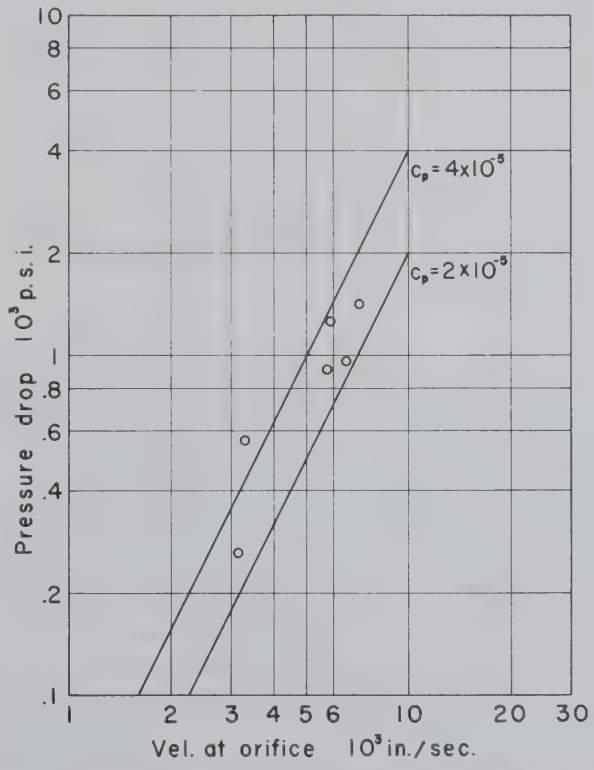

Fig. 6. Pressure drop vs. velocity through orifice from drop-test record.

The relationship between the two coefficients is

$$c_p = 3.9 \times 10^{-5}/c_d^2 \tag{32}$$

The velocity of flow through the orifice is dependent upon piston velocity and net orifice area, both of which

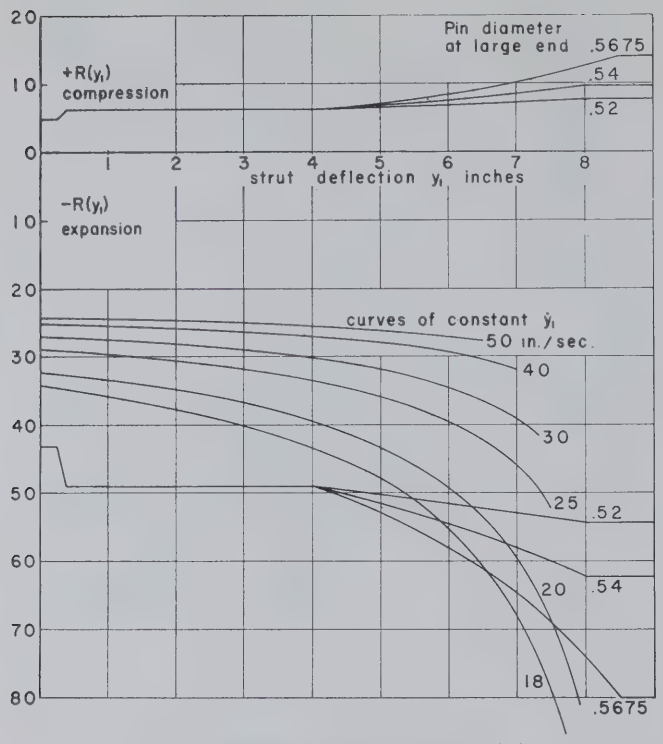

FIG. 7. Orifice damping function $R(y_1)$.

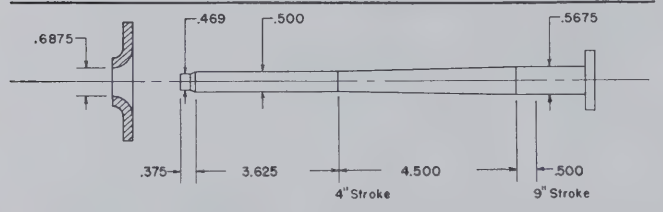

FIG. 8. Metering pin and orifice.

may be determined from the piston displacement trace and metering-pin dimensions.

$$V_o = (a_f/A_o)\dot{y}_1 \tag{33}$$

The pressure drop may be found if we know the damping force. In analyzing the records, this force was assumed to be the difference between the total compressive force on the piston and that due to the air pressure already determined. This neglects the effects of friction, which should be taken into account at this point. Attempts to evaluate the frictional force were not successful because the test data were not sufficiently complete for this purpose. However, near the end of the compression stroke where the damping force approaches zero, friction was found to be unimportant, as indicated by the fact that the measured force due to air pressure was nearly equal, in all cases, to the total force. Computed pressure drops were plotted against orifice velocity. A typical plot is shown in Fig. 6. The points are widely scattered but fall between $c_p = 2 \times 10^{-5}$ and $c_p = 5 \times 10^{-5}$. An average value of 3.5×10^{-5} is used in the majority of the differential analyzer solutions, although for comparison partial solutions of the drop-test condition were made using values ranging between 2.5×10^{-5} and 4.6×10^{-5}. For reverse flow through the main orifice, c_d is taken as 0.52, which is the value generally used for re-entrant tubes. The snubber orifices are small drilled holes with square edges, for which the coefficient is 0.61. The remaining data required to determine $F(y_1)$ and $R(y_1)$ depend on the dimensions of the shock strut and are listed in Table 1. Curves of $R(y_1)$ as used on the differential analyzer input table are shown in Fig. 7 and represent the function as derived for the metering pin shown in Fig. 8, as well as for pins having slightly smaller diameters at the large end. The latter curves were included to study the effect of metering-pin taper.

TABLE 1
Numerical Data

Total stroke of shock strut	9.00	in.
Static to fully compressed	1.66	in.
Air piston diameter, d_p	5.5	in.
Air volumes: Compressed	19.67	cu.in.
Static	59.02	cu.in.
Extended	233.49	cu.in.
Fluid piston diameter, d_f	4.75	in.
Main orifice diameter	0.6875	in.
Rebound check: Inside diameter of cylinder, d_c	5.75	in.
Number of snubber orifices	2	
Diameter of snubber orifices	0.0625	in.
Specific gravity of fluid	0.834	
Airplane gross weight	46,460	lbs.
Weight on main wheels in static position	40,580	lbs.
Weight of unsprung mass, per wheel	420	lbs.

Differential Analyzer Solutions

Inasmuch as several excellent papers[3-5] are available which describe machines of the type used in the solution of the present problem, no further description is included here. A schematic diagram of the machine circuit is shown in Fig. 9. Equipment used included eleven integrators; two input tables for introducing the functions $G(y_2)$ and $R(y_1)$; and three output tables on which were plotted y_1, y_2, $\dot{y}_1$, $\dot{y}_2$, and F_s/Mg as functions of time. The function $F(y_1)$ was generated in the machine by using two integrators—one with inverted input and output connections for generating the logarithm of $(1 - k_p y_1)$.

In order to begin the solutions on the differential analyzer, the initial conditions to be imposed must be known. These conditions determine the initial displacements of the integrators and the input and output tables. In the landing conditions, the motion consists of two phases: the first beginning at the instant of contact between the tire and the ground and consisting of tire deflection only. The shock-strut piston does not move relative to the cylinder during this phase because the initial force F_o is greater than the external force applied to the strut. The solution in this case may be found by making minor modifications to the machine circuit such that $\ddot{y}_1 = \dot{y}_1 = y_1 = 0$ during this period. The initial conditions, then, for the landing conditions are those that exist at the instant of ground contact.

$$\dot{y}_1 = y_1 = 0, \quad y_2 = 0, \quad \dot{y}_2 = \sqrt{2gh}$$

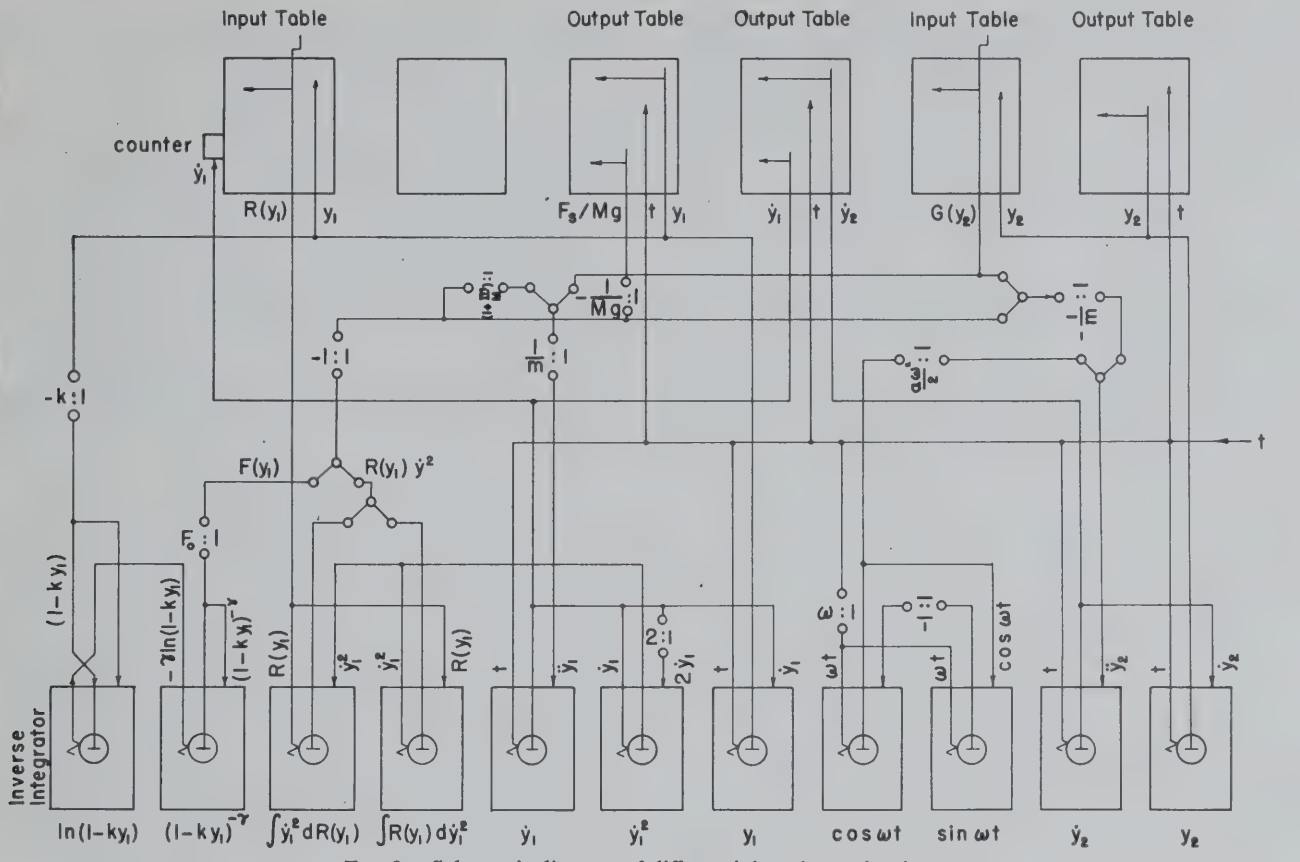

FIG. 9. Schematic diagram of differential analyzer circuit.

In the taxiing cases, the initial conditions were determined by considering the airplane to roll into the sinusoidal ground surface from a smooth horizontal plane. The system was considered to be in static equilibrium initially, and the deflections y_1 and y_2 were found as follows. The tire deflection was taken from the static load-deflection curve of Fig. 4 for the condition

$$G(y_2) = (M + m)g - L$$

The initial piston deflection was determined by considering the air to have undergone an isothermal compression from the extended position. This permits expressing y_1 in terms of the equilibrium force on the piston which, in turn, is equal to $Mg - L$. Thus, we write

$$y_{1_i} = \frac{1}{k_p}\left[1 - \frac{F_o/Mg}{1 - (L/Mg)}\right]$$

The remaining arbitrary initial values are $\dot{y}_1 = \dot{y}_2 = 0$. These four initial values, together with those for $\ddot{y}_1$ and $\ddot{y}_2$ which may be determined from Eqs. (12) and (13), are sufficient to set all the initial displacements in the machine. The solutions are obtained by setting the machine in motion and by allowing it to continue until the desired information is obtained. In the drop-test solutions, curves were plotted through the compression and subsequent expansion strokes to the point at which the tire left the ground on rebound. Beyond this point, the equations are no longer valid. In the taxiing solutions, the objective was to obtain steady-state oscillations of the system. Therefore, the solutions were continued until the transients were damped out and the motion during one oscillation was reproduced, or nearly reproduced, in the next.

RESULTS

The drop-test solutions were carried out in anticipation of an experimental drop-test program on the same system. Accordingly, the data used in the solutions were chosen to agree with the anticipated experimental conditions. It is unfortunate for the purpose of comparison that the experimental tests, which were conducted nearly a year after the numerical solutions were obtained, were carried out under somewhat different conditions so that exact comparisons cannot be made. However, some conclusions can be drawn which indicate that the analytical approach using the equations derived in this paper can be used with good results.

Differential analyzer solutions were obtained for the metering pin shown in Fig. 8, as well as for the variations in this pin indicated on the $R(y_1)$ curves of Fig. 7. Curves for a representative solution are shown in Fig. 10. In addition, partial solutions were made for a slightly different pin, not shown, which was subsequently used in the experimental tests and to which we shall refer as the "test pin." Solutions for this pin were not completed because they indicated that, for the gross weight considered and for the 27-in. free

drop, the tire would completely bottom, producing a peak load in excess of that permitted in the design specification. However, the "test pin" was used in the experimental tests with a lower gross weight, which permitted it to be used without causing the tire to bottom. Our comparison, then, must be made for different gross weights and only over that interval of time for which the differential solution was carried out. Curves A and B of Fig. 11 show, respectively, the experimental and analytical results for the "test pin" and show close agreement up to the point at which the tire bottoms. The weight difference does not nullify the comparison, inasmuch as experiments show that weight is a secondary factor in determining the load-factor curve provided given static tire and piston deflections are maintained. Curve C in the same figure is the analytical solution for the metering pin shown in Fig. 8. This pin is 0.1 in. larger in diameter at the end, which causes the load to increase more rapidly at the beginning of the stroke and gives the higher efficiency necessary to absorb the energy without bottoming the system. This curve is included to show the correspondence with the experimental curve during the expansion stroke. Reasonable agreement may be expected here, inasmuch as the expansion stroke is controlled largely by the snubber orifices, which were the same for both curves. In Fig. 12, the same three curves are shown plotted against piston position.

The primary objective in carrying out the solutions for the taxiing case was to determine the maximum response amplitudes corresponding to a state of resonance. Calculations carried out for a linearized system in which damping was neglected indicated that the lower natural frequency was near $\omega = 10$ rad. per sec.; therefore, a frequency range of $5 \leqq \omega \leqq 20$ was investigated. It was found that a value of 0.25 for $a\omega^2/2g$ represented the maximum excitation that could be permitted without bottoming the system or causing the tire to rebound. The response curves for this value of $a\omega^2/2g$ plotted over the above frequency range are shown in Fig. 13. A maximum response at $\omega = 10$ rad. per sec. is clearly shown. A representative solution as plotted by the differential analyzer is shown in Fig. 14. The amplitude of the ground sinusoid corresponding with the maximum excitation at resonance may be calculated.

$$a = \frac{2g}{\omega^2}\left(\frac{a\omega^2}{2g}\right) = \frac{2(386)}{100}(0.25) = 1.93 \text{ in.}$$

It is of some interest to compare the natural frequencies of the system as obtained from the differential analyzer solutions with those calculated using an idealized system in which no damping is present and linear tire and shock-strut spring characteristics are assumed. In this linear system, the actual tire load-deflection curve is replaced by a straight line tangent to the curve at the point of equilibrium. The shock-strut function $F(y_1)$ is replaced by a linear function whose slope is obtained

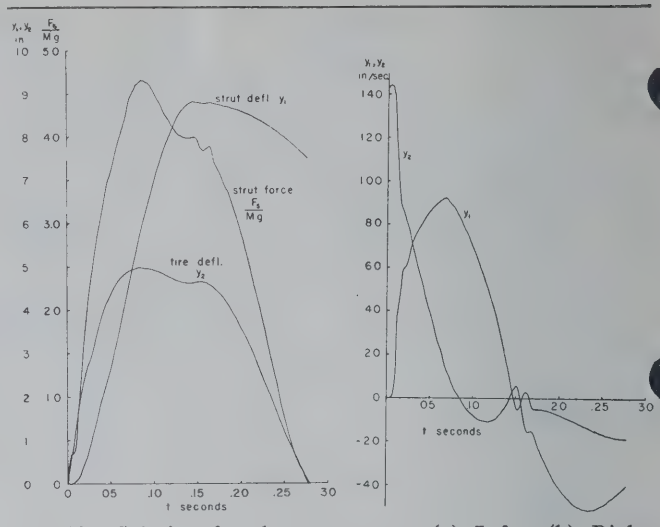

FIG. 10. Solution for drop-test case. (a) Left. (b) Right.

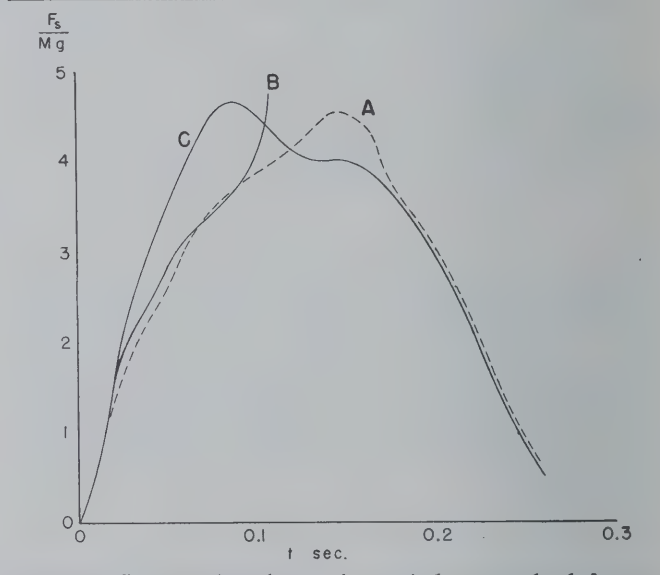

FIG. 11. Calculated and experimental drop-test load factors plotted as functions of time.

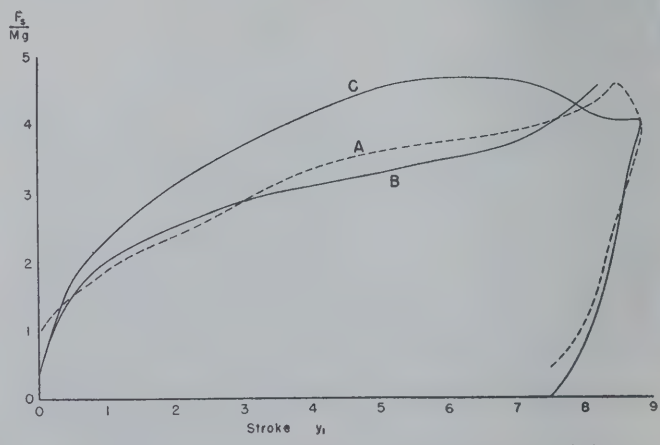

FIG. 12. Calculated and experimental drop-test load factors plotted as functions of piston position.

by substituting the equilibrium value of y_1 in the first derivative of Eq. (22). The differential equations obtained for such a system are linear, and their solution yields, for this example, angular frequencies of 10 and 157 rad. per sec. The lower frequency may be verified by measuring the period of oscillation from Fig. 14. In this mode, the motions of the piston and tire are essentially in phase. The higher frequency oscillation can be detected during the first 0.2 sec. of motion, particularly on the velocity curves. The measured period is approximately 0.04 sec., which agrees well with the calculated frequency. It is seen that in this mode the tire deflection and piston deflection are 180° out of phase.

Conclusions

By means of the equations and methods given in this paper, the response of, and loads on, a conventional airplane landing gear in landing and taxiing may be found.

Comparison of the differential analyzer solutions for the landing condition with experimental drop-test results show good correlation for the example treated. More extensive and exact comparisons should be made for further verification of the method and numerical data used. In this connection, the use of more complete instrumentation in drop-test programs to aid in the evaluation of strut air pressures, temperatures, and frictional forces would be extremely valuable. On the basis of present available data, values of 1.1 and 3.5×10^{-5}, respectively, were chosen for γ and c_p.

The natural frequencies of the landing-gear system can be calculated with good accuracy by considering an idealized system with no damping and linear spring characteristics.

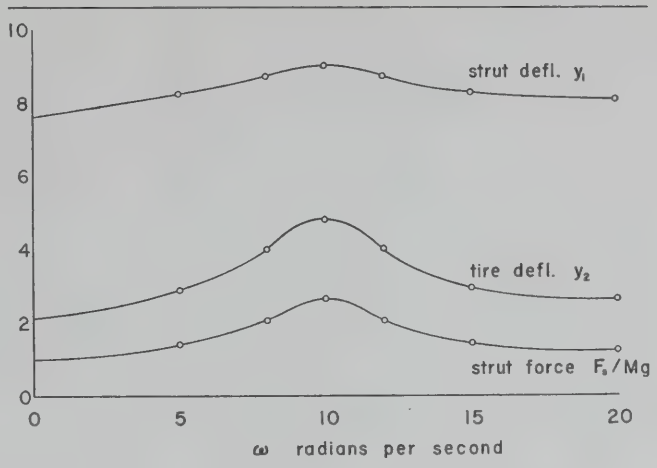

Fig. 13. Response curve for taxiing conditions.

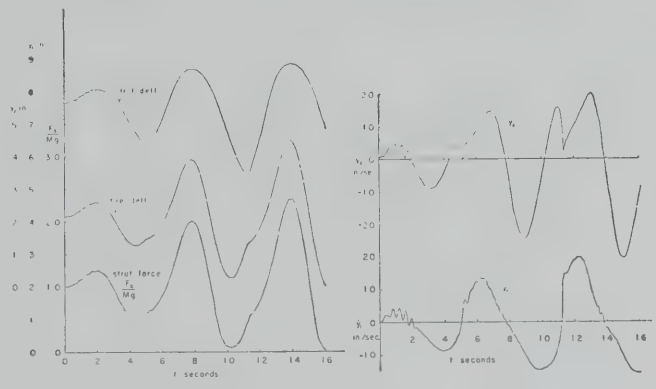

Fig. 14. Solution for taxiing case. (a) Left. (b) Right.

References

[1] Biot, M. A., and Bisplinghoff, R. L., *Dynamic Loads on Airplane Structures During Landing*, N.A.C.A. A.R.R. 4H10, October, 1944.

[2] Stowell, E. Z., *Evaluation of Some Approximate Methods of Computing Landing Stresses in Aircraft*, N.A.C.A. T.N. No. 1584 May, 1948.

[3] Bush, V., and Caldwell, S. H., *A New Type of Differential Analyzer*, Journal of Franklin Institute, Vol. 240, No. 4, October, 1945.

[4] *The Differential Analyzer of the University of California*, published by University of California at Los Angeles, 1947.

[5] Crank, J., *The Differential Analyzer*, Longmans, Green and Company, New York, 1947.

[6] Marks, Lionel S., Mechanical Engineer's Handbook, 4th Ed., p. 253; McGraw-Hill Book Company, Inc., New York, 1941.

Reprinted from JOURNAL OF APPLIED PHYSICS, Vol. 21, No. 4, 298–301, April, 1950
Copyright 1950 by the American Institute of Physics
Printed in U. S. A.

The Summation of Fourier Series by Operational Methods

LOUIS A. PIPES
Department of Engineering, University of California, Los Angeles, California
(Received September 26, 1949)

A method for the summation of certain types of Fourier series by the use of Laplace transforms is presented. The procedure enables one to easily obtain graphical representations of functions defined by Fourier series in many cases of practical importance.

I. INTRODUCTION

IN the mathematical analysis of problems in electric circuit theory, mechanical vibrations, heat conduction, and other branches of mathematical physics, one frequently arrives at solutions that are expressed in the form of infinite Fourier series. In many cases, it is more convenient to have the solutions of these problems expressed in closed form for purposes of calculation.

Oliver Heaviside[1] in the second volume of his *Electromagnetic Theory* used his rather informal "resistance operator" methods to interpret and sum Fourier series. As is well known, his mathematical processes were sometimes open to question. However, his methods frequently lead to useful results most simply, and he himself said in several instances, "I feel quite certain that this could be shown by conventional mathematics."

It is the purpose of this discussion to present a method for summing certain types of Fourier series of frequent occurrence in applied mathematics by the use of the modern Laplace method of the "Operational Calculus."

II. FUNDAMENTAL TRANSFORMATIONS

The method to be described is based upon the fact that certain hyperbolic functions can be expressed as an infinite series of exponential functions. If we use the notation,

$$A_k = e^{-kap} = \exp(-kap) \tag{2.1}$$

then the following expansions may be written

$$\tanh(ap) = 1 - 2A_2 + 2A_4 - 2A_6 + \ldots, \tag{2.2}$$

$$\coth(ap) = 1 + 2A_2 + 2A_4 + 2A_6 + \ldots, \tag{2.3}$$

$$\frac{1}{\sinh(ap)} = 2(A_1 + A_3 + A_5 + A_7 + \cdots) \tag{2.4}$$

$$\frac{1}{\cosh(ap)} = 2(A_1 - A_3 + A_5 - A_7 + \cdots), \tag{2.5}$$

a is a positive real number, and p is a number whose real part is positive.

By the use of a method due to Mittag-Leffler,[2] it is possible to obtain the following expansions,

$$\tanh(ap) = \frac{2}{ap}\left\{\frac{1}{1+(\pi/2ap)^2} + \frac{1}{1+(3\pi/2ap)^2} + \frac{1}{1+(5\pi/2ap)^2} + \cdots\right\} = \frac{2}{ap}\sum_{n=1}^{\infty}\frac{1}{1+\{[(2n-1)\pi]/2ap\}^2}, \tag{2.6}$$

$$\coth(ap) = \frac{1}{ap}\left\{1 + \frac{1}{1+(\pi/ap)^2} + \frac{2}{1+(2\pi/ap)^2} + \cdots\right\} = \frac{1}{ap}\left\{1 + \sum_{n=1}^{\infty}\frac{2}{1+(n\pi/ap)^2}\right\}, \tag{2.7}$$

$$\frac{1}{\cosh(ap)} = \frac{1}{a^2p^2}\left\{\frac{\pi}{1+(\pi/2ap)^2} - \frac{3\pi}{1+(3\pi/2ap)^2} + \cdots\right\} = \frac{1}{a^2p^2}\sum_{n=1}^{\infty}\frac{(-1)(2n-1)\pi}{1+(n\pi/2ap)^2}, \tag{2.8}$$

$$\frac{1}{\sinh(ap)} = \frac{1}{ap}\left\{1 - \frac{2}{1+(\pi/ap)^2} + \frac{2}{1+(2\pi/ap)^2} - \cdots\right\} = \frac{1}{ap}\left\{1 + \sum_{n=1}^{\infty}(-1)^n\frac{2}{1+(n\pi/ap)^2}\right\}. \tag{2.9}$$

It is possible to expand other combinations of hyperbolic functions in a similar manner, however, the above expansions are sufficient to illustrate the general principles of the method to be described.

III. THE LAPLACE TRANSFORMATION

Modern rigorous "operational calculus" is based upon the Fourier-Mellin integral equations.[3]

[1] O. Heaviside, *Electromagnetic Theory* (D. Van Nostrand Company, Inc., New York, 1925), Vol. II, pp. 107–119.
[2] E. T. Whittaker, and G. N. Watson, *Modern Analysis* (Cambridge University Press, London, 1927), pp. 134–136.
[3] L. A. Pipes, *Applied Mathematics for Engineers and Physicists* (McGraw-Hill Book Company, Inc., New York, 1946), Chapter XXI.

These equations state that, if

$$g(p)=p\int_0^\infty e^{-pt}h(t)dt, \tag{3.1}$$

then

$$h(t)=\frac{1}{2\pi j}\int_{c-j\infty}^{c+j\infty}\frac{g(p)e^{pt}dp}{p}, \tag{3.2}$$

where $j=(-1)^{\frac{1}{2}}$ and c is a real constant of such magnitude that the poles of the integrand lie entirely to the left of the path of integration. For brevity, the notation

$$g(p)=Lh(t) \quad \text{or} \quad h(t)=L^{-1}g(p) \tag{3.3}$$

is used to denote the above relations between the functions $g(p)$ and $h(t)$. The function $g(p)$ is said to be the Laplace transform of $h(t)$ and the function $h(t)$ is said to be the inverse Laplace transform of $g(p)$. Extensive tables of Laplace transforms have been compiled.[3] In this discussion we require the transforms of the sine and the cosine. These transforms are given by

$$L\sin(nwt)=\frac{nwp}{p^2+n^2w^2}=\frac{nw}{p}\cdot\frac{1}{1+(nw/p)^2} \tag{3.4}$$

and

$$L\cos(nwt)=\frac{p^2}{p^2+(nw)^2}=\frac{1}{1+(nw/p)^2}. \tag{3.5}$$

Another result of the theory of Laplace transform that is required is the following one.[3]

If

$$L^{-1}g(p)=h(t) \tag{3.6}$$

then

$$L^{-1}e^{-kp}g(p)=\begin{cases}0 & t<k\\ h(t-k) & t>k,\end{cases} \tag{3.7}$$

where k is a positive constant.

IV. SUMMATION OF FOURIER SERIES

The general method of summation will now be illustrated by applying it to several special cases.

Example I

In certain investigations of physical problems the following Fourier series is obtained:

$$F_1(t)=4[(\sin t/1)+(\sin 3t/3)+(\sin 5t/5)+\cdots]$$

$$=4\sum_{n=1}^{\infty}\frac{\sin(2n-1)t}{(2n-1)} \quad t>0. \tag{4.1}$$

The Laplace transform of the function $F(t)$ represented by the series (4.1) may be obtained by taking the Laplace transform of each term of the series using (3.4). In this manner one obtains

$$LF_1(t)=\frac{4}{p}\left[\frac{1}{1+(1/p)^2}+\frac{1}{1+(3/p)^2}+\frac{1}{1+(5/p)^2}+\cdots\right]. \tag{4.2}$$

We now note that, if in Eq. (2.6) we let

$$a=\pi/2, \tag{4.3}$$

then we can express the series term of (4.2) in the following form:

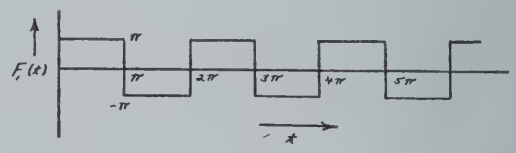

FIG. 1.

$$\left[\frac{1}{1+(1/p)^2}+\frac{1}{1+(3/p)^2}+\frac{1}{1+(5/p)^2}+\cdots\right]$$

$$=ap/2\tanh(ap). \tag{4.4}$$

Hence, comparing (4.2) and (4.4) we see that

$$LF_1(t)=2a\tanh(ap)=\tanh(\pi p/2). \tag{4.5}$$

We now use the expansion (2.2) and obtain

$$LF_1(t)=\pi[1-2e^{-\pi p}+2e^{-2\pi p}-2e^{-3\pi p}+\ldots]. \tag{4.6}$$

This is the Laplace transform of the Fourier series (4.1). To obtain the inverse Laplace transform of (4.6) and then obtain a representation of the series (4.1) we use the result (3.7). The inverse Laplace transform of the first term of (4.6) is a step function of height π formed at $t=0$. The inverse transform of the second term is a step function of height -2π formed at $t=\pi$. The inverse transform of the third term is a step function of height $+2\pi$ formed at $t=2$ and so on. The sum of all these step functions is illustrated in Fig. 1.

Example II

As a second example let it be required to interpret the following Fourier series that occurs in certain electrical and heat conduction problems.

$$F_2(t)=-\frac{2}{\pi}\sum_{n=1}^{\infty}\frac{1}{n}\sin\left(\frac{n\pi t}{s}\right). \tag{4.7}$$

By the use of (3.4), the Laplace transform of (4.7) is obtained and is given by:

$$LF_2(t)=-\frac{2}{\pi}\sum_{n=1}^{\infty}\frac{n\pi}{nsp}\frac{1}{1+(n\pi/sp)^2}$$

$$=-\frac{1}{sp}\sum_{n=1}^{\infty}\frac{2}{1+(n\pi/sp)^2}. \tag{4.8}$$

If we now compare (4.8) with (2.7) it is seen that we have,

$$LF_2(t)=\coth(sp)-1/sp. \tag{4.9}$$

By the use of (2.3) this may be written in the following form,

$$LF_2(t)=(1-1/sp+2e^{-2sp}+2e^{-4sp}+2e^{-6sp}+\ldots). \tag{4.10}$$

To obtain the inverse transform of F_2 we note that the inverse transform of the first term is a unit step function, the inverse transform of the term $-1/sp$ is $-t/s$, the inverse transform of $+2e^{-2sp}$ is a step function of height that begins at $t=2s$, etc. The sum of the various transforms gives the function $F_2(t)$. The result is given graphically in Fig. 2.
This figure is a graphical representation of the Fourier series $F_2(t)$.

Example III

As another example, let it be required to obtain the graph of the following Fourier series:

$$F_3(t)=(\sin t-\tfrac{1}{2}\sin 2t+\tfrac{1}{3}\sin 3t-\cdots)$$

$$=-\sum_{n=1}^{\infty}(-1)^n\frac{1}{n}\sin(nt). \tag{4.11}$$

In this case we transform (4.11) by the use of Eq. (3.4) and note the similarity to Eq. (2.8). Then the expansion (2.4) gives the result

$$LF_3(t)=(1/p-2\pi e^{-\pi p}-2\pi e^{-3\pi p}-2\pi e^{-5\pi p}+\ldots). \tag{4.12}$$

Now the inverse transform of $1/p$ is t, the inverse transform of $-2\pi e^{-\pi p}$ is a step function of height -2π that begins at $t=\pi$, etc. The sum of the various inverse transforms is $F_3(t)$. This function is given graphically in Fig. 3.

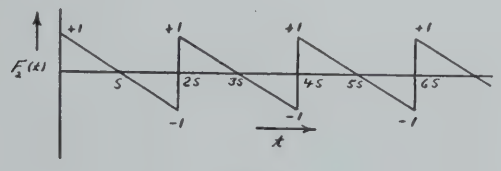

FIG. 2.

Example IV

An interesting series which arises in the analysis of the propagation of charge along a cable will now be considered. This series represents a row of impulses and the function it represents is important in the analysis of the disturbances created when lightning hits a transmission line. The series to be considered is the following one:

$$F_4(x)=-\frac{2}{s}\sum_{n=1}^{n=\infty}\sin\left(\frac{n\pi x}{s}\right)\sin\left(\frac{n\pi b}{s}\right). \tag{4.13}$$

To study this series more easily, the product of sines may be transformed into two cosines and written in the following form:

$$F_4(x)=-\frac{1}{s}\sum_{n=1}^{n=\infty}\left[\cos\frac{n\pi(x-b)}{s}-\cos\frac{n\pi(x+b)}{s}\right]. \tag{4.14}$$

Let us first consider the first series of (4.14) and let,

$$t=x-b. \tag{4.15}$$

This series may be written in the form:

$$\phi(t)=-\frac{1}{s}\sum_{n=1}^{\infty}\cos\left(\frac{n\pi st}{s}\right). \tag{4.16}$$

By (3.5) it can be transformed to:

$$L\phi(t)=-\frac{1}{s}\sum_{n=1}^{\infty}\cos\frac{1}{1+(n/sp)}. \tag{4.17}$$

By the use of Eqs. (2.7) and (2.3) this may be written in the form,

$$L\phi(t)=p/s(1+2e^{-2sp}+2e^{-4sp}+\ldots). \tag{4.18}$$

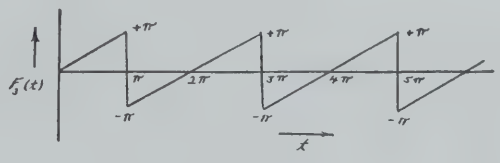

FIG. 3.

To obtain the inverse transform of this function we note that,[3]

$$L^{-1}p=\delta(t). \tag{4.19}$$

The function, $\delta(t)$, is an impulse function known in the literature as the Dirac function. It has the following properties:

$$\delta(t)=\begin{cases}0 & t\neq 0\\ \infty & t=0\end{cases} \tag{4.20}$$

and

$$\int_{-\infty}^{+\infty}\delta(t)dt=1. \tag{4.21}$$

As a consequence of (3.7), the inverse transform of (4.18) is

$$\phi(t)=1/s[\delta(t)+2\delta(t-2s)+2\delta(t-4s)+\ldots]. \tag{4.22}$$

We note that the first term is an impulse at $t=x-b=0$ or at $x=b$. The second term is an impulse located at $t=2s$ or $x=2s+b$, and so forth. The second series of (4.14) may be transformed in a similar manner if the substitution $t=x+b$ is made and it can be shown that this series represents a row of negative impulses at $x=-b$, $x=2s-b$, etc. A graphical representation of the function $F_4(x)$ defined by (4.13) is given in Fig. 4.

The function $F_4(x)$ is zero for all values of x except at the places where it has the values of positive and negative pulses of the Dirac type.

V. GENERAL CONSIDERATIONS

The general Fourier series may be written in the form:

$$F(t)=A_0+\sum_{n=1}^{\infty} A_n \cos(nwt)+\sum_{n=1}^{\infty} B_n \sin(nwt). \quad (5.1)$$

The coefficients A_n and B_n are known functions of n. By the use of Eqs. (3.4) and (3.5), it is possible to transform (5.1) into

$$LF(t)=A_0+\sum_{n=1}^{\infty} \frac{An}{1+(nw/p)^2}+\frac{w}{p}\sum_{n=1}^{\infty} \frac{nBn}{1+(nw/p)^2}. \quad (5.2)$$

The success of the method of interpretation described in this discussion depends upon the possibility of effecting the summations of (5.2) by the use of the Eqs. (2.6)–(2.9) or by formulas derivable from them.

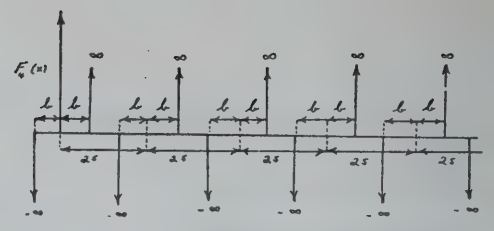

FIG. 4.

The interpretation of the Fourier series can then be carried out by the use of Eqs. (2.2)–(2.5) or combinations of these expansions.

In many cases, however, the summation of the fractions of (5.2) may present insurmountable difficulties and in such cases, this method of interpretation is not applicable.

A Time-Motion Study by Methods of High-Speed Cinematography

By Henry W. Baer, Bernard F. Cohlan and Arthur R. Gold

In this paper an attempt has been made to evaluate a method of motion study pertaining to moving machinery. The test object was a 13-ton capacity punch press and the motion study was performed with a high-speed motion picture camera. It is shown that the motion picture camera produces: (1) a visual indication of the actual occurrence which allows an understanding that nonvisual means could not afford; (2) a method of study which does not influence the system studied in the least; and (3) a record of the occurrence which has very little inherent error.

THE ADVENT of high-speed cinematography places a valuable tool in the hands of the research worker. Motion picture photography has already proved itself in many phases of science, but in some cases it is necessary to test its applicability and determine the error in the resulting record.

A common method of investigation of moving machinery has been the use of recording devices such as strain gage bridges, oscillographs, photoelectric cells, and others. In this investigation an attempt has been made to determine the merits of data obtained from a high-speed motion picture camera.

All tests were conducted in one of the Engineering Research Laboratories of the University of California, Los Angeles campus. The research was conducted by the writers who were under the general direction of Professor D. Rosenthal, and with technical advice of Mr. A. Keller for the use of high-speed photographic equipment.

A contribution submitted August 28, 1950, by Henry W. Baer, Bernard F. Cohlan and Arthur R. Gold, as a report of experiments conducted in the Engineering Research Laboratories, Dept. of Engineering, University of California, Los Angeles 24, Calif.

Description of Equipment

A standard 13-ton capacity punch press was chosen as a typical example of moving machinery. As a result of a previous investigation,* it was possible to operate the press near its full capacity. The load simulator consisted of a steel, cone-shaped indentor penetrating an aluminum block. Aluminum was chosen to reduce wear on the indentor, thus eliminating a variable due to changes in indentor form. The punch

* The previous investigation consisted of a thorough stress analysis of the entire punch-press structure to determine the maximum allowable load for continuous operation.

Copyrighted, 1951, by the Society of Motion Picture and Television Engineers, Inc.

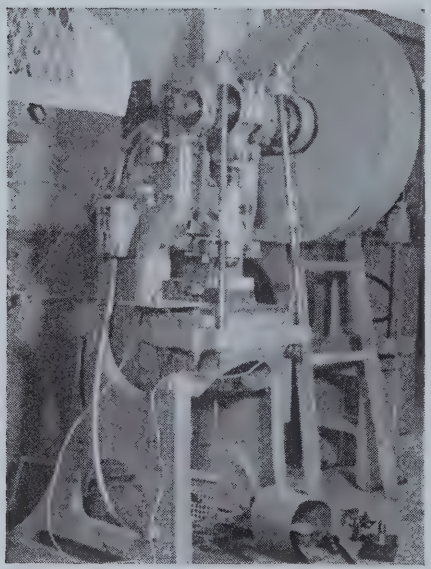

Fig. 1. Punch press.

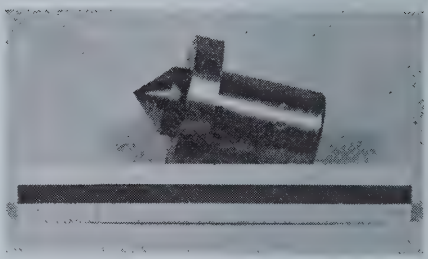

Fig. 2. Load simulator.

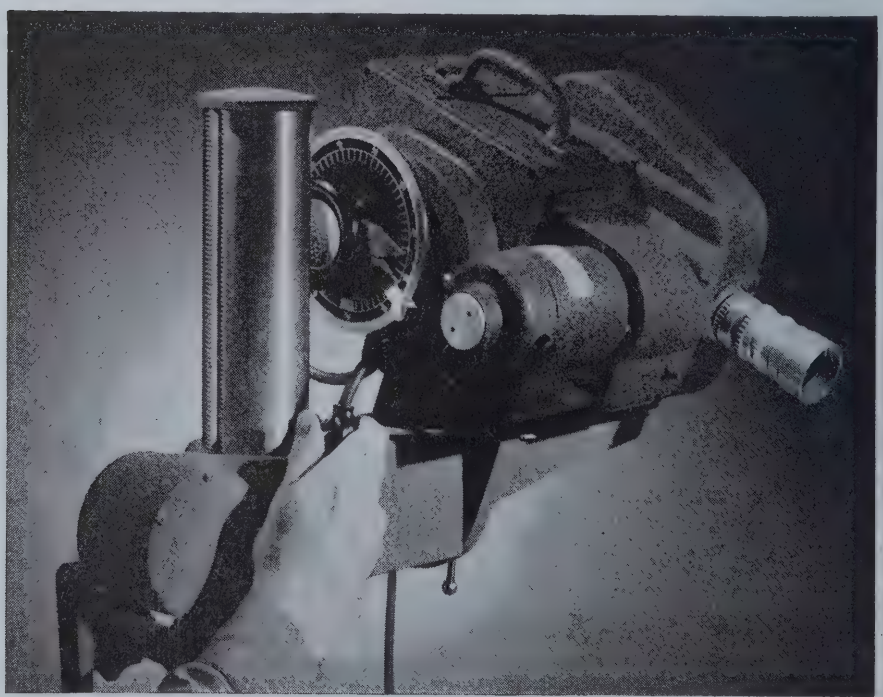

Fig. 3. Kodak High-Speed Camera.

press and load simulator are shown in Figs. 1 and 2.

The photographic measurements were obtained by a Kodak High-Speed Camera (see Fig. 3). This camera uses 16-mm film and has a maximum speed of 3000 frames/sec. The lens used was of 2½-inch focal length.

Only ram displacements were recorded. A pointer attached to the ram was photographed against a stationary scale along with a small clock marking time (Fig. 4). The clock was calibrated in milliseconds which proved to be of sufficient sensitivity for the purpose. High-speed motion pictures of the pointer, the scale, and the clock were taken while the press was in motion.

The force exerted by the ram was determined by an inked stylus oscillograph with a null-type strain gage bridge input. This force was determined from the elastic strain induced in the press tie rods (Fig. 1). To this end a pair of electric strain gages was mounted on each tie rod (Fig. 5). The strain gages in each pair were connected in series to eliminate the effect of accidental bending. The record of force was calibrated by loading the ram statically. This calibration of force was considered as an approximation only since the actual loads were dynamic ones. The time constant of the oscillograph was such that only the average value of force could be measured with reasonable accu-

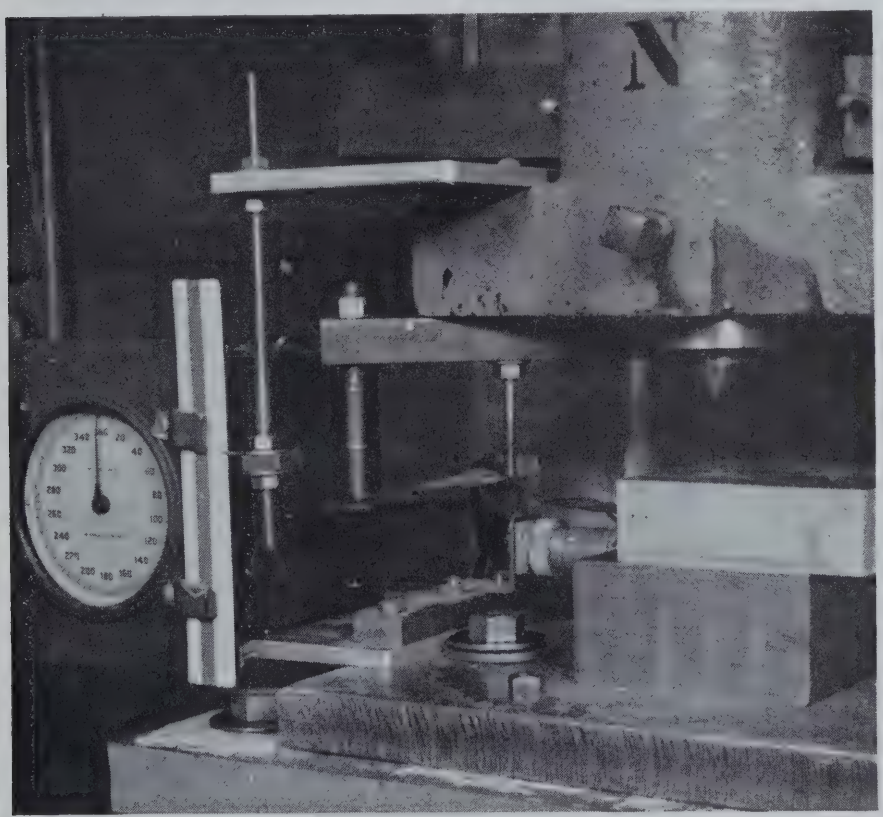

Fig. 4. Ram, pointer, stationary scale and clock.

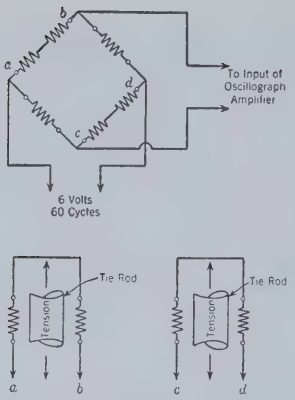

Fig. 5. Schematic arrangement of electric strain gages.

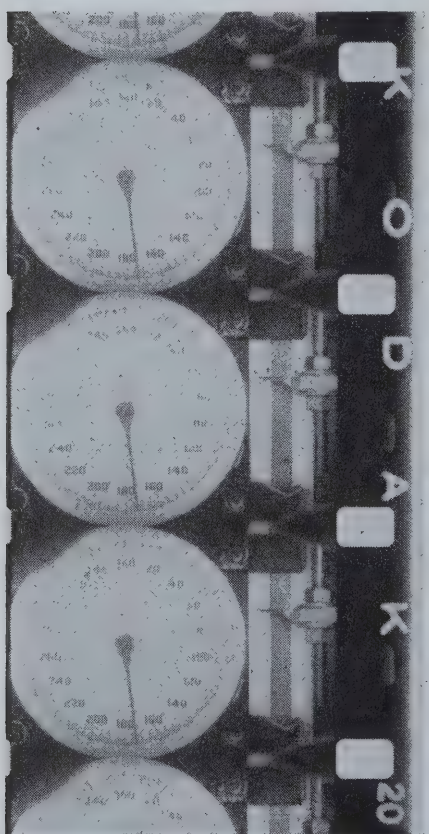

Fig. 6. Section of recording film (×4).

racy; therefore, the force indication was used only as a guide to operation within the capacity of the press.

Experimental Procedure

Experimental data were obtained from photographic recordings of the press operation. The operation consisted of repeated impacts between the indentor and the aluminum specimen, simulating an actual punch-press operation. The resulting films were translated into ram displacement vs. time curves to facilitate study.

These data were reduced by taking readings of time and displacement from the film (see Fig. 6) by means of a low-power binocular microscope. The maximum error incurred in the time measurement was estimated to be 1 msec (millisecond) and the maximum error in the displacement measurement was estimated to be 0.005 in. The reduced photographic data are shown in Fig. 7. Two curves are shown, one for load, and one for no-load motion of the ram.

Experimental Results

The no-load curve is essentially a cosine curve with an amplitude of 1.25 in. and a period of 460 msec. The load curve departs from a cosine curve during impact and after impact it returns to a cosine curve as the flywheel returns to no-load energy conditions. The displacement amplitude due to this load is 1.19 in. and its period is 480 msec. The difference of 0.06 in. in amplitude between load and no-load curves can be attributed to clearance between press components which manifests itself as backlash. The load curve indicates that the ram came to rest upon impact and remained at rest until the backlash was taken up. Upon absorption of the backlash the indentor was driven into the specimen. This portion of the stroke actually did the plastic and elastic work. At completion of the work interval the ram force was removed and the

stored elastic energy raised the ram. Here again the ram remained stationary during the absorption of the backlash and then accelerated to a normal energy condition with respect to its position.

Analysis of Results

The value of a photographic analysis of this type can be demonstrated in two ways: (1) by a comparison of the experimental findings with the expected theoretical performance; and (2) by the detection of occurrences that would not ordinarily be expected from theoretical considerations. In accordance with the first principle the following theoretical discussion will indicate a good correlation between the experiment and theory.

Since it is reasonable to assume backlash in the driving mechanism—and a simple calculation reveals that the indentor velocity is relatively small when impact occurs—, it can readily be seen that little work can be done until all backlash has been taken up. Therefore, it is reasonable to believe that the indentor comes to rest for a short period of time, while the backlash is absorbed. At the end of this time further penetration occurs until the limit of the stroke has been reached. Before the ram can again be lifted the backlash must once more be taken up. During this time the indented metal gives up its elastic energy to the ram, thus lifting it a short distance. Here again the ram remains at rest while the backlash is absorbed. At this point the ram undergoes motion which does not seem consistent with the predicted path indicated by the no-load curve. This is an occurrence which was not predicted from theory and which indicates the sensitivity of the method. At first thought it would seem that the ram could not be lifted until a time later than that indicated by the no-load curve for the same displacement. The subsequent discussion appears to substantiate the experimental findings just described.

During the impact of the ram with the specimen the flywheel and motor speed greatly decrease. Consideration of the torque-speed characteristics (Fig. 8) of an induction motor shows that slightly decreased speed is associated with a

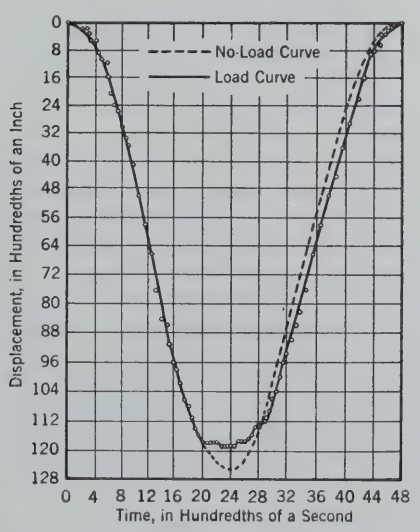

Fig. 7. Displacement-time curves.

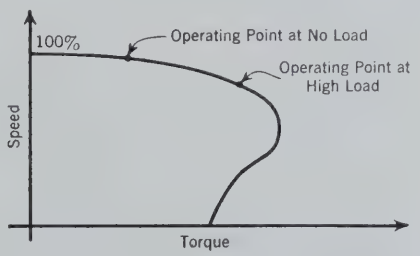

Fig. 8. Speed-torque characteristics.

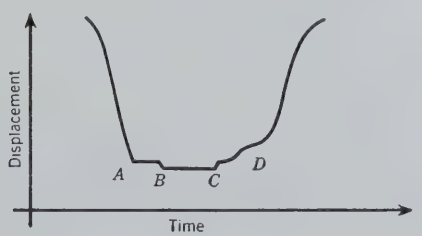

Fig. 9. Schematic displacement-time curve.

highly increased torque. Since in induction motors the assumption is made that the torque is proportional to the current, it seems reasonable that a torque requirement change will cause a current change. This shows that during impact a current surge occurs.

Examination of Fig. 9 shows that the flywheel and motor see no load from points A to B and a large load from points B to C. During the period A–B the motor tends toward zero slip and during period B–C the slip increases to some large value. This change in speed and torque causes a large surge of current which tends to continue into the period C–D due to the inductive properties of the motor. This surge current could accelerate the driving system to a point where it could lift the ram at an earlier time than that indicated by the no-load curve. Under this high acceleration the flywheel would return to a normal energy level in an extremely short time after impact, as was actually indicated by the experiment.

Thus the high-speed camera has shown an occurrence that could have been overlooked by a recording system which possesses a lesser degree of perception.

Final Evaluation of High-Speed Cinematography

1. Versatile; can be adapted to a wide variety of uses.
2. The photographic equipment is stable and unaffected by surrounding conditions.
3. The film provides a reliable and permanent data record.
4. The equipment requires a minimum of installation time for time-motion studies.
5. The method allows direct visual study of high-speed occurrences.
6. The photographic method does not alter the system being studied as the system is completely isolated from the recording device.
7. The error introduced in translation from the film to the reduced form is negligible in most applications.
8. The ability of the photographic method to detect rapid changes is limited predominantly by the maximum camera speed. Its ability to detect small magnitude changes is limited primarily by the magnifying and resolving power of the lens and also by the grain size of the film. These limits far exceed the limits of other recording systems of comparable cost and complexity.
9. The photographic method has a disadvantage in that the experimental record cannot be used until the film has been processed which means delay and increased research cost.

Recommended Further Studies

In subsequent studies of the problem an attempt should be made to use high-speed cinematography in the determination of the following factors related to a punch-press operation:

1. What are the energy-time relations between flywheel and ram under several kinds of simulated loads?
2. What percentage of its kinetic energy does the flywheel lose during the interval of maximum work?
3. Is there a lag between minimum flywheel energy and maximum force exerted on the ram?

The above factors should be investigated by high-speed cinematography methods by establishing relationships of time functions of displacement, force, and flywheel revolution rates. It is hoped that a satisfactory answer to the above additional questions in conjunction with the data as presented in this paper could serve as a guide in future punch-press design. The recommended experiments would also demonstrate the utility of high-speed cinematography.

Reprinted from JOURNAL OF THE AERONAUTICAL SCIENCES
Copyright, 1950, by the Institute of the Aeronautical Sciences and reprinted by permission of the copyright owner
OCTOBER, 1950 VOLUME 17, NO. 10

Transient Loading of Supersonic Rectangular Airfoils*

JOHN W. MILES†

University of California at Los Angeles

SUMMARY

The results of earlier papers are used to calculate the lift and moment coefficients for a rectangular airfoil that experiences a sudden change in angle of attack (without rotation) in an otherwise uniform supersonic stream or which enters a sharp-edged gust. The results are valid when the Mach lines from the leading-edge corners do not intersect the opposite side edges. Numerical results are given in the form of curves.

(1) INTRODUCTION

THE INDICIAL ADMITTANCE of a system is defined as its response to a step function excitation. In the present situation, it is desired to calculate the pressure distribution along a spanwise strip x of a rectangular airfoil due to an angle of attack along a second spanwise strip ξ, which has the value zero before $t = t_0(\xi)$ and unity thereafter. This result, which is essentially the Green's function for the problem, may then be used to find the response of the airfoil to an excitation that has an arbitrary distribution in space and time.

NOTATION

A.R. = aspect ratio (ratio of span to chord)
C_L = lift coefficient, Eq. (2.10)
C_M = moment coefficient, Eq. (2.11)
J_0 = Bessel function, first kind, zero order
M = Mach Number (ratio of free-stream velocity to sonic velocity)
U = free-stream velocity
T = time required to reach steady state, Eq. (4.3)
a = indicial admittance, Eqs. (2.7), (3.4), and (3.6)
f = chordwise velocity distribution, Eq. (2.3)
k = Green's function for harmonic excitation, Eq. (2.2)
m = $(M - 1)/M$
n = $(M + 1)/M$
p = gage pressure
t = time
t_0 = time at which disturbance arises at point ξ, Eq. (2.5)
w = $(x - \xi)/U(t - t_0)$
x = chordwise coordinate (Fig. 1)
α = downwash angle (Fig. 1)
β = $(M^2 - 1)^{1/2}$
γ = dimensionless pressure, Eqs. (2.8) and (2.9)
δ = Dirac delta function, Eq. (2.4)
ϵ = small, positive, real constant, Eq. (2.5b)
θ = Mach angle ($\sin^{-1} 1/M$, Fig. 1)
ξ = running value of x
ρ = air mass density
τ = dimensionless time, Eq. (4.4)
ω = angular frequency

The indicial admittance for the two-dimensional supersonic airfoil has been obtained by several writers[1–5] through a variety of approaches. The method to be used in the present analysis is that of reference 4, wherein the indicial admittance was determined from the transfer function—which is to say that the response to a step function excitation was obtained from the response to a harmonic excitation. This method is chosen principally because of the availability of the latter result[6] but also because of the pedagogic emphasis that it places on the equivalence of the two results, either of which may be used to analyze arbitrary distributions of the excitation in time, by virtue of the Duhamel and Fourier methods of superposition, respectively, for linearized systems.

(2) STATEMENT OF PROBLEM

The chordwise (gage) pressure distribution—i.e., the force per unit chord acting on a spanwise strip at x—on a rectangular airfoil of aspect ratio A.R., leading edge

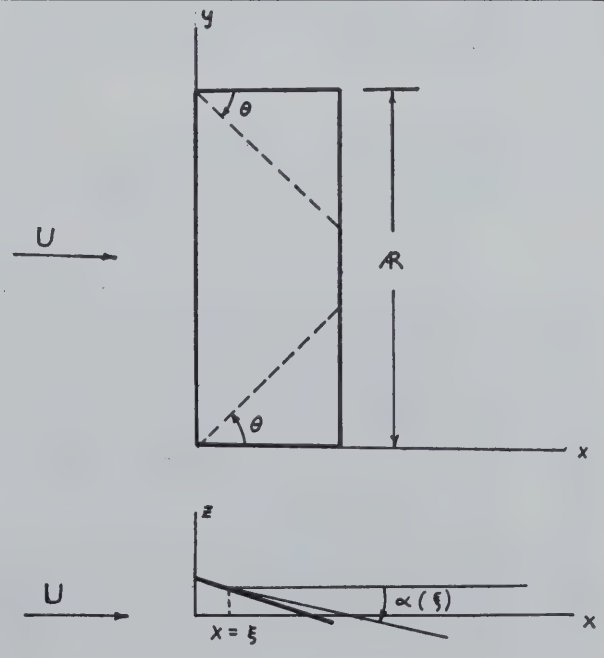

FIG. 1. Rectangular airfoil.

Received September 28, 1949.

* The author wishes to thank Irven Naiman, of the Aerodynamics Section, USNOTS, for his assistance in editing and checking the manuscript and in supervising the computation and preparation of the graphs.

† Associate Professor of Engineering. Also, Consultant, U.S. Naval Ordnance Test Station, Inyokern, Calif.

$x = 0$, and trailing edge $x = 1$ in a supersonic flow directed along the positive x axis with velocity U and Mach angle θ (Mach Number, $M = \csc\theta$), as shown in Fig. 1, due to a downwash *angle* distribution

$$\alpha(\xi, t) = \alpha(\xi) \exp(i\omega t)$$

is given by[6]

$$p(x, t) = -\left(\frac{\rho U^2}{\beta}\right)\int_0^x k(x-\xi)\alpha(\xi, t)d\xi \quad (2.1)$$

$$k(x) = k_0(x) - (\beta\text{A.R.})^{-1}k_1(x) \quad (2.2a)$$

$$k_0(x) = \delta(x-\xi) + \left(\frac{\partial}{\partial x} + \frac{i\omega}{U}\right)\times \left[\exp\left(\frac{-i\omega M^2 x}{\beta^2 U}\right) J_0\left(\frac{\omega M x}{\beta^2 U}\right)\right] \quad (2.2b)$$

$$k_1(x) = \left(\frac{\partial}{\partial x} + \frac{i\omega}{U}\right)\times \left[\left(\frac{\beta^2 U}{\omega M}\right)\exp\left(\frac{-i\omega M^2 x}{\beta^2 U}\right)\sin\left(\frac{\omega M x}{\beta^2 U}\right)\right] \quad (2.2c)$$

$$\beta = (M^2 - 1)^{1/2} \quad (2.3)$$

$$\lim_{\epsilon \to 0+}\int_{x-\epsilon}^{x+\epsilon}\delta(x-\xi)d\xi = 1 \quad (2.4)$$

where J_0 is Bessel's function of the first kind and order zero and $\delta(x-\xi)$ is the Dirac delta function. The unit of length is taken as the chord of the airfoil, the notation having been slightly modified from that of references 4 and 6. The result is linearized and holds only when the Mach lines from the leading-edge corners do not intersect on the wing. The latter restriction is met by demanding the inequality $\beta\text{A.R.} \geq 2$, although it can be shown[6] that the final results for the lift and moment coefficients are valid provided only that $\beta\text{A.R.} \geq 1$, which implies that the aforementioned Mach lines do not intersect the opposite wing edges.

The downwash distribution to be considered is given by

$$\alpha(\xi, t) = f(\xi)\,1[t - t_0(\xi)] \quad (2.5a)$$

$$= \frac{f(\xi)}{2\pi}\lim_{\epsilon \to 0+}\int_{-\infty}^{\infty} d\omega(\epsilon + i\omega)^{-1}\exp[i\omega(t - t_0)] \quad (2.5b)$$

$1(t - t_0)$ is the Heaviside step function, and Eq. (2.5b) introduces its Fourier representation in the ω spectrum. This distribution is introduced in Eq. (2.1), and the pressure may be expressed in the form

$$p(x, t) = -\left(\frac{\rho U^2}{\beta}\right)\int^x a[x-\xi, t - t_0(\xi)]f(\xi)d\xi \quad (2.6)$$

$$a(x, t) = a_0(x, t) - (\beta\text{A.R.})^{-1}a_1(x, t) \quad (2.7a)$$

$$a_{0,1}(x, t) = \frac{1}{2\pi}\lim_{\epsilon \to 0+}\int_{-\infty}^{\infty} d\omega\,(\epsilon + i\omega)^{-1}k_{0,1}(x)\exp(i\omega t) \quad (2.7b)$$

The function $a[x - \xi, t - t_0(\xi)]$ is defined as the indicial admittance of the airfoil and gives the (dimensionless) pressure at station x due to a downwash increment at station ξ, which vanishes for time earlier than $t_0(\xi)$ and has the magnitude $f(\xi)$ for time later than $t_0(\xi)$. The first term, a_0, gives the two-dimensional response, and the second term, a_1, gives the defect in the three-dimensional response, relative to its two-dimensional value, due to induction effects. Since the two-dimensional problem has been solved previously,[1–5] it suffices herein to consider the three-dimensional effects as described by a_1.

In the remainder of this paper it will be convenient to make the pressure dimensionless by writing

$$p(x, t) = -(\rho U^2/\beta)\gamma(x, t) \quad (2.8)$$

$$\gamma(x, t) = \gamma_0(x, t) - (\beta\text{A.R.})^{-1}\gamma_1(x, t) \quad (2.9a)$$

$$\gamma_{0,1}(x, t) = \int_0^x a_{0,1}[x - \xi, t - t_0(\xi)]f(\xi)d\xi \quad (2.9b)$$

The problem to be solved may now be posed as: Given $f(\xi)$, find $\gamma_1(x, t)$; this problem has been reduced to two successive quadratures, as indicated by Eqs. (2.7) and (2.9).

While some applications may require a direct knowledge of the pressure over the airfoil, the lift and moment coefficients are generally the items of principal interest. The increments in these coefficients are given by

$$-\delta C_L(t) = (\rho U^2/2)^{-1}\int_0^1 [-2p_1(x, t)]dx \quad (2.10a)$$

$$= (4/\beta^2\text{A.R.})\int_0^1 \gamma_1(x, t)\,dx \quad (2.10b)$$

$$-\delta C_M(t) = (\rho U^2/2)^{-1}\int_0^1 [-2p_1(x, t)](1/2 - x)dx \quad (2.11a)$$

$$= -\frac{1}{2}\delta C_L - \left(\frac{4}{\beta^2\text{A.R.}}\right)\int_0^1 x\gamma_1(x, t)\,dx \quad (2.11b)$$

The moment coefficient is taken about the mid-chord, and the reference moment arm is the chord ($= 1$).

(3) Indicial Admittance

Consider first the integration of Eq. (2.7b), assuming that reversing the order of the integrations with respect to ξ and ω is justifiable, which may be verified a posteriori. Carrying out the indicated differentiation in Eq. (2.2c) and substituting in Eq. (2.7b) yields

$$a_1(x, t) = (1/2\pi)\lim_{\epsilon \to 0+}\int_{-\infty}^{\infty}(\epsilon + i\omega)^{-1}\times \exp\left[i\omega\left(t - \frac{M^2 x}{\beta^2 U}\right)\right]\times \left[\cos\frac{\omega M x}{\beta^2 U} - \left(\frac{i}{M}\right)\sin\left(\frac{\omega M x}{\beta^2 U}\right)\right]d\omega \quad (3.1)$$

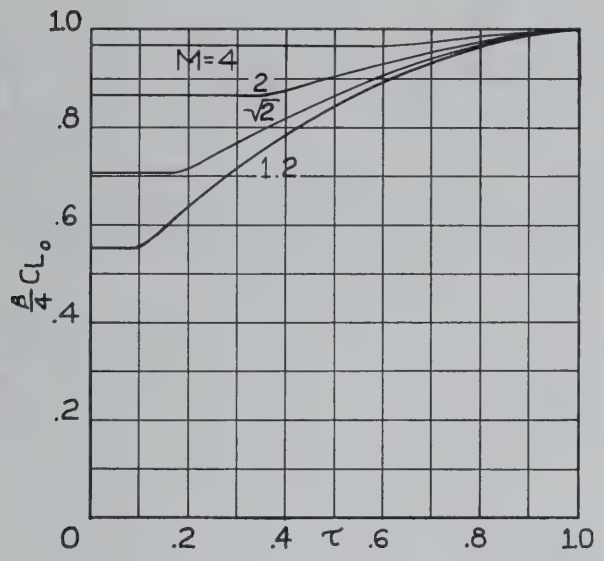

FIG. 2. Two-dimensional lift coefficient for sudden (unit) change in angle of attack.

If the trigonometric functions in Eq. (3.1) are replaced by their exponential equivalents, the result may be written

$$a_1(x, t) = \frac{1}{4\pi} \lim_{\epsilon \to 0+} \int_{-\infty}^{\infty} (\epsilon + i\omega)^{-1} \times \left\{ m \exp\left[i\omega \left(t - \frac{x}{nU} \right) \right] + n \exp\left[i\omega \left(t - \frac{x}{mU} \right) \right] \right\} d\omega \tag{3.2}$$

$$m = (M - 1)/M \tag{3.3a}$$

$$n = (M + 1)/M \tag{3.3b}$$

The integrals may be directly interpreted as step functions [cf., Eq. (2.5)], whence

$$a_1(x, t) = \frac{m}{2} 1\left(Ut - \frac{x}{n} \right) + \frac{n}{2} 1\left(Ut - \frac{x}{m} \right) \tag{3.4}$$

It is evidently convenient to introduce the single variable (x/Ut) and restate Eq. (2.9) in the form

$$\gamma_1(x, t) = \int_0^x a_1 \left\{ \frac{x - \xi}{U[t - t_0(\xi)]} \right\} f(\xi) d\xi \tag{3.5}$$

$$a_1(w) = 0, \quad w < 0 \tag{3.6a}$$

$$= 1, \quad 0 \leq w \leq m \tag{3.6b}$$

$$= m/2, \quad m \leq w \leq n \tag{3.6c}$$

$$= 0, \quad w \geq n \tag{3.6d}$$

(4) Sudden Change in Angle of Attack

The simplest transient problem of practical interest is the sudden change of angle of attack (without rotation) over the entire wing. [Physically this might arise from a suddenly imposed, vertical (downward) velocity, but the primary value of the solution is as a basis for Duhamel integration.] Consider, therefore, the downwash distribution [cf. Eq. (2.5)],

$$f(\xi) \equiv 1 \tag{4.1a}$$

$$t_0(\xi) \equiv 0 \tag{4.1b}$$

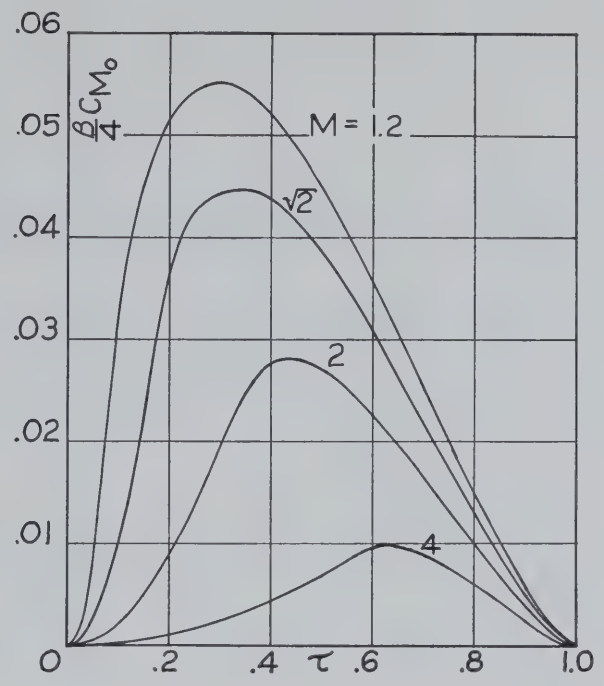

FIG. 3. Two-dimensional moment coefficient for sudden (unit) change in angle of attack.

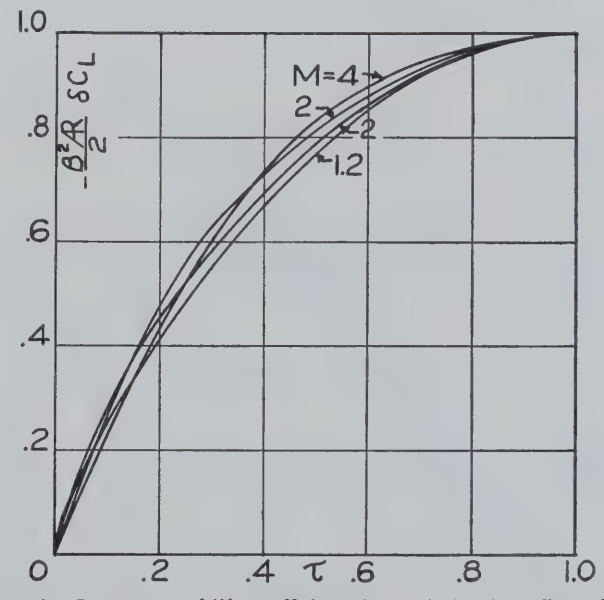

FIG. 4. Increment of lift coefficient due to induction effects for sudden (unit) change of angle of attack.

for which Eq. (3.4) reduces to

$$\gamma(x, t) = \int_0^x a_1 \left(\frac{x - \xi}{Ut} \right) d\xi \tag{4.2}$$

It is evident that the steady-state pressure will exist over the entire airfoil $(0 < x < 1)$ after a time T given by

$$T = M \times (\text{chord})/(M - 1)U \tag{4.3}$$

and it is convenient to introduce the dimensionless time parameter

$$\tau = (t/T) = m\ Ut = [(M - 1)/M]\, Ut \tag{4.4}$$

By substituting the indicial admittance from Eq. (3.5), Eq. (4.2) yields

$$\gamma_1(x, t) = x, \quad x \leq \tau \tag{4.5a}$$

$$= \frac{m}{2} x + \frac{n}{2} \tau, \quad \tau \leq x \leq (n/m)\tau \tag{4.5b}$$

$$= n\tau, \quad x \geq (n/m)\tau \tag{4.5c}$$

The lift and moment coefficients due to the pressure distribution [Eq. (4.5)] are given by Eqs. (2.10) and (2.11). Adding to these results the two-dimensional coefficients of reference 4 (allowing for the differences in notation), it is found that

$$\frac{\beta}{4} C_L = (mn)^{1/2} - (2\beta \text{A.R.})^{-1} \left[2n\tau - \left(\frac{n}{m}\right)\tau^2 \right], \quad \tau \leq \frac{m}{n} \tag{4.6a}$$

$$= \frac{1}{\pi} \cos^{-1} [M(1 - n\tau)] + \frac{(mn)^{1/2}}{\pi} \cos^{-1} \left[M \left(1 - \frac{m}{\tau}\right) \right] + \frac{1}{\pi} (2n\tau - n^2\tau^2 - mn)^{1/2} - (2\beta \text{A.R.})^{-1} \times \left[\frac{m}{2} + n\tau - \frac{n}{2}\tau^2 \right], \quad \frac{m}{n} \leq \tau \leq 1 \tag{4.6b}$$

$$= 1 - (2\beta \text{A.R.})^{-1}, \quad \tau \geq 1 \tag{4.6c}$$

$$\frac{\beta}{4} C_M = \frac{m^{-3/2} n^{1/2} (1 - m)^2}{4} \tau^2 + (12\beta \text{A.R.})^{-1} \left[3 \left(\frac{n}{m}\right) \tau^2 - 2 \left(\frac{n}{m^2}\right) (2 - 2m + m^2) \tau^3 \right], \quad \tau \leq \frac{m}{n} \tag{4.7a}$$

$$= \frac{m^{-3/2} n^{1/2} (1 - m)^2}{4\pi} \tau^2 \cos^{-1} \left[M \left(1 - \frac{m}{\tau}\right) \right] + \frac{1}{4\pi} \left(1 - \frac{\tau}{m}\right) (2n\tau - n^2\tau^2 - mn)^{1/2} + (12\beta \text{A.R.})^{-1} \left(\frac{m}{2} + \frac{3n}{2} \tau^2 - n\tau^3 \right), \quad \frac{m}{n} \leq \tau \leq 1 \tag{4.7b}$$

$$= (12\beta \text{A.R.})^{-1}, \quad \tau \geq 1 \tag{4.7c}$$

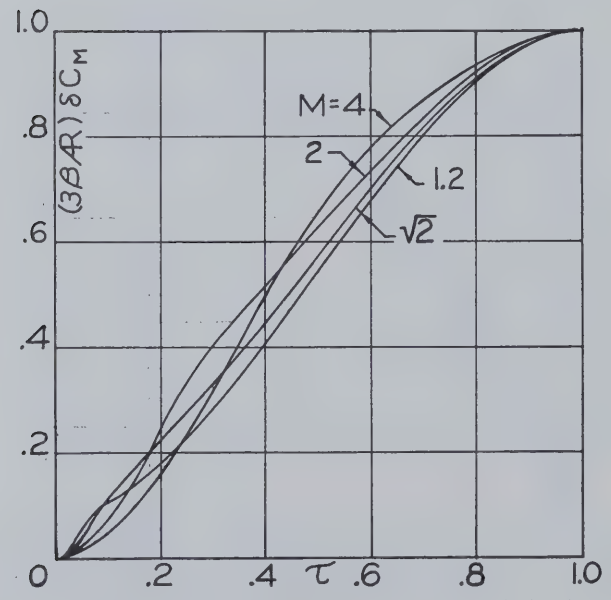

FIG. 5. Increment of moment coefficient due to induction effects for sudden (unit) change of angle of attack.

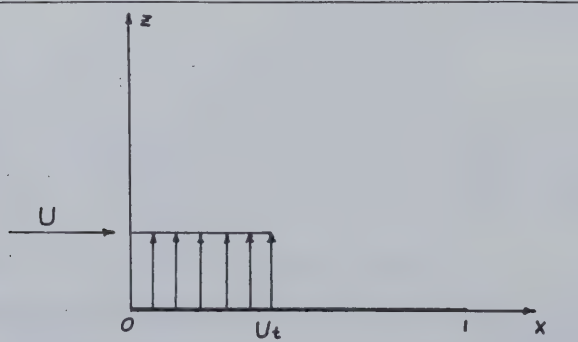

FIG. 6. Velocity distribution on airfoil at time t after entering sharp-edged gust.

The two-dimensional results C_{L_0} and C_{M_0}, as taken from reference 4, are plotted in Figs. 2 and 3. The three-dimensional increments δC_L and δC_M, defined in

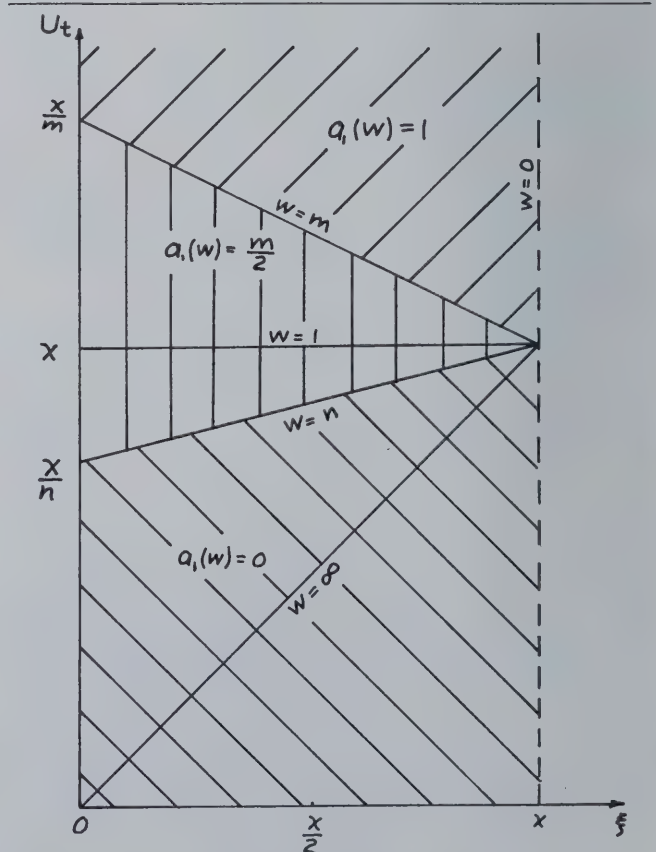

FIG. 7. Ut vs. ξ, as given by Eq. (5.3b), and $a_1(w)$, as given by Eq. (3.5).

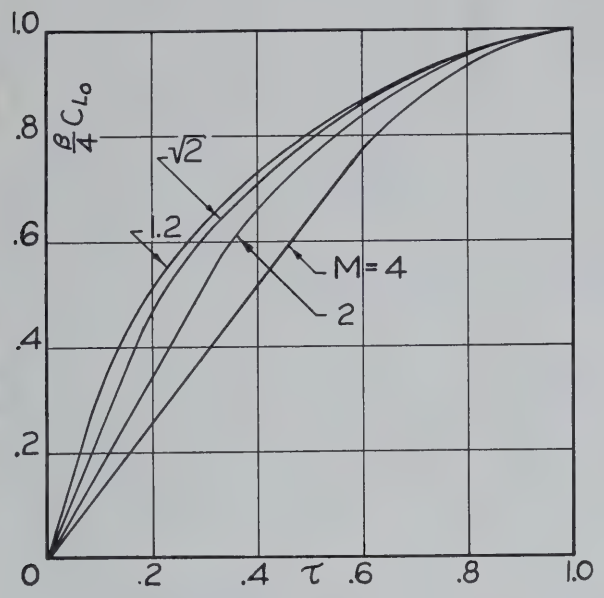

FIG. 8. Two-dimensional lift coefficient for uniform (unit) gust entry.

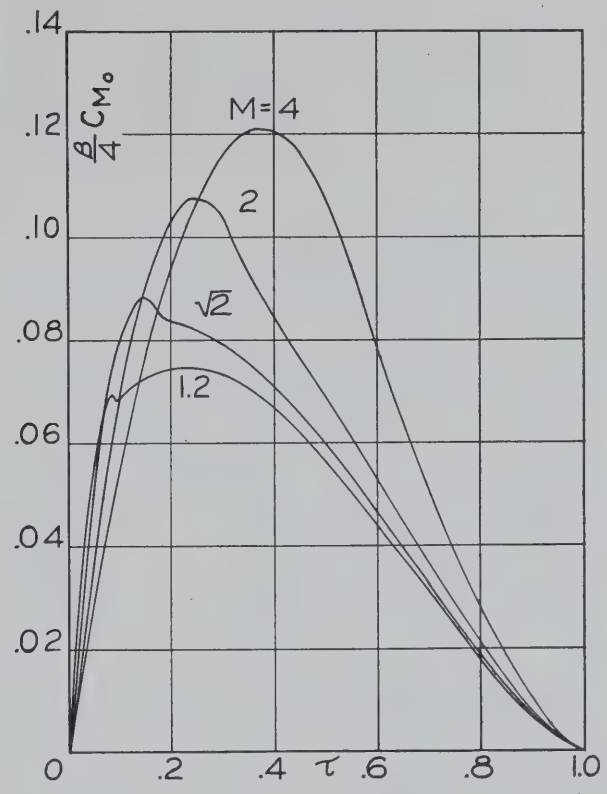

FIG. 9. Two-dimensional moment coefficient for uniform (unit) gust entry.

accordance with the relations

$$C_L = C_{L_0} + \delta C_L \tag{4.8a}$$
$$C_M = C_{M_0} + \delta C_M \tag{4.8b}$$

are plotted in Figs. 4 and 5.

(5) Gust Loading

A second special case of practical importance is the entry of the airfoil into a sharp-edged gust. In this case, the downwash distribution, which is depicted in Fig. 6, is given by Eq. (2.5), where

$$f(\xi) \equiv 1 \tag{5.1a}$$
$$Ut_0(\xi) \equiv \xi \tag{5.1b}$$

and Eq. (3.5) reduces to

$$\gamma_1(x, t) = \int_0^x a_1\left(\frac{x-\xi}{Ut-\xi}\right) d\xi \tag{5.2}$$

In carrying out the integrations in Eq. (5.2), it is expedient to examine the behavior of w in the (Ut, ξ) plane—viz.,

$$w = (x - \xi)/(Ut - \xi) \tag{5.3a}$$
$$Ut = [x + (w - 1)\xi]/w \tag{5.3b}$$

Eq. (5.3b) represents a one-parametric family of straight lines, the lines of dominant importance being shown in Fig. 7, together with the domains of $a_1(w)$ which they delineate.

Carrying out the integration indicated by Eq. (5.2) with the aid of Fig. 6 yields

$$\gamma(x, t) = x, \quad x \le \tau \tag{5.4a}$$
$$= \frac{1}{2}\left(\frac{m}{m-1}\right)x + \frac{1}{2}\left(\frac{n}{n-1}\right)\tau, \quad \tau \le x \le \frac{n}{m}\tau$$
(5.4b)
$$= 0, \quad x \ge (n/m)\tau \tag{5.4c}$$

Adding the results of substituting this result [Eq. (5.4)] in Eqs. (2.10) and (2.11) to the two-dimensional lift and moment coefficients of reference 4* yields

$$\frac{\beta}{4}C_L = \left(\frac{n}{m}\right)^{1/2}\tau - (2\beta\text{A.R.})^{-1}\left(\frac{n}{m}\right)\tau^2, \quad \tau \le \frac{m}{n} \tag{5.5a}$$
$$= \frac{1}{\pi}\cos^{-1}[M(1-n\tau)] + \frac{1}{\pi}\left(\frac{n}{m}\right)^{1/2}\tau\,\cos^{-1}\left[M\left(1-\frac{m}{\tau}\right)\right] - (2\beta\text{A.R.})^{-1}M\left(-\frac{m}{2} + n\tau - \frac{n}{2}\tau^2\right),$$
$$m/n \le \tau \le 1 \tag{5.5b}$$
$$= 1 - (2\beta\text{A.R.})^{-1}, \quad \tau \ge 1 \tag{5.5c}$$

* Eq. (28b) of reference 4 should have contained an additional factor of $1/\pi$ in the last term, for which reason Fig. 6 therein is incorrect.

$$\frac{\beta}{4} C_M = \frac{1}{2}\left(\frac{n}{m}\right)^{1/2} \tau\left(1 - \frac{\tau}{m}\right) + (12\beta \text{A.R.})^{-1}\left[-3\left(\frac{n}{m}\right)\tau^2 + 4\left(\frac{n}{m^2}\right)\tau^3\right], \quad \tau \leq \frac{m}{n} \tag{5.6a}$$

$$= \frac{1}{2\pi}\left(\frac{n}{m}\right)^{1/2} \tau\left(1 - \frac{\tau}{m}\right) \cos^{-1}\left[M\left(1 - \frac{m}{\tau}\right)\right] + \frac{1}{2\pi}\frac{\tau}{m}(2n\tau - n^2\tau^2 - mn)^{1/2} +$$

$$(12\beta \text{A.R.})^{-1} M\left[-\frac{m}{2} + \left(\frac{3n}{2}\right)\tau^2 - n\tau^3\right], \quad \frac{m}{n} \leq \tau \leq 1 \tag{5.6b}$$

$$= (12\beta \text{A.R.})^{-1}, \quad \tau \geq 1 \tag{5.6c}$$

The results of Eqs. (5.5) and (5.6) are plotted in Figs. 8–11, in accordance with Eqs. (4.8).

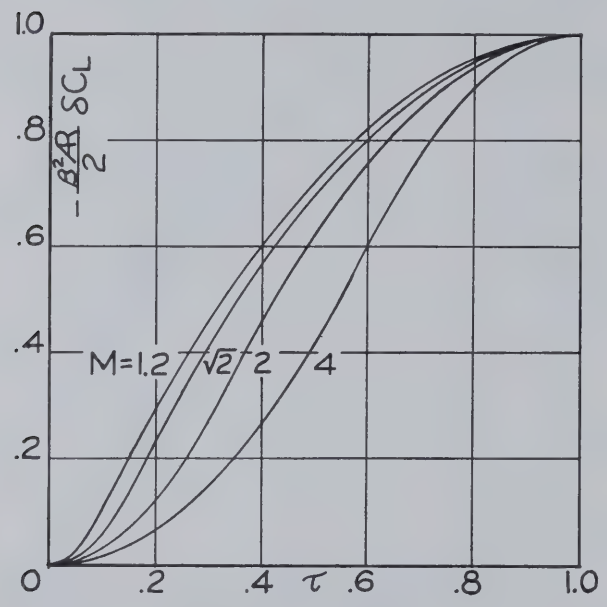

FIG. 10. Increment of lift coefficient due to induction effects for uniform (unit) gust entry.

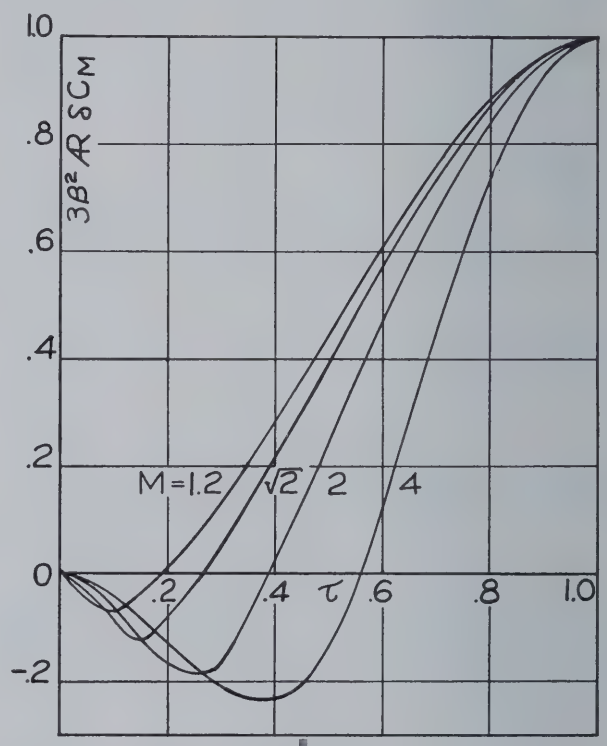

FIG. 11. Increment of moment coefficient due to induction effects for uniform (unit) gust entry.

REFERENCES

[1] Biot, M. A., *Loads on a Supersonic Wing Striking a Sharp-Edged Gust*, Journal of the Aeronautical Sciences, Vol. 16, pp. 296–301, 1949.

[2] Chang, C. C., *The Transient Reaction of an Airfoil Due to Change in Angle of Attack at Supersonic Speed*, Journal of the Aeronautical Sciences, Vol. 15, pp. 635–655, 1948.

[3] Heaslet, M. A., and Lomax, H., *Two-Dimensional Unsteady Lift Problems in Supersonic Flight*, N.A.C.A. T.N. No. 1621, 1948.

[4] Miles, J. W., *Transient Loading of Airfoils at Supersonic Speeds*, Journal of the Aeronautical Sciences, Vol. 15, pp. 592–598, 1948.

[5] Schwarz, L., *Plane Non-Stationary Theory of the Wing at Supersonic Speed*, U.S.A.A.F. Translation, F-TS-934-RE, Wright Field, Dayton, Ohio, 1947.

[6] Naval Ordnance Test Station, *The Oscillating Rectangular Airfoil at Supersonic Speeds*, by J. W. Miles, Inyokern, Calif., NOTS, 1 June, 1949 (Technical Memorandum RRB-15). (Also in press, Quart. Appl. Math.)

[Reprinted from The Journal of The American Ceramic Society, Vol. 33, No. 8. August, 1950.]

Wetting Properties of Some Enamel Glasses and Relation to Impact Resistance

by W. J. KNAPP, C. C. SHAH, and T. J. PLANJE

Department of Ceramic Engineering, School of Mines and Metallurgy, The University of Missouri, Rolla, Missouri

The wetting properties of some enamel glasses on commercially pure enameling iron were determined and compared with correlated impact resistance test results. The rate of change of wetting characteristics with temperature seemed to influence the impact resistance of the enameled metal.

I. Introduction

THE nature of the adherence of enamel glasses to iron or steel has been discussed by various investigators[1]; factors such as the coefficient of thermal expansion of the glass, solubility of iron oxide in the glass, reduction of constituents and subsequent plating of metal, formation of dendrites, development of an interfacial layer, and others have been considered. The part played by adherence-promoting oxides, such as cobalt oxide, nickel oxide, and manganese oxide, in developing adherence has been studied and related to the foregoing factors.

The effects of wetting agents in liquids are commonly known, and usually only very small additions of the agent are necessary to improve the wetting properties of the liquid. Scott[2] reports that the wetting abilities of cryolite melts on platinum at elevated temperatures were changed abruptly by minute additions of certain oxides, such as lead or bismuth oxides. An addition of lead oxide in the proportions of 1:5000 changed the nature of the melt from wetting to nonwetting. Since adherence-promoting additions to enamel batches are usually made in amounts under 2%, a study of the wetting properties of enamel glasses containing similar additions seemed desirable. King[3] has suggested that adherence is produced when the enamel glass wets the metal. The improvement of the wetting ability of an enamel glass should promote adherence by obtaining intimate contact of glass on metal, but the actual mechanism of adherence probably cannot be explained by wetting properties alone.

Absolute surface tension values for an enamel glass have been obtained by Ellefson and Taylor[4] at about 1000°C. It was noted that the glass wetted platinum when oxygen was present, but was nonwetting *in vacuo*. Harrison and Moore[5] measured the surface tension of a number of typical commercial frits at enameling temperatures by weighing the liquid supported by the meniscus adhering to a platinum cylinder.

Amberg[6] determined the surface tension of enamel glasses containing various oxide additions at 1380°C. by the drop-weight method. He suggested the possibility of a relation between surface tension and adherence. A number of other investigators[7] have reported on methods for measuring absolute surface tension.

The observations[2, 4] made on wetting properties of melts at elevated temperatures indicate the necessity of distinguishing between the surface tension of a glass and its wetting ability on a specific metal, since wetting ability is a function not only of the surface tension of the glass, but also of the specific attraction between the metal and the glass. It seemed desirable, therefore, to investigate the wetting properties of some enamel glasses on enameling iron and to compare the results with correlated impact resistance values. It was assumed that impact resistance and adherence are related to some extent.

II. Experimental Procedure

(1) *Wetting Properties*

The test procedure was somewhat similar to the sessile-drop method of Ellefson and Taylor,[4] and was conducted as follows: a 2-gm. portion of −100-mesh glass was pressed to form a cylindrical specimen 1/2 in. in diameter. The specimen was placed upon a 2 1/2- by 3 1/2-in. piece of prepared 18-gauge enameling iron, and both were placed in a tube furnace. Nitrogen was introduced into the furnace, and a small continuous flow of nitrogen was maintained during the test period to prevent further oxidation of the metal surface. The ends of the refractory tube of the furnace were covered with glass plates so that visual study of the sample was possible.

The temperature of the furnace was increased at the rate of 6° to 8°C. per minute. The glass specimen was observed with a low power telescope; and above 600°C., the drop shape was photographed at about 25°C. increments of temperature.

The contact angle values and heights of the drop were determined by measurements on enlarged photographic prints. The ratio of photographic enlargement was determined by

---

Presented at the Fifty-Second Annual Meeting, The American Ceramic Society, New York, N. Y., April 26, 1950 (Enamel Division, No. 15). Received August 1, 1949.

This investigation was conducted at The University of Missouri in partial fulfillment of the requirements of Mr. Shah for a Master of Science degree. At the time of the investigation, Mr. Knapp was assistant professor in the Department of Ceramic Engineering, The University of Missouri; he is now assistant professor in the Department of Engineering, University of California. Mr. Planje is assistant professor in the Department of Ceramic Engineering, The University of Missouri.

[1] (*a*) M. J. Bahnsen, "Review of Theories on Adherence of Sheet-Steel Enamels," *Enamelist*, **12** [12] 16–17 (1935); *Ceram. Abstracts*, **15** [1] 11 (1936).

(*b*) W. A. Deringer, "Relation of Hydrogen to Adherence of Sheet-Steel Enamels," *J. Am. Ceram. Soc.*, **26** [5] 151–59 (1943).

(*c*) J. O. Lord, "Critical Analysis of Some Statements and Experiments on the Adherence of Sheet-Steel Ground Coats," *ibid.*, **20** [4] 111–25 (1937).

(*d*) Karl Kautz, "Further Data on Enamel Adherence," *ibid.*, **19** [4] 93–108 (1936).

(*e*) H. F. Staley, "Electrolytic Reactions in Vitreous Enamels and Their Relation to the Adherence of Enamels to Steels," *ibid.*, **17** [6] 163–67 (1934).

(*f*) G. C. Priddey, "Influence of Cobalt and Nickel on Vitreous Enamel Ground Coats," *Foundry Trade J.*, **80** [1578] 263–71; [1581] 351–52 (1946); *Ceram. Abstracts*, **1947**, March, p. 62*i*.

(*g*) G. H. Spencer-Strong and R. M. King, "Mechanics of Enamel Adherence: IX, Equilibrium Studies in Some Systems of Enamel Glass and Cobalt, Nickel, and Iron Oxides," *J. Am. Ceram. Soc.*, **17** [7] 208–14 (1934).

[2] T. R. Scott, "Anomalous Behavior of Fused Cryolite," *Nature*, **157**, 480–81 (1946).

[3] R. M. King, "Nature of Enamel Adherence," *Finish*, **4** [9] 37–39, 56 (1947); *Ceram. Abstracts*, **1948**, Jan., p. 4*a*.

[4] B. S. Ellefson and N. W. Taylor, "Surface Properties of Fused Salts and Glasses: I, Sessile-Drop Method for Determining Surface Tension and Density of Viscous Liquids at High Temperatures," *J. Am. Ceram. Soc.*, **21** [6] 193–205 (1938).

[5] W. N. Harrison and D. G. Moore, "Surface Tension of Vitreous Enamel Frits at Near Firing Temperatures," *J. Research Natl. Bur. Standards*, **21** [3] 337–46 (1938); RP 1133; *Ceram. Abstracts*, **18** [1] 12 (1939).

[6] C. R. Amberg, "Effect of Molybdenum and Other Oxides on Surface Tension of Silicate Melts and on Properties of Refractories and Abrasives," *J. Am. Ceram. Soc.*, **29** [4] 87–93 (1946)

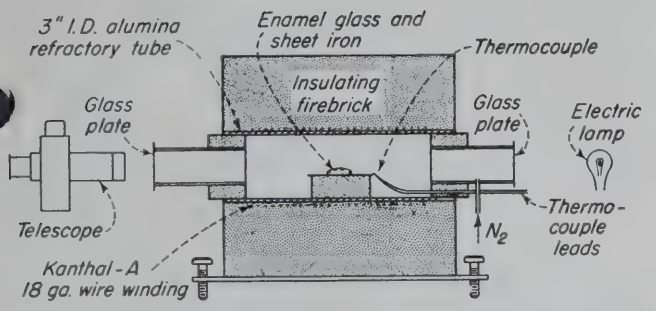

Fig. 1. Diagram of furnace and apparatus for measuring apparent interfacial tension.

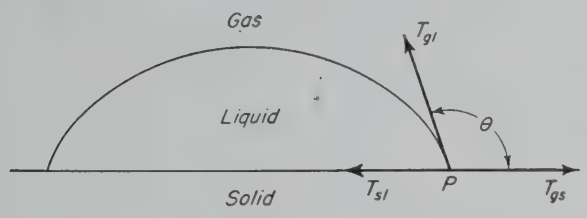

Fig. 2. Diagram showing the three principal forces which act at a point (P) in a drop. The subscript letters g, l, and s, stand for gas, liquid, and solid, respectively.

photographing a mm. scale placed in the normal sample position. The furnace and associated apparatus are shown in Fig. 1.

The experimentation was designed to determine the wetting characteristics of an enamel glass on enameling iron by observing the drop shape at several temperatures. Three principal forces act at point P (Fig. 2) of a drop, and are the interfacial tensions T_{gs}, T_{sl}, and T_{gl}. The subscript letters, g, l, and s, stand for gas, liquid, and solid, respectively. At equilibrium,

$$T_{sl} = T_{gs} + T_{gl} \cos \theta \quad (1)$$

For a large drop at equilibrium, the interfacial tension between gas and liquid (T_{gl}) may be calculated by means of the approximation formula of Quincke:[7(a)]

$$T_{gl} = \frac{g' \rho z^2}{2(1 - \cos \theta)} \quad (2)$$

g' = gravitational constant.
ρ = density of glass.
z = depth below apex of drop.
θ = contact angle.

For the interface between the solid and the liquid, the work of adhesion may be calculated by means of the following equation:[8]

$$W = T_{gl} (1 - \cos \theta) \quad (3)$$

W = work of adhesion.
θ = contact angle (measured through the gas phase; see Fig. 2).

Since the measurements were made instantaneously as the temperature was continuously increased, the glass drop did not develop an equilibrium shape at any specific point of determination. The time required for the drop to assume its equilibrium shape is dependent on glass viscosity. Viscosities of the test glasses were not determined, and the extent of the influence of viscosity was not evaluated. Values were calculated for T_{gl} and W by means of equations (2) and (3), and were termed "apparent," in view of the nonequilibrium conditions.

(2) *Glass Properties*

The relative fusibilities of the glasses used were determined by the porcelain-fusion-block method.[9] The glasses were crushed and passed through a 100-mesh sieve; portions were packed into fusion blocks and heated rapidly in a furnace to 600°C., and thereafter at the rate of 6° to 8°C. per minute. Temperature readings were taken when the glass flowed past the top and bottom reference marks.

Glass density determinations were made by the pycnometer method at room temperature.

(3) *Impact Resistance*

Samples of the glass frits were milled with 6% clay and sufficient water to bring the specific gravity to about 1.70. Two- by four-inch specimens of the 18-gauge enameling iron were dipped into the slip, so that an application weight of about 20 gm. per sq. ft. per side was obtained. The specimens were fired for 3 minutes at 840°C. (Enamels containing As_2O_3 and Ni_3O_4 were fired for $3\frac{1}{2}$ minutes.) The falling-weight test[10] was used with modification to evaluate impact resistance for five specimens of each type. A steel ball was dropped from a small height upon a supported specimen, and repeated drops were made from regularly increased heights until failure was indicated by visual observation. The kinetic energy of the ball at the impact producing failure was calculated and was designated "impact resistance." The thickness of the fired enamels was measured with a magnetic-type thickness tester (General Electric Type B).

---

[7] (*a*) G. Quincke, Ueber die Capillaritäts Constanten geschmolzener Körper," *Am. Phys. Chemie*, **135**, 621 (1868), "Ueber die Capillaritäts Constanten geschmolzener Chemischer Verbindungen," *ibid.*, **138**, 141 (1869).

(*b*) G. Autonow, "Surface Tension in Different States of Aggregation," *Ann. Physik*, **35**, 84–96 (1939); *Ceram. Abstracts*, **18** [11] 312 (1939).

(*c*) C. L. Babcock, "Surface Tension Measurements on Molten Glass by Modified Dipping Cylinder Method," *J. Am. Ceram Soc.*, **23** [1] 12–17 (1940).

(*d*) A. E. Badger, C. W. Parmelee, and A. E. Williams, "Surface Tension of Various Molten Glasses," *ibid.*, **20** [10] 325–29 (1937).

(*e*) A. Dietzel, "Practical Importance and Calculation of Surface Tension in Glasses, Glazes, and Enamels," *Sprechsaal*, **75**, 82 (1942).

(*f*) A. Dietzel, "Relations Between Surface Tension and Structure of Molten Glass," *Kolloid-Z.*, **100**, 368–80 (1942); *Ceram. Abstracts*, **22** [11] 191 (1943).

(*g*) N. E. Dorsey, "New Equation for the Determination of Surface Tension from the Form of a Sessile Drop or Bubble," *J. Wash. Acad. Sci.*, **18** [19] 505–509 (1928); *Ceram. Abstracts*, **8** [2] 148 (1929).

(*h*) F. M. Jaeger, "Temperature Coefficient of Free Molecular Surface Energy of Liquids Between 80°C. and 1650°C.," *Z. anorg. u. allgem. Chem.*, **101**, 1–214 (1917).

(*i*) C. M. Lampman, "Effect of Different Bodies on Some Wetting and Flow Characteristics of Glazes," *J. Am. Ceram. Soc.*, **21** [7] 252–58 (1938).

(*j*) H. K. Livingston, "Contact Angles and Adsorption on Solid Surfaces," *J. Phys. Chem.*, **48**, 120–24 (1944).

(*k*) G. W. Morey, Properties of Glass. American Chemical Society Monograph Series, Reinhold Publishing Corp., New York, 1938. 561 pp.; *Ceram. Abstracts*, **18** [2] 48 (1939).

(*l*) C. W. Parmelee and K. C. Lyon, "Maximum Bubble Pressure (Jaeger) Method for Measuring Surface Tension of Molten Glass," *J. Soc. Glass Technol.*, **21** [83] 44–52 (1937); *Ceram. Abstracts*, **17** [8] 275 (1938).

(*m*) A. D. Prater and A. E. Badger, "Correction Factor for Surface Tension of Glass by the Drop-Weight Method," *Glass Ind.*, **27** [7] 339, 367 (1946); *Ceram. Abstracts*, **1946**, Oct., p. 172.

(*n*) L. Shartis and A. W. Smock, "Surface Tensions of Some Optical Glasses," *J. Am. Ceram. Soc.*, **30** [4] 130–36 (1947).

(*o*) E. W. Tillotson, "Surface Tensions of Molten Glasses," *J. Ind. Eng. Chem.*, **4**, 651–52 (1912).

[8] E. K. Rideal, Introduction to Surface Chemistry, pp. 5–6. Cambridge Univ. Press, 1930.

[9] A. I. Andrews, Enamels, p. 330. Twin City Printing Co., Champaign, Ill., 1935; 428 pp.; *Ceram. Abstracts*, **14** [7] 158 (1935).

[10] C. J. Kinzie, "Physical Tests for Vitreous Enamels," *J. Am. Ceram. Soc.*, **12** [3] 188–92 (1929).

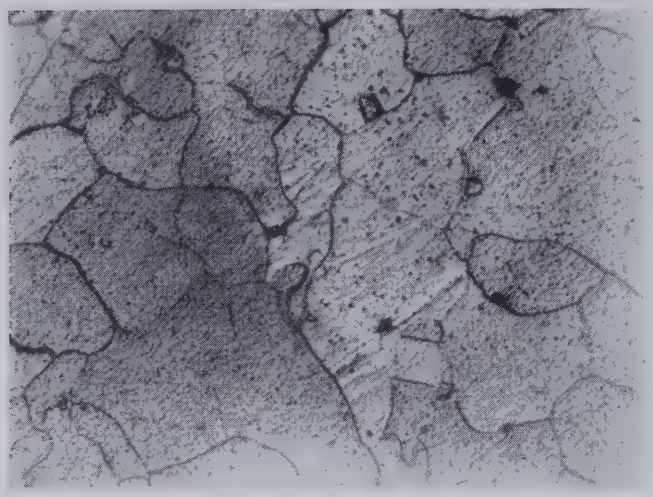

Fig. 3. Microstructure of enameling iron; 250×; 2% nital etch.

Fig. 4. Typical enamel glass drop (Base + As_2O_3–750°C.).

III. Materials

(1) *Enamel Glasses*

A base glass composition, similar to a typical ground coat without the adherence agents, was used (Table I). Adherence-agent additions, consisting of Co_3O_4, CuO, MnO_2, MoO_3, Ni_3O_4, WO_3, As_2O_3, V_2O_5 and TiO_2, were made to similar batches in the amount of 3%. These oxides were chemically pure, and the base glass ingredients were ceramic-grade materials. The batches were melted in an air-gas pot furnace at 1150° to 1200°C., temperatures being measured with an optical pyrometer, and the melts were fritted.

Table I. Composition of Base Enamel Glass

Batch composition (%)		Calculated oxide composition (%)	
Buckingham feldspar	24.9	SiO_2	48.2
Hydrated borax	34.8	Al_2O_3	6.7
Flint	19.9	B_2O_3	11.6
Sodium carbonate	6.5	Na_2O	13.4
Sodium nitrate	3.9	K_2O	6.2
Fluorspar	7.0	CaO	6.1
Adherence oxide	3.0	F	4.1
		Adherence oxide	3.7

(2) *Enameling Metal*

Commercially pure, 18-gauge sheet enameling iron was used. The microstructure of the metal is shown in Fig. 3. The metal was prepared by being cleaned in a boiling, commercial cleaner solution, rinsed, pickled in sulfuric acid (7% H_2SO_4, 60°C., 15 minutes) and neutralized (0.30% borax solution, 60°C., 10 minutes).

Table II. Apparent Interfacial Tension (Gas-Liquid—T_{gl}) and Apparent Work of Adhesion (W)

Glass	Temp. (°C.)	Apparent interfacial tension, T_{gl} (dynes/cm.)	Apparent work of adhesion W (ergs/cm.²)
Base	636	212	212
	650	127	168
	675	72	108
	700	27	48
	725	5	10
	750	Very small	Very small
Base + 3% Co_3O_4	650	168	168
	675	87	83
	700	25	47
	725	3	5
	750	Very small	Very small
Base + 3% MnO_2	636	241	256
	650	193	252
	675	84	127
	700	29	53
	725	7	13
	750	Very small	Very small
Base + 3% CuO	650	238	238
	685	176	188
	700	116	144
	725	46	80
	750	14	27
	775	9	19
Base + 3% Ni_3O_4	675	382	332
	716	381	338
	725	182	217
	750	16	31
	775	5	10
Base + 3% As_2O_3	650	324	324
	688	244	230
	700	179	184
	725	48	81
	750	41	71
	775	37	65
	800	35	63
	825	33	59
	850	31	56
	875	11	22
	900	Very small	Very small
Base + 3% WO_3	636	198	198
	650	127	152
	673	45	61
	700	22	41
	725	8	15
	750	4	8
Base + 3% TiO_2	650	246	246
	675	154	242
	700	47	77
	725	18	34
	750	10	19
	775	Very small	Very small
Base + 3% MoO_3	642	256	256
	650	163	172
	675	91	113
	700	28	51
	725	7	13
	750	Very small	Very small
Base + 3% V_2O_5	640	249	206
	650	132	116
	675	54	81
	700	26	46
	725	15	29
	750	4	8
	775	Very small	Very small

IV. Results

A photograph of a typical enamel glass drop is shown in Fig. 4. Values for apparent interfacial tension between gas-liquid (glass), T_{gl}, and for apparent work of adhesion, W, are given in Table II. Values of T_{gl} are plotted for several temperatures in Fig. 5.

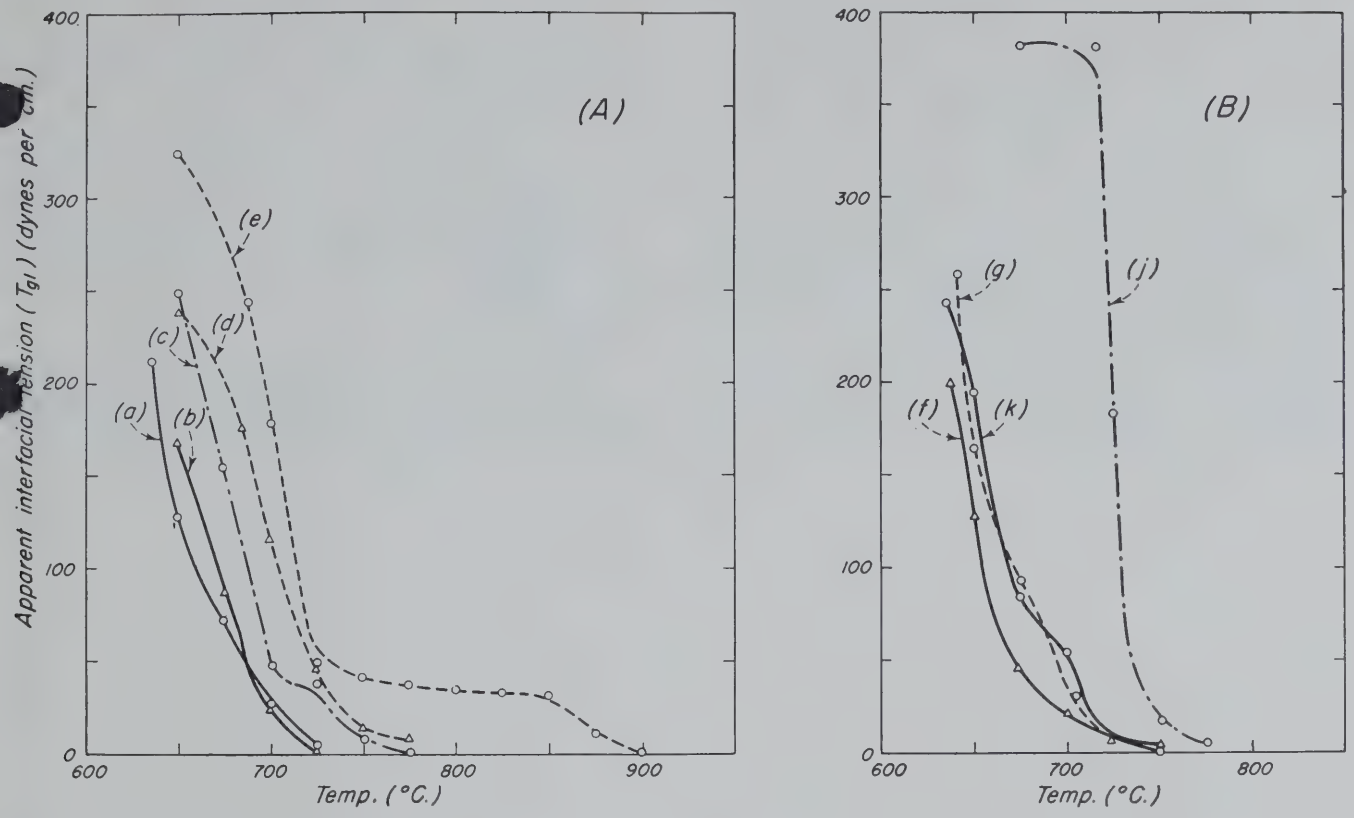

Fig. 5. Apparent interfacial tension—gas-liquid vs. temperature: *A*, (*a*) base; (*b*) base + Co_3O_4; (*c*) base + TiO_2; (*d*) base + CuO; (*e*) base + As_2O_3; *B*, (*f*) base + MnO_2; (*g*) base + MoO_3; (*j*) base + Ni_3O_4; (*k*) base + WO_3.

Table III. Enamel Fusibility and Impact Resistance Values

Enamel glass	End point (°C.), fusion block test	Temp. interval (°C.), for flow	Impact resistance (× 10^6) (ergs)
Base	750	46	5.8
Base + 3% Co_3O_4	735	4	11.7
Base + 3% CuO	755	35	7.1
Base + 3% MnO_2	720	28	6.5
Base + 3% MoO_3	745	36	4.6
Base + 3% Ni_3O_4	820	84	4.5
Base + 3% WO_3	740	62	4.5
Base + 3% As_2O_3	880	151	2.7
Base + 3% V_2O_5	725	37	2.1
Base + 3% TiO_2	750	41	1.5

Table IV. Rate of Change of Apparent Interfacial Tension (Gas-Liquid) with Temperature vs. Impact Resistance

Glass type	Rate of change of apparent T_{gl} with temp. $\left(\frac{\delta T_{gl}}{\delta \text{ temp.}}\right)$ (dynes/cm./°C.)	Impact resistance (ergs) (× 10^6)
Base	3.22	5.8
Base + 3% Co_3O_4	2.92	11.7
Base + 3% CuO	2.56	7.1
Base + 3% MnO_2	3.34	6.5
Base + 3% MoO_3	3.44	4.6
Base + 3% Ni_3O_4	18.5	4.5
Base + 3% WO_3	3.91	4.5
Base + 3% As_2O_3	5.16	2.7
Base + 3% V_2O_5	4.12	2.1
Base + 3% TiO_2	4.16	1.5

Enamel impact resistance and fusibility results are given in Table III.

V. Discussion

Enameling iron usually is thought to possess a surface layer of iron oxide after metal preparation for commercial enameling. As a typical commercial method was used to prepare the iron used in experimentation, the results actually concern the wetting behavior of some enamel glasses on a surface which was composed chiefly of iron oxide.

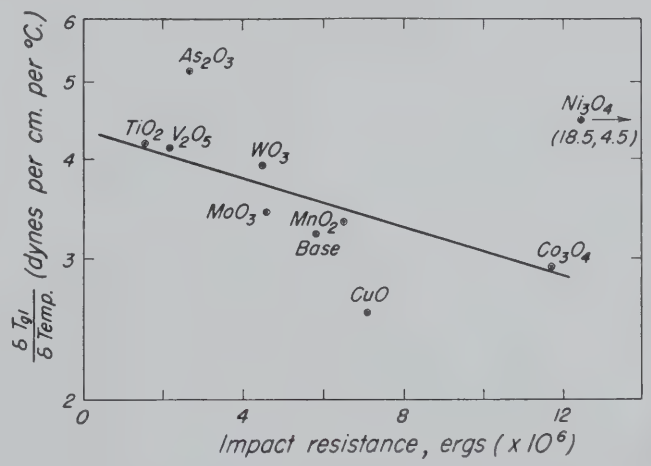

Fig. 6. Impact resistance and rate of change of apparent interfacial surface tension (gas-liquid) with temperature.

In discussing the wetting behavior of a liquid drop, Barrett and Taylor[11] define a contact angle of 90° as the criterion of the temperature at which wetting begins; and this precedent was accepted for the considerations presented herewith.

Most of the curves presented in Fig. 5 have portions which display approximately linear relations of apparent T_{gl} and temperature. Table IV and Fig. 6 show values for the mean

[11] E. P. Barrett and J. A. Taylor, "Method for Studying Flow Characteristics of Glasses and Slags at Elevated Temperatures," *J. Am. Ceram. Soc.*, **19** [2] 39–44 (1936).

rate of change of apparent T_{gl} with temperature $\left(\frac{\delta T_{gl}}{\delta \text{ temp.}}\right)$ and impact resistance. $\frac{\delta T_{gl}}{\delta \text{ temp.}}$ values were obtained by calculating the slopes of the linear portions of the curves in Fig. 5. Some possibility of a relation between impact resistance and $\frac{\delta T_{gl}}{\delta \text{ temp.}}$ is indicated in Fig. 6; this may be due to the existence of temperature ranges of varying magnitudes over which wetting may occur. If the mechanism responsible for adherence were made operative over a longer temperature interval of firing by virtue of an increased period of wetting, better adherence and impact resistance might result.

No relations or conclusions could be made with values obtained for apparent work of adhesion; this suggested that the mechanism of adherence may not be accounted for entirely by wetting properties alone.

VI. Conclusions

(1) It is desirable to distinguish between the absolute surface tension of a glass relative to air and its wetting ability on a specific surface for correlation with the adherence of enamel glasses on metal.

(2) The rate of change of wetting ability with temperature of glasses may influence the progress of the mechanism responsible for adherence.

(3) The experimental procedure described may suggest a control method for evaluating the wetting properties of enamel glasses.

Acknowledgment

The authors wish to express their appreciation to P. G. Her S. T. Yuster, and D. Rosenthal for their advice and critici They also wish to thank J. S. Winston for his assistance in making photomicrographs of the metal.

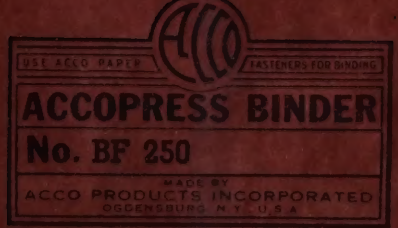
USE ACCO PAPER FASTENERS FOR BINDING
ACCOPRESS BINDER
No. BF 250
MADE BY
ACCO PRODUCTS INCORPORATED
OGDENSBURG N.Y. U.S.A.

UNIVERSITY OF ILLINOIS-URBANA
620C122R C001
REPRINTS IN ENGINEERING
1-47
3 0112 007897645